PDR

ORNL/NRC/LTR-89/13

THE RESPONSE OF BWR MARK II AND MARK III CONTAINMENTS TO SHORT-TERM STATION BLACKOUT SEVERE ACCIDENT SEQUENCES

S. R. Greene
S. A. Hodge
C. R. Hyman
A. E. Levin*
B. W. Patton
A. Sozer
M. L. Tobias

BWR Mark II and Mark III Parametrics Program
Oak Ridge National Laboratory
Oak Ridge, Tennessee

Letter Report

December 29, 1989

Research sponsored by the U.S. Nuclear Regulatory Commission Office of Nuclear Regulatory Research under Interagency Agreement DOE 1886-8082-8B with the U.S. Department of Energy under contract DOE-AC05-840R21400 with the Martin Marietta Energy Systems, Inc.

NOTICE

This report was prepared as an account of work sponsored by an agency of the United States Government. Neither the United States Government nor any agency thereof, or any of their employees, makes any warranty, expressed or implied, or assumes any legal liability or responsibility for any third party's use, or the results of such use, of any information apparatus, product or process disclosed in this report, or represents that its use by such third party would not infringe privately owned rights.

*Georgia Institute of Technology

NOTICE: This document contains information of a preliminary nature. It is subject to revision or correction and therefore does not represent a final report.

9001300186 900122
PDR TOPRP EXIORNL
B PDC

ORNL/NRC/LTR-89/13

THE RESPONSE OF BWR MARK II AND MARK III CONTAINMENTS TO SHORT-TERM STATION BLACKOUT SEVERE ACCIDENT SEQUENCES

S. R. Greene
S. A. Hodge
C. R. Hyman
A. E. Levin*
B. W. Patton
A. Sozer
M. L. Tobias

BWR Mark II and Mark III Parametrics Program
Oak Ridge National Laboratory
Oak Ridge, Tennessee

Letter Report

December 29, 1989

Research sponsored by the U.S. Nuclear Regulatory Commission Office of Nuclear Regulatory Research under Interagency Agreement DOE 1886-8082-8B with the U.S. Department of Energy under contract DOE-AC05-84OR21400 with the Martin Marietta Energy Systems, Inc.

NOTICE

This report was prepared as an account of work sponsored by an agency of the United States Government. Neither the United States Government nor any agency thereof, or any of their employees, makes any warranty, expressed or implied, or assumes any legal liability or responsibility for any third party's use, or the results of such use, of any information apparatus, product or process disclosed in this report, or represents that its use by such third party would not infringe privately owned rights.

*Georgia Institute of Technology

NOTICE: This document contains information of a preliminary nature. It is subject to revision or correction and therefore does not represent a final report.

CONTENTS

		Page
FOREWORD		v
EXECUTIVE SUMMARY		ES-1
1. INTRODUCTION		1-1
2. BWR-4/MARK II ANALYSES		2-1
2.1 Introduction		2-2
2.2 BWR-4 Short-term Station Blackout Core Degradation Analyses		2-4
	2.2.1 Introduction	2-4
	2.2.2 BWR-4 BWRSAR Model	2-6
	2.2.3 Short-term Station Blackout Response (with ADS and simplified eutectics)	2-8
	2.2.4 Short-term Station Blackout Response (with ADS and best-estimate eutectics)	2-31
	2.2.5 Short-term Station Blackout Response (simplified eutectics and no ADS)	2-39
2.3 Mark II Containment Response to Unmitigated Short-term Station Blackout		2-61
	2.3.1 Mark II Containment Design Description	2-61
	2.3.2 Mark II Containment Failure Modes and Mechanisms	2-67
	2.3.3 MELCOR Mark II Containment Model Description	2-68
	2.3.4 Mark II Containment Response: Short-term Station Blackout With ADS, Simplified Eutectics, and All Core Debris Retained in Drywell Pedestal	2-73
	2.3.5 Mark II Containment Response: Short-term Station Blackout With ADS, Simplified Eutectics, and Pool-Debris Interaction	2-84
2.4 Response of Mark II Downcomers to Contact With Core Debris		2-98
	2.4.1 Introduction	2-98
	2.4.2 Mark II Downcomer Design Description	2-98
	2.4.3 Description of the HEATING Thermal Analysis Code	2-99
	2.4.4 HEATING-6 Downcomer/Debris Model	2-99
	2.4.5 Analysis Results	2-104
3. BWR-6/MARK III ANALYSES		3-1
3.1 Introduction		3-1
3.2 BWR-6 Short-term Station Blackout Core Degradation Analyses		3-1

CONTENTS (continued)

		Page
3.2.1	Introduction	3-1
3.2.2	BWRSAR BWR-6 Model	3-1
3.2.3	Short-term Station Blackout Response (with ADS)	3-6
3.3	Mark III Short-term Station Blackout Containment Response to Unmitigated Short-term Station Blackout	3-27
3.3.1	Introduction	3-27
3.3.2	Mark III Containment Design Description	3-27
3.3.3	Mark III Containment Failure Modes and Mechanisms	3-42
3.3.4	Mark III Containment Model Description	3-43
3.3.5	Mark III Containment Response: Short-term Station Blackout With ADS	3-49
APPENDIX A.	MELCOR Defect Investigation Reports Forwarded to SNL	A-1
APPENDIX B.	MELCOR Code Corrections/Modifications Implemented at ORNL	B-1
APPENDIX C.	BWRSAR/MELCOR Interface	C-1
APPENDIX D.	Mark II Steam Explosion Issues	D-1
APPENDIX E.	Code Input Decks for the Mark II Containment Response Calculations	E-1
APPENDIX F.	Code Input Decks for the Mark III Containment Response Calculations	F-1

FOREWORD

This letter report is the second in a series of draft reports to be published by the NRC-sponsored ORNL BWR Mark II and III Parametrics Program.

The purpose of this letter report is to provide an update on the status of ongoing work, and to provide a summary of the results obtained to date. The intent of the Mark II and III Parametrics Program is to apply the best available BWR severe accident simulation tools and detailed plant models to provide best-estimate analyses of generic Mark II and III severe accident behavior, and to assess the potential value of plant and procedural modifications. No single computer code provides the best-available treatment of all aspects of BWR severe accident phenomena. Some potentially important BWR Mark II severe accident phenomena cannot be modeled by any existing computer code. The BWRSAR, MELCOR, and HEATINC computer codes are being employed for the analyses discussed in this report. Considerable effort has been expended to develop detailed plant models (i.e., code input decks) which accurately reflect the most important design features of Mark II and Mark III containments, while maximizing the generic applicability of the analyses results. In this regard, the cooperation of the Pennsylvania Power and Light Company (PP&L), and System Energy Resources Incorporated (SERI) [the owners of the Susquehanna and Grand Gulf nuclear power plants] is greatly appreciated. Both PP&L and SERI have provided site visits and access to detailed plant design and procedural data which has contributed significantly to the quality and applicability of these analyses.

This report focuses on the results of the analyses completed before November 7, 1989.

Sherrell R. Greene, Manager
Mark II and III Parametrics
Program

EXECUTIVE SUMMARY

This report is the second in a series of letter reports to be published by the NRC-sponsored ORNL BWR Mark II and III Parametrics Program. The report focuses on the results of analyses conducted prior to November 7, 1989 to investigate the response of BWR Mark II and Mark III containments to an unmitigated short-term station blackout severe accident sequence.

The BWRSAR, MELCOR, and HEATING computer codes are being employed for the analysis of BWR-4/Mark II and BWR-6/Mark III reactor/containment systems. BWRSAR is being employed to characterize the mass and energy sources from the reactor to the containment for the scenarios of interest. MELCOR is employed to calculate the response of the containment to these sources. HEATING is used to conducted detailed analyses of the response of Mark II downcomers to core-concrete debris impingement.

BWRSAR calculations have been completed for the first 900 min. of the short-term station blackout sequence with automatic depressurization system (ADS) actuation for both the BWR-4/Mark II and the BWR-6/Mark III designs. Reactor vessel (bottom head penetration) failure is predicted to occur in the BWR-4 case at 263 min. into the transient. Reactor vessel failure is predicted to occur in the BWR-6 case at 218 min. into the transient. BWRSAR calculations have also been completed for the BWR-4/Mark II short-term station blackout accident sequence without ADS actuation. Reactor vessel (bottom head penetration) failure is predicted to occur in the BWR-4 case at 246 min. into the transient (17 min. before vessel failure in the case with ADS).

BWRSAR calculations have also been conducted to examine the potential impact of the most recent experimental findings regarding BWR debris eutectic formation in the lower head of the reactor vessel. [Debris relocation into the BWR bottom head would cause boiloff of the water there; after dryout, reheating of the collected debris would promote the formation of eutectic mixtures.] These calculations indicate that more unoxidized zirconium would be expected to enter the containment early in the accident than is predicted by traditional modeling methods. This unoxidized zirconium would oxidize on the containment floor, heating the debris and providing a direct source of hydrogen to the drywell atmosphere. However, the calculations also indicate that any significant differences in the predicted containment response would be limited to the first two hours after initial reactor vessel penetration failure.

MELCOR calculations have been completed for the BWR-4/Mark II short-term station blackout accident with ADS initiation. The Mark II containment model utilized in this study incorporates a deep inpedestal drywell cavity similar to that of WNP-2 (flooded inpedestal wetwell region). The results of the calculations conducted to date indicate that the inpedestal drywell floor would be completely ablated at 810 min. for the case where all of the debris is held inpedestal, and at 846 min. for the

case where 5% of the reactor vessel debris pour is assumed to flow directly into the wetwell. The containment pressure at the time of drywell floor failure in the first case is predicted to be approximately 120 psig, which is below the expected containment failure pressure of 135 psig. The containment pressure in the second case (5% debris enters the wetwell pool) is approximately 125 psig. No assessment of the containment pressure pulse resulting from gross debris/pool interactions following drywell floor failure has been made. These results are not applicable to Mark II designs such as Limerick and Susquehanna which do not have an inpedestal drywell cavity. Additional MELCOR Mark II calculations are in progress at the present time.

Detailed HEATING-6 calculations have been conducted to examine the response of a typical Mark II downcomer to debris impingement. The debris conditions employed for this analysis are based on the MELCOR/CORCON results for the short-term station blackout accident sequence with ADS actuation, and are representative of the most challenging debris conditions observed throughout the calculation. The results of these analyses suggest that the downcomers may be able to withstand debris heights of six inches without failing for the specific initial and boundary conditions utilized in the study. Firm conclusions regarding downcomer survivability cannot be made, however, since several potentially-important transient effects are ignored by these analyses.

MELCOR calculations are underway for the BWR-6/Mark III short-term station blackout sequence with ADS actuation. No calculations were complete as of November 7, due to several MELCOR code problems and MELCOR/BWRSAR interface issues that have slowed progress in this area.

Several MELCOR code bugs and suggested improvements have been identified to date, and forwarded to the Sandia MELCOR code development team. Three of these problems could not be corrected via creative use of code input options. These three problems were addressed by modifying MELCOR directly and creating new local (ORNL) versions of the code.

Finally, a short-term study (funded by Oak Ridge Associated Universities) has been completed to assess the state of knowledge regarding core-concrete-water interactions, the potential significant of such interactions in Mark II containment systems, and the efficacy of incorporating more comprehensive models for these phenomenon in MELCOR. The conclusions of this study are that experimental data for core-concrete-water interactions is virtually non-existent. The presence of hot or molten concrete and concrete decomposition products in core debris could significantly alter the dynamics of fuel-coolant interactions. MELCOR's current capability to simulate these phenomena is extremely simplistic and limited in scope. The incorporation of concrete properties and the ability to treat core-concrete-water interactions could be added in a straight-forward way to MELCOR to provide a more versatile parametric tool for simplistic analyses of this potentially-important Mark II severe accident issue.

THE RESPONSE OF BWR MARK II AND MARK III CONTAINMENTS TO SHORT-TERM STATION BLACKOUT SEVERE ACCIDENT SEQUENCES

1. INTRODUCTION

The ORNL BWR Mark II and III Parametrics Program is sponsored by the Severe Accident Issues Branch of the NRC's Office of Nuclear Regulatory Research, and is a major element of the NRC's Mark II and III Containment Performance Improvement (CPI) Program. The CPI Program is intended to complement the ongoing Individual Plant Examination (IPE) effort by identifying and providing an understanding of generic Mark II and III severe accident containment challenges. ORNL's primary responsibility is to perform best-estimate analyses of severe accident core degradation and containment response phenomena.

Venting for Boiling Water Reactor (BWR) containments has been suggested as a way to prevent some types of core melt accidents or to avoid catastrophic containment failure and large consequences resulting from others. A study (Ref. 1) performed at the Idaho National Engineering Laboratory (INEL) has evaluated venting procedures that were in draft form for the Peach Bottom Atomic Power Station (a Mark I containment). A main conclusion from that study on post-core-melt mitigation was that "based on the draft procedure and equipment in place at the time of the analyses, containment venting has limited potential for further reducing the risk associated with accident sequences currently identified as being important to risk." More recently, Vermont Yankee Nuclear Power Corporation (Ref. 2) and the Boston Edison Company (Ref. 3) have submitted to the Nuclear Regulatory Commission (NRC) potential plans for venting procedures at the Vermont Yankee and Pilgrim plants, respectively. These proposals have also been assessed by INEL (Ref. 4). The ORNL BWRSAT Program has assessed a Mark I plant (Peach Bottom) using the BWRSAR and CONTAIN codes for the more risk significant (based on draft NUREG-1150, dated February 1987) sequences with and without assumptions related to improvements in the Automatic Depressurization System, containment sprays, and venting (Ref. 5). Similar assessments of Mark II and Mark III plants are to be made in this Program.

The fundamental design characteristics of Mark I, II, and III containments are significantly different (Table 1.1). With respect to size, the major design difference is that the total containment free volume of the Mark II is 30-40% larger than that of the Mark I, while the total containment free volume of the Mark III is 500-600% greater than that of the Mark I. This difference alone would suggest that the basic severe accident performance of the Mark II and III plants might be significantly different than the Mark I plants. However, the three containment designs also differ in shape and the location of the pressure suppression pool relative to the drywell floor. The objective of this study is, therefore, to assess the impact of various severe accident parameters on the survivability of Mark II and III containments. Parametric analyses are performed to determine the impact of a range of important parameter values on core melt progression and containment failure timing.

Table 1.1. BWR Mark I, II, and III Containment Characteristics

PARAMETER	MARK I BROWNS FERRY	MARK II LIMERICK	MARK III GRAND GULF
Drywell Design Pres. (psig)	56	55	30
Drywell Design Temp. (°F)	281	340	330
Drywell Free Volume (ft^3)	159,000	248,900	270,000
Wetwell Design Pres. (psig)	56	55	15
Wetwell Design Temp. (°F)	281	220	185
Min. Wetwell Free Vol. (ft^3)	126,200	149,400	1,400,000
Max. Wetwell Pool Vol. (ft^3)	127,800	127,800	136,000
Total Containment Free Vol. (ft^3)	285,200	398,300	1,670,000

This report focuses on the short-term station blackout sequence. Historically, the station blackout accident has been considered to be the sequence initiated by loss of offsite power and reactor scram combined with failure of the station diesels to start and load. Today, this accident sequence is classified as long-term Station Blackout, in which water is injected into the reactor vessel by the steam turbine-driven HPCI or RCIC systems as necessary to keep the core covered for as long as DC power for turbine governor control remains available from the unit batteries, a period of about six hours. The reason for today's "long-term" designation is that the definition of station blackout implemented by the NRC-sponsored Accident Sequence Evaluation Program (ASEP) has been expanded to include two cases that heretofore would have been classified as Loss of Injection, or TQUV in WASH-1400 parlance. In these short-term station blackout sequences, the capability for water injection to the reactor vessel is lost at the inception of the accident sequence. (The short-term designation derives from the fact that the core is uncovered relatively quickly in these sequences.)

The early total loss of injection hallmark of BWR short-term Station Blackout might be initiated in either of two ways. First, there might be independent failures of both the HPCI and RCIC systems when they are called upon to keep the core covered during the period while DC power remains available. Second, there might be a common-mode failure of the DC battery systems that, upon loss of offsite power, precludes starting of the diesel generators and thereby is the cause of the Station Blackout; without DC power for valve operation and turbine governor control, the steam turbine-driven injection systems would not be operable.

With respect to the basic characteristics of the severe accident sequence, the difference between long-term and short-term Station Blackout can be summarized as follows: DC power remains available during the period of core degradation for short-term Station Blackout; the decay heat level is relatively high and the reactor vessel is depressurized during the period of core degradation and material relocation within and from the vessel. For long-term Station Blackout, the core remains covered for more than six hours so the decay heat level is approximately 30% less during the period of core degradation and, since the SRVs cannot be manually operated without DC power, the reactor vessel is pressurized at the time of bottom head penetration failure and initial release of debris from the vessel.

Much of the impetus for basing these BWR containment response studies upon the short-term station blackout severe accident sequence derives from the most recent findings of the ASEP in support of the NUREG-1150 effort (Ref. 6). These findings provide the estimate that 49% of the overall risk of core damage at Peach Bottom and 97% of the core damage risk at Grand Gulf can be attributed to the overall threat of Station Blackout. Although no BWR Mark II containment was considered in the NUREG-1150 effort, there is no reason to suspect that station blackout would not be a dominant sequence for Mark II facilities. For Peach Bottom, the recent ASEP program findings assign 44% of the overall core

damage frequency to long-term Station Blackout, 5% to short-term Station Blackout, 42% to ATWS, and 11% to all other possible accident sequences (Ref. 7). A recently completed study by INEL (Ref. 8) finds base-case core damage frequencies for a generic BWR Mark II containment plant to be 29% for long-term Station Blackout, 12% for short-term Station Blackout, 28% for ATWS, and 31% for all other possible sequences.

A series of BWR-4/Mark II and BWR-6/Mark III calculations are currently underway at ORNL. The BWR-LTAS (Ref. 9), BWRSAR (Ref. 10), and MELCOR (Ref. 11) codes are being employed for analysis of the reactor and primary containment response for a variety of short-term station blackout scenarios. This report describes the results and status of calculations for (a) a BWR-4/Mark II short-term station blackout sequence in which the automatic depressurization system (ADS) is initiated in the optimum manner to delay the onset of hydrogen generation and core damage and relocation, (b) a BWR-4/Mark II short-term station blackout sequence in which the reactor is not depressurized, and (c) a BWR-6/Mark III short-term station blackout sequence in which the ADS is initiated in the optimum manner to delay the core damage process. Although no calculation directly addresses the long-term station blackout accident sequence, it should be noted that the accident sequence analyzed in case (b) can also be considered to represent a worst-case long-term station blackout. [The reactor vessel remains pressurized during the period of core degradation, but the decay heat levels are higher than those normally associated with the long-term case.]

Chapter 2 describes the results of the BWR-4/Mark II analyses. Section 2.2 describes the BWRSAR BWR-4 reactor model utilized to define the invessel accident sequence progression, debris pours, and safety/relief valve (SRV) flows necessary to drive the containment model, and the invessel accident progression and debris pours for the short-term blackout sequences analyzed to date. Section 2.3 presents a description of the Mark II containment design and containment failure mechanisms, the MELCOR Mark II containment model and the MELCOR containment response calculations conducted to date. Section 2.4 describes the results of detailed heat transfer calculations currently underway at ORNL to assess the impact of core debris impingement on and interaction with Mark II downcomers.

Chapter 3 describes the results of the BWR-6/Mark III analyses. Section 3.2 describes the BWRSAR BWR-6 reactor model utilized to define the invessel accident sequence progression, debris pours, and safety/relief valve (SRV) flows necessary to drive the containment model, and the invessel accident progression and debris pours for the short-term blackout sequences analyzed to date. Section 3.3 presents a description of the Mark III containment design and containment failure mechanisms, the MELCOR Mark III containment model and the MELCOR containment response calculations conducted to date.

The MELCOR computer code is currently under active development at Sandia National Laboratories. The current version of the code (version 1.8.0) does not treat some of the BWR-specific severe accident phenomena such

as core plate failure modes, multi-eutectic debris formation invessel, corium spreading on the drywell floor, steam explosions in Mark II wetwells, and others important to the current analyses. Many of these limitations are a consequence of MELCOR's use of other pre-existing severe accident analysis codes (CORCON and VANESA) as physics modules. The successful completion of the work described in this report has also involved identification and/or clarification of several additional code deficiencies and limitations that had initially prevented application of MELCOR to the sequences of interest in this study. Many of these problems are artifacts of differences in MELCOR's and BWRSAR's assumptions regarding the manner in which core debris is formed invessel and discharged from the vessel following vessel failure. Appendix A presents a summary of the various problems identified and reported to the MELCOR code development staff at SNL during the course of this study. Appendix B describes the local MELCOR code modifications implemented at ORNL for three cases in which a basic code application problem could not, to an acceptable degree, be circumvented via manipulation of code input.

Appendix C presents a brief description of the BWRSAR/MELCOR interface written at ORNL to provide an automated method for driving the MELCOR containment models with the BWRSAR SRV flows, vessel leakage flows, debris pours, and exvessel decay heat levels. Appendix D presents the results of a brief investigation (funded by Oak Ridge Associated Universities) conducted to evaluate the state of knowledge concerning core-concrete-water interactions, the impact of such interactions on Mark II containments, and the efficacy of implementing modifications to MELCOR's Fuel Dispersal Interaction module to allow the code to provide some analysis capability for this Mark II severe accident phenomenon. Representative examples of the various code input decks used for the analyses are provided in Appendix E (Mark II calculations) and Appendix F (Mark III calculations).

Chapter 1 References

1. D. J. Hanson et al., "Containment Venting Analysis for the Peach Bottom Atomic Power Station," NUREG/CR-4696, EGG-2464, December 1986.

2. Vermont Yankee Nuclear Power Corporation, *Vermont Yankee Containment Safety Study*, August 1986.

3. R. G. Bird, Boston Edison, *Information Regarding Pilgrim Station Safety Enchancement Program*, BECo ltr. 87-111 to S. A. Varga, USNRC, July 8, 1987.

4. K. C. Wagner, R. J. Dallman, and W. J. Galyean, "An Overview of BWR Mark-I Containment Venting Risk Implications," NUREG/CR-5225, EGG-2548, November 1988.

5. "Primary Containment Response Calculations for Unmitigated Short-Term Station Blackout at Peach Bottom," letter report to Dr. Thomas J. Walker, Accident Evaluation Branch, Division of Systems Research, USNRC, dated November 28, 1988. NUREG/CR-5317 (to be published).

6. "Severe Accident Risks: An Assessment for Five U.S. Nuclear Power Plants," NUREG-1150, Vol. 1, Summary Report, Second Draft for Peer Review, U.S. Nuclear Regulatory Commission, (June, 1989).

7. Personal Communication with Teresa Sype of the ASEP Program, Sandia National Laboratory, November 1988.

8. "Preliminary Risk Quantification for BWR Mark II Containment Improvements," Draft Report by Idaho National Engineering Laboratories, October 24, 1989.

9. R. M. Harrington and L. C. Fuller, "BWR-LTAS: A Boiling Water Reactor Long-Term Accident Simulation Code," NUREG/CR-3764, ORNL/TM-9163, February 1985.

10. S. A. Hodge and L. J. Ott, "Boiling Water Reactor Severe Accident Response (BWRSAR) Code Description and Assessment," NUREG/CR-5381 (to be published).

11. F. E. Haskin et al., "Development and Status of MELCOR," presented at the Fourteenth Water Reactor Safety Information Meeting, Gaithersburg, MD (October 1988).

2. BWR-4/MARK II ANALYSES

2.1 Introduction

There are nine domestic BWR Mark II units (six plants): Limerick-1 and -2, Susquehanna-1 and -2, La Salle-1 and -2, WNP-2, Nine Mile Point-2, and Shoreham. Limerick, Susquehanna, and Shoreham (five units) employ the BWR-4 reactor design; while La Salle, WNP-2, and Nine Mile Point-2 (four units) employ the BWR-5 reactor design. The basic design characteristics of these plants are summarized in Tables 2.1 and 2.2. Although these plants share many generic containment features, the drywell reactor pedestal/cavity design is highly plant-specific (see Section 2.3.1). For the purpose of these analyses, a synthetic "Mark II CPI Plant" design is being utilized. This CPI Plant integrates Susquehanna's BWR-4 reactor with a primary containment which incorporates elements of the Susquehanna, La Salle, and WNP-2 designs. This combination of features was chosen, in part, to minimize the impact of current core-concrete interaction analysis code (CORCON) limitations by utilizing a drywell pedestal/cavity design (La Salle/WNP-2) that prevents spreading of the core debris to the expedestal region of the drywell.

This chapter presents the results of the Mark II calculations performed for this study. Section 2.2 describes the results of the BWRSAR calculations conducted to evaluate the response of the BWR-4 to (a) a short-term station blackout in which the automatic depressurization system (ADS) is activated in a manner consistent with (but modified slightly from) existing plant operating procedures, and (b) a short-term station blackout case in which the reactor vessel is not depressurized. These BWRSAR calculations define the SRV and vessel leakage flows and the debris pours needed to drive the containment response calculations.

The vessel debris pours calculated by the BWRSAR code depend upon a user-input definition of the pure species and eutectic mixtures that will form in the vessel bottom head and their melting points. Two distinct cases were evaluated for the short-term station blackout scenario in which the ADS is actuated. A "best-estimate" debris pour calculation was performed in which BWRSAR was directed to generate multiple eutectic species in the lower head in a manner consistent with the results of the small-scale BWR Core Debris Eutectic Formation and Melting Experiment (Ref. 1) performed at ORNL by G. W. Parker in December 1987. However, the CORCON module within MELCOR can not accommodate this multi-eutectic treatment. A second case was, therefore, evaluated in which BWRSAR was directed to form bottom head debris constituents consistent with those utilized by CORCON. The results of both these calculations are described in Section 2.2, along with the results of the case in which the ADS is not actuated.

Section 2.3 describes the results of the Mark II containment response calculations, and Section 2.4 presents the results of analyses conducted

Table 2.1. Domestic BWR Mark II Units

NAME	MWe	LOCATION	REACTOR TYPE[a]	COMMERCIAL OPERATION
La Salle 1	1036	Seneca, IL	5	10/82
La Salle 2	1036	Seneca, IL	5	6/84
Limerick 1	1055	Pottstown, PA	4	2/86
Limerick 2	1055	Pottstown, PA	4	89%
Nine Mi. Pt. 2	1080	Scriba, NY	5	3/88
Shoreham	809	Brookhaven, NY	4	100%
Susquehanna 1	1032	Berwick, PA	4	6/83
Susquehanna 2	1032	Berwick, PA	4	2/85
WNP-2	1095	Richland, WA	5	12/84

[a]The BWR-4 plants employ a High Pressure Coolant Injection (HPCI) steam-turbine pumping system to provide high pressure makeup to the reactor vessel via a feedwater line. In the BWR-5 plants, this system is replaced by a High Pressure Core Spray (HPCS) system, which is driven by an electric motor.

Table 2.2. Domestic BWR Mark II Design Parameters

PARAMETER	Lim	LaS	Sus	9Mi	Sho	WNP
Power (Mwt)	3293	3293	3293	3300	2436	3293
Design Psig	55	45	53	45	48	45
	-5	-5	-5	-5	-5	-2
Drywell Design Temp (°F)	340	340	340	340	340	340
Wetwell Design Temp (°F)	220	275	220	212	225	225
Drywell Free Volume Ft^3	248900	229500	239600	303400	192500	200500
Wetwell Free Volume Ft^3	289100	297000	281500	346800	215400	256400
Tot. P.C. Ft^3/Mwt	163	160	158	197	167	139
No. Downcomers	87	98	82	123	82	102
Downcomer Dia (in)	24	23.5	24	23.3	23.3	24
Tot. Downcomer Ft^2	257	295	242	363	242	309

Lim = Limerick
LaS = La Salle
Sus = Susquehanna
9Mi = Nine Mile Point-2
Sho = Shoreham
WNP = WNP-2
P.C. = Primary Containment

to examine the response of Mark II downcomers to core debris impingement. Appendix D discusses Mark II core-concrete-pool interaction issues.

2.2 BWR-4 Short-term Station Blackout Core Degradation Analyses

2.2.1 Introduction

The purpose of these BWRSAR code calculations is to provide the debris pour rates and compositions for an unmitigated short-term station blackout accident sequence that proceeds beyond the point of reactor vessel bottom head failure. The BWRSAR code results are being used to drive a detailed MELCOR code simulation of the BWR Mark II containment response.

The core degradation analyses performed in support of the studies discussed in this chapter have been calculated with the Boiling Water Reactor Severe Accident Response (BWRSAR) code and are based upon the unmitigated short-term station blackout accident sequence at a prototypic BWR of the Mark II containment design. (Initial conditions for the calculation were provided by the BWR-LTAS code, as discussed in Section 2.2.2.) The purpose of these BWRSAR calculations is to provide the reactor vessel gas blowdown rates and the core and structural debris pour rates from the vessel for use as input to subsequent MELCOR calculations of the detailed containment response. Information concerning the BWRSAR code and its applications to short-term station blackout is provided in the following discussion.

The BWRSAR code implements the BWR severe accident modeling strategy outlined in Table 2.3. It should be recognized that this methodology, developed at ORNL by L. J. Ott, involves significantly longer times to reactor vessel bottom head penetration failure than previous analytical approaches because of the contention that after the onset of core degradation and the initial local failures of the core plate, the very large amount of water in the BWR reactor vessel bottom head must first be boiled away and the quenched debris must then reheat (to about 1900°F) before the reactor vessel bottom head penetrations can fail. It should also be noted that, in general, very little of the debris in the bottom head is molten at the time of penetration failure and, therefore, the subsequent debris pours from the reactor vessel are controlled by the rate of debris melting and begin sometime after penetration failure. However, if the reactor vessel were pressurized at the time of penetration failure, then the metal-water reactions associated with the vessel blowdown through the bottom head debris would produce a large amount of hydrogen and associated energy release within the debris bed, and significant debris pours would begin almost immediately after bottom head penetration failure.

Additional and more detailed information concerning the operation of the BWRSAR code and its capabilities and limitations can be found in References [2] and [3].

Table 2.3 BWRSAT Program Calculational Methodology Employed to Represent Events Between Onset of Core Degradation and Pour of Molten Materials from Reactor Vessel for BWRs

1. As canister and control blade material becomes molten, it is relocated onto the core plate. This causes:
   a. a temporarily increased steaming rate
   b. core plate dryout and cessation of steaming
   c. buildup of mass on the core plate and core plate heatup.

2. Each radial region of the core plate fails due to loss of strength when its calculated temperature reaches a user-specified value. Each core plate region and its accumulated debris falls into the lower plenum, producing a burst of steam and lowering the water level there as the fallen material is quenched.

3. Molten Zr metal flows downward over the lower core fuel rod nodes, leaving the UO_2 fuel pellets encased in thin ZrO_2 sheaths. Steam rising from the lower plenum cools the core nodes from which all unoxidized Zr has been removed. On the other hand, the rising steam causes energy release in the core peripheral nodes where Zr metal at elevated temperature still remains.

4. The standing portions of the core fall into the lower plenum by radial column. Each core column collapses when its average clad temperature reaches a user-input value, at which time very little of the UO_2 mass in the region has become molten. (The actual failure mechanism is weakening, by overtemperature, of the ZrO_2 sheaths surrounding the UO_2 fuel pellets.) The falling mass is quenched by the water in the lower plenum until the time of bottom head dryout. After bottom head dryout, the debris begins to reheat.

5. The structure of the control rod guide tubes in the lower plenum is heated by the surrounding core debris and is weakened to the point of failure when its temperature reaches a user-specified value. Failure of the control rod guide tubes causes all remaining standing portions of the core to immediately collapse. The control rod guide tube mass is added to the bottom head debris.

6. Bottom head penetrations fail by a simulated creep-rupture mechanism as the debris mass in their vicinity reaches about 2100°F. The reactor vessel depressurizes and equalizes with drywell pressure. When standing molten metal pools develop within debris nodes remote from the vessel wall, leakage pathways are opened through the wall via the instrument guide tubes.

7. The individual components of the debris mass leave the vessel in the order that they reach their melting points and become liquid. Solid metallic material surrounding the lower portion of the original instrument guide tube locations is ablated into the molten material flowing from the reactor vessel via these pathways.

2.2.2 BWR-4 BWRSAR Model

The BWRSAR code input deck for the BWR Mark II calculations is based upon the Susquehanna Plant. Construction of the input deck was greatly facilitated by information provided by the Pennsylvania Power and Light (PP&L) Company with regard to plant-specific design features.

One of the information items provided by PP&L in support of this study has general application to accident studies based upon all types of BWRs and is considered to be of sufficient importance to warrant a brief description here. This item involves Susquehanna Plant data recorded during a plant test in which the main steam isolation valves were tripped with the reactor at power (Ref. 4). Recorded data includes reactor vessel pressure and water level, feedwater flow, HPCI and RCIC system injected flow, and core inlet flow. It has been necessary in previous studies to neglect the effect of reactor vessel injection during feedwater turbine coastdown because information on which to base a reasonable estimate of this effect was not available. As a result of this test, however, we now have the Susquehanna data, which show that the injection associated with feedwater pump coastdown is sufficient to increase the reactor vessel water level by about 57 in. The higher initial reactor vessel water level, in turn, causes a delay of about 16 min. in the time of uncovering of the top of the core and corresponding delays in the subsequent events of the accident sequence.

Additional detailed plant-specific information provided by PP&L combined with the experience and insight gained from previous BWR severe accident studies at Oak Ridge and recent advances in the state of severe accident research have been utilized to construct a BWRSAR code input deck that is considered to be an improvement over previous efforts in the following ways:

1. Representation of 9 × 9 fuel assemblies,

2. Axial conduction calculated for the fuel and cladding,

3. Reduced reactor vessel leakage to conform to measured leak rates for Susquehanna,

4. Safety relief valve (SRV) leakage per Susquehanna experience with Crosby valves,

5. Reduced control blade melting temperature (2450°F) in accordance with recent experimental (DF-4, CORA) observations,

6. Increased core plate and control rod guide tube creep rupture failure temperatures (2100°F) as recommended by recent group discussions with representatives from EPRI, Sandia National Laboratories, and Idaho National Engineering Laboratory concerning BWR severe accident modeling (as explained in Table 2.3, core plate failure permits debris relocation into the reactor vessel lower plenum),

7. Decreased ablation temperature (2660°F) for the debris material in the vessel bottom head,

8. End-of-cycle axial power profile as provided by PP&L for Susquehanna Unit 1 Cycle 4 (equilibrium core),

9. Decay heat release from fuel in accordance with current recommendations of R. A. Lorenz (see the discussion in Appendix A, page A-13. Based on recent experiments, current release is slower than before), and

10. Operator actions, with regard to reactor vessel pressure control in accordance with Susquehanna procedures.

The BWRSAR calculation was initiated at time 35 min. into the short-term station blackout accident sequence. The initial conditions for the BWRSAR input deck were taken from the results of a BWR-LTAS (Ref. 5) calculation that covers the period of the accident sequence from 0.6 min. to 35.0 min. The initial conditions for the BWR-LTAS calculation were taken from the results of the Susquehanna main steam isolation valve closure test discussed in the preceding paragraph. Operator control of reactor vessel pressure during the period of the BWR-LTAS calculation and the period of the BWRSAR calculation before ADS actuation is modeled as follows:

Event	Time (min)
Begin manual control of reactor vessel pressure and begin depressurization to 765 psia.	2.00
Complete controlled depressurization; maintain vessel pressure in range 715–865 psia.	2.00–33.33
With water level near the top of the core, allow vessel pressure to increase. Then maintain vessel pressure in the range 935–1075 psia.	33.33–78.0
With water level at 257.5 in. above vessel zero, open one SRV; when vessel pressure falls to 715 psia, manually actuate the ADS.	78.0

The pressure control strategy described above reflects a final adjustment to the BWRSAR input deck for the purpose of increasing the general applicability of the calculated results. This adjustment was to represent earlier (manual) actuation of the Automatic Depressurization System (ADS) than currently specified by the Susquehanna emergency procedures. Under short-term station blackout conditions, the Susquehanna procedures require the operators to manually actuate ADS at a reactor

vessel water level equivalent to 28% of core height, which occurs at 84.25 min. after scram. However, BWRSAR calculations indicate that a substantial amount of hydrogen (about 80 lb.) would be generated by clad metal-steam reactions by this time. It is believed that the general adherence to Revision 3 of the BWR Owners Group Emergency Procedures Guidelines (EPGs) is better represented by earlier actuation of the ADS, before significant hydrogen has been generated. Accordingly, the BWRSAR calculations have been repeated for use in this study to represent manual ADS actuation at time 78.0 min., when the reactor vessel water level is at 33% of core height and less than 10 lb. of hydrogen has been generated. ADS actuation at this time provides steam cooling of the uncovered portion of the core and delays any further hydrogen generation for a period of about 20 minutes.

2.2.3 Short-term Station Blackout Response (with ADS and simplified eutectics)

2.2.3.1 Calculated events prior to reactor vessel bottom head penetration failure

The sequence of events and event timing for the BWR Mark II short-term station blackout with ADS actuation accident sequence as calculated by the BWRSAR code are provided in Table 2.4. It is assumed that the reactor had been operating at 100% power at the time of scram and that no reactor vessel injection source is ever recovered. As indicated, the ADS maneuver is carried out in two steps in accordance with the provisions of Revision 3 of the EPGs. First, a single SRV member of the ADS family is manually opened when the reactor vessel water level has fallen to one-third core height. Then, as the vessel pressure decreases through 715 psia, the ADS is actuated, opening the remainder of the ADS family of valves. This results in a total of six open SRVs.

Plots of key parameters representing events within the reactor vessel as predicted by the BWRSAR code are provided in Figures 2.1-2.12. These plots represent events from time 35 min., when the BWRSAR calculation is initiated, until time 300 min., which is about 37 min. after reactor vessel bottom head penetration failure. As indicated in Figure 2.1, the ADS maneuver is initiated at time 78 min, when the reactor vessel water level (Figure 2.2) is at about one-third core height; this causes the opening of six SRVs. Since the SRVs are modeled as Crosby valves, the ADS valves remain open once actuated. [This would not be true of the Target Rock-type SRVs installed at earlier BWR plants such as Peach Bottom and Browns Ferry for which the open or closed status depends upon the differential pressure between reactor vessel and drywell.] The associated SRV flows from the reactor vessel to the pressure suppression pool are shown in Figure 2.3.

The swollen reactor vessel water level, the calculation of which includes consideration of the effects of voids, is shown in Figure 2.2. The calculated water level rapidly falls below the core plate as a result of the water loss by flashing when the ADS valves are

Table 2.4. Calculated sequence of events for BWR (Mark II) Short-Term Station Blackout with ADS Actuation

Event	Time (min)
Station blackout-initiated scram from 100% power. Independent loss of the steam turbine-driven HPCI and RCIC injection systems	0.0
Swollen water level falls below top of core	37.2
Open one SRV	78.0
ADS system actuation	79.5
Core plate dryout	81.2
Relocation of core debris begins	124.1
First local core plate failure	129.2
Collapse of fuel pellet stacks in central core	220.0
Reactor vessel bottom head dryout; structural support by control rod guide tubes fails; remainder of core falls into reactor vessel bottom head	263.2
Initial failure of bottom head penetrations	263.3

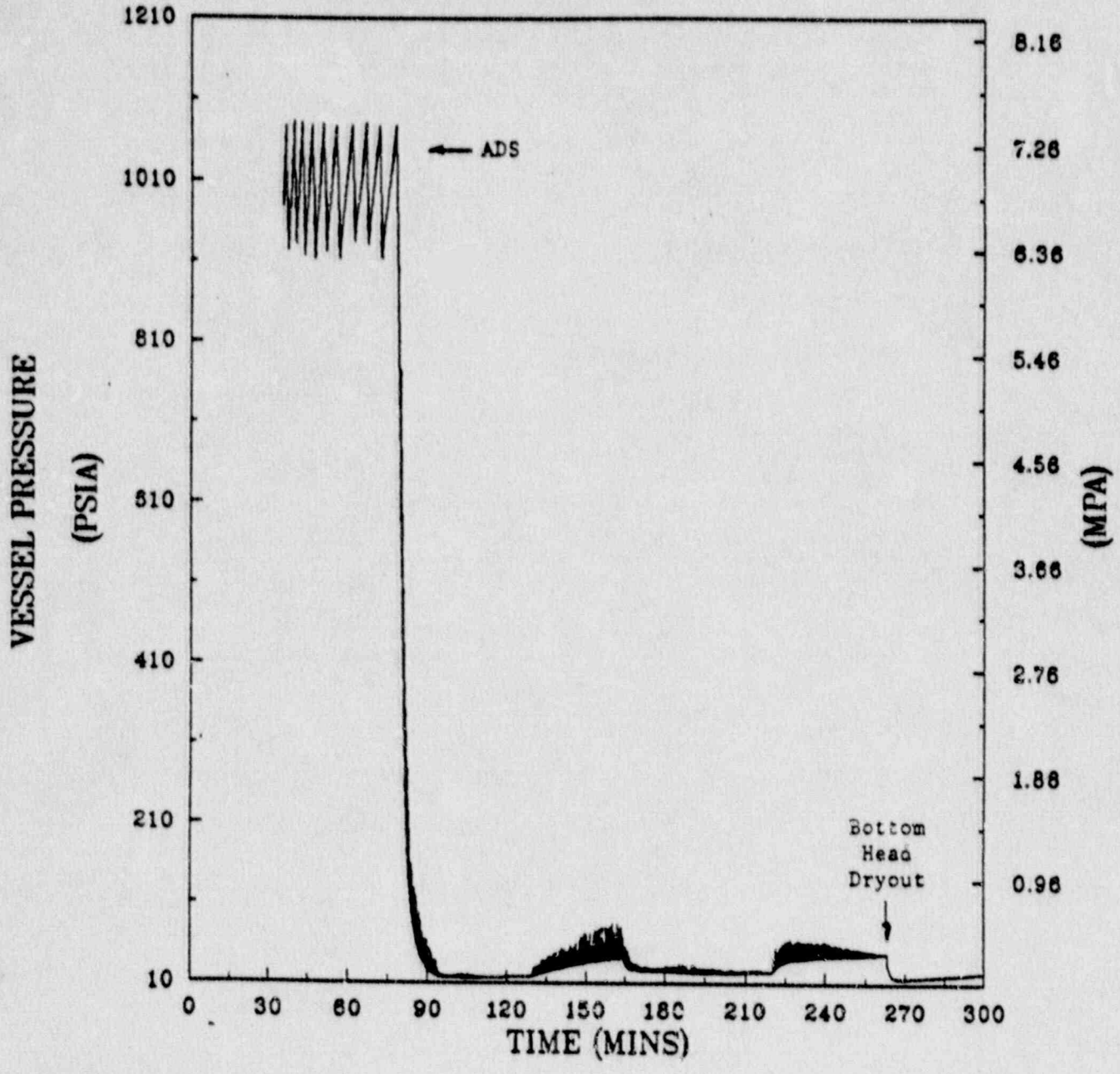

Fig. 2.1. Reactor vessel pressure for BWR-4/Mark II short-term station blackout accident sequence with ADS (simple eutectics).

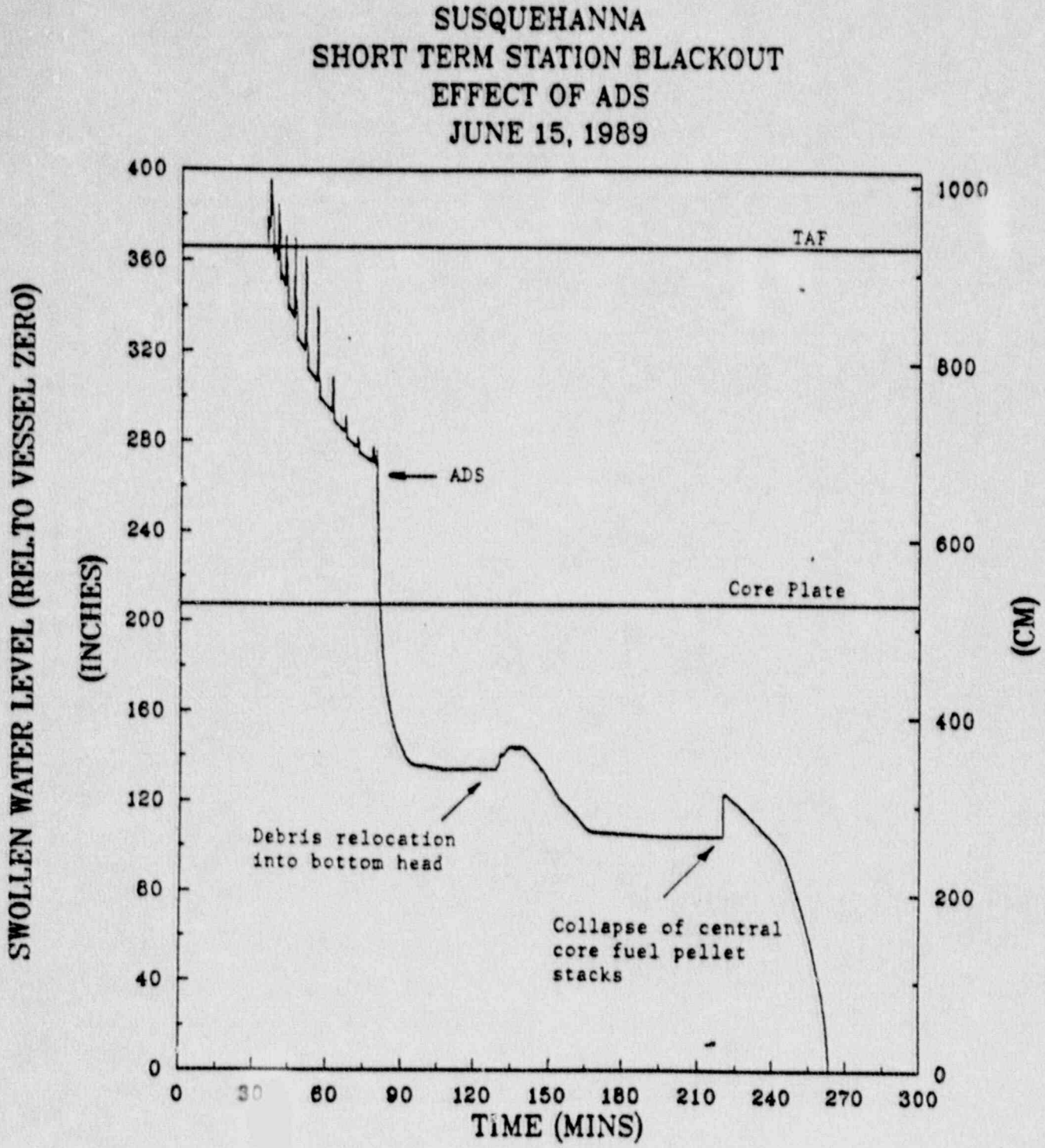

Fig. 2.2. Swollen reactor vessel water level for BWR-4/Mark II short-term station blackout accident sequence with ADS (simple eutectics).

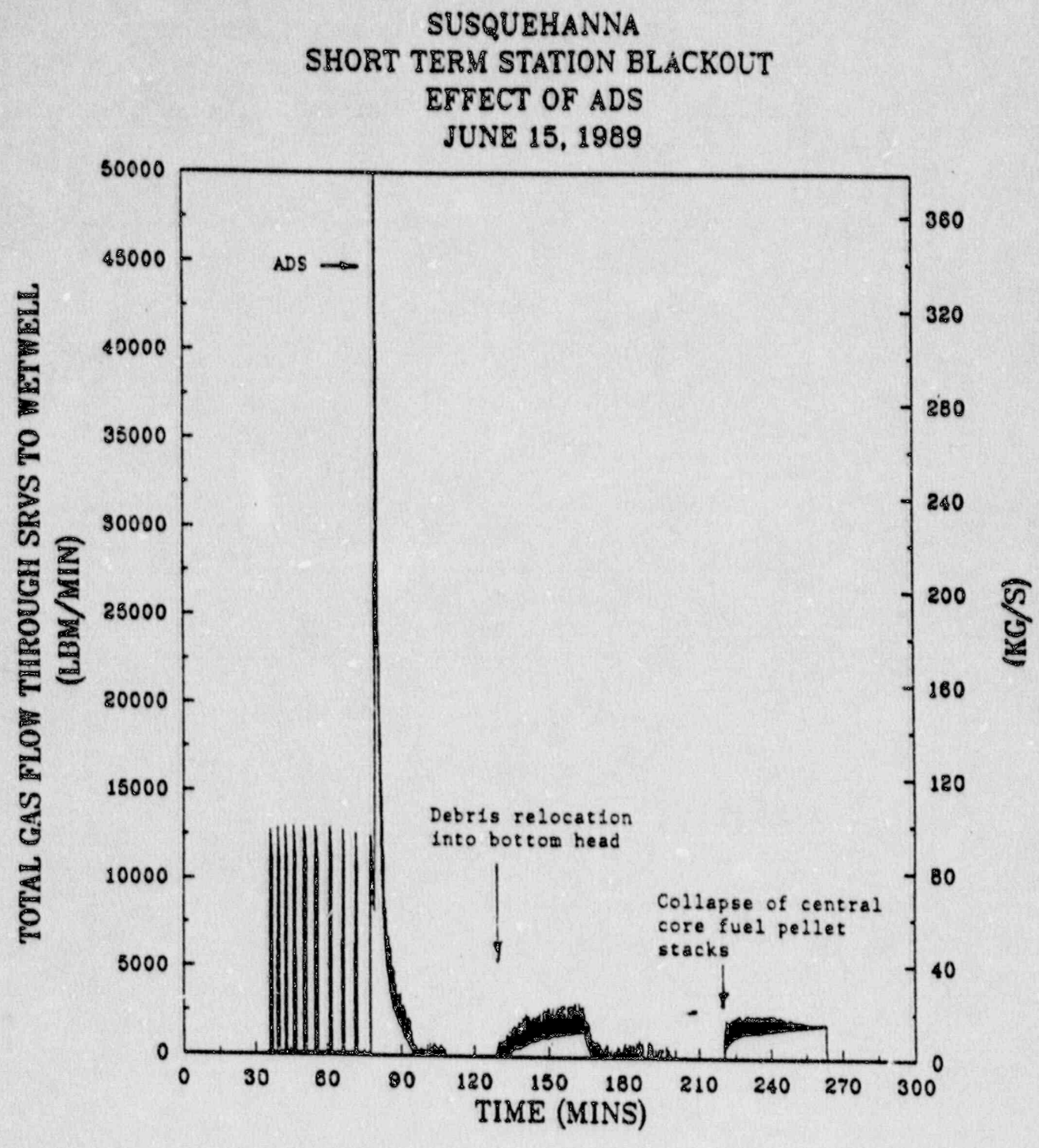

Fig. 2.3. Total SRV gas flow for BWR-4/Mark II short-term station blackout accident sequence with ADS (simple eutectics).

opened. Small temporary increases in level subsequently occur because of displacement of water in the bottom head whenever large masses of core debris are introduced after core plate failure. The decay heat associated with the fuel pellets relocated into the bottom head at time 220 min. causes a boiloff of the remaining water in the reactor vessel; bottom head dryout is predicted at time 263 min.

Figure 2.4 shows the extent of hydrogen generation by metal-steam reaction in the core region. Approximately 23% of the clad, 10% of the channel box walls, and 1% of the control blade stainless steel is predicted to be oxidized during the portion of the accident sequence before bottom head penetration failure, producing about 1060 lb. of hydrogen in the core region within the reactor vessel. This hydrogen does not accumulate within the reactor vessel, but rather is transferred into the wetwell via the open SRVs.

Selected primary containment response characteristics predicted by the BWRSAR code for the period until one-half hour after reactor vessel bottom head penetration failure are provided in the individual plots of Figures 2.5 through 2.12. (The results of a more detailed MELCOR calculation of containment response for this same period as well as for the remainder of the accident sequence when significant amounts of core debris have entered the drywell are discussed in Section 2.3.)

As indicated in Figure 2.5, ADS actuation causes a small increase in drywell pressure, but this pressure increase is soon erased as the containment heat sinks soak up energy after core plate dryout. The containment pressure does increase notably in response to debris relocation into the reactor vessel bottom head and again after collapse of the central fuel pellet stacks. (For both of these occasions, hydrogen generated within the reactor vessel is swept into the pressure suppression pool together with the steam release, which is condensed.) On the other hand, bottom head penetration failures do not significantly increase the containment pressure because the reactor vessel was previously depressurized by means of the ADS actuation.

The drywell atmosphere temperature, shown in Figure 2.6, increases by means of compression and increased heat transfer from the reactor vessel whenever flow is initiated from the safety/relief valves (Figure 2.3), then decreases as the drywell heat sinks absorb the energy of the atmosphere. The effect of bottom head penetration failure is slight. At the completion of the reactor vessel blowdown, neither the drywell pressure nor the calculated drywell shell temperature (Figure 2.7) is of sufficient magnitude to threaten the integrity of the drywell pressure boundary.

The temperature of the wetwell atmosphere responds to the events occurring within the reactor vessel as shown in Figure 2.9, but does not increase to a threatening value. The wetwell atmosphere temperature increases after reactor vessel bottom head penetration failure because of the fission products and associated decay heat release within the pressure suppression pool and in the wetwell atmosphere. (The pool remains subcooled, however. Its response is shown in Figure 2.12.)

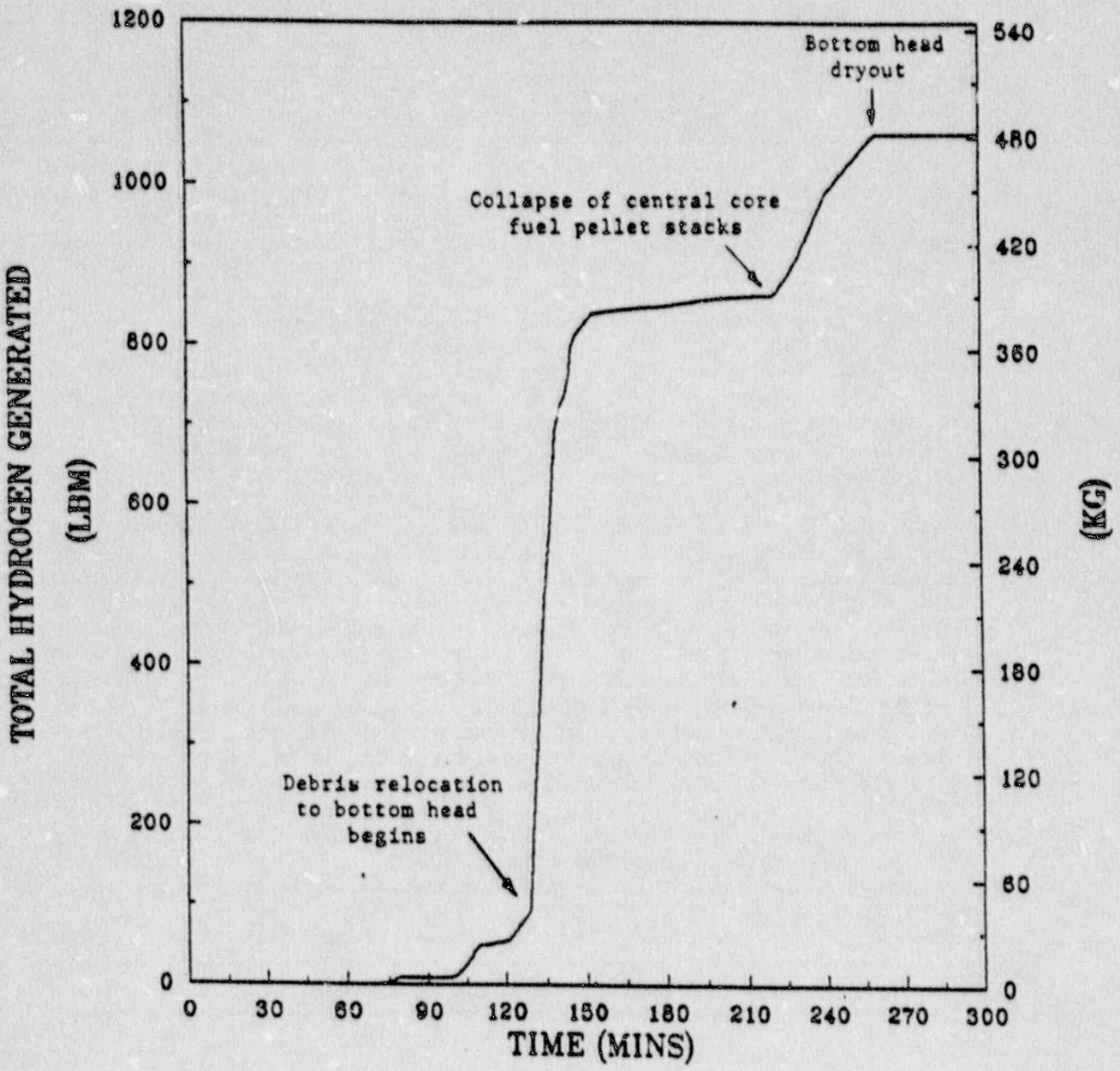

Fig. 2.4. Total hydrogen generated invessel for BWR-4/Mark II short-term station blackout accident sequence with ADS (simple eutectics).

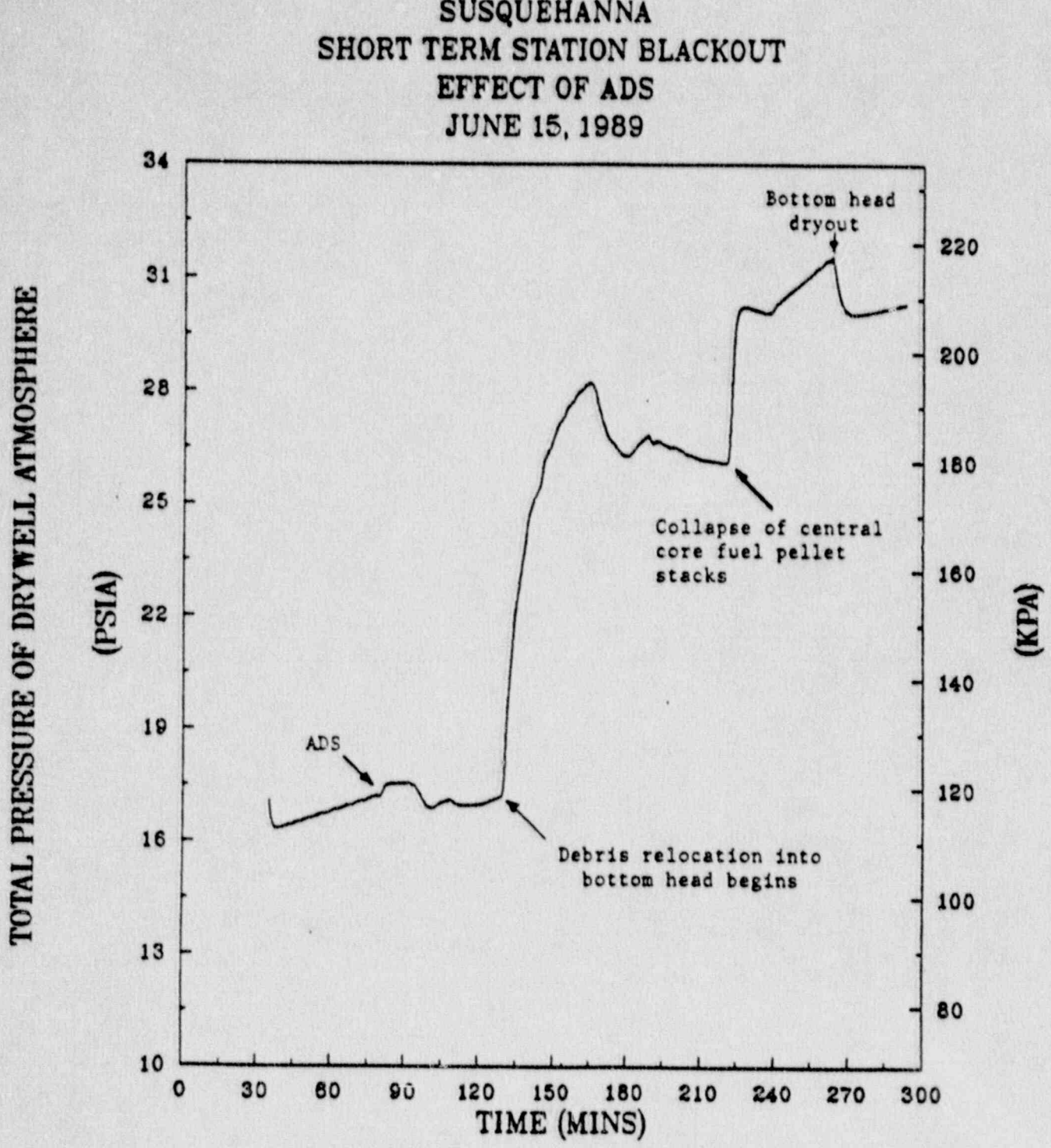

Fig. 2.5. Drywell atmosphere pressure for BWR-4/Mark II short-term station blackout accident sequence with ADS (simple eutectics).

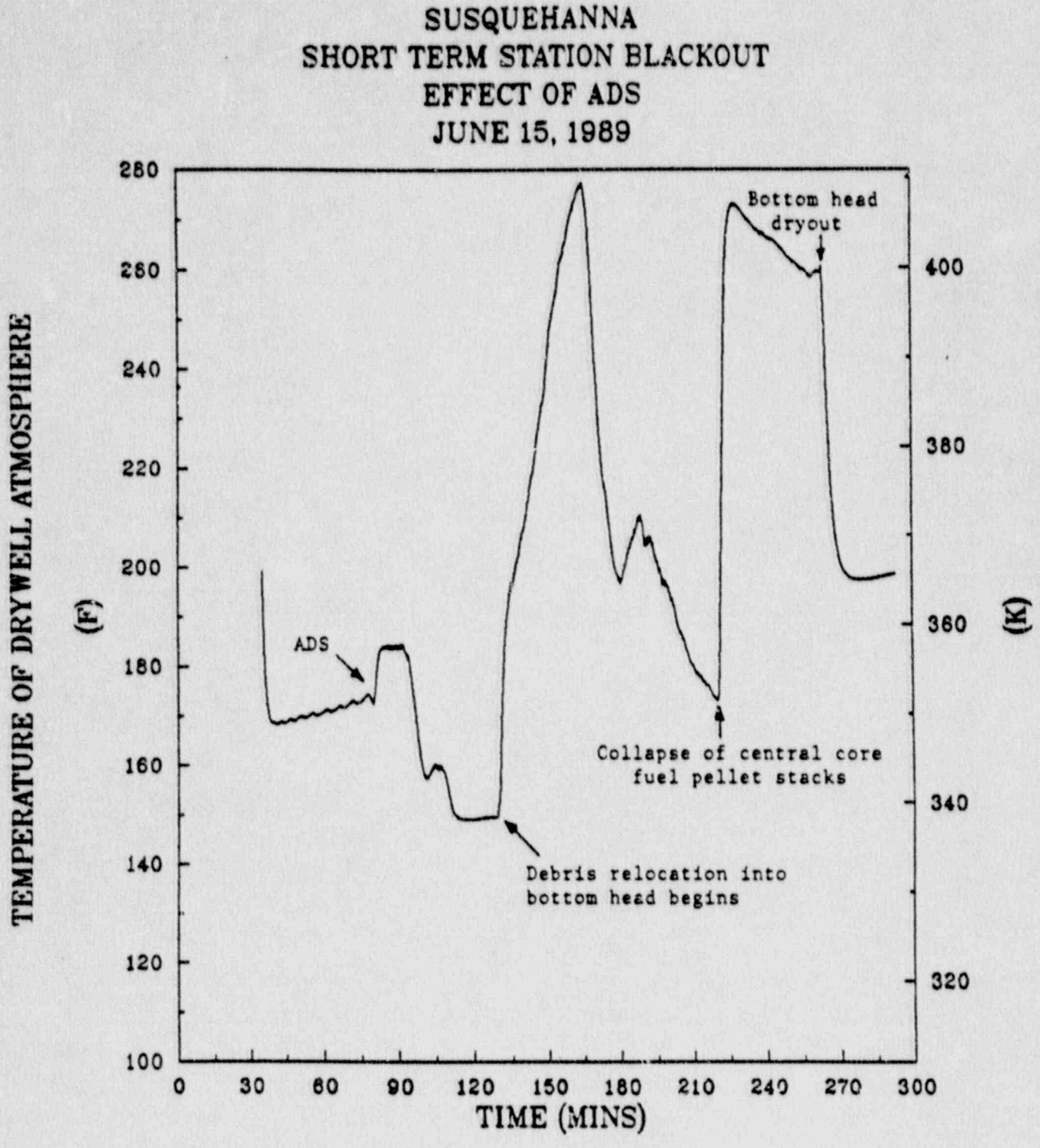

Fig. 2.6. Drywell atmosphere temperature for BWR-4/Mark II short-term station blackout accident sequence with ADS (simple eutectics).

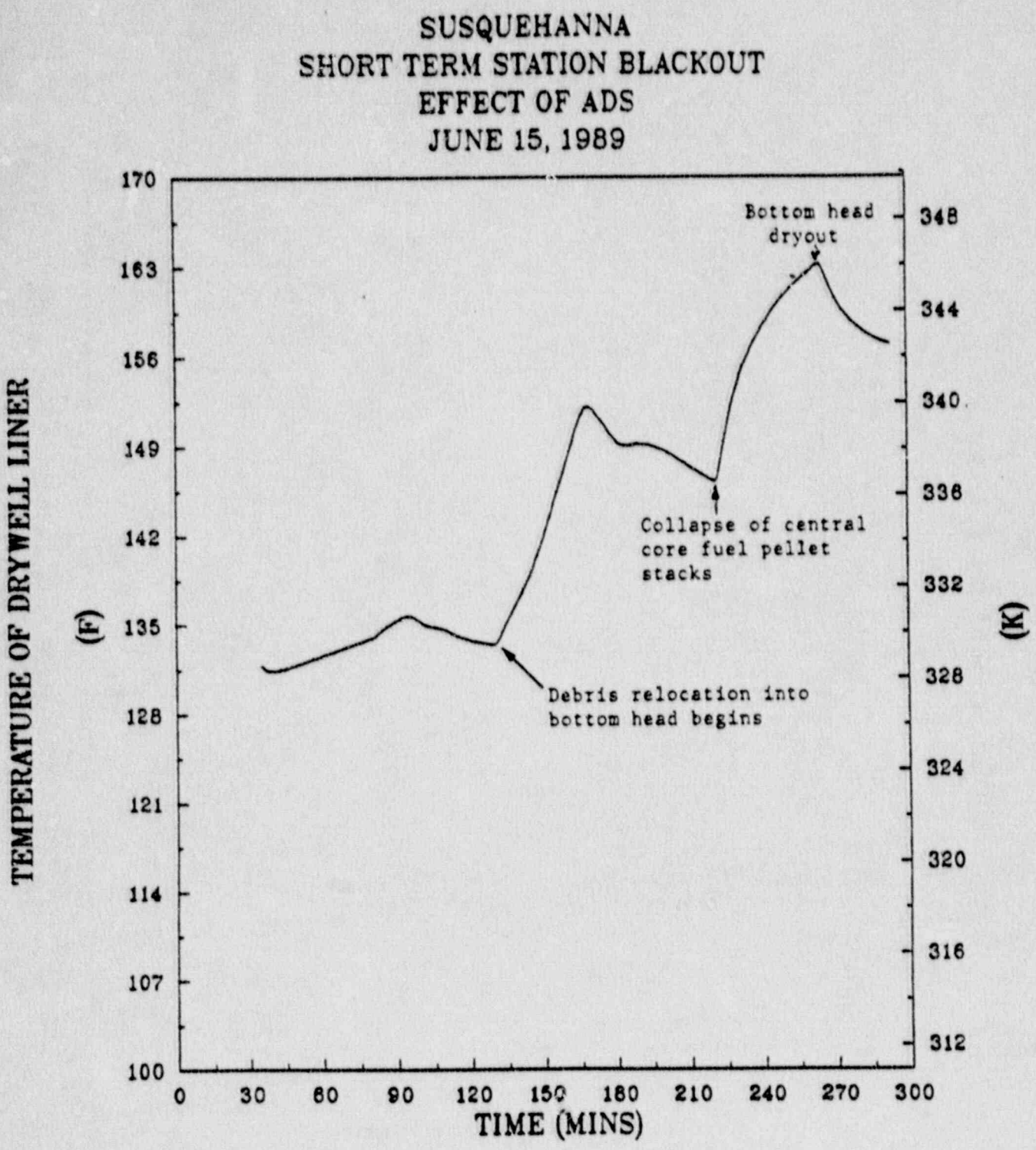

Fig. 2.7. Drywell liner temperature for BWR-4/Mark II short-term station blackout accident sequence with ADS (simple eutectics).

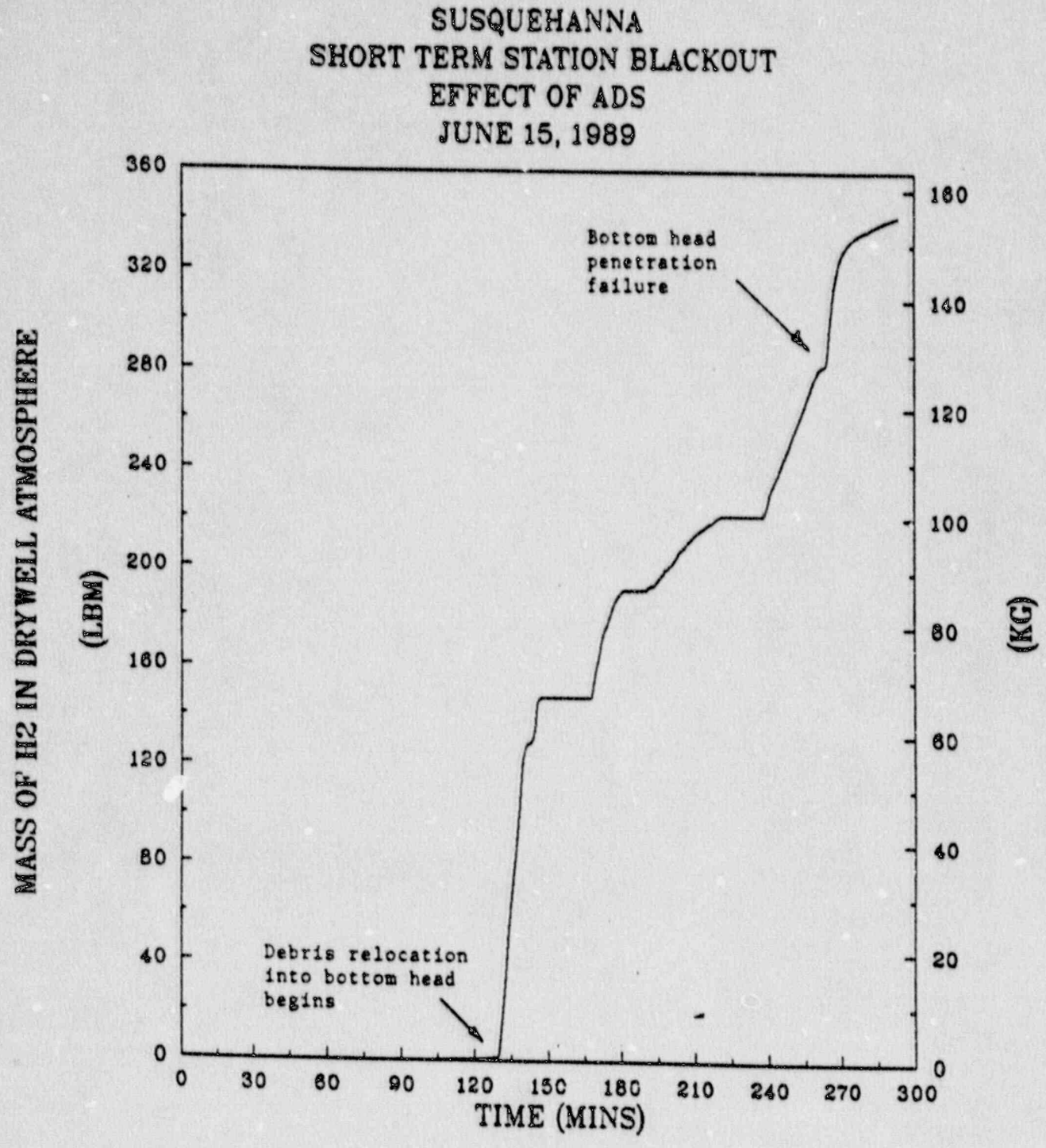

Fig. 2.8. Hydrogen mass in drywell atmosphere for BWR-4/Mark II short-term station blackout accident sequence with ADS (simple eutectics).

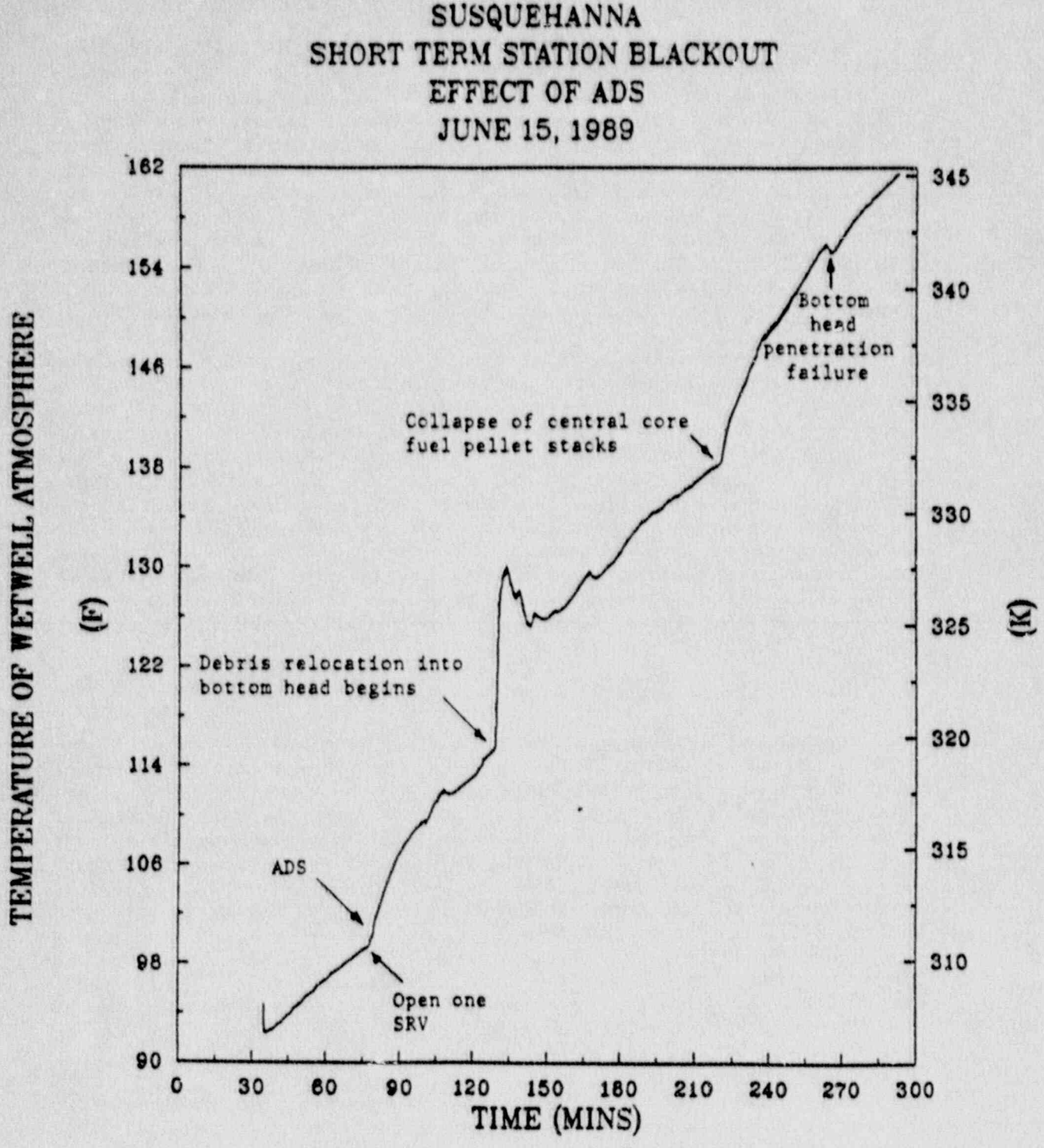

Fig. 2.9. Wetwell atmosphere temperature for BWR-4/Mark II short-term station blackout accident sequence with ADS (simple eutectics).

The calculated interchange of gas volumes between the drywell and wetwell as necessary to maintain the pressure differential within the user-specified range is shown in Figure 2.10. Since all of the indicated volume transfers are negative, the calculated gas transfers are exclusively from wetwell to drywell. In the Mark II containment design, these transfers are through vacuum-breaker valves that open mechanically to permit flow whenever the wetwell pressure exceeds the drywell pressure by some minimum amount (0.5 psi was assumed for these BWRSAR calculations). As indicated, the necessary gas transfers are largest during the initial periods of debris relocation into the reactor vessel lower plenum when the attendant steam generation flushes large amounts of hydrogen from the vessel atmosphere into the wetwell.

A large amount of hydrogen is predicted to have accumulated within the wetwell airspace (Figure 2.11) and the drywell (Figure 2.8) by the time of reactor vessel bottom head penetration failure. Some additional hydrogen (about 25 lb.) is generated by metal-water reactions instigated by the passage of steam through the bottom head debris bed during the first 60 min. after penetration failure. A slow rate of hydrogen generation by this mechanism continues as long as water remains in the downcomer region of the reactor vessel. This water is boiled by radiative and conductive (through the vessel wall) heat transfer from the bottom head debris; since passage through the SRVs would require dislocation of the water occupying the lower 16 ft. of the SRV tailpipes, the steam follows the path of least resistance and passes through the debris bed on its way out of the vessel.

2.2.3.2 Calculated reactor vessel debris pours

The reactor vessel debris pours calculated by the BWRSAR code depend upon a user-input definition of the pure species and eutectic mixtures that will form in the vessel bottom head and their melting points. The "best-estimate" debris pour calculation performed for the BWR Mark II study is based upon code input specifying that multiple eutectic species are formed in the lower head of the BWR reactor vessel in a manner consistent with the results of the small-scale BWR Core Debris Eutectic Formation and Melting Experiment[1] performed at ORNL by G. W. Parker in December 1987. The debris components and melting temperatures assumed in the "best-estimate" calculation are shown in Table 2.5. In the experiment, metal pours occurred in three mixtures over the range 2640°F to 2920°F. An oxide pour occurred at 4172°F, leaving the majority of the UO_2 pellets within the simulated lower plenum regions. This remaining UO_2 would be expected to melt at approximately 4800°F.

The CORCON module within MELCOR can not accommodate this multi-eutectic treatment. Currently, CORCON can accept only UO_2, Zr, steel, ZrO_2, steel oxide, and B_4C. Accordingly, for the purposes of this study, the BWRSAR code input was modified as necessary to specify the formation of two eutectic mixtures that are compatible with the CORCON module within the MELCOR code. These are:

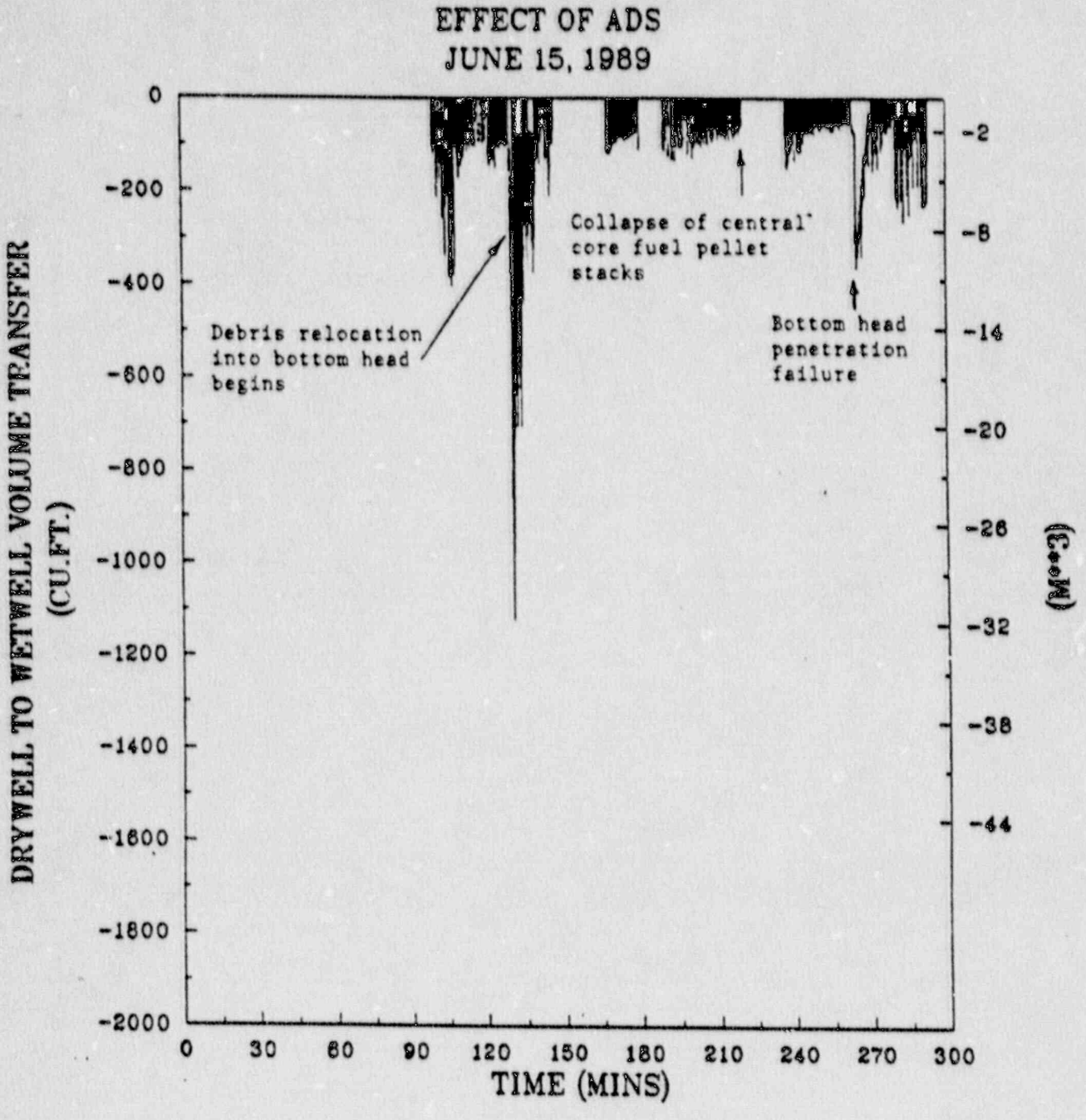

Fig. 2.10. Drywell-to-wetwell atmosphere transfers for BWR-4/Mark II short-term station blackout accident sequence with ADS (simple eutectics).

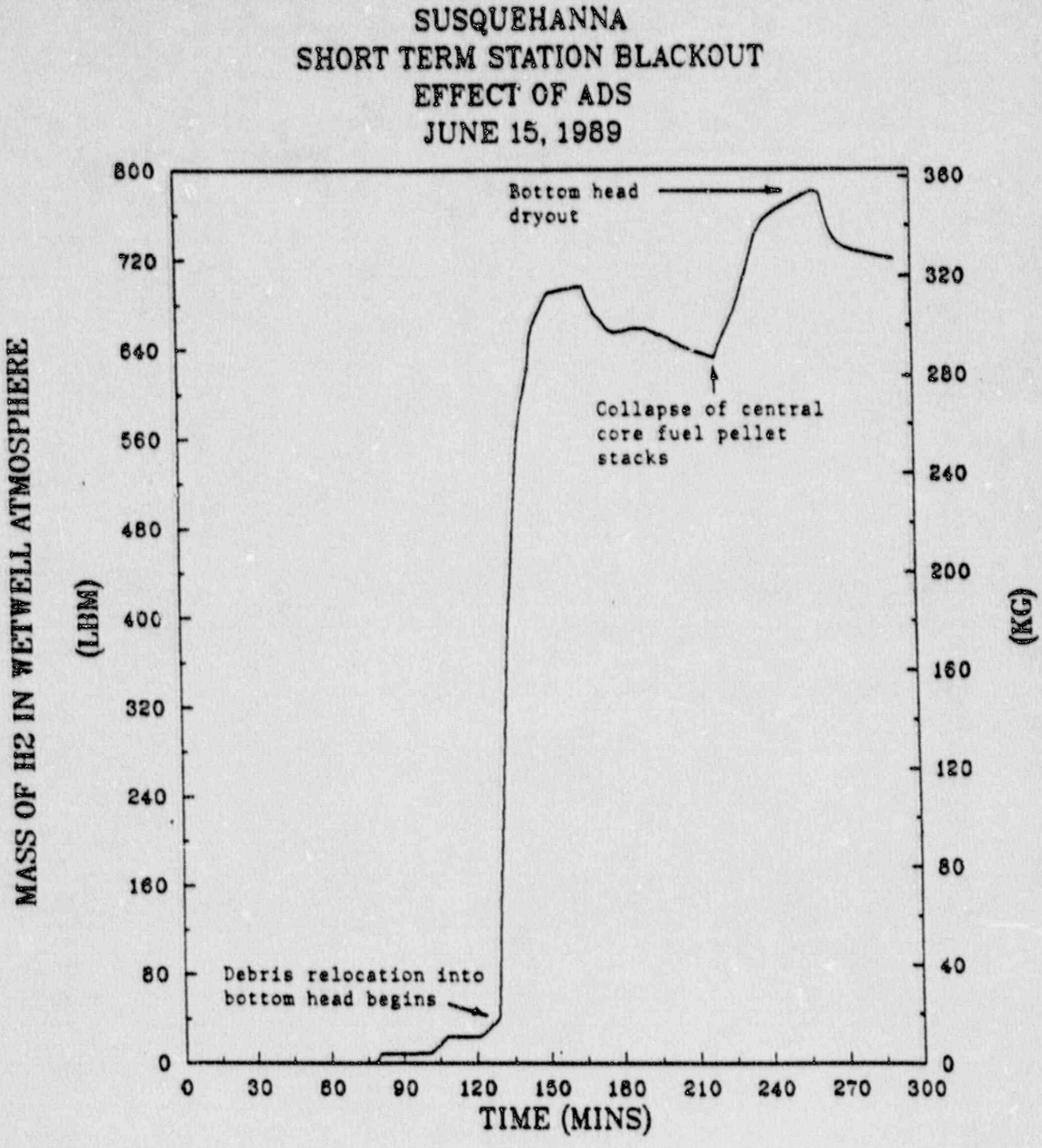

Fig. 2.11. Hydrogen mass in wetwell atmosphere for BWR-4/Mark II short-term station blackout accident sequence with ADS (simple eutectics).

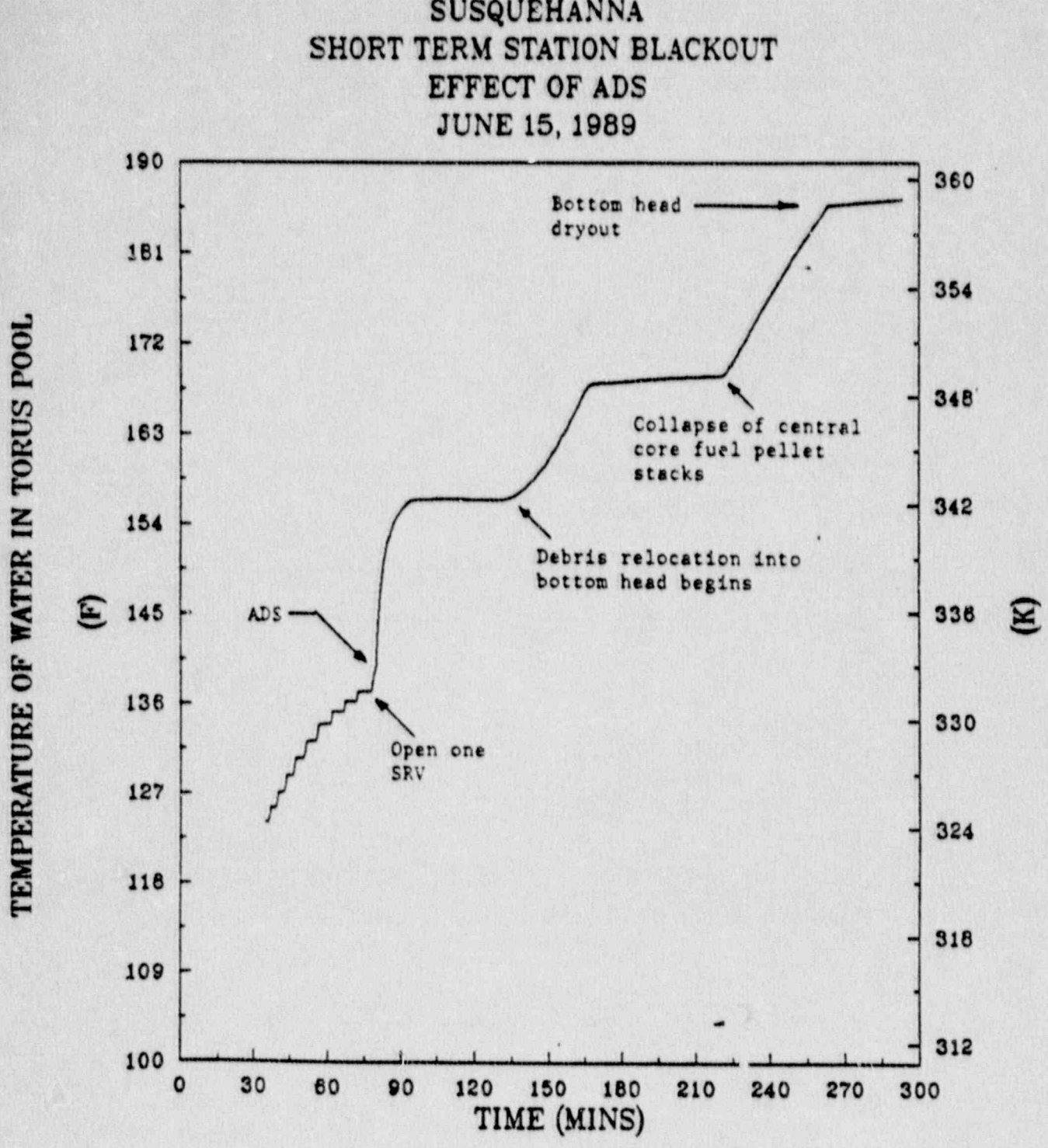

Fig. 2.12. Suppression pool temperature for BWR-4/Mark II short-term station blackout accident sequence with ADS (simple eutectics).

Table 2.5. Best-estimate BWR bottom head debris compositions

Component	Composition	Melting Temperature (°F)
Eutectic 1	Zr - Fe - Cr	2642
Eutectic 2	Fe - Cr - Ni	2660
Eutectic 3	Zr - Fe - Ni	2912
Remaining Metals	Zr/Fe/Cr/Ni	2920
Eutectic 4	ZrO_2 - UO_2	4172
Remaining Non-fuel Oxides	FeO/Fe_3O_4 NiO/B_4C	4172
Fuel Pellets	UO_2	4800

1. All metals in one mixture melting at 2750°F (mole fractions Zr 0.210, Fe 0.579, Cr 0.151, Ni 0.060),

2. All ZrO_2 and UO_2 in a mixture melting at 4800°F material (mole fractions ZrO_2 0.170, UO_2 0.830).

The remaining oxides are also specified to melt at 4800°F.

While these melting temperatures are significantly higher than those of some of the pours observed in the small-scale experiment, temperatures of this magnitude are necessary with the current version of CORCON within MELCOR. Otherwise, the containment calculation would initially treat these introduced pours as frozen material and the latent heat of fusion would be lost from the calculation. At any rate, use of these higher melting temperatures is conservative in that a more severe challenge to the containment is introduced at the time of the initial pour.

The integrated mass of material that has left the reactor vessel for the BWR Mark II calculations based upon Susquehanna is shown as a function of time in Figure 2.13. Although the initial bottom head penetration failure occurs at time 263 min., the initial debris pour does not begin until time 270 min. because of the time interval required for the metallic debris to heat to its assumed melting temperature of 2750°F. [The mass-averaged temperature of the release is shown in Figure 2.14.] About 850,000 lb. of debris is predicted to have left the vessel by the end of the calculation, at time 900 min. This is equivalent to about 98% of the total original mass of bottom head debris. The composition of the released debris is provided in Table 2.6. The decay heat (proportional to the mass of UO_2) included in the released debris is shown in Figure 2.15.

It should be noted that the BWRSAR code predicts that the portion of the reactor vessel bottom head beneath the point of attachment of the support skirt has been completely removed by time 483 min. [The removal is by the process of ablation of surrounding wall structure by the molten debris pouring through the failed bottom head penetration sites.] There are no specific models within BWRSAR to address this phenomenon since it is believed that the 340,000 lb. of debris remaining within the vessel at this time would merely relocate downward about three feet onto the control rod drive housing support structure (see Figure 2.16). After relocation, the debris would continue to melt, with the molten portion flowing down onto the drywell floor in the same manner as if the portion of the bottom head surrounding the penetrations had remained intact. [This statement is true even if the debris were not held up by the housing support structure; the rate of release of molten material over the drywell floor is determined by the rate at which the debris melts, regardless of where the debris is located.] Within the BWRSAR code, heat transfer from the debris to the reactor vessel wall by convection and conduction is discontinued at the time that the debris is predicted to relocate onto the CRD housing support structure.

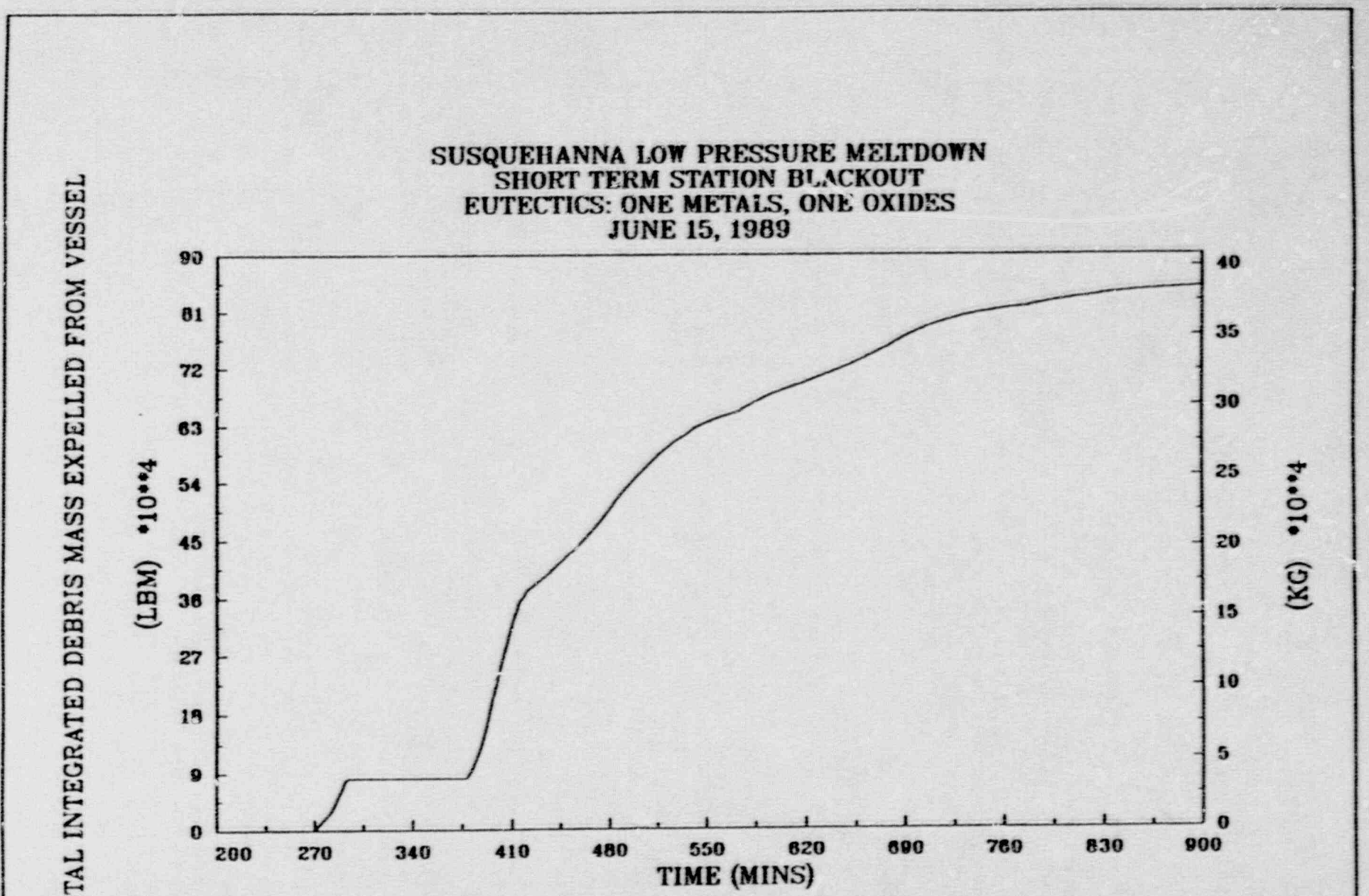

Fig. 2.13. Integrated debris mass expelled from reactor vessel for BWR-4/Mark II short-term station blackout accident sequence with ADS (simple eutectics).

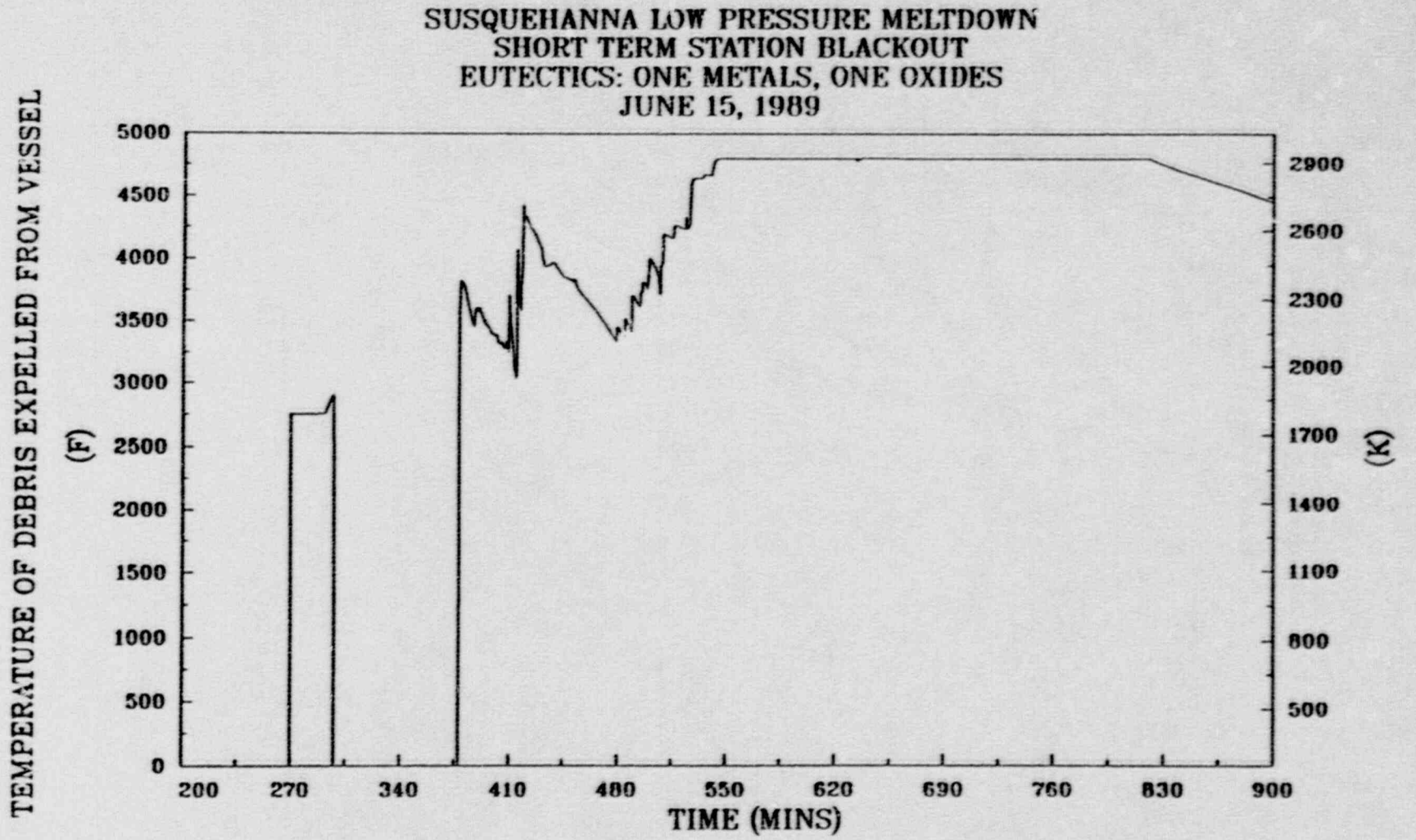

Fig. 2.14. Mass-averaged debris pour temperature for BWR-4/Mark II short-term station blackout accident sequence with ADS (simple eutectics).

Table 2.6 Composition of the debris released from the reactor vessel by the end of the BWR Mark II calculation with ADS

Constituents	Integrated Mass (lbs)
Metals	
Zr	113,869
Fe	283,737
Cr	47,702
Ni	21,218
B_4C	768
Total	467,294
Oxides	
ZrO_2	33,565
FeO	96
Fe_3O_4	184
Cr_2O_3	74
NiO	11
B_2O_3	39
UO_2	347,379
Total	381,348
Grand Total	848,642

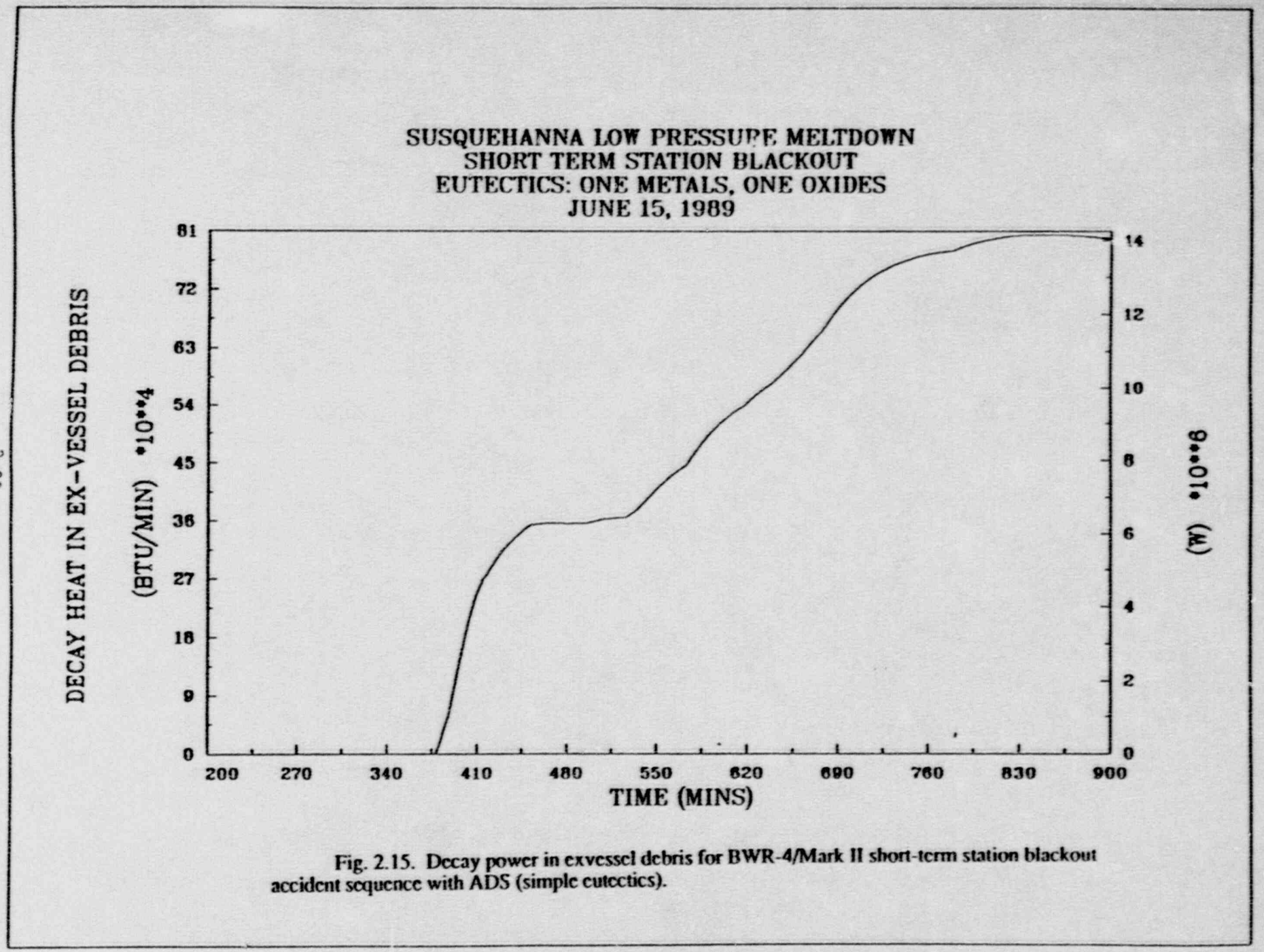

Fig. 2.15. Decay power in exvessel debris for BWR-4/Mark II short-term station blackout accident sequence with ADS (simple eutectics).

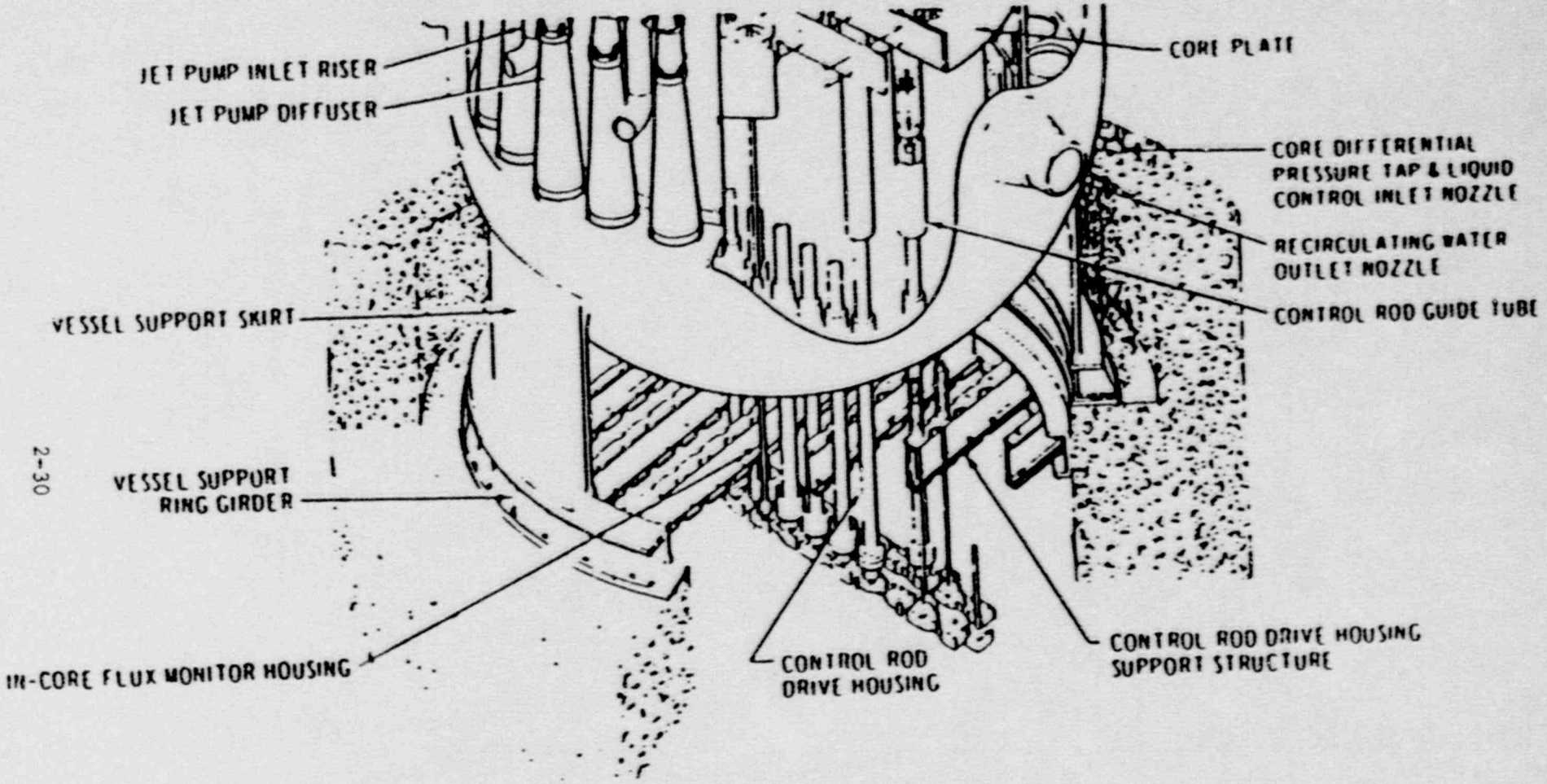

Figure 2.16. Downward movement of separated portions of the bottom head beneath the skirt would be limited to about 34 inches by the CRD housing support structure.

2.2.4 Short-term Station Blackout Response (with ADS and best-estimate eutectics)

It is obviously necessary to consider the differences in the debris pours predicted by BWRSAR when the best-estimate (Parker) bottom head debris compositions are used as opposed to the two-eutectic mixture compositions that drive the MELCOR calculations of containment response described in Section 2.2.3, and to attempt to determine if these differences are important. The two debris composition sets are compared in Table 2.7. The characteristics of the two resulting debris pours are compared in Tables 2.8 and 2.9 and in Figures 2.17 through 2.20. The calculated results are identical through the time of initial reactor vessel bottom head penetration failure, which is predicted to occur at 263 min. after scram.

As indicated in Table 2.8, the best-estimate debris pours precede the two-eutectic debris pours during both the early metallic melting period (263-275 min.) and the early oxidic melting period (345-385 min.). There is, however, no significant difference in the debris masses accumulated on the drywell floor during the other periods of the pour calculation.

The differences in the rates of debris pour from the reactor vessel are shown in Table 2.9. The pour rates for the unoxidized zirconium metal are of special significance, since this metal will be oxidized on the drywell floor. (The zirconium metal pours are listed separately, but are also included in the adjacent "Metals" column.) The oxidation of zirconium releases large amounts of energy and increases the temperature of the debris that attacks the concrete floor, floor drains, and (in some Mark II designs) the stainless steel downcomers.

As expected, the best-estimate eutectic representation of the lower-head debris results in a broader (and more finely structured) spectrum of pours (as predicted by BWRSAR) from the reactor vessel. The zirconium metal, UO_2, and total debris pours are shown in Figures 2.17 through 2.19 for both sets of debris compositions. The mass-averaged temperatures of the pours are compared in Figure 2.20.

The important question is, of course, "What is the significance of the differences in the two debris pour spectrums with respect to the calculated containment response?" Unfortunately, a satisfactory answer to this question could only be obtained by performing the associated MELCOR containment response calculations for both sets of pours. For the reasons discussed previously, the MELCOR calculation for the best-estimate case cannot be run until improvements are implemented into the CORCON module. Nevertheless, it does seem probable that any significant difference in the predicted containment response would be limited to the two-hour period after initial penetration failure when the major metallic pours occur and the oxidic pours are being initiated. During this period, the best-estimate debris pours are more rapid and thereby provide a more severe containment loading; however, the total released masses are not sufficient to threaten the Mark II containment

Table 2.7. Bottom head debris composition sets utilized in the two BWRSAR calculations

The Two-Eutectic Mixture		The Best-Estimate (Parker) Eutectics	
Component	Melting Temperature °F	Component	Melting Temperature °F
		Zr-Fe-Cr	2642
		Fe-Cr-Ni	2660
All metals	2750		
		Zr-Fe-Ni	2912
		Remaining metals	2920
		ZrO_2-UO_2	4172
		Remaining non-fuel oxides	4172
All oxides	4800	Fuel pellets	4800

Table 2.8. Integrated masses (lbs) of debris expelled from the reactor vessel for the two sets of debris compositions

Time* (min)	The Two-Eutectic Mixture			The Best-Estimate (Parker) Eutectics		
	Zr	Metals	Oxides	Zr	Metals	Oxides
265	0	0	0	926	3279	0
275	3499	11482	0	7871	27736	0
285	12610	41383	0	13055	45993	0
345	40108	80928	0	41036	82319	3606
365	40108	80928	0	50741	107475	31538
385	45792	95236	14782	53778	115726	35899
405	84273	192090	82745	85266	195405	79657
885	113869	466323	380184	113518	469493	384959

*The initial bottom head penetration failure occurs at 263 minutes after scram.

Table 2.9. Debris pour rates (lbs/min) for the two sets of debris compositions

Period (Min)	The Two-Eutectic Mixture			The Best-Estimate (Parker) Eutectics		
	Zr	Metals	Oxides	Zr	Metals	Oxides
263-265	0	0	0	463	1640	0
265-275	350	1148	0	695	2446	0
275-285	911	2990	0	518	1826	0
285-305	1375	1977	0	1399	1816	180
305-325	0	0	0	0	0	0
325-345	0	0	0	0	0	0
345-365	0	0		485	1258	1397
365-385	284	715	739	152	413	218
385-405	1924	4843	3398	1574	3984	2188
405-425	1221	3371	1767	1157	3479	2243

*The initial bottom head penetration failure occurs at 263 minutes after scram.

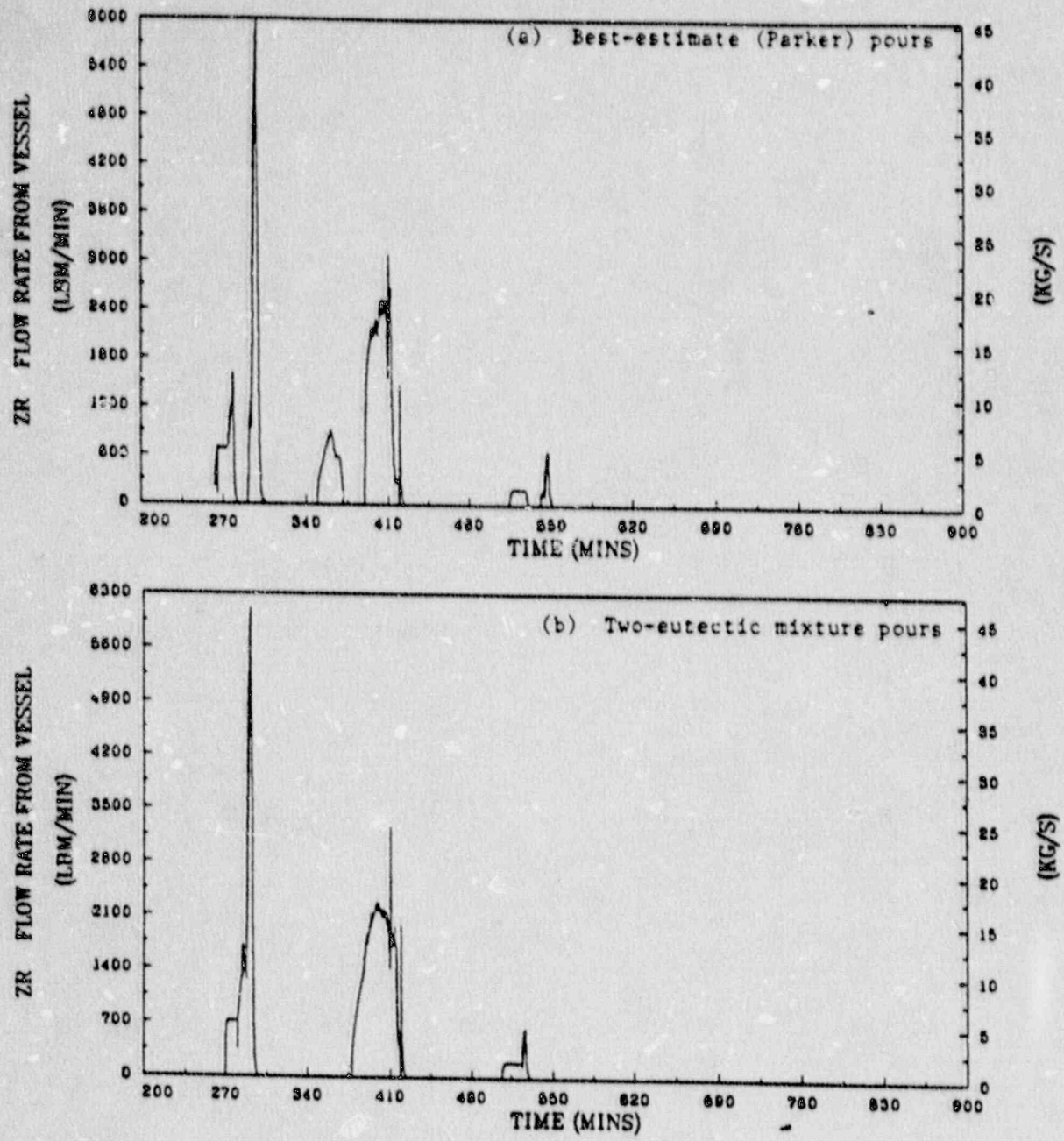

Figure 2.17. Zirconium metal pours from the reactor vessel for the short-term station blackout accident sequence with ADS actuation.

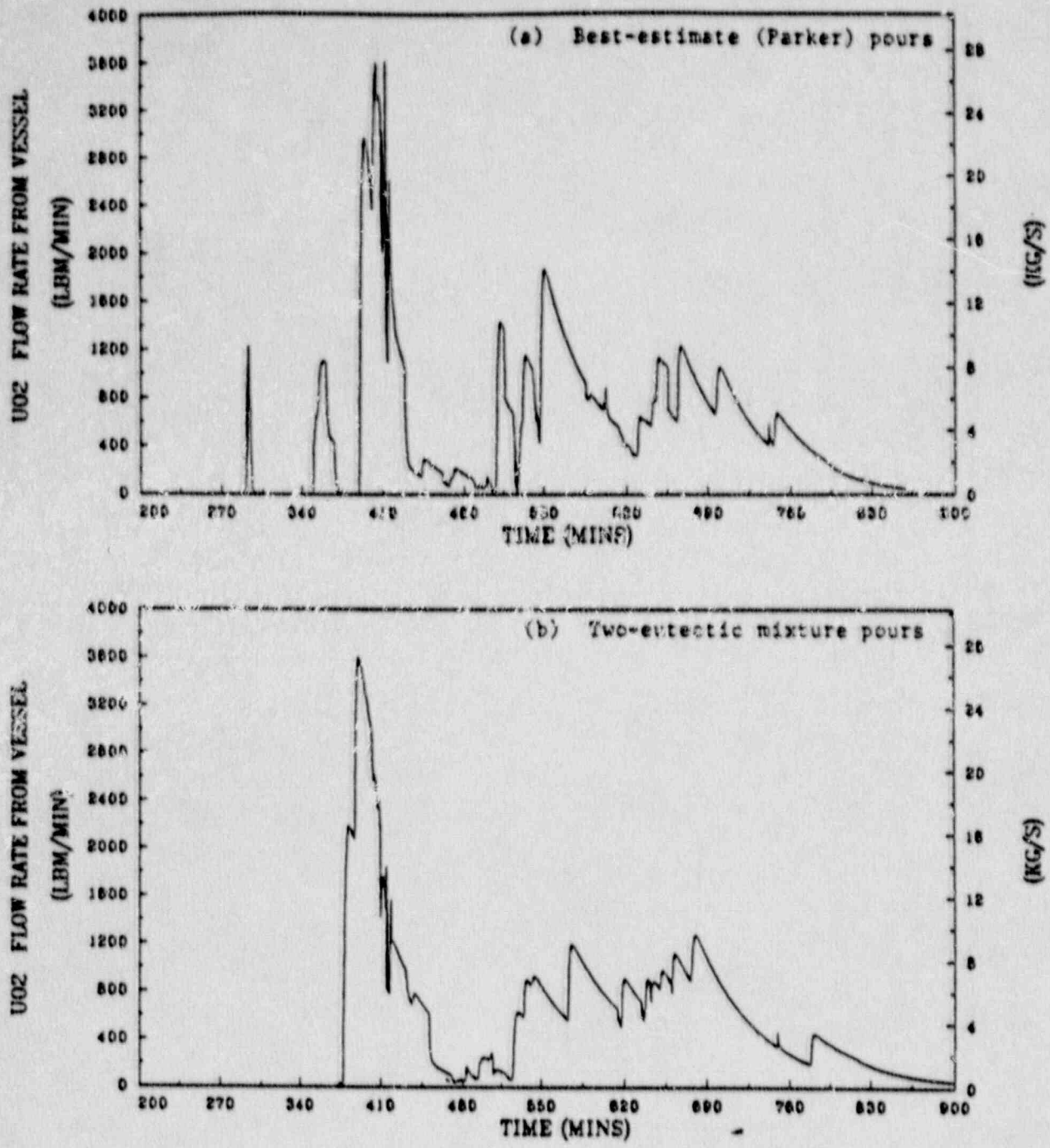

Figure 2.18. Uranium dioxide pours from the reactor vessel for the short-term station blackout accident sequence with ADS actuation.

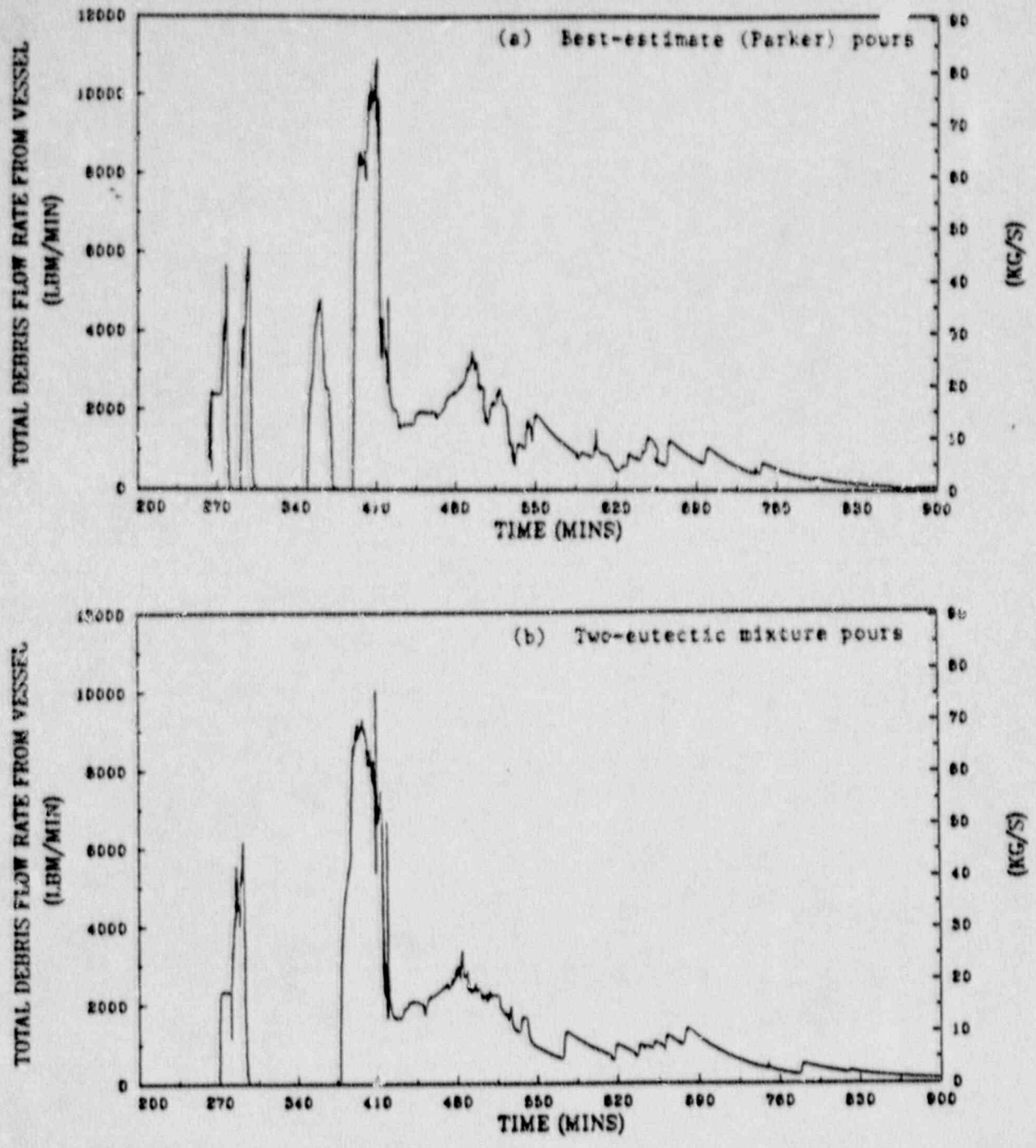

Figure 2.19. Total debris pours from the reactor vessel for the short-term station blackout accident sequence with ADS actuation.

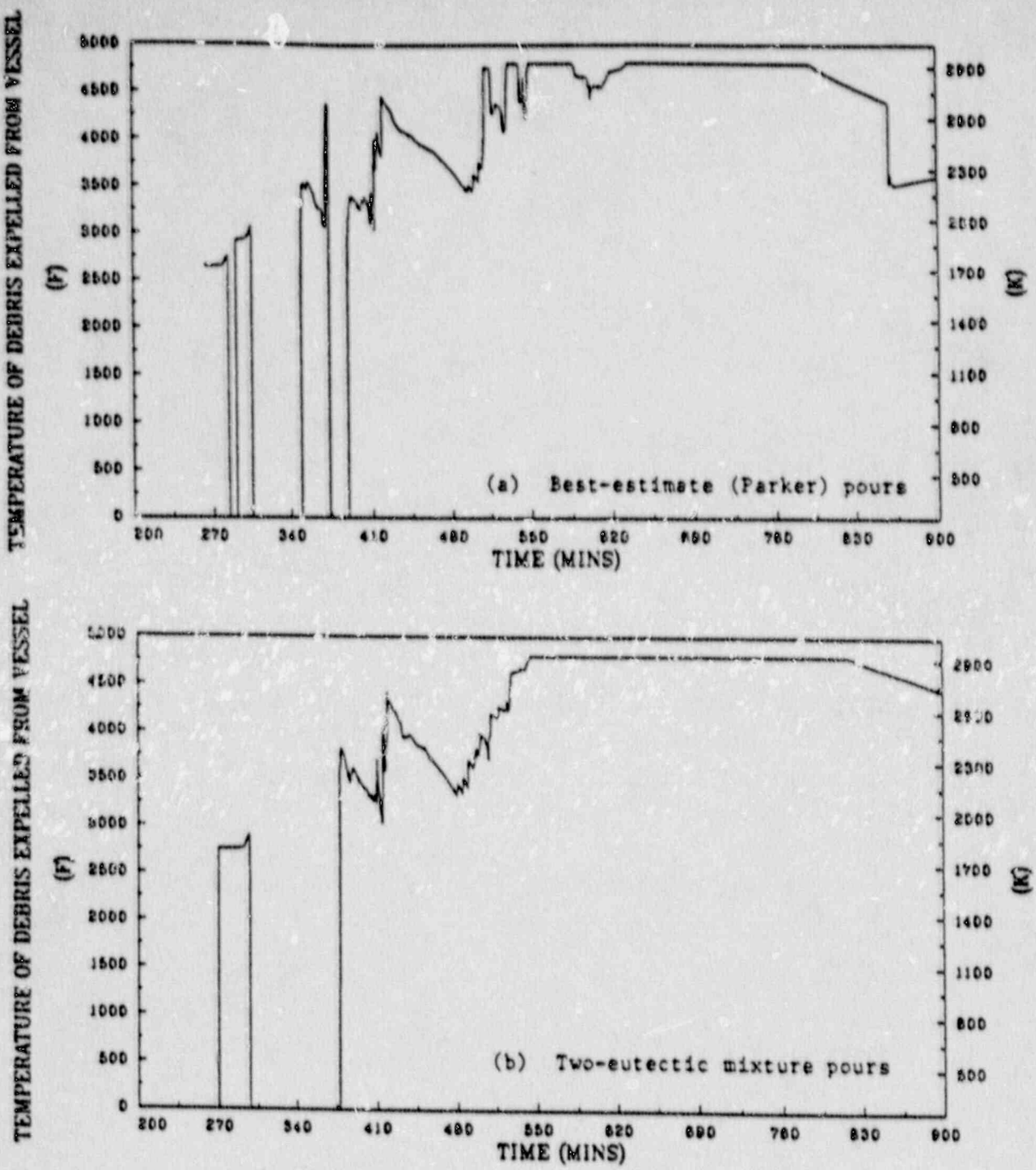

Figure 2.20. Mass-averaged temperature of the debris pours from the reactor vessel for the short-term station blackout accident sequence with ADS actuation.

integrity. (These differences in initial debris pour characteristics would be of much more significance in the smaller Mark I containments.) As indicated in Figures 2.19 and 2.20, differences in the overall characteristics of the two debris pour spectrums are small after 390 min. into the accident sequence.

2.2.5 Short-term Station Blackout Response (simplified eutectics and no ADS)

2.2.5.1 Calculated Events prior to reactor vessel bottom head penetration failure

If the reactor vessel depressurization initiated by manual actuation of the ADS does not occur, either by system malfunction or by failure of the operator to follow procedures, then liquid water would remain in the lower core region during the early portion of the core degradation phase of the short-term station blackout accident sequence. As will be demonstrated, the result is a much-higher degree of metal-water reaction within the core region and an accelerated core degradation rate by means of the associated energy release.

The calculated sequence of events for short-term station blackout without ADS is provided in Table 2.10. For consistency with the assumption that the ADS is either not available or not actuated by the operators, the code input deck for this calculation has no provision for manual SRV actuation of any kind, including operator control of vessel pressure during the early part of the accident sequence. As indicated by a comparison of Tables 2.10 and 2.4, the absence of operator pressure control causes a one-minute delay in the calculated time of uncovering of the top of the core. This is in itself, of course, not significant.

Plots of key parameters as calculated by BWRSAR for events within the reactor vessel for the case without actuation of the ADS are shown in Figures 2.21-2.24. These plots represent events from 35 min. after the inception of the accident sequence, when the BWRSAR calculation is initiated, to time 250 min., which is about four min. after the predicted initial failure of reactor vessel bottom head penetrations and onset of debris pours onto the drywell floor. As indicated in Figure 2.21, the calculated vessel pressure decreases significantly after core plate dryout; this occurs because steam generation ceases within the core region while steam leakage and heat transfer from the vessel to the drywell atmosphere continue. Subsequently, the vessel pressure is restored to the range of the safety/relief valve setpoints after local core plate failures introduce core debris into the water in the lower plenum and restore invessel steam generation. The associated SRV flows are shown in Figure 2.23.

The predicted swollen reactor vessel water level for the case without ADS is shown in Figure 2.22. The decreasing water level initially traces a smooth curve through the core region, punctuated by spikes at each SRV actuation. Subsequently, after the onset of downward material

Table 2.10. Calculated sequence of events for BWR (Mark II) Short-Term Station Blackout without ADS Actuation. The bottom head debris is modeled to separate into a mixture of metals melting at 2750°F and a mixture of oxides melting at 4350°F

Event	Time (min)
Station blackout-initiated scram from 100% power. Independent loss of the steam turbine-driven HPCI and RCIC injection systems	0.0
Swollen water level falls below top of core	38.2
Relocation of core debris begins	90.6
Core plate dryout	135.3
First local core plate failure	155.8
Collapse of fuel pellet stacks in central core	163.8
Reactor vessel bottom head dryout; structural support by control rod guide tubes fails; remainder of core falls into reactor vessel bottom head	193.8
Initial failure of bottom head penetrations	246.1
Pour of molten debris from reactor vessel begins	246.5

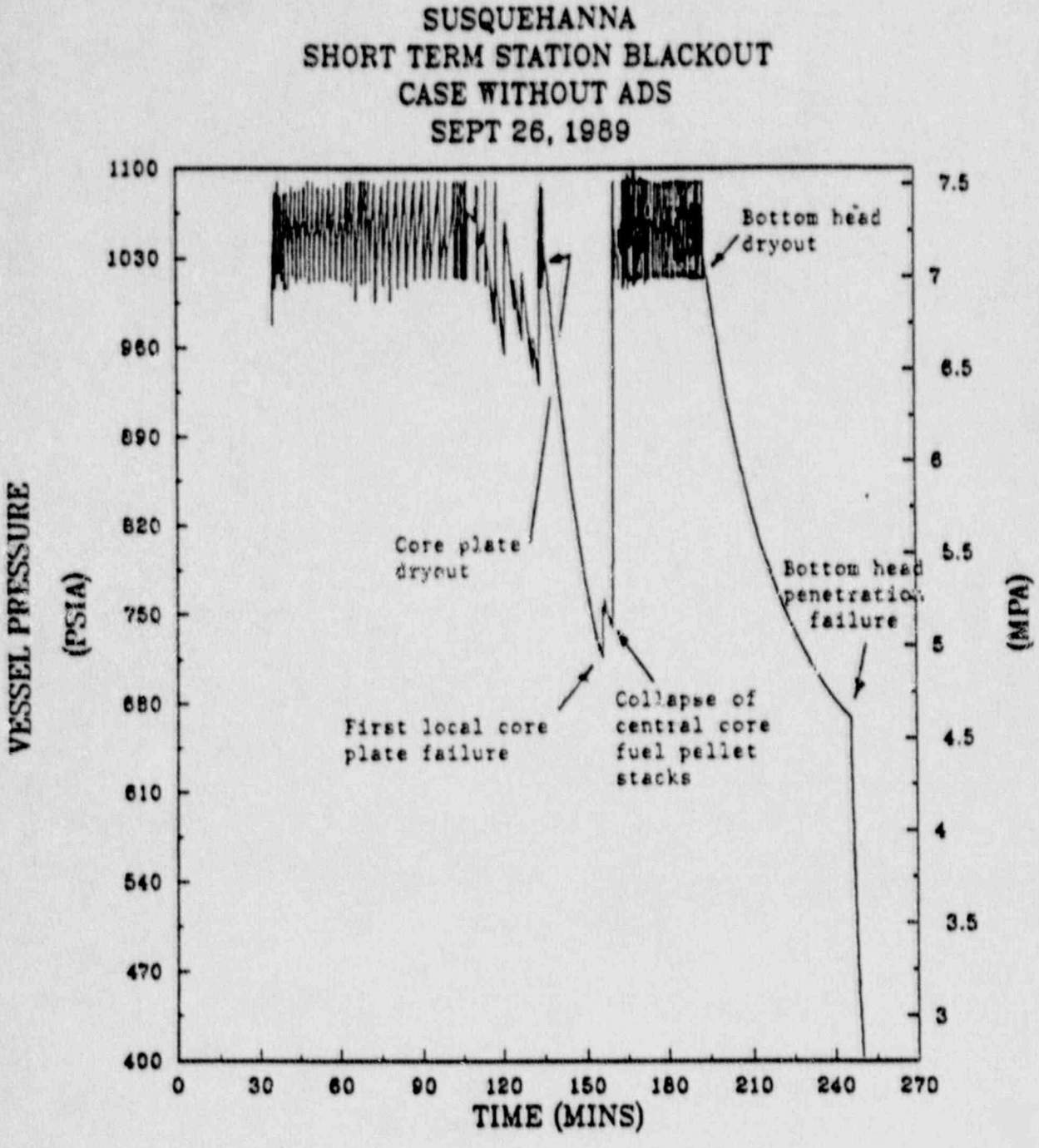

Fig. 2.21. Reactor vessel pressure for BWR-4/Mark II short-term station blackout accident sequence without ADS (simple eutectics).

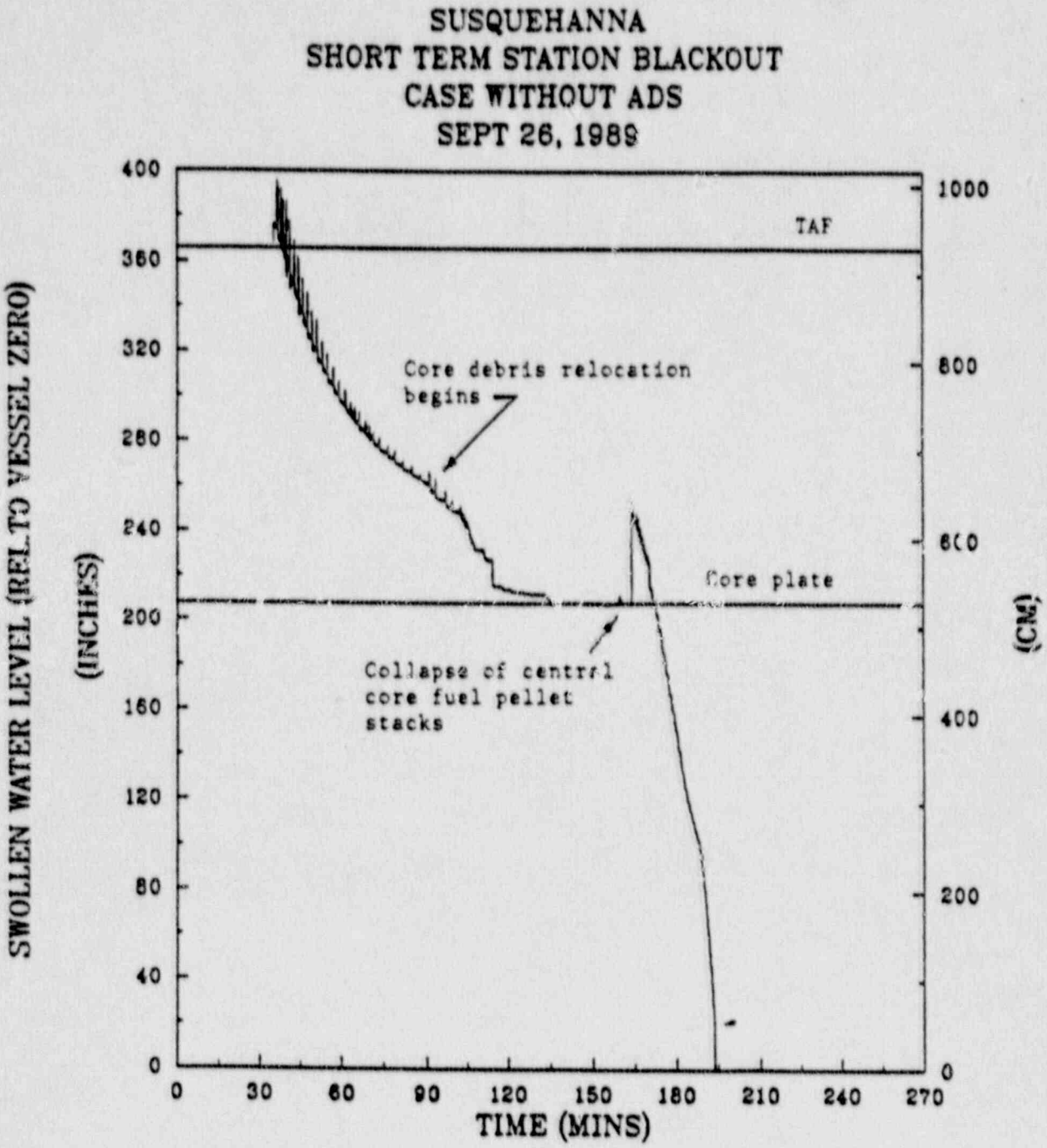

Fig. 2.22. Swollen reactor vessel water level for BWR-4/Mark II short-term station blackout accident sequence without ADS (simple eutectics).

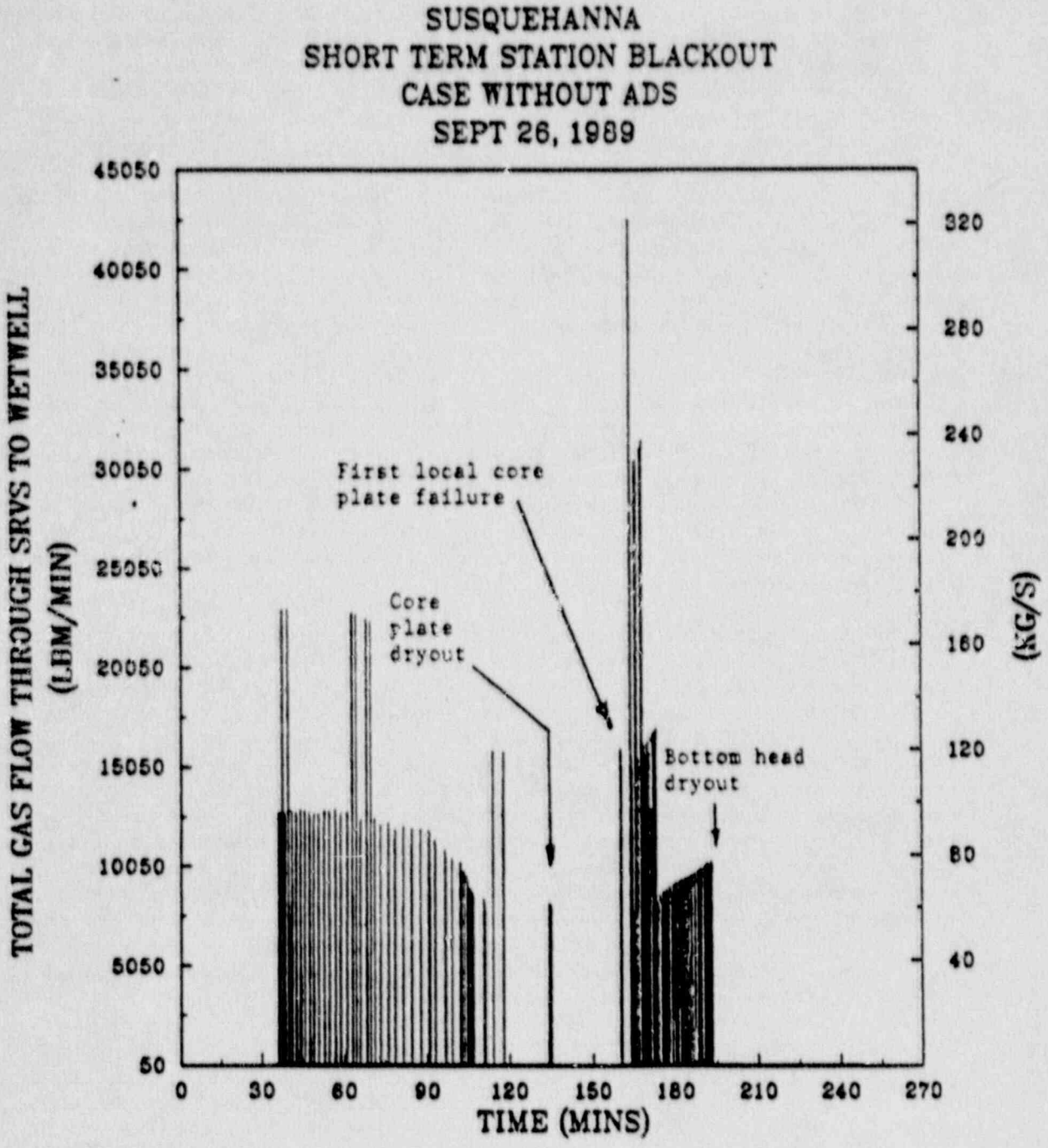

Fig. 2.23. Total SRV gas flow for BWR-4/Mark II short-term station blackout accident sequence without ADS (simple eutectics).

relocation and quenching, the rate of level decrease is accelerated and proceeds in a more steplike fashion. Core plate dryout occurs with the water level just below the core plate (rather than several feet below as in the case with ADS actuation); consequently, water again enters the core region after core plate failure as a result of displacement of water in the lower plenum by the falling debris from the central region of the core. The decay heat associated with the fuel pellet stack collapse at time 164 min. causes a rapid boiloff of the remaining water and bottom head dryout occurs at time 194 min.

Figure 2.24 shows the total hydrogen generated in the core region as a function of time. Approximately 53% of the clad, 12% of the channel box walls, and 1% of the control blade stainless steel is predicted to be oxidized in the core region during the accident sequence, producing about 2210 lb. of hydrogen. Comparison with Figure 2.4 reveals that this is slightly more than twice the hydrogen produced in the core region during the accident sequence with ADS actuation. As indicated previously, the primary reason for this great increase in calculated hydrogen generation during core degradation is that liquid water remains in the lower portion of the core region at the time that large portions of the core have exceeded the runaway zirconium oxidation temperature. Steam generation by heat transfer to this water from the submerged portion of the core and by the mechanism of quenching of the relocating debris then provides a steam-rich atmosphere (rather than the steam-starved atmosphere in the case with ADS actuation) to fuel the metal-water reactions in the core region.

The selected primary containment response characteristics as predicted by the BWRSAR code for the case without ADS are provided in the individual plots of Figures 2.25 through 2.32. Since the BWRSAR code has no models to represent the effect of core debris entering the drywell, the plotted code results are terminated at time 250 min., which is about four min. after the initial reactor vessel bottom head penetration failure. In this accident sequence without ADS actuation, the reactor vessel is pressurized at the time of vessel penetration failure so that there is a rapid blowdown of steam from the vessel atmosphere through the debris bed. The consequent hydrogen generation as the entering steam reacts with the unoxidized zirconium metal within the bed and attendant energy release induces rapid melting of the metals within the bed. The result is a large amount of hydrogen generation and a significant release of molten metals onto the drywell floor almost immediately after the initial bottom head penetration failure.

The drywell pressure trace as calculated by BWRSAR is provided in Figure 2.25. As shown, the containment pressure is predicted to be about 40 psia at the time of reactor vessel bottom head failure and to then increase rapidly in response to vessel blowdown and the large amount of hydrogen generated in the bottom head debris bed during blowdown. A more precise MELCOR calculation of the drywell (and wetwell) pressure response will be discussed in a later section of this report; however, it is evident from Figure 2.25 that the peak containment pressure immediately following reactor vessel blowdown would not exceed 120 psia.

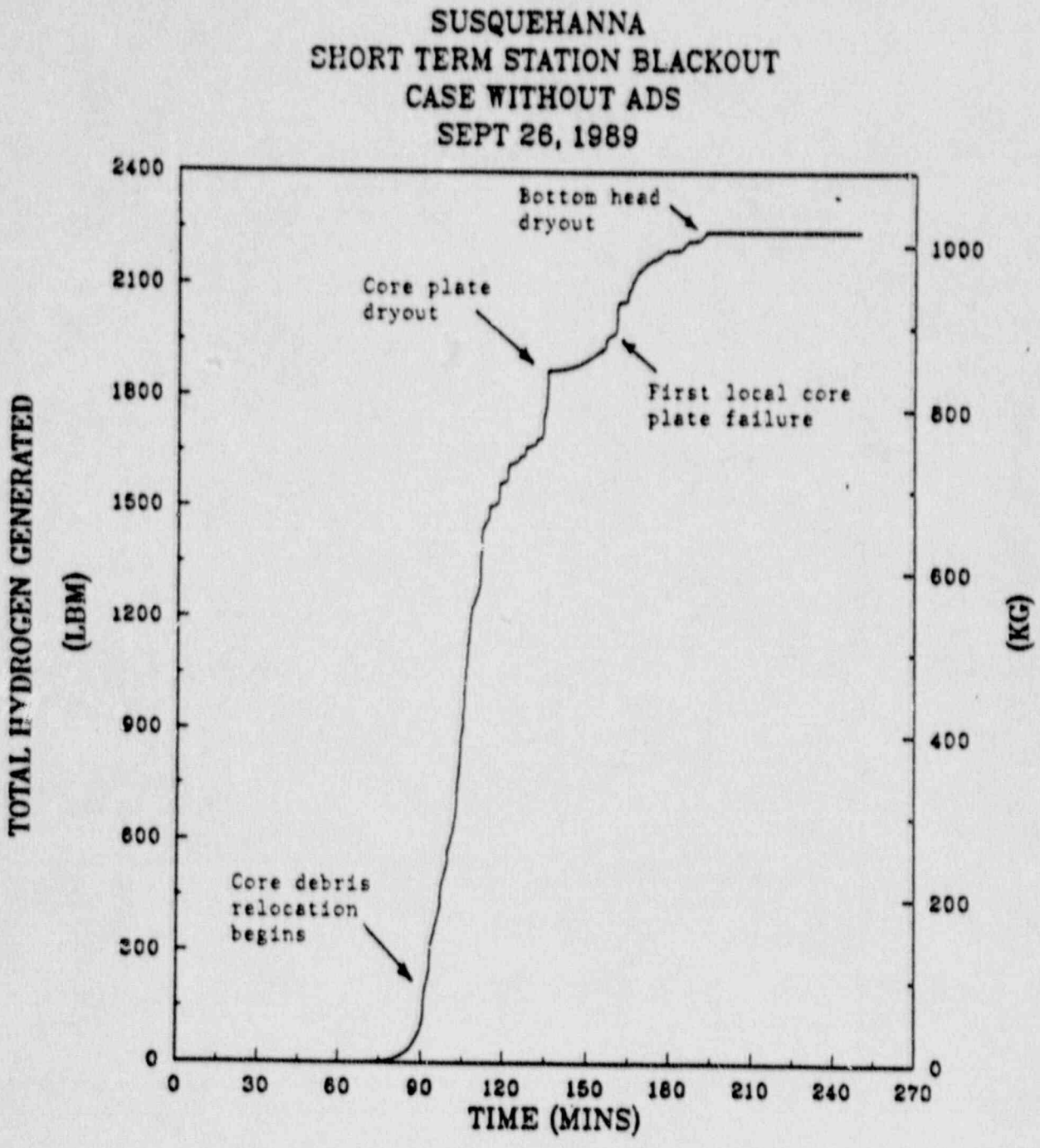

Fig. 2.24. Total hydrogen generated invessel for BWR-4/Mark II short-term station blackout accident sequence without ADS (simple eutectics).

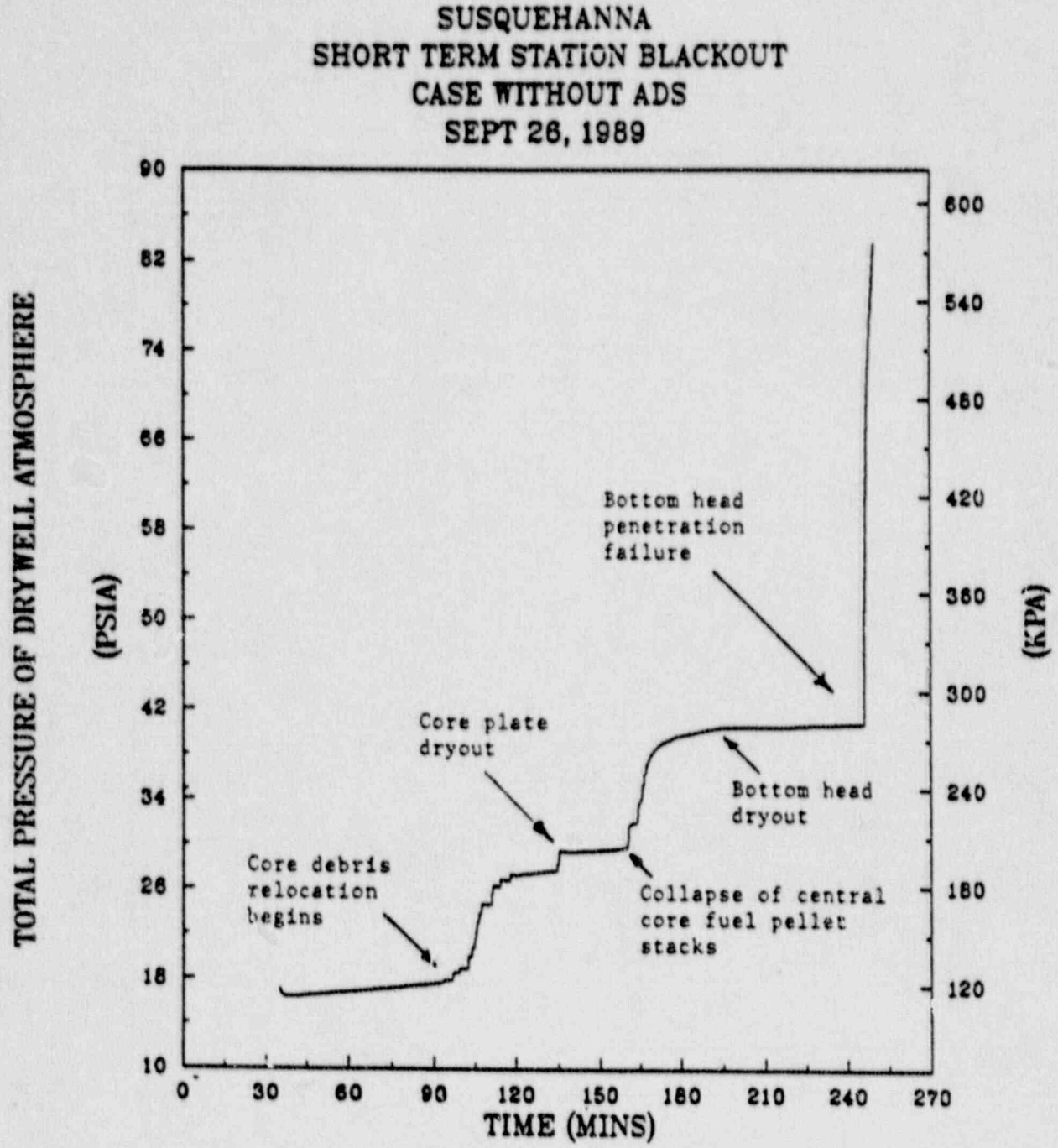

Fig. 2.25. Drywell atmosphere pressure for BWR-4/Mark II short-term station blackout accident sequence without ADS (simple eutectics).

There is also a large increase in the predicted drywell atmosphere temperature at the time of reactor vessel blowdown as shown in Figure 2.26. This is caused by the large energy release within the vessel bottom head by metal-water reactions during vessel blowdown and the associated heating of the escaping gases. Again, the MELCOR calculation of the drywell response, which employs a multi-cell representation of the drywell volume, provides a much more precise description of containment temperatures than does the single-cell BWRSAR representation of the drywell. The BWRSAR containment results discussed here are intended only to provide the reader with a general introduction to the containment response, to be refined in later sections of this report.

The calculated temperature of the drywell shell, shown in Figure 2.27, increases rapidly after the onset of reactor vessel blowdown, but does not approach threatening values. The mass of hydrogen in the drywell atmosphere (Figure 2.28) increases during vessel blowdown as hydrogen generated in the bottom head debris bed directly enters the drywell atmosphere.

The temperature of the wetwell atmosphere responds to the events occurring in the reactor vessel and, after vessel bottom head failure, to events in the drywell as indicated in Figure 2.29, but is not predicted to approach threatening values. A large flow is initiated from the drywell to the wetwell as the drywell is pressurized after reactor vessel bottom head failure, as shown in Figure 2.30. The calculated pressure suppression pool temperature does not exceed 180°F, as indicated in Figure 2.32.

The amount of hydrogen predicted to have accumulated in the drywell and wetwell for the case without ADS actuation (Figures 2.28 and 2.31) is much greater than the corresponding amounts predicted for the same accident sequence when the reactor vessel is depressurized (Figures 2.8 and 2.11). Much of the additional hydrogen (about 2200 lb.) is predicted to be generated by the passage of steam through the debris bed during the period of reactor vessel blowdown. [It is emphasized that this hydrogen generated within the bottom head debris bed is in addition to the approximately 2210 lb of hydrogen predicted to be generated in the core region, as discussed previously.] The uncertainties associated with this BWRSAR calculation are large, but it is obvious that much more metal-water reaction would occur within the bottom head debris bed if the vessel were pressurized at the time of penetration failure than if it were not.

2.2.5.2 Calculated reactor vessel debris pours for the case without ADS

Based upon the two-eutectic-mixture approach described in Section 2.2.3.2, for which all metals melt at 2750°F and all oxides melt at 4800°F, characteristics of the reactor vessel debris flows as calculated by the BWRSAR code for the case without ADS actuation are shown in Figures 2.33 through 2.38. Once again, the very important effect of the

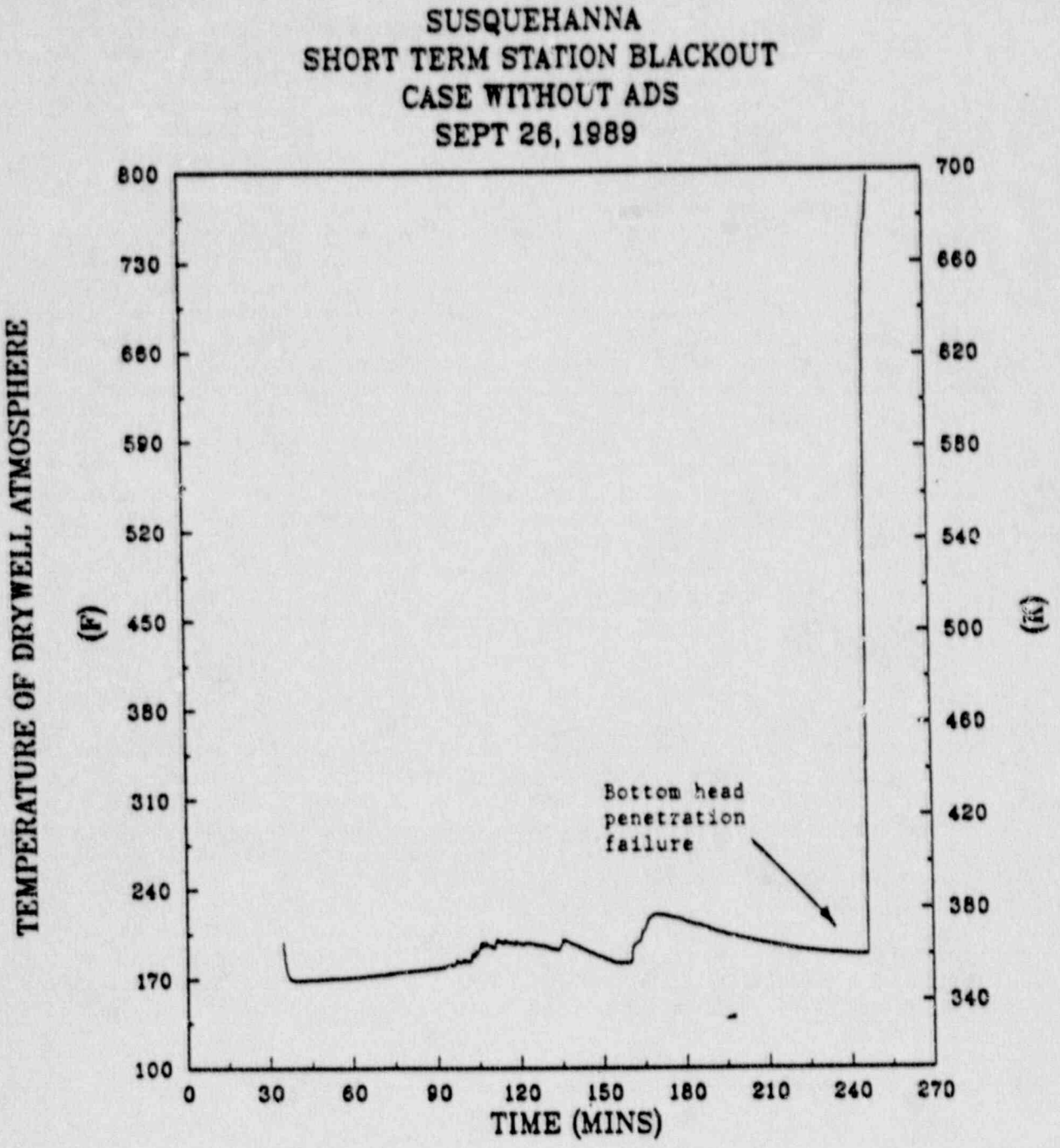

Fig. 2.26. Drywell atmosphere temperature for BWR-4/Mark II short-term station blackout accident sequence without ADS (simple eutectics).

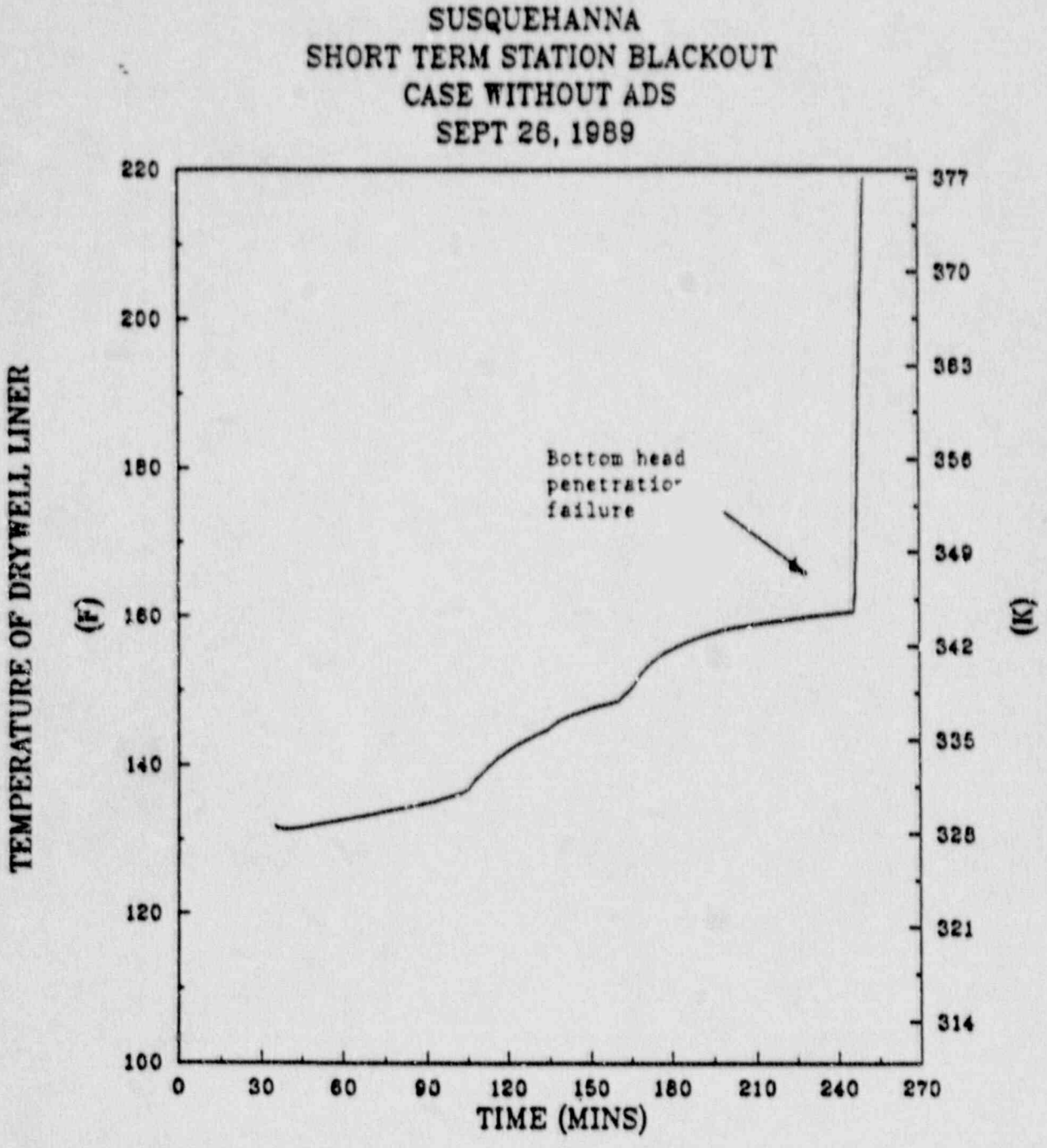

Fig. 2.27. Drywell liner temperature for BWR-4/Mark II short-term station blackout accident sequence without ADS (simple eutectics).

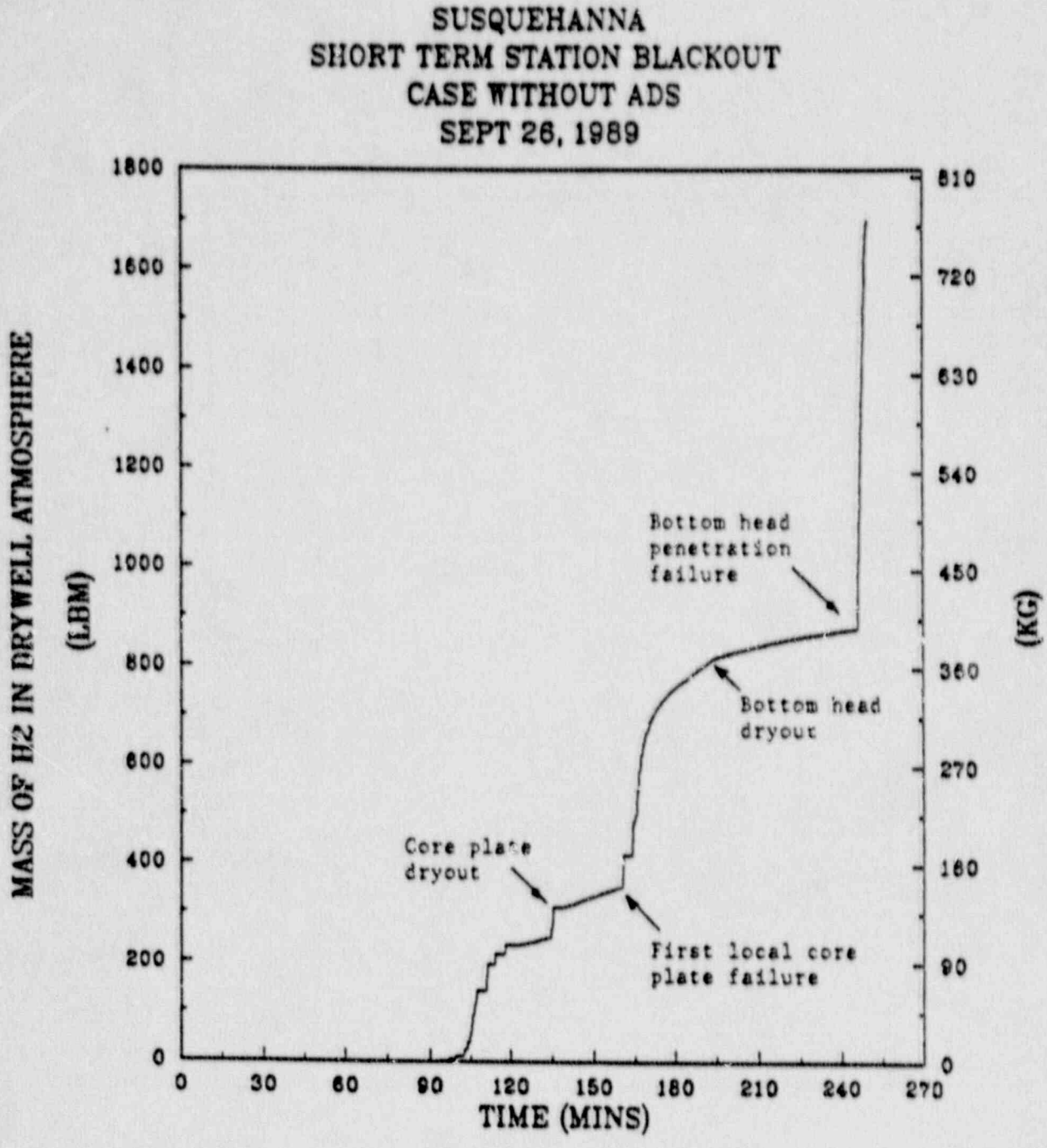

Fig. 2.28. Hydrogen mass in drywell atmosphere for BWR-4/Mark II short-term station blackout accident sequence without ADS (simple eutectics).

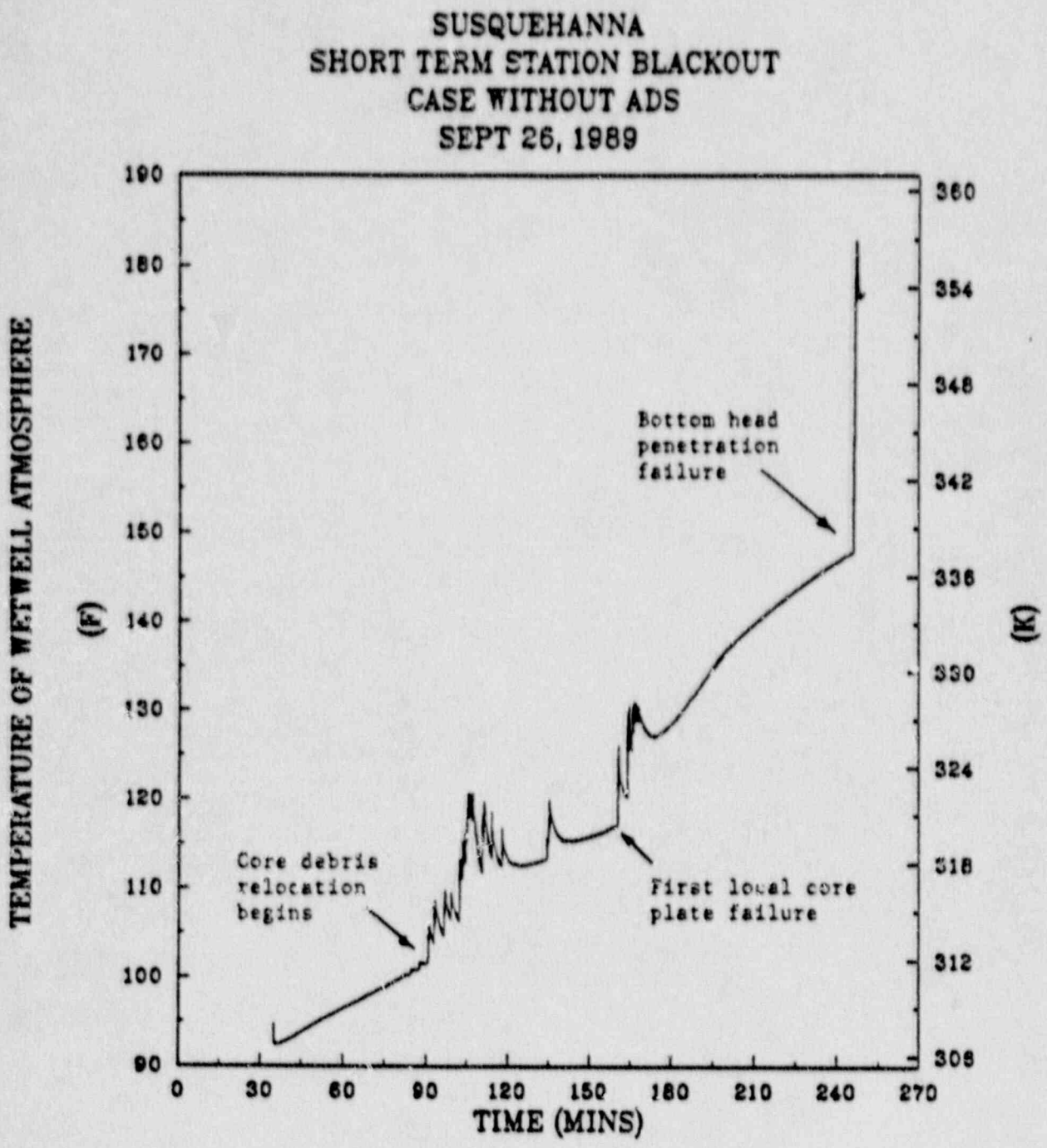

Fig. 2.29. Wetwell atmosphere temperature for BWR-4/Mark II short-term station blackout accident sequence without ADS (simple eutectics).

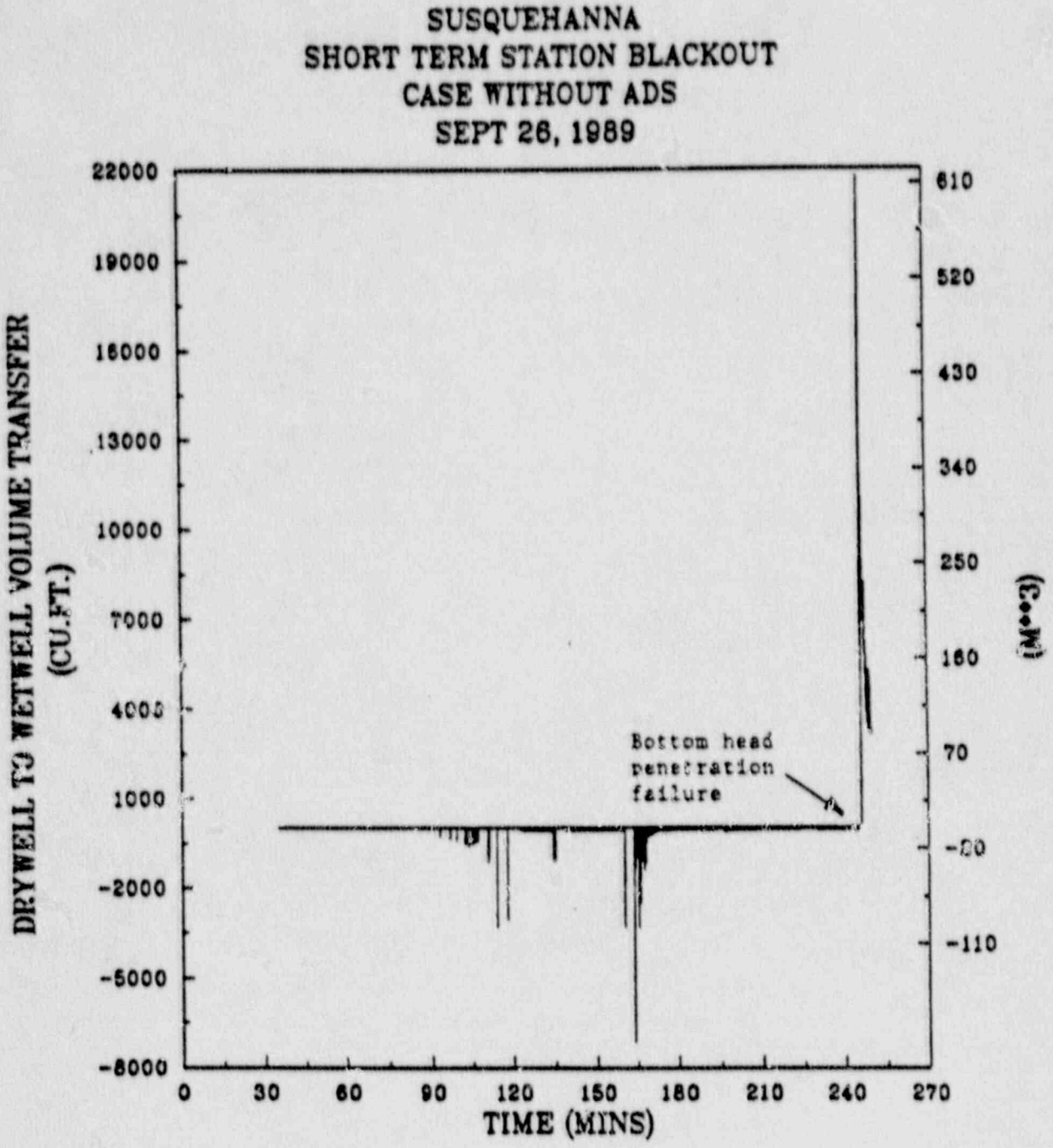

Fig. 2.30. Drywell-to-wetwell atmosphere transfers for BWR-4/Mark II short-term station blackout accident sequence with ADS (simple eutectics).

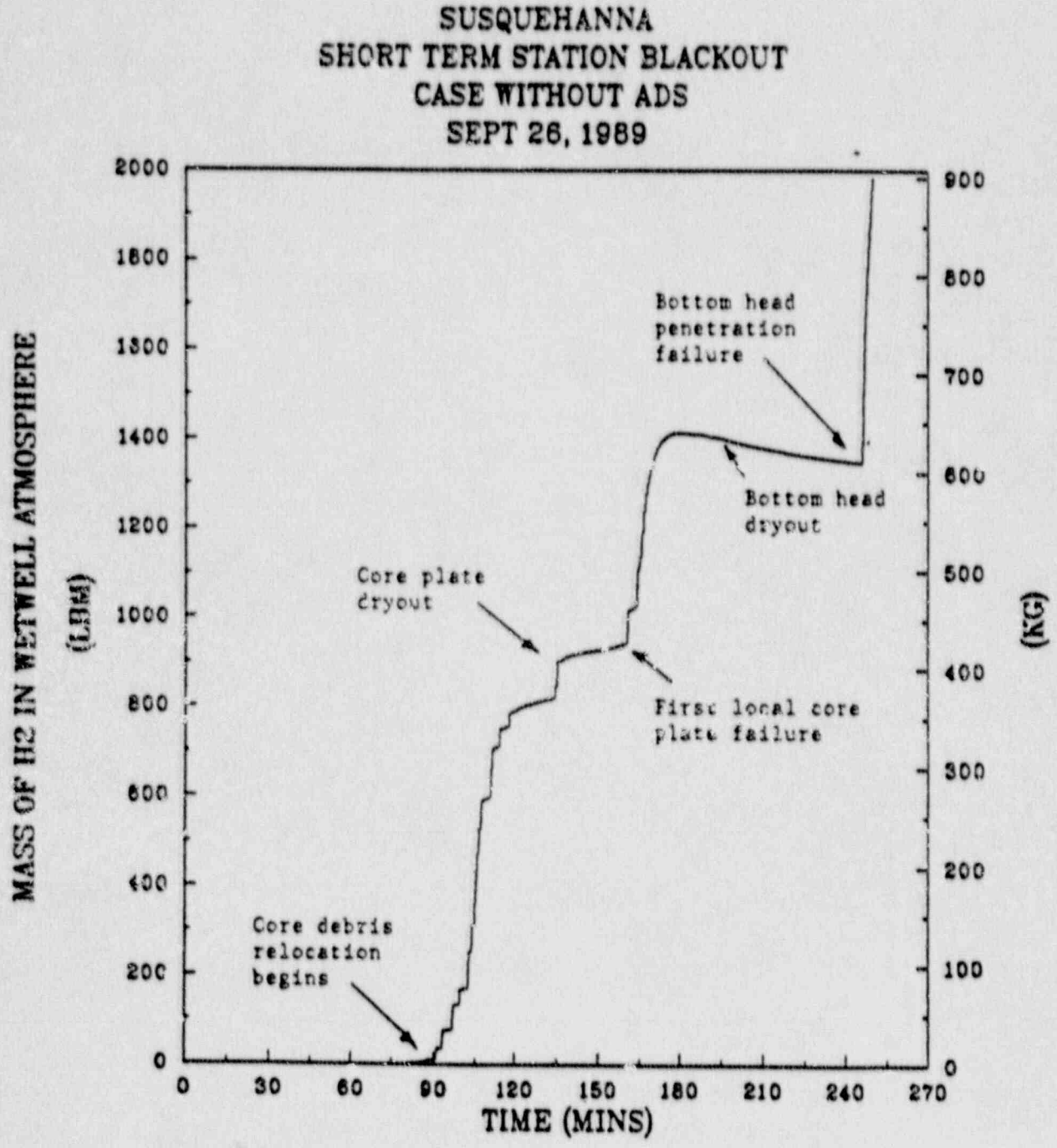

Fig. 2.31. Hydrogen mass in wetwell atmosphere for BWR-4/Mark II short-term station blackout accident sequence without ADS (simple eutectics).

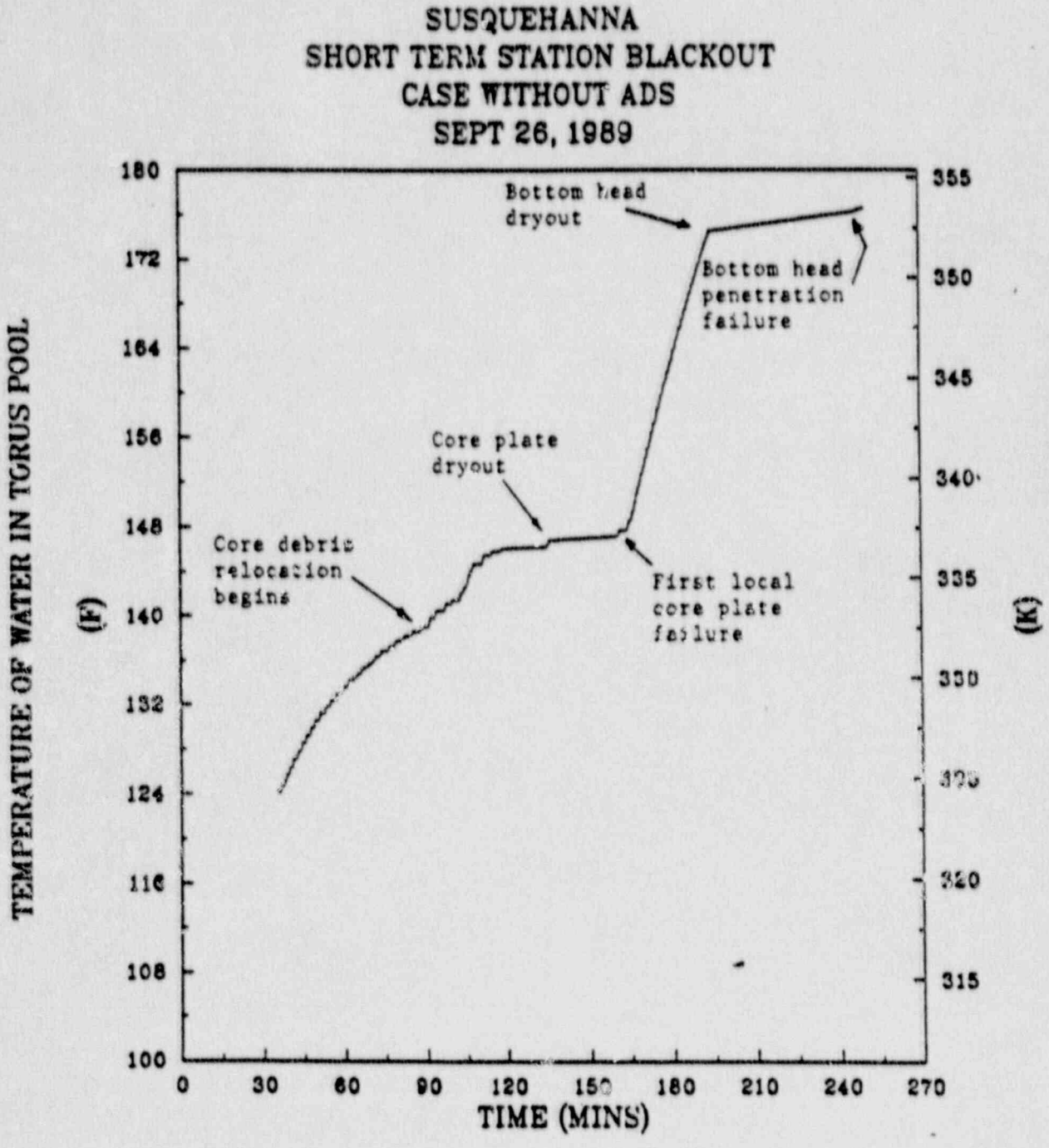

Fig. 2.32. Suppression pool temperature for BWR-4/Mark II short-term station blackout accident sequence without ADS (simple eutectics).

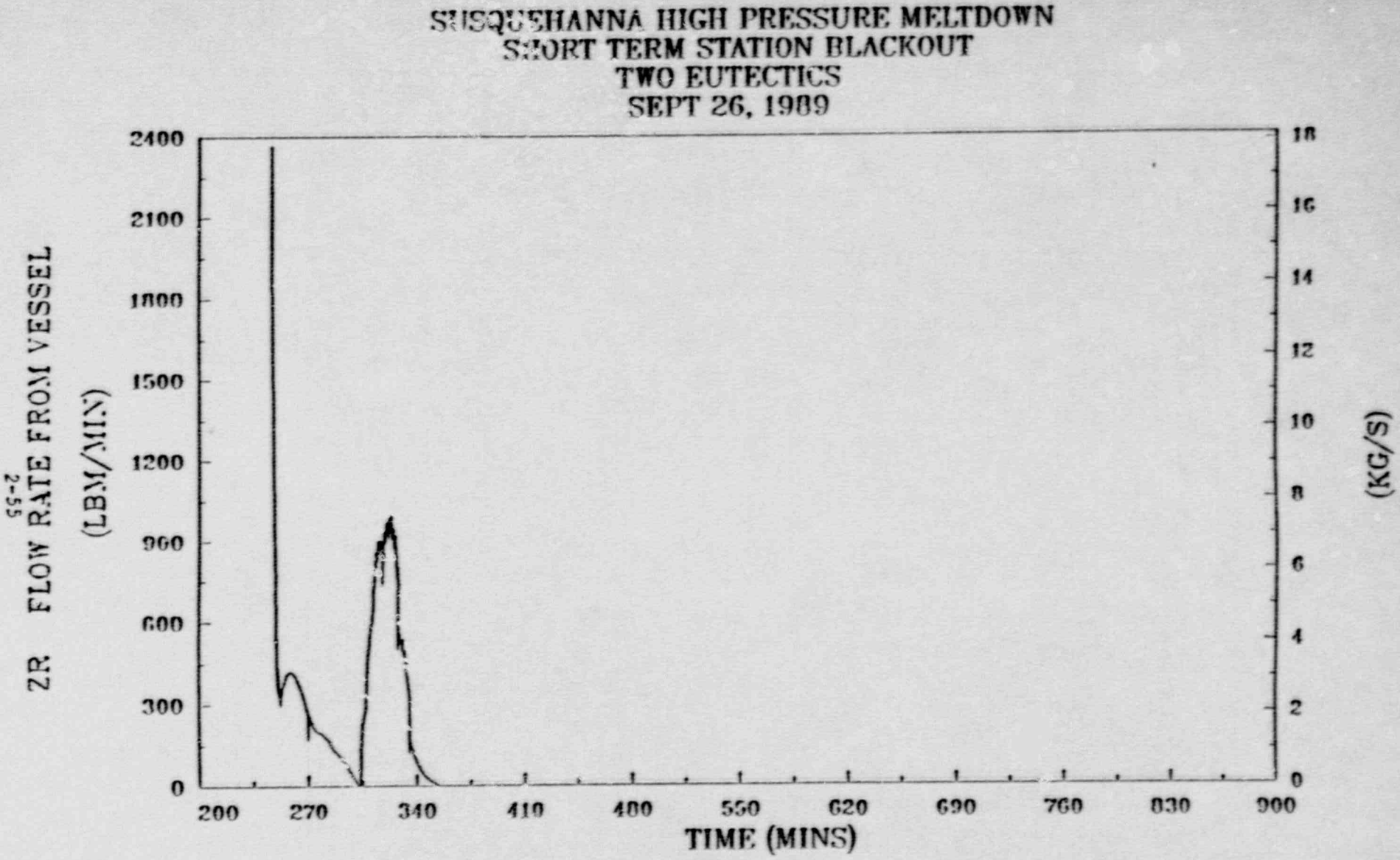

Fig. 2.33. Zirconium metal pours from the reactor vessel for BWR-4/Mark II short-term station blackout accident sequence without ADS (simple eutectics).

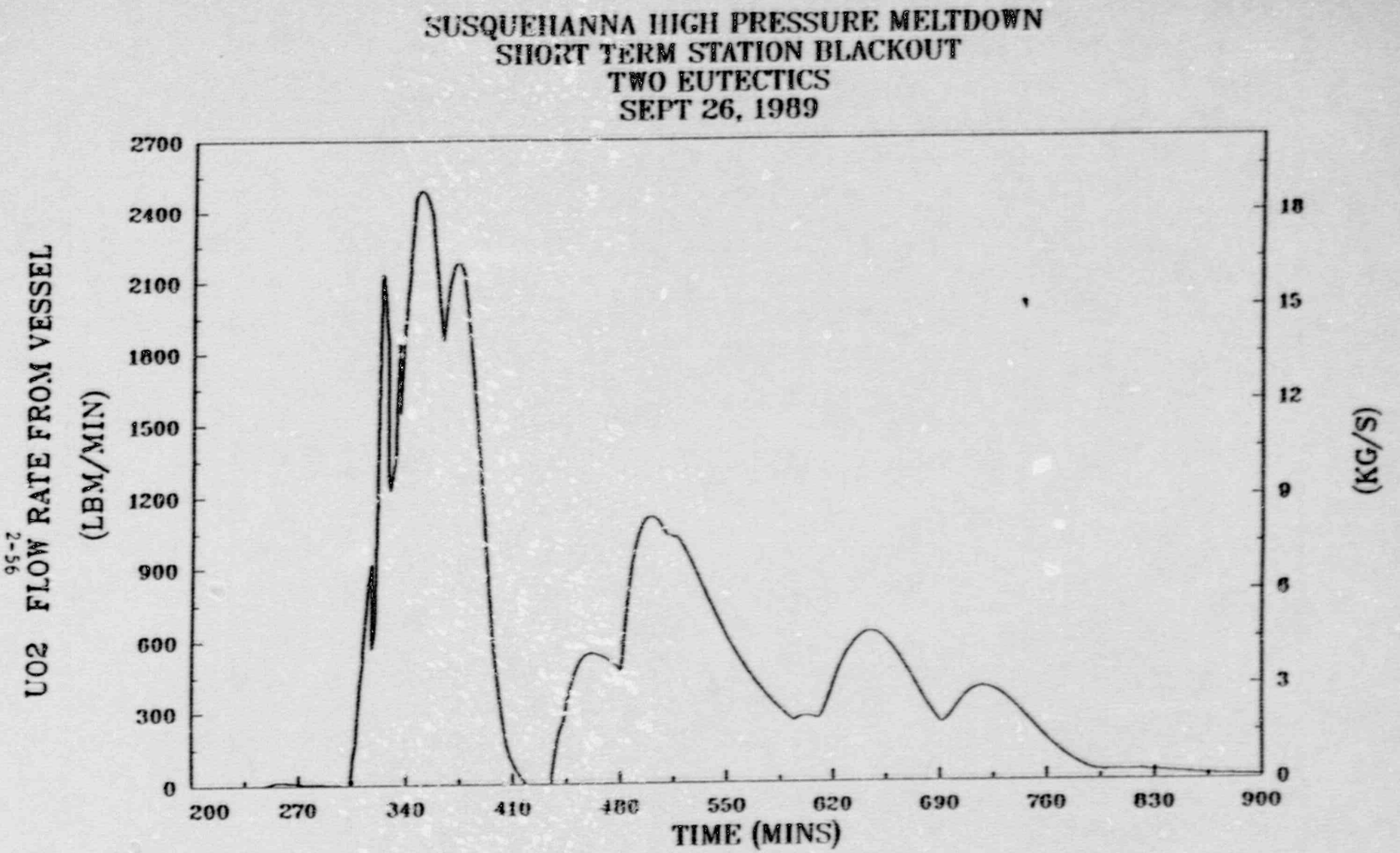

Fig. 2.34. Uranium dioxide pours from the reactor vessel for BWR-4/Mark II short-term station blackout accident sequence with ADS (simple eutectics).

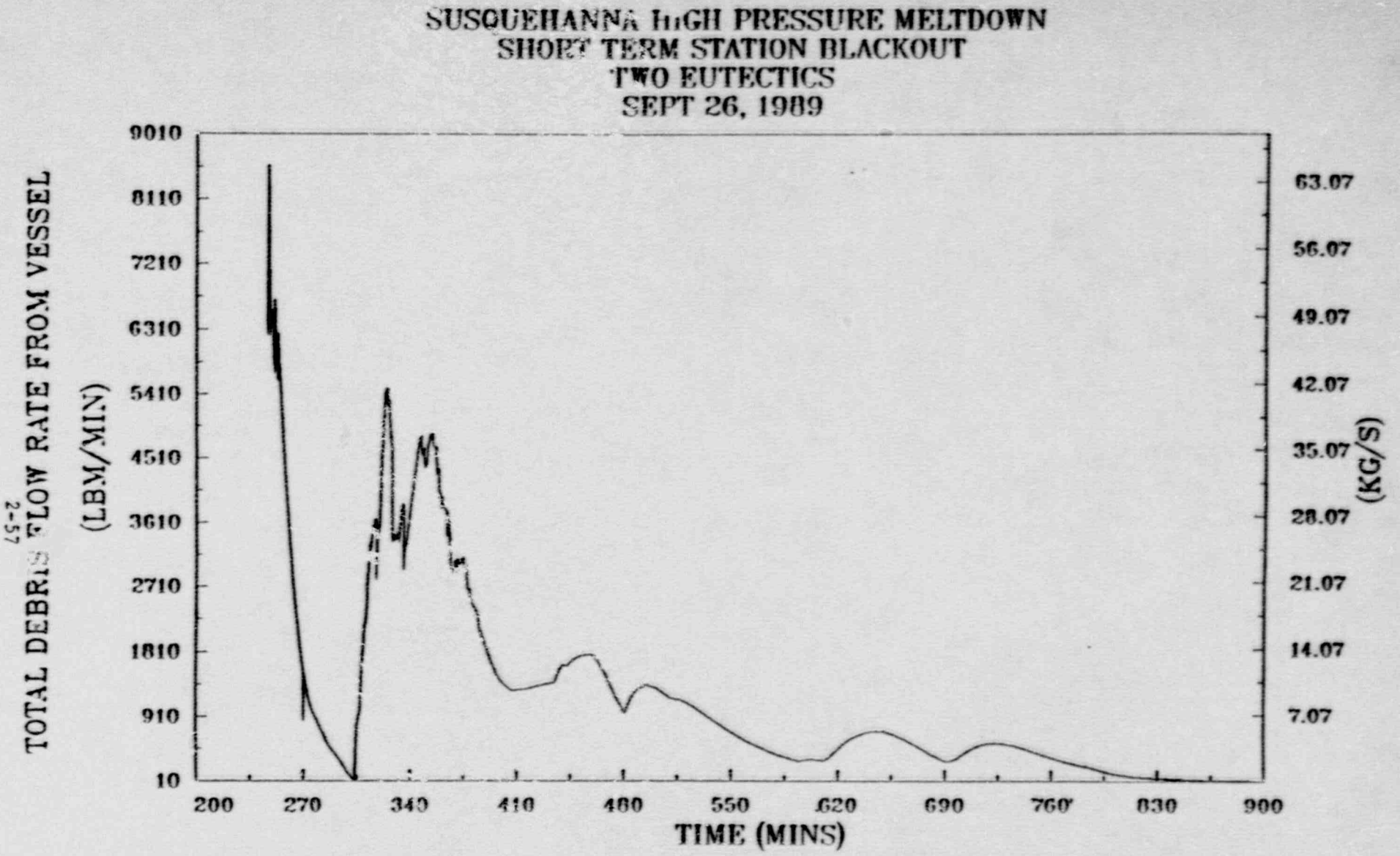

Fig. 2.35. Total debris pours from the reactor vessel for BWR-4/Mark II short-term station blackout accident sequence without ADS (simple eutectics).

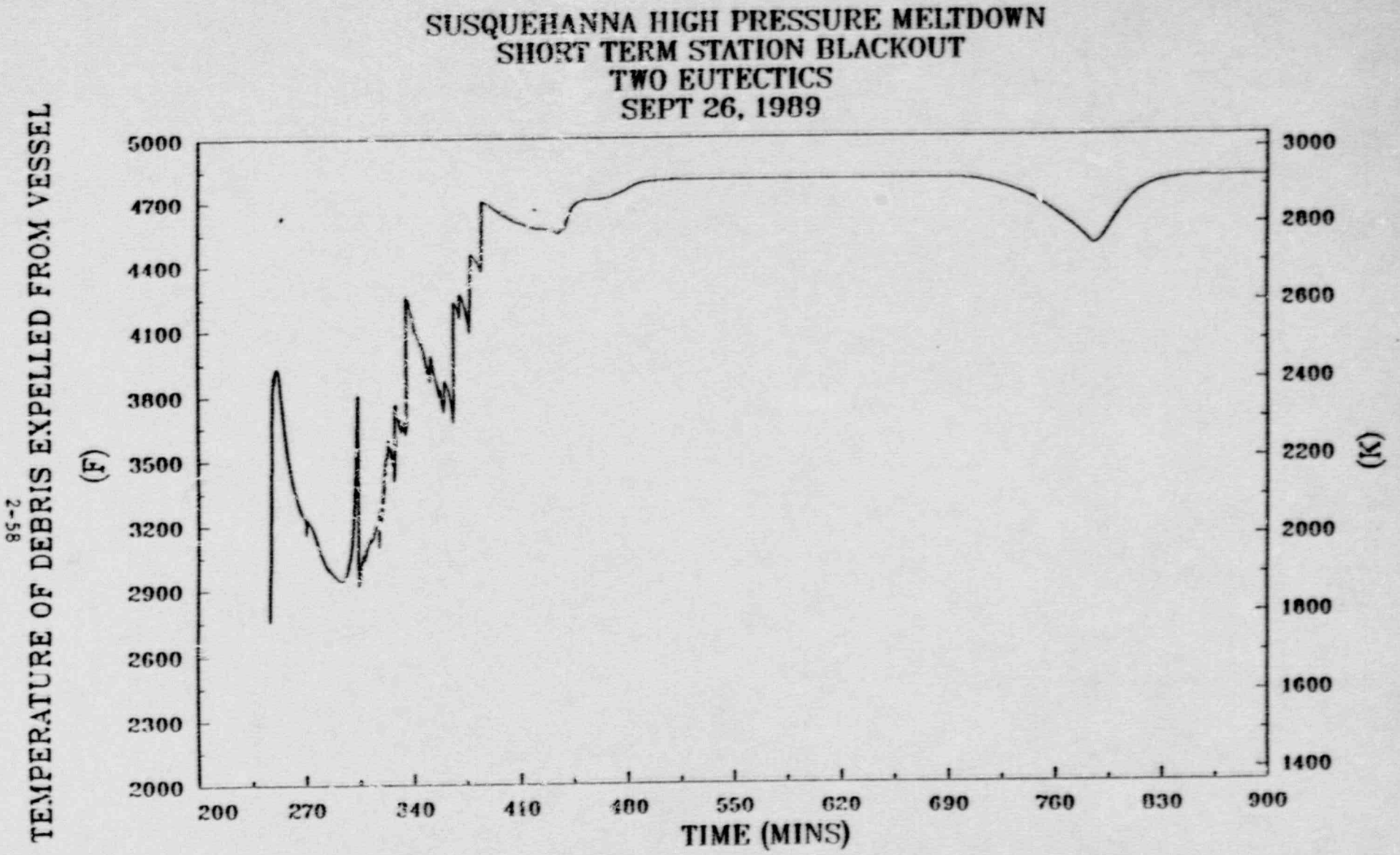

Fig. 2.36. Zirconium metal pours from the reactor vessel for BWR-4/Mark II short-term station blackout accident sequence without ADS (simple eutectics).

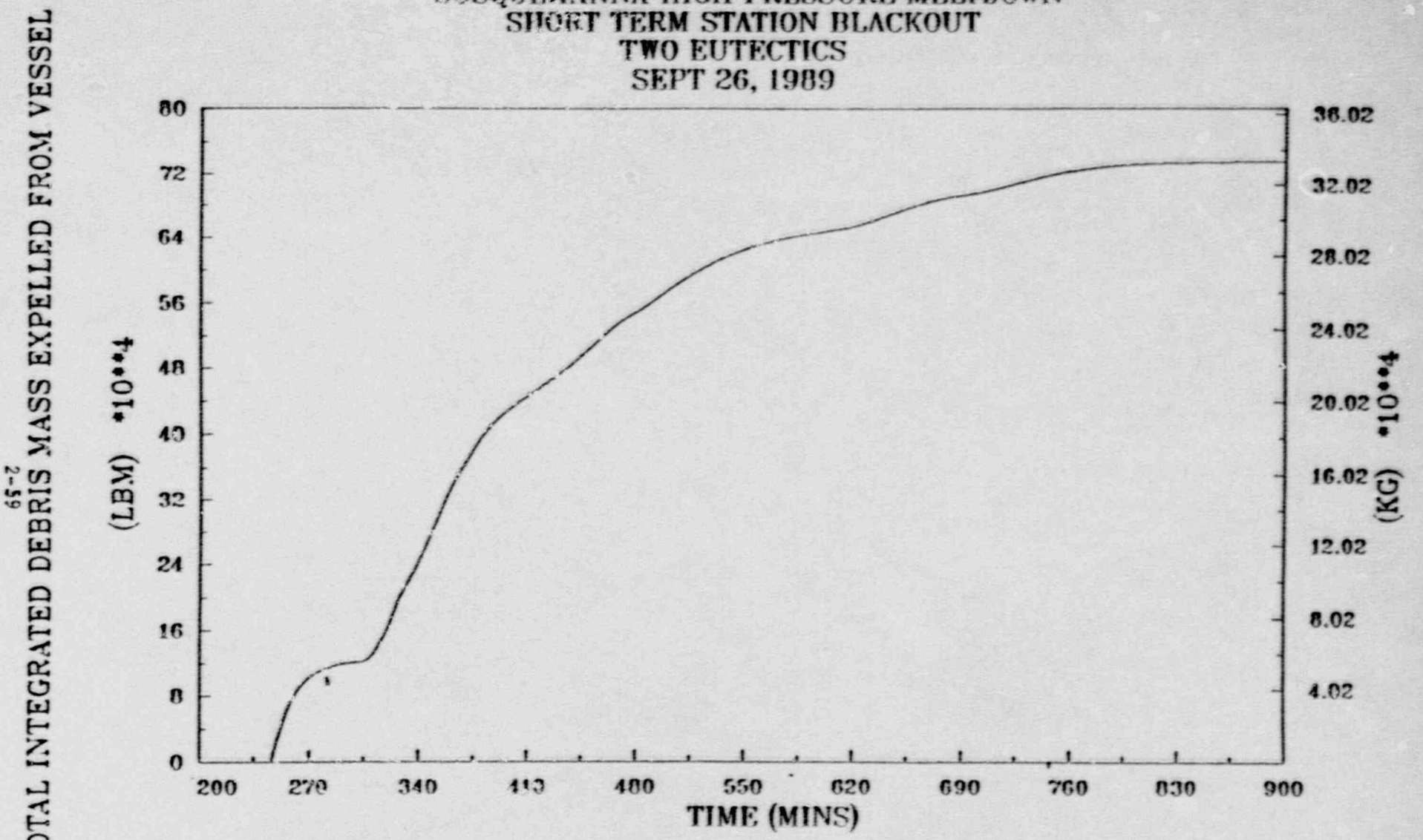

Fig. 2.37. Integrated debris mass expelled from the reactor vessel for BWR-4/Mark II short-term station blackout accident sequence with ADS (simple eutectics).

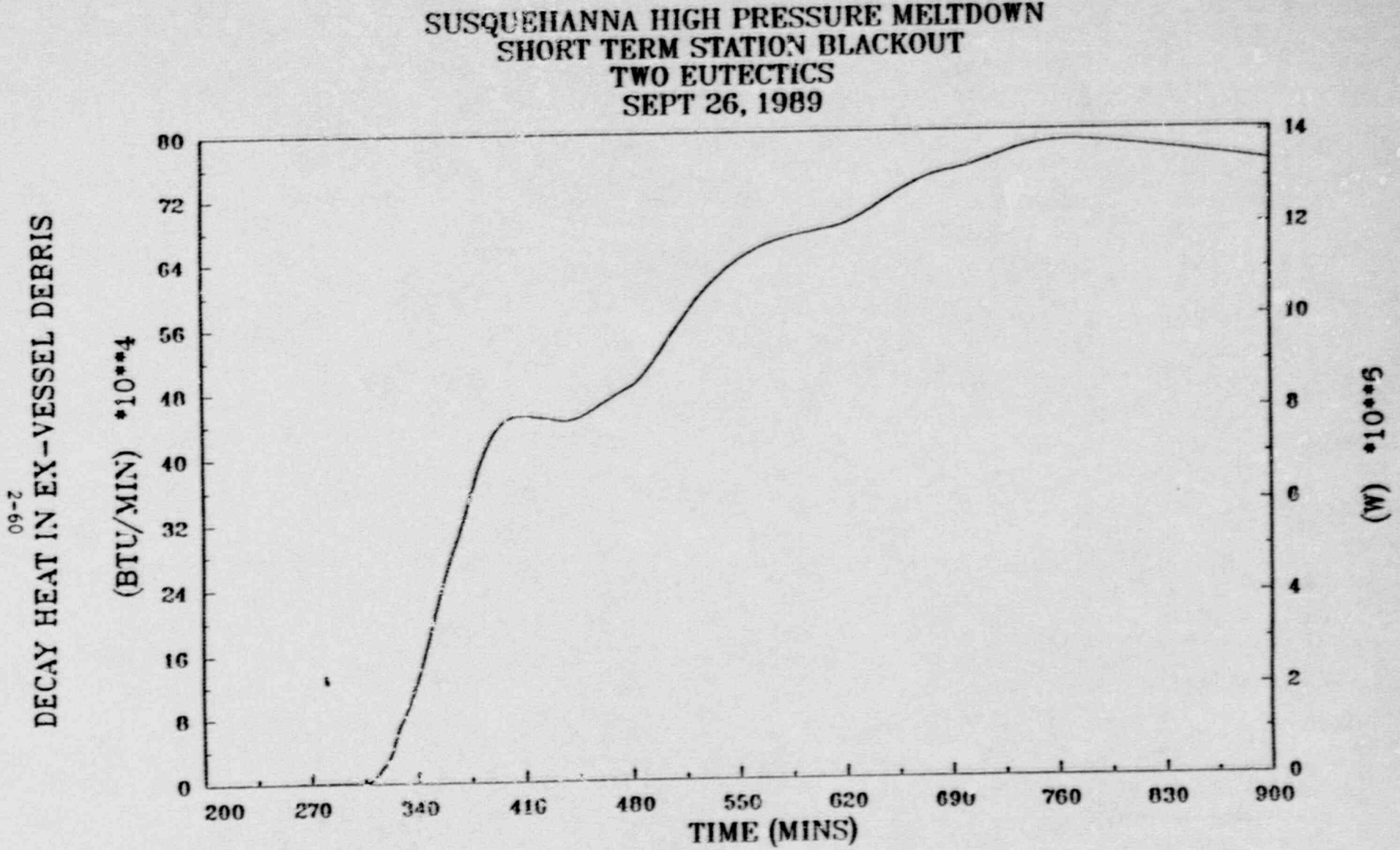

Fig. 2.38. Decay power in exvessel debris for BWR-4/Mark II short-term station blackout accident sequence without ADS (simple eutectics).

large energy release associated with the blowdown of steam through the bottom head debris bed and the associated metal-water reactions is evident, this time manifested by the very large initial pours of molten metals. Subsequent to the effects of the vessel blowdown, the releases of additional molten materials onto the drywell floor are controlled simply by the magnitude of the decay heat and the melting temperatures of the component mixtures.

The composition of the debris that has been released from the reactor vessel by the end of the BWRSAR calculation at time 900 min. is provided in Table 2.11. Comparison with the similar information for the case with ADS actuation provided in Table 2.6 shows that significantly less debris is predicted to have left the vessel at time 900 min. for the case without ADS actuation. The reason for this can be discerned by noting the large difference in predicted zirconium metal release. The pressurized blowdown of steam through the bottom head debris bed for the case without ADS actuation converts much of the zirconium metal to ZrO_2 within the bed. Since the ZrO_2 is modeled to melt with the other oxides at 4800°F, whereas the zirconium metal melts with the metals at 2750°F, it will take longer (for the same decay heat rate) for the ZrO_2 to melt and pour from the vessel. Indeed, the BWRSAR calculation predicts that 102,000 lb. of ZrO_2 remains in the vessel at time 900 min. for the case without ADS.

2.3 Mark II Containment Response to Unmitigated Short-term Station Blackout

2.3.1 Mark II Containment Design Description

The Mark II Containment utilizes the 'over-under' design in its suppression pool arrangement. This type of containment is used on only a limited number of late model BWR/4 and all BWR/5 reactors (Table 2.1). Typical Mark II containments are illustrated in Figures 2.39 and 2.40. Typical Mark II containment design specifications are listed in Table 2.2.

The Mark II design provides a more compact arrangement of the pressure suppression system and reactor building than does the Mark I design. The containment is constructed of prestressed or reinforced concrete with the suppression chamber located directly below the drywell in the same structure. The base foundation slab is a reinforced concrete mat approximately seven feet thick. The top of the base foundation slab within the containment is lined with stainless steel plate that serves as the suppression pool floor.

The drywell and suppression pool are steel lined structures constructed of either prestressed or reinforced concrete in the shape of a truncated cone and cylinder, respectively. The drywell head is bolted to a steel ring girder which is attached to the top of the concrete containment wall. The floor of the drywell serves as a pressure barrier between the drywell and suppression chamber and provides lateral positioning for the

Table 2.11. Composition of the debris released from the reactor vessel by the end of the BWR Mark II calculation without ADS

Constituents	Integrated Mass (lbs)
Metals	
Zr	38,045
Fe	263,391
Cr	49,062
Ni	21,825
B_4C	189
Total	372,512
Oxides	
ZrO_2	37,217
FeO	25
Fe_3O_4	44
Cr_2O_3	18
NiO	2
B_2O_3	8
UO_2	326,073
Total	363,387
Grand Total	735,899

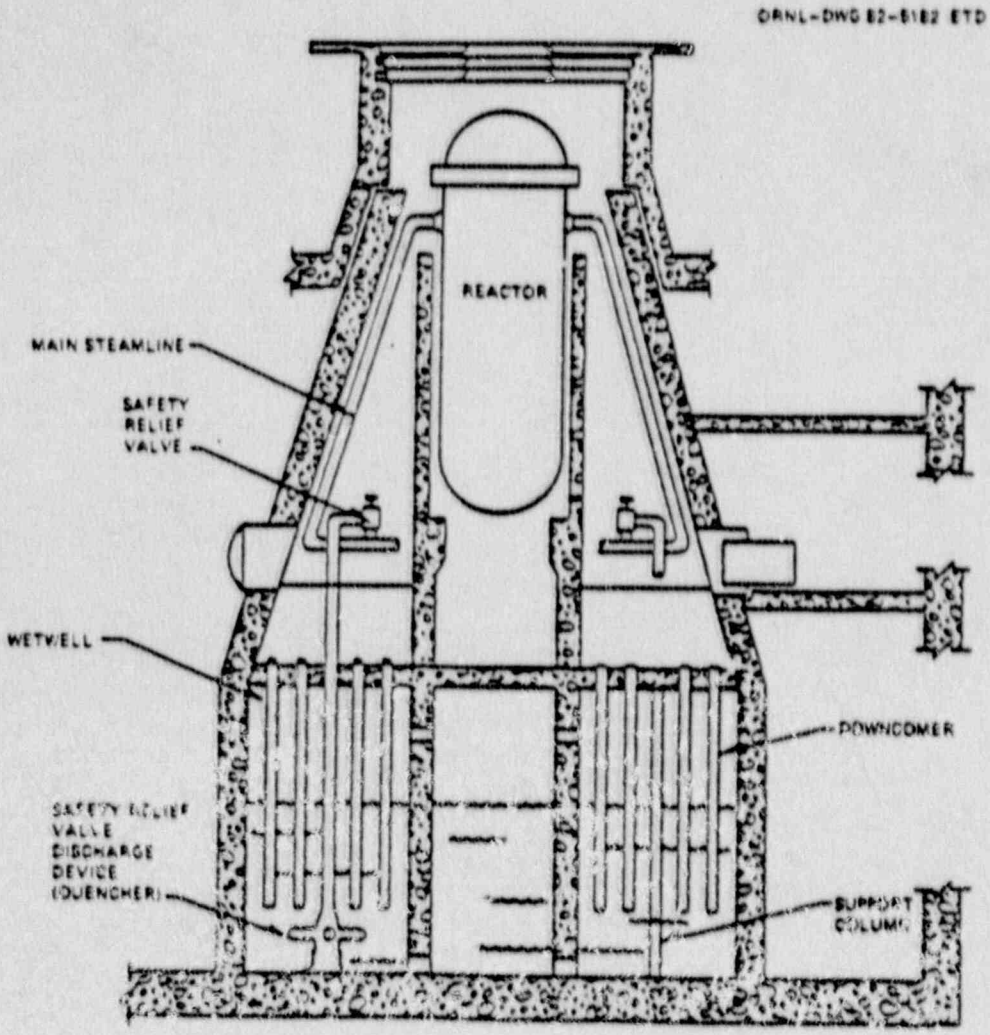

Fig. 2.39. Limerick Mark II containment

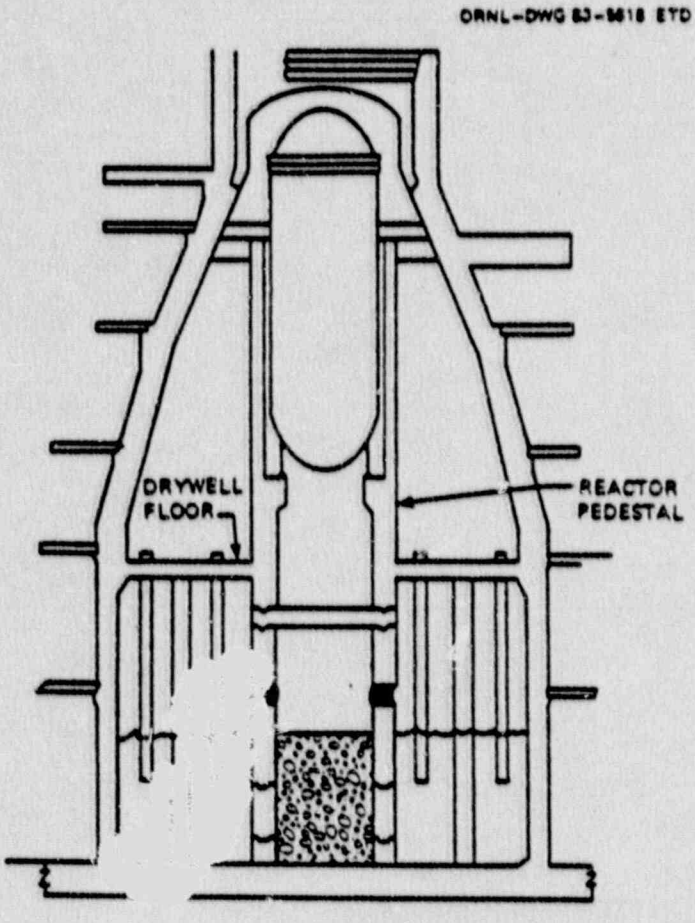

Fig. 2.40. La Salle Mark II containment.

reactor pedestal and support for the downcomers. The drywell cone and suppression pool cylinder are eighty feet and sixty feet high, respectively. The drywell floor is approximately three feet thick.

The reactor pedestal wall thickness in the drywell region varies between four and six feet thick. The reactor pedestal stands 84 ft tall from its base to the vessel support lip. The pedestal may be either hollow (Figure 2.39) or solid (Figure 2.40) in the suppression pool region (plant dependent). Figure 2.41 depicts the reactor pedestal designs employed in each of the six Mark II plants. All Mark II plants except La Salle have hollow pedestals in which the wetwell inpedestal volume is open to the suppression pool via openings in the pedestal wall, and the region inside the pedestal is partially filled with water. The hollow pedestal region directly beneath the vessel in the drywell is accessible through open manways. In some plants, the drywell floor elevation inside the reactor pedestal is several feet lower than that outside the pedestal, forming a concrete cavity directly beneath the reactor vessel (Figure 2.41). Shoreham and Nine Mile Point-2 have downcomers located within their reactor pedestal directly beneath the reactor vessel (four at Shoreham, eight at Nine Mile Point-2). At Shoreham, an inpedestal curb has been fitted around the inner circumference of the pedestal to prevent the escape of core debris into the expedestal region above the drywell floor. La Salle, Limerick, and WNP-2 have inpedestal drain lines which penetrate the inpedestal drywell floor.

Vacuum breakers are provided to equalize the static pressures between the suppression chamber and the drywell. They accomplish this by providing a controlled return flow path from the suppression chamber to the drywell to assure design operation of the suppression chamber in the event of a small steam leak. In contrast to the Mark I system, only one of the Mark II plants (WNP-2) provides vacuum relief between the inside of the primary containment and the reactor building atmosphere. The concrete containment structure has the ability to accommodate subatmospheric (negative) pressures of about five pounds per square inch absolute.

The reactor building completely encloses the reactor and its primary containment. The structure provides secondary containment when the primary containment is closed and in service, and primary containment when the primary containment is open, as it is during the refueling period. The reactor building houses the refueling and reactor servicing equipment, the new and spent fuel storage facilities, and other reactor auxiliary or service equipment, including the reactor core isolation cooling system, reactor water cleanup system, standby liquid control system, control rod drive system, the emergency core cooling systems, and electrical equipment components.

The reactor building exterior walls and superstructure up to the refueling floor are constructed of reinforced concrete. Above the level of the refueling floor, the building structure is fabricated of structural steel members, insulated siding, and a metal roof. Joints in the superstructure paneling are designed to assure leak tightness. Penetrations

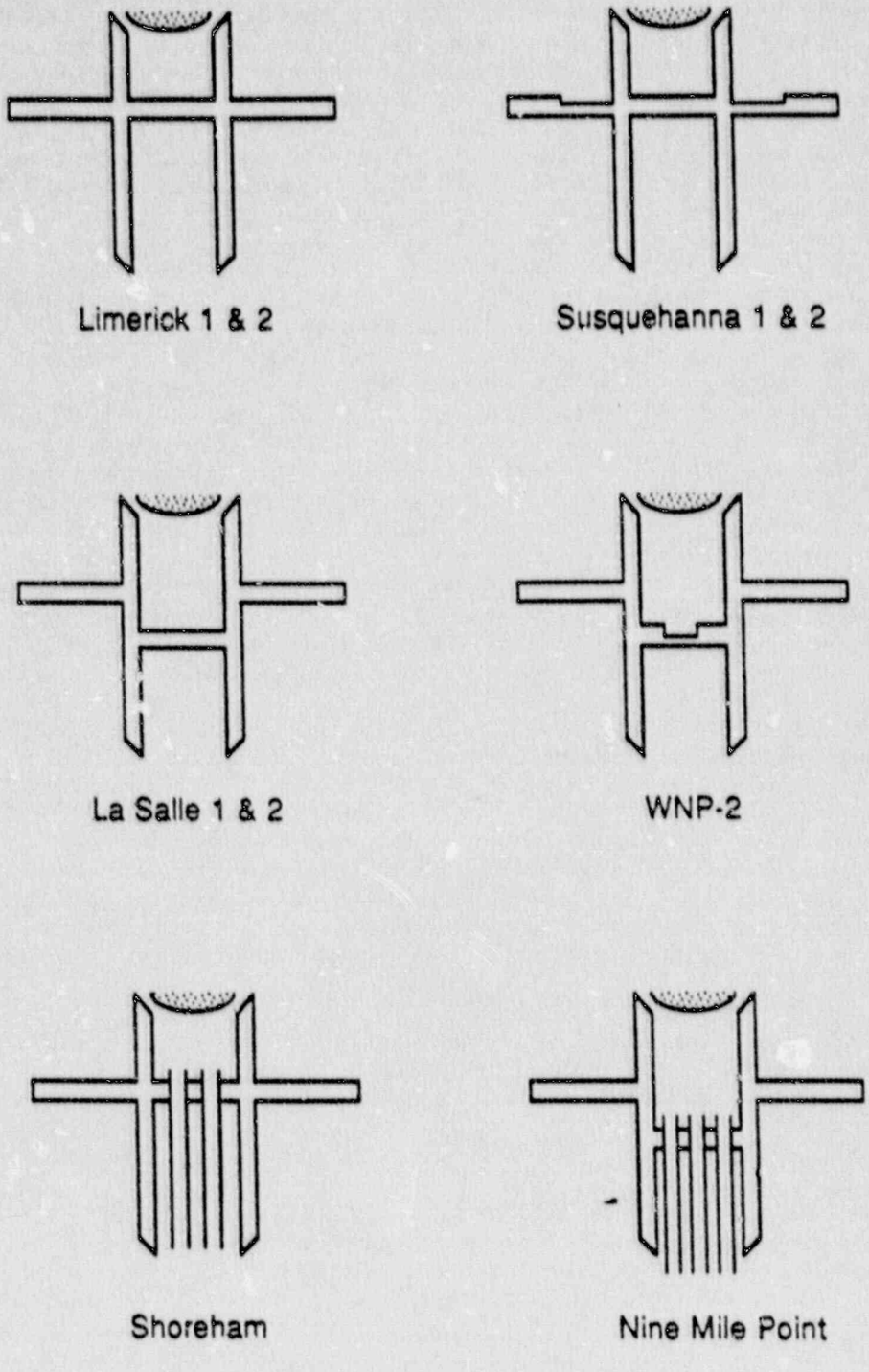

Fig. 2.41. Mark II reactor pedestal designs.

of the reactor building are designed with leakage characteristics consistent with leakage requirements of the entire building. The reactor building is designed to limit the inleakage to 100% of the reactor building free volume per day at negative 0.25 in. H_2O gauge, while operating the standby gas treatment system. The building structure above the refueling floor is also designed to contain a negative interior pressure of 0.25 in. H_2O gauge.

2.3.2 Mark II Containment Failure Modes and Mechanisms

Historically, the dominant primary containment failure mechanism considered in BWR severe accident analyses was over-pressure failure of the steel primary containment shell (Refs. 6 and 7). The pressure and location at which failure would occur are plant-dependent. Failure pressures for Mark II containments have been predicted to range between 133 and 140 psig (Refs. 7-9). The most probable over-pressure failure location for Mark II plants appears to be the primary containment liner in the wetwell airspace above the surface of the pressure suppression pool. A potentially-important feature of this failure location is that primary containment blowdown would enter the lowest portions of the reactor building, thus affording the maximum opportunity for scrubbing of fission products and aerosols prior to their release to the environment. However, the associated release of steam into the building would also preclude the performance of any subsequent equipment recovery efforts in that locale.

A second potential mechanism for BWR primary containment failure is primary containment shell or penetration failure due to collapse of the reactor vessel caused by ablation of the reactor's concrete support pedestal or the drywell floor. Recent ORNL studies have revealed that more than 75% of the reactor pedestal wall thickness may be eroded due to concrete ablation in some cases (Ref. 10). The probability of the failure mode is a strong function of the amount of zirconium metal available for oxidation on the drywell floor. It should be noted that the weight of the reactor vessel and internals would be decreased prior to pedestal failure due to expulsion of the core and core support materials following reactor vessel failure. The resulting load on the reactor pedestal would, therefore, be significantly reduced. Unfortunately, the most probable location for primary containment failure following pedestal or drywell floor collapse is not known with certainty (and is probably plant-specific).

A third type of primary containment failure in Mark I and II plants is failure of the drywell head flange seals (Ref. 11). The Idaho National Engineering Laboratory and Sandia National Laboratories have recently conducted thermal performance tests of seals similar to those employed in BWRs (Refs. 12 and 13). These experiments indicate that the seals lose their elasticity and structural integrity when subjected to temperatures of 700 to 750°F. Recent ORNL calculations indicate that drywell head flange temperatures of 900 to 1068°F may be reached in some Mark I accident sequences. Failure of these head flange seals is a

particular concern, since drywell blowdown via this pathway would enter the region between the drywell head and the drywell shield plugs located in the floor of the refueling bay - and then directly into the refueling bay itself. This is a particularly undesirable path, because the reactor building and the various reactor building fission product retention mechanisms would be bypassed. The actual flow area available for leakage through this path is a function of both the seal elasticity (springback) and the drywell head flange clamping force (Ref. 11). The clamping force is, in turn, a function of the reactor system pressure, head closure design (type of closure arrangement, number of closure bolts or pins, bolt length, bolt diameter, etc.), the thermal gradient across the closure fixtures, and the head flange bolt preload (Refs. 11, 14, and 15). Reference 11 indicates that head seal leakage at the Peach Bottom Plant would begin at 82 psig for zero gasket springback. These results are widely applied by other plants, but are probably applicable only to Peach Bottom since the head closure designs (Table 2.12) and head flange bolt preload are highly variable, plant-specific characteristics. It is, therefore, probable that the actual conditions under which the drywell head closure would leak are very plant-dependent.

2.3.3 MELCOR Mark II Containment Model Description

The Mark II primary containment model employed for these calculations is based on a synthetic containment that incorporates elements of the Susquehanna, La Salle, and WNP-2 designs. The containment volume and heat sink surface areas are based on the Susquehanna design, while the inpedestal region of the drywell is based on the WNP-2 design. The WNP-2 and La Salle designs incorporate a deep inpedestal drywell cavity with a volumetric capacity substantially larger than the volume of core debris resulting from a 100% core-melt accident. This cavity design was selected primarily to minimize the impact of core-concrete interaction modeling limitations associated with the application of CORCON (stand-alone or as module in MELCOR) to pedestal designs that do not incorporate a cavity (such as the Limerick and Susquehanna designs). CORCON, which was originally developed to model the results of core-concrete interaction experiments that were performed in well defined crucible geometries, does not have the capability to model the flow and spreading of core/concrete debris that would occur in flat-floored designs.

Figure 2.42 is a schematic representation of the ORNL MELCOR Mark II containment model employed in these analyses. Table 2.13 summarizes some of the more-important model parameters. The model consists of nine control volumes representing the interior pedestal region of the wetwell, the remainder of the wetwell, the 87 downcomers (single cell), the interior pedestal region of the drywell, the remainder of the drywell (4 cells), and the annular gap between the reactor vessel and the inside of the reactor shield wall.

Fifteen flow paths are employed to represent the architectural features (such as ports in the reactor pedestal and shield wall) which facilitate circulation between the drywell and wetwell, and between the inpedestal

Table 2.12. Mark II drywell head closure design data

Plant	Closure Type	Head Diam. (ft)	No. Bolts/ Pins	Bolt Diam. (in.)	Bolt Length (in.)
Peach Bottom*	Bolted Flange	32.25	68	2-1/2	44
Limerick	Bolted Flange	37.63	80	2-3/4	32
La Salle	Bolted Flange	31.45	60	3	30
Shoreham	Bolted Flange	30.17	128	2	19
Susquehanna	Bolted Flange	37.63	80	2-3/4	32
9-Mi Point 2	Horizontal Finger Pin Joint	34.00	48	3	-

*Peach Bottom (Mark I) shown for reference only. (Other Mark I Plants have different drywell head closure designs.)

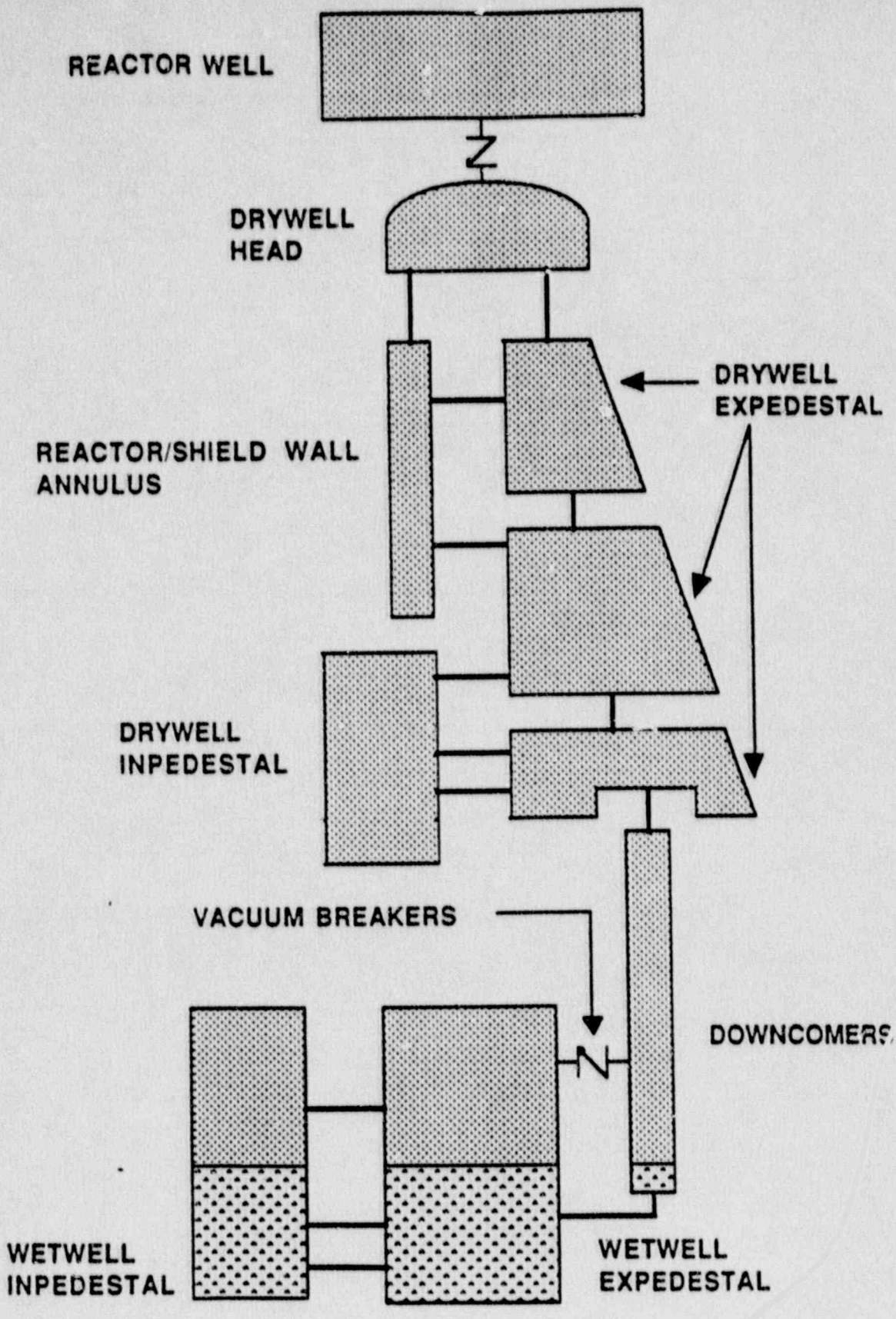

Fig. 2.42. ORNL Mark II containment model

Table 2.13 ORNL Mark II containment model parameters

Control Volume Name	Free Volume (ft^3)	Heat Slab Name	Material inner/middle/outer
Drywell:			
Inpedestal	11,018	pedestal wall 1	concrete
		pedestal wall 2	concrete
		RPV bottom head	steel.
		floor	steel/concrete/steel
Expedestal 705'-723'	65,685	exterior wall	steel/concrete
		floor	steel/concrete/steel
		misc. steel	steel
Expedestal 723'-758'	91,677	exterior wall	steel/concrete
		shield wall	steel/concrete/steel
		misc. steel	steel
Expedestal 758'-779'	25,497	exterior wall	steel/concrete
		misc. steel	steel
Expedestal 779'-809'	37,151	drywell head	steel
		drywell head flange	steel
		RPV head	steel
		exterior wall	steel/concrete
		misc. steel	steel
Reactor-Shield Wall Annulus	636	shield wall	steel/concrete/steel
		RPV wall	steel
Downcomers	11,689	downcomer wall (airspace)	steel
		downcomer wall (submerged)	steel
Wetwell			
Inpedestal	15,821	pedestal wall (airspace)	steel/concrete/steel
		pedestal wall (submerged)	steel/concrete/steel
		floor	steel/concrete
Expedestal	264,330	exterior wall (airspace)	steel/concrete
		exterior wall (submerged)	steel/concrete
		support columns (airspace)	steel
		support columns (submerged)	steel
		floor	steel/concrete
Reactor Well	11,159	exterior wall	steel/concrete
		shield plugs	concrete

and expedestal regions of the drywell and wetwell. Special care was taken in the modeling of the wetwell-to-drywell vacuum breakers in an attempt to provide a means to estimate the number of valve opening and closing cycles that would be associated with the accident sequence. To do this, it is necessary to consider that, although the valves are of the same design, small variations in the as-manufactured status of the valves would ensure that small pressure differences developing over periods of several minutes would cause the opening of only one (lowest-set) vacuum breaker. With this in mind, the following strategy is employed for these calculations.

The five wetwell-to-drywell vacuum breakers are modeled as six independent, parallel flow paths between the wetwell airspace and the drywell. The first four flow paths each represent 25% of the flow area of a single vacuum breaker, and are staged to open over the first 20% of the actual measured pressure differential required for full opening of a vacuum breaker valve. The fifth flow path represents a second vacuum breaker (100% of the flow path area of a single vacuum breaker), and is programmed to open over the second 20% of the actual measured vacuum breaker opening pressure interval. The sixth flow path represents the remaining three vacuum breakers (300% of the flow area of a single vacuum breaker), and is programmed to open over the last 60% of the total opening pressure differential. Thus, if the pressure differential between the wetwell and drywell reaches 40% of the differential required for full opening, the model would provide that five flow paths are open, representing that two vacuum breakers are fully open while the remaining three are totally closed. This is in lieu of a more straightforward (but less accurate) model that would represent that all five valves would each be 40% open.

The relative complexity of the vacuum breaker model was dictated by the desire to provide a detailed analysis of the expected number of opening and closing cycles during an accident sequence, and to provide the input necessary to estimate the likelihood of a stuck-open vacuum breaker. The vacuum breaker models are based on actual test data supplied to ORNL by Pennsylvania Power and Light (PP&L), and may not be representative of those employed in other Mark II plants.

Thirty-one heat slabs are incorporated in the model to represent the various floors, walls, and structures that provide heat sinks within the primary containment (Table 2.13). Water vapor and CO_2 is released from concrete structures as the structures are heated. The outgassing model implemented in the ORNL model assumes that the free water is released from concrete structures over an interval of 190°F to 221°F. The chemically-bound water is released from concrete structures over the interval of 221°F to 968°F. The CO_2 is assumed to be released from concrete structures over the interval of 1021°F to 1472°F. These input assumptions are based on experimental data from Sandia National Laboratories (Ref. 16).

The model incorporates two primary containment failure modes. The first failure mode is a simple over-pressure failure which opens a 0.1 ft^2

hole in the wetwell airspace region when the pressure in that region exceeds 135 psig. The second failure mode simulates the combined over-pressure/over-temperature failure of the drywell head flange seals (see Section 2.3.2). The model is constructed in accordance with the Chicago Bridge and Iron Company results for Peach Bottom (Ref. 11) so that the drywell head flange seals begin leaking when the drywell pressure is greater than 82 psig if the head flange temperature has ever exceeded 700°F at any previous time in the transient. The seal leakage area ramps from 0.0 in.^{2} at 82 psid to 662 in.^{2} at 200 psid. This leak enters the reactor well in the region between the reactor shield plugs (in the refueling bay floor) and the drywell head. This region is modeled as a separate control volume in the ORNL model (Figure 2.42).

Both a "single-cavity" and a "dual-cavity" version of the model was developed. The single-cavity version of the model employs a single active CORCON cavity (for core-concrete interaction simulation) in the inpedestal region of the drywell. This model is useful for examination of scenarios in which all of the debris escaping the reactor vessel is held within the inpedestal drywell region. The dual-cavity version of the model employs both the inpedestal drywell cavity as well as a cavity representing the inpedestal region of the wetwell. This model is useful for examination of scenarios in which debris enters the inpedestal region of the wetwell via inpedestal downcomers, or due to melt-through of the drywell floor drains.

The interface between the BWRSAR and MELCOR codes is provided via use of the External Data File (EDF) option in MELCOR. The utilization of the EDF option necessitated (a) modification of an existing BWRSAR Post Processor code, and (b) the addition of an "interface" control volume to the ORNL primary containment model.

The MELCOR code input is constructed to source the BWRSAR-generated SRV flows into the interface cell, the vessel leakage flows into the inpedestal region of the drywell, and the debris pours into the appropriate CORCON cavity (inpedestal drywell or inpedestal wetwell), as required for the specific case under investigation. Because MELCOR will not permit externally-sourced hydrogen to be injected into water pools, a special interface cell was required for the containment structure. The details of the method employed to interface BWRSAR and MELCOR are provided in Appendix C.

2.3.4 Mark II Containment Response: Short-term Station Blackout With ADS, Simplified Eutectics, and All Core Debris Retained in Drywell Pedestal

This Section presents the containment response results obtained by MELCOR analysis of the short term station blackout scenario assuming operation of the ADS system and retention of all core debris in the drywell pedestal. The scenario is described in Chapter 1 and the invessel BWRSAR analysis is reported in Section 2.2. The ORNL Mark II primary containment MELCOR model is described in Section 2.3.3. The

containment failure models described in Section 2.3.3 were disabled for this calculation.

The MELCOR analysis of the containment response was performed subsequent to completion of the BWRSAR calculations and represents the same period of the accident sequence. The initial containment atmospheric conditions for MELCOR were specified to be the same as those used by BWRSAR and the time dependent conditions were calculated in response to the mass and energy sources generated by BWRSAR. These sources consist of SRV steam and hydrogen into the wetwell pool, leakage of water from the reactor coolant system, discharge of steam and hydrogen flows from the bottom head of the reactor vessel after the head penetrations fail, and core/bottom head structural material debris pours from the failed reactor vessel bottom head. The containment calculation progressed from the time of core uncovery (35 min.) and continued throughout the core degradation and relocation period. The calculation was terminated when the drywell floor within the inpedestal region cavity was calculated to have been completely ablated in the axial direction (3.6 feet at time 810 min.).

Because BWRSAR models the Mark II drywell as a single cell, it is not possible to specify the initial atmospheric temperature and composition spatial distributions. Likewise, it is not possible to specify the corresponding spatial temperature distributions of the drywell structures. For the current MELCOR analyses, uniform initial atmosphere temperatures and compositions were specified consistent with the BWRSAR results. (This is reasonable since significant intercell differences would not develop by time 35 minutes.) The thermal conditions for the structures were conservatively initialized to the steady state values consistent with the input atmospheric temperatures. This leads to a somewhat higher energy state of the structures than that corresponding to BWRSAR at the beginning of the calculation. This is conservative with respect to calculated containment pressures as the following paragraphs indicate.

The phenomena of concrete degassing at elevated temperatures provides a source of containment water vapor in addition to the BWRSAR sources described above. Because containment atmosphere temperatures are elevated in the latter phases of severe accidents, the structures may reach temperatures high enough to cause significant gas loss and containment pressurization. Figure 2.43 presents the calculated expedestal wetwell pressure for similar calculations differing only in whether or not degassing is modeled. The degassing case exhibits an initial pressure rise not calculated by the case in which structural degassing is not considered. This initial degassing pulse is due to the initial drywell concrete structural temperatures which are slightly above the threshold for steam evolution. The pressure rise is approximately 10 psi and is maintained/increased throughout the remainder of the calculation. This approach is conservative because the degassing calculation provides a continuous source of gas which pressurizes the containment. Thus, the MELCOR Mark II analyses were performed with this conservatively high initial structure temperature and degassing approach.

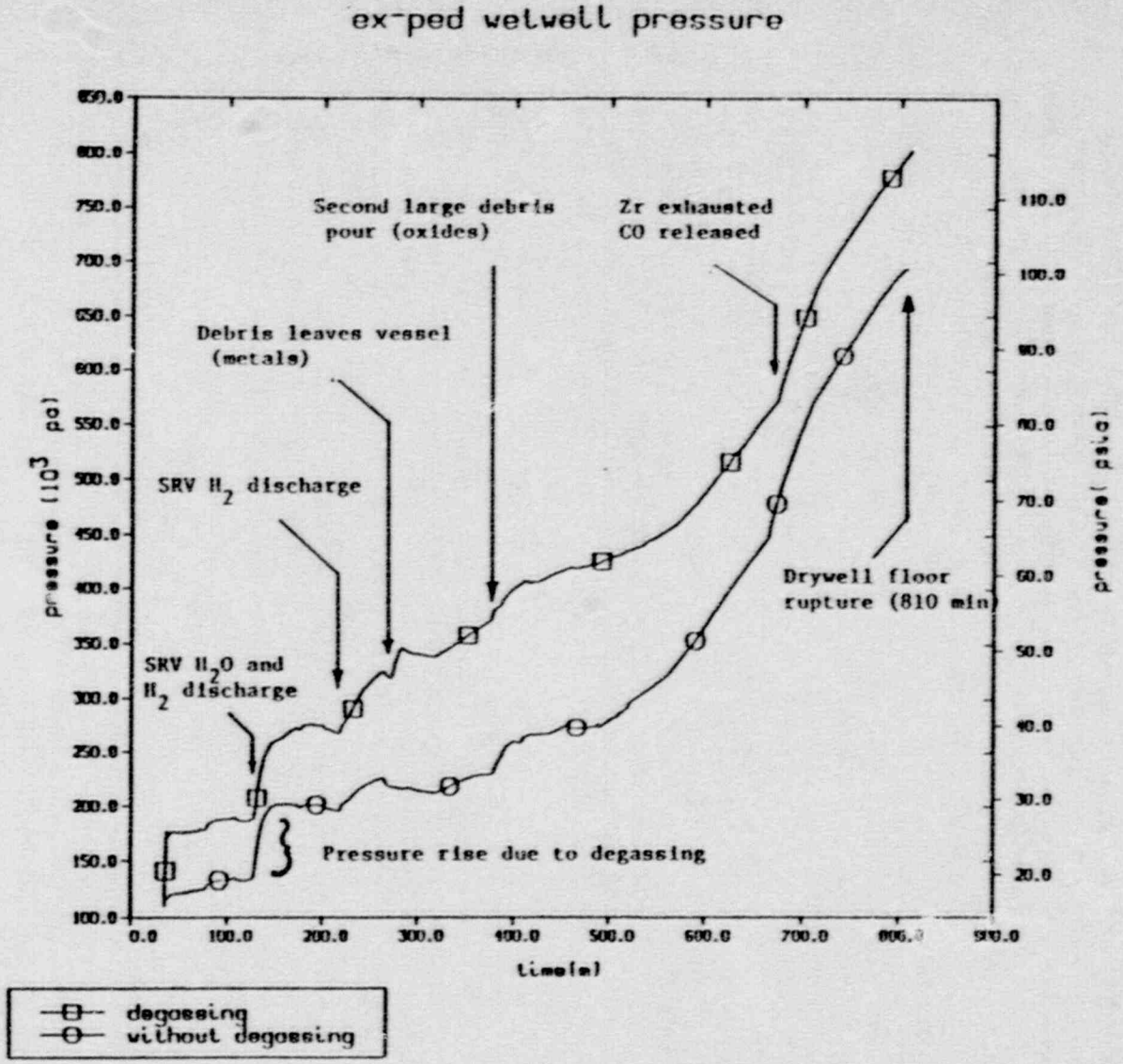

Fig. 2.43. Case 1 effect of concrete structure degassing on wetwell expedestal pressure as calculated by MELCOR for the single cavity Mark II analysis of short term station blackout with ADS actuation.

Figure 2.44 presents the time dependent pressure distribution calculated for the Mark II primary containment. As can be seen, the pressure for the inpedestal drywell region experiences a large pressure spike (35 psi) due to the initial gas release from the concrete reactor pedestal. However, the containment does not reach the 135 psig level required for wetwell failure at any time during the calculation. Because the pressure is continuing to rise at the time of floor rupture, it would not be reasonable to conclude that the maximum pressure had been reached or that the containment would not fail due the the steam spike which is expected to occur when the drywell debris falls into the suppression pool. (An estimate of the magnitude of this steam spike and the resulting containment pressure spike will be included in a future report.)

There are distinct discontinuities exhibited by the pressure traces of Figure 2.44. These are caused by significant events in the progression of the transient. At times 130 and 220 min., the pressure increases markedly due to the discharge of steam and hydrogen gases through the SRVs into the wetwell pool. At 270 min., another rise occurs as the reactor vessel bottom head is calculated to fail and debris begins to pour onto the drywell floor. Another break occurs as the second debris pour commences at 380 min. A final pressure increase is noted at 675 min. This corresponds to the rapid release of carbon monoxide from the debris as the carbon from the coking reaction begins to burn with the carbon dioxide and water vapor released from the concrete (see discussion below).

Figure 2.45 depicts the primary containment atmospheric temperature distribution as a function of time. Once again, there are noticeable discontinuities in the temperature traces. At times 130 and 220 min., the temperatures rapidly increase in response to the SRV discharges mentioned earlier. It is also interesting to note that the maximum temperature occurs in the annulus between the biological shield and the outer surface of the reactor vessel. The reason for this is the boundary condition employed at the inner surface of the reactor vessel wall. For these calculations, it was assumed that the inner surface was at the SRV gas discharge temperature.

Notice also that there is no obvious increase in the inpedestal air temperature at the time of reactor vessel bottom head failure (270 min.). This is because the debris falls into a shallow pool of water created by normal primary coolant system water leakage prior to failure of the bottom head. By 290 min. however, this water has been vaporized and the debris immediately begins to heat the inpedestal atmosphere so that the temperature increases rapidly. At 380 min., the second major debris pour commences and the inpedestal air temperature rapidly increases. At about 550 min., the upper oxide layer top crust melts, and rapid heat transfer to the inpedestal atmosphere ensues.

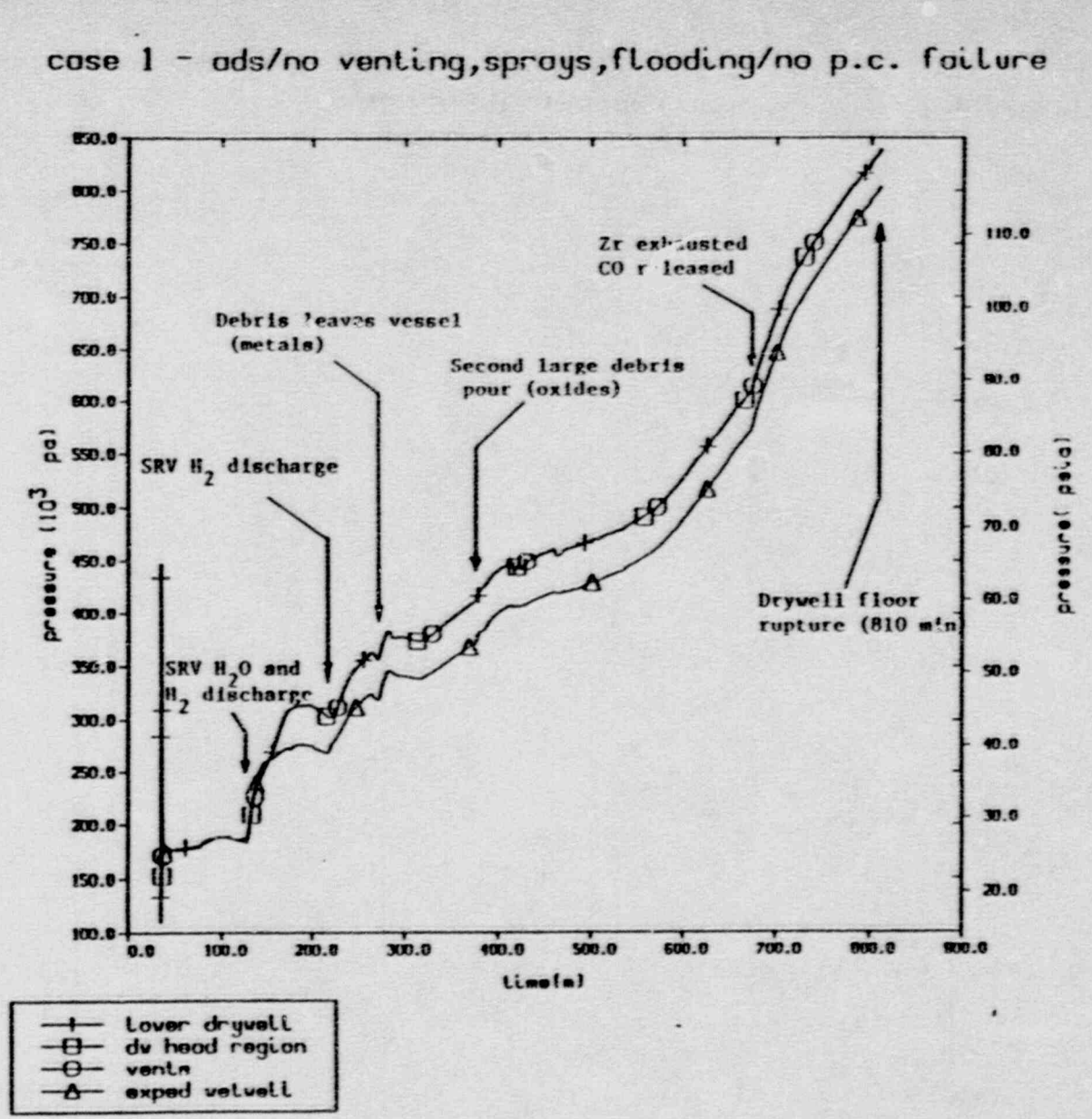

Fig. 2.44. Case 1 primary containment pressure distribution as predicted by MELCOR for single cavity Mark II analysis of short term station blackout with ADS actuation.

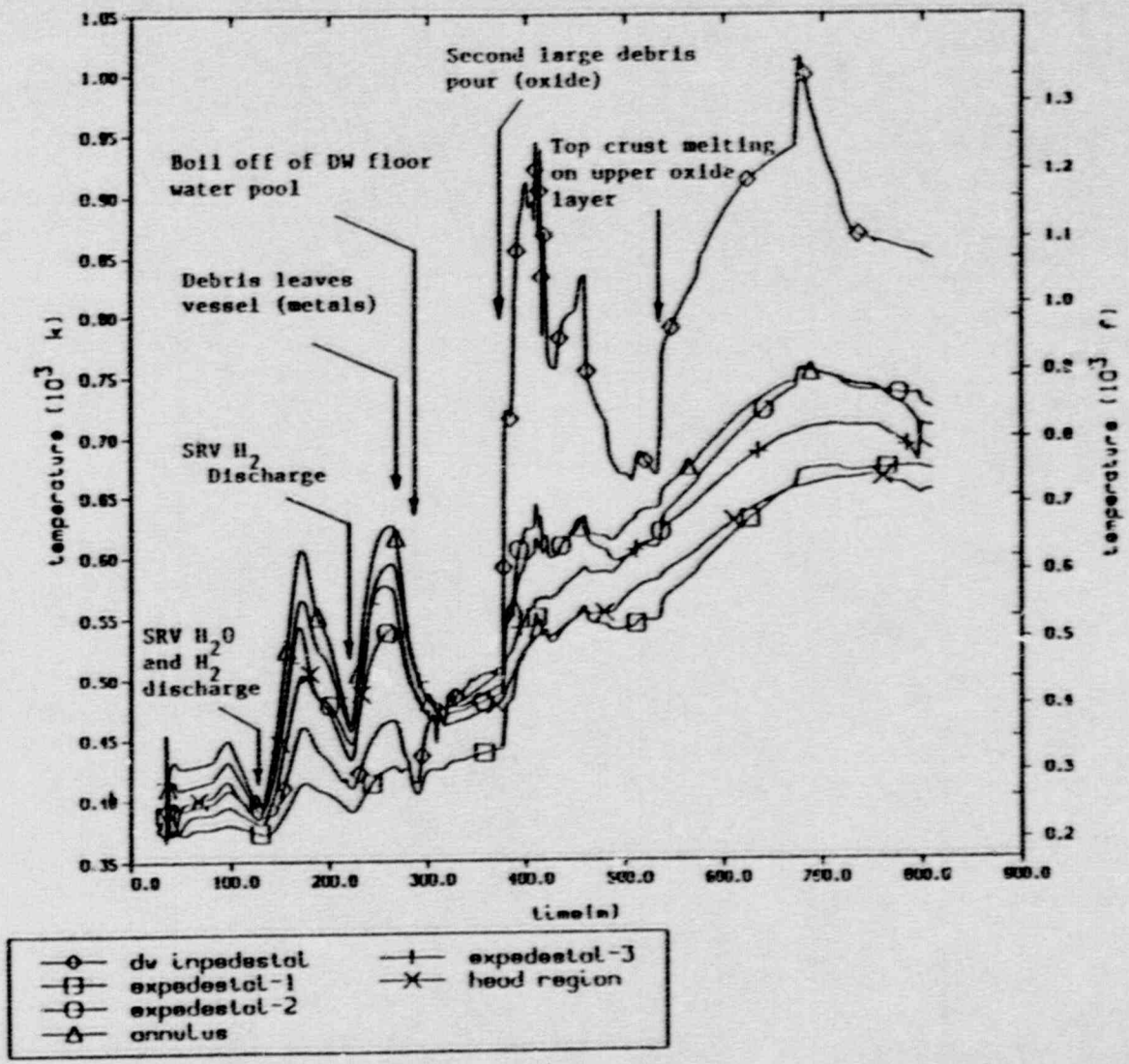

Fig. 2.45. Case 1 primary containment temperature distribution as predicted by MELCOR for single cavity Mark II analysis of short term station blackout with ADS actuation.

A final note on the atmosphere temperature distribution: as shown in Figure 2.45, the drywell head atmosphere temperature reaches approximately 720°F by the end of the calculation at 810 min. In contrast, the calculated results also indicate that the drywell head flange reaches only 573°F. This is because the head flange is bounded on the inner surface by the drywell head atmosphere but on the outside by the cooler atmosphere within the reactor well (see Fig. 2.42). Although the calculated temperature of the atmosphere within the reactor well increased from 109 to 427°F due to the modeled heat transfer during this accident sequence, the head failure criteria as described in Section 2.3.3 were not met and the head flange was not predicted to leak.

It is also to be noted that there is a substantial temperature difference (350°F at 810 min.) between the hottest and coldest regions of the primary containment. The ability to consider regional temperature differentials within the containment is a result of the detailed nodalization scheme employed for the Mark II containment and these could not be calculated if simpler nodalizations were used. Determination of regional temperatures within the drywell is necessary if judgements concerning local effects such as failure or survival of drywell head flange seals are to be made.

Figure 2.46 reports the calculated debris temperatures for the drywell floor inpedestal cavity. It is seen that both the heavy oxide and metal layer temperatures rapidly increase as the debris begins pouring from the failed reactor vessel at 270 min. The layer temperatures reach a local peak of about 1900°F at 300 min. due to the termination of the pour from the reactor vessel (Figure 2.14). The debris accumulated on the drywell floor up to this point consists mostly of metals and contains very little decay heat. Because there is no additional pour from 300 to 380 min., the debris cools and the temperatures decrease. The debris temperatures once again begin to increase as the second massive debris pour commences at 380 min.

At about 400 min., the debris reaches the ablation temperature of the limestone common sand concrete (2245°F) and concrete ablation begins. Because the pouring debris contains a mixture of low melting temperature metals (2750°F) and higher melting temperature oxides (4800°F), the debris pour temperature is intermediate between the two melting temperatures and the cavity debris temperatures continue to rise. Because the heavy oxide layer is at the bottom of the debris pool and because it has a much higher melting temperature than the overlying metal layer, it initially develops thick crusts that insulate the bulk of the oxide layer and the oxide layer temperature increases more rapidly than the overlying metals. This is the reason for the diverging layer temperatures between 400 and 490 min.

At around 460 min., it is noted that a light oxide layer formed on top of the metal layer. This is due to the small content of UO_2 in the debris pour after 460 min. Because UO_2 is extremely dense and because it constituted a large fraction of the earlier portion (380–460 min.) of the second pour, all of the oxide pouring from the reactor vessel from 300 to 460 min. settled to the bottom of the debris pool and no upper

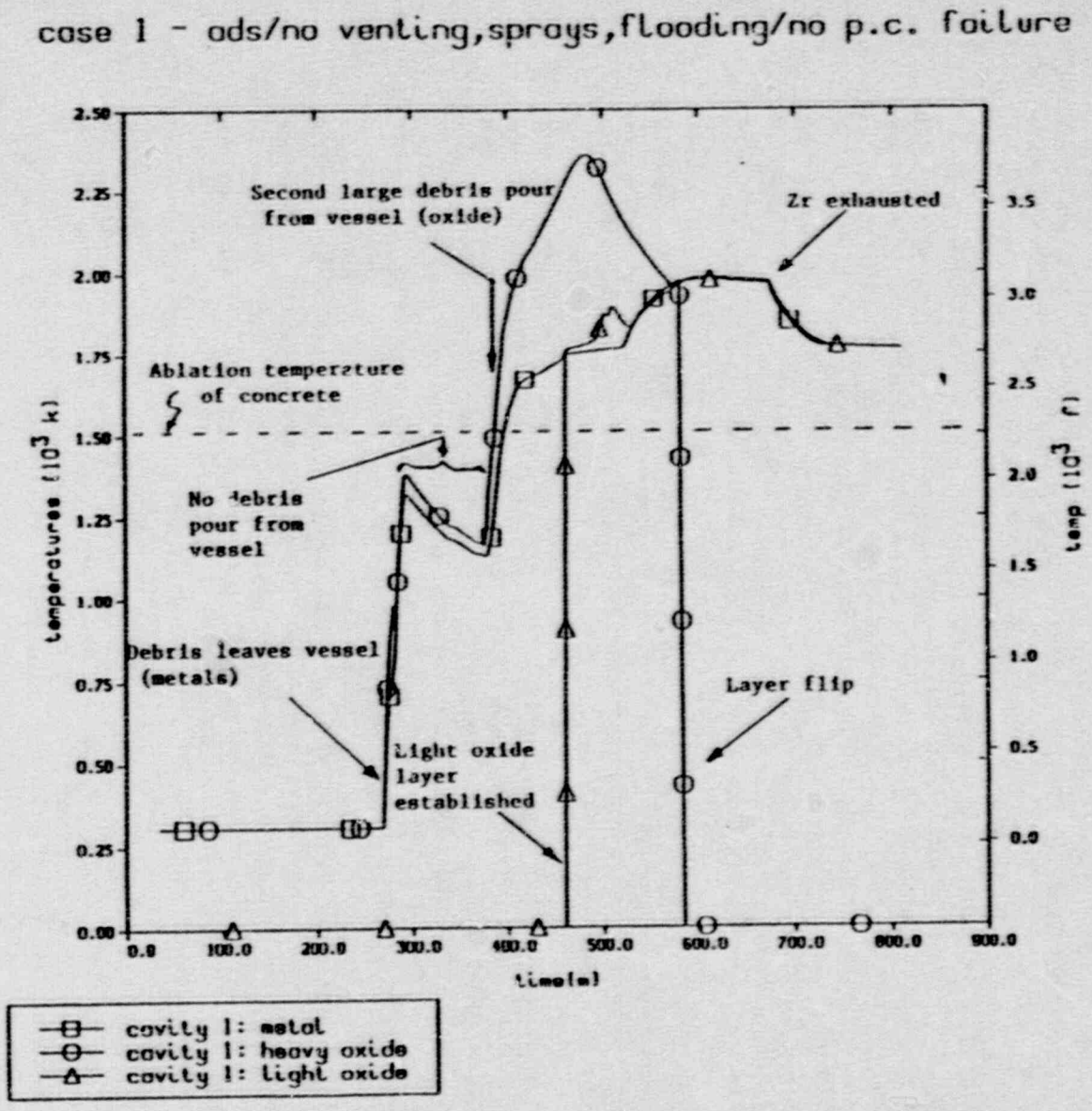

Fig. 2.46. Case 1 debris layer temperatures as predicted by MELCOR for single cavity Mark II analysis of short term station blackout with ADS actuation.

oxide layer could form. After 460 min., the UO_2 content of the debris pour is small and when the debris pour oxide combines with the concrete oxide rising through the metal layer, a buoyantly stable upper oxide layer formed.

After 490 min., the heavy oxide layer temperature begins to decrease due to the increased heat losses from the heavy oxide layer. The increased heat losses stem from the melting of the heavy oxide and metal layer crusts resulting in the calculation of large intralayer convective heat transfer coefficients. This resulted in effective homogenization of the debris temperature distribution-decreasing the heavy oxide layer temperature while increasing the metal and light oxide layer temperatures. The melting of the heavy oxide layer in turn is due to the increasing concentration of the concrete oxides in the heavy oxide layer. Since the concrete oxides (SiO_2 and CaO) melt at lower temperatures than the core debris oxides (UO_2 and ZrO_2), mixing the two oxides results in a lowering of the heavy oxide solidus temperature. Thus the heavy oxide layer experiences thinning of its crusts which lowered the thermal resistance to conduction heat transfer at the boundaries of the layer and the heavy oxide layer temperature began to decrease.

Concrete oxide dilution of the heavy oxide layer continued until about 585 min. At this time, the heavy oxide layer density was calculated to be less than the overlying metal layer density and the code performed a "layer flip" of the metal and heavy oxide layers. In addition, the material of the formerly heavy oxide layer was combined with that of the light oxide layer so that the resulting mixture of light oxides was placed on top of the metal layer.

At 675 min. the debris temperatures drop due to the exhaustion of the unoxidized zirconium and the reduction of the chemical power supplied to the debris. At this time the carbon inventory which had been accumulating in the metal layer begins to react with the CO_2 released by the ablation of concrete and produces large quantities of CO according to the following reaction:

$$C + CO_2 \rightarrow 2CO \ .$$

As can be seen, there are two moles of gas produced by this reaction for every mole of gas consumed. Figure 2.47 shows the cumulative debris gas releases for CO, CO_2, H_2, and H_2O. The CO release is very rapid and occurs only after the oxidation of all of the zirconium. This is the reason for the increased rate of pressure rise at 675 min. as shown in Figure 2.44.

Figure 2.48 depicts the axial and radial concrete ablation distances calculated for this transient. The concrete floor of the drywell is 3.74 feet thick and the cavity is 9.55 feet deep. Thus the bottom (lower surface) of the drywell floor is located at the depth of 13.29 feet. It is seen that the floor is penetrated at 810 min. Because the floor is ruptured, the calculation is terminated.

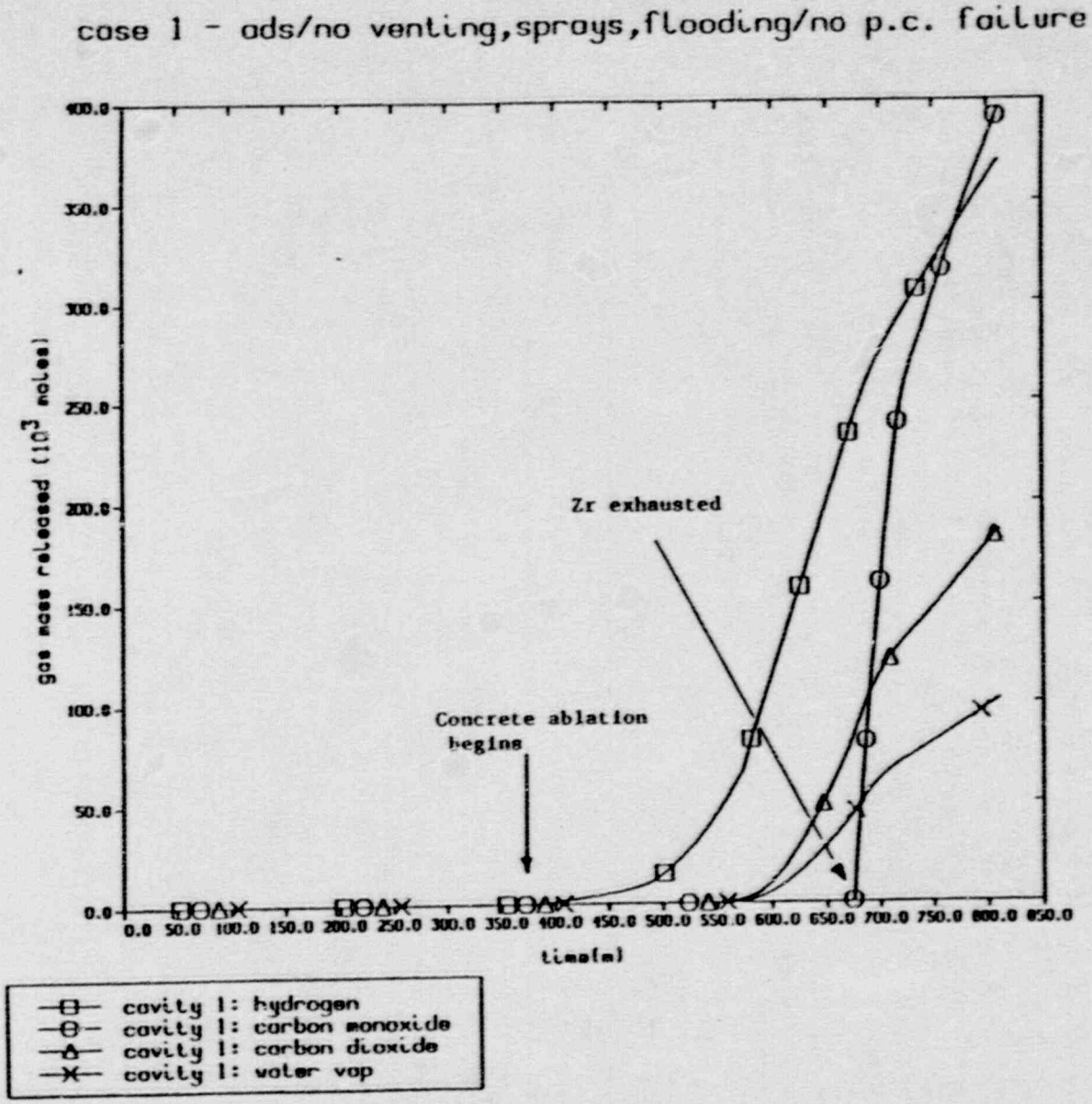

Fig. 2.47. Case 1 debris gas releases as predicted by MELCOR for single cavity Mark II analysis of short term station blackout with ADS actuation.

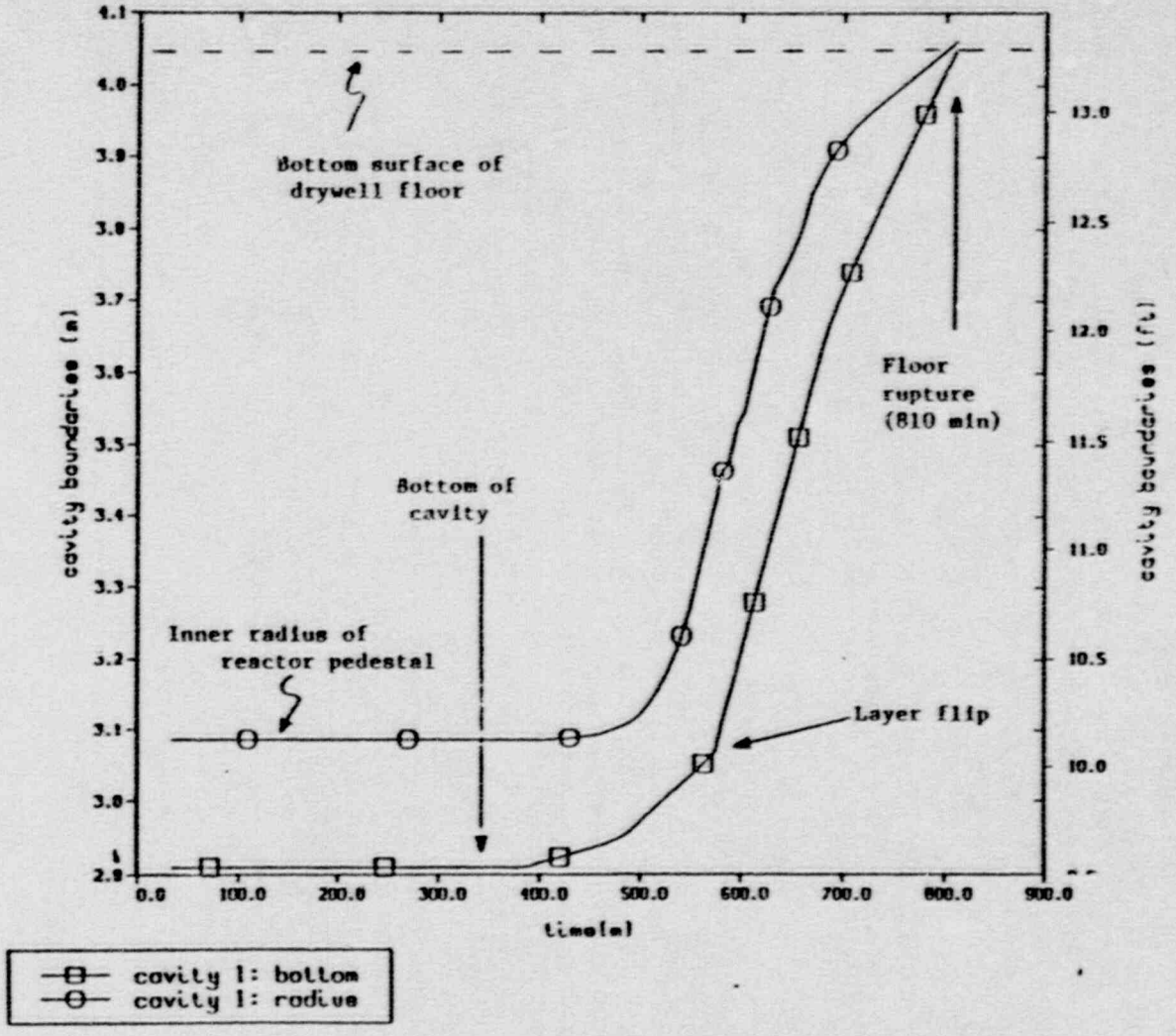

Fig. 2.48. Case 1 maximum cavity dimensions as predicted by MELCOR for single cavity Mark II analysis of short term station blackout with ADS actuation.

It must be realized, however, that one should not generalize this result and conclude that all Mark II drywell floors would be completely ablated for a depressurized short term station blackout scenario. The main reason for this is that the current calculation assumes that a deep cavity exists such that the core debris will be maintained in a crucible type geometry. In the current calculation, Figure 2.49 shows that the total debris thickness is about 8.2 feet at 810 min. and is well below the 13.3 feet thickness required before overflow onto the remaining drywell floor can occur. In this configuration, the debris has limited surface area through which it can lose heat to the atmosphere. Thus more heat is transferred downwards into the underlying concrete and more concrete is ablated. Axial (downward) ablation would be less severe in Mark II designs (such as Limerick and Susquehanna) that do not incorporate a deep inpedestal cavity.

2.3.5 Mark II Containment Response: Short-term Station Blackout With ADS, Simplified Eutectics, and Pool-Debris Interaction

This Section presents containment response results obtained by MELCOR analysis of the short term station blackout scenario assuming operation of the ADS system and entrance of some core debris into the pressure suppression pool. The transient addressed is identical to the one discussed in Section 2.3.4 except that it is further assumed that an arbitrarily small fraction of the core debris leaving the reactor vessel is immediately transferred into the water pool of the wetwell. This is an important consideration because most Mark II containments have inpedestal drywell floor drains (and some have inpedestal downcomers) which could provide an avenue for early entry of core debris into the wetwell pool.

Because the extent of debris relocation to the wetwell is highly uncertain, a parametric analysis approach is being employed. This section presents results of the first such study, in which 5% (by mass) of the time dependent debris pour is directed into the wetwell pool while the remaining 95% of the debris pour is assumed to remain on the inpedestal floor of the drywell. (Future calculations will examine cases in which 20%, 50%, 80%, and 95% of the pour directly enters the wetwell pool.)

The debris/pool interaction is calculated by the Fuel Dispersal Interactions (FDI) package within MELCOR. The documentation of the package is incomplete. As a result, considerable effort was expended to utilize the package in a manner consistent with the approach which would have been employed if the MELCOR COR package had been used to generate the debris transfers to FDI. Since the COR package was not used to calculate the debris pours leaving the reactor vessel, additional information that is not normally required from BWRSAR was needed as input to the MELCOR FDI calculation. This information consists of the hole diameter through which the debris leaves the drywell, the debris speed through the hole (assuming the hole is completely filled with flowing debris), and the time-integrated total enthalpy of debris having passed through the hole.

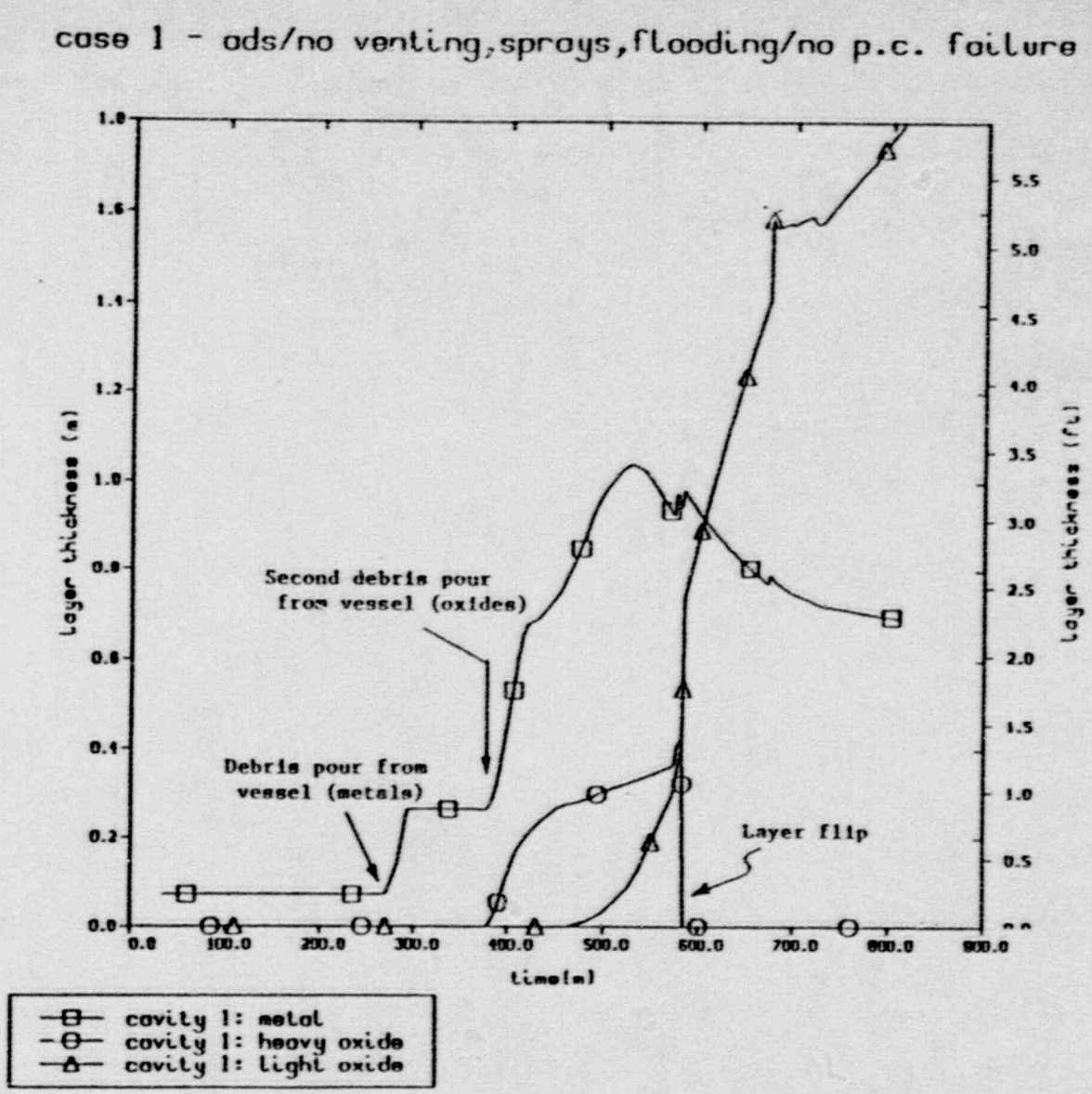

Fig. 2.49. Case 1 debris layer thicknesses as predicted by MELCOR for single cavity Mark II analysis of short term station blackout with ADS actuation.

For the current application, it is desired that the initial velocity of the flowing debris as it passes through the drywell floor be small. Accordingly, it was assumed that the hole diameter was 4.6 feet. The debris speed is then that corresponding to 5% of the total debris volume flow leaving the reactor vessel flowing through this assumed hole. Finally, the cumulative debris enthalpy was evaluated by time integrating the enthalpy flow leaving the reactor vessel (see Appendix C). The specific enthalpy of each debris species was evaluated as a function of temperature utilizing the enthalpy tables employed by MELCOR so that consistency in enthalpy definition was assured. (Subsequently, after consultation with the MELCOR code development staff, it was found that this cumulative enthalpy parameter has no effect on the calculation.)

It is important to note that MELCOR does not have the capability to directly model the flow of molten debris from above the drywell floor through openings (downcomers or failed drain pipes) in the drywell floor, the subsequent acceleration of the debris as it falls through the wetwell airspace, the debris-coolant interaction as the debris then falls through water, the debris bed formation as the quenched material accumulates on the wetwell floor, and the debris/concrete interaction at the bed-floor interface. What can and has been done by manipulation of code input is to direct part of the debris pour from the reactor vessel directly into the wetwell pool and to then utilize the FDI package for debris/water interactions. A second cavity is specified in order to calculate the debris/concrete interaction occurring once the debris has settled to the bottom of the wetwell inpedestal water pool. The geometric characteristics of the CORCON cavity representing the wetwell inpedestal region were assumed identical to that employed in the drywell CORCON cavity.

A further distinction between this analysis and that reported in Section 2.3.4 consisted of the provision to allow the containment to either leak or fail. As discussed in Section 2.3.3, two failure modes are modeled. First, is the failure of the wetwell by direct overpressurization at a pressure difference between primary and secondary containments of 135 psi. Second, is the leakage through the drywell head flange. This is modeled to occur once the drywell head seals have thermally degraded (temperature of 700°F) and the drywell-to-refueling bay pressure difference has reached 82 psi.

Figure 2.50 presents the time dependent pressure distribution calculated for the Mark II primary containment. As can be seen, the pressure does not reach the 135 psig level required for wetwell failure. The calculation is terminated when the drywell concrete floor is calculated to have been ruptured by axial concrete ablation at 846 min. [This is 36 min. later than for the case in which all debris is represented to remain within the inpedestal region.] Because the pressure is continuing to rise at the time of floor rupture, it should not be assumed that the maximum pressure had been reached or that the containment would not fail by the steam spike incurred when the drywell debris inventory dumps into the wetwell pool.

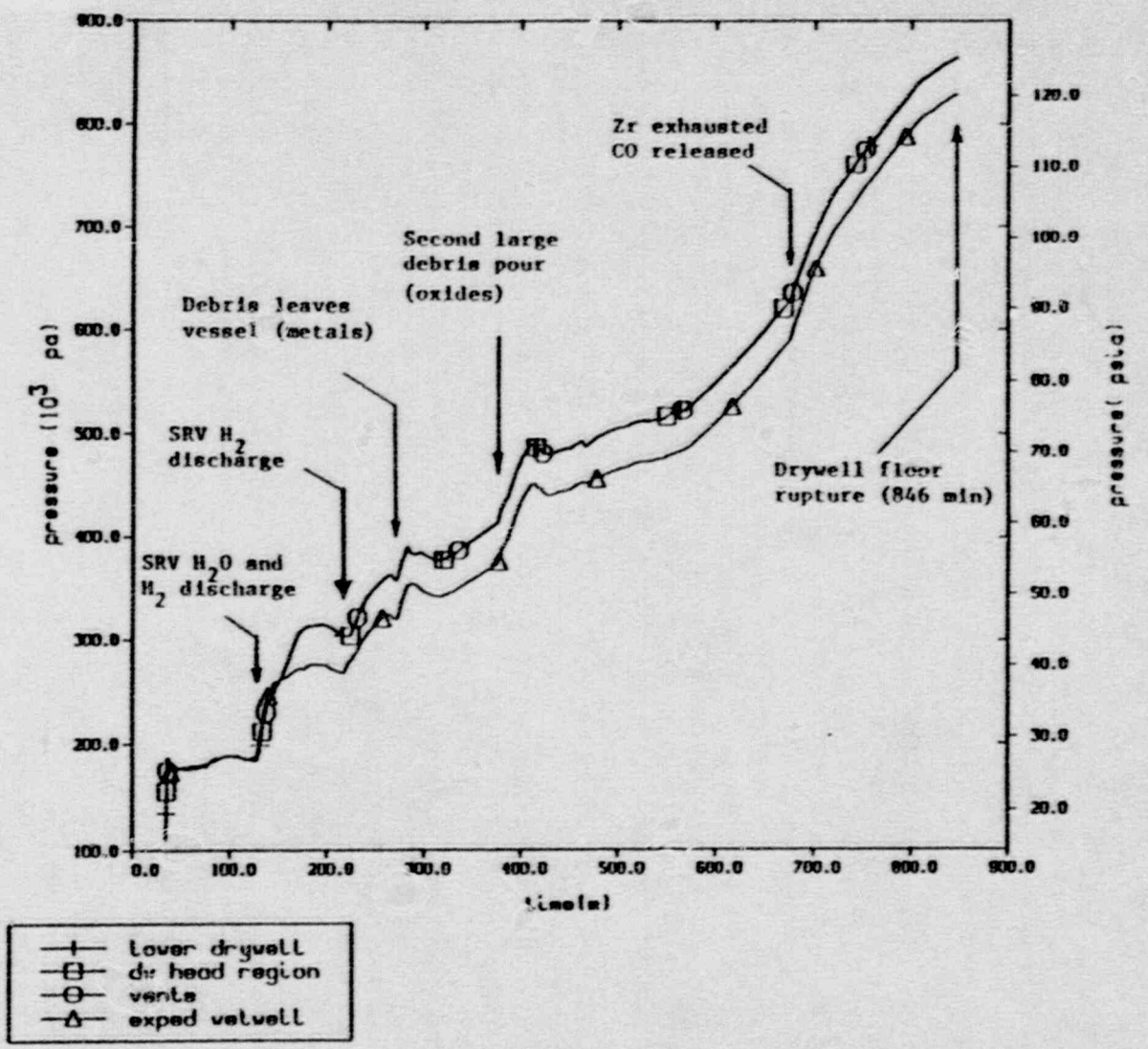

Fig. 2.50. Case 3 primary containment pressure distribution as predicted by MELCOR for dual cavity (95% drywell/5% wetwell) Mark II analysis of short term station blackout with ADS actuation.

There are distinct discontinuities exhibited by the pressure trace of Figure 2.50. These are caused by significant events in the progression of the transient. At times 130 and 220 min., the pressure increases markedly due to the discharge of steam and hydrogen gases through the SRVs into the wetwell pool. At 270 min., another rise occurs as the reactor vessel bottom head is calculated to fail and debris begins to pour onto the drywell floor. Another break occurs as the second debris pour commences at 380 min. A final pressure increase is noted at 675 min. This corresponds to the rapid release of carbon monoxide from the debris as the carbon from the coking reaction begins to burn with the carbon dioxide and water vapor released from the concrete (see discussion below).

Figure 2.51 depicts the primary containment atmospheric temperature distribution as a function of time. Once again there are noticeable discontinuities in the temperature traces. At times 130 and 220 min., the temperatures are predicted to increase rapidly in response to the SRV discharges mentioned earlier. It is also interesting to note that the maximum temperature occurs in the annulus between the biological shield and the outer surface of the reactor vessel. The reason for this is the boundary condition employed at the inner surface of the reactor vessel wall. For these calculations, it was assumed that th inner surface of the reactor vessel was at the SRV gas discharge temperature.

Notice also that there is no obvious increase in the inpedestal air temperature at the time of reactor vessel bottom head failure (270 min.). This is because the debris falls into a shallow pool of water created by primary coolant system water leakage prior to failure of the bottom head. At 290 min. however, this water has been vaporized and the debris immediately begins to heat the inpedestal atmosphere and the temperature jumps. At 380 min., the second major debris pour commences and the inpedestal air temperature rapidly increases. At about 550 min., the upper oxide layer top crust melts and heat transfer to the inpedestal atmosphere increases.

As shown in Figure 2.51, the drywell head atmosphere temperature reaches approximately 700°F by the end of the calculation at 846 min. In contrast however, the results also indicate that the drywell head flange reaches only 590°F. This is because the head flange is bounded on the inner surface by the drywell head atmosphere but on the outside is bounded by the cooler surrounding atmosphere. Thus the head failure criteria as described earlier are not satisfied and the head is not allowed to leak.

It is also to be noted that there is a substantial temperature difference (350°F at 846 min.) between the hottest and coldest regions of the primary containment. This is calculated as a result of the detailed nodalization scheme employed for the Mark II containment and would not be calculated if simpler nodalizations were used.

Figure 2.52 reports the calculated debris temperatures for the drywell floor inpedestal cavity. It is seen that both the heavy oxide and metal

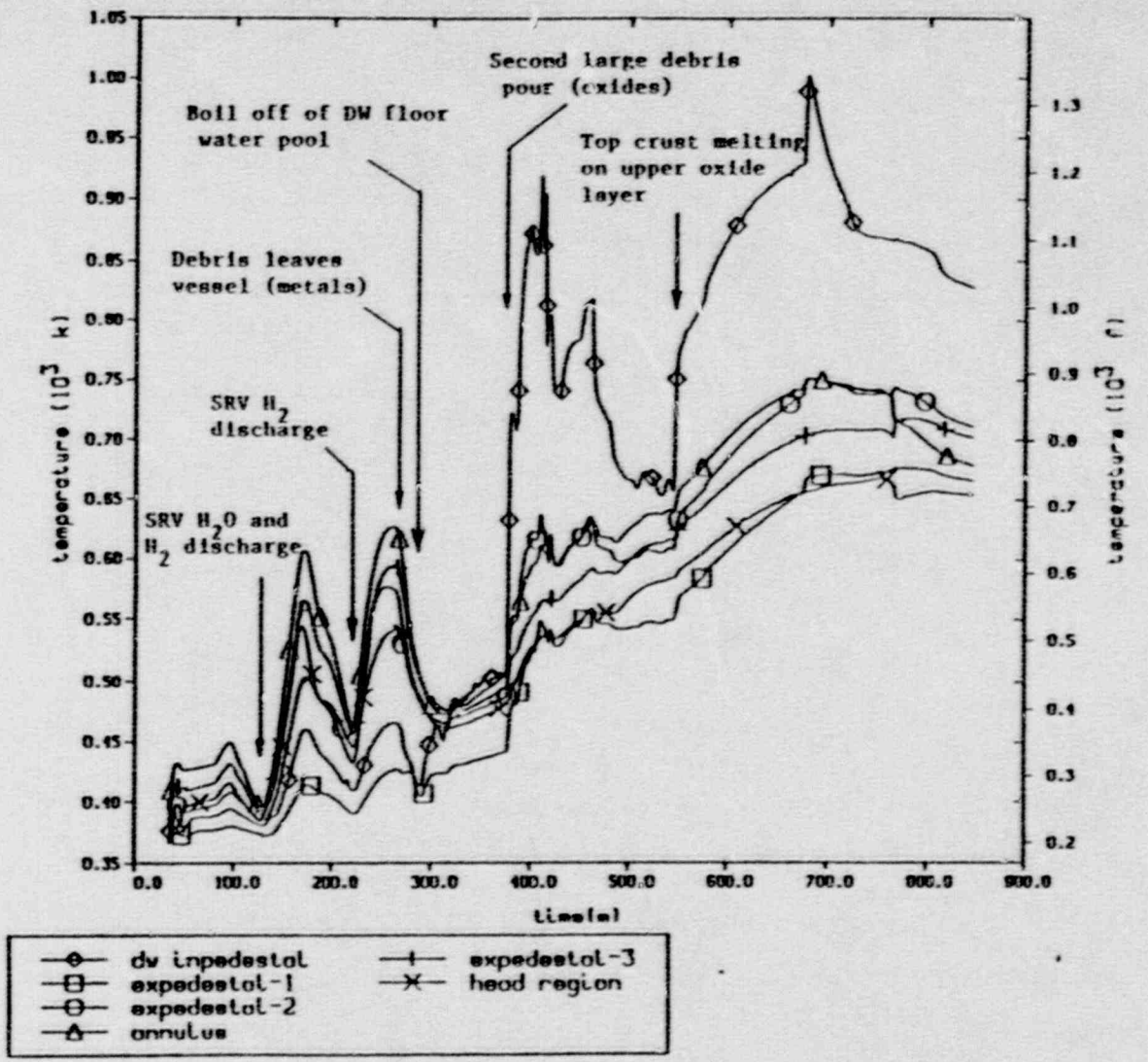

Fig. 2.51. Case 3 primary containment temperature distribution as predicted by MELCOR for dual cavity (95% drywell/5% wetwell) Mark II analysis of short term station blackout with ADS actuation.

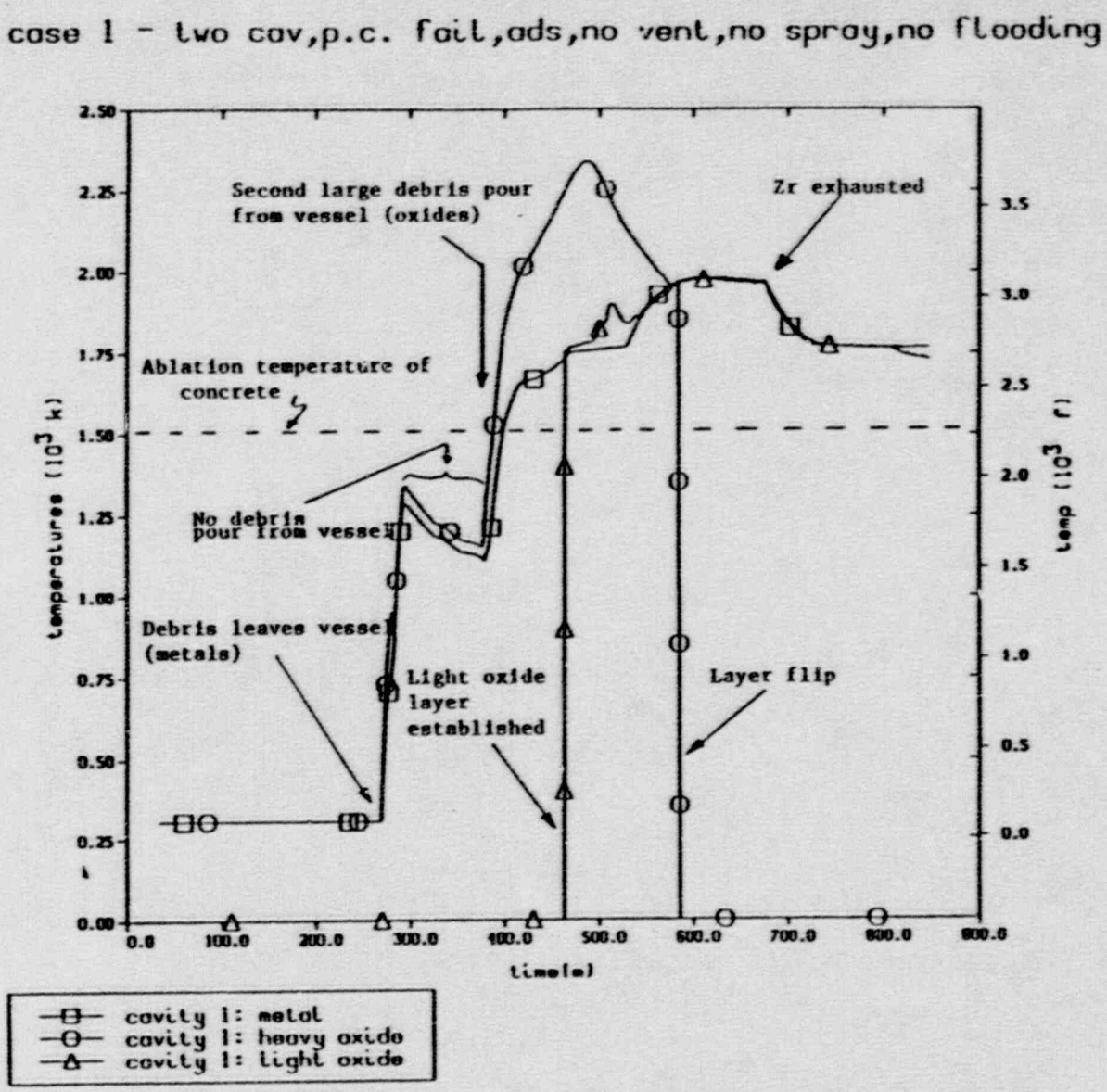

Fig. 2.52. Case 3 inpedestal drywell debris layer temperatures as predicted by MELCOR for dual cavity (95% drywell/5% wetwell) Mark II analysis of short term station blackout with ADS actuation.

layer temperatures rapidly increase as the debris begins pouring from the failed reactor vessel at 270 min. The layer temperatures reach a local peak of about 1900°F at 300 min. due to the termination of the pour from the reactor vessel (Figure 2.14). Because there is no additional pour from 300 to 380 min., the debris cools and the temperatures decrease. The debris temperatures once again begin to increase as the second massive debris pour commences at 380 min.

At about 400 min., the debris reaches the ablation temperature of the limestone common sand concrete (2245°F) and concrete ablation begins. Because the pouring debris contains a mixture of low melting temperature metals (2750°F) and higher melting temperature oxides (4800°F), the debris pour temperature is between the two melting temperatures and the cavity debris temperatures continue to rise. Because the heavy oxide layer is at the bottom of the debris pool and because it has a much higher melting temperature than the overlying metal layer, it initially develops thick crusts which insulate the bulk of the oxide layer and the oxide layer temperature increases more rapidly than the overlying metals. This is the reason for the diverging layer temperatures between 400 and 490 min.

At around 460 min., it is noted that a light oxide layer forms on top of the metal layer. This is due to the small content of UO_2 in the debris pour after 460 min. Because UO_2 is extremely dense and because it constitutes a large fraction of the earlier portion (380-460 min.) of the second pour, all of the oxide pouring from the reactor vessel from 380 to 460 min. settles to the bottom of the debris pool and no upper oxide layer can form. After 460 min., the UO_2 content of the debris pour is small and when the debris pour oxide combined with the concrete oxide rising through the metal layer, a buoyantly stable upper oxide layer is formed.

After 490 min., the heavy oxide layer temperature begins to decrease due to the increased heat losses from the heavy oxide layer. The increased heat losses stem from the melting of the heavy oxide and metal layer crusts, resulting in the calculation of large intralayer convective heat transfer coefficients. This results in effective homogenization of the debris temperature distribution--decreasing the heavy oxide layer temperature while increasing the metal and light oxide layer temperatures. The melting of the heavy oxide layer in turn is due to the increasing concentration of the concrete oxides in the heavy oxide layer. Since the concrete oxides (SiO_2 and CaO) melt at lower temperatures than the core debris oxides (UO_2 and ZrO_2), mixing the two oxides results in a lowering of the heavy oxide layer solidus temperature. Thus, the heavy oxide layer experiences thinning of its crusts which lowers the thermal resistance to conduction heat transfer at the boundaries of the layer and the layer temperature begins to decrease.

Concrete oxide dilution of the heavy oxide layer continues until about 585 min. At this time, the heavy oxide layer density is calculated to be less than the overlying metal layer density and the code performs a "layer flip" of the metal and heavy oxide layers. In addition, the

material of the formerly heavy oxide layer is combined with that of the light oxide layer so that the resulting mixture of light oxides is placed on top of the metal layer.

At 675 min., the debris temperatures drop due to the exhaustion of the unoxidized zirconium and the reduction of the chemical power supplied to the debris. At this time the carbon inventory which has been accumulating in the metal layer begins to react with the CO_2 released by the ablation of concrete and produces large quantities of CO according to the following reaction:

$$C + CO_2 \rightarrow 2CO \ .$$

As can be seen, there are two moles of gas produced by this reaction for every mole of gas consumed. Figure 2.53 shows the cumulative debris gas releases for CO, CO_2, H_2, and H_2O. The CO release is very rapid and occurs only after the oxidation of all of the zirconium. This is the reason for the increased rate of pressure rise at 675 min. as shown in Figure 2.50.

Figure 2.54 depicts the axial and radial concrete ablation distances calculated for this transient. The concrete floor of the drywell is 3.74 feet thick and the cavity is 9.55 feet deep. Thus the bottom of the cavity is located at the depth of 13.3 feet. It is seen that the floor is penetrated at 846 min. Because the floor is ruptured, the calculation is terminated.

It must be realized that one should not generalize this result and conclude that all Mark II drywell floors will be completely ablated for a depressurized short term station blackout scenario. The main reason for this is that the current calculation assumes that a deep cavity exists such that the core debris will be maintained in a crucible type geometry. In the current calculation, Figure 2.55 shows that the total debris thickness is about 7.9 feet at 846 min. and is well below the 13.3 feet thickness required before overflow onto the remaining drywell floor can occur. In this configuration, the debris has limited surface area through which it can lose heat to the atmosphere. Thus, more heat is transferred downwards into the underlying concrete and more concrete is ablated. For Mark II drywell floor geometries that do not incorporate a deep cavity, the core debris would spread into a configuration having a much larger surface area. Thus less heat would be transferred into the concrete and less ablation would result.

Figure 2.56 exhibits the cumulative steam generation by the falling debris through the water pool as a function of time. Only 19,100 lb of steam are predicted to be produced as a result of this interaction. The conclusion to be made is that a 5% debris relocation to the wetwell inpedestal pool does not result in pressures that threaten the containment. Figure 2.57 shows the calculated temperatures of the debris lying on the wetwell floor. It is seen that they are very low and that there is no calculated debris/concrete interaction.

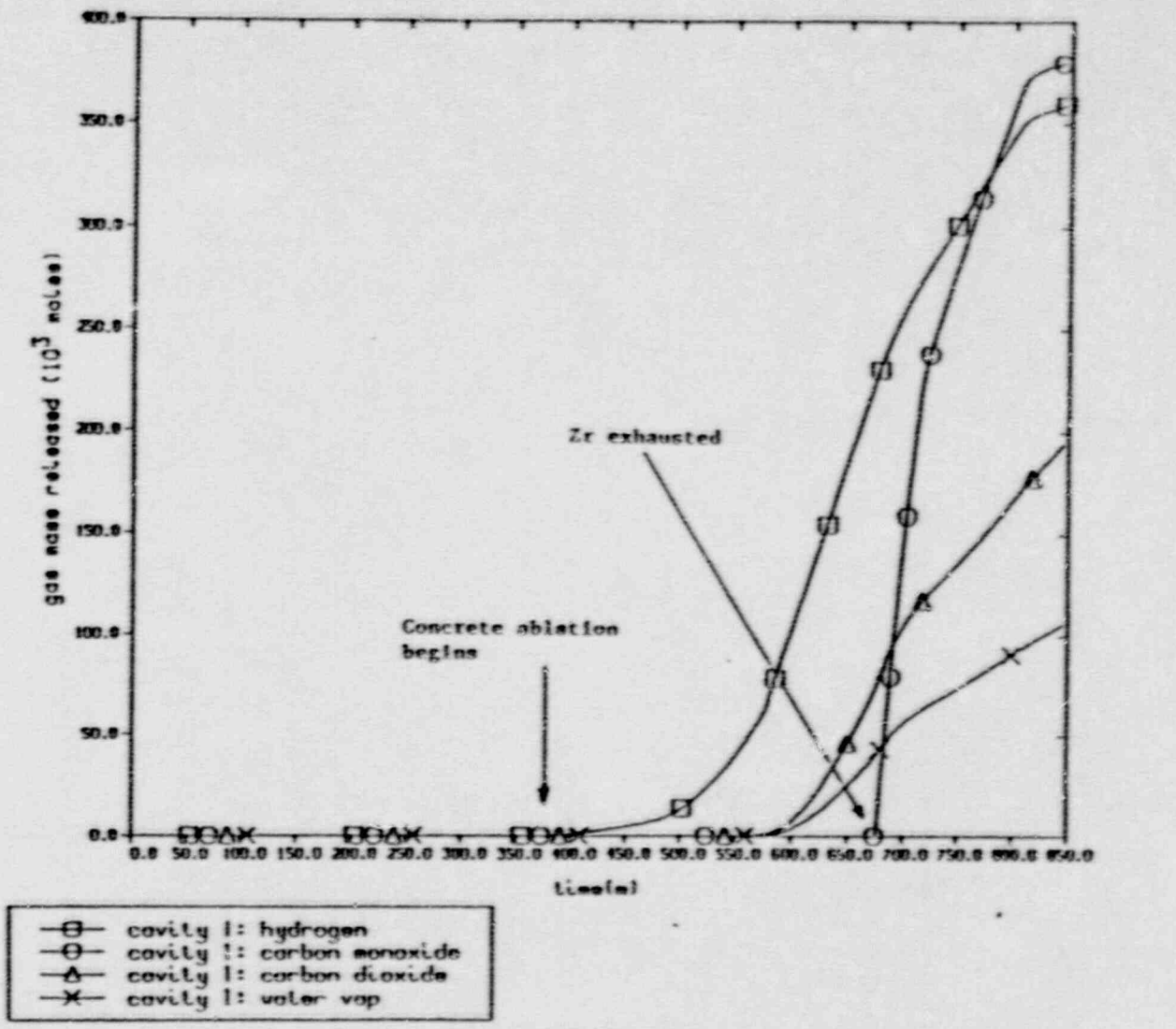

Fig. 2.53. Case 3 inpedestal drywell debris gas releases as predicted by MELCOR for dual cavity (95% drywell/5% wetwell) Mark II analysis of short term station blackout with ADS actuation.

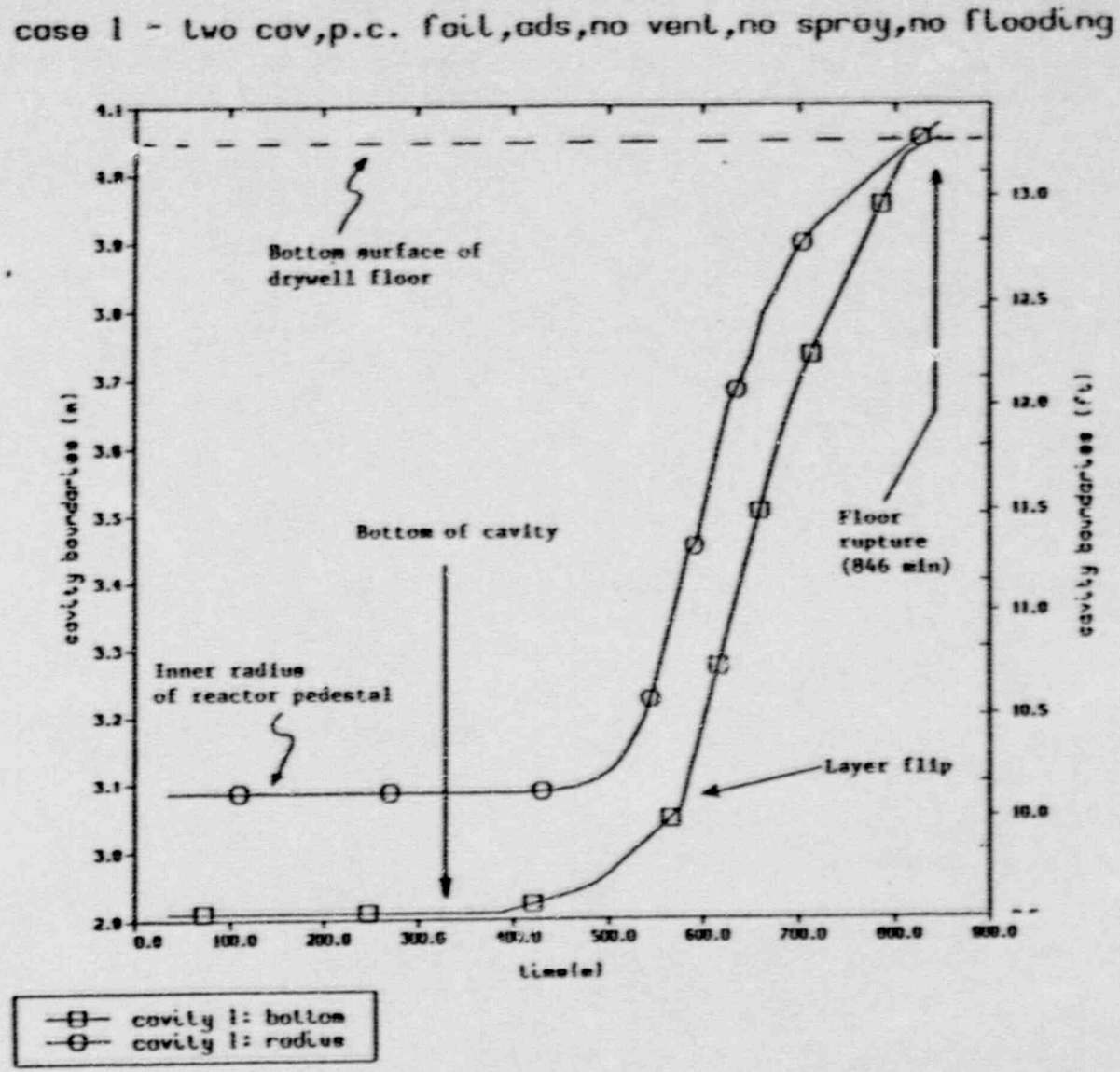

Fig. 2.54. Case 3 inpedestal drywell maximum cavity dimensions as predicted by MELCOR for dual cavity (95% drywell/5% wetwell) Mark II analysis of short term station blackout with ADS actuation.

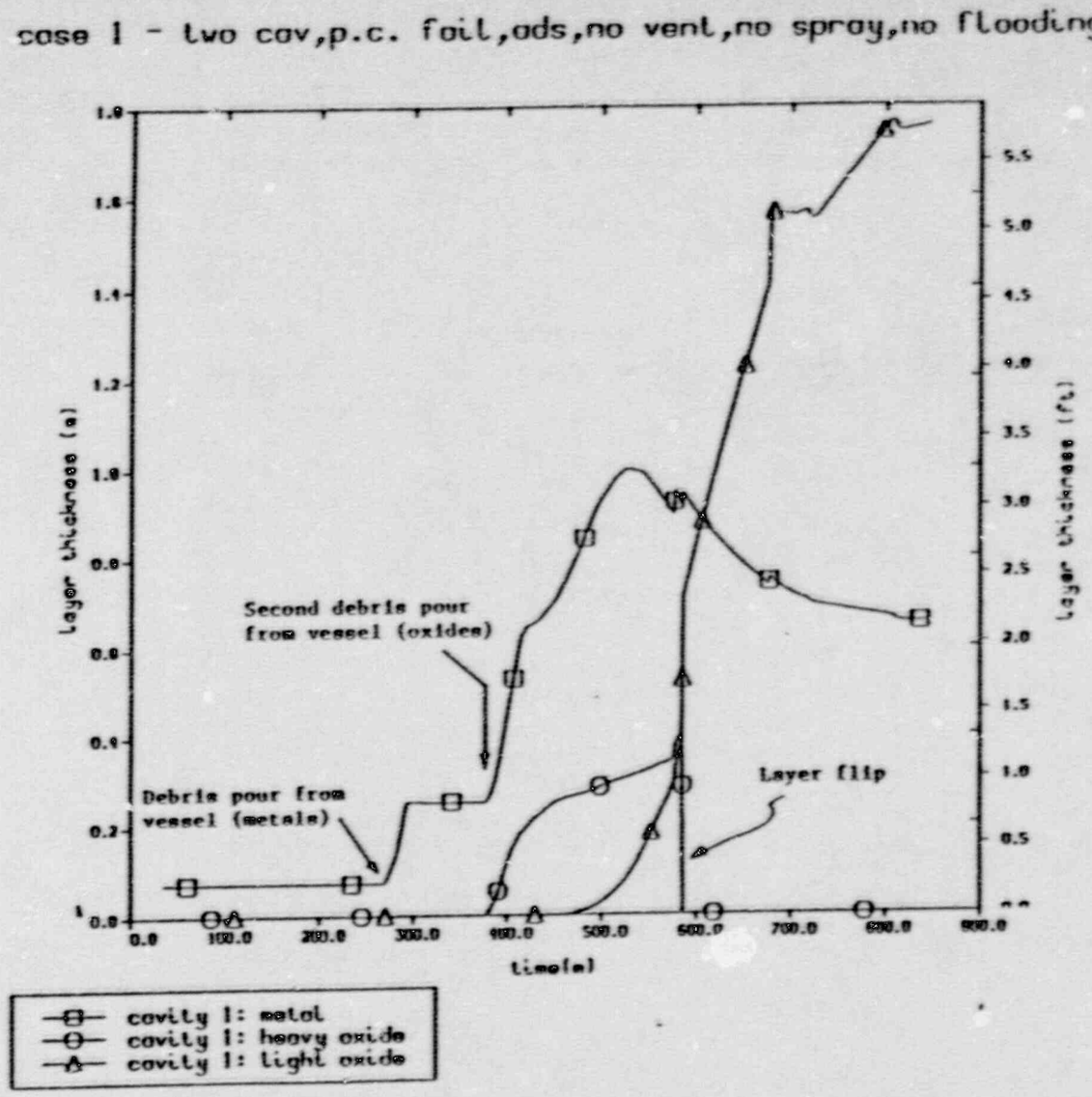

Fig. 2.55. Case 3 inpedestal drywell debris layer thicknesses as predicted by MELCOR for dual cavity (95 % drywell/5% wetwell) Mark II analysis of short term station blackout with ADS actuation.

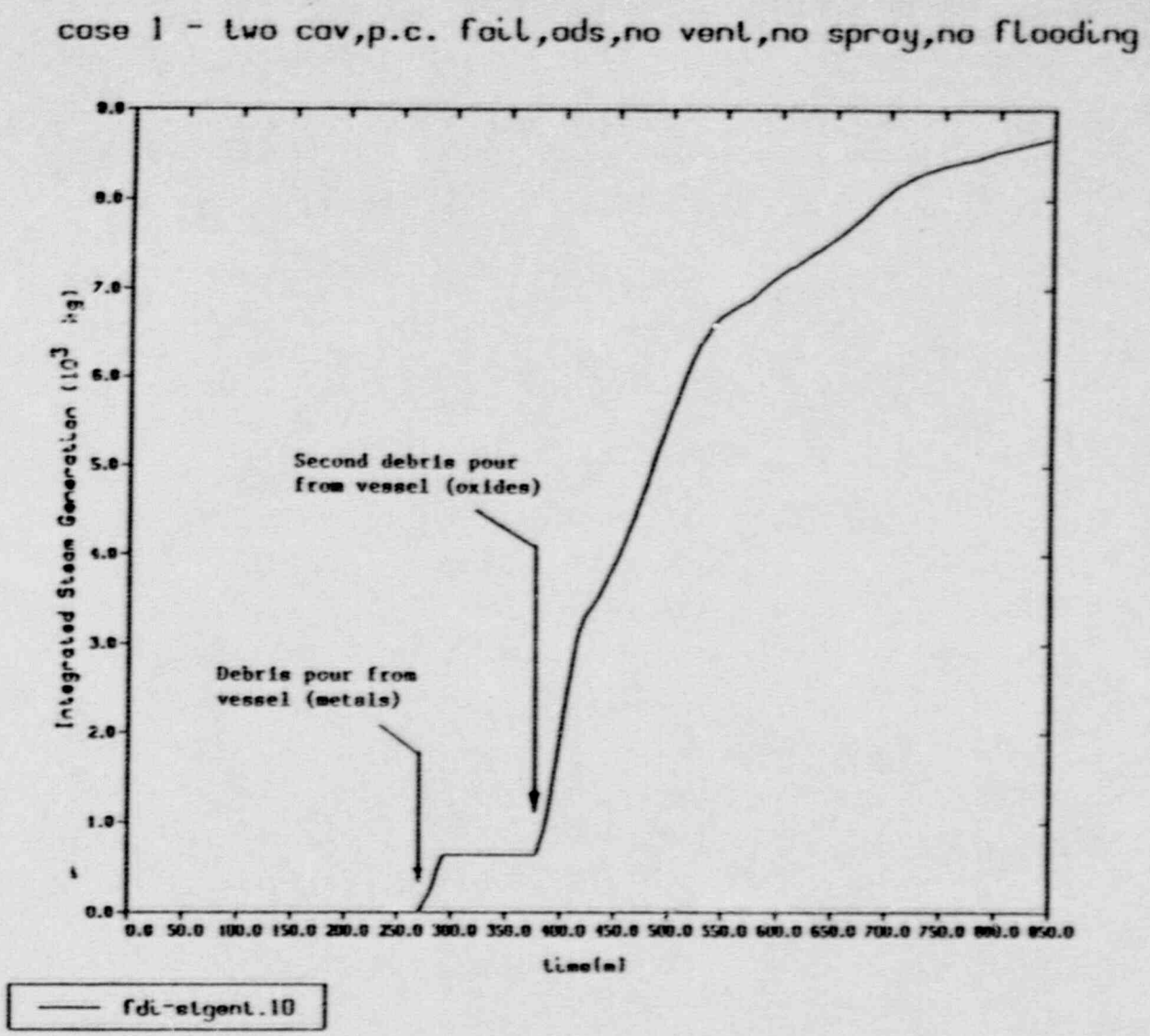

Fig. 2.56. Case 3 integrated steam generation from debris/wetwell pool interaction as predicted by MELCOR for dual cavity (95% drywell/5% wetwell) Mark II analysis of short term station blackout with ADS actuation.

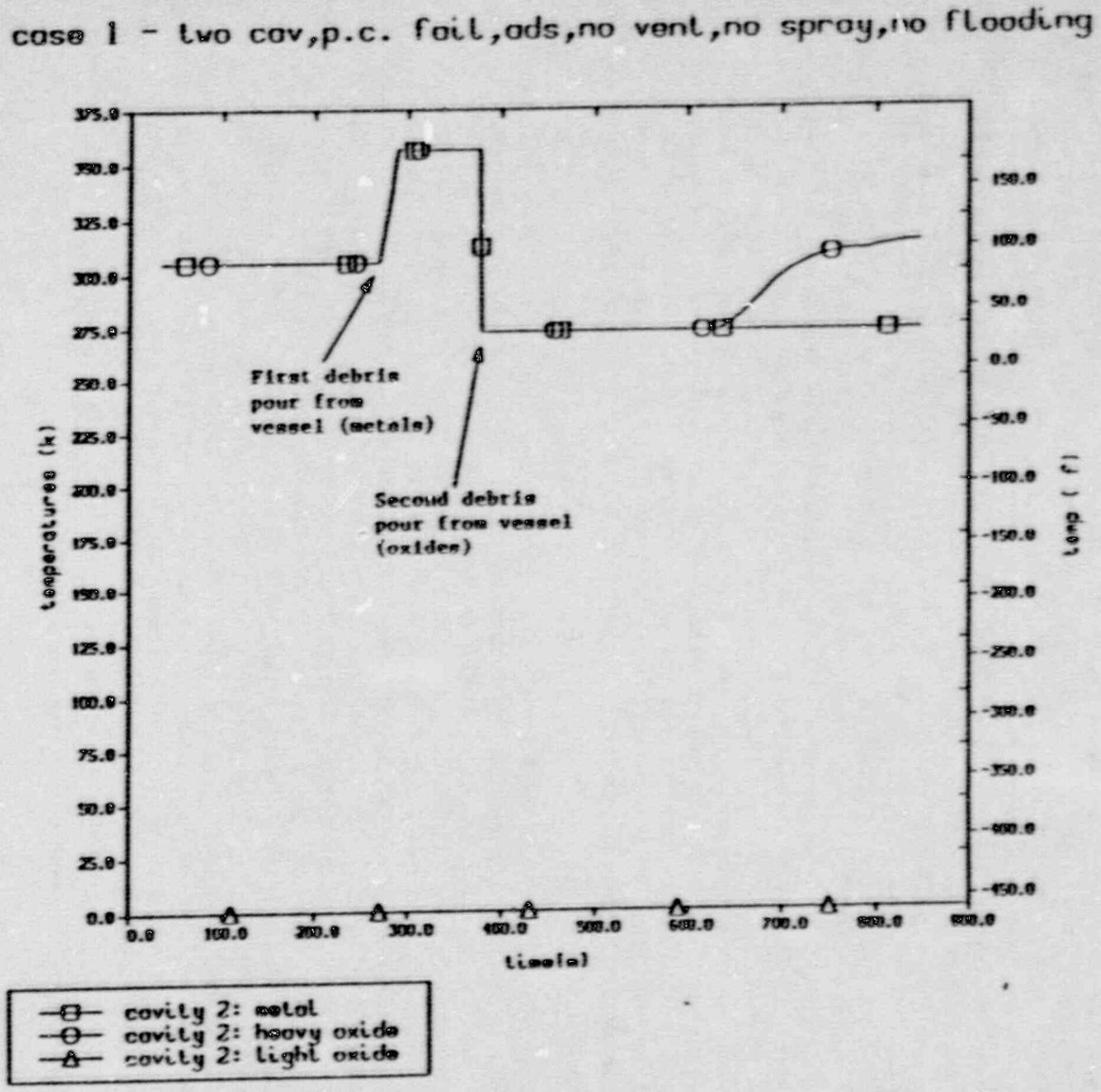

Fig. 2.57. Case 3 inpedestal wetwell debris layer temperatures as predicated by MELCOR for dual cavity (95% drywell/5% wetwell) Mark II analysis of short term station blackout with ADS actuation.

2.4 Response of Mark II Downcomers to Contact With Core Debris

2.4.1 Introduction

As previously noted in Section 2.3.1, two Mark II containments (Shoreham and Nine Mile Point-2) incorporate downcomers inside the reactor pedestal. Shoreham's downcomers extend only 1/2 in. above the floor of the drywell, while Nine Mile Point's downcomers extend 3-6 in. above the drywell floor. All Mark II plants employ downcomers in the expedestal region of the drywell. Susquehanna's downcomers extend the farthest above the drywell floor (18 in.) of any of the plants. Given an unmitigated severe accident, it is highly likely that core debris would enter the pressure suppression pool via the downcomers in the Shoreham and Nine Mile Point-2 facilities. However, in the other Mark II plants core debris would have to either (a) melt-through inpedestal floor drains, or (b) spread into the expedestal region of the drywell and either spill over the top of the downcomers or melt-through the sides of the downcomers, or (c) melt-through the inpedestal drywell floor prior to entering the pressure suppression pool. This is a potentially significant issue, since the entrance of core debris into a downcomer could result in downcomer failure via either direct ablation or due to a steam explosion in the submerged region of the downcomer when the core debris enters the pool. Failure of a downcomer or floor drain is an extremely undesirable event, since such failures constitute pressure suppression pool bypass.

The purpose of the effort described in this Section is to investigate the impact of core debris-downcomer interactions on Mark II downcomer survivability. The focus of these investigations is the question of how deep the debris surrounding the upper portion of the downcomer (the portion extending above the drywell floor) must be to melt-through the downcomer wall. This is an extremely complicated problem, since debris composition, depth, and temperature are actually plant-, sequence-, and time-dependent parameters. The approach adopted for these analyses is to perform time-dependent downcomer thermal response calculations for selected prototypical debris conditions based upon BWRSAR/MELCOR/CORCON results from the short-term station blackout case with ADS as described in Section 2.3.4. For the purpose of these calculations, the debris characteristics are assumed to be time-independent, and the debris height is varied in a parametric manner. These analyses are performed with the HEATING-6 three-dimensional thermal analysis code (Ref. 17).

2.4.2 Mark II Downcomer Design Description

Downcomers (vent pipes) connect the drywell airspace to the wetwell pool. These downcomers are designed to facilitate condensation of steam in the event of a design-basis loss of coolant accident. The majority of these vent pipes are approximately two feet in internal diameter, but the pipe sizes do vary within some containments (WNP-2 utilizes both 24 in. and 28 in. downcomers). This analysis is performed for the most common expedestal vent pipe (Susquehanna's type II downcomer with an

inner diameter of 24 in. and a wall thickness of 3/8 in). The downcomers are surrounded with a steel ring or collar, with a thickness of 3/4 in. and outer radius of 21-in. at the upper surface of the drywell floor. The vent pipe penetrates the 3.74 ft concrete drywell floor slab, and extends far below the surface of the suppression pool (Fig. 2.58). A long portion of the pipe is exposed to the atmosphere in the wetwell airspace. The vent pipe extends 1.5 ft. above the concrete drywell floor. The top of the vent pipes are open, but shielded by a downcomer jet deflector plate. Any accumulation of molten debris above the 1.5 ft depth would, in this configuration, result in immediate flow of molten debris down into the vent pipe.

2.4.3 Description of the HEATING Thermal Analysis Code

The following paragraph taken from the HEATING (version 6.1) manual briefly describes capabilities of the HEATING code (Ref. 17):

> "HEATING is a FORTRAN program designed to solve steady-state and/or transient heat conduction problems in one-, two-, or three-dimensional Cartesian, cylindrical, or spherical coordinates. A model may include multiple materials, and the thermal conductivity, density, and specific heat of each material may be both time- and temperature-dependent. The thermal conductivity may be anisotropic. Materials may undergo a change of phase. Thermal properties of materials may be input or may be extracted from material properties library. Heat generation rates may be dependent on time, temperature, and position, and boundary temperatures may be time- and position dependent. The boundary conditions, which may be surface-to-boundary or surface-to-surface, may be specified temperatures or any combination of prescribed heat flux, forced convection, natural convection, and radiation. The thermal effectiveness of certain finned surfaces may be modeled. The boundary condition parameters may be time- and/or temperature-dependent. General gray body radiation problems may be modeled with user-defined factors for radiant exchange. The mesh spacing may be variable along each axis. HEATING is variably dimensioned and utilizes free-form input."

2.4.4 HEATING-6 Downcomer/Debris Model

A schematic drawing of the model geometry is shown in Fig. 2.59. The model is set up in two-dimensional (r,z) cylindrical coordinates (no angular dependency is considered). This geometry represents a typical vent pipe surrounded by molten debris. The outer boundary of the modeled region coincides with the outer radius of the steel ring. The debris is above the steel ring and divided into several regions. Near cold surfaces where thermal gradients are large (cold as compared to the initial temperature of the molten debris) such as near the vent pipe exterior surface and above the steel ring, debris regions have smaller nodes than the other regions do. The portion of the vent pipe in contact with the molten debris is also highly nodalized compared to its

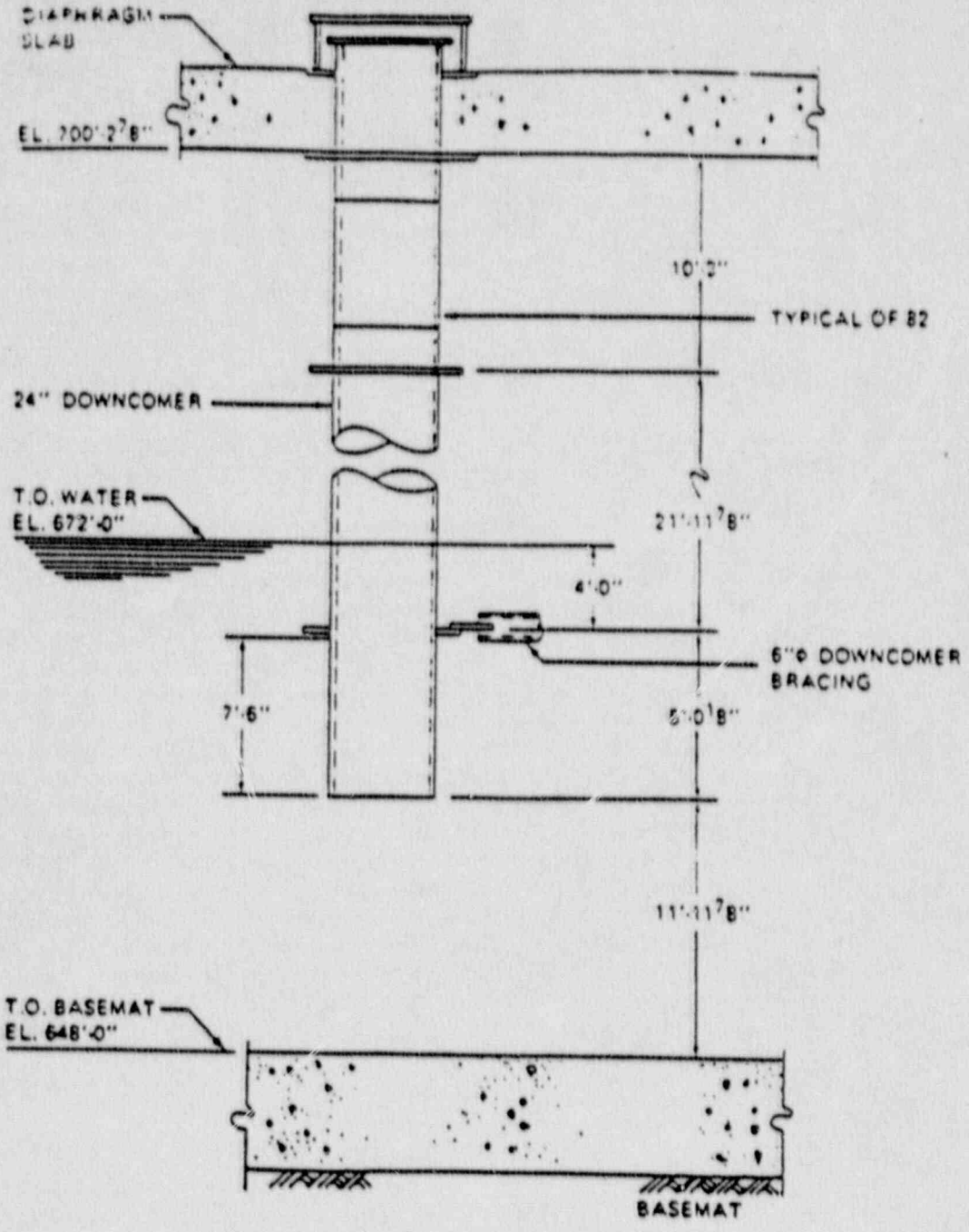

Fig. 2.58. Susquehanna downcomer design.

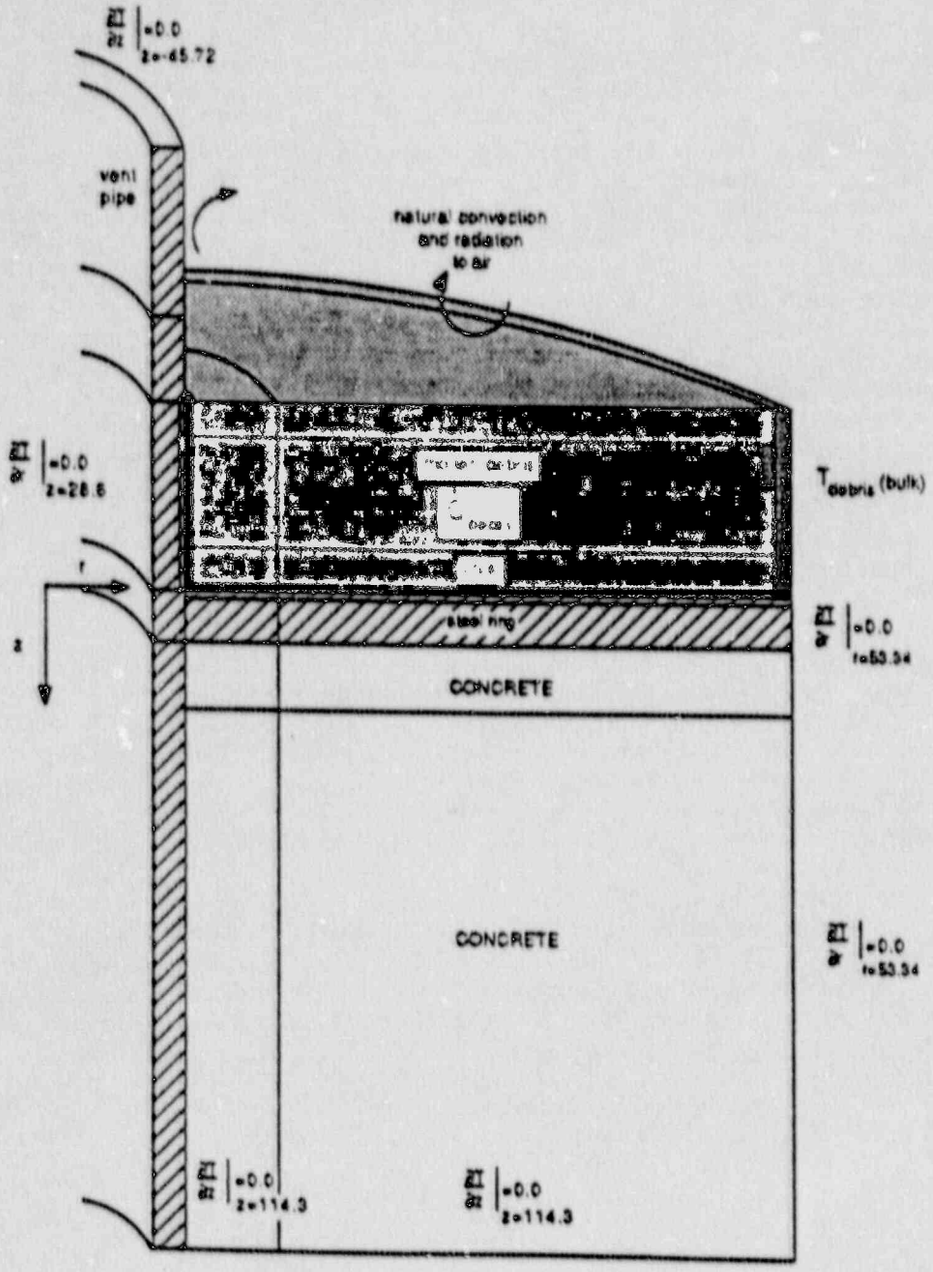

Fig. 2.59. HEATING-6 Downcomer/debris model.

remaining regions. Dark thin areas on initially cold steel surfaces represent crust. Beneath the steel ring, there is a thick concrete diaphragm slab (45 inch) which acts as a heat sink.

The HEATING-6 model of a vent pipe surrounded by debris is considered to be "a typical region" in the expedestal area. The neighboring regions are represented by boundary conditions. No heat losses are considered from the concrete to its surrounding (indicated by zero derivatives in Fig. 2.59). The steel ring does not transfer heat from its outer surface to the surrounding concrete (indicated by a zero derivative in the radial direction). The debris from its top surface and the vent pipe from its outer vertical surface can transfer heat to air by natural convection and radiation. Because vent pipes are submerged in the pressure suppression pool, air flow from the bottom of the vent pipes is not possible. Heat transfer to air inside the vent pipes is neglected because of low heat capacity of air. Heat losses through small top and bottom surfaces of the vent pipe are neglected. The debris outer surface temperature is fixed by a bulk debris temperature and heat transfer into the modeled debris region depends on local thermal gradients at this boundary.

Internal heat generation occurs only in the debris and crust regions due to decay heat. Chemical heat generation is not considered because the floor is covered by the steel ring in the model. No chemical heat generation due to debris-concrete reaction can therefore occur. The initial debris, structure and air temperatures, decay heat generation rate, material properties and boundary conditions were based on the results of the short-term station blackout discussed in Section 2.3.4.

When hot debris suddenly comes in contact with cold surfaces at time zero, a crust is formed. The HEATING-6 model of the vent pipe/debris interaction reserves a thin layer of crust on the steel surfaces. Assuming perfect contact between molten debris and cold steel surfaces, an interfacial temperature is calculated from the following equation which is based on conduction heat transfer and material properties:

$$T_i = \frac{T_m + T_s (k_s \rho_s C_{ps})^{0.5}/(k_m \rho_m C_{pm})^{0.5}}{1 + (k_s \rho_s C_{ps})^{0.5}/(k_m \rho_m C_{pm})^{0.5}}$$

where

C_{ps}, C_{pm} = specific heat of steel and molten debris respectively,
k_s, k_m = thermal conductivity of steel and molten debris respectively,
r_s, r_m = density of steel and molten debris respectively,
T_i = interfacial temperature,
T_m = molten debris temperature, and
T_s = steel temperature.

Initial temperatures of the thin steel layers and the crust are specified as arithmetic averages of the steel temperature and interfacial temperature. The initial crust thickness is x_m = 0.1 mm in the model. Thickness of the thin steel layer (x_s) whose temperature is increased due to initial contact with molten debris is calculated from

$$x_s = x_m \frac{(\rho_s C_{ps}/k_s)^{0.5}}{(\rho_m C_{pm}/k_m)^{0.5}}$$

The top surface of the molten debris transfers heat to air by natural convection and radiation. Natural convection heat transfer coefficients for horizontal surfaces cooled from the top are calculated from (Ref. 18)

$$Nu_m = 0.14\ (Gr_L Pr)^{0.33} \text{ for } 2 \times 10^7 < Gr_L Pr < 3 \times 10^{10}$$

where

Gr_L = Grashof number,
Nu_m = mean Nusselt number = h L/k
Pr = Prandtl number,
h = heat transfer coefficient,
L = characteristic length, and
k = thermal conductivity of air.

Natural convection heat transfer coefficients for the vertical surfaces of the vent pipe are calculated from the correlation for vertical plates (Ref. 18):

$$Nu_m = 0.10\ (Gr_L Pr)^{0.33} \text{ for } Gr_L Pr > 10^9 .$$

Radiation heat transfer coefficients between the surfaces and air is calculated from

$$h_r = \frac{C}{(1/e_s + 1/e_a - 1)} (T_s + T_a) (T^2_s + T^2_a)$$

where

C = Stefan-Boltzmann constant (5.675 10-12 W/cm^2 K^4),
h_r = radiation heat transfer coefficient,
e_s = surface emissivity,
e_a = air emissivity,
T_a = air temperature, and
T_s = surface temperature.

The emissivity values used in calculations are

e_s = 0.6 , and
e_a = 0.6 for air above the molten debris (MELCOR's default value).

2.4.5 Analysis Results

A series of calculations have been conducted to investigate the response of the downcomer to debris impingement. The initial structure and debris temperatures for these analyses are specified, and the atmosphere temperature and debris decay heat rate are treated as constant boundary conditions. Chemical heat generation due to debris-concrete and metal-water reactions is not considered since the steel collar around the vent pipe would (at least initially) impede the flow of concrete decomposition products into the debris that is in close proximity to the downcomer wall.

Four sets of calculations have been conducted. The first set is intended to identify the "critical debris height" (the maximum debris height at which the downcomers would not be expected to melt-through within 30 min.) for the specified initial and boundary conditions. The choice of a 30-min. period is intended to provide insight into the expected behavior of the downcomer during the initial (metallic) period of the debris pour from the reactor vessel. The boundary conditions are based on the BWRSAR/MELCOR/CORCON results for the short-term station blackout case with ADS, as described in Section 2.3.4, and are appropriate for a point in time in the accident at which the debris is near its maximum temperature, and contains a significant amount of UO_2. The actual initial values assumed in the analysis are:

Downcomer melting temperature = 2796°F,

Constant debris decay heat rate = 1144.1 Btu/min/ft^3,

Initial (constant) debris temperature = 3715°F,

Initial downcomer temperature = 291°F,

Initial collar temperature = 291°F,

Initial concrete temperature = 219°F, and

Initial (constant) air temperature = 869°F.

A set of scoping calculations were performed in which various fixed debris heights were assumed, and the response of the downcomer/debris system was predicted. After the hot debris comes into contact with the cool vent pipe, heat is transferred from the debris into the vent pipe, steel ring, and surrounding atmosphere. The structures rapidly heatup in response to large temperature differences. As thermal gradients become small, heat transfer to the downcomer is reduced. The results of these calculations indicate that the critical debris height for the initial and boundary conditions predicted by MELCOR is approximately 6.3 inches. Figure 2.60 depicts the downcomer/debris temperature contours at 30 min. for this case. The maximum downcomer temperature at the end of 30 min. is predicted to be 2670°F (130°F below the downcomer melting temperature). The calculation for a similar case in which the

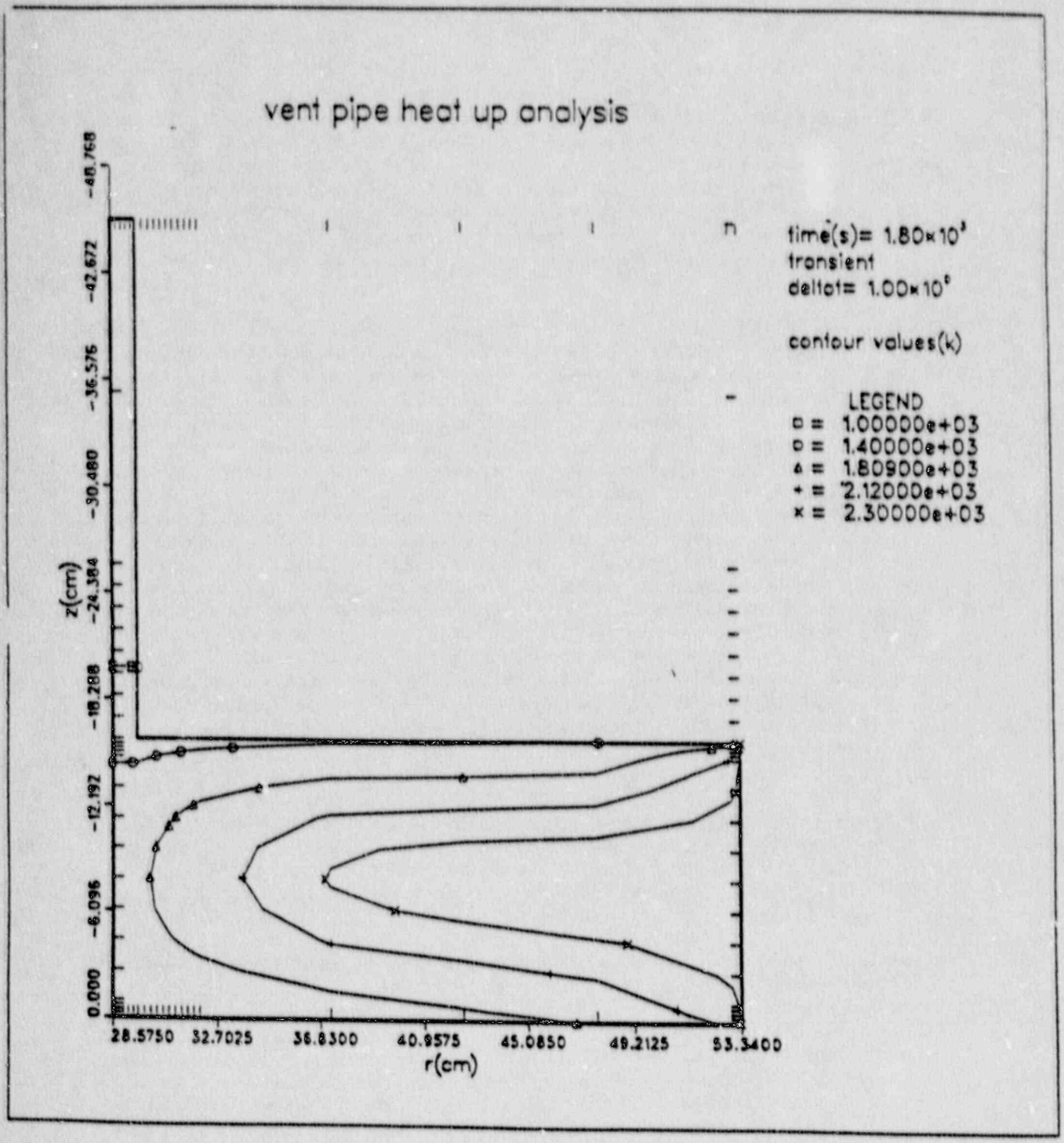

Fig. 2.60. Temperature contours in the debris and vent pipe for containment air temperature equal to 738.4 K at 30 minutes.

debris height is 12.6 in. indicates that the downcomer would reach its melting temperature in about seven minutes.

A second calculation was conducted to investigate the downcomer's response for a "limiting" critical debris height (6.3 in.) case in which there is no heat transfer from the downcomer and debris to the surrounding air. Figures 2.61, 2.62, and 2.63 depict the downcomer/debris temperature contours at 10, 20, and 30 min., respectively, for this case. The maximum inner surface temperature for this case is predicted to be 2787°F (very near the melting point of carbon steel) at the inner surface of the downcomer. This temperature was reached at about 20 min. into the transient, and remained roughly at that value for the remaining 10 minutes.

A third set of calculations was performed to investigate the impact of the containment atmosphere temperature on the debris/downcomer response for a debris height of 6.3 inches. Since the air temperature is fixed in the calculations, it acts as an infinitely large heat sink. In actuality, the air temperature, debris composition, and debris height would all vary with time. Depending on the magnitude of the air temperature, heat loss to the atmosphere can become equivalent to decay heat generation because radiation heat transfer becomes very effective at high debris temperatures. This renders the results of calculations such as those discussed here potentially sensitive to the assumed air temperature, air emissivity, and debris surface emissivity. Two calculations were performed in which the containment atmosphere temperature was assumed to be 1160°F and 1340°F, respectively. The inner surface temperature of the downcomer at the end of 30 min. were predicted to be 2694°F and 2713°F (compared to the base case of 2670°F). Thus, a large increase in assumed air temperature results in only a small increase in downcomer temperature during the 30-min. analysis period. Modest variations in the atmosphere temperature alone, do not, therefore, appear to significantly influence the peak downcomer temperature for a debris depth of 6.3 inches.

Finally, a calculation was performed to investigate the combined effect of low atmosphere temperature (480°F) and high air emissivity (e_{air}=1.0), on the downcomer's response for a debris height of 12.6 inches. Peak downcomer temperatures remained below 2600°F during the 30-min. analysis period.

In summary, the limited-scope calculations performed to date suggest that the downcomers may be able to withstand contact with core-concrete debris of depths less than six inches for the specific initial conditions and boundary conditions assumed in the analyses. While the boundary conditions employed for debris temperature and internal heat generation rate were selected to represent the most conservative debris conditions predicted by BWRSAR/MELCOR/CORCON for a short-term station blackout with ADS, the initial downcomer and concrete temperatures may be non-conservative. This non-conservatism is due to the fact that the debris would actually buildup around the outer surface of the downcomer throughout the accident. Thus, the initial downcomer and concrete

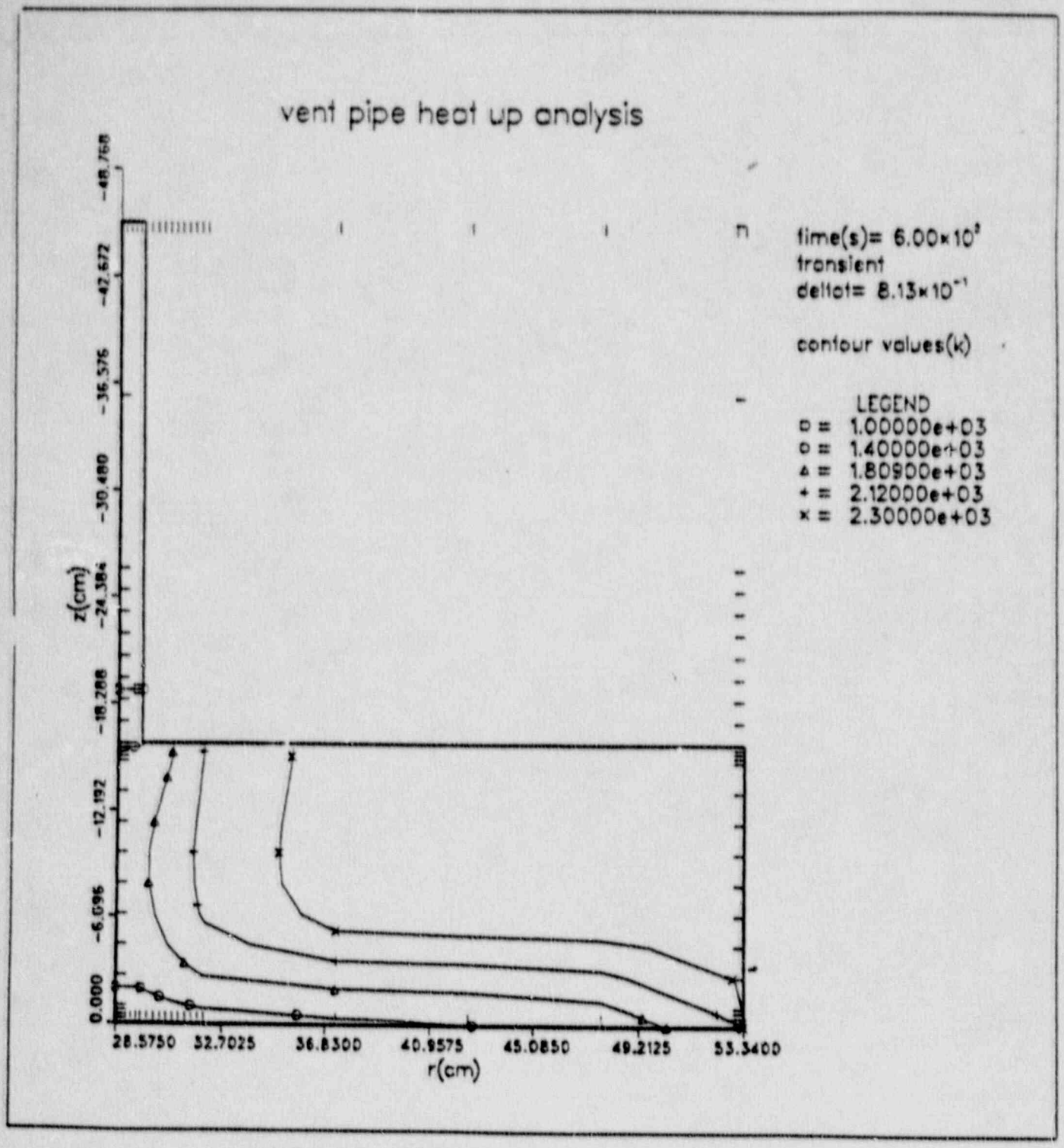

Fig. 2.61. Temperature contours in the debris and vent type at 10 minutes (no heat loss to air).

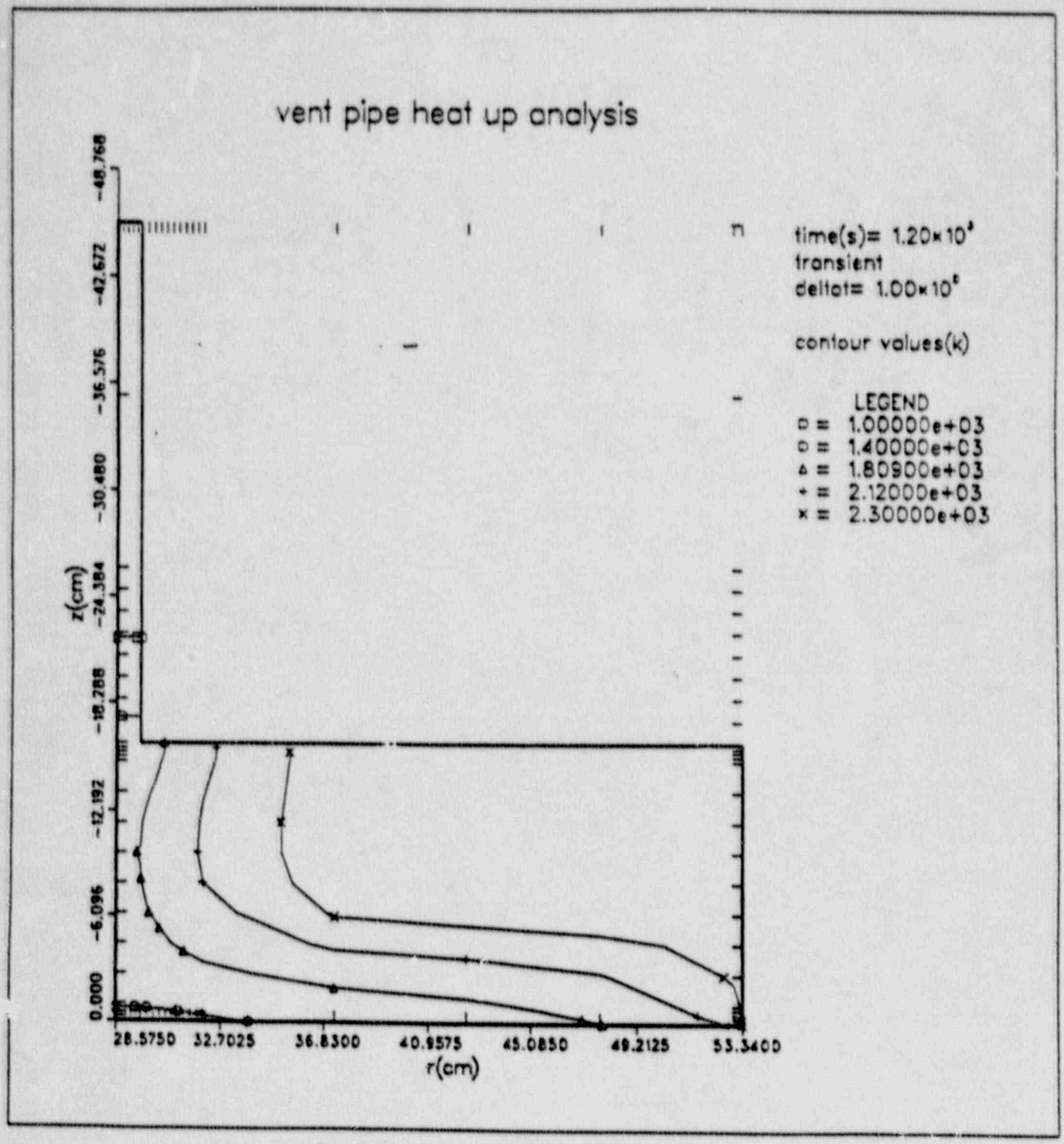

Fig. 2.62. Temperature contours in the debris and vent pipe at 20 minutes (no heat loss to air).

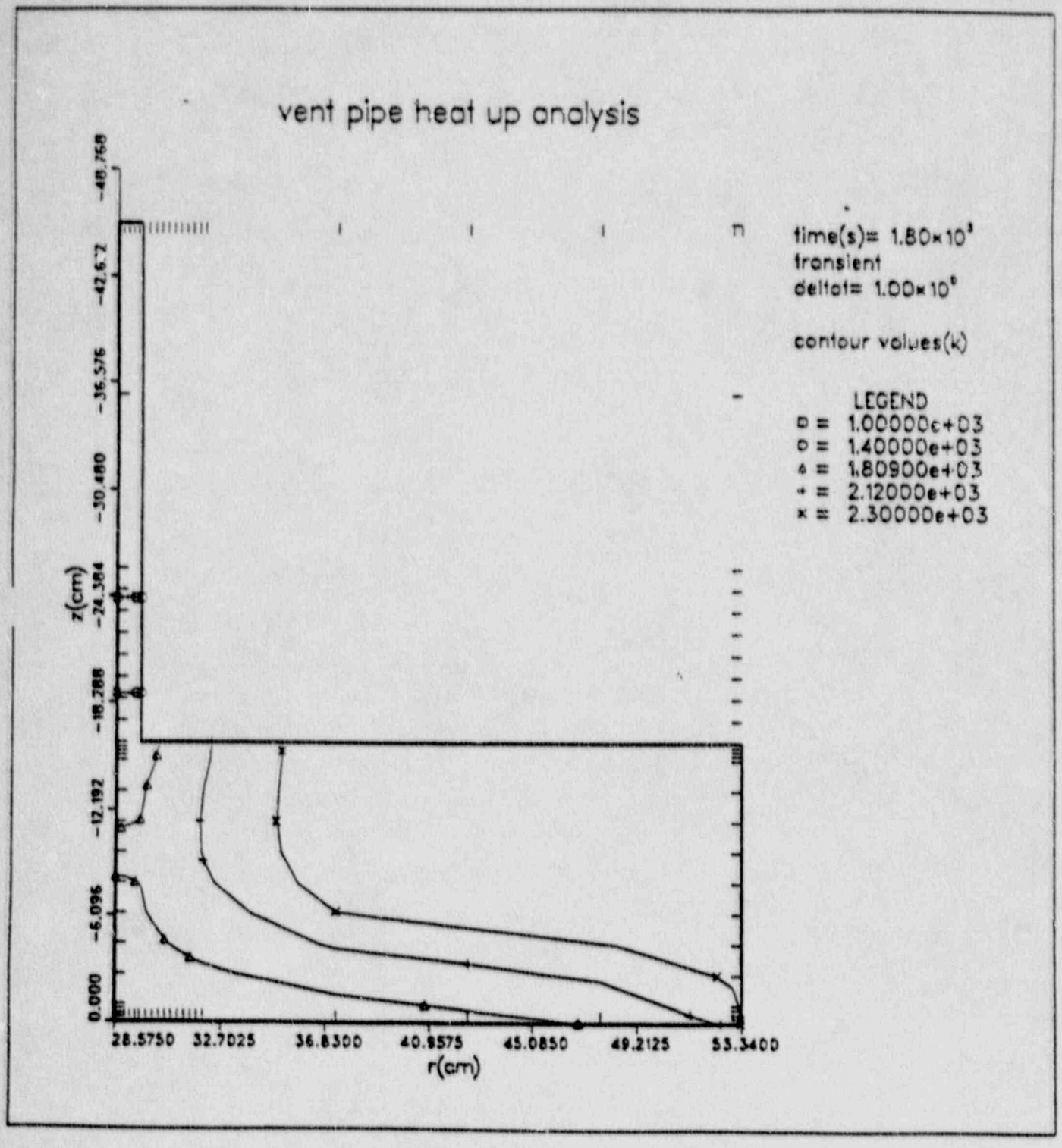

Fig. 2.63. Temperature contours in the debris and vent pipe at 30 minutes (no heat loss to air).

temperatures for the present analyses cannot be accurately known. It is, therefore, inappropriate to draw firm conclusions regarding downcomer survivability from these calculations.

Chapter 2 References

1. C. W. Parker, L. J. Ott, and S. A. Hodge, Small-Scale BWR Core Debris Eutectics Formation and Melting Experiment, Nuclear Engineering and Design (to be published) North-Holland, Amsterdam.

2. S. A. Hodge and L. J. Ott, "Boiling Water Reactor Severe Accident Response (BWRSAR) Code Description and Assessment," NUREG/CR-5318 (to be published).

3. L. J. Ott, Advanced Severe Accident Response Models for BWR Application, Nuclear Engineering and Design 115 (1989) 289-303, North-Holland, Amsterdam.

4. C. A. Kukielka, S. Seyedhosseini, and M. P. Carr, Feedwater Coast-Down Measurement of a BWR, Proceedings of the U.S. NRC Sixteenth Water Reactor Safety Information Meeting, Gaithersburg, MD, NUREG/CP-0097, Vol. 6, February 1989.

5. R. M. Harrington and L. C. Fuller, "BWR-LTAS: A Boiling Water Reactor Long-Term Accident Simulation Code," NUREG/CR-3764, February 1985.

6. Reactor Safety Study, WASH-1400, Appendix VII, U.S. Nuclear Regulatory Commission, October 1975.

7. L. G. Greimann, et al., "Reliability Analysis of Steel Containment Strength," NUREG/CR-2442, Ames Laboratory, Iowa State University, June, 1982.

8. "Ultimate Pressure Capacity of Shoreham Primary Containment," Appendix M, Shoreham Nuclear Power Station Probabilistic Risk Assessment, Stone & Webster Engineering Corp., 1982.

9. "Ultimate Pressure Capacity of Limerick Primary Containment," Appendix J, Limerick Generating Station Probabilistic Risk Assessment, Bechtel Power Corporation, September 1982.

10. S. A. Hodge, C. R. Hyman, and L. J. Ott, "Primary Containment Response Calculations for Unmitigated Short-Term Blackout at Peach Bottom," letter report to Dr. Thomas J. Walker, Accident Evaluation Branch, Division of Reactor Accident Analysis, RES, USNRC, dated May 2, 1989.

11. "Mark I Containment Severe Accident Analysis," CBI NA-CON, Inc. for the BWR Mark I Owners' Group, April 1987.

12. T. L. Bridges, "Containment Penetration Elastomer Seal Leak Rate Tests," NUREG/CR-4944, Idaho National Engineering Laboratory, July 1987.

13. D. A. Brinson and G. H. Graves, "Evaluation of Seals for Mechanical Penetrations of Containment Buildings," NUREG/CR-5096, ERC International, August 1988.

14. R. F. Kulak, et al., "Structural Response of Large Penetrations and Closures for Containment Vessels Subjected to Loading Beyond Design Basis," NUREG/CR-4064, Argonne National Laboratory, February 1985.

15. David B. Clauss, "Failure Mechanism of LWR Steel Containment Buildings Subject to Severe Accident Loadings," Proceedings of the Third Workshop on Containment Integrity, NUREG/CP-0076, August 1986.

16. Reactor Safety Research Semi-annual Report - July—December 1986, NUREG/CR-4805 (2 of 2), SAND86-2752 (2 of 2), November 1987.

17. K. W. Childs, et al., Heating: A Computer Program for Multidimensional Heat Transfer Analysis, (Version 6.1), NUREG/CR-0200, January 1988.

18. M. Ozisik, Basic Heat Transfer, pp. 303, McGraw-Hill, 1977.

3. BWR-6/MARK III ANALYSES

3.1 Introduction

There are currently four domestic BWR Mark III units in operation: Grand Gulf 1, Clinton 1, Perry 1, and River Bend 1. All four units employ the BWR-6 reactor design (Table 3.1). Grand Gulf and Clinton employ a steel-lined, reinforced concrete cylindrical containment structure, while Perry and River Bend employ a free-standing steel containment shell which is enclosed by a cylindrical concrete structure (Figure 3.1). The NRC Technical Monitor has requested that ORNL conduct some preliminary limited-scope Mark III severe accident analyses to provide information desired for resolution of near-term Mark III severe accident issues. The Grand Gulf Mark III design is being employed for these evaluations. This choice is dictated, in part, by the short time frame available for these analyses, as well as the desire to employ a plant design for which a PRA has been conducted. (The Grand Gulf plant is being utilized as the prototypical Mark III plant in the NRC's NUREG-1150 PRA effort.)

3.2 BWR-6 Short-term Station Blackout Core Degradation Analyses

3.2.1 Introduction

The Boiling Water Reactor Severe Accident Response (BWRSAR) code has been applied to perform the core degradation analyses described in this section. Information concerning the operation of this code is provided in Section 2.2.1, and a more detailed discussion of the code and its capabilities and limitations can be found in References 1 and 2. The accident sequence considered is short-term station blackout, which is described in Chapter 1. The accident is assumed to occur at the end of core life, and to be unmitigated.

3.2.2 BWRSAR BWR-6 Model

The BWRSAR code input deck for the BWR Mark III containment calculations is based upon the dimensions and emergency procedures of the Grand Gulf Plant with modifications as described in the following paragraph. Plant-specific information was provided by System Energy Resources, Inc., as necessary to define reactor vessel SRV setpoints, main steam isolation valve leakage rates, core radial and axial power factors, reactor vessel leakage rates, and heat transfer from the reactor vessel to the drywell atmosphere.

The BWRSAR calculations were performed, however, with one very important difference in assumed operator action as opposed to the procedures currently in effect at Grand Gulf. This difference has to do with the

Table 3.1. Domestic Mark III plants

Name	MWe	Location	Reactor Type	Commercial Operation
Clinton 1	930	Clinton, IL	6	4/87
Grand Gulf 1	1142	Port Gibson, MS	6	7/85
Grand Gulf 2	1142	Port Gibson, MS	6	33%
Perry 1	1205	North Perry, OH	6	11/87
Perry 2	1205	North Perry, OH	6	57%
River Bend 1	936	St. Francisville, LA	6	6/86

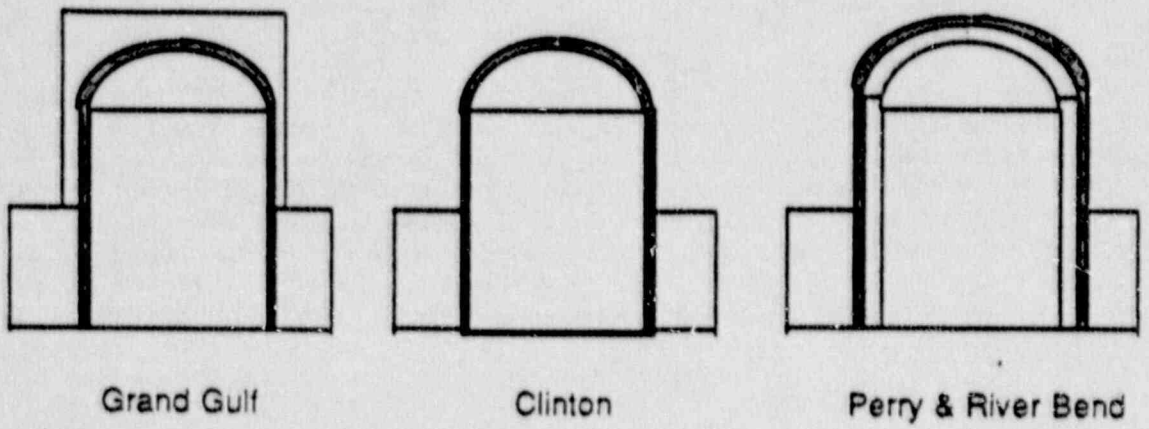

Fig. 3.1. Domestic Mark III containment designs.

time in the short-term station blackout accident sequence at which the operators would manually actuate the ADS. Grand Gulf has implemented Revision 4 of the BWR Owners Group Emergency Procedures Guidelines (EPGs), which provide [Contingency #3 (Steam Cooling) and WS-10 (RPV Variables Worksheet)] for manual ADS actuation at a water level equivalent to 71.33% of core height, or 323 in. above vessel zero. In contrast, the Susquehanna (Mark II) procedures are based upon Revision 3 of the EPGs and call for manual ADS actuation under station blackout conditions at a water level of 28% of core height and, as explained in Section 2.2, the BWR Mark II degraded core analyses performed for this study were based upon ADS actuation at a water level of 33% core height or 266 in. above vessel zero.

In considering the question of the optimum time to manually actuate the ADS under conditions in which the core is partially uncovered and no reactor vessel water injection systems are available, it is important to consider both the temporary core cooling to be achieved and the effect upon the subsequent metal-water reactions when the core has reheated to runaway oxidation temperatures. With the core partially uncovered at the time of ADS actuation, the flashing attendant to vessel depressurization will cause the water level to fall below the core plate so that the core will later be in a steam-starved condition during the period of runaway metal-water reaction.

Although actuation of the ADS with the reactor vessel water level at either 71% or 33% of core height will result in rapid dryout of the core region, there is a significant difference in the amount of core cooling that is achieved during the blowdown. By the time that coolant boiloway has reduced the reactor vessel water level to 33% of core height, BWRSAR predicts the highest clad temperature in the uncovered portion of the core to be about 1650°F. Three min. later, the steam cooling provided by the ADS actuation is predicted to have reduced the maximum clad temperature to about 950°F. The ADS maneuver thus delays the onset of core degradation, buying time for the operators to continue efforts to restore reactor vessel water injection capability. The maximum clad temperature does not again reach 1650°F until about 15 min. after the time of ADS actuation.

If the ADS is actuated with the reactor vessel water level at 71% of core height, the maximum clad temperature in the uncovered portion of the core at the time is only about 700°F. Therefore, only a small temperature reduction is achieved by steam cooling. Table 3.2 provides a comparison of the times at which major core damage events occur for the two ADS strategies. As indicated, delaying the manual ADS actuation until the water level has decreased to about one-third core height results in a corresponding delay of 25 to 30 min. in the onset of debris relocation and the subsequent core degradation events. Obviously, the delay should not be too long; it would be very undesirable to have the core already in the process of runaway metal-water reaction at the time that ADS was actuated.

Table 3.2. Calculated timing of significant events for two ADS actuation strategies for the short-term station blackout accident sequence at Grand Gulf

	Time (min.)	
	ADS at 33% core height	ADS at 71% core height
Station blackout-initiated scram from 100% power. Independent loss of the steam turbine-driven HPCI and RCIC injection systems	0.0	0.0
Swollen water level falls below top of core	42.0	42.0
ADS system actuation	75.0	48.2
Core plate dryout	75.6	50.3
Relocation of core debris begins	106.9	79.0
First local core plate failure	111.0	82.8
Collapse of fuel pellet stacks in central core	184.2	153.1

The BWRSAR calculations performed for this study are based upon an assumption that the manual ADS actuation for the BWR Mark III plant is delayed until the reactor vessel water level has decreased to one-third core height. This was done at the direction of the NRC Technical Monitor for the purpose of evaluating the efficacy of what is believed to be the most effective accident management procedure.

3.2.3 Short-term Station Blackout Response (with ADS)

3.2.3.1 Calculated events prior to reactor vessel bottom head penetration failure

The sequence of events and event timing as calculated by the BWRSAR code for the BWR Mark III short-term station blackout accident sequence with ADS actuation are provided in Table 3.3. It is assumed that the reactor had been operating at 100% power at the time of scram, that the accident is initiated at the end of core life, and that no reactor vessel water injection source is ever recovered.

Plots of key parameters representing events within the reactor vessel as predicted by the BWRSAR code are provided in Figures 3.2-3.5. The BWRSAR calculation was begun at time five min. after the main steam isolation valve closure and reactor scram that immediately follow the initiating loss of electric power for this accident sequence. The initial conditions for the BWRSAR input deck were taken from the results of a BWR-LTAS (Ref. 3) calculation that covers the period from 0.60 min. to 5.0 min. The initial conditions for the BWR-LTAS calculation were taken from the results of the Susquehanna main steam isolation valve closure test discussed in Section 2.2.2.

Reactor vessel pressure, shown in Figure 3.2, is maintained by automatic SRV cycling until time 75 min., when the ADS is manually actuated with the reactor vessel water level at about one-third core height. This causes the opening of eight SRVs, which then remain open throughout the remainder of the accident sequence. After the initial depressurization, the vessel pressure increases slightly during periods of rapid steam generation initiated by the quenching of molten debris relocated into the water in the vessel lower plenum. The associated SRV flows from the reactor vessel are shown in Figure 3.4.

The swollen reactor vessel water level is shown in Figure 3.3. The BWRSAR input deck for this calculation provides an initial collapsed water level of 524 in. above vessel zero and the swollen level, which reflects the presence of steam bubbles within the water, fluctuates significantly with the pressure changes induced by SRV cycling. It is the calculated height of the swollen level within the core shroud and steam separators that is actually plotted in Figure 3.3 and therefore the upper limit for the plotted points is the top of the steam separators, 607.5 in. above vessel zero.

Table 3.3. Calculated sequence of events for BWR Mark III Short-Term Station Blackout with ADS Actuation. The bottom head debris is modeled to separate into a mixture of metals melting at 2750°F and a mixture of oxides melting at 4350°F

Event	Time (min)
Station blackout-initiated scram from 100% power. Independent loss of the steam turbine-driven HPCI and RCIC injection systems	0.0
Swollen water level falls below top of core	42.0
ADS system actuation	75.0
Core plate dryout	75.6
Relocation of core debris begins	106.9
First local core plate failure	111.0
Collapse of fuel pellet stacks in central core	184.2
Reactor vessel bottom head dryout; structural support by control rod guide tubes fails; remainder of core falls into reactor vessel bottom head	218.1
Initial failure of bottom head penetrations	218.2

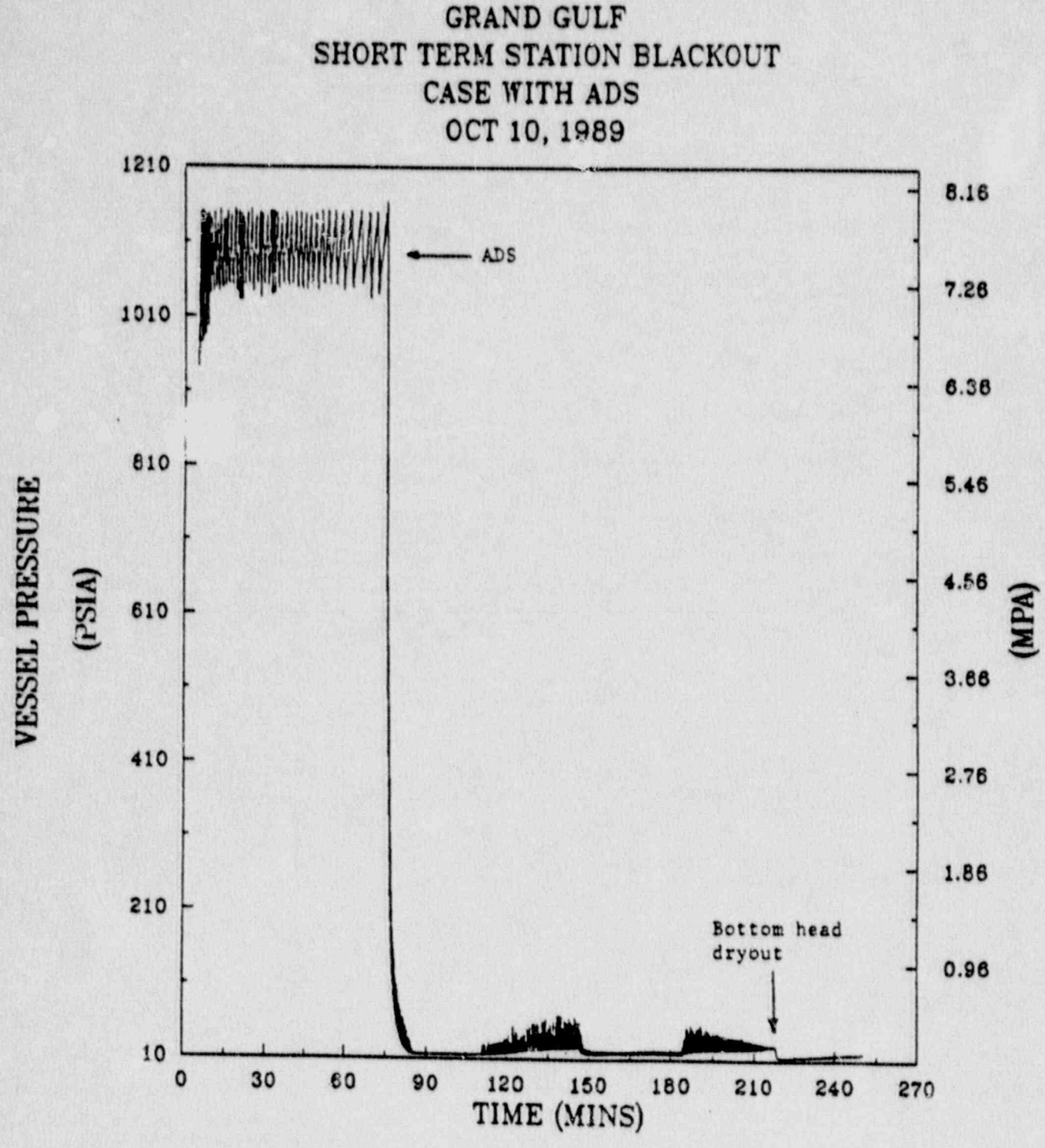

Fig.3.2. Reactor vessel pressure for the BWR-6/Mark III short-term station blackout with ADS actuation (simple eutectics).

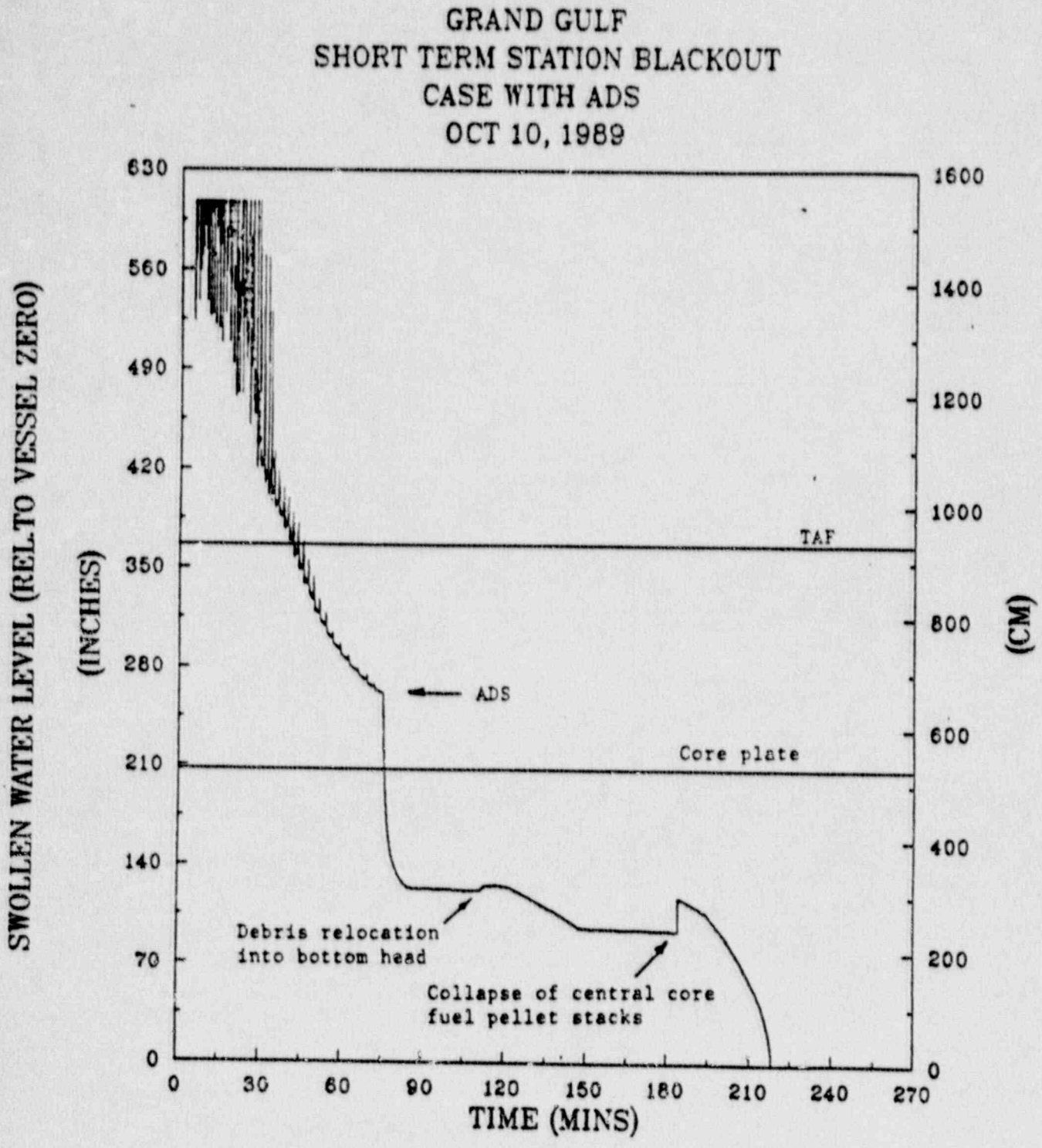

Fig. 3.3. Swollen reactor vessel water level for the BWR-6/Mark III short-term station blackout with ADS actuation (simple eutectics).

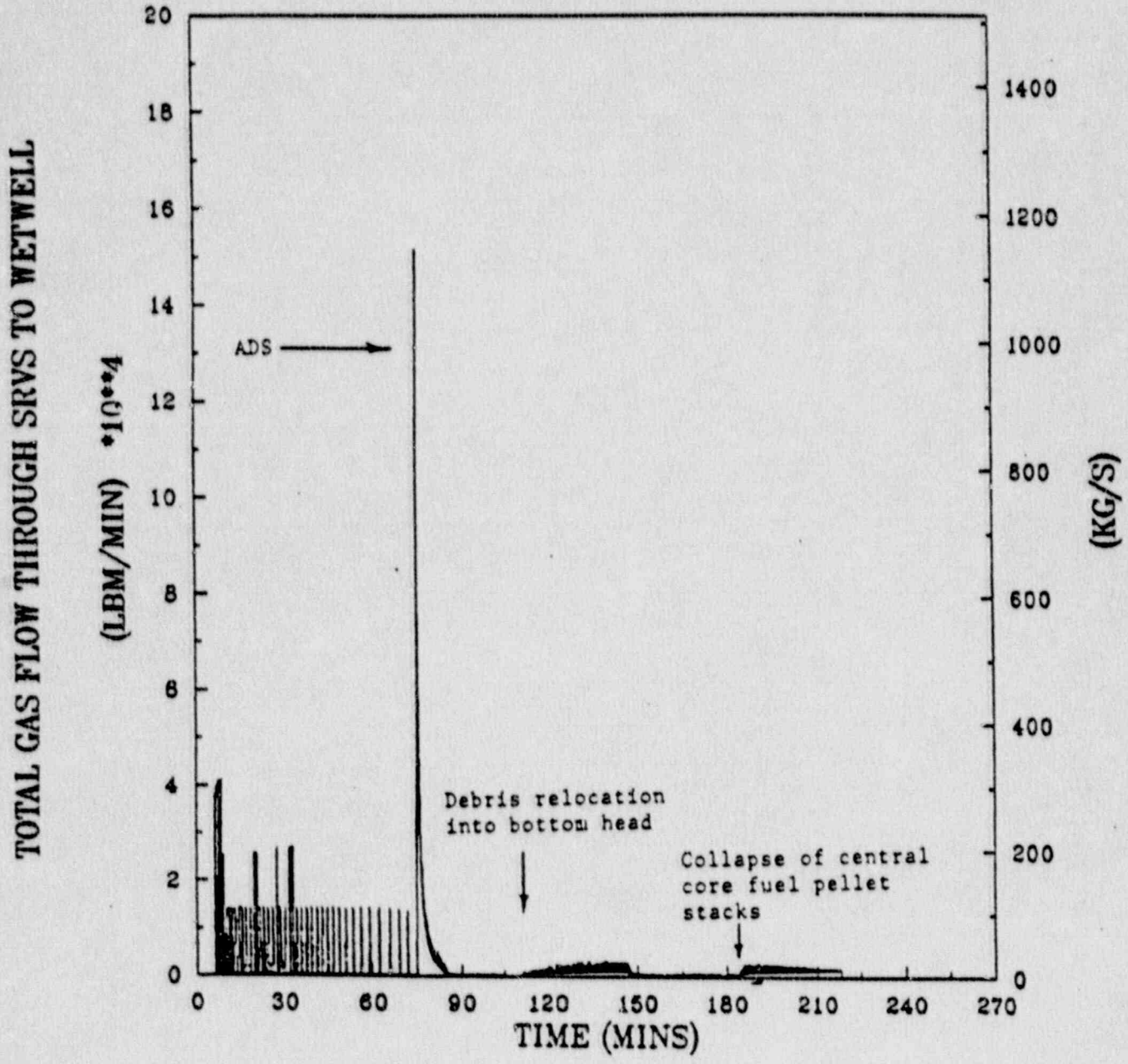

Fig. 3.4. Total gas flow through SRVs for the BWR-6/Mark III short-term station blackout with ADS actuation (simple eutectics).

Since manual control of reactor vessel pressure during the period before ADS actuation is not represented in the BWRSAR calculation for the BWR Mark III plant but was represented in the BWR Mark II calculation, the top of the core is predicted to be uncovered about five min. later for the BWR Mark III case, as may be seen by a comparison of the event timings listed in Tables 3.3 and 2.4. When the SRVs are manually actuated, they are held open longer for each opening than when they actuate automatically so as to achieve a greater reduction in reactor vessel pressure per valve operation and thereby reduce the total number of valve actuations (compare the pressure traces before ADS actuation as shown on Figures 2.1 and 3.2). The additional loss of coolant from the reactor vessel associated with the manual valve actuation strategy hastens the uncovering of the core. However, it should be noted that the purpose of the strategy is to more evenly distribute the release of steam into the pressure suppression pool and to reduce the probability that a SRV will stick open. When the vessel pressure control is left to automatic SRV actuation, the lowest set valve repeatedly discharges into the same location within the pool. When the SRVs are manually actuated, a different valve is selected for each opening.

The calculated water level rapidly drops below the core plate as a result of flashing when the ADS valves are opened [Figure 3.3]. Subsequently, small temporary level increases occur as a result of water displacement in the lower plenum whenever large masses of debris are introduced after core plate failure. The decay heat associated with the fuel pellets introduced into the lower plenum at time 182 min. causes a boiloff of the remaining water in the reactor vessel and bottom head dryout is predicted at time 218 minutes.

The integrated amount of hydrogen generated in the core region is shown in Figure 3.5. Approximately 25% of the clad, 12% of the channel box walls, and 3% of the control blade stainless steel sheaths are predicted to be oxidized during the accident sequence, producing about 1300 lbs of hydrogen in the process. The generated hydrogen does not in general accumulate within the reactor vessel but rather is passed to the pressure suppression pool via the SRVs.

Selected primary containment response characteristics as predicted by the BWRSAR code for the period of the accident sequence ending one-half hour after reactor vessel bottom head penetration failure are provided in Figures 3.6 through 3.13. (A more detailed calculation of containment response for this accident sequence performed with the MELCOR code is provided in Section 3.3.) Since the free volume of the Mark III containment (1,670,000 ft^3) is more than four times the free volume of the Mark II containment (380,000 ft^3), it is not surprising that significantly smaller containment pressure and temperature increases are predicted to occur during the same accident sequence. For example, the Mark III drywell pressure [Figure 3.6] is only about 18.5 psia at the time of bottom head dryout as opposed to 31.5 psia for the Mark II drywell [Figure 2.5]. Neither of these pressures is of sufficient magnitude to pose any threat to containment integrity, but with the reactor vessel floating on the containment pressure through the open SRVs after

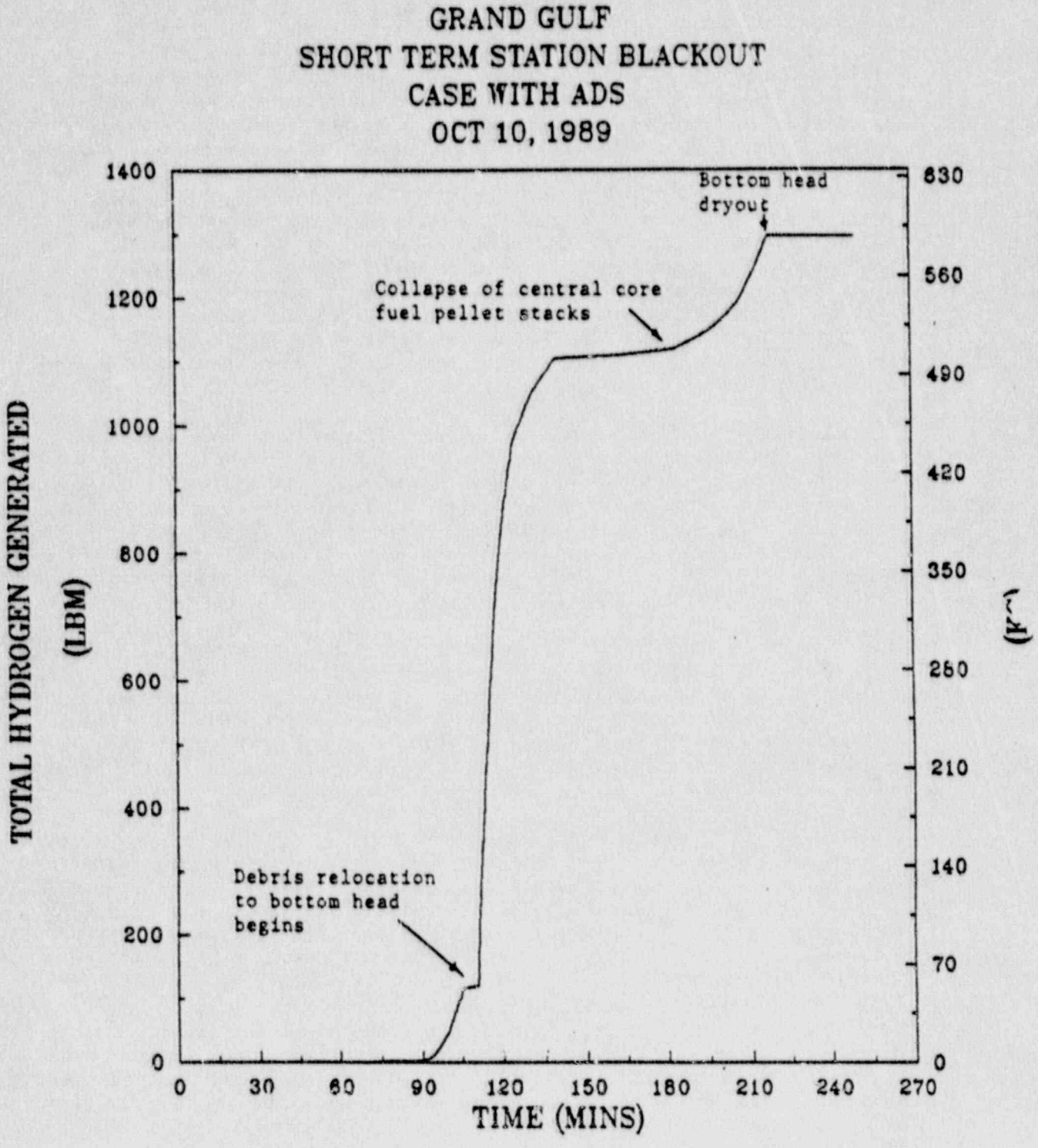

Fig. 3.5. Total hydrogen generated invessel for the BWR-6/Mark III short-term station blackout with ADS actuation (simple eutectics).

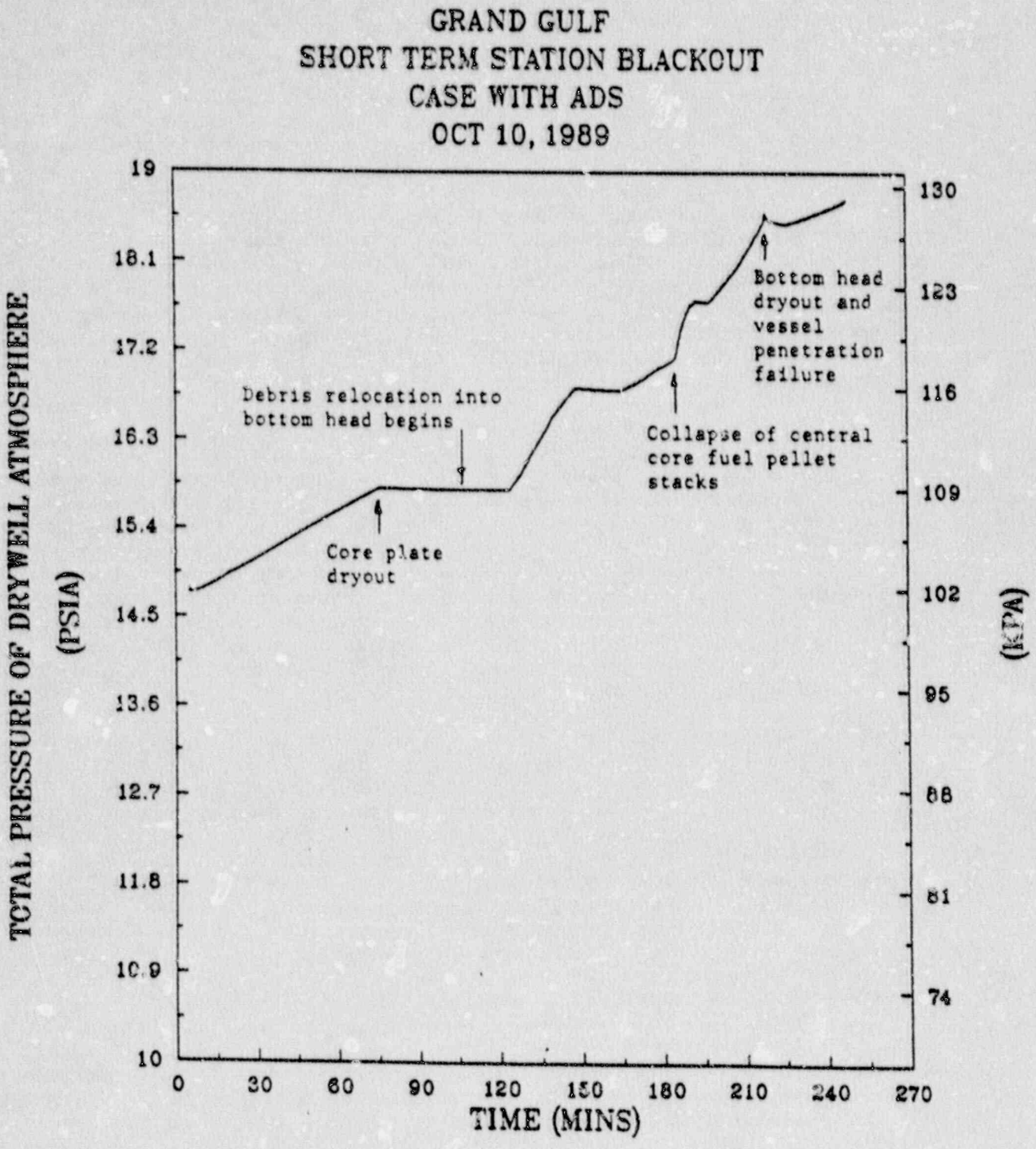

Fig. 3.6. Drywell atmosphere pressure for the BWR-6/Mark III short-term station blackout with ADS actuation (simple eutectics).

ADS actuation, the difference in containment backpressure will affect events within the reactor vessel. The effect of this lower containment backpressure for the Mark III case as well as the faster coolant boiloff as a result of having a larger core (800 vs 764 fuel assemblies) in the same size vessel may be seen by a comparison of the timings of events after ADS actuation listed on Tables 2.4 and 3.3.

The drywell atmosphere temperature, shown in Figure 3.7, varies less than 6°F during the portion of the accident sequence represented; nevertheless, there is an observable response to invessel events. The time delay between the onset of debris relocation into the reactor vessel bottom head and the associated increase in drywell pressure (Figure 3.6) should be noted. This delay occurs because the wetwell-to-drywell vacuum breakers require electric AC power for operation and hence gas flow into the drywell as the wetwell pressure increases must be by leakage through the drywell wall. [This is not true of the Mark II containment design]. As indicated in Figure 3.8, the temperature of the drywell liner is virtually unchanged during this period.

Very little hydrogen is predicted to accumulate within the Mark III containment drywell during the period before bottom head penetration failure, as indicated in Figure 3.9. Since the path for hydrogen release from the reactor vessel is via the SRVs into the pressure suppression pool and from there upward into the wetwell atmosphere, the movement of hydrogen into the drywell during this period is limited by the leakage rate through the drywell wall. After reactor vessel bottom head penetration failure, a direct path exists from the vessel to the drywell and the increase in drywell hydrogen by this pathway is apparent (starting at time 218 min.) in Figure 3.9. Much more hydrogen is subsequently generated by the core debris-concrete interaction on the drywell floor, as described in Section 3.3.

The calculated temperature of the wetwell atmosphere does respond directly to the invessel events as indicated on Figure 3.10, but does not increase to threatening values during the period of the BWRSAR calculation. The gas volume transfers representing leakage between the wetwell and drywell are shown in Figure 3.11. It should be noted that the calculated volume transfers are very small relative to the wetwell free volume of 1,400,000 ft^3. Inleakage to the drywell is predicted to continue after reactor vessel bottom head penetration failure. BWRSAR predicts this continued inleakage for two reasons. First, the reactor vessel is depressurized at the time of penetration failure so there is no vessel blowdown into the drywell (see Figure 3.6). Second, BWRSAR has no models to calculate the effect of core debris-concrete interactions and the associated release of gases into the drywell atmosphere. The MELCOR calculation of containment response, discussed in Section 3.3, does represent the effects of core debris-concrete interaction as well as provide a more detailed calculation of containment events during the period before reactor vessel bottom head penetration failure.

As previously discussed, most of the hydrogen released from the reactor vessel during the short-term station blackout accident sequence for the

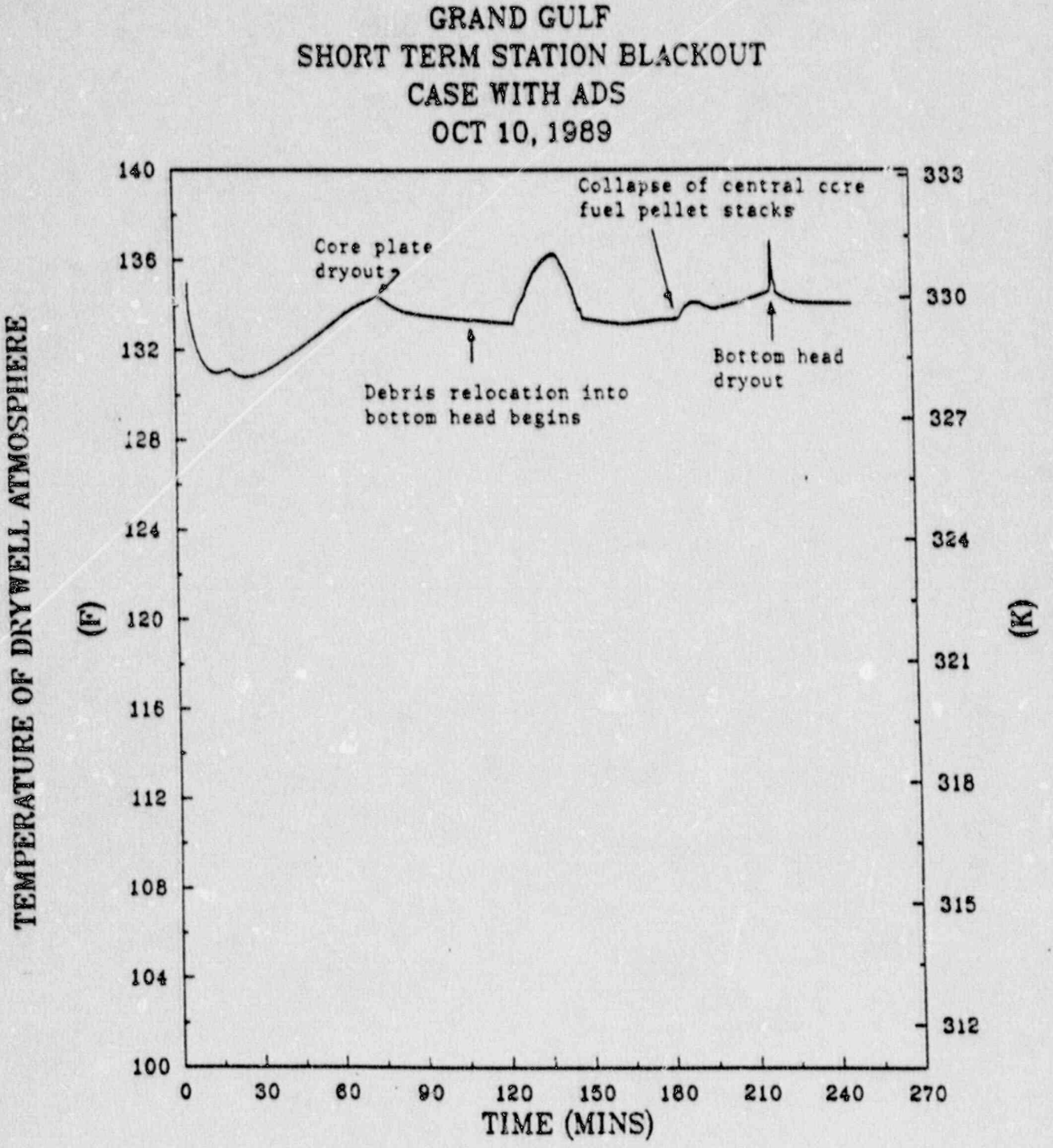

Fig. 3.7. Drywell atmosphere temperature for the BWR-6/Mark III short-term station blackout with ADS actuation (simple eutectics).

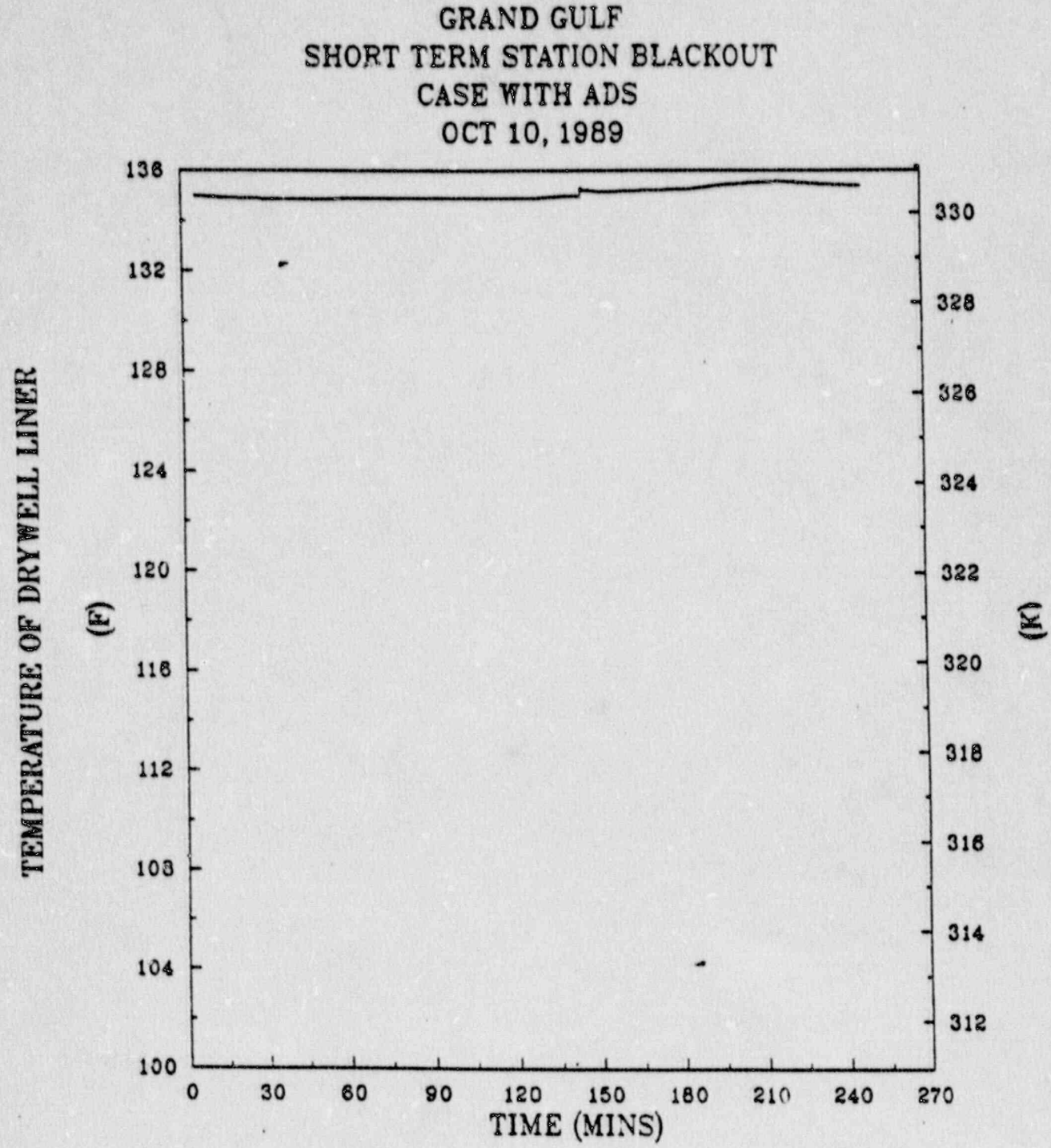

Fig. 3.8. Drywell liner temperature for the BWR-6/Mark III short-term station blackout with ADS actuation (simple eutectics).

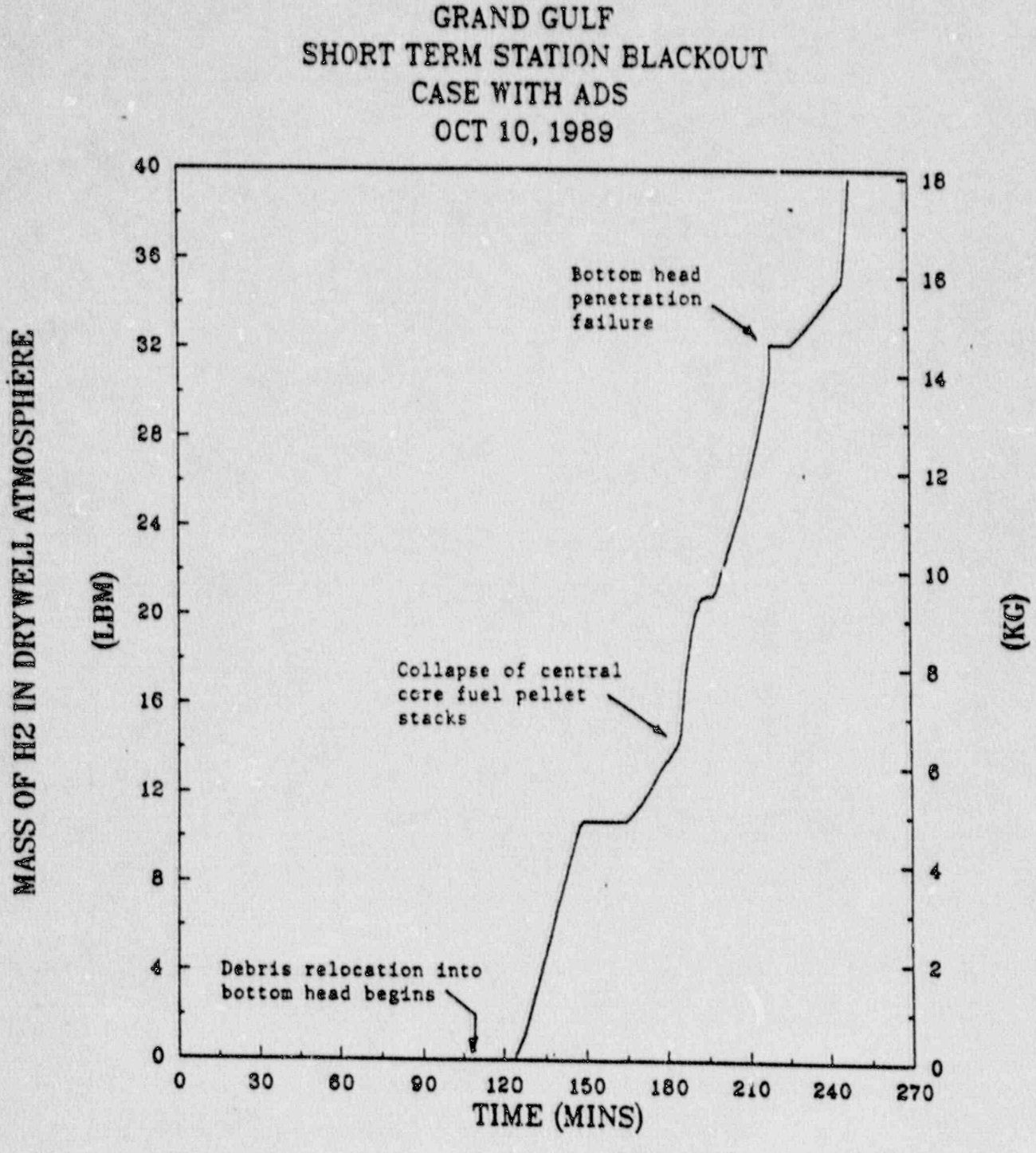

Fig. 3.9. Mass of hydrogen in drywell atmosphere for the BWR-6/Mark III short-term station blackout with ADS actuation (simple eutectics).

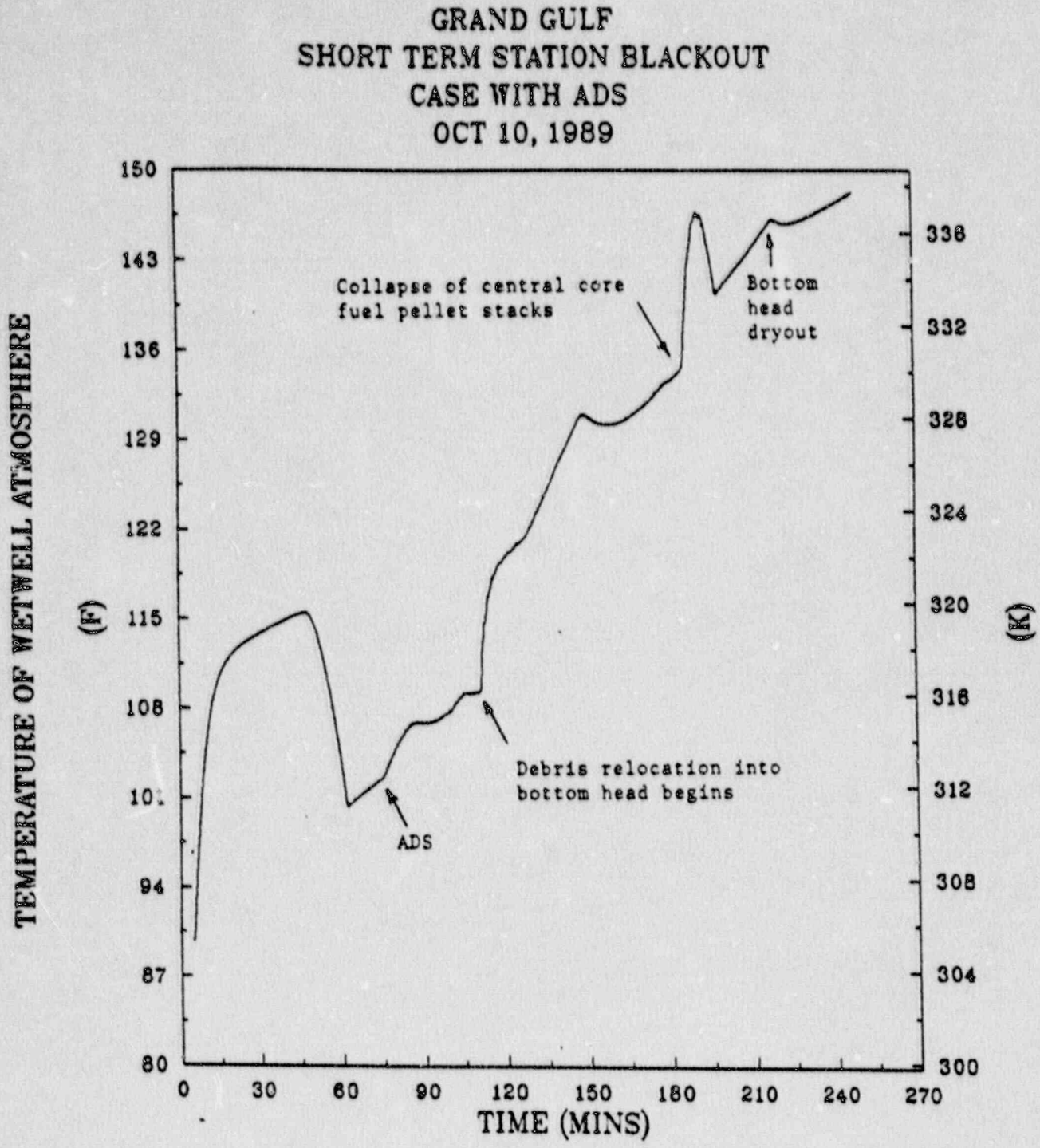

Fig. 3.10. Wetwell atmosphere temperature for the BWR-6/Mark III short-term station blackout with ADS actuation (simple eutectics).

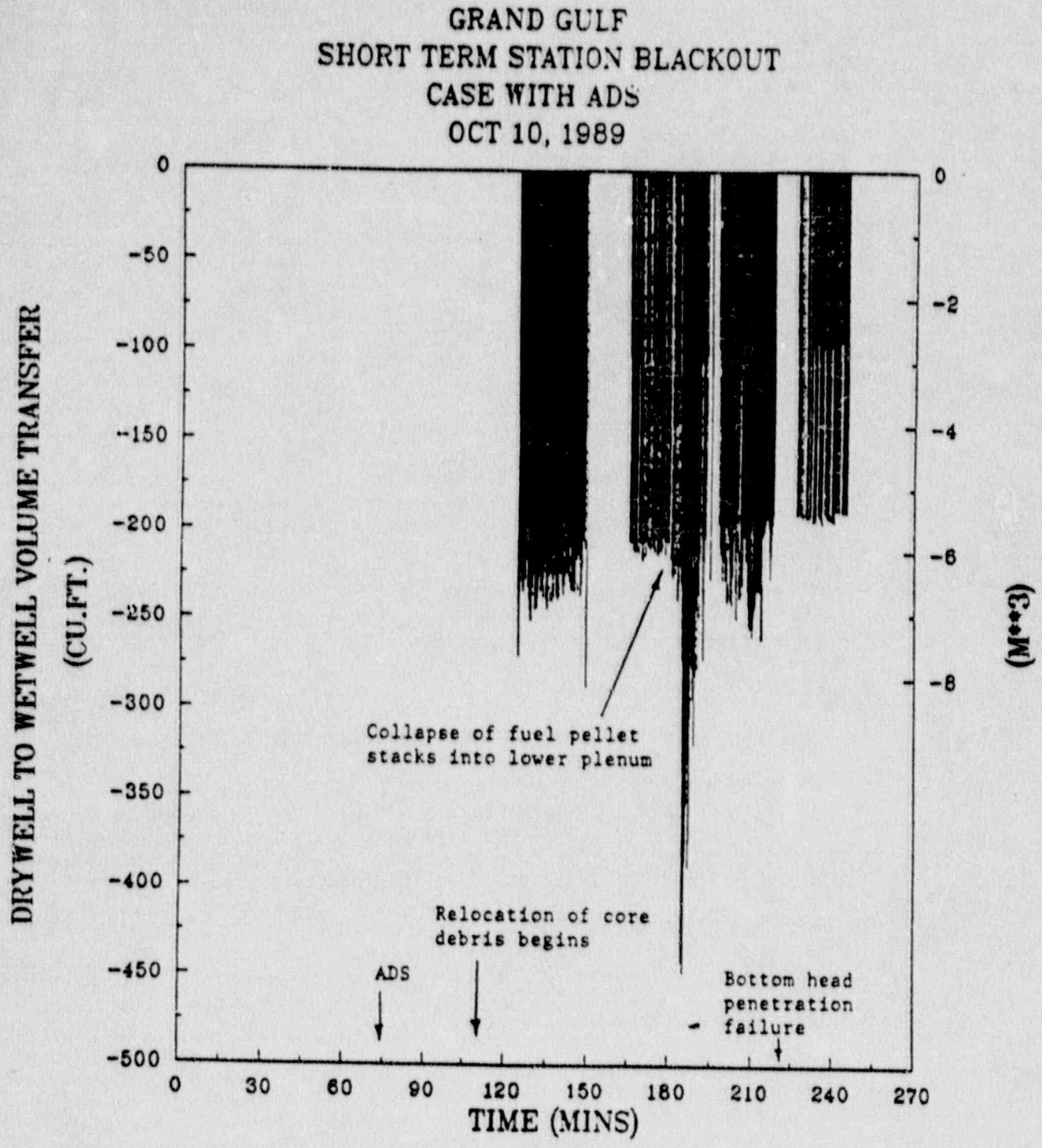

Fig. 3.11. Drywell-to-wetwell volume transfers for the BWR-6/Mark III short-term station blackout with ADS actuation (simple eutectics).

BWR Mark III containment is predicted to accumulate in the wetwell atmosphere (compare Figures 3.12 and 3.9). Since the Mark III containment is not inerted during reactor operation (as are the smaller BWR Mark I and Mark II containments), there are obvious concerns with respect to hydrogen deflagrations; this issue is discussed in conjunction with the more detailed results of the MELCOR containment response calculations in Section 3.3.

The temperature response of the Mark III containment pressure suppression pool is shown in Figure 3.13. Although the free volume of the Mark III containment is much larger than that of the Mark II containment, the pressure suppression pool water volumes are similar; therefore, the pool temperature increases associated with the short-term station blackout accident sequence with ADS actuation are similar (compare Figures 3.13 and 2.12).

3.2.3.2 Calculated reactor vessel debris pours

After reactor vessel dryout, the conversion of the constituents of the bottom head debris bed from solid to liquid is determined for the BWRSAR calculation by user-input defining the eutectic mixtures to be formed and their melting points.

For the reasons discussed in Section 2.2.3, the BWRSAR code input used in this study to provide the reactor vessel gas blowdown rates and debris pours for the MELCOR calculations of detailed containment response are based upon formation of one metallic eutectic mixture melting at 2750°F and one oxidic eutectic mixture melting at 4800°F. This approach is consistent for both the BWR Mark II containment (Section 2.2) and BWR Mark III containment (Section 3.2) calculations.

The predicted pour rates of zirconium metal for the BWR Mark III calculation are shown in Figure 3.14. The release of unoxidized zirconium metal onto the drywell floor is of special significance in BWR severe accident studies since this metal then becomes available for oxidation (and the associated energy release) on the drywell floor.

The predicted release of molten UO_2 is shown in Figure 3.15. The initial oxide release lags the molten metal release because of the higher melting temperature of the oxides. The combined flow of molten metals (zirconium and stainless steel) and oxides (primarily ZrO_2 and UO_2) is provided in Figure 3.16.

The mass-averaged temperature of the debris pour (Figure 3.17) increases with the oxidic fraction of the pour. It should be recognized that the BWRSAR code does not treat the bottom head debris bed as a homogeneous mixture; rather, models provide that melting of oxides can be occurring in the center of the bed at the same time that melting of metals is continuing in cooler regions near the upper surface of the bed and near the vessel walls. In addition, molten metal formed in the upper part of the bed will become superheated as it flows downward through the hotter center of the bed on its way out of the vessel.

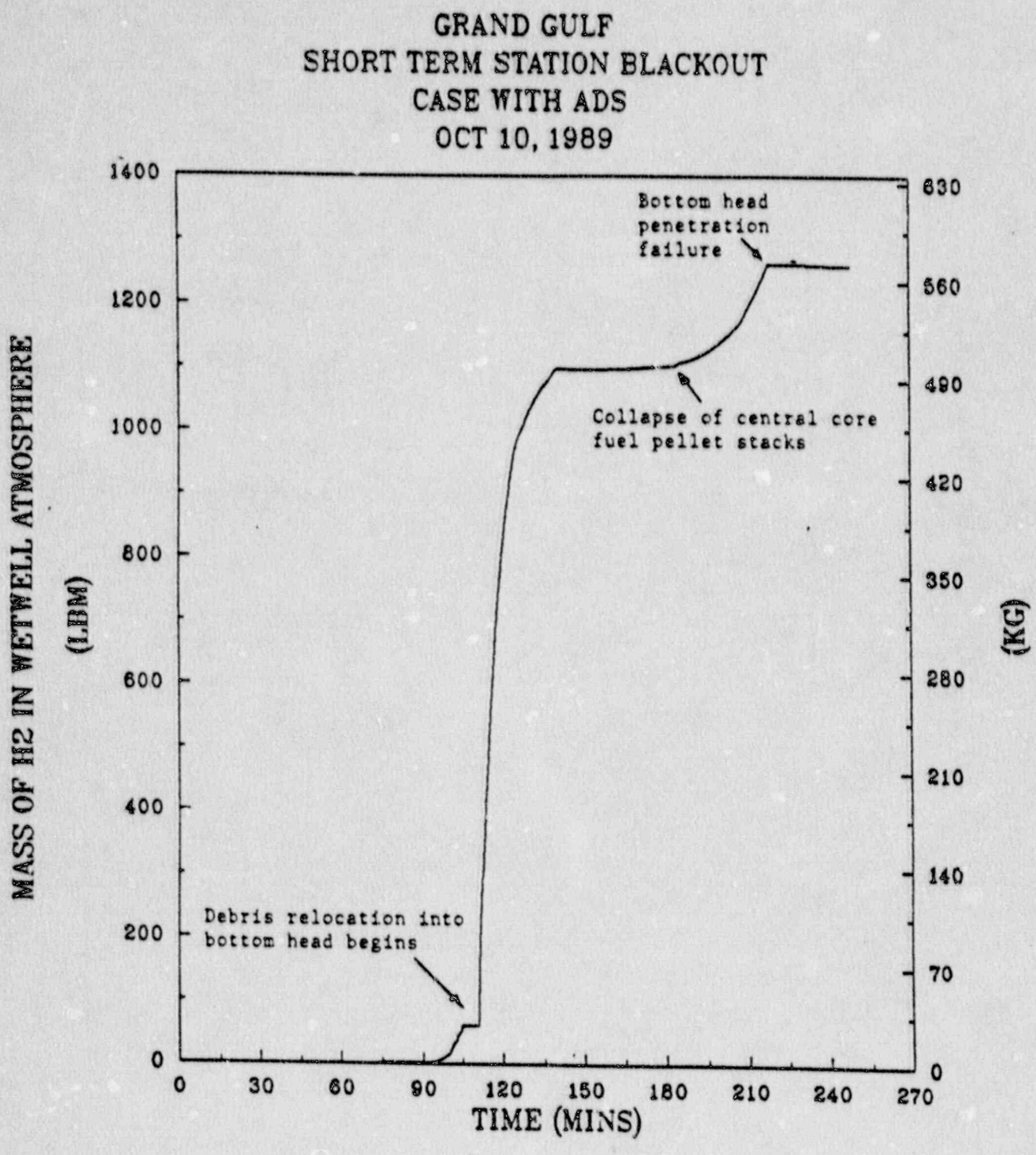

Fig. 3.12. Mass of hydrogen in wetwell atmosphere for the BWR-6/Mark III short-term station blackout with ADS actuation (simple eutectics).

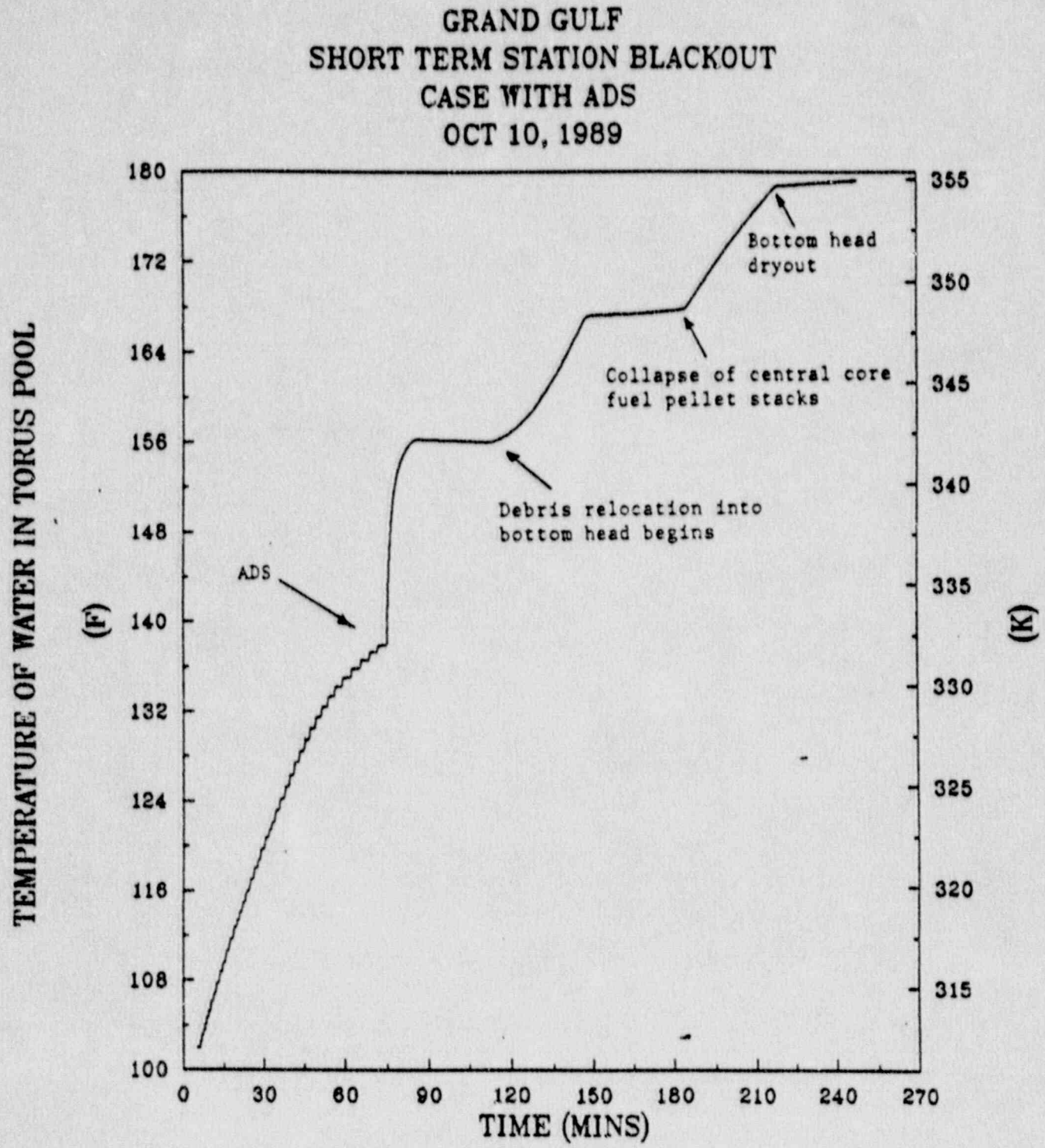

Fig. 3.13. Suppression pool temperature for the BWR-6/Mark III short-term station blackout with ADS actuation (simple eutectics).

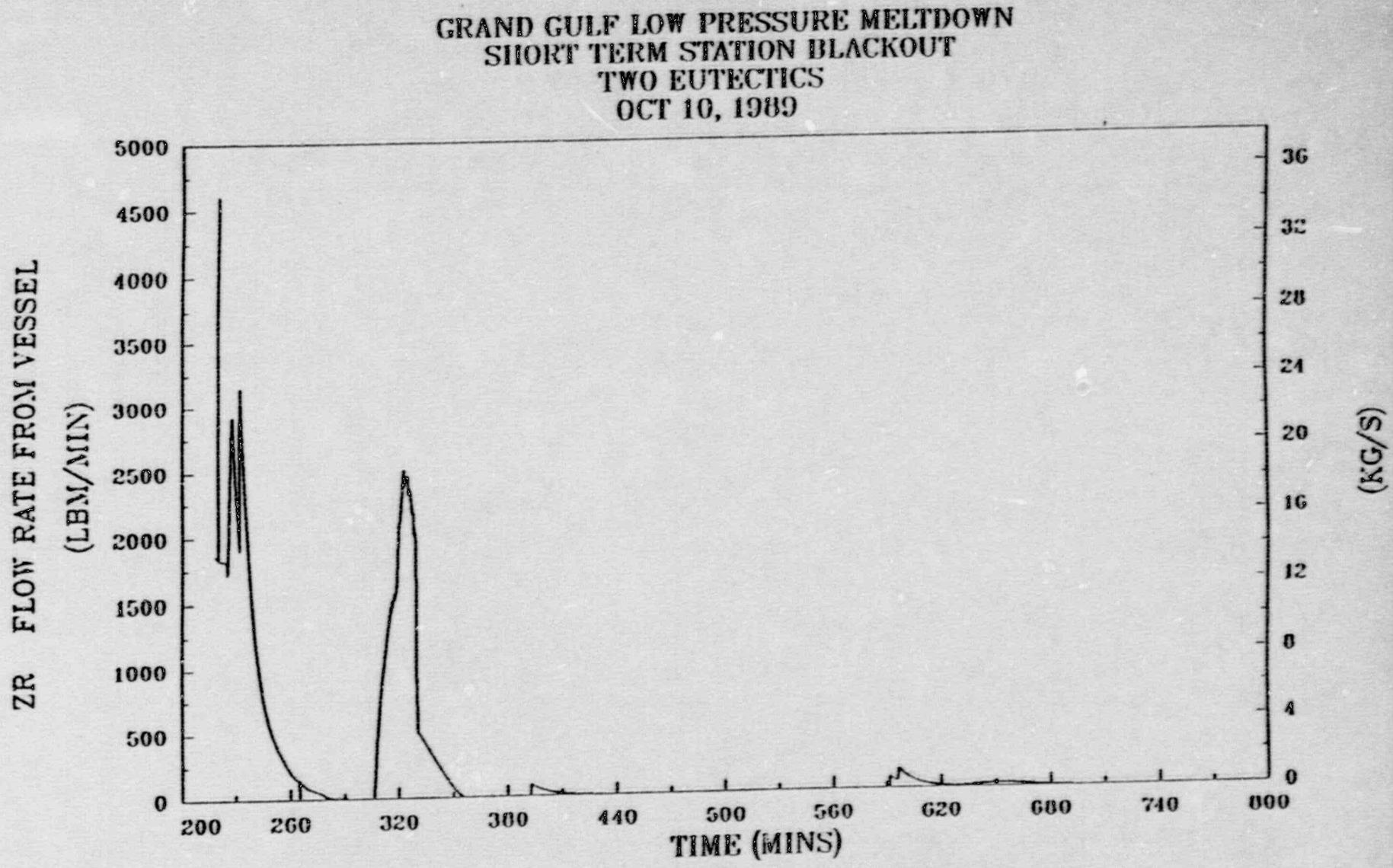

Fig. 3.14. Zirconium flow rate from reactor vessel for the BWR-6/Mark III short-term station blackout with ADS actuation (simple eutectics).

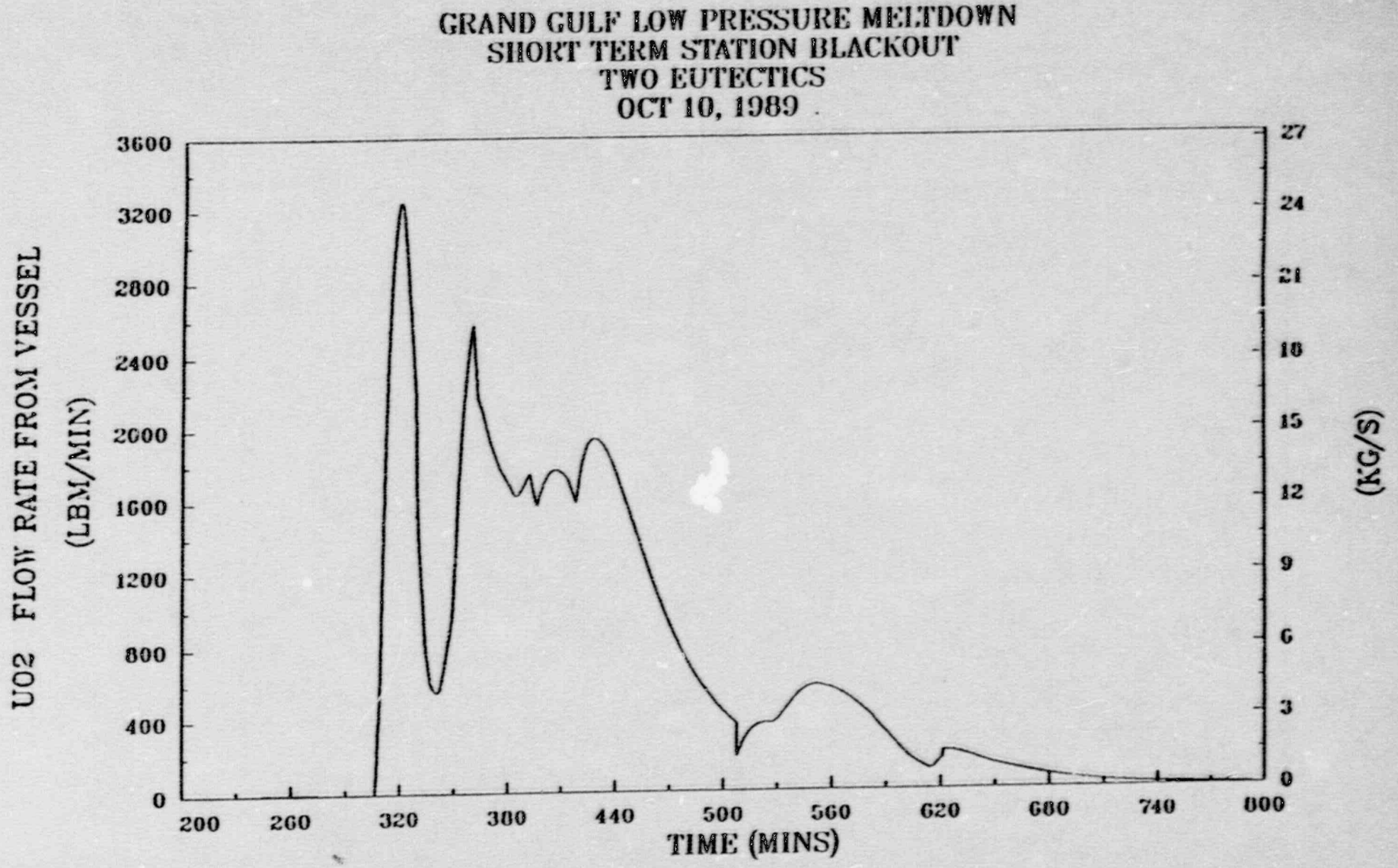

Fig. 3.15. Uranium dioxide flow rate from reactor vessel for the BWR-6/Mark III short-term station blackout with ADS actuation (simple eutectics).

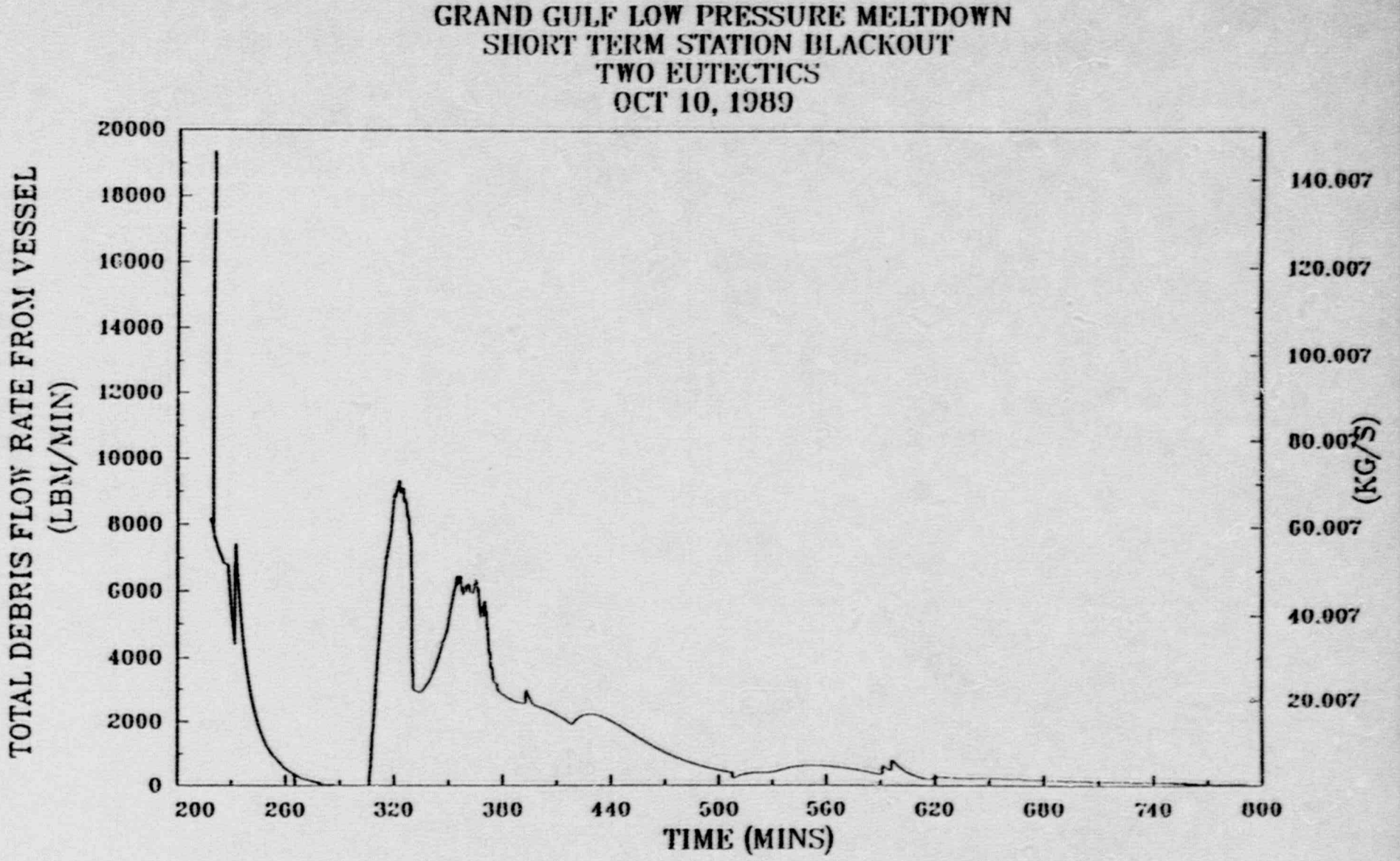

Fig. 3.16. Total debris flow rate from reactor vessel for the BWR-6/Mark III short-term station blackout with ADS actuation (simple eutectics).

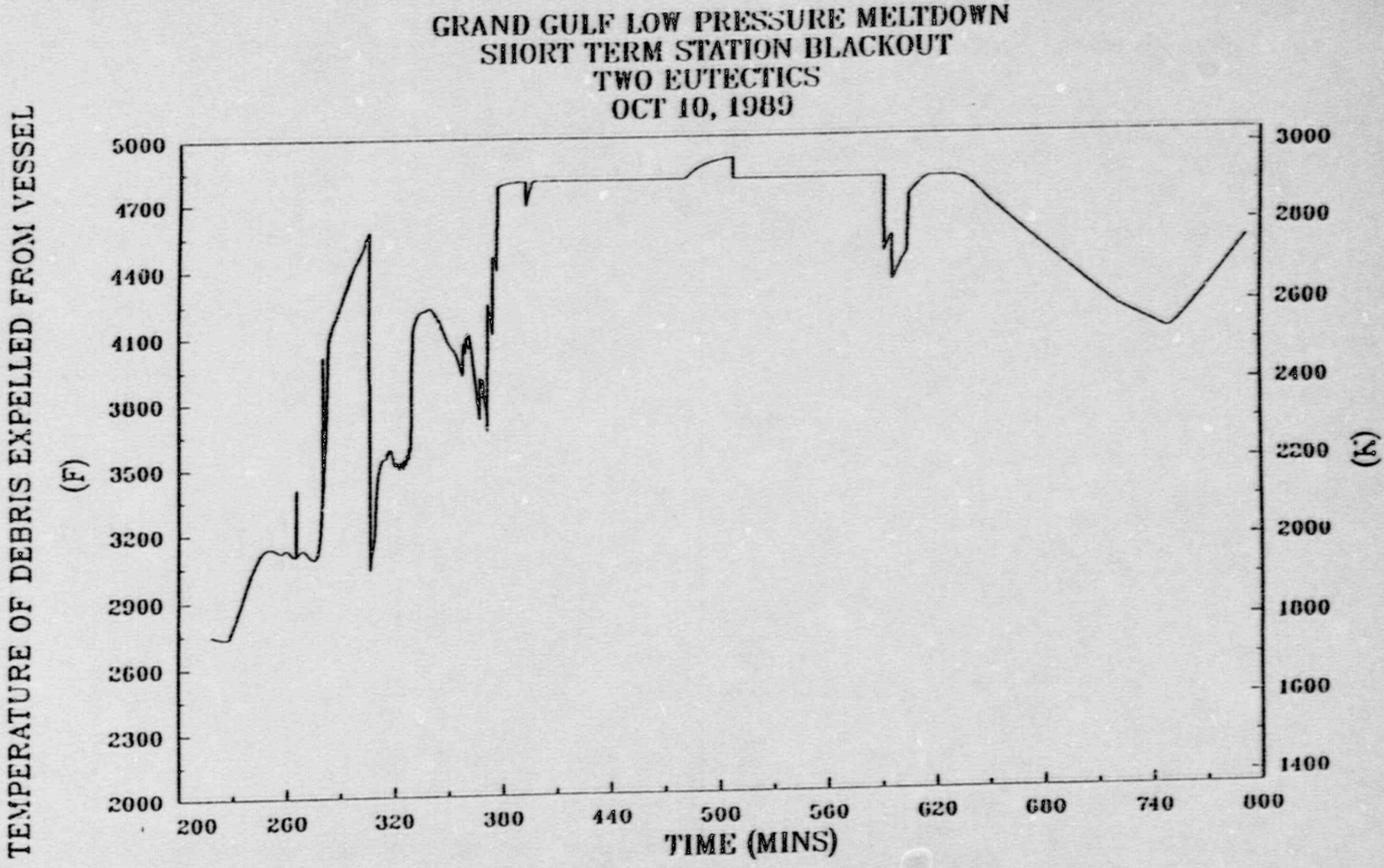

Fig. 3.17. Temperature of debris pours from the reactor vessel for the BWR-6/Mark III short-term station blackout with ADS actuation (simple eutectics).

The integrated mass of material that has left the reactor vessel for the BWR Mark III calculations based upon Grand Gulf is shown as a function of time in Figure 3.18. About 850,000 lbs of debris is predicted to have left the vessel by the end of the calculation; the composition of the released debris is provided in Table 3.4. The decay heat (proportional to the mass of UO_2) included in the exvessel debris is shown in Figure 3.19. It should be noted that the exvessel decay heat is predicted to pass through a maximum at about time 640 min.; subsequently, the reduction of the decay heat with time is greater than the rate at which decay heat is added to the exvessel debris by the release of additional UO_2 from the vessel.

3.3 Mark III Short-term Station Blackout Containment Response to Unmitigated Short-term Station Blackout

3.3.1 Introduction

Mark III containment systems are employed on all BWR-6 plants. These Mark III containments are the only BWR containments that are not inerted. Figures 3.20 and 3.21 are illustrations of two versions of the Mark III containment concept. Figure 3.21 is the Mark III design utilized at the Grand Gulf nuclear plant. The designs differ in that the Grand Gulf approach utilizes a reactor enclosure building as part of the secondary containment system rather than a shield building. Tables 3.5 and 3.6 summarize a listing of typical Mark III primary containment design specifications.

3.3.2 Mark III Containment Design Description

3.3.2.1 Mark III containment design - Perry and River Bend

The containment vessel is a free standing, vertical, cylindrical steel pressure vessel with an ellipsoidal head and a flat bottom steel liner plate. The cylindrical shell has horizontal external stiffeners and is anchored 5 ft into the concrete mat foundation. The containment is a seismic Category I structure. The flat bottom liner plate is approximately 3/4 in. thick and is continuously supported by the concrete mat.

The containment has an inside diameter of 120 ft and is 183 ft in overall height with an internal volume of 1,168,000 ft^3. It is designed to withstand an internal differential pressure of 15 psi, an external differential pressure of 0.8 psi, and an internal temperature of 185°F. The containment vessel surrounds the drywell and suppression pool and forms the primary leaktight barrier to limit fission product leakage during a LOCA. To avoid exceeding the containment design negative pressure, redundant AC-powered vacuum breaker systems are provided to connect the containment volume to the annulus volume bounded by the steel containment and the shield building.

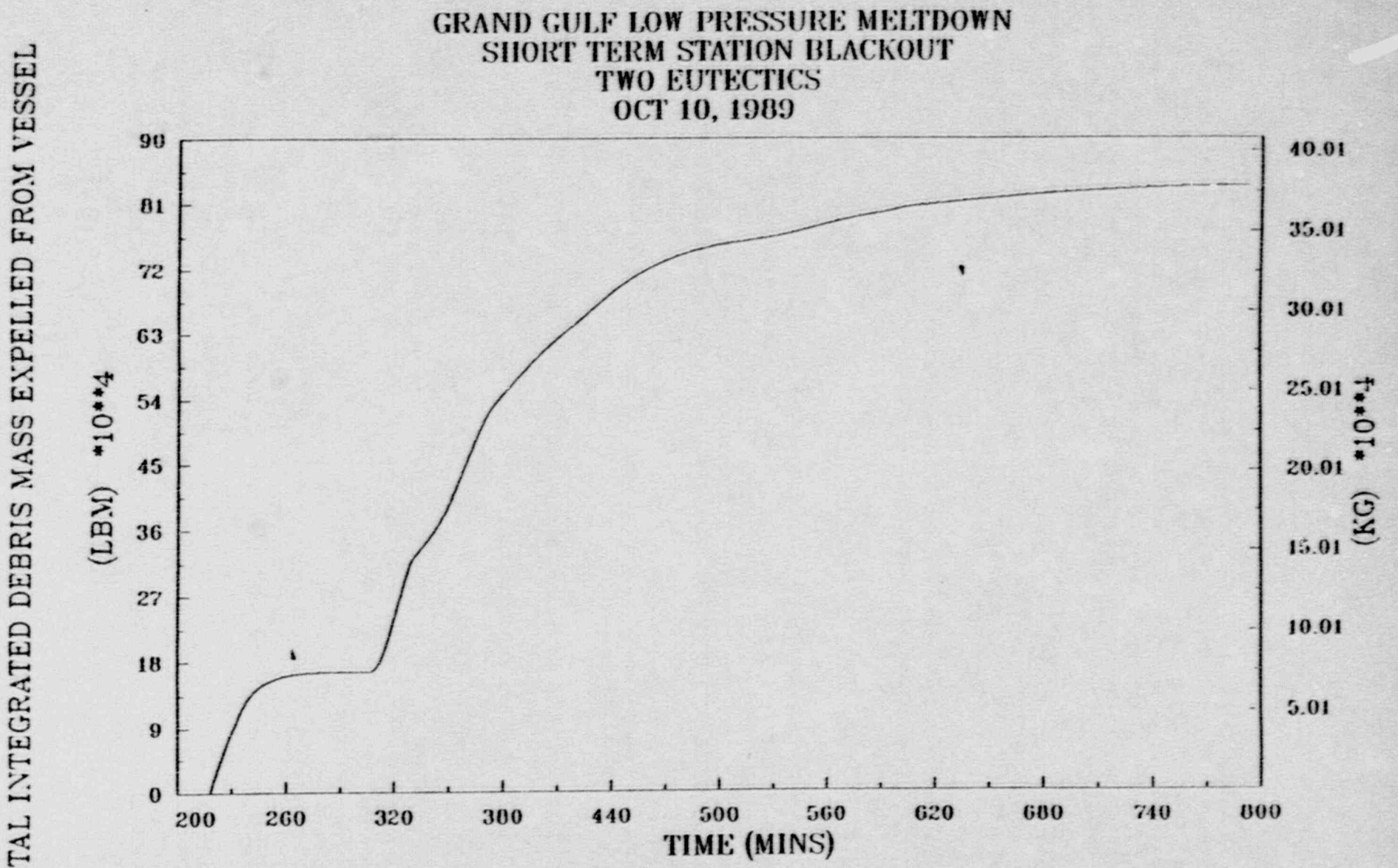

Fig. 3.18. Integrated debris mass expelled from vessel for the BWR-6/Mark III short-term station blackout with ADS actuation (simple eutectics).

Table 3.4. Composition of the debris released from the reactor vessel by the end of the BWR Mark III Calculation

Constituents	Integrated mass (lbs.)
Metals	
Z	105,335
Fe	268,131
Cr	50,216
Ni	22,391
B_4C	672
Total	446,745
Oxides	
ZrO_2	37,773
FeO	195
Fe_3O_4	94
Cr_2O_3	78
NiO	8
B_2O_3	7
UO_2	359,567
Total	397,722
Grand Total	844,467

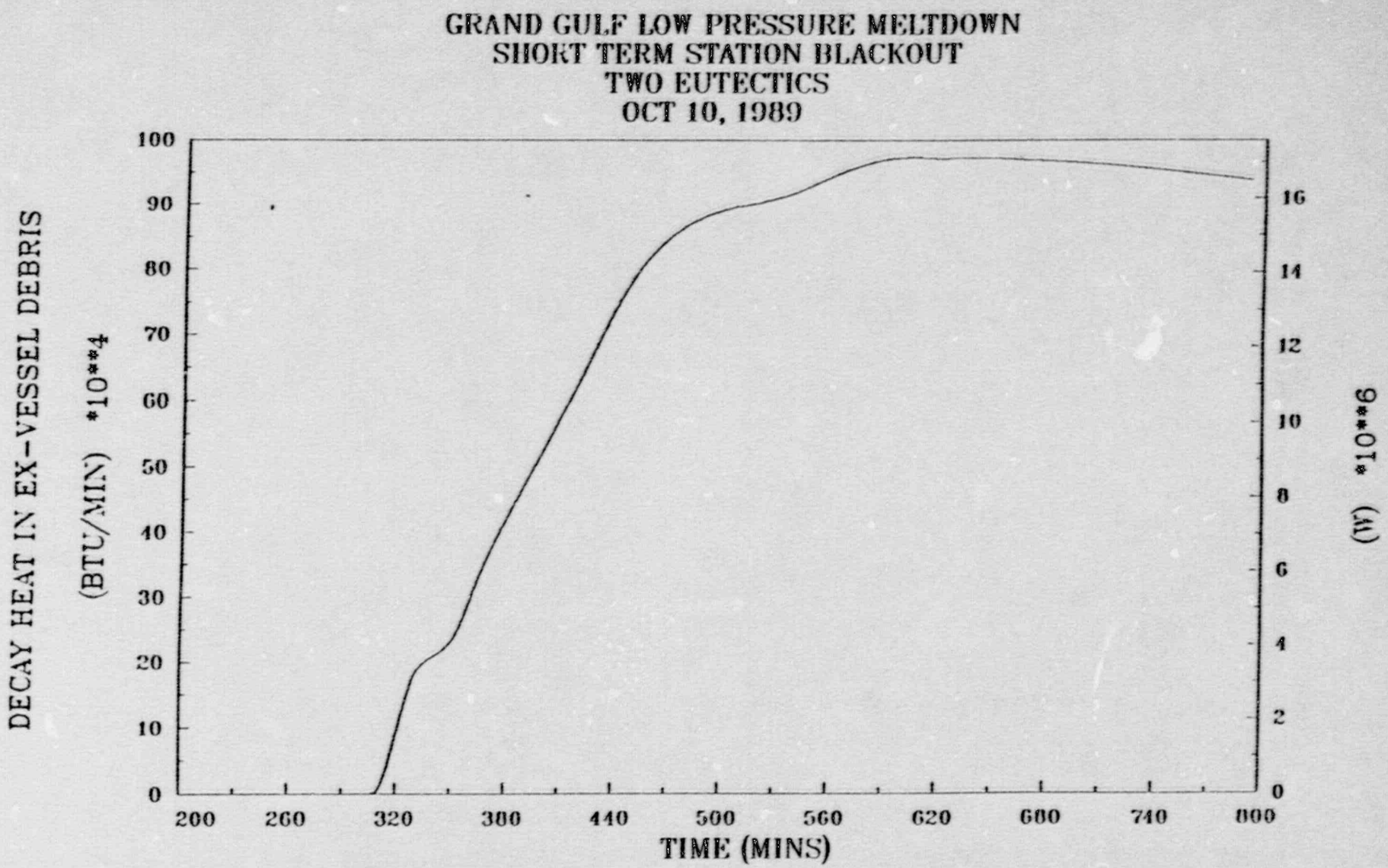

Fig. 3.19. Decay heat in exvessel debris for the BWR-6/Mark III short-term station blackout with ADS actuation (simple eutectics).

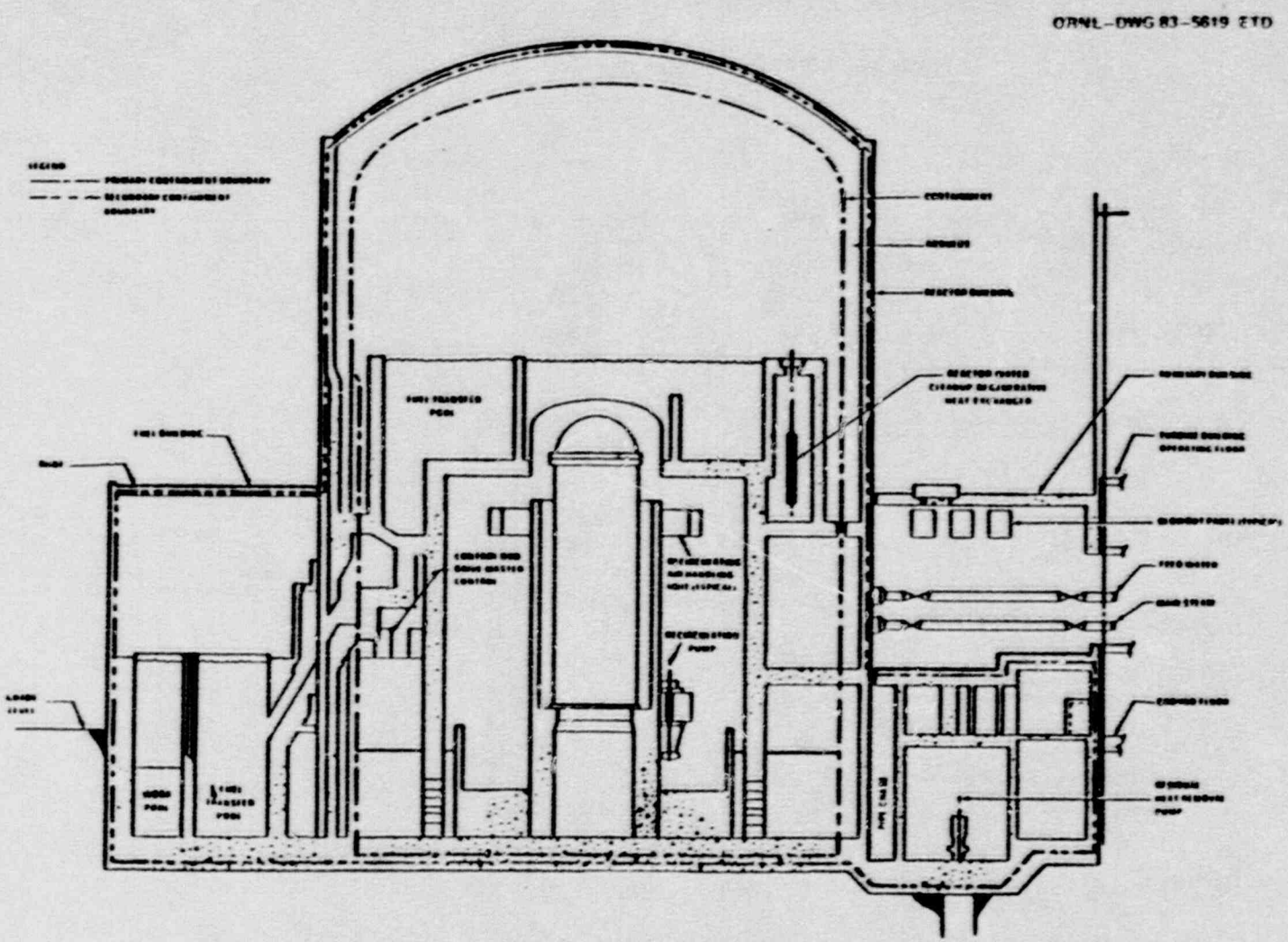

Fig. 3.20. Mark III containment design as employed at River Bend and Perry.

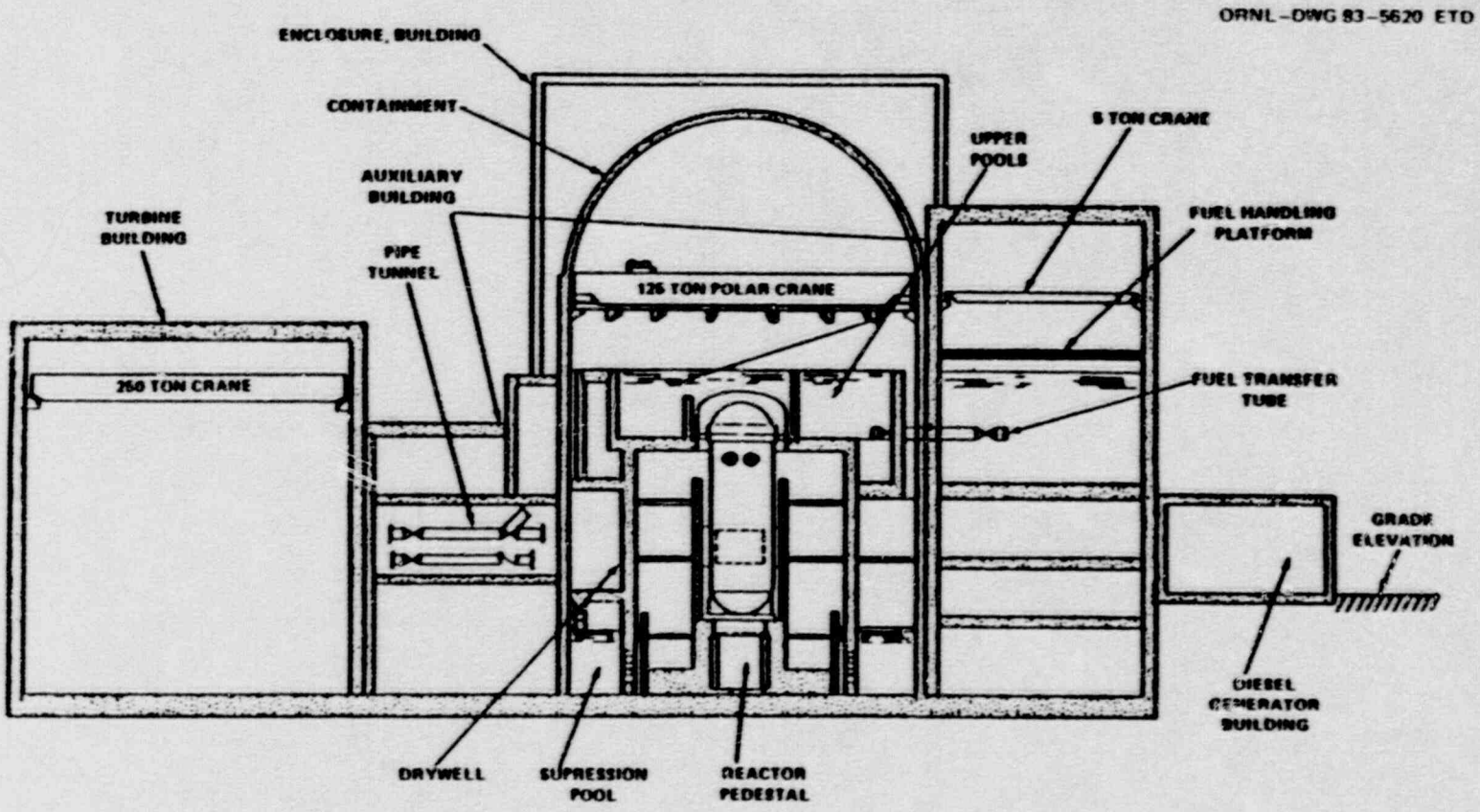

Fig. 3.21. Grand Gulf Mark III containment design.

Table 3.5. Typical MK III containment design characteristics - Perry and River Bend

	Drywell		Suppression chamber
Internal design pressure, psig	30		15
External design pressure, psid	21		0.8
Design temperature, °F	330		185
Free volume, ft^3	275,000		168,000
Suppression pool water volume, ft^3 (max.)	12,000		120,000
Shield building volume, ft.		400,000	

Table 3.6. Typical MK III containment design characteristics

	Drywell		Suppression chamber
Internal design pressure, psig	30		15
External design pressure, psid	21		3
Design temperature, °F	330		185
Free volume, ft^3	275,000		1,400,000
Suppression pool water volume, ft.	13,000		125,000
Auxiliary building volume, ft^3		3,000,000	
Enclosure building volume, ft^3		600,000	

The containment vessel is free standing and receives no structural support except at the embedment in the foundation mat. Likewise, the containment provides no major structure support. The containment shell has an average thickness of 1 3/4 inch. Major platforms and floors within the containment are supported by the drywell. However, the containment walls do support an overhead 125 ton capacity polar crane, some attached piping such as the containment spray headers, and miscellaneous electrical connections, personnel locks, fans, ladders, and walkways.

Some postulated loss of coolant accidents may require flooding the containment to remove the fuel from the reactor and affect repairs. Although it is anticipated that defueling of the reactor for most accident sequences would be accomplished by the normal procedures and equipment, the containment can be flooded to [illegible] above the top of the active fuel in the core as a contingency [illegible] over undefined damage resulting from a LOCA.

The drywell (Figure 3.22) is a cylindrical reinforced concrete structure with a removable steel head to allow vertical access to the reactor vessel for refueling or maintenance. The drywell is constructed of 5 ft thick reinforced concrete walls and roof, has an inner diameter of 73 ft, a height of 91 ft, and has a volume of 274,500 cubic feet. The drywell is designed for an internal pressure of 30 psi gauge, an external differential pressure of 21 psi, and an internal temperature of 330°F.

Two reinforced concrete walls 4 ft thick and 25 ft high are located across the drywell top slab. These comprise the longitudinal walls of the upper containment pools and serve as the supporting structure for the operating floor and structural stiffeners for the drywell top slab.

The ruppression pool, both inside and outside the drywell, is an open top, steel lined structure. The carbon steel of the containment vessel is clad with stainless steel up to about 1 ft above the normal suppression pool level. This clad provides a maintenance free, easily decontaminated surface and eliminates the need for a protective paint coating. The water used to fill the pool is either condensate or demineralized water. The water is generally air saturated and stagnant, but retains high purity. The suppression pool contains 129,550 ft^3 of water at the low water level. The normal pool level may vary between a depth of about 20.5 ft (high level) and about 20 ft (low level). This condition allows a normal vent submergence of nearly six feet (minimum) and a minimum freeboard height of about 5.5 feet. A weir wall forms the inner boundary of the suppression pool, and is located inside the drywell. The wall is built of reinforced concrete two feet thick and lined with steel plate on the suppression pool side. The weir wall height is 25 feet.

The Mark III arrangement uses horizontal vents to conduct the steam from the drywell during a LOCA to the suppression pool. In the vertical section, the drywell wall is penetrated by a series of 27.5 in. diameter

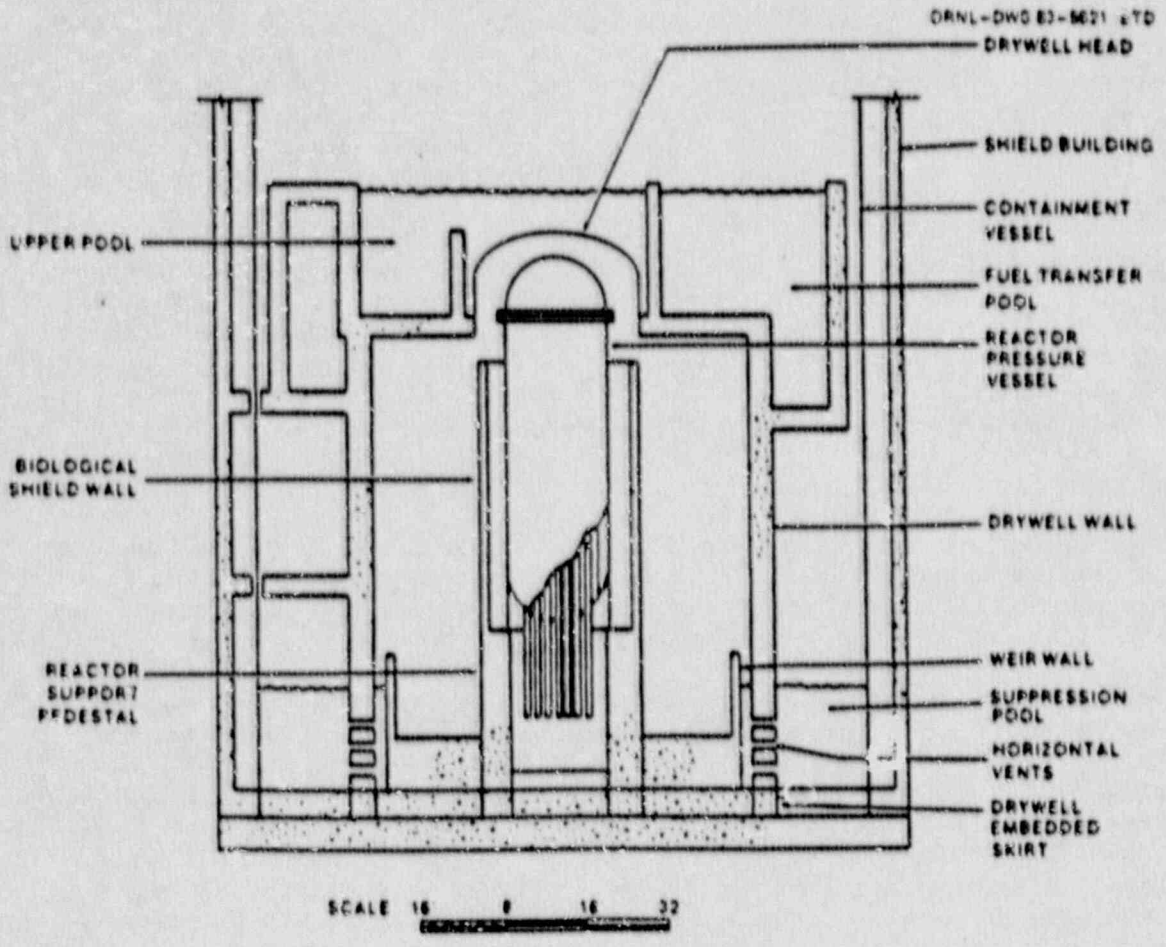

Fig. 3.22. Mark III primary containment structures.

horizontal pipes. There are three rows of these horizontal vent pipes with their centerlines 7.5, 12, and 16.5 ft below the surface of the suppression pool. Any buildup of pressure in the drywell forces the water down in the vent annulus. When the water is depressed to the level of the first row of horizontal vents, steam is vented to the suppression pool. If the pressure in the drywell is high enough, the water in the annulus is depressed further, thereby uncovering the second and third row of vents. In addition to the LOCA steam condensing function, the pool provides a heat sink for SRV and RCIC exhaust steam, and an alternative source of water for the emergency core cooling systems.

The reactor vessel support pedestal is located below the reactor vessel and the reactor shield wall. The pedestal, which is supported by a massive concrete base located on the containment base slab, supports both the reactor vessel and reactor shield wall. The support pedestal is a reinforced concrete circular cylinder about 21 ft high with a constant outside diameter of 32 ft and an inside diameter which varies from about 21 ft at the lower part to about 19 ft at the upper part. It has openings for access, control rod drive piping, and neutron monitoring instrumentation. The vessel support skirt is attached to the pedestal. Due to the recessed floor level inside the pedestal, a cavity is formed which would receive any material leaving the reactor vessel in the event of a melt-through of the lower vessel head.

The reactor shield wall, which rests on the reactor pedestal, has a cylindrical-shape and surrounds the reactor vessel up to the main steam line penetrations. The shield wall is penetrated by numerous pipes which connect to the reactor vessel. Because of the number of piping penetrations, the reactor shield wall is made of composite structural steel and concrete. Both surfaces of the shield wall are lined with carbon steel plate for strength. High-density concrete is placed between the plate surfaces for shielding. The reactor shield wall effectively reduces radiation levels in the drywell to permit inspection and maintenance when the unit is shut down.

The containment upper pool walls are above the drywell and within the containment volume. The outer walls form a rectangular pool which is subdivided by two interior sections. All of these walls are joined to the drywell roof slab which constitutes the pool base slab. The pool is completely lined with stainless steel plates. The pool consists of five regions: a moisture separator storage area; the reactor well; a steam dryer storage area; a temporary fuel storage area; and a fuel transfer region. The overall pool is 36 ft wide, 96 ft long, and 24 ft deep, while the fuel transfer and storage area is 42 ft deep. The upper pool provides the following functions: radiation shielding when the reactor is in operation; storage space for the dryer, separator, and fuel assemblies during refueling; an area for fuel transfer during refueling; and a large volume of water as a suppression pool makeup water source.

The suppression pool makeup system (SPMS) provides additional water from the upper containment pool to the suppression pool by gravity flow during accident conditions. The SPMS piping consists of two lines that penetrate the drywell end of the upper containment pool through the side-walls. The elevation of the pool penetrations limits the volume of water that can be dumped to a 13 ft 7.75 in. thick slice across the entire upper pool surface area.

The upper pool is dumped by gravity flow after opening two normally closed motor operated valves in series on each dump line. The upper pool dumps on receipt of a suppression pool low-low level signal [18 in. below low water level] or 30 min. after receipt of concurrent low reactor vessel level and high drywell pressure signals (i.e., a LOCA signal). The 30-min delay in the LOCA-induced pool dump is implemented by means of a timer, which is tripped on receipt of the LOCA signal.

The secondary containment is the physical boundary which encloses the primary containment boundary, those systems external to the primary containment which would contain reactor coolant after a LOCA, and the areas in which spent fuel is stored and handled. The purpose of the secondary containment is to prevent the uncontrolled ground level release of fission products to the environment in the event of a LOCA or a fuel handling accident. It serves as a dilution and holdup volume for fission products which may leak from the primary containment following an accident. Structurally, this is accomplished by the leak tight design of the secondary containment buildings, which are designed to leak no more than 100% of their contained volume in a 24-hour period at design negative pressure. These buildings are constructed to maintain this leak tight functional integrity in the event of an earthquake.

The external walls of the secondary containment also provide tornado missile protection for enclosed safety related components. The double doors which connect portions of the secondary containment to other areas of the auxiliary building are designed so that one door can always remain closed. During normal operation the secondary containment areas are maintained at a pressure slightly less than atmospheric by the heating, ventilating and air conditioning (HVAC) systems serving these areas. The fuel building and the auxiliary building are maintained at a minimum of 0.325 in. of water below ambient pressure.

The normal exhaust air flow from the secondary containment is to the plant vent exhaust. This exhaust air flow is diverted to the Standby Gas Treatment System (SGTS) during abnormal or emergency conditions. There are, however, potential LOCA fission product leakage paths through the primary containment boundary that could bypass the secondary containment and thus be released to the environment without filtration by the SGTS. These consist of process piping containment penetrations that are routed through or terminated outside the secondary containment areas.

Several containment design features are provided in order to eliminate the potential for secondary containment bypass leakage. A system is

provided to either collect any leakage past the MSIVs or to prevent leakage altogether by providing back pressure downstream of the valves. The feedwater lines are provided with a positive water seal from the Residual Heat Removal (RHR) System to preclude leakage past the feedwater containment isolation valves. The HVAC supply and exhaust ductwork penetrating the containment is provided with three containment isolation valves (two outside and one inside) in which the duct between the two isolation valves outside containment is vented to the annulus.

The secondary containment structural boundaries encompass the shield building-to-containment annulus (hereafter referred to simply as "the annulus"), all of the fuel building except the stairwells and elevator vestibules, and the portions of the auxiliary building housing the emergency core cooling system (ECCS) pumps, the Residual Heat Removal (RHR) System heat exchangers, and the Reactor Water Cleanup (RWCU) System pumps. It encloses the primary containment boundary (except for the reactor building foundation mat, portions of the main steam and feedwater guard pipes and the main steam isolation valves in the steam tunnel), those systems external to the primary containment which would contain reactor coolant after LOCA, and areas in which spent fuel is stored and handled.

The shield building is a 130 ft diameter cylindrical-shaped, conventionally reinforced concrete structure with a shallow domed roof, three-feet thick wall, and an overall height of 197 feet. The radial annulus, the space between the containment vessel and shield building, is five feet wide with a minimum dome clearance of 7.5 ft and a volume of 433,000 ft^3. The walls of the shield building, which encompass the containment vessel, function as a secondary containment barrier, form the annular space for the collection and filtration of fission product leakage from the steel containment vessel, and provide biological shielding for plant personnel and the public. During normal and emergency operations, this annulus space is maintained at a slightly negative pressure relative to atmospheric pressure [approximately minus 5 in. of water] so that any leakage through the shield building or containment vessel will be into this space.

The auxiliary building is located adjacent to the reactor building and opposite the fuel building. It is supported by a reinforced concrete mat. Concrete walls and structural steel members carry vertical loads, provide lateral stability, and afford missile protection. Steel framing and grating platforms provide support to interior equipment compartments. The principal structural requirement of the auxiliary building is the support and protection of the safety and operating systems, equipment, and piping it encloses.

The emergency core cooling system (ECCS) pumps and equipment and Reactor Core Isolation Cooling (RCIC) system equipment are supported at the foundation level of the auxiliary building in watertight compartments fitted with bulkhead doors. The exhaust duct penetrations from these rooms are constructed to prevent flooding of an adjacent compartment if one of the compartments is flooded due to a pipe break. The RHR System

heat exchangers are situated in vertical compartments on either side of the steam tunnel (the compartment through which the main steam lines are routed to the turbines).

The auxiliary building steam tunnel and RHR system rooms are designed to handle the consequences of high energy pipe breaks. The RHR system rooms are designed for a differential pressure of two psi and the associated temperature changes and jet forces. Blowout panels in the steam tunnel walls are provided to relieve pressure following a steam line rupture within the RHR system compartments.

The auxiliary building is divided into zones for ventilation purposes. The zones are necessary because of the possibility of radioactive releases or extreme environments in the secondary containment portions of the building. The ductwork routes air flow from areas of low radioactive levels to areas of potentially higher contamination. Backdraft dampers are provided in the ducts serving areas of high radioactivity levels. A pressure gradient is maintained between areas of low and potentially high radioactivity levels by exhausting more air from areas of potentially high radiation than is supplied. This prevents migration of the radioactive contaminants from the rooms.

The fuel building is the structure located adjacent to the reactor building and opposite to the auxiliary building. The fuel building houses equipment and facilities for receiving, storing, shielding, shipping, and handling fuel. A continuous reinforced concrete foundation mat supports the fuel building. The fuel building is enclosed by concrete walls and a concrete roof which are designed for tornado and missile protection. The central part of the building is occupied by the fuel pool and equipment compartments formed by concrete walls and slabs. Stainless steel liner plates seal the interior pool surfaces. The fuel building personnel and equipment entrances are provided with airtight doors to maintain the leak tightness of the building. The access doors are provided with an electrical system indicating when a door is open. A transfer tube passes fuel from the transfer compartment to the reactor building. The fuel building exhaust fans, the SGTS equipment, and the annulus recirculation/exhaust fan equipment are located in separate compartments within the building.

3.3.2.2 Mark III containment design differences – Grand Gulf

The Grand Gulf nuclear plant incorporates a containment design that differs in several respects from the design employed at Perry and River Bend. The Grand Gulf design consists of an auxiliary building that completely surrounds the lower portion of the concrete containment and an enclosure building that completely surrounds the containment above the auxiliary building roofline.

The containment is a reinforced concrete structure consisting of a flat circular foundation mat, a right circular cylinder, and a hemispherical dome. Its internal surface is completely lined with welded steel plate which forms a leaktight barrier. The containment wall is a right circular cylinder, 3-6 ft thick, with an internal diameter of 124 ft and a height of about 145 feet. The containment dome is a hemispherical shell 2-6 ft thick, with an internal diameter of 124 feet. The containment provides vertical support for a number of intermediate platforms and directly supports a 125 ton polar bridge crane. Two personnel access locks with double, interlocked doors, and one equipment hatch are provided for access into the containment.

There are three vacuum relief systems associated with the Grand Gulf Mark III containment design. The Normal Drywell Vacuum Relief System, consisting of a valved penetration from the containment to the drywell, is provided to relieve a vacuum in the drywell which may occur due to normal temperature and humidity changes in the drywell that cannot be accommodated by the Drywell Cooling System. This is not a safety system and is not connected with the other vacuum relief systems. An interlock is provided through the Drywell Purge System to keep the normal vacuum relief line closed during a LOCA.

The second vacuum relief system is part of the Drywell Purge System. Each drywell purge air compressor discharge line has a vacuum relief line tied into it. This vacuum relief function is provided only after a LOCA. Each of these two vacuum relief lines would draw air from the containment volume and discharge into the drywell to relieve the vacuum in the drywell due to steam condensation following LOCA blowdown. The vacuum breakers in the drywell purge compressor discharge lines open automatically when drywell pressure falls to within one psi above containment pressure.

The third vacuum relief system is the Post-LOCA Vacuum Relief System. This system consists of two separate vacuum relief lines which share a common penetration to the drywell. This vacuum relief function is also provided only after a LOCA and serves to backup the vacuum relief lines associated with the Drywell Purge System. The post-LOCA vacuum relief lines open to draw air from the containment to the drywell when drywell pressure falls 0.5 psi below that of the containment.

The auxiliary building is a reinforced concrete structure with walls several feet thick. The building, which is a multilevel structure, houses both normal and emergency auxiliary systems, the nuclear steam supply system and fuel handling facilities. The normal auxiliary systems include the Residual Heat Removal (RHR) System, Reactor Core Isolation Cooling (RCIC) System, Low Pressure Core Spray (LPCS) System, and Standby Gas Treatment System (SGTS). The building also houses electrical and instrumentation piping penetration rooms; ventilation equipment for the auxiliary building, containment, fuel handling area, and SGTS; electrical equipment such as load centers, motor control centers, and emergency cable trays; and normal and emergency process piping.

The enclosure building is a limited leakage, steel-framed, seismic Category I structure with un-insulated metal siding and insulated roof deck. It completely encloses the portions of the containment above the auxiliary building roof levels and is designed and constructed to limit leakage of radioactive materials into the environment following a loss-of-coolant accident. The structural steel frame is supported solely by struts attached on the containment shell. To maintain the required leakage limits, a flexible seal is provided around the entire periphery of the enclosure/auxiliary building interface. This seal is designed to absorb all anticipated differential seismic movements between the containment and the auxiliary building without loss of the seals' leaktight integrity.

The annulus area between the containment and the enclosure building is maintained at a slightly negative pressure (0.25 in. w.g.) during accident conditions by the Standby Gas Treatment System.

3.3.3 Mark III Containment Failure Modes and Mechanisms

As indicated in Tables 3.5 and 3.6, the design pressure of domestic Mark III containments is +30 psid for the drywell, and +15 psid for the wetwell. The actual containment failure pressures are, however, expected to be significantly higher than the design pressure, and would be plant dependent (since Grand Gulf and Clinton employ a steel-line concrete containment, while Perry and River Bend utilize free-standing steel containments).

Few Mark III containment strength analyses have been documented in the open literature. However, Reference 4 reports the results of a static pressure capability analysis for the Perry plant which yielded an estimated outer containment (wetwell) shell failure pressure estimate of 100 psig. A uniform static internal pressure was used and strain ductility was taken as the failure criterion. The failure was predicted to occur just above the junction of the hemispherical containment head and the cylindrical sidewall. A preliminary dynamic study was conducted to investigate the response of explosively (dynamically) loaded hemispherical heads. Approximate analysis methods were developed, compared to element results, and applied to the containment heads. It was determined that the containment's dynamic resistance for a 500 microsecond pulse is approximately ten times the static strength.

Reference 5 reports the results of an analysis conducted for the Grand Gulf Nuclear Station, which yielded an ultimate static containment pressure capability estimate of 56 psig. The ultimate capacity was defined in this analysis as the pressure at which a general yield state is reached at a critical structural section. This report also indicates that the ultimate pressure capability of the upper containment air lock could be as low as 32.7 psig. Dynamic pressure effects were not considered in the Grand Gulf analyses.

3.3.4 Mark III Containment Model Description

The modeling of the Grand Gulf Mark III containment has been governed by two basic principles:

1. Compartmentalize the building as necessary to represent the actual physical layout,

2. Represent all containment system components (i.e. sprays, vacuum breakers, etc.), even if these components are not operational in the initial cases, so that only minor changes will be required to investigate new scenarios.

The ORNL Mark III containment model employed for these analyses is illustrated in Figures 3.23 and 3.24 (drywell and wetwell, respectively). The model consists of 26 control volumes and 35 flow paths. A tabular listing of the control volumes and flow paths is given in Tables 3.7. and 3.8.

A control volume noding scheme was selected for the drywell that duplicated the noding used in the "steam line break in the drywell head area" analysis referenced in the Grand Gulf FSAR. This was done so that previously calculated parameters such as friction factors, loss coefficients, etc., could be employed in the model. The only changes from the FSAR noding scheme are that the cavity is a separate control volume, and nodes 1, 2, and 3 in the FSAR have been combined into a single control volume.

The main criteria used for selecting the noding scheme of the wetwell is the physical compartmentalization resulting from the equipment, gratings, and solid concrete structures present at various elevations within the outer containment. Thus, the control volumes represent the physical space between floors in the wetwell. Various smaller rooms such as the main steam tunnel, filter demineralizer rooms, etc., are modeled as separate control volumes. Since the FSAR had analyzed a steam line break in each of these areas, flow path characterization information from the FSAR could be used directly in the MELCOR model.

The large, relatively open area above the upper pool poses a difficult modeling problem. There are no floors or other physical structures to subdivide the volume into smaller compartments and the use of a single large control volume would not accurately represent the local conditions near the hydrogen ignitors in the dome area. To resolve this issue, the hemispherical portion of the containment was modeled as a single control volume. The regions directly above the upper pool floor and the annulus between the upper pool support structures and the containment are modeled as concentric cylindrical volumes, the radial area of each corresponding to the physical area of the modeled portion (floor or annulus). The flow paths between these volumes are equivalent to the open air space between each control volume. The goal of this modeling approach is to capture the effects of any natural circulation currents that might enhance hydrogen mixing.

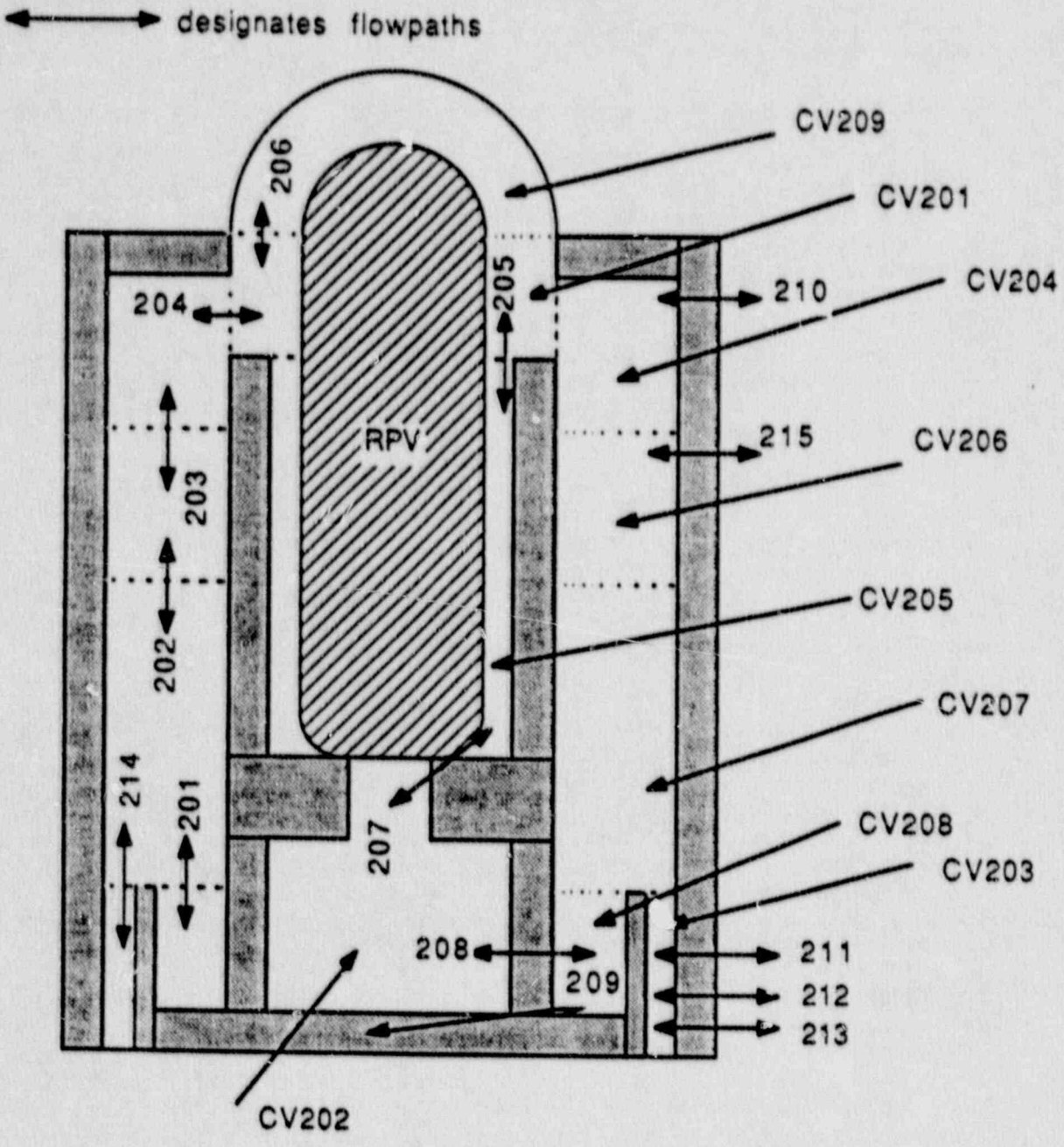

Fig. 3.23. ORNL Mark III containment model (outer containment nodalization).

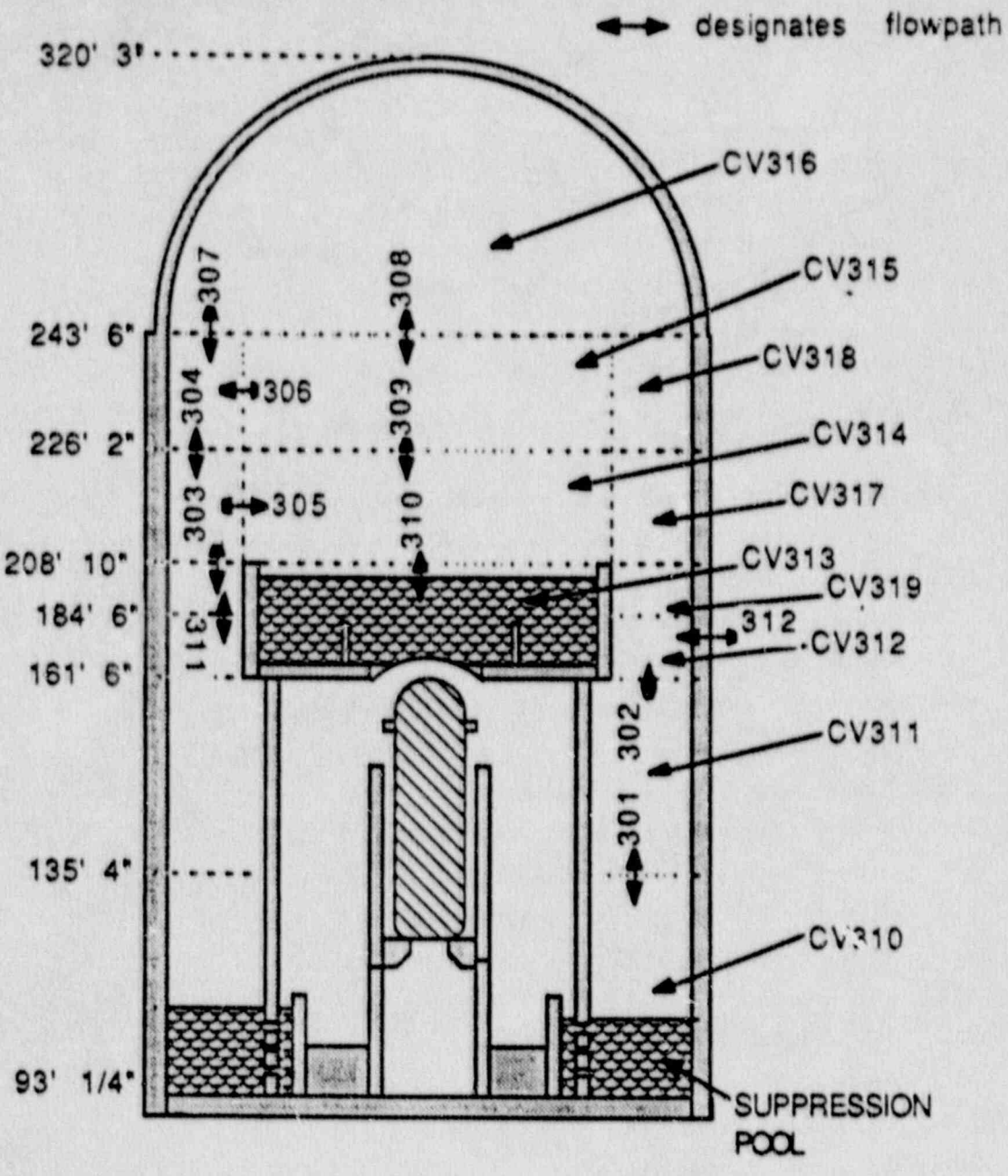

Fig. 3.24. ORNL Mark III containment model (drywell nodalization).

Table 3.7. Mark III containment model control volume

CV No.	Physical description
201	area between top of shield wall and drywell head seals
202	pedestal cavity beneath reactor pressure vessel
203	annulus between weir wall and drywell containment wall
204	area from grating at 161'10" to 180'3"
205	RPV - shield wall annular region
206	area from grating at 147' 7" to 161'10"
207	area from top of weir wall to grating at 147' 7"
208	area from drywell floor to top of weir wall
209	RPV - drywell head annular region
310	suppression pool floor to bottom of concrete floor at 135' 4"
311	wetwell annular region from 135' 4" to 161' 6"
312	drywell-wetwell annular region from 161' 6" to 184' 6"
313	upper pool/ refueling pool
314	wetwell airspace above upper pool (208' 10" to 226' 2")
315	wetwell airspace above upper pool (226' 2" to 243' 6")
316	hemispherical dome airspace
317	wetwell airspace next to containment wall (208' 10" to 226' 2")
318	wetwell airspace next to containment wall (226' 2" to 243' 6")
319	drywell-wetwell annular region from 184' 6" to 208' 10"
320	holding pump room
321	main steam room
322	RWCU heat exchanger room
323	valve room
324	filter/demineralizer room
325	RWCU pump room
326	RWCU tank room
327	Equipment hatch access from 135' 4" to 208' 10"

Table 3.8. Mark III containment model flow path summary

Flow Path No.	Physical Description
201	vertical flow path from cv 208 to cv 207
202	vertical flow path from cv 207 to cv 206
203	vertical flow path from cv 206 to cv 204
204	horizontal flow path from cv 204 to cv 201
205	vertical flow path from cv 205 to cv 201
206	vertical flow path from cv 201 to cv 209
207	vertical flow path from cavity (cv 202) to weir wall annulus (cv 205)
208	door in cavity pedestal (cv 208 to cv 202)
209	drains from dw floor (cv 208) to cavity sumps (cv202)
210	drywell to wetwell vacuum breakers (cv 204 to cv 312)
211	top row of weir wall vents (cv 203 to cv 310)
212	middle row of weir wall vents (cv 203 to cv 310)
213	bottom row of weir wall vents (cv 203 to cv 310)
214	vertical flow path from weir wall annulus (cv 203) to drywell area (cv 207)
215	drywell to wetwell nominal leakage flow path
301	vertical flow path from suppression pool (cv 310) to dw-ww annulus region (cv 311)
302	vertical flow path in annulus region at elevation 161' 6" (cv 311 to cv 312)
303	vertical flow path in annulus region at elevation 208' 10" (cv 319 to cv 317)
304	vertical flow path from cv 317 to cv 318
305	horizontal flow path from cv 317 to cv 314
306	horizontal flow path from cv 318 to cv 315
307	vertical flow path from cv 318 to cv 316
308	vertical flow path from cv 315 to cv 316
309	vertical flow path from cv 314 to cv 315
310	vertical flow path from cv 313 to cv 314
311	vertical flow path in annulus from at elevation 184' 6" (cv 312 to cv 319)
312	20" vent lines (supply and exhaust) from cv 312 to cv 400 (environment)
313	horizontal flow path between holding pump room (cv 320) and containment (cv 319)
314	vertical flow path between main steam tunnel and RWCU heat exchanger room.
315	horizontal flow path between RWCU heat exchanger room and containment (cv 322 to cv 319)
316	suppression pool dump from upper pool (cv 313 to cv 310)
317	horizontal flow path from valve room to containment
318	horizontal flow path between RWCU demineralizer room (cv 324) and containment (cv 319).
319	vertical flow path between RWCU pump room (cv 325) and containment (cv 312).
320	horizontal flow path between RWCU pump room (cv 325) and RWCU tank room (cv 326)

Table 3.8 (continued)

Flow Path No.	Physical Description
321	Flowpath between equipment hatch (cv 327) and suppression pool (cv 310)
322	Flowpath between equipment hatch and cv 311
323	Flowpath between equipment hatch and cv 312
324	Flowpath between equipment hatch and cv 319
325	Flowpath between equipment hatch and cv 317

Other flow paths of interest include the installed 20" vent lines, the drains from the weir wall annulus floor to the equipment drain sump in the drywell pedestal, the drywell-wetwell vacuum breakers, drywell-wetwell nominal leakage paths, access door to drywell pedestal, holes in the reactor support skirt allowing hot gases from the concrete-corium reactions to rise up to the drywell head region, and the top, middle, and bottom rows of weir wall vents.

Heat slabs were modeled as they presently exist in the plant, with the exception of some of the concrete floors and walls in the miscellaneous rooms around the upper pool. Due to the relatively large cooling capability of the suppression pool, the contribution to steam condensation from these heat slabs would be negligible. Total amounts of miscellaneous steel for both the drywell and wetwell had already been calculated in the FSAR. These heat sinks were equally distributed among the control volumes in the drywell and wetwell, with the exception of the relatively open airspaces above the upper pool.

The insulation surrounding the reactor pressure vessel is neglected since the properties of the insulation (thermal conductivity, etc.,) under accident conditions are unknown. This is a conservative assumption since it allows for maximum heat transfer to the shield wall (and hence, maximum generation of gases from concrete degassing) as well as heating of the drywell atmosphere. The inside surface of the reactor vessel is assumed to be at the temperature of the gas and steam exiting the safety relief valves. The temperature of the inside surface will therefore vary with time, but the thermal lag of the pressure vessel will tend to delay the overall effect on the drywell atmosphere temperature.

The containment ignitors are modeled using the BURN package in MELCOR. The value of minimum H_2 concentration at which the burns occurred from the 1/4 scale Hydrogen Control Owner's Group (HCOG) tests is used as the default hydrogen ignition concentration when the ignitors are operational.

3.3.5 Mark III Containment Response: Short-term Station Blackout With ADS

Due to time constraints, only a few important highlights of the base case run will be discussed in the current draft of this report. (A complete and thorough discussion of all of the results will be provided in the next draft.)

Selected preliminary results from this case are shown in Figures 3.25 through 3.28. As indicated in Figure 3.25, the Mark III containment design pressure (15 psig) is exceeded at approximately 8.3 hrs (30,000 s) into the accident. However, subsequently the containment pressure reaches only about 30 psig at the end of the 24 hr (86,400 s) period represented by the calculation. This is significantly less than

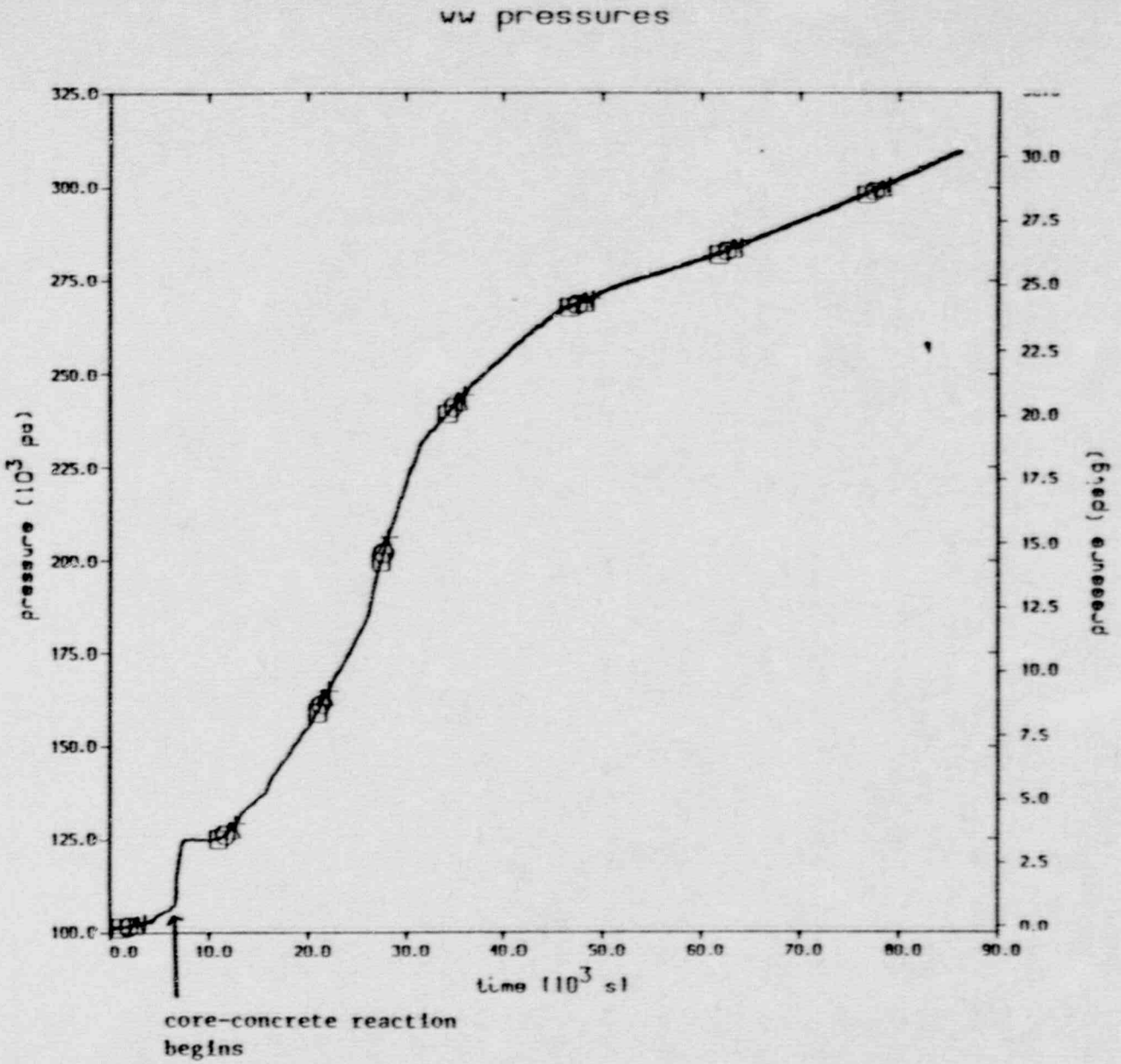

Fig. 3.25. Containment pressure for BWR-6/Mark III short-term station blackout with ADS.

the ultimate static containment pressure capability estimate of 56 psig discussed in Section 3.3.3. From the results of the current calculation, it is conceivable that the containment pressure would never reach the capability estimate, since the total decay heat release rate for the debris decreases steadily after about 11 hrs (40,000 s) into the accident.

To prevent the calculation of artificial hydrogen stratification in the outer containment, the equipment access hatch region for these calculations is represented as a separate control volume, with distinct flowpaths to adjacent control volumes in the drywell-to-wetwell annulus. This allows natural circulation currents to be established that provide rapid mixing of the hydrogen in the wetwell. Figure 3.27 shows how the natural circulation currents have reduced the temperature differences between control volumes to less than 10 degrees F. As shown in Figure 3.28, the hydrogen concentrations in the wetwell control volumes are so nearly identical that the plots lie essentially on top of each other. This agrees with the 1/4 scale tests conducted by the utilities Hydrogen Control Owners Group (HCOG) organization. With no hydrogen ignitors active, the hydrogen concentration reaches a steady state value of 20-25% after approximately 7-8 hrs into the accident.

The suppression pool level never exceeds the weir wall height at any time during the 24 hr transient. After the initial swell due to the reactor vessel depressurization initiated by ADS actuation, the pressure generated by corium-concrete gas release keeps the weir wall annulus level depressed during the rest of the accident sequence. The supression pool level versus time is shown in Figure 3.26.

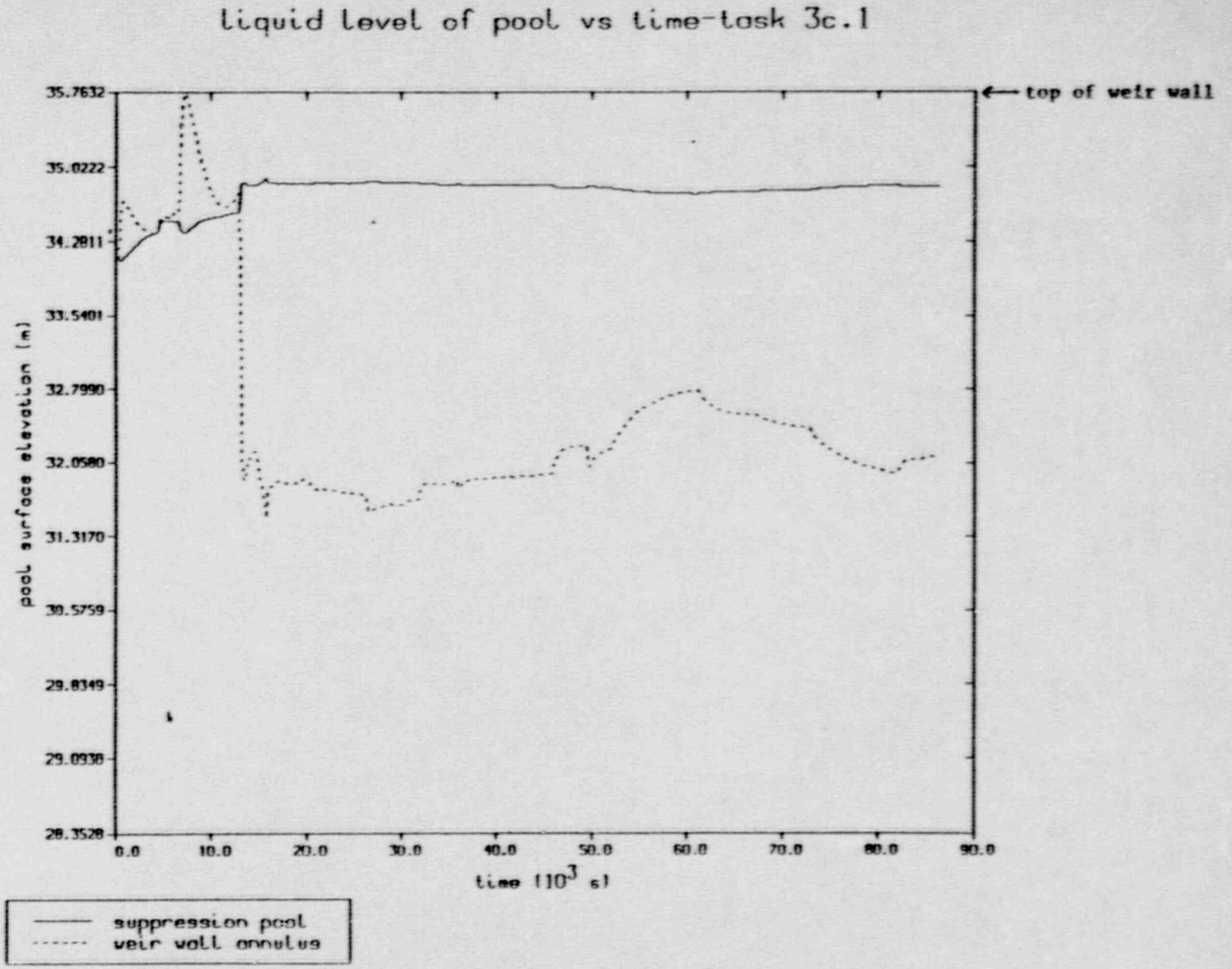

Fig. 3.26. Suppression pool surface elevation for BWR-6/Mark III short-term station blackout with ADS.

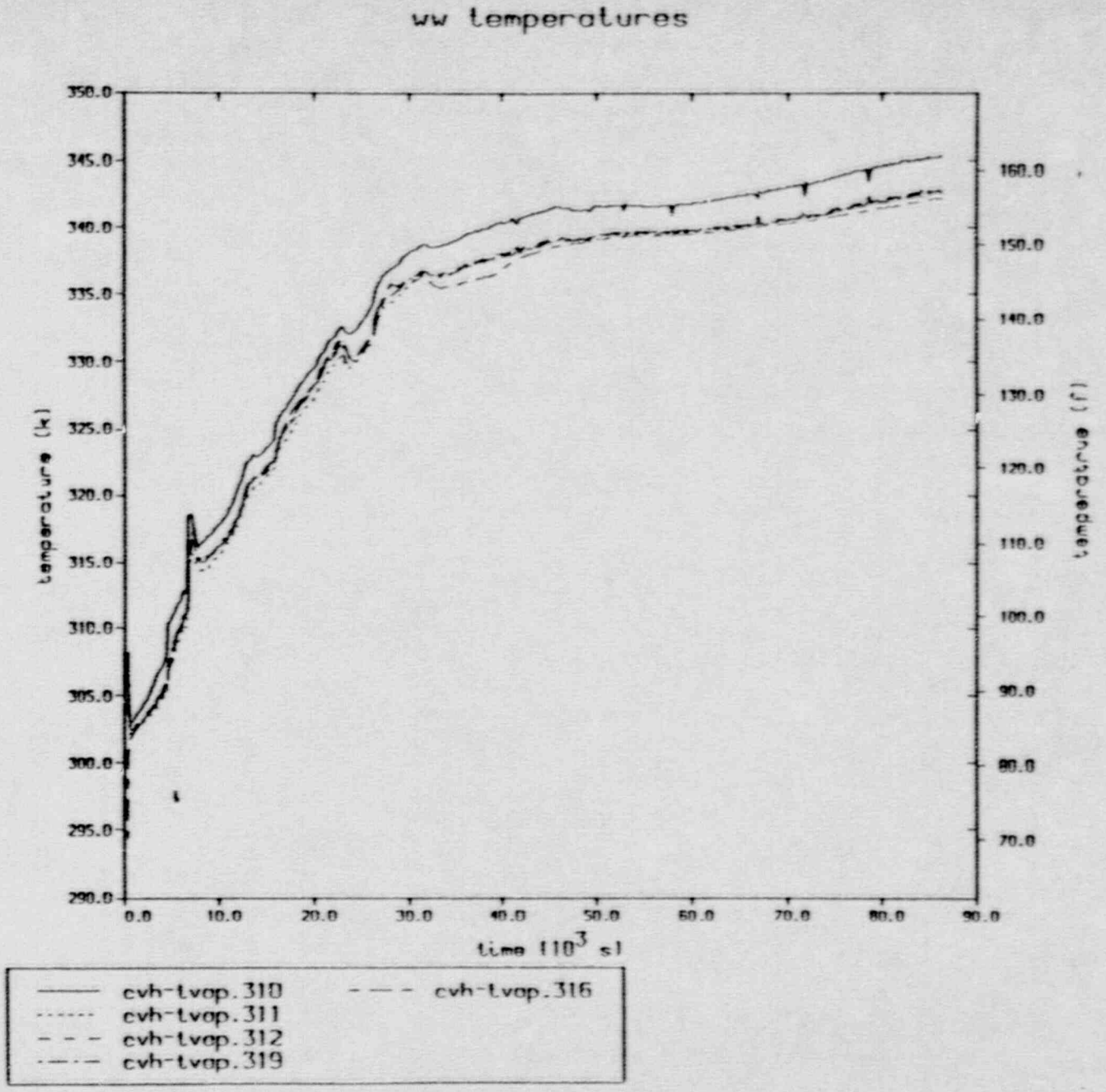

Fig. 3.27. Containment atmosphere temperatures for BWR-6/Mark III short-term station blackout with ADS.

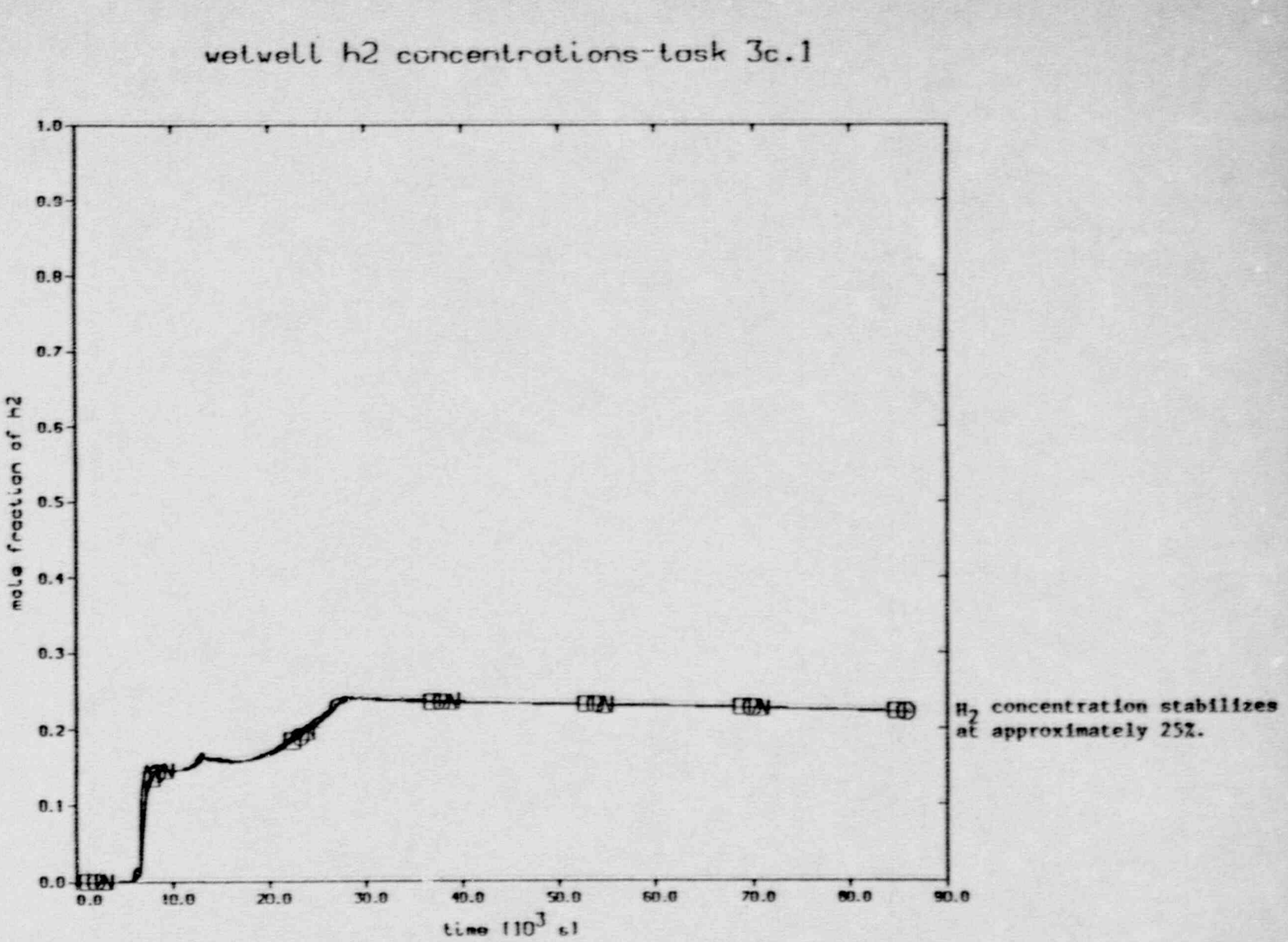

Fig. 3.28. Containment atmosphere hydrogen mole fractions for BWR-6/Mark III short-term station blackout with ADS.

Chapter 3 References

1. S. A. Hodge and L. J. Ott, "Boiling Water Reactor Severe Accident Response (BWRSAR) Code Description and Assessment," NUREG/CR-5318 (to be published).

2. L. J. Ott, Advanced Severe Accident Response Models for BWR Application, Nuclear Engineering and Design 115 (1989) 289-303, North-Holland, Amsterdam.

3. R. M. Harrington and L. C. Fuller, "BWR-LTAS: A Boiling Water Reactor Long-Term Accident Simulation Code," NUREG/CR-3764, February 1985.

4. L. C. Greimann, et al., "Reliability Analysis of Steel Containment Strength," NUREG/CR-2442, Ames Laboratory, Iowa State University, June, 1982.

5. Letter from L. F. Dale, Manager of Nuclear Services, Mississippi Power and Light Company to Mr. Robert L. Tedesco, US NRC, dated June 19, 1981.

APPENDIX A:

MELCOR DEFECT INVESTIGATION REPORTS FORWARDED TO SNL

Several MELCOR code defects and desirable code improvements have been identified via the work described in this report. Some of the defects have been circumvented via expeditious and creative use of existing code user-input options. Some have required extensive code debugging efforts at ORNL and the development and implementation of MELCOR code modifications to address the deficiencies. The MELCOR Code Development Program at SNL has an established and effective mechanism for reporting and documenting code errors, deficiencies, and desired improvements. The mechanism for transmittal and documentation of this information is the MELCOR Defect Investigation Report (DIR). This Appendix presents a compilation of the DIRs submitted to Sandia National Laboratories by ORNL's BWR Mark II and III Parametrics Program researchers since January 1989. DIRs submitted by other ORNL research programs in which MELCOR is being utilized are not included in this compilation. The various MELCOR code versions created at ORNL in conjunction with this work are described in Appendix B. The following paragraphs summarize the contents of the DIRs. Interested readers are encouraged to examine the individual DIRs (included in this Appendix) for additional details.

Six MELCOR Defect Investigation Reports (DIRs) were submitted to SNL during April 1989. The first two DIRs request improvements in MELGEN's ability to detect and flag anomalous External Data File data prior to initiation of the MELCOR run. The third DIR identifies a MELPLT problem which results in confusing and undesirable plot output for cases in which the value of an EDF variable does not change over the time frame of the plot. The fourth DIR identifies an inconsistency in the RN Package's default utilization of heat slabs as settling surfaces for aerosols. The fifth DIR identifies an inconsistency in the CVH Package's handling of pool mass/elevation initialization data. The sixth DIR transmits information relative to ongoing CORSOR improvements at ORNL and desirable improvements in MELCOR's fuel fission product release modeling.

Four DIR's were forwarded to SNL during May 1989. The first DIR requested a code modification to allow the user to specify, via control functions, the debris phase diagram employed within the CORCON module. The second DIR requested a code modification to allow the user to connect an External Data File mass/energy source directly to a flow path. This modification would address a current code limitation which prevents the user from sourcing externally-calculated SRV hydrogen flows directly into the pressure suppression pool. The third DIR requested a code modification to allow the user to select separate failure temperatures for the control blades, core plate, and lower head penetrations. Currently, the user must specify a single, universal failure temperature for these three structures. The fourth DIR identified a code error in which the sensitivity coefficient employed to "tune" the code for correct calculation of CRAY CTSS cpu usage is not correctly implemented.

One DIR was forwarded to SNL during June 1989. This DIR identifies an undesirable logic feature which requires the code to obtain physical properties for mass sources which are not active, resulting in an abnormal code termination. While this problem can be over-ridden via

ingenious use of user-defined control functions, implementation of this correction is desirable to improve the generality of the EDF mass source option. This error has been corrected by SNL in subsequent versions of the code.

One DIR was forwarded to SNL during July 1989. This DIR dealt with an error that MELCOR (VANESA) generates for cases in which there is no UO_2 in the debris pour. This error is not normally encountered in a MELCOR run in which the COR module is used to simulate the core melt process since MELCOR's core melt models typically generate debris pours which always contain some UO_2. A substantial effort was expended in isolating the problem prior to transmitting the DIR to SNL.

One DIR was transmitted to SNL during September 1989. This DIR dealt with an error that occurs in one of the Fuel Dispersal Interactions (FDI) Package routines for cases in which there is no UO_2 in the debris pour.

Six DIRs were forwarded to SNL during October 1989. The first DIR reported another problem in the VANESA subroutine of MELCOR, which results in a code bomb whenever the core-concrete debris contains very small amounts of certain species. The second DIR reports a problem with the FDI routine that results in an abnormal code termination if the integrated amount of any debris constituent (as provided in the EDF file) does not increase continually with time. The third DIR reported a series of problems with the MELPLT (MELCOR plotting package), which generates confusing and misleading plotted output under some circumstances. The fourth DIR reported a limitation in MELCOR's heat slab degassing model that restricts the user's ability to realistically model degassing of laminated or layered structures such as steel-clad concrete structures. The fifth DIR submitted during October reported an error in the code's calculation and plotting of the maximum radial cavity ablation variable in the Cavity Package. The sixth DIR requested that the capability to plot additional CORCON parameters be added to the code.

DEFECT INVESTIGATION REPORT (DIR) NUMBER: -PG. 1/

TITLE: EDF ERROR HANDLING - DETECTION OF CHARACTER DATA CODE:1.8.0

REQUESTOR/ORG.: S. R. GREENE - ORNL, FTS-624-0626 DATE:4/18/89

A. REQUEST:

The EDF package does not correctly flag character data in an EDF file. The following data file was employed:

```
'bwrsar pour'
 0.00000000E+00 0.00000000E+00 0.00000000E+00 0.00000000E+00 0.00000000E+00
 0.00000000E+00 0.00000000E+00 0.00000000E+00 0.00000000E+00 0.00000000E+00
 0.00000000E+00 0.00000000E+00 0.00000000E+00 0.00000000E+00 0.00000000E+00
 0.00000000E+00 0.00000000E+00
 0.60000000E+03 0.78500425E+05 0.13787065E+05 0.13172418E+04 0.50978260E+02
 0.10081224E+02 0.80364700E+03 0.54380165E+11 0.18294596E+04 0.55975560E+01
 0.54241974E+02 0.74000001E+00 0.18000001E+00 0.79999998E-01 0.72291990E+00
 0.19977519E+00 0.77304803E-01
```

The MELGEN execution and error handling looked like this:

```
x180g77 newgin / 10 .21
  input file name containing melgen input
   (carriage return uses melgin)
     opening file newgin for user input
 $*$*$  70 - error -maximum record size exceeded
 file in error is sarpour
 ('file name = ',a)
               ^
 called by SQTCBK   at 00776652d (line    3)
 called by QIOERR   at 00641312d (line  240)
 called by $IOERP   at 00403604c
 called by $WFF     at 00334361d (line  240)
 called by QWRITE   at 01257477d (line  437)
 called by XERRORM  at 00776313a (line   26)
 recursive traceback
 the current dropfile name is    +x180g$b
x180g77  ctss time    40.346     seconds
cpu=    7.624   i/o=   14.463   mem=   18.260
```

The same file was accepted after the first line ('bwrsar pour') of the file was deleted.

Can the EDF error handling routine be modified to detect and correctly flag this error ?

REQUEST BASIS/.....	CHANGES REQUIRED/.....	SEVERITY._____
E = error	N = none	MIN = minor
N = new	C = coding	MED = medium
R = revised feature	D = documentation	MAJ = major
O = other	I = input deck	

DEFECT INVESTIGATION REPORT (DIR) NUMBER: -PG. 1/ /

TITLE: EDF Doesn't Detect Decreasing Time Values CODE:1.8.0

REQUESTOR/ORG.: S. R. GREENE - ORNL, FTS-624-0626 DATE:4/24/89

A. REQUEST:

The MELGEN EDF input editor does not detect and flag the situation in which an EDF contains decreasing time values. MELCOR will not flag the situation either if the calculation is terminated prior to reaching the point in time at which the decreasing time value occurs.

REQUEST BASIS/.....CHANGES REQUIRED/.....SEVERITY._____

E = error	N = none	MIN = minor
N = new	C = coding	MED = medium
R = revised feature	D = documentation	MAJ = major
O = other	I = input deck	

STEP	PAGES	BY	DATE	CK'D	DATE	APPR	DATE
A. Request	1						
B. Diagnosis							
C. Plan							
D. Changes							
E. Release							

DEFECT INVESTIGATION REPORT (DIR) NUMBER: -PG. 1/ 3

TITLE: MELPLT/EDF Interface CODE:1.8.0

REQUESTOR/ORG.: S. R. GREENE - ORNL, FTS-624-0626 DATE:4/27/89

A. REQUEST:

MELPLT has trouble plotting a variable read in from EDF, when the ordinate of the data does not change over the time frame of the plot. There is no problem with the plot when IDENTICAL data is input to MELCOR via a Tabular Function.

The first attached plot displays the MELPLT results for the case where a Tabular Function was employed to input data for the temperature of an external mass source to the CVH Package. The temperature (in the Tabular Function) of the material was variable with time, but was constant at 557.0 K over the duration of this plot. The plot is OK. The second plot illustrates the results rendered when the same data is input as an EDF file. There is no range on the ordinate axis (557.000 to 557.000) and the plot oscillates back and forth between the upper and lower boundary.

This should be corrected, since (I would think) it would not be an uncommon desire to plot results over a selected time period in which EDF parameter values would not change.

REQUEST BASIS/.....	CHANGES REQUIRED/.....	SEVERITY._____
E = error	N = none	MIN = minor
N = new	C = coding	MED = medium
R = revised feature	D = documentation	MAJ = major
O = other	I = input deck	

STEP_____	PAGES	BY	DATE	CK'D	DATE	APPR	DATE
A._Request	1						
B._Diagnosis							
C._Plan							
D._Changes							
E._Release							

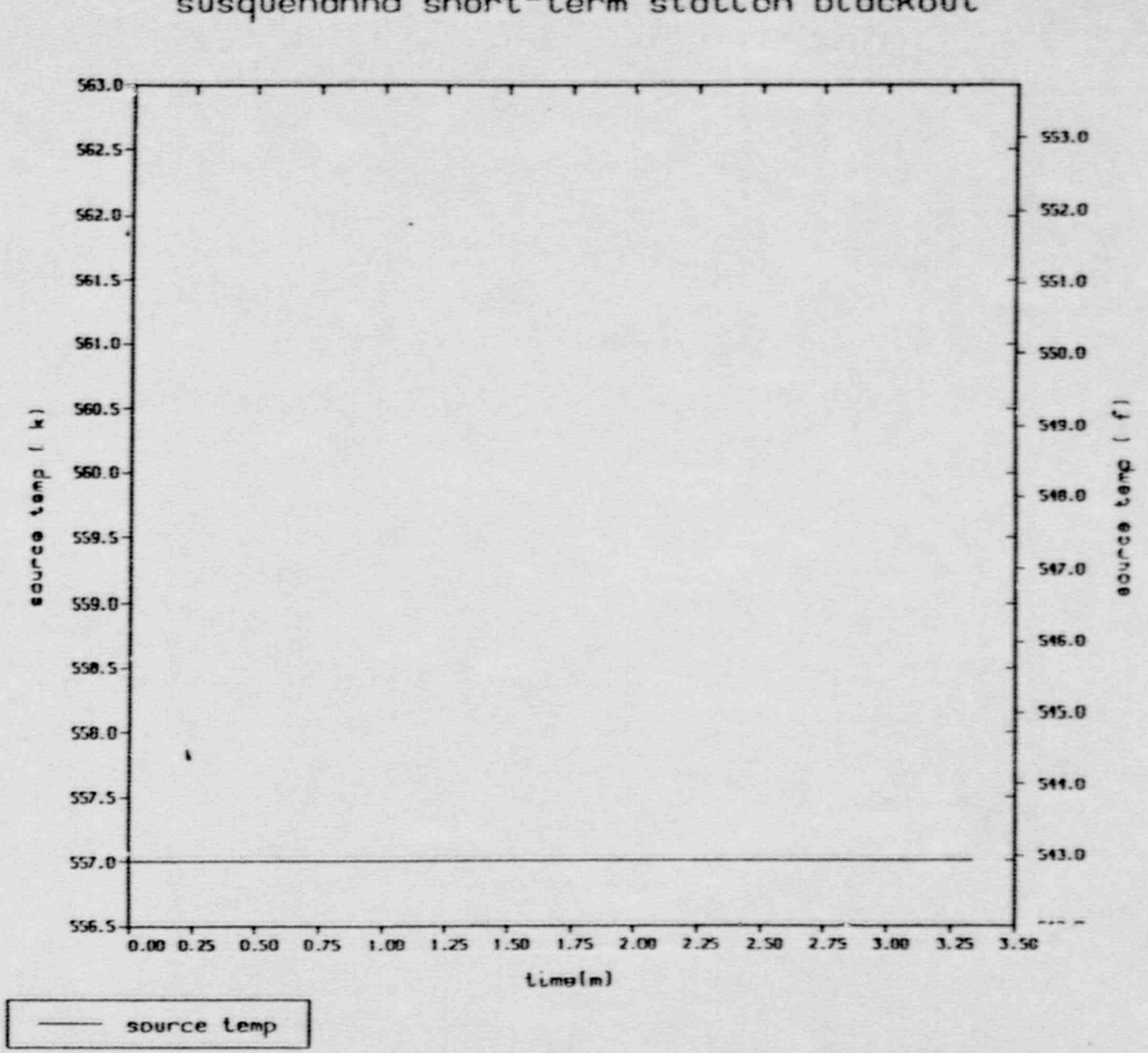
susquehanna short-term station blackout
source temp (k)
source temp (f)
563.0
562.5
562.0
561.5
561.0
560.5
560.0
559.5
559.0
558.5
558.0
557.5
557.0
556.5
553.0
552.0
551.0
550.0
549.0
548.0
547.0
546.0
545.0
544.0
543.0
0.00 0.25 0.50 0.75 1.00 1.25 1.50 1.75 2.00 2.25 2.50 2.75 3.00 3.25 3.50
time(m)
source temp

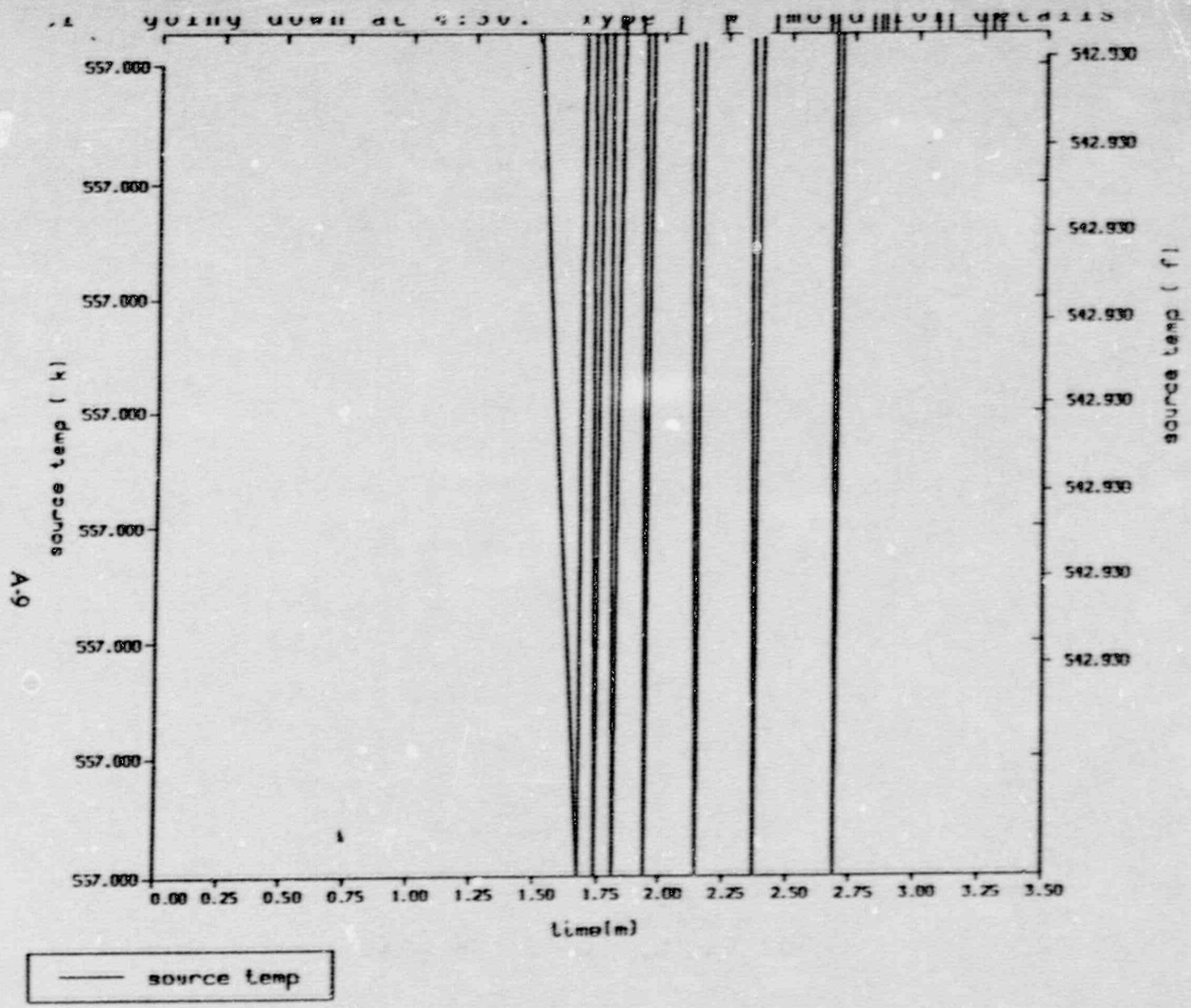
557.000
557.000
557.000
557.000
557.000
557.000
557.000
source temp (k)
542.930
542.930
542.930
542.930
542.930
542.930
542.930
source temp (f)
0.00 0.25 0.50 0.75 1.00 1.25 1.50 1.75 2.00 2.25 2.50 2.75 3.00 3.25 3.50
time(m)
source temp

DEFECT INVESTIGATION REPORT (DIR) NUMBER: -PG. 1/2

TITLE: Inconsistent RN & HS Package Treatment of Surfaces CODE:1.8.0

REQUESTOR/ORG.: S. R. GREENE - ORNL, FTS-624-0626 DATE:4/27/89

A. REQUEST:
The RN Package does not consistently pickup the default horizontal heat slabs as settling surfaces. Example MELGEN input:

```
cv40000     'wetwell cavity'    2    2    3
cv40001     0    0
cv400a0     3
cv400a1     pvol    109006.      rhum    .95    * 15.81 psia
cv400a2     tatm    307.83         tpol   324.11
cv400a3     zpol    204.52
cv400a4     mass.2   0.0
cv400a5     mlfr.4  0.0          mlfr.5   1.0      mlfr.6   0.0
cv400a6     mlfr.7  0.0          mlfr.8   0.0
cv400b1      197.5          0.0   *  648'
cv400b2      213.5124        447.7  *  703'11" - 3.5' = 700.42 = 213.5124 m
*                                   *  pedestal ID = 19'7"
*
*hs40001xnn   wet  well inpedestal   floor
*
hs40001000  12  1  1  0
hs40001001  'ww inped floor'
hs40001002  197.5  0.0  *elevation=648'
hs40001003  1.0
hs40001100  40101  1  0.0 * slab geometry
hs40001200  40101
hs40001300  0
hs40001400  1  400  'ext'  0.0  0.0
hs40001500  27.98  27.983  2.9845 * floor dia. = 19'7" (5.97 m)
hs40001600    0  -400
hs40001800  -1
hs40001801  294.26  11       * room temperature  =  70f
hs40001802   285.8   12      *  average  room temperature=55
```

CONTINUED

REQUEST BASIS/.....CHANGES REQUIRED/.....SEVERITY._____

E = error	N = none	MIN = minor
N = new	C = coding	MED = medium
R = revised feature	D = documentation	MAJ = major
O = other	I = input deck	

STEP	PAGES	BY	DATE	CK'D	DATE	APPR	DATE
A. Request	1						
B. Diagnosis							
C. Plan							
D. Changes							
E. Release							

The input for heat slab 40001 is accepted by the heat slab package, but rejected by the RN package as a valid settling surface. The following MELGEN diagnostic file is generated:

```
 error - no flow through or horizontal heat slab for volume   400

    rnl package error in pass 2

   message from subroutine meggdb
   error encountered in generate pass 2 - no restart file written
```

The problem is eliminated by introducing an RNDS card for heat slab 40001:

```
rnds001      40001     lhs       floor
```

Why is this slab not accepted as a valid settling surface ?

DEFECT INVESTIGATION REPORT (DIR) NUMBER: -PG. 1//

TITLE: CVH Pool Mass/Elevation Specification CODE:1.8.0

REQUESTOR/ORG.: S. R. GREENE - ORNL, FTS-624-0626 DATE:4/27/89

A. REQUEST:

I recently had a case in which the following CVH cell input was utilized:

```
cv40000     'wetwell cavity'    2    2    3
cv40001     0    0
cv400a0     3
cv400a1     pvol    109006.      rhum    .95    *  15.81 psia
cv400a2     tatm    307.83         tpol   324.11
cv400a3     zpol    204.52
cv400a4     mass.1  0.0          mass.2   0.0
cv400a5     mlfr.4  0.0          mlfr.5   1.0      mlfr.6   0.0
cv400a6     mlfr.7  0.0          mlfr.8   0.0
cv400b1      195.022           0.0   *  648'
cv400b2      213.5124        447.7   *  703'11" - 3.5' = 700.42 = 213.5124 m
*                                    *  pedestal ID = 19'7"
```

Notice that this input contains both a "zpol" and a "mass.1" input, and that the two values are inconsistent.

MELGEN accepted the input and (as I had intended) initilized the pool elevation at 204.52 m. The mass.1 input (which I had forgotten to remove when I added the pool) was ignored. When I noticed the faulty input, I was surprised that MELGEN did not flag the use of both zpol and mass.1 for the same volume, and (failing that) that the code did not over-ride the earlier zpol input with the latter mass.1 input.

MELGEN should be modified to flag the use of any combination of zpol, vpol, and mass.1.

REQUEST BASIS/.....	CHANGES REQUIRED/.....	SEVERITY._____
E = error	N = none	MIN = minor
N = new	C = coding	MED = medium
R = revised feature	D = documentation	MAJ = major
O = other	I = input deck	

STEP_____	PAGES	__BY__	_DATE_	_CK'D_	_DATE__	_APPR_	_DATE_
A._Request	1						
B._Diagnosis							
C._Plan							
D._Changes							
E._Release							

DEFECT INVESTIGATION REPORT (DIR) NUMBER: -PG. 1/15

TITLE: Improved CORSOR Modeling CODE:1.8.0

REQUESTOR/ORG.: S. R. GREENE - ORNL, FTS-624-0626 DATE:4/27/89

A. REQUEST:

Recent ORNL fission product transport work have shown convincingly that all of the various CORSOR release rates for the volatile fission products are a factor of 3 or 4 too high. I have attached a short paper by Dick Lorenz which describes our latest information regarding fuel fission product release rates and the CORSOR modifications required. ORNL is currently working on an improved version of CORSOR.

I have also attached a copy of a plot Dick prepared for Steve Hodge, which illustrates vividly the difference between present CORSOR fission product release rates for cesium, and the release rates predicted by the latest (Booth diffusion) model currently under development. "T/100" is the temperature in K divided by 100 (for a transient recently predicted by BWRSAR). The HODGE values represent BWRSAR's prediction of volatile release for this same transient. The Booth different most significantly from the current CORSOR values for low burnups, but are still significantly different for high burnups.

I thought you should be aware of this information. I would be happy to arrange for discussions between Dick Lorenz, Tony Wright, and others, if you wish to discuss this further.

REQUEST BASIS/.....	CHANGES REQUIRED/.....	SEVERITY._____
E = error	N = none	MIN = minor
N = new	C = coding	MED = medium
R = revised feature	D = documentation	MAJ = major
O = other	I = input deck	

STEP_____PAGES	__BY__	_DATE_	_CK'D_	_DATE__	_APPR_	_DATE_
A._Request____1						
B._Diagnosis						
C._Plan						
D._Changes						
E._Release						

CORSOR - History and Status
R. A. Lorenz
3/3/89

CORSOR is the common name for the NRC computer program used to calculate fission product, structural material, and control rod material releases from reactor cores during severe accidents. It is based on the "fractional release rate model" first used in NUREG-0772 (1981), and is based on the equation F = 1-EXP(-k(dt)), where F is the fraction of current inventory released, k is a release-rate coefficient (fraction/min), and dt is the time interval (min). The release coefficient, k, is different for most fission product, structural material, and control material elements and has a strong temperature dependence. A dependence of k on atmosphere (oxidizing vs reducing) for some elements has been long recognized but is used only for tellurium (retention of Te by unoxidized cladding) in response to an ORNL review, NUREG/CR-0027, Vol. 2 (1983). There have been significant changes in the mathematical expressions used to determine k, but the basic release rate equation has been in use since 1981. Discussion of CORSOR is easier by separating it into three parts: 1) volatile fission product release, 2) non-volatile fission product release, and 3) structural and control material release.

Volatile Fission Products. Release rates (the values of k) for the volatile fission products Kr, Xe, Cs, and I have remained essentially unchanged since the 1981 NUREG-0772 version of CORSOR. CORSOR-M (NUREG/CR-4173, 1985) used a convenient and logical 1/T correlation to express the values of k, but the correlation for the volatile fission products was such that there was essentially no difference from previous values of k. This was done because there was not sufficient quantity of new release results to justify a change, and it therefor premitted essentially direct comparison of accident calculation results for volatile fission products regardless of whether the NUREG-0772, CORSOR, or CORSOR-M release rate coefficients were used. Results from the ORNL HI and VI test series now show convincingly that all of the various CORSOR release rates for the volatile fission products are of factor of 3 or 4 too high. ORNL test VI-2 showed that the release rates (values of k) for the volatile fission products decrease even more as the total fraction released exceeds about 30%. ORNL developed an expedient correlation for this deficiency by dividing the initial inventory into three parts, the first part released at the highest rate (highest values of k) and the third part release at the lowest rate. This method was called CORSOR-3 (Severe Fuel Damage Meetings 1985) but has not been widely adopted. The Source Term Code Package (NUREG-0956, July 1986) did not employ the factor of 3 or 4 reduction in k values indicated by current high temperature experiments, and did not include a needed further reduction when large total fractional releases occur.

Non-Volatile Fission Products. There is a genuine scarcity of data for the release of the less-volatile fission products, especially from tests conducted under the conditions expected for severe accidents. CORSOR-M (1985) made significant changes to the values of k (in addition to using the 1/T format) for several of the less-volatile elements, but there were few "good" data to evaluate these changes. The ORNL high temperature tests (2700 K) will provide these data.

The new data in hand do show the importance of atmosphere (H_2 or H_2O)

and its effect on the chemical form of a number of fission products: Ba, Sr, Mo, Eu, Ru, and the more volatile Sb, Sn (cladding), and Te. CORSOR as used in the Source Term Code Package follows the oxidation of the cladding so that the proper release of Te is calculated, and a similar (probably) correlation could be developed for Sb release. It appears that oxidation or reduction of the fuel itself must be calculated in order to predict correctly the releases of the above atmosphere-dependent fission product releases.

Structural and Control Materials. There are two problems with using the CORSOR-type fractional release rate model with structural and control materials. First, many of them melt at relatively low temperatures and run down out of the heated zone. Second, most of them are present in such large quantity that saturation of the flowing steam/hydrogen atmosphere will occur. If either of these is neglected, there will be an over-calculation of the released amount since all of the reference data for release coefficients were obtained from small tests in which there was no runoff and no vapor saturation.

The only attempt in any CORSOR version to account for the above is with silver alloy in the current Source Term Code Package (NUREG-0956). Earlier accident calculations (probably the BMI-2104 series) indicated very high releases of Ag, In, and Cd. It was found that the code did not account for rundown. ORNL suggested an expedient remedy in the form of reducing the fraction release-vs-maximum temperature correlation previously used. Note that the Ag, In, and Cd control alloy releases are not calculated using the fractional release rate model.

An ORNL review of CORSOR (ORNL/TM-8842, 1985) pointed out the need for a vaporization-based model for structural components (including UO_2) and for an accommodation for rundown, deposition in the cooler paortions of the core, aerosol formation, etc. A quantitative empirical method was proposed that worked within the fractional release rate model framework. The summary page from that review is attached.

It is well known that there is an effect fo burnup on fission product release, but that has not been included in any CORSOR version and was not mentioned in the ORNL/TM-8842 review.

In summary, CORSOR is out of date in most respects, but can be altered to produce results much closer to reality while still using the fractional release rate format. ORNL has shown that Booth-type diffusion equations can be adapted to reproduce experimental release rates quite closely. A change from the fractional release rate model to the use of diffusion equations by themselves will represent only a small improvement. CORSOR-3 reproduces test data just as well and can be incorporated much more easily. A major missing link is the proper accommodations for atmosphere, geometry, vaporization, and condensation, where appropriate. High quality data for determining release of the less-volatile species must await the performing of tests in the ORNL fission product release program.

CORSOR SUMMARY (FROM ORNL/TM - 8842)

1. The fractional rate release model as used in CORSOR appears satisfactory for the calculation of fission product release from fuel and cladding. As the experimental data base and our theoretical knowledge are expanded, more comprehensive models may be beneficial.

2. Significant reductions in release rates for fission products Ba, Sr, Mo, and Ru are recommended. Minor changes are suggested for other fission products in order to use a uniform mathematical format.

3. A partition of the released fission products into 60% as aerosol solids and 40% vapor along with simple provisions for particle deposition and vapor condensation in the cool portions of the core is suggested.

4. A vaporization model for structural materials (stainless steel and Inconel), fuel rod cladding and UO_2, and control rod silver alloy is proposed. A simple method of accounting for the effects of exposed surface area, degree of saturation, phase changes, partitioning between aerosol particles and vapor fractions, deposition of particles and condensation of vapor in the cool upper portions of the core is suggested. Fraction release rates of these materials are recommended for use until the vaporization model can be implemented.

5. Additional data needs are for the release of fission products, Te, Sb, Ba, Sr, Mo, and Ru. The release rates for these species are sensitive to the composition of the atmosphere and/or the extent of oxidation of the Zircaloy cladding.

6. Verfication of the vaporization release of structural material components is impossible because of lack of inclusion of these materials in the more realistic experiments.

CALCULATED RELEASE, HODGE CASE

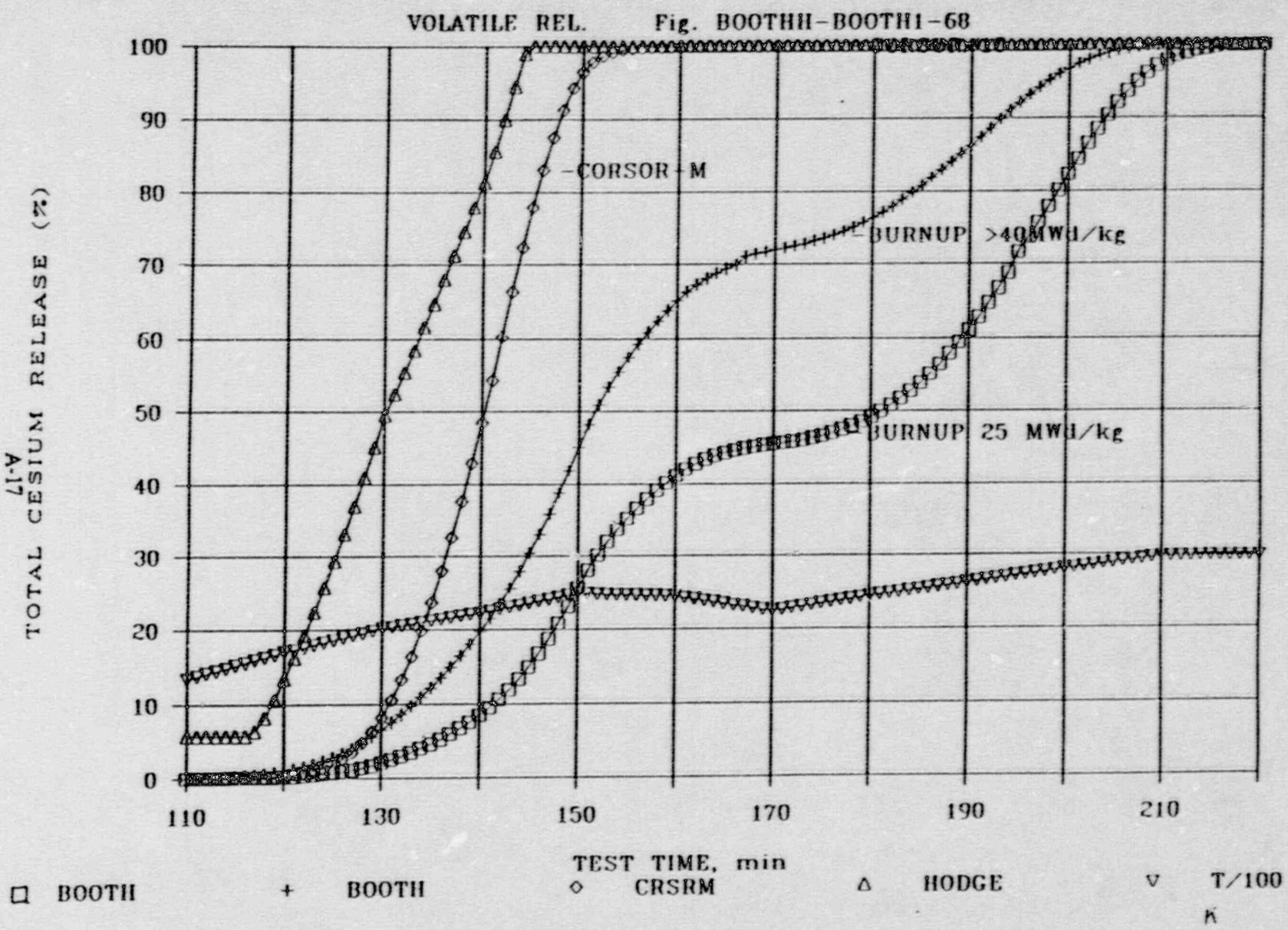

DEFECT INVESTIGATION REPORT (DIR) NUMBER: -PG. 1/

TITLE:Cavity Debris Phase Diagram Link To CF CODE:1.8.0

REQUESTOR/ORG.: S. R. GREENE - ORNL, FTS-624-0626 DATE:5/26/89

A. REQUEST:

It would be very useful to allow the user to program his/her own debris phase diagram with control functions. How-bout-it ?

REQUEST BASIS/.....	CHANGES REQUIRED/.....	SEVERITY._____
E = error	N = none	MIN = minor
N = new	C = coding	MED = medium
R = revised feature	D = documentation	MAJ = major
O = other	I = input deck	

STEP_____PAGES	__BY__	_DATE_	_CK'D_	_DATE__	_APPR_	_DATE_
A._Request____1						
B._Diagnosis						
C._Plan						
D._Changes						
E._Release						

DEFECT INVESTIGATION REPORT (DIR) NUMBER: -Pg. 1/

TITLE: Flow Path Connection To EDF Source CODE:1.8.0

REQUESTOR/ORG.: S. R. GREENE - ORNL, FTS-624-0626 DATE:5/26/89

A. REQUEST:

A code modification to allow the user to connect a flow path directly to an EDF source file is badly needed. One example use of this feature would be to allow a user to source hydrogen and steam from a previous MELCOR or BWRSAR run directly into the pressure suppression pool. The hydrogen source cannot be correctly handled correctly without this modification.

REQUEST BASIS/.....	CHANGES REQUIRED/.....	SEVERITY._____
E = error	N = none	MIN = minor
N = new	C = coding	MED = medium
R = revised feature	D = documentation	MAJ = major
O = other	I = input deck	

STEP	PAGES	BY	DATE	CK'D	DATE	APPR	DATE
A. Request	1						
B. Diagnosis							
C. Plan							
D. Changes							
E. Release							

DEFECT INVESTIGATION REPORT (DIR) NUMBER: -PG. 1/

TITLE:Separate Failure Temp for Other Structure Penetrations CODE:1.8.0

REQUESTOR/ORG.: S. R. GREENE - ORNL, FTS-624-0626 DATE:5/26/89

A. REQUEST:

The code currently employs a single failure temperature for all "other structure" and the lower head penetrations. The recent DF-4 experiments clearly demonstrate that the melt/failure temperature of the BWR control blades is lowered significantly by chemical reactions between the melt and the B_4C. Since "other structure" is used to represent both the control blades and the core plate, the use of a single failure temperature for these two structures is not appropriate, nor is it desirable to use the same failure temperature for the penetrations.

I suggest:

A. The penetration failure temperature be independent of the "other structure" failure temperature;

and,

B. The user be allowed to input either spatially-dependent failure temperatures for the "other structure", or allowed a choice of two or three different values.

REQUEST BASIS/.....	CHANGES REQUIRED/.....	SEVERITY._____
E = error	N = none	MIN = minor
N = new	C = coding	MED = medium
R = revised feature	D = documentation	MAJ = major
O = other	I = input deck	

STEP_____	PAGES	BY	DATE	CK'D	DATE	APPR	DATE
A. Request	1						
B. Diagnosis							
C. Plan							
D. Changes							
E. Release							

DEFECT INVESTIGATION REPORT (DIR) NUMBER: -PG. 1/1

TITLE:Sensitivity coefficient # 10 doesn't work CODE:1.8.0

REQUESTOR/ORG.: S. R. GREENE - ORNL, FTS-624-0626 DATE:6/2/89

A. REQUEST:

The code does not accept input for sensitivity coefficient # 10 (ctss weighting factors for cpu, I/O, and memory).

REQUEST BASIS/.....CHANGES REQUIRED/.....SEVERITY._____

E = error	N = none	MIN = minor
N = new	C = coding	MED = medium
R = revised feature	D = documentation	MAJ = major
O = other	I = input deck	

STEP	PAGES	BY	DATE	CK'D	DATE	APPR	DATE
A. Request	1						
B. Diagnosis							
C. Plan							
D. Changes							
E. Release							

DEFECT INVESTIGATION REPORT (DIR) NUMBER: -PG. 1/1

TITLE:Unnecessary Calls to Water Properties Pkg CODE:1.8.0

REQUESTOR/ORG.: S. R. GREENE - ORNL, FTS-624-0626 DATE:6/5/89

A. REQUEST:

I recently encountered a case in which the code was bombing in a call to the water properties package, indicating that it was passing the package a temperature above the upper limit of the correlations. .nis was occurring in conjunction with the use of a BWRSAR-generated EDF file in which we had written out the upper internal reactor vessel gas temperature for the water, steam, and hydrogen, along with zero values for the integrated flow for the liquid water. In this particular case, the code was attempting to obtain liquid water properties even-though no water had been released.

Randy Cole identified the problem over the phone and supplied a control function patch which basically clamps the water temperature to the maximum of the critical temperature or the temperature in the EDF file. This has us running for now.

I suggest the code logic be modified to cause the code to call the properties package only when it has a non-zero source mass to deal with. (Randy may have already done this.)

REQUEST BASIS/.....	CHANGES REQUIRED/.....	SEVERITY._____
E = error	N = none	MIN = minor
N = new	C = coding	MED = medium
R = revised feature	D = documentation	MAJ = major
O = other	I = input deck	

STEP_____PAGES	BY	DATE	CK'D	DATE	APPR	DATE
A._Request____1						
B._Diagnosis						
C._Plan						
D._Changes						
E._Release						

DEFECT INVESTIGATION REPORT (DIR) NUMBER: -PG. 1/1

TITLE: VANESA Error When Debris Has No UO_2 CODE: 1.8.0

REQUESTOR/ORG.: S. R. GREENE - ORNL, FTS-624-0626 DATE: July 7, 1989

A. REQUEST:

A floating point error is encountered in VANESA, and the code bombs for the case in which there is no UO_2 in the debris and the concrete has reached the ablation temperature. This error was encountered when the BWRSAR debris pours were sourced in via the EDF package. The early pours are Zr- and Fe- rich, but contain no UO_2. Everything is fine until the concrete first reaches the ablation temperature. It is at this point that VANESA is first called and immediately bombs.

The problem appears to occur in line 102 of VANESA:

QOXP = SOXP/POXP.

POXP is zero (confirmed via debugger) and a floating point divide error is encountered.

REQUEST BASIS/.....	CHANGES REQUIRED/.....	SEVERITY._____
E = error	N = none	MIN = minor
N = new	C = coding	MED = medium
R = revised feature	D = documentation	MAJ = major
O = other	I = input deck	

STEP_____	PAGES	BY	DATE	CK'D	DATE	APPR	DATE
A. Request	1						
B. Diagnosis							
C. Plan							
D. Changes							
E. Release							

DEFECT INVESTIGATION REPORT (DIR) NUMBER: **-PG. 1/**

TITLE:Problem in subroutine FDILOW **CODE:1.8**

REQUESTOR/ORG.: C R HYMAN/ORNL **DATE:Sept 18,1989**

A. REQUEST:

This DIR is for documentation only. The information in this DIR was orginally passed to Ed Boucheron on or about Sept 18,1989.

MELCOR encountered a floating point error in FDILOW due to lack of UO2 in the initial portion of the EDF file generated by the BWRSAR code.

It appears that when the COR package is used to generate the materials calculated to leave the failed reactor vessel, there is always some amount of UO2 present in the discharge. The FDI package was developed incorporating this assumption. Since BWRSAR calculates the initial pour to be entirely metallic,the difficulty immediately presented itself.

The following UPDATE instructions were proposed by Ed Boucheron as a fix of the problem.

```
*/
*ident,*diornl
*d,fdilow.283,fdilow.285
    if(fmassi(i).ne.0.0) then
      xfrac(1)=fmspl2(1)/(fmspl2(1)+fmcavn(1))
      call rn1fdr(ntpcc,ntpcor,xmsfdi,xmrfdi,xfrac,
   +              xcord,numcls,nfdi,ifdi)
    end if
```

These instructions have been incorporated into ORNL's version of MELCOR and the code no longer exhibits the difficulty.

DEFECT INVESTIGATION REPORT (DIR) NUMBER: **-PG. 1/1**

TITLE: Subroutine SRPP error. **CODE:1.6**

REQUESTOR/ORG.: C R HYMAN/ORNL **DATE:Oct 10,1989**

A. REQUEST:

This DIR is for documentation only. This information was orginally passed via telephone to Ed Boucheron and Randy Cole of the MELCOR code development staff on or about Oct 10,1989.

MELCOR tried to take the square root of a negative number at UPDATE line SRPP.18. MELCOR had calculated tens of thousands of seconds of the transient when this error was produced. SNL MELCOR staff were contacted and they suspected that the moles of some particular VANESA species was probably being calculated as very small negative number. They recommended that debug of the various variables be performed so that their values were known at the time of the error. Dave Bradley of the CORCON and VANESA code development staff was also contacted and he corroborated the MELCOR staff suspicion. Debug print statements were inserted into the subroutine SRPP and it was found that the variable xm(3,2) had the value of -0.460692e-13, a very small negative number.

The following conditional check was placed into SRPP immediately after line SRPP.15:

```
If (abs(xm(3,2).lt.1.0e-6) xm(3,2)=0.0
```

MELCOR was restarted with the above modification inserted and no difficulty was encountered.

In discussions with Dave Bradley, it was learned that a more recent version of VANESA has been developed and is ready for use. It was also learned that the new version of VANESA contained a check for the exact situation causing the current difficulty. Additional checks have been developed in the new version of VANESA to preclude difficulties of this type. The MELCOR staff has been informed of this and the priority of incorporating the newer version of VANESA into MELCOR remains low.

DEFECT INVESTIGATION REPORT (DIR) NUMBER: -PG. 1/

TITLE: Abnormal Stop When Using FDI Package in MELCOR CODE: 1.8.0

REQUESTOR/ORG.: M. L. Tobias - ORNL, FTS 624-0574 DATE: 10/16/89

This report is for record purposes only, the information concerning this case (input filed and output listings) having been furnished to M. Carmel of SNL on or about 10/13/89.

A. REQUEST:

A case came to an abnormal stop when the FDI package was being used. The pour data were input as an external data file. The failure appears to be associated with a pause in the flow of molten materials. The same case runs satisfactorily if the FDI package is not invoked.

REQUEST BASIS/.....	CHANGES REQUIRED/.....	SEVERITY._____
E = error	N = none	MIN = minor
N = new	C = coding	MED = medium
R = revised feature	D = documentation	MAJ = major
O = other	I = input deck	

STEP	PAGES	BY	DATE	CK'D	DATE	APPR	DATE
A. Request	1						
B. Diagnosis							
C. Plan							
D. Changes							
E. Release							

DEFECT INVESTIGATION REPORT (DIR) NUMBER: -PG. 1/

TITLE: Three Problems With MELPLT Package CODE: 1.8.0

REQUESTOR/ORG.: M. L. Tobias - ORNL, FTS-624-0574 DATE: 10/18/89

This report is for record purposes only, the information below having been communicated to R. Summers on or about August 4, 1989.

A. REQUEST:

Problem 1: If the GRID instruction is given, the grid appears not on the axes but over the entire plotting area. (Example 1 and input listing are attached.)

Problem 2: If the ploti or eploti command is given with i ranging from 4 through x, the data points themselves are not plotted but rather the markers seem to be placed at positions spaced equidistantly along the curve length. The markers are not placed at data coordinates whether or not a connecting curve is drawn. See example 2 and example 3. The lists accompanying these say 8 points are plotted, yet only 6 markers appear.

Problem 3: If user supplied input data are used and the data i command is given with "i" from 4 to 9 or a through i, the markers are placed equidistantly along the curve. In Example 4, 17 markers are used, yet only 6 points were supplied. In example 3, however, where "i" in data i was set to "0", a points only choice, the markers are placed at the coordinates that were supplied.

REQUEST BASIS/.....	CHANGES REQUIRED/.....	SEVERITY._____
E = error	N = none	MIN = minor
N = new	C = coding	MED = medium
R = revised feature	D = documentation	MAJ = major
O = other	I = input deck	

STEP	PAGES	BY	DATE	CK'D	DATE	APPR	DATE
A. Request	1						
B. Diagnosis							
C. Plan							
D. Changes							
E. Release							

MELCOR dr4 modeling: case 31; v.f. s=0.4
Bypass Temperature (10^3 K)
Time (10^3 s)
114 mm plane
254 mm plane
368 mm plane
495 mm plane

Example 4

```
 RECORDS REPLACED (7/86) BY DISSPLA

CARD   1 SET  1 : FILE1 MELPIF31
CARD   2 SET  1 : TITLE, MELCOR DFA MODELING: CASE 31; V F 'S:0.4
CARD   3 SET  1 : YLABEL, BYPASS TEMPERATURE, (K)
CARD   4 SET  1 : YLIM 7400  7600
CARD   5 SET  1 : YLIM 200  1200
CARD   6 SET  1 : LEGEND 114 MM PLANE
CARD   7 SET  1 : * POSITION  15  85
CARD   8 SET  1 : LIST
CARD   9 SET  1 : GRID
CARD  10 SET  1 : PLOT COR TSVR 107
CARD  11 SET  2 : LEGEND 25A MM PLANE
CARD  12 SET  2 : LIST
CARD  13 SET  2 : CPLOT3 COR-TSVB 113
CARD  14 SET  3 : LEGEND 56B MM PLANE
CARD  15 SET  3 : LIST
CARD  16 SET  3 : CPLOT* COR TSVB 117
CARD  17 SET  4 : LEGEND 695 MM PLANE
CARD  18 SET  4 : LIST
CARD  19 SET  4 : CPLOTL COR TSVB 127
CARD  20 SET  5 : .
     THE PRECEDING COMMAND IS UNKNOWN - DELETED


OPENING FILE 1  MELPIF31
TITLE BLOCK : MELCOR   /87/08/01 /14.21.56 /DFA MODELING: CASE 31
PROCESSING FILE 1  MELPIF31
KEY BLOCK AFTER TIME=  0.00000E+00  EXCEL=         0  KEY RECORD SETS =      100 /     2515
END OF FILE ENCOUNTERED
FILE TITLE  : MELCOR   /87/08/01 /14.21.56 /DFA MODELING: CASE 31
              80 RECORDS PROCESSED
ALL FILES PROCESSED


INFORMATION LIST FOR PLOT   1

Y PLOT VARIABLE :COR TSVB 107
X PLOT VARIABLE :TIME 0
TITLE  :MELCOR DFA MODELING: CASE 31; V F 'S:0.4
XLABEL :TIME (0)_S)
YLABEL :BYPASS TEMPERATURE ((K)
LEGEND :114 MM PLANE
PLOT DATA SOURCE (CALC(3)/EXPC(3)/EXP WITH 0000NDS(0)) :C
PLOT CURVE CHARACTER FLAG  0
FRAME (NEW(1)/LAST(0)) 1
XLIMITS =     7.40000E+03    7.60000E+03
YLIMITS =     2.00000E+02    1.20000E+03
NUMBER OF DATA PAIRS =    0
DATA FROM FILE  :  1  MELPIF31
LEGEND POSITION : 0.0045 0.1187
DATA PRINT LIST (OFF(0)/ON(1))   :

     0 POINTS PLOTTED


LIST OF DATA

        X             Y             Z             Y             Z             Y             Z             Y             Y             Y
  7.4005E+03    6.6226E+02    7.4400E+03    6.6566E+02    7.4802E+03    6.5207E+02    7.5202E+03    6.4166E+02
  7.4203E+03    6.6403E+02    7.4603E+03    6.6806E+02    7.5001E+03    3.0105E+02    7.5236E+03    7.6692E+02


INFORMATION   ST FOR PLOT   2
```

```
Y PLOT VARIABLE :CON-TSVB 113
X PLOT VARIABLE :TIME_0
TITLE :HELIOS OF& MODELING: CASE 31, V.I 'S-0 &
XLABEL :TIME ((}_S)
YLABEL :CON-TSVB 113 ((}K)
LEGEND :25& MM PLANE
PLOT DATA SOURCE (CAL(C)/EXP(C)/EXP WITH BOUNDS(B)) :C
PLOT CURVE CHARACTER FLAG :J
FRAME (NEW(I)/LAST(B)) B
NUMBER OF DATA PAIRS =    8
DATA FROM FILE :    1  HELPFIL1
LEGEND POSITION : 0.0045 0.1182
DATA PRINT LIST (OFF(0)/ON(1))    1

     8 POINTS PLOTTED


LIST OF DATA

        X             Y             X             Y             X             Y             X             Y             X             Y
  7.408'E+03  9.5202E+02  7.4400E+03  9.6054E+02  7.4802E+03  9.5998E+02  7.5202E+03  8.1915E+02
  7.4203E+03  9.5522E+02  7.4603E+03  9.6504E+02  7.5001E+03  6.1642E+02  7.5234E+03  8.1958E+02


INFORMATION LIST FOR PLOT    5

Y PLOT VARIABLE :CON-TSVB 117
X PLOT VARIABLE :TIME_0
TITLE :HELIOS OF& MODELING: CASE 31, V.I 'S-0 &
XLABEL :TIME ((}_S)
YLABEL :CON-TSVB 117 ((}K)
LEGEND :368 MM PLANE
PLOT DATA SOURCE (CAL(C)/EXP(C)/EXP WITH BOUNDS(B)) :C
PLOT CURVE CHARACTER FLAG :K
FRAME (NEW(I)/LAST(B)) B
NUMBER OF DATA PAIRS =    8
DATA FROM FILE :    1  HELPFIL1
LEGEND POSITION : 0.0045 0.1182
DATA PRINT LIST (OFF(0)/ON(1))    1

     8 POINTS PLOTTED


LIST OF DATA

        X             Y             X             Y             X             Y             X             Y             X             Y
  7.408'E+03  1.0N4AE+03  7.4400E+03  1.1014E+03  7.4802E+03  1.1024E+03  7.5202E+03  1.0127E+03
  7.420'E+03  1.0924E+03  7.4603E+03  1.1035E+03  7.5001E+03  1.1419E+02  7.5234E+03  8.8935E+02


INFORMATION LIST FOR PLOT    6

Y PLOT VARIABLE :CON-TSVB 122
X PLOT VARIABLE :TIME_0
TITLE :HELIOS OF& MODELING: CASE 31, V.I 'S-0 &
XLABEL :TIME ((}_S)
YLABEL :CON-TSVB 122 ((}K)
LEGEND :495 MM PLANE
PLOT DATA SOURCE (CAL(C)/EXP(C)/EXP WITH BOUNDS(B)) :C
PLOT CURVE CHARACTER FLAG :L
FRAME (NEW(I)/LAST(B)) B
NUMBER OF DATA PAIRS =    8
DATA FROM FILE :    1  HELPFIL1
LEGEND POSITION : 0.0045 0.1182
```

[illegible] PLOTTER

LIST OF DATA

7.48051E+01	1.10465E+01	7.44881E+01	1.12675E+01	7.48027E+01	1.14835E+01	7.52825E+01	1.08451E+01	
7.42671E+01	1.11481E+01	7.46851E+01	1.13651E+01	7.50011E+01	1.02781E+01	7.52561E+01	9.99511E+00	

PLOTTER CONTROLS FOR 2 DISSPLA FRAMES AND ON DCP METAFILE TAPE55

MELCOR df4 modeling: case 31; metaoub

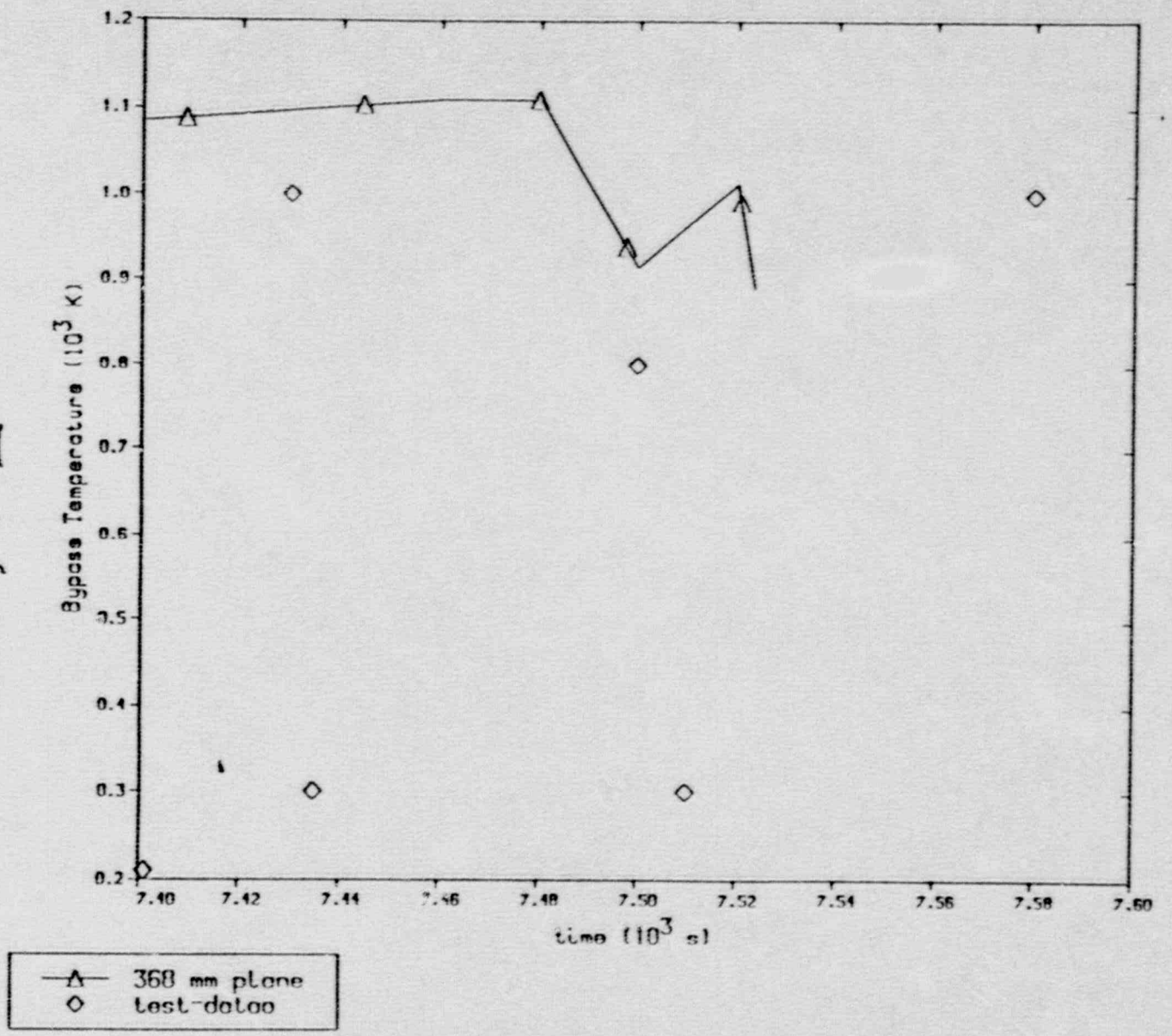

Example 2

```
MET.9108.MS-8088     * JOB 1970 MET01970 AA 1        001 001 R67     START 10.01 04 AUG 89 R67.PRT   X10A ****** *     MET.9108.MS-8088
MET.9108.MS-8088     * JOB 1970 MET01970 AA 1        001 001 R67     START 10.01 04 AUG 89 R67.PRT   X10A ****** *     MET.9108.MS-8088
MET.9108.MS-8088     * JOB 1970 MET01970 AA 1        001 001 R67     START 10.01 04 AUG 89 R67.PRT   X10A ****** *     MET.9108.MS-8088
MET.9108.MS-8088     * JOB 1970 MET01970 AA 1        001 001 R67     START 10.01 04 AUG 89 R67.PRT   X10A ****** *     MET.9108.MS-8088
MET.9108.MS-8088     * JOB 1970 MET01970 AA 1        001 001 R67     START 10.01 04 AUG 89 R67.PRT   X10A ****** *     MET.9108.MS-8088
MET.9108.MS-8088     * JOB 1970 MET01970 AA 1        001 001 R67     START 10.01 04 AUG 89 R67.PRT   X10A ****** *     MET.9108.MS-8088
MET.9108.MS-8088     * JOB 1970 MET01970 AA 1        001 001 R67     START 10.01 04 AUG 89 R67.PRT   X10A ****** *     MET.9108.MS-8088



***************************************************************
*                                                             *
*            M V S   J E S 2   H O T   N E W S                *
*                                                             *
***************************************************************
*                                                             *
*  REVISED: 07/27/89 14:58:21      BY S7H                     *
*  07/27 BOTH THE IBM 3033S WILL BE DOWN TONIGHT FROM         *
*        6:00-8:00PM FOR SYSTEM WORK                          *
*                                                             *
*  07/27 MICROSOFT REPRESENTATIVES WILL BE AVAILABLE TO DEMON-*
*        STRATE MICROSOFT EXCEL SPREADSHEET SOFTWARE FOR THE PC *
*        THURS., 7/27 AT ORNL CONF. ROOM, BLDG. 3047, AT 10:00 *
*        AM AND 2:00 PM AND FRIDAY, 7/28 AT Y12 BLDG. 9709, RM *
*        133 AT 10:00AM AND 2:00PM                            *
*                                                             *
*  07/24 BOTH IBM 3033S WILL BE DOWN THIS MORNING, MONDAY     *
*    FROM 11:30A-12:30P TO RESTORE TWO DISK PACKS             *
*                                                             *
*  07/21 DCA SYSTEM SELECT 9 (THE SERIES/1 AT X-10) WILL BE   *
*        REPLACED WITH AN IBM 7171 (SIMILAR TO SYSTEM SELECT  *
*        47) ON TUESDAY EVENING, JULY 25. SEE THE MAY-JUNE    *
*        CAT NEWS FOR DETAILS. IF YOU HAVE PROBLEMS, CONTACT  *
*        PROGRAMMING ASSISTANCE                               *
*                                                             *
*  07/21 SYSTEM SELECT 9 (SERIES 1) WILL NOT BE AVAILABLE FROM *
*    17:00-19:00, JULY 25, TUESDAY, DUE TO INSTALLATION OF    *
*    7171 PROTOCOL CONVERTER.                                 *
*                                                             *
*                                                             *
*                                                             *
*                                                             *
*                                                             *
*                                                             *
***************************************************************
```

```
 USING INPUT FILE  NELPLT VERSION 1.02 (2/21/85)
  1SCORS REPLACED (2/86) BY DISSPLA

CARD    1 SET   1 : FILE1 HELPIF3)
CARD    2 SET   1 : TITLE, HELCOR DF& MODELING: CASE 3); METABOR
CARD    3 SET   1 : YLABEL, BYPASS TEMPERATURE, ((3K)
CARD    4 SET   1 : XLIM 7ABB  7ABB
CARD    5 SET   1 : YLIM 7BB  12BB
CARD    6 SET   1 : LEGEND 3&B MM PLANE
CARD    7 SET   1 : LIST
CARD    8 SET   1 : PLOT& CBR TSVB 11)
CARD    9 SET   2 : DATAB TEST-DATAB
                      B    B
                    XLABEL.
                    YLABEL.
                      7.4B1BBE+B3   7.1BBBBE+B2
                      7.45BBBE+B3   1.BBBBBE+B3
                      7.43BBBE+B3   1.BBBBBE+B2
                      7.5BBBBE+B1   B.BBBBBE+B2
                      7.51BBBE+B1   1.BBBBBE+B2
                      7.5BBBBE+B1   1.BBBBBE+B3
                     -1.214BBE+B4  -1.234BBE+B4


OPENING FILE 1  HELPIF3)
TITLE BLOCK : HELCOR    /B9/B9/B1 /14.21.54 /DF& MODELING, CASE 1(
PROCESSING FILE 1  HELPIF3)
KEY BLOCK AFTER TIME=  B.BBBBE+BB  CYCLE=         B  KEY RECORD SIZES =       1RR /      2115
END OF FILE ENCOUNTERED
FILE TITLE  : HELCOR    /B9/BB/B1 /14.21.54 /DF& MODELING, CASE 3(
              BB RECORDS PROCESSED
ALL FILES PROCESSED
READING DATA FOR CURVE     2 FROM FILE BRINPUT
FOUND TEST-DATAB


INFORMATION LIST FOR PLOT    1

* PLOT VARIABLE :CBR-TSVB 11)
* PLOT VARIABLE :TIME B
TITLE  :HELCOR DF& MODELING: CASE 3(; METABOR
XLABEL :TIME ((),S)
YLABEL :BYPASS TEMPERATURE ((3K)
LEGEND :3&B MM PLANE
PLOT DATA SOURCE (CALL(C)/EXP(E)/EXP WITH BOUNDS(B)) :C
PLOT CURVE CHARACTER FLAG :&
FRAME (NEW(1)/LAST(B)) 1
XLIMITS :    7.ABBBE+B3    7.6BBBE+B1
YLIMITS :    2.BBBBE+B2    1.2BBBE+B1
NUMBER OF DATA PAIRS =    B
DATA FROM FILE :  1  HELPIF3)
LEGEND POSITION : B.BB4( B.11B7
DATA POINT LIST (OFF(B)/BN(1)) :  1

      B POINTS PLOTTED


LIST OF DATA

          X             Y             X             Y             X             Y             X             Y             X             Y
  7.4B3E+B3  1.B84E+B1  7.44BBE+B3  1.1B14E+B1  7.4B27E+B3  1.1B4E+B1  7.52B7E+B3  1.B12E+B1
  7.42B3E+B3  1.B72E+B1  7.4CB3E+B3  1.1B2BE+B1  7.5BBBE+B3  9.141BE+B7  7.525BE+B3  B.B29BE+B7


INFORMATION   S1 FOR PLOT    2
```

```
DATA RECORD NAME :LIST-DATA0
TITLE  :RECCOR DFA MODELING: CASE 11; RETARDR
YLABEL  YLABEL,
YLABEL  XLABEL,
LEGEND :LIST-DATA0
PLOT DATA SOURCE (CALLC)/EXPEE)/EXP WITH BOUNDS(B)) :C
PLOT CURVE CHARACTER FLAG :B
FNAME (NEWEL)/LASTEN)) B
NUMBER OF DATA PAIRS =    6
DATA FROM FILE :   B  UNIMPUT
LEGEND POSITION : 0.0BAS 0.11NZ
DATA POINT LIST (OFF(B)/NPC1)) : B

     6 POINTS PLOTTED


PLOTTER CONTROLS FOR   2 DISSPLA FNAMES ARE ON NCP RETAFILE TAPE55
```

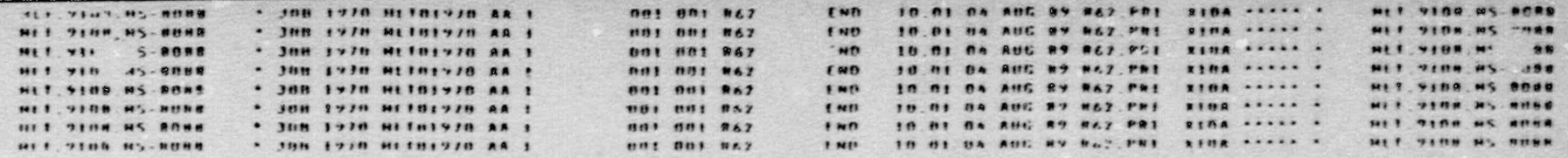

MELCOR df4 modeling: case 31; metaoud

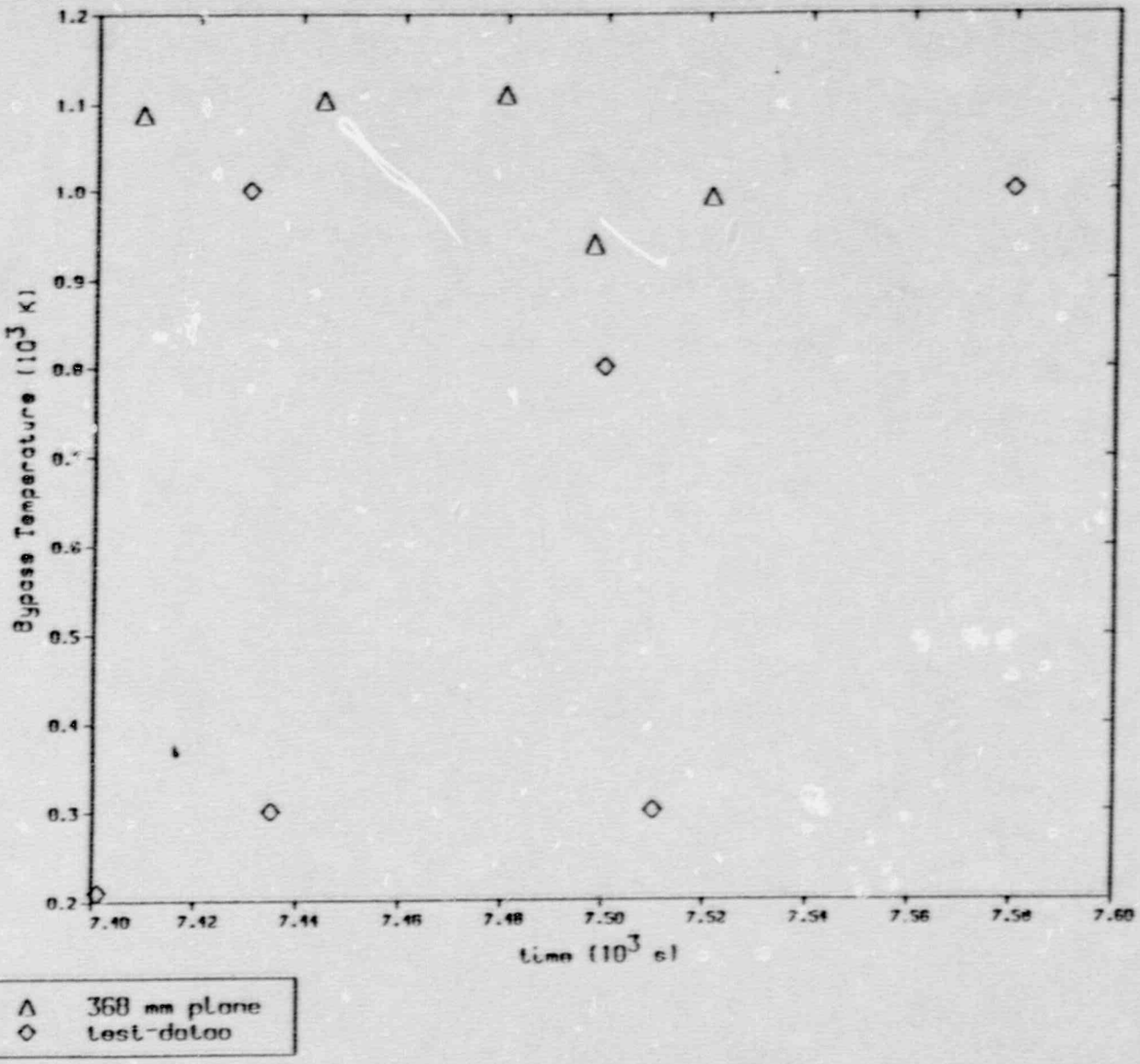

Example 3

```
MLT.9108.MS-8088     * JOB 1972 MLTH1972 AA 1          001 001 R67     START 10.06 04 AUG 89 R67.PR1   X10A ****** *     MLT.9108.MS-8088
MLT.9108.MS-8088     * JOB 1972 MLTH1972 AA 1          001 001 R67     START 10.06 04 AUG 89 R67.PR1   X10A ****** -     MLT.9108.MS-8088
MLT.9108.MS-8088     * JOB 1972 MLTH1972 AA 1          001   1 R67     START 10.06 04 AUG 89 R67.PR1   X10A ****** *         9108.MS-8088
MLT.9108.MS-8088     * JOB 1972 MLTH1972 AA 1          001  .1 R67     START 10.06 04 AUG 89 R67.PR1   X10A ****** *       . 9108.MS-8088
MLT.9108.MS-8088     * JOB 1972 MLTH1972 AA 1          001 001 R67     START 10.06 04 AUG 89 R67.PR1   X10A ****** *     MLT.9108.MS-8088
MLT.9108.MS-8088     * JOB 1972 MLTH1972 AA 1          001 001 R67     START 10.06 04 AUG 89 R67.PR1   X10A ****** *     MLT.9108.MS-8088
MLT.9108.MS-8088     * JOB 1972 MLTH1972 AA 1          001 001 R67     START 10.06 04 AUG 89 R67.PR1   X10A ****** *     MLT.9108.MS-8088
MLT.9108.MS-8088     * JOB 1972 MLTH1972 AA 1          001 001 R67     START 10.06 04 AUG 89 R67.PR1   X10A ****** *     MLT.9108.MS-8088
```

```
****************************************************************
*                                                              *
*              MVS-JES2 HOT NEWS                               *
*                                                              *
****************************************************************
*                                                              *
*  REVISED: 07/27/89 14:56:23        BY SJM                    *
*  07/27 BOTH THE IBM 3033S WILL BE DOWN TONIGHT FROM          *
*        6:00-8:00PM FOR SYSTEM WORK                           *
*                                                              *
*  07/27 MICROSOFT REPRESENTATIVES WILL BE AVAILABLE TO DEMON- *
*        STRATE MICROSOFT EXCEL SPREADSHEET SOFTWARE FOR THE PC *
*        THURS., 7/27 AT ORNL CONF. ROOM, BLDG. 3047, AT 10:00 *
*        AM AND 2:00 PM AND FRIDAY, 7/28 AT Y12 BLDG. 9704, RM *
*        133 AT 10:00AM AND 2:00PM.                            *
*                                                              *
*  07/24 BOTH IBM 3033S WILL BE DOWN THIS MORNING, MONDAY      *
*    FROM 11:30A-12:30P TO RESTORE TWO DISK PACKS.             *
*                                                              *
*  07/21 DCA SYSTEM SELECT 9 (THE SERIES/1 AT X-10) WILL BE    *
*        REPLACED WITH AN IBM 7171 (SIMILAR TO SYSTEM SELECT   *
*        #7) ON TUESDAY EVENING, JULY 25. SEE THE MAY JUNE     *
*        CAT NEWS FOR DETAILS. IF YOU HAVE PROBLEMS, CONTACT   *
*        PROGRAMMING ASSISTANCE.                               *
*                                                              *
*  07/21 SYSTEM SELECT 9 (SERIES 1) WILL NOT BE AVAILABLE FROM *
*    17:00-19:00  JULY 25, TUESDAY, DUE TO INSTALLATION OF     *
*    7171 PROTOCOL CONVERTER.                                  *
*                                                              *
*                                                              *
*                                                              *
*                                                              *
*                                                              *
*                                                              *
****************************************************************
```

```
.USER INPUT ECHO  MELPLT VERSION 1.02 (2/3/85)
  ASSUMES REPLACED 4//865 BY DISSPLA

CARD    1 SET  1 : FILE1 MELPLT1;
CARD    2 SET  1 : TITLE, MELCOR DFA MODELING  CASE 31, METAMOD
CARD    3 SET  1 : YLABEL, BYPASS TEMPERATURE, (K)*
CARD    4 SET  1 : YLIM 7400  7600
CARD    5 SET  1 : YLIM 200  1200
CARD    6 SET  1 : LEGEND 368 MM PLANE
CARD    7 SET  1 : LIST
CARD    8 SET  1 : PLOT CON-TSVB 117
CARD    9 SET  2 : DATA8 TEST-DATA8
                     0     0
                   YLABEL,
                   YLABEL,
                     7.400E+03  2.100E+02
                     7.430E+03  1.000E+03
                     7.435E+03  5.000E+02
                     7.500E+03  0.000E+02
                     7.510E+03  3.000E+02
                     7.580E+03  1.000E+03
                    -1.234E+04  1.234E+04


OPENING FILE 1  MELPLT1
TITLE BLOCK : MELCOR    /89/08/01 /14.21.54 /DFA MODELING, CASE 31    -
PROCESSING FILE 1  MELPLT1
KEY BLOCK AFTER TIME=  0.000E+00  CYCLE=         0  KEY RECORD SIZES =      100 /     2115
END OF FILE ENCOUNTERED
FILE TITLE  : MELCOR    /89/08/01 /14.21.54 /DFA MODELING, CASE 31
              80 RECORDS PROCESSED
ALL FILES PROCESSED
READING DATA FOR CURVE     2 FROM FILE UNINPUT
FOUND TEST-DATA8


INFORMATION LIST FOR PLOT    1

* PLOT VARIABLE :CON-TSVB 117
* PLOT VARIABLE :TIME 0
TITLE  :MELCOR DFA MODELING, CASE 31, METAMOD
XLABEL :TIME (S)_S)
YLABEL :BYPASS TEMPERATURE (K)*
LEGEND :368 MM PLANE
PLOT DATA SOURCE (CAL(C)/EXP(E)/EXP WITH BOUNDS(B)]  C
PLOT CURVE CHARACTER FLAG :1
FRAME (NEW(1)/LAST(0)] 1
XLIMITS :    7.400E+03   7.600E+03
YLIMITS :    2.000E+02   1.200E+03
NUMBER OF DATA PAIRS =    8
DATA FROM FILE :  1  MELPLT1
LEGEND POSITION : 0.0045 0.1167
DATA PRINT LIST (OFF(0)/ON(1)]  1

     8 POINTS PLOTTED

LIST OF DATA

  7.400E+03  1.084E+03  7.440E+03  1.101E+03  7.480E+03  1.107E+03  7.520E+03  1.112E+03
  7.470E+03  1.092E+03  7.460E+03  1.105E+03  7.500E+03  1.141E+03  7.576E+03  8.995E+02


INFORMATION   ST FOR PLOT    2
```

```
DATA RECORD NAME :TEST DATA0
TITLE    :ICON DFA MODELING: CASE 11; METAFILE
FRAME#   :FRAME1.
FRAME1   :FRAME1.
LEGEND :TEST DATA0
PLOT DATA SOURCE (CALC)/FILE(1)/TAP WITH BOUNDS(N) :2
PLOT CURVE CHARACTER FLAG :0
FNAME (N:W(1)/LAST(0)) 0
NUMBER OF DATA PAIRS =    6
DATA FROM TAPE :  9  BRINPUT
LEGEND POSITION : 0.0045 0 1182
DATA PRINT LIST (BIT(0)/BNF(1))   0

     6 POINTS PLOTTED


PLOTTER CONTROLS FOR   2 DISSPLA FRAMES ARE ON BCP METAFILE TAPE55
```

```
MLT.9108.MS-8088    * JOB 1972 MLT01972 AA 1      001 001 R67    END   10.06.04 AUG 89 R67.PR1   X10A ****** *     MLT.9108.MS-8088
MLT.9108.MS-8088    * JOB 1972 MLT01972 AA 1      001 001 R67    END   10.06.04 AUG 89 R67.PR1   X10A ****** *     MLT.9108.MS-8088
MLT.9108.MS-8088    * JOB 1972 MLT01972 AA 1      001 001 R67    END   10.06.04 AUG 89 R67.PR1   X10A ****** *     MLT.9108.MS-8088
MLT.9108.MS-8088    * JOB 1972 MLT01972 AA 1      001 001 R67    END   10.06.04 AUG 89 R67.PR1   X10A ****** *     MLT.9108.MS-8088
MLT.9108.MS-8088    * JOB 1972 MLT01972 AA 1      001 001 R67    END   10.06.04 AUG 89 R67.PR1   X10A ****** *     MLT.9108.MS-8088
MLT.9108.MS-8088    * JOB 1972 MLT01972 AA 1      001 001 R67    END   10.06.04 AUG 89 R67.PR1   X10A ****** *     MLT.9108.MS-8088
MLT.9108.MS-8088    * JOB 1972 MLT01972 AA 1      001 001 R67    END   10.06.04 AUG 89 R67.PR1   X10A ****** *     MLT.9108.MS-8088
MLT.9108.MS-8088    * JOB 1972 MLT01972 AA 1      001 001 R67    END   10.06.04 AUG 89 R67.PR1   X10A ****** *     MLT.9108.MS-8088
```

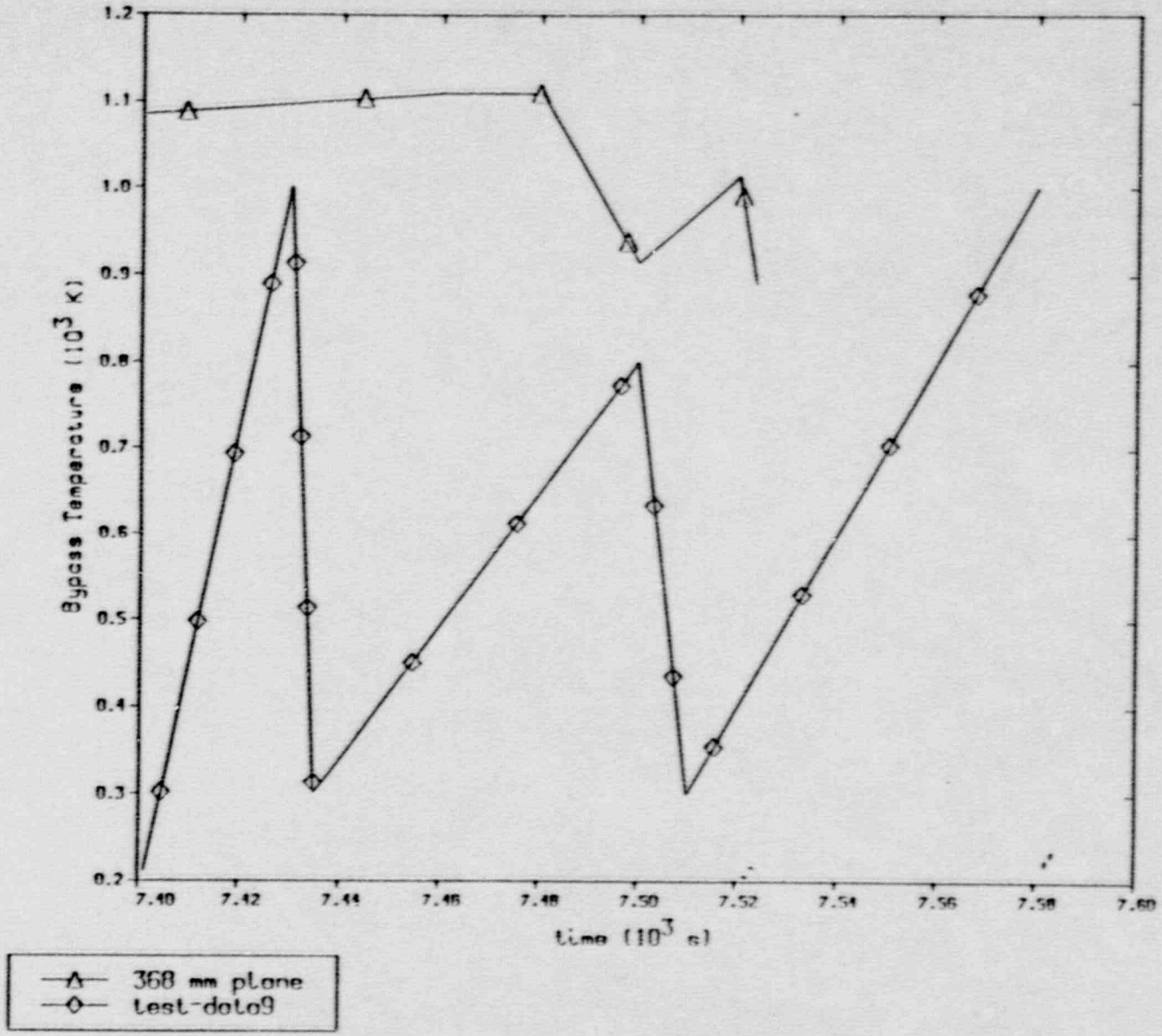
MELCOR df4 modeling: case 31; metaoub
Bypass Temperature (10^3 K)
time (10^3 s)
1.2
1.1
1.0
0.9
0.8
0.7
0.6
0.5
0.4
0.3
0.2
7.40
7.42
7.44
7.46
7.48
7.50
7.52
7.54
7.56
7.58
7.60
368 mm plane
test-data9

Example 4

```
HLT 9103 MS-8088     * JOB 1968 HLT801968 AA 1      001 001 R67    START  9 17 04 AUG 89 R67 PM1   X10A ***** -    HLT 9108 MS-8088
HLT 9108 MS-8088     * JOB 1968 HLT801968 AA 1      001 001 R67    START  9 17 04 AUG 89 R67 PM1   X10A ***** -    HLT 9108 MS-8088
HLT 9108 MS-8088     * JOB 1968 HLT801968 AA 1      001 001 R67    START  9 17 04 AUG 89 R67 PM1   X10A ***** -    HLT 9108 MS-8088
HLT 9108 MS-8088     * JOB 1968 HLT801968 AA 1      001 001 R62    START  9 17 04 AUG 89 R62 PM1   X10A ***** -    HLT 9108 MS-8088
HLT 9108 MS-8088     * JOB 1968 HLT801968 AA 1      001 001 R67    START  9 17 04 AUG 89 R62 PM1   X10A ***** -    HLT 9108 MS-8088
HLT 9108 MS-8088     * JOB 1968 HLT801968 AA 1      001 001 R67    START  9 17 04 AUG 89 R67 PM1   X10A ***** -    HLT 9108 MS-8088
HLT 9108 MS-8088     * JOB 1968 HLT801968 AA 1      001 001 R67    START  9 17 04 AUG 89 R67 PM1   X10A ***** -    HLT 9108 MS-8088
HLT 9108 MS-8088     * JOB 1968 HLT801968 AA 1      001 001 R67    START  9 17 04 AUG 89 R62 PM1   X10A ***** -    HLT 9108 MS-8088
```

```
*****************************************************************
*                                                               *
*                    M V S - 3 F S Z   H O T   N E W S          *
*                                                               *
*****************************************************************
*                                                               *
*  REVISED: 07/27/89 14:56:25      BY SZH                       *
*  07/27 BOTH THE IBM 3033S WILL BE DOWN TONIGHT FROM           *
*        6:00-8:00PM FOR SYSTEM WORK                            *
*                                                               *
*  07/27 MICROSOFT REPRESENTATIVES WILL BE AVAILABLE TO DEMON-  *
*        STRATE MICROSOFT EXCEL SPREADSHEET SOFTWARE FOR THE PC *
*        THURS., 7/27 AT OMNI CONF. ROOM, BLDG. 3047, AT 10:00  *
*        AM AND 2:00 PM AND FRIDAY, 7/28 AT 932 BLDG. 9709, RM  *
*        139 AT 10:00AM AND 2:00PM.                             *
*                                                               *
*  07/24 BOTH IBM 3033S WILL BE DOWN THIS MORNING, MONDAY       *
*    FROM 11:30A-12:30P TO RESTORE TWO DISK PACKS.              *
*                                                               *
*  07/21 DCA SYSTEM SELECT 9 (THE SERIES/1 AT X'10') WILL BE    *
*        REPLACED WITH AN IBM 7171 (EMULEX IC SYSTEM SELECT     *
*        47) ON TUESDAY EVENING, JULY 25. SEE THE MAY JUNE      *
*        CAT NEWS FOR DETAILS. IF YOU HAVE PROBLEMS, CONTACT    *
*        PROGRAMMING ASSISTANCE.                                *
*                                                               *
*  07/21 SYSTEM SELECT 9 (SERIES 1) WILL NOT BE AVAILABLE FROM  *
*    17:00-19:00  JULY 25, TUESDAY, DUE TO INSTALLATION OF      *
*    7171 PROTOCOL CONVERTER.                                   *
*                                                               *
*                                                               *
*                                                               *
*                                                               *
*                                                               *
*****************************************************************
```

```
 RSCORS REPLACED (2/86) BY DISSPLA

CARD    1 SET   1 : FILE1 MELPTF3)
CARD    2 SET   1 : TITLE, MELCOR DFA MODELING: CASE 3); METAOOB
CARD    3 SET   1 : YLABEL, BYPASS TEMPERATURE, ((3K)
CARD    4 SET   1 : YLIM 7400, 7600
CARD    5 SET   1 : XLIM 200, 1200
CARD    6 SET   1 : LEGEND 360 MM PLANE
CARD    7 SET   1 : LIST
CARD    8 SET   1 : PLOT& COR-TSVR )))
CARD    9 SET   2 : DATA9 TEST DATA9
                    "     "
                  XLABEL,
                  YLABEL,
                    7.401OOE+03   2.140000E+02
                    7.410OOE+03   1.000001E+03
                    7.435OOE+03   1.000001E+02
                    7.500000E+03   0.000001E+02
                    7.510000E+03   5.000000E+02
                    7.580000E+03   1.000001E+03
                   -1.234500E+04  -1.234500E+04


OPENING FILE 1  MELPTF3)
TITLE BLOCK :  MELCOR    /89/08/01 /14.21.54 /DFA MODELING; CASE 3)
PROCESSING FILE 1  MELPTF3)
KEY BLOCK AFTER TIME=  0.000E+00  CYCLE=         0  KEY RECORD SIZES =      198 /     2315
END OF FILE ENCOUNTERED
FILE TITLE   : MELCOR    /89/08/01 /14.21.54 /DFA MODELING; CASE 3)
               80 RECORDS PROCESSED
ALL FILES PROCESSED
READING DATA FOR CURVE     2 FROM FILE DRINPUT
FOUND TEST-DATA9


INFORMATION LIST FOR PLOT    1

* PLOT VARIABLE :COR-TSVR )))
* PLOT VARIABLE :TIME,0
TITLE   :MELCOR DFA MODELING; CASE 3); METAOOB
XLABEL :TIME ((),S)
YLABEL :BYPASS TEMPERATURE ((3K)
LEGEND :360 MM PLANE
PLOT DATA SOURCE [CAL(C)/(FxP(I)/(FxP WITH BOUNDS(R)] :C
PLOT CURVE CHARACTER FLAG :6
FRAME [NEW(1)/LAST(0)] 1
XLIMITS :    7.400OE+03    7.600OE+03
YLIMITS :    7.0000E+02    1.200OE+03
NUMBER OF DATA PAIRS =    8
DATA FROM FILE :   1  MELPTF3)
LEGEND POSITION : 0.0045 0.1182
DATA PRINT LIST [OFF(0)/ON(1)] :  1

     8 POINTS PLOTTED


LIST OF DATA

       X             Y             Z             W             V             U             T             S             R             Q
  7.400SE+03   1.0P65E+03   7.640OE+01   1.1016E+01   7.600ZE+03   2.1094E+03   7.520ZE+03   1.0129E+03
  7.4203E+03   1.097AE+03   7.4603E+01   1.1093E+01   7.5001E+03   9.1419E+02   7.5256E+03   8.8991E+02


INFORMATION   ST FOR PLOT    2
```

```
DATA RECORD NAME :TEST-DATA9
TITLE  :MFICON DFA MODELING: CASE 11, METADUR
YLABEL : YLABEL,
YLABEL : YLABEL,
LEGEND :TEST-DATA9
PLOT DATA SOURCE (CALLED)/EXP(E3)/EXP WITH BOUNDS(B)) :E
PLOT CURVE CHARACTER FLAG :9
FRAME (NEW(1)/LAST(0)) 0
NUMBER OF DATA PAIRS =    6
DATA FROM FILE :   0  UNIMPUT
LEGEND POSITION : 0.0045 0.1182
DATA PRINT LIST (OFF(0)/ON(1)) : 0

     6 POINTS PLOTTED


PLOTTER CONTROLS FOR   2 DISSPLA FRAMES ARE ON DCP METAFILE TAPE55
```

```
MLT_9108_MS-8088   - 308 1968 MLT81968 AA 1   001 001 R67   END   9_37 04 AUG 89 R67_PR1   $10A ***** -   MLT_9108_MS_8088
MLT_9108_MS-8088   - 308 1968 MLT81968 AA 1   001 001 R67   END   9_37 04 AUG 89 R67_PR1   $10A ***** -   MLT_9108_MS-8088
MLT_9'   MS-8088   - 308 1968 MLT81968 AA 1   001 001 R67   END   9_37 04 AUG 89 R67_PR1   $10A ***** -   MLT_9108_'   8088
MLT_9.   MS-8088   - 308 1968 MLT81968 AA 1   001 001 R67   END   9_37 04 AUG 89 R67_PR1   $10A ***** -   MLT_9108_M   .088
MLT_9108_MS-8088   - 308 1968 MLT81968 AA 1   001 001 R67   END   9_37 04 AUG 89 R67_PR1   $10A ***** -   MLT_9108_MS_8088
MLT_9108_MS-8088   - 308 1968 MLT81968 AA 1   001 001 R67   END   9_37 04 AUG 89 R67_PR1   $10A ***** -   MLT_9108_MS-8088
MLT_9108_MS-8088   - 308 1968 MLT81968 AA 1   001 001 R67   END   9_37 04 AUG 89 R67_PR1   $10A ***** -   MLT_9108_MS_8088
MLT_9108_MS-8088   - 308 1968 MLT81968 AA 1   001 001 R67   END   9_37 04 AUG 89 R67_PR1   $10A ***** -   MLT_9108_MS_8088
```

DEFECT INVESTIGATION REPORT (DIR) NUMBER: -PG. 1/1

TITLE:REQUEST FOR MORE CAV PACKAGE PLOT INFO CODE:1.8+

REQUESTOR/ORG.: C R HYMAN/ORNL DATE:OCT19,1989

A. REQUEST:

I would like to be able to plot the following additional CORCON parameters as functions of time:

- Chemical power(watts)
- Individual debris species masses(kg):
  - Fe
  - Cr
  - Ni
  - Zr
  - UO_2
  - ZrO_2
  - SiO_2
  - CaO
  - C

Having this information from plots speeds the understanding of MELCOR analysis. It also would be usefui in understanding the relative importance of the various chemical effects being calculated by CORCON.

DEFECT INVESTIGATION REPORT (DIR) NUMBER: -PG. 1/1

TITLE: DEFECT IN DEGASSING MODEL CODE:1.8+

REQUESTOR/ORG.: C R HYMAN/ORNL DATE:Oct 24,1989

A. REQUEST:

As currently implemented in MELCOR (manual page HS-UG-22), the user does not have the flexibility to explicity specify the noding intervals of a structure which are to be evaluated for degassing. The user can only control the side of the structure, i.e. the inside or outside, from which the gas emerges(the ISRCHS parameter) and the number of noding intervals to be evaluated(the ISDIST parameter). The code then assumes that the nodes that are actually degassed are the ISDIST nodes nearest the side chosen by the ISRCHS parameter.

For a structure which is composed of one material, this poses no problem. However, for structures for which degassing occurrs only in the interior of the structure, this limitation may be significant.

Mike Carmel has been informed of this (by phone on 10/23/89) and he informed me that they are aware of this defect, but that work priorities do not permit them to address it at this time.

REQUEST BASIS/.....CHANGES REQUIRED/.....SEVERITY._____

E = error	N = none	MIN = minor
N = new	C = coding	MED = medium
R = revised feature	D = documentation	MAJ = major
O = other	I = input deck	

STEP	PAGES	BY	DATE	CK'D	DATE	APPR	DATE
A. Request	1						
B. Diagnosis							
C. Plan							
D. Changes							
E. Release							

DEFECT INVESTIGATION REPORT (DIR) NUMBER: -PG. 1/1

TITLE:ERROR IN RMAX DETERMINED BY CAV PACKAGE CODE:1.8+

REQUESTOR/ORG.: C R HYMAN DATE:Oct 24,1989

A. REQUEST:

This DIR serves as documentation only. Randy Cole is aware of the problem and is currently developing an UPDATE set to correct it.

An error was found in the RMAX variable calculated by the cavity package. It was made apparent by plotting the variable and noticing several non-physical steps downward. Cole suggested a temporary fix as follows:

```
* /
*ident,hym3
*/  fix the dermination of rmax for cav package
*d,cavrup.63
*i,cavrup.65
          end if
* /
*compile,cavrup
```

The above fix was inserted into the ORNL version of MELCOR and the problem has been resolved.

REQUEST BASIS/.....	CHANGES REQUIRED/.....	SEVERITY._____
E = error	N = none	MIN = minor
N = new	C = coding	MED = medium
R = revised feature	D = documentation	MAJ = major
O = other	I = input deck	

STEP_____PAGES	BY	DATE	CK'D	DATE	APPR	DATE
A._Request____1						
B._Diagnosis						
C._Plan						
D._Changes						
E._Release						

APPENDIX B:

MELCOR CODE CORRECTIONS/MODIFICATIONS IMPLEMENTED AT ORNL

This Appendix provides a brief history of ORNL's local MELCOR code versions. Where appropriate, reference is made to the DIRs included in Appendix A. As indicated in Appendix A, the completion of the work described in this letter report has resulted in the identification of several MELCOR code defects and desired code improvements. These problems may be conveniently grouped into four classes: (1) problems which effect only the plotting of the output [three DIRs], (2) problems which would effect the numerical results of the calculation, but that do not result in abnormal code aborts [seven DIRs], (3) problems which do result in abnormal code aborts or failure to start, but that were subsequently avoided via creative use of code input parameters or modification of the external data files prior to their use by MELCOR [six DIRs], and (4) problems which resulted in abnormal code aborts and that required code modifications to address the deficiency [three DIRs]. Significant effort was expended, in some cases, to determine the source of those problems which fall into the first three classes. A substantial effort was frequently required to diagnose and implement fixes for the Class 3 problems. Those efforts will not, however be discussed further in this Appendix. Rather, the purpose of this Appendix is to briefly identify the code bugs which did required local code modifications, and to describe the nature of the code modifications required to address these errors.

Three fixes have been made to the local ORNL version of MELCOR 1.8.0 and have also been forwarded to SNL for incorporation into subsequent versions of MELCOR. The first fix stems from an error in subroutine FDILOW and is similar in nature to the VANESA requirement of non-zero UO_2 mass in the debris pool reported in Appendix A. It appears that when the COR package is used to generate the materials calculated to leave the failed reactor vessel, there is always some amount of UO_2 present in the discharge. The FDI package was developed incorporating this assumption. Since BWRSAR calculates the initial pour to be entirely metallic, the difficulty immediately presented itself. The following UPDATE instructions were proposed by Ed Boucheron of SNL's MELCOR Code Development staff as a fix to the problem.

```
*/
*ident,fdiornl
*d,fdilow.283,fdilow,285
  if(fmassi(i).ne.0.0)then
   xfrac(1)=fmspl2(1)/(fmspl2(1)+fmcavn(1))
   call rnlfdr(ntpcc,ntpcor,xmsfdi,xmrfdi,xfrac,
    +          xcorcl,numcls,nfdi,ifdi)
    end if
```

These instructions have been incorporated to ORNL's version of MELCOR and the code no longer exhibits the difficulty.

The second modification addressed an error in which MELCOR attempts to take the square root of a negative number at UPDATE line SRPP.18. MELCOR had calculated tens of thousands of seconds of the transient when this error was produced. SNL MELCOR staff were contacted and they

suspected that the moles of some particular VANESA species was probably being calculated as very small negative numbers. They recommended that debug of the various variables be performed so that their values were known at the time of the error. Dave Bradley of the CORCON and VANESA code development staff was also contacted and he corroborated the MELCOR staff suspicion. Debug print statements were inserted into the subroutine SRPP and it was found that the variable xm(3,2) had the value of -0.460692e-13, a very small negative number.

The following conditional check was placed into SRPP immediately after line SRPP.15:

```
If (abs(xm(3,2).lt1.0e-6) xm(3,2)=0.0
```

MELCOR was restarted with the above modification inserted and no difficulty was encountered.

In discussions with Dave Bradley, it was learned that a more recent version of VANESA has been developed and is ready for use. It was also learned that the new version of VANESA contained a check for the exact situation causing the current difficulty. Additional checks have been developed in the new version of VANESA to preclude difficulties of this type. The MELCOR staff has been informed of this, but the priority of incorporating the newer version of VANESA into MELCOR remains low.

The third modification dealt with an error in the RMAX variable calculated by the cavity package. It was made apparent by plotting the variable and noticing several non-physical steps downward. Randy Cole, of SNL's MELCOR Code Development staff, suggested a temporary fix as follows:

```
*/
*ident,hym3
*/ fix the determination of rmax for cav package
*d,cavrup.63
*i,cavrup.65
        end if
*/
*compile,cavrup
```

The above fix was inserted by the ORNL version of MELCOR and the problem has been resolved.

APPENDIX C:

BWRSAR/MELCOR Interface

The use of BWRSAR for simulation of the invessel phase of the severe accident scenarios discussed in this report was predicated on (a) the perception that BWRSAR provides a more detailed treatment of the BWR core melt-down process and bottom head/debris interactions than does MELCOR, and (b) the fact that ORNL's experience with BWRSAR provided a basis for more rapid response to the reactor analysis needs of the Mark II and III Parametrics Program. The use of BWRSAR for these analyses does, however, present a code interface problem, since the MELCOR containment models must be driven with the BWRSAR-generated SRV discharge, vessel leakage, and debris pour results. The interface between the BWRSAR and MELCOR codes is provided via use of the External Data File (EDF) option in MELCOR. The utilization of the EDF option necessitated (a) modification of an existing BWRSAR Post Processor code, and (b) the addition of an "interface" control volume to the ORNL primary containment model.

The EDF Package serves as a MELCOR utility to allow the code to communicate with external data files that may define sources and/or boundary conditions which vary with time. The EDF Package has the capability to both read and write data files. SNL's development of the EDF package was driven, in part by ORNL's need to interface BWRSAR and MELCOR for the calculations described in this report. The addition of the EDF Package to MELCOR is responsive to a request (DIR) originally submitted to SNL by ORNL on March 20, 1987.

Four external data files are required to interface BWRSAR and MELCOR for the types of calculations described in this report. The first file consists of five parameters: time, integrated SRV flows (water, steam, and hydrogen) and instantaneous SRV gas temperature at monotonically-increasing times throughout the accident. The second external data file also consists of five parameters: time, integrated reactor vessel and recirculation loop leakage (water, steam, and hydrogen) and the instantaneous temperature of this leakage at monotonically-increasing times throughout the accident.

The third external data file contains all of the information necessary to characterize the debris pours entering the containment throughout the accident. This file contains seventeen parameters: time, integrated mass of UO_2 in the debris, integrated mass of zirconium (Zr) in the debris, integrated mass of steel in the debris, integrated ZrO_2 in the debris, integrated mass of steel oxide in the debris, integrated mass of control rod poison in the debris, integrated enthalpy of the debris, debris temperature, debris pour column diameter (i.e., reactor vessel hole size if calculated by MELCOR), debris velocity as it enters the containment cavity (normally calculated by MELCOR as the debris ejection velocity from the reactor vessel), mass fraction of iron (Fe) in the steel, mass fraction of chromium (Cr) in the steel, mass fraction of nickel (Ni) in the steel, mass fraction of iron oxide (FeO) in the steel oxide, mass fraction of chromium oxide (Cr_2O_3) in the steel oxide, and the mass fraction of nickel oxide (NiO) in the steel oxide, at monotonically-increasing times throughout the accident.

The fourth external data file contains the total exvessel debris decay heat history. This file contains only two parameters: time, and total exvessel debris decay heat at monotonically-increasing times throughout the accident.

Two separate BWRSAR post-processor codes are employed to generate the four external data files required to drive MELCOR. The first post-processor reads the BWRSAR-generated data files and generates both the plotted BWRSAR results for SRV and vessel leakage flows and the MELCOR SRV and vessel leakage external data files described above. Since this information is generated directly by BWRSAR, no manipulation or other modification of the BWRSAR results are performed by this post-processor.

The second BWRSAR post-processor (SARCON2) reads the BWRSAR-generated data files and generates the MELCOR external data files for the debris pour characteristics and the external data file for the debris pour decay heat. As currently written, the debris pour characteristics file contains 0.0 in the data fields for the integrated debris enthalpy, debris pour column diameter, and the debris pour velocity. These three parameters are required as input to MELCOR's Fuel Dispersal Interactions (FDI) Package, which determines the amount of steam generated by the debris as it falls through a pool of water. Initial consultations with the SNL MELCOR code development team indicated that all three parameters are required to be non-zero if FDI calculations are to be performed. (It has since been determined that the integrated enthalpy parameter is not actually utilized by MELCOR.)

To complete this file, a third code (MELCOR EDF pre-processor) was written to calculate the debris enthalpy using the materials properties functions of the MELCOR code. These were obtained from the Material Properties User's Guide for Version 1.8.0 of the MELCOR code. The data are in the form of tables of temperature vs. enthalpy per unit mass. The values of enthalpy at intermediate temperatures were obtained by linear interpolation between the tabulated values, just as is done in the MELCOR code itself.

The file generated by SARCON2 contains values of the integrated flow of each material up to time t_i. At time t_i, the temperature of the pour is T_i. The integrated flow of material j up to time t_i is denoted as $M_{j,i}$. The code calculates the enthalpy, $h_{j,i}$, per unit mass of each material j at temperature T_i. The total enthalpy to be inserted in the new EDF for a particular time, t_k, is the sum of all enthalpy additions up to time t_k:

$$\text{Total Enthalpy} = \sum_i \sum_j h_{j,i} \left[M_{j,i} - M_{j,i-1}\right] \qquad (1)$$

The summation over j is over all materials. The summation over i is from $i=2$ to $i=k$. For the initial time, t_1, the enthalpy value is taken as the sum of $h_{j,1}M_{j,1}$ for all the materials j, but is actually zero

since at the first time in the SARCON2 file, the $M_{j,1}$ values are all zero. If it should happen that values of $M_{j,i}$ are the same for successive values of i, a small increase is forced in order to prevent an interruption of the calculation, as discussed below.

The EDF pre-processor code also provides for a constant value of the flow diameter to be inserted. For the purpose of these calculations, it is the diameter of a circle whose area is a user-determined percent of the total inpedestal drywell floor area, A. The velocity of the flow at time t_i is calculated from the integrated mass flows and the component densities, d_j:

$$\text{Flow Velocity} = \Sigma_i \Sigma_j [M_{j,i} - M_{j,i-1}]/(Ad_j) \qquad (2)$$

The values for the densities were also obtained from the Material Properties User's Guide. Code results for enthalpies, velocities, debris pour column and diameter were checked with hand calculations.

The new external data files generated by the code were checked by exercising them in several short MELCOR calculations. A base case was first run for 2400 s of problem time. Next, the case was run with the integrated enthalpy set to zero. The answers were identical except for the listings of the values in the external data file. (It appears that the inserted value is intended to be available for checking purposes.) Third, the case was run for an extended period of time. An abnormal termination occurred in MELCOR at that point at which the input data for the integrated flows became constant, corresponding to a temporary pause in the flows. A DIR describing the problem was forward to SNL (see Appendix A). For present purposes, the problem was dealt with by changing the integrated flows by successive multiplication by a factor of (1.0 + 1.0e-6) during the constant integrated flow period, thus ensuring that the flows always increase slightly. Several cases have since been run successfully with the files created using this method.

The routines implemented in the MELCOR EDF pre-processor code will eventually be implemented directly into SARCON2. This will eliminate the need for post-processing the external data files generated by SARCON2.

In addition to the external data files, an additional MELCOR model "interface cell" was required because MELCOR 1.8.0 does not possess the capability to inject externally-sourced hydrogen into a pool of water. Thus, it is not possible to provide a realistic treatment of the impact of externally-calculated SRV hydrogen flows on pressure suppression pool temperature or wetwell pressure. A partially-flooded interface volume, which is connected to the pressure suppression pool (sub-surface) via a flow path is utilized to provide this function. The use of such an interface volume is undesirable, since the utilization of a small volume for this interface cell results in small code time steps and long cpu times, while the use of large cell volumes can result in a distortion of the pool's response due to the time delay associated with material

transport through the cell. Nevertheless, such a cell was incorporated in the model to provide the necessary interface between BWRSAR and MELCOR.

APPENDIX D:

MARK II STEAM EXPLOSION ISSUES*

*The work described in this Appendix was conducted by Dr. A. E. Levin, of the Georgia Institute of Technology and was funded by the Oak Ridge Associated Universities (ORAU).

Severe accidents in boiling water reactors (BWRs) are considered to be of extremely low probability. Nevertheless, because of the potential for widespread release of radioactive material outside of the limits of the reactor site, these accidents contribute significantly to the overall risk due to plant operation. As a result, the Nuclear Regulatory Commission (NRC) has sponsored a large, multi-disciplinary program to model such severe accidents.

One aspect of severe accident analysis that has received considerable attention in the NRC program is that of steam explosions. These events may occur when molten core materials, structural materials, or both come into contact with water. Steam explosions are characterized by extremely rapid vaporization of the water, resulting in very large pressures in the melt-water mixture. The pressure pulse is relieved by expansion of the mixture at high velocities. The resultant forces on the rest of the system, whether inside the reactor vessel or outside, can cause considerable damage. Steam explosions occurring invessel can potentially develop enough energy to propel the reactor vessel head into the containment. Exvessel explosions can generate missiles that may penetrate the containment building, or develop high enough pressures to cause containment failure. An exvessel explosion occurring in a BWR suppression pool could cause severe damage to the structure surrounding the pool (wetwell) and contribute to overall containment failure.

This Appendix discusses the issue of steam explosions in the pressure suppression pool in BWRs with Mark II containments. The Mark II design, which was described in Chapter 2, is uniquely susceptible to the ingress of molten core materials into the pressure suppression pool, in the event of a core-melt accident. Moreover, the core material may also be mixed with molten concrete and concrete decomposition products. The effect of the concrete on the dynamics of a melt-water interaction, i.e., whether the concrete increases or decreases the probability that a steam explosion may occur, is at present unknown.

After a description of the Mark II containment, the subject of steam explosions is discussed, with particular attention to the potential effects resulting from the presence of molten concrete. Current modeling techniques for melt-water interactions and steam explosions are then examined, with emphasis of the MELCOR computer code. Modifications to MELCOR that would permit more realistic modeling of melt-water interactions in Mark II suppression pools are explored, and recommendations are made for experimental work that would provide data to test the models.

BWR Mark-II Containment Design

Boiling water reactors in the United States have been constructed using three containment designs: Mark I, Mark II, and Mark III. While the Mark III is the most recent and most advanced configuration, there are nine BWRs at five sites which employ the Mark II design (Ref. 1). The basic Mark II configuration in shown in Fig. D.1. The reactor is supported on a pedestal near the top of the containment. The pressure

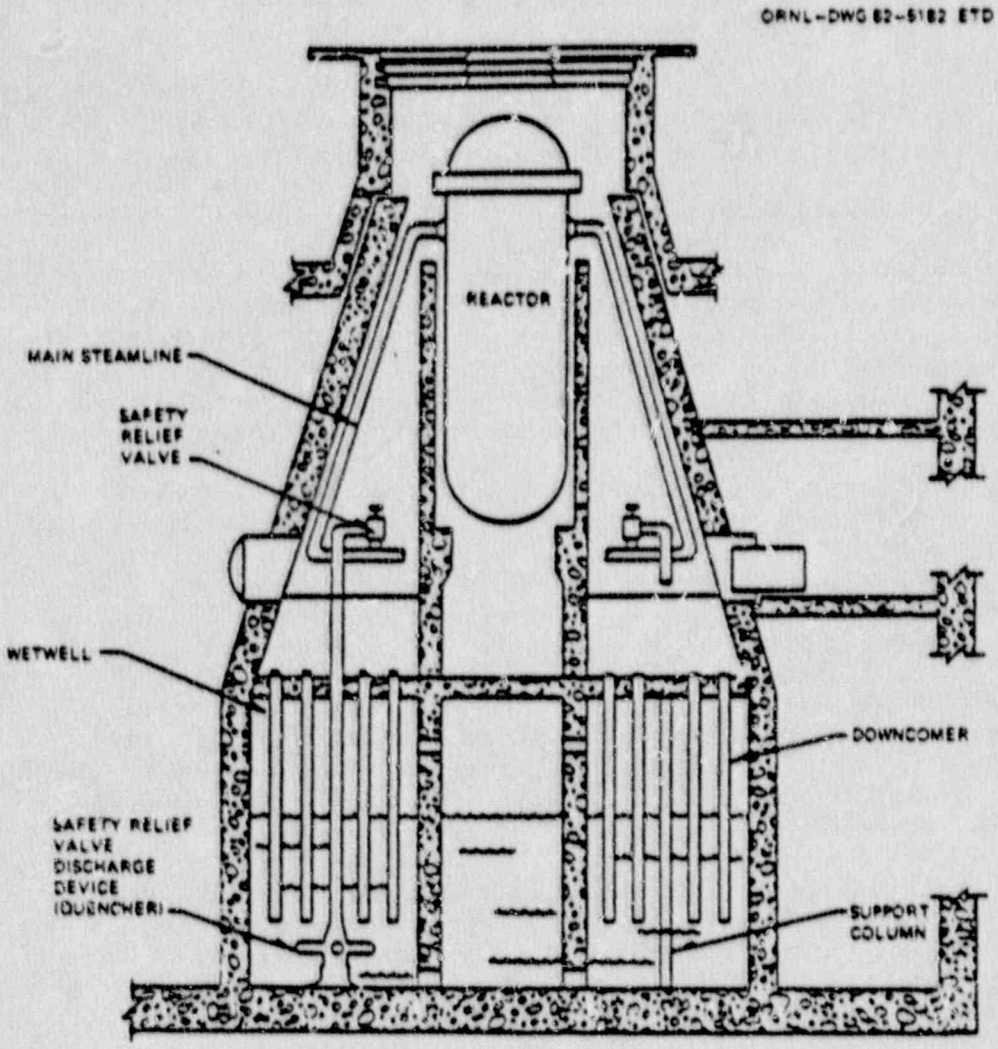

Fig. D.1. Limerick Mark II containment.

suppression pool comprises the lower part of the structure, with a slab of reinforced concrete separating the upper region, or drywell, from the wetwell. As can be seen, in the event of an unmitigated core-melt accident, molten metal (steel, zirconium), or oxides (UO_2, ZrO_2), or both will fall onto the concrete slab. Since these materials, referred to generically as corium, may be heated by the decay of fission products in the fuel, they can proceed to melt through the concrete, releasing carbon dioxide and water vapor into the drywell atmosphere while the concrete decomposition products become part of the molten mass. Upon melt-through of the concrete slab, (or inpedestal drains or downcomers) the molten material can fall into the pressure suppression pool. It is also possible for the molten corium to flow out of the area immediately below the reactor vessel, in which case it could flow into the wetwell through or around the downcomers shown in Fig. D.1. The corium could melt through the downcomers where they penetrate the drywell floor, or flow directly into the pipes if the molten pool is deep enough.
Figure D.2 shows the Mark II containment used at the LaSalle plant. In this design, the drywell floor within the reactor pedestal is recessed. The volume of the resultant cavity is large enough to contain an entire molten core. In addition, the wetwell does not extend into the inpedestal region under the cavity, so that the probability of a melt-water interaction in the wetwell is substantially smaller than in the design shown in Fig. D.1. Another variation on this containment design is similar to that shown in Fig. D.1, but with downcomers in the inpedestal region of the drywell floor in addition to those shown in the expedestal region. All of the Mark II designs except Susquehanna also incorporate 4"-6" diameter inpedestal floor drains which penetrate the drywell floor. In the event of a vessel breach, the molten core material would be able to reach the suppression pool via the downcomers as described previously, via melt-through of the floor drains, or via melt-through of the concrete floor.

The possibility of molten corium, possibly combined with molten concrete, reaching the suppression pool raises the possibility of steam explosions. The following section provides an overview of this subject, and discusses how the presence of concrete may affect the system's behavior.

Steam Explosions

Steam explosions can occur when molten core materials come into contact with water. The explosion can be considered as passing through four distinct phases (Ref. 2):

1. *Fuel-coolant mixing*, in which the molten fuel and liquid cool and become intermixed on a coarse scale. The heat transfer mode is relatively quiescent, and is considered to be film boiling.
2. *Triggering*, in which the fuel and coolant are brought into intimate contact. The vapor film collapses and heat transfer rates escalate rapidly, as the fuel fragments and the heat transfer area increases.

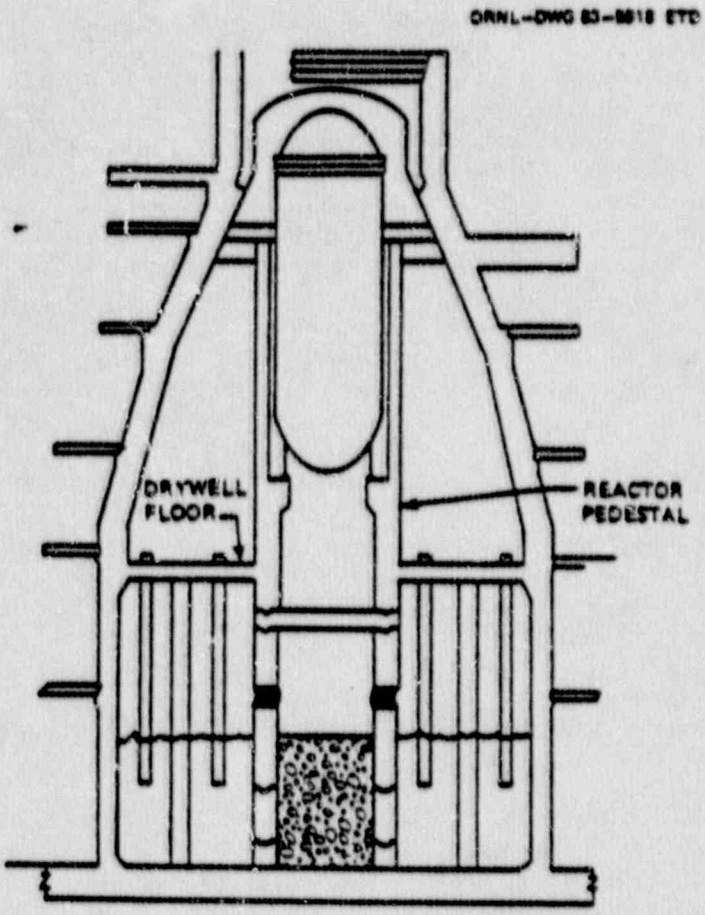

Fig. D.2. La Salle Mark II containment.

3. *Explosion propagation*, in which the fuel fragmentation process spreads rapidly through the fuel-coolant mixture. Large quantities of vapor are produced at extremely high pressure.
4. *Expansion*, in which the high-pressure vapor expands against the surrounding liquid and structure. It is in this phase that destructive mechanical work can be performed. It must be emphasized that these four phases proceed very rapidly, with the time between triggering and expansion on the order of 2 ms.

Considerable work has been done in the field of steam explosion phenomenology. An extensive experimental program was carried out at Sandia National Laboratories (Refs. 3-6), in which experiments were performed using core simulant materials and molten corium. Additiona information on steam explosions is available outside of the nuclear industry; both the foundry and paper production industries have considerable operating experience with steam explosions in process equipment (Refs. 7-8).

The possibility of steam explosions in Mark II wetwells is of concern for several reasons. The forces generated during a steam explosion can cause severe damage to the wetwell structure and components. It is conceivable that the pressure spike that might occur would of sufficient magnitude to fail the containment. Should such a failure occur, it is also possible that the explosion would resuspend into the containment atmosphere radioactive material that had been deposited previously in both the wetwell and the drywell. These aerosols would then escape into the environment, where they might comprise a significant source term. It must be noted in this connection that the elapsed time between the beginning of a severe accident and the occurrence of a steam-explosion could be several hours, since the core material must first penetrate the reactor vessel and then melt-through the floor drains or floor slab, or overflow the downcomers. Steam explosions in Mark II containments could, therefore, provide the mechanism for a long-delayed, but large, fission product source term.

Effect of Concrete on Steam Explosions

Despite the large body of experimental data that is available on steam explosions, there is virtually no information on how the presence of concrete in the molten material might affect the possibility of the event or its subsequent behavior. The inclusion of molten concrete and its decomposition products in the melt potentially affects both the properties of the molten material and the manner in which it interacts with the water in the suppression pool.

Concrete is basically a mixture of ceramic materials with water and carbon dioxide trapped within its matrix. The type of concrete used in most nuclear power plants consists largely of calcium oxide (CaO) and silicon dioxide (SiO_2), with small amounts of alumina (Al_2O_3) and other minerals. The CO_2 content is approximately 20% by weight, with water comprising about 7% of the mixture. Concrete is able to withstand very high loadings in compression, but has relatively little mechanical

strength in tension. Its properties are also highly temperature dependent; if it is raised to a temperature near the boiling point of water, the water in the matrix begins to evaporate and the concrete loses substantial mechanical strength.

When it is heated to high temperatures, concrete begins to lose not only its water, but its entrapped CO_2 as well. By the time it reaches ~2240°F, almost all of the CO_2 and water vapor has been driven out. Concrete's melting temperature varies according to its composition. In general, the melting temperature ranges between ~2096 and 2546°F (Ref. 9); it should be noted that this temperature is somewhat below the melting temperature of its individual components.

When molten concrete is cooled, it does not re-solidify into an aggregate similar to its original state. Instead, it becomes a vitreous material, with a glass transition temperature around 1466°F. When cooled below this temperature, the material turns into a glass.

While there is no information available on steam explosions with corium-concrete mixtures, experiments and analytical modeling have been performed on molten core-concrete interactions (Refs. 9-12). This work may give some insight into the composition of the material that would enter the wetwall in a Mark II. Most of the tests on molten core-concrete interactions has been performed at SNL. As in the steam explosion tests, both simulant materials and corium have been used for these experiments. When the molten material consists only of metal (e.g., molten steel), the concrete decomposes into molten oxides that tend to stratify and float on top of the molten metal. It has been hypothesized that if sufficient CO_2 and water vapor were released from the decomposing concrete, the gases sparging through the molten pool would cause the two layers to become thoroughly mixed (Ref. 9). However, this type of behavior has not generally been observed (Ref. 10). The individual layers are well-mixed within themselves, but the layers remain distinct from one another.

In contrast to the behavior described above, contact between molten oxidic material and concrete has resulted in a well-mixed pool with no apparent stratification (Ref. 11). The concrete constituents dissolve readily into the core oxides, changing the thermophysical properties of the mixture. Complex chemical interactions may also occur in these mixtures; for instance, the calcium oxide in concrete can react with uranium dioxide to form calcium uranate.

One experimental series of particular interest with respect to core/concrete/water interactions is the SWISS tests (Ref. 13). In these experiments, an iron-alumina melt, simulating molten corium, was brought into contact with a limestone-common sand concrete disk. The molten metal was heated throughout the test by inductive means. At a specified point in each test, water was allowed to flow onto the melt and concrete, forming a pool on top of the mixture. Water was supplied continuously to the pool to maintain a constant subcooling and constant water head. Heating was maintained until the melt penetrated through

the bottom of the concrete disk. In the SWISS-1 test, water was introduced about 35 minutes after deposition of the melt on the concrete; in SWISS-2, the water was introduced shortly after the melt deposition.

No steam explosions were seen in the two SWISS tests, and, in fact, the water appeared to have relatively little effect on the erosion of the concrete by the melt.

The lack of experimental data on steam explosions involving molten corium and concrete has also led to investigation of steam explosions in industrial practice. Steam explosions have been noted in both the foundry industry, when molten metal comes into contact with water [7], and in the paper production industry, where the explosions are caused by contact between water and molten smelt [8]. The latter experiences are of some interest with regard to Mark II steam explosion issues, and are explained here in more detail.

Smelt is a mixture of salts, primarily sodium carbonate and sodium sulfide, that result from the chemical processes involved in paper production. The smelt is initially dissolved in a solution referred to "black liquor". This liquid is sprayed into a boiler and is burned to produce process heat. The smelt becomes molten in this process, and runs to the bottom of the boiler, from which it is subsequently drained. The molten smelt then flows into a water pool, where it is reconstituted into its original components, to be reused in production. Molten smelt-induced steam explosion can occur in two places. If a boiler tube breaks or if water leaks into the boiler, the molten smelt on the floor of the boiler can cause a steam explosion. When the molten smelt is drained from the boiler and flows into water for reconstitution, steam explosions can also occur. Of the two types of explosions, those occurring in boilers tend to be the most violent and the most destructive. It is of particular note that, in many cases, steam explosions did not occur immediately upon contact of water and molten smelt. Rather, significant delays, up to several tens of minutes, can occur between water ingress and a steam explosion. It has been hypothesized that a layer of char and solidified smelt can overlay the molten smelt on the boiler floor. When water enters the boiler, it first encounters the solid crust. The crust acts as an insulator, keeping some smelt molten, while the water tends to percolate downward. Eventually, water comes into contact with molten smelt, initiating an explosion.

This experience is relevant, in some respect, to the SWISS tests, in which water was poured over a melt-concrete mixture, as described previously. Although no steam explosions were observed in the SWISS tests, the water was in contact with the moltent mixture for only about 6 minutes in SWISS-1 and 35 minutes in SWISS-2. The results of the SWISS tests indicate that a core of molten material was overlain by a solidified, vitreous mixture of concrete and melt constituents. It can be speculated that a steam explosion might have occurred in either or both SWISS runs had the water remained in contact with the melt-concrete mixture longer, allowing water to penetrate the solidified upper crust

and to come into contact with the inner, molten material. The possibility of this sequence of events is also relevant to BWR Mark II steam explosion questions, as will be discussed in a later section.

Because the physical properties and configuration of the molten mass depend on the composition of the material deposited on the concrete, the course of a severe accident is of considerable importance. In particular, it is recognized that, upon melt-through of the vessel lower head, the composition of material falling from the vessel onto the drywell floor will vary as a function of time. Calculations have been performed for an unmitigated station blackout at the Peach Bottom reactor, a BWR in a Mark I containment. Initially, the molten debris entering the drywell is almost entirely metal; most of the oxidic material remains solid, since its temperature is not high enough to allow it to melt. After a considerable period has elapsed, about 250 minutes in the referenced calculation, the oxide temperature in the vessel reaches the liquidus temperature, and subsequent oxidic debris is considered to be molten.

If a Mark II containment is now considered, assuming the course of the accident is similar to that described above, the composition of the molten material on the drywell floor can be discussed. The initial pour of molten metal would first degas the concrete and then begin to erode it. Gases released from the concrete would oxidize some of the metal, and molten oxides from the concrete would be present, as well. These molten oxides would tend to form a stratified layer on top of the metal, although the gas being released from the concrete could serve to mix these layers to some extent. The molten metal would create a cavity in the floor and continue to erode underlying concrete. When molten core oxides finally begin to spill from the reactor vessels, they might also tend to form a stratified layer on the molten metal, depending on the relative densities of the two materials. If the prior metal-oxide system is stratified, the core oxides could combined with the lighter oxides already present. In addition, if the oxide layer remains on top of the metal layer, it can erode the side walls of the cavity in the drywell floor, with the concrete decomposition products also becoming part of the molten oxidic layer.

The process of ablation of the concrete on the drywell floor is relatively slow, and it is hypothesized that it would take some hundreds of minutes for the molten corium to penetrate through the drywell floor and its reinforcing members. The point at which the molten material would enter the wetwell is not clear, because of the lack of information on fundamental processes as the accident progresses. It is possible that some of the molten corium would solidify, particularly near the top of the pool, where it is in contact with the drywell atmosphere.

In addition, it should be remembered that the degassification and dewatering of the concrete occurs at temperatures far below that at which the material is ablated. Therefore, a "front" can be thought of as proceeding into the concrete, behind which the floor is dry and essentially degassed. The front will reach the bottom of the floor

before it is melted through. Concrete loses most of its structural strength when it is dry, and does not resist tensile forces well in any case. The molten core debris exerts a load on the floor of many tons; it is therefore entirely possible that the drywell floor will give way well before the molten material has eroded its complete thickness.

At this point, a mixture of molten metal and molten oxides, possibly mixed with frozen metal, frozen oxides, and hot, dry concrete, can fall into the wetwell. Again, because of a lack of fundamental data, it is difficult to determine the configuration of this material as it enters the wetwell and the suppression pool. The behavior of the debris as it interacts with the suppression pool is also not known. Depending upon the composition of the debris, it is possible that a steam explosion may occur. Even if an energetic explosion does not occur, it is possible that the rapid generation of steam as the hot debris enters the suppression pool will produce pressures sufficient to fail the containment. The containment will be at an elevated temperature and pressure prior to the melt-pool interaction because of the gases and water vapor released during the core-concrete interaction. A steam explosion may create missiles which can penetrate the containment walls and cause significant damage to structures inside and around the wetwell, while a non-energetic steam spike might cause a more gradual containment failure by overpressurization of the containment. The course of the accident at this point will also affect the resuspension of radioactive material deposited in both the containment and the wetwell, and its subsequent dispersal inside and outside of the containment. The behavior of the corium-concrete mixture when it interacts with the suppression pool is, therefore, important to understand, in order to determine severe accident progression in Mark II BWR plants.

Modeling of Steam Explosions

Although the four basic phases of a steam explosion are understood qualitatively, most quantitative modeling of the phenomenology currently employs relatively simple models. The reasons for this approach are both physical and practical. From the physical standpoint, the processes involved in steam explosions are difficult to model. The detailed mixing behavior of the molten material and the coolant, heat transfer, triggering and propagation, and the thermodynamics and hydrodynamics the expansion process must all be described mathematically if a complete explosion model is to be developed. To this point, there is not enough detailed data on steam explosions to permit more than primarily empirical or semi-empirical models. The stochastic nature of these events – why seemingly identifical initial conditions can result in different behavior – is also not well understood. From a practical point of view, the resolution of any model that is developed to predict steam explosion dynamics must be considerably shorter than the duration of the physical events themselves. Significant events in steam explosions can occur on a time scale of tens of microseconds. The timesteps that must be used in a computer model to resolve this detailed behavior must probably be of the order of 10^{-6} to 10^{-7} seconds. In the

calculation of a severe accident over a period of hours, it is impractical to perform some calculations using time steps this small. As a result, integrated severe accident codes do not employ detailed steam explosion models. A detailed code for fuel-coolant interaction and steam explosions is currently under development; this code has not been released for general use at this time.

The MELCOR computer code [15] is a large, integrated, severe accident model. It includes modules for the calculation of most of the important phenomena involved in core-melt events. One of these modules is the Fuel Dispersal Interaction (FDI) Package. The FDI package contains a simplistic model for the initiation (mixing) phase of a steam explosion. This model will be explored in detail in the following section, with subsequent discussion regarding how the model can be altered to accommodate BWR Mark II analysis. Suggestions for improvement of the FDI modeling approach will also be discussed.

Summary of MELCOR-FDI Modeling Approach

The FDI package in MELCOR consists of approximately 50 subroutines, and contains calls to approximately 20 additional subroutines in other MELCOR packages. FDI models the hydrodynamic and thermal behavior of molten corium that is dropped into a reactor cavity filled with water. It calculates the fragmentation of the molten material during the initial mixing phase resulting from hydrodynamic interaction with the water, the heat transfer between the corium and the water, and the steam generation resulting from the heat transfer. It does not, however, calculate the process of a steam explosion; in fact, the calculation ends at about the completion of the initiation phase. It should be noted that some modeling has apparently been done to continue the calculation into the triggering and propagation phases. However, these routines are not presently accessed when the FDI package is executed.

The execution of the package is initiated by a call the subroutine FDIRN1, which in turn calls two other subroutines: a control routine, FDICON, and subroutine FDILOW, which handles the execution of additional subroutines that model the events occurring during an ejection of molten corium from a reactor vessel at low pressure. This is the case of interest for BWR Mark II modeling, since it is assumed that the reactor primary system will be depressurized long before vessel melt-through. FDILOW calls the subroutines in FDI that calculate heat transfer, enthalpy change, and, thereafter, thermal behavior of the melt and steam generation. Figure D.3 shows the call sequence for major subroutines in the FDI package.

The overall calculational procedure for the FDI package is relatively simple. The heat transfer from the molten corium to the water is calculated, based on a simple heat transfer model, with the heat transfer area determined from hydrodynamic breakup of the melt stream. The mixing volume (volume of water into which the melt transfers energy) is taken to be all of the water in the cavity, and the steam generation

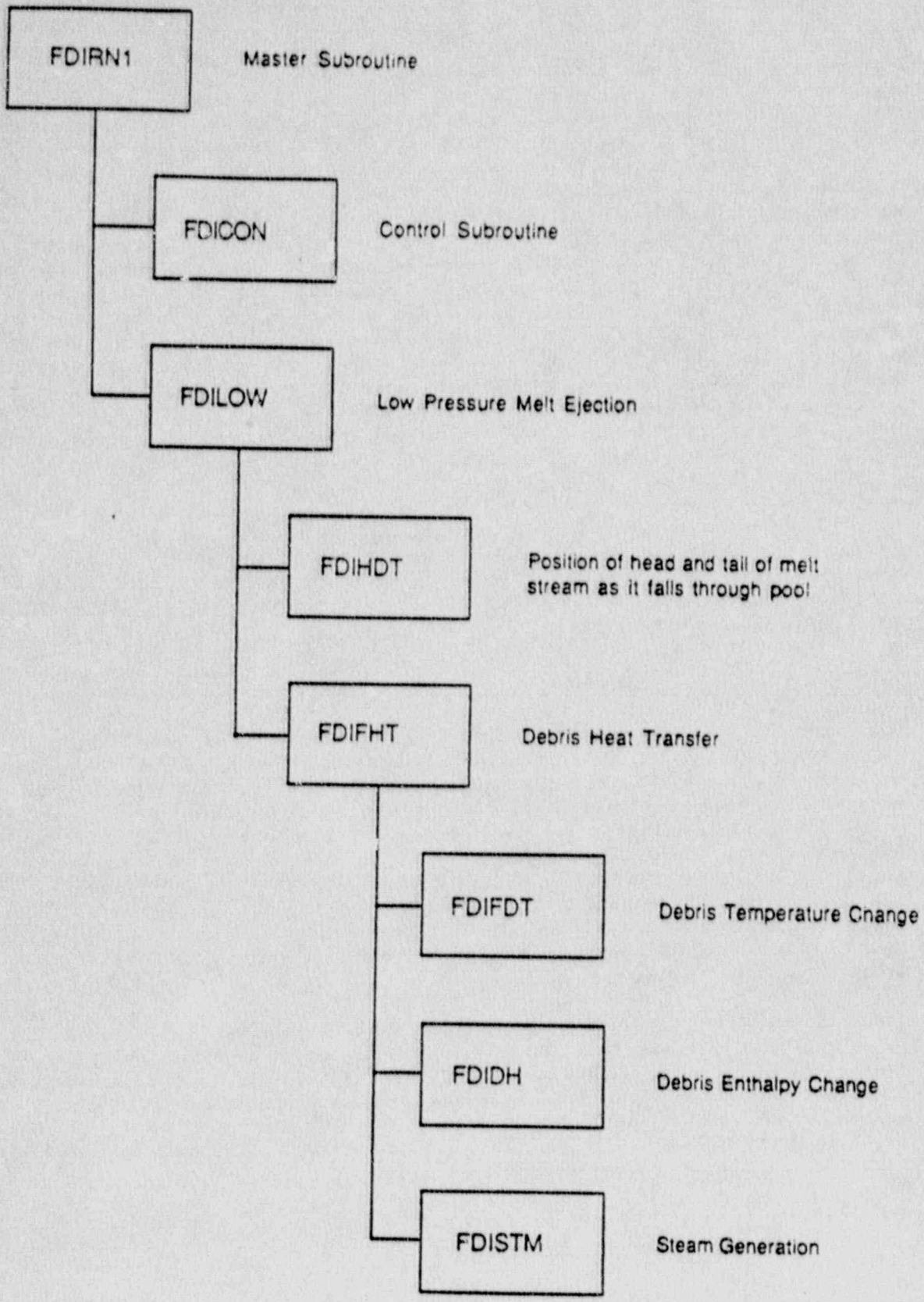

Fig. D.3. MELCOR Fuel Dispersal Interactions Package flow chart.

resulting from the heat transfer is found, as well as the change in fuel temperature. The calculation continues until the melt stream comes into contact with the cavity floor. If the corium is above its liquidus temperature, FDI assumes that a steam explosion is triggered by melt-cavity contact. This assumption is based on experimental evidence that contact between the melt-water-steam mixture and the floor of the cavity is one way in which a steam explosion is triggered. At this point in FDI, the calculation ends. As mentioned previously, some modeling has been performed and coded into the FDI package to carry out actual steam explosion calculations. If corium contacts the cavity floor and triggers a steam explosion during a given time step, the code logic would nominally move to a series of calls to subroutines that are meant to find fuel fragment size and coolant mixing volume, based on empirical correlations. The previous mixing calculation would be ignored, and a new calculation would be initiated to determine the explosion process. However, the routines comprising this section of the code are not accessed; calls to a controlling subroutines, FDISXI, are "commented out" of FDIRN1, and the models in a second subroutine, FDISEX, are also "commented out." Therefore, a mixing calculation is carried out only as long as no steam explosion is triggered, ending either when all of the water in the cavity is boiled away, or when the melt contacts the cavity floor. In the latter case, since the code cannot transfer control to the steam explosion routines, the calculation does not really progress to the end of the mixing phase.

Heat Transfer Calculation

The heart of the FDI package is the corium temperature calculation, carried out largely in subroutine FDIFDT. This routine calculates not only the heat transfer, but the corium breakup as it falls through the water-filled reactor cavity (or any water pool, such as the Mark II wetwell). The heat transferred to the water in the water-corium mixture determines the amount of steam generated in the initial mixing process. In addition, the amount of energy transferred from the corium to the water must, of course, reduce the corium temperature. It is ultimately this temperature, i.e., whether the corium is molten or solid upon contact with the cavity floor, that determines the likelihood of a steam explosion in MELCOR.

The corium heat transfer calculation employs a relatively simple model. It is assumed that the corium breaks up into small spherical fragments as it drops through the water pool. These fragment are treated in a lumped fashion, as bodies without temperature gradients, which transfer their energy to an essentially infinite heat sink. The primary mode of heat transfer is assumed to be radiation, though a bounding calculation is done for film boiling.

The diameter (d_f) of the corium fragments is calculated as

$$d_f(z) = d_o e^{-Cz} \qquad (1)$$

where z is the distance from the top of the pool, and d_o is the initial diameter of the melt stream. The constant, C, is taken from an empirical model, not referenced in the code manual:

$$C = \left[\left(0.1232 - 0.15\sqrt{\frac{\rho_c}{\rho_f}}\right) We^{1/4}\sqrt{\frac{\rho_c}{\rho_f}}\right]/d_o \tag{2}$$

where ρ_c and ρ_f are the coolant and fuel (corium) densities, respectively, and We is the Weber number, defined as

$$We = \frac{\rho_c d_o u^2}{\sigma_f}, \tag{3}$$

where u is the velocity of the corium as it falls through the pool and σ_f is the corium surface tension.

The equation for the fuel temperature, T_f, as a function of time, t, assuming radiation heat transfer, is

$$-\frac{dT_f}{dt} = \frac{\sigma A (T_f^4 - T_c^4)}{\rho_f c_f V} \tag{4}$$

where σ is the Stefan-Boltzman constant for radiation heat transfer, c_f is the corium specific heat, T_c is the coolant temperature, and A and V are the corium fragment area and volume, respectively.

Since the geometry is spherical,

$$\frac{A}{V} = \frac{\pi d^2}{\frac{\pi d^3}{6}} = \frac{6}{d}. \tag{5}$$

It is now assumed that

$$T_c^4 << T_{f,b}^4 \tag{6}$$

where $T_{f,b}$ is the corium temperature at the cavity floor. The temporal derivative of the corium temperature can also be transformed into a spatial derivative by the chain rule:

$$\frac{dT}{dt} = \frac{dz}{dt}\frac{dT}{dz} = u\frac{dT}{dz} \tag{7}$$

Substituting Eqs. (1), (5), and (7) into Eq. (4), and eliminating T_c using Eq. (6), the differential equation for corium temperature becomes:

$$-\frac{dT}{dz} = \frac{6\sigma T_f^4}{\rho_f c_f d_o e^{-Cz_u}} \tag{8}$$

The solution to this equation, with $T_f = T_{f,o}$ at the top of the pool at $T_f = T_{f,b}$ at the bottom of the pool ($z=0$), is

$$T_{f,b} = \left[\frac{1}{3\,\frac{6\sigma}{\rho_f c_f u d_o C}\left(e^{Cz}-1\right) + \frac{1}{T_{f,o}^3}}\right]^{1/3} \tag{9}$$

Equation (9) assumes that the corium particles stay molten, and therefore continue to break up, until they reach the cavity floor. If at any point the corium temperature drops below its solidus, the particles are assumed to solidify, and the diameter is held constant from that elevation to the cavity floor.

As noted previously, a bounding calculation is performed to determine whether the corium temperature is such that film boiling is important. The film boiling correlation is:

$$h_{fb} = \frac{k_g}{2(k_g \mu_g d_o (T_v - T_{sat})/[\rho_g (\rho_c - \rho_g) g h_{fg}])^{1/4}} \tag{10}$$

where

h_{fb} = film boiling heat transfer coefficient
k_g = steam thermal conductivity
μ_g = steam viscosity
ρ_g = steam density
T_{sat} = steam saturation temperature
T_v = $1/2\ (T_f + T_{sat})$
h_{fg} = latent heat of vaporization
g = gravitational acceleration

Using this correlation, the temperature at which the radiation heat flux, q''_r, is equal to the film boiling heat flux, q''_{fb}, is determined. If the corium temperature is greater than the intersection point, film boiling is ignored. For most cases, as long as the corium is molten, $q''_r >> q''_{fb}$. If, however, the corium temperature drops below the intersection point (referred to in MELCOR as the "conversion temperature"), radiation heat transfer is eliminated and the calculation is carried forward from that elevation using the film boiling correlation.

The actual heat transfer calculation – transfer of the energy in the corium to the coolant – is performed in subroutine FDIFHT. Here, equation-of-state subroutines are called to calculated the enthalpy change of the fuel as it changes temperature during the process described above. The fuel enthalpy change is then used to determine the enthalpy change in the coolant. As explained in the previous Section, the

coolant mixing volume is taken to be the entire volume of water in the cavity. The steam generation can therefore be found very simply, since the fuel mass and coolant volume and mass are known, and the total enthalpy transfer has been calculated.

The heat transfer model in the FDI package has the advantage of being relatively simple and easy to use. It does, however, have some apparent shortcomings. In particular, the manner in which the change in fuel enthalpy is calculated is not entirely consistent from the physical standpoint. The equation of state for the fuel, found in Subroutine FEOSIN, includes the latent heat of fusion, which is released as the corium solidifies during the energy change between liquid and solid states. Rather than holding the temperature constant while a change of state occurs, it appears that the latent heat is "spread out" over a range of temperatures. If the corium mixture does not undergo a change of state - that is, if it stays molten - or if it changes state completely - solidifies entirely - the total enthalpy change is calculated reasonably accurately. However, if the corium reaches an "in-between" stage, where some has solidified and some remains molten, it is not clear that MELCOR can calculate accurately the total enthalpy change.

In addition to the above inconsistency, the way in which the heat transfer "conversion" is calculated appears to have the potential for ignoring significant contributions to the energy transport from corium to coolant. The film boiling contribution is considered only if the corium temperature drops below the so-called "conversion" temperature, at which $q''_{fb} = q''_r$. However, since by definition q''_r is of the same magnitude as q''_{fb}, it seems that half of the heat transfer is ignored. In addition, if the temperature is only slightly above or below the "conversion" point, only one mode of heat transfer is considered (radiation if $T > T_{conv}$; film boiling if $T < T_{conv}$). However, the alternative mode may still be a significant contributor to the energy transport under these conditions, so that MELCOR may underestimate the total heat transfer from corium to coolant.

Possible modeling changes in MELCOR that would permit more accurate calculation of the corium to coolant energy transfer will be discussed in a later section.

Inclusion of Molten Concrete in MELCOR FDI Calculations

The FDI package uses a set of material property subroutines to determine the mass-averaged thermophysical properties of the corium in steam explosion calculations. Included in the MELCOR library of materials are the main constituents of corium, such as uranium, zirconium, stainless steel, and the oxides of these materials. Also included are properties of concrete, for use primarily in calculations of molten corium-concrete interactions. While these properties are not presently included in the input to the FDI package - that is, concrete is not considered as a constituent in the material entering the coolant pool - there is no reason why it could not be added, also on a mass-average basis. The basic procedure for the calculation would therefore be

1. Determine constituents of material entering wetwell, using the molten corium-concrete interaction module present in MELCOR.
2. Determine, if possible, specific constituents of melt "pour" as a function of time.
3. Calculate properties of molten material on mass-averaged basis.

It must be mentioned here that some internal logic in MELCOR would require alteration to permit the transfer of results from the molten corium-concrete calculation to the FDI package.

The largest uncertainty in the procedure detailed above, with respect to a Mark-II calculation, lies in the detailed make-up of the material entering the water pool. Since there is virtually no experimental data in this area, it is not known whether or how the material would be stratified as the corium melts through the drywell floor. It it is not stratified, it may be possible to assume that the corium and concrete enter the pool as a relatively homongeneous mixture. If the material is stratified, however, the constituents of the melt may enter the pool separately, so that molten metal and molten oxides would not be well mixed. The thermophysical properties of the melt as it interacts with the pool would therefore be affected by the presence or absence of homogeneity, and the way in which a steam explosion might be triggered and propagate could also be affected.

Because of the way the FDI package is now configured, it is likely that a homogeneous mixture could be accommodated. A heterogeneous, stratified melt, in which the properties of the material might vary as a function of time or position, would be significantly more difficult to accommodate.

Suggested Alterations to the MELCOR FDI Package for Initiation Phase Modeling

As described in previous sections, the FDI scheme for calculating the initial (mixing) phase of a steam explosion is extremely simple. Several assumptions are made regarding the thermophysical properties of the molten corium, the mode of heat transfer, and the volume of coolant involved in the mixing phase - and therefore the steam generation - that are in some cases difficult to justify on a physical basis. In addition, the FDI package is not well documented with respect to hydrodynamic and heat transfer models, although the code listing itself contains considerable useful information in the form of comment statements. It is therefore suggested that changes and additions to the FDI models be considered to allow more physically realistic calculation of the initial phase of a steam explosion. Suggested alterations are listed below.

1. Improve the heat transfer calculation logic so that both radiation and film boiling can be taken into account, when appropriate.

2. Improve the equation-of-state calculation for the molten corium. Specifically, the temperature of the corium should be modeled accurately during the solidification process, and the latent heat fusion accounted for explicitly in that calculation. This would allow a more accurate determination of the amount of molten material available to participate in a steam explosion.
3. Complete the package so that the complete initiation phase of a steam explosion is accomplished, and an explosion calculation can be performed. The current version of the package has some key subroutines removed, so that equations for corium fragmentation and mixing are not accessed. Instead, the fuel is simply mixed with all available coolant, and the calculation ends when a steam explosion is triggered.
4. Addition of the capability to handle non-homogeneous melt products should be considered. This would allow variations in melt properties as a function of time and space, which may be necessary for BWR Mark II simulations.

It is recognized, in making these recommendations, that the data base for steam explosions is not particularly large. It is also recognized that a great deal about steam explosion dynamics is not well understood. While the four phases can be described qualitatively, quantitative models for parameters such as the corium mass participating in an explosion, mixture volumes, conversion ratios (corium thermal energy to destructive expansion work), explosion triggering, and explosion propagation are difficult to find, and tend to be highly empirical. In addition, because of the time scale on which such explosions occur, detailed modeling may be neither appropriate nor desirable in a code such as MELCOR. Instead, bounding calculations based on empirical models may be the best approach, one that will allow reasonable conclusions to be drawn while maintaining faster-than-real-time calculations. The suggested improvements, however, should improve the physical basis of the FDI package, while having a relatively small impact on calculation time.

A Model for Peak Pressures in Steam Explosions

Although the FDI package in MELCOR currently calculates only the first phase of a steam explosion, a simple model for the peak pressures reached during a steam explosion could be added to the code with little difficulty. It must be emphasized that this model does not predict whether a steam explosion will actually occur; the stochastic nature of these events makes such predictions extremely difficult. However, since the FDI package does in fact contain the logic to determine if a steam explosion *might* occur – i.e., the corium is molten when it comes in contact with the cavity floor – the peak pressure model represents a means by which to estimate a factor related to the destructive potential of the event.

The basic model is one proposed by Corradini [2] and modified by Taleyarkhan [16]. The primary assumptions in the model are that the

corium mixes with a specified mass of coolant in a coolant volume (isochoric) process, coming to thermodynamic equilbrium. The equilbrium temperature, T_e, is calculated by assuming that the total internal energy of the corium-water-steam system is conserved, so that

$$T_e = \frac{T_f + \left[\frac{m_c c_c}{m_f c_f}\right] T_c}{1 + \frac{m_c c_c}{m_f c_f}} \qquad (11)$$

The heat capacity of the coolant, $m_c c_c$, is a weighted average of the water and steam components of the coolant. Since this model is applied after the mixing phase of the corium-water interaction, the mixture volume will have some characteristic void fraction. Using the initial void fraction, a mixture specific volume, v_m, can be calculated:

$$v_m = \frac{1}{\rho\,(1-\alpha) + \rho_g \alpha} \qquad (12)$$

where ρ, ρ_g, and α are the liquid density, vapor density, and void fraction.

The process is assumed to proceed at constant volume, and since mass is conserved, as is implied in Eq. (11), the specific volume of the mixture must be constant. Therefore, an equation of state can be applied to the system at T_e and v_m, to find the pressure when the corium-coolant system reaches equilibrium. This pressure represents the peak value (pre-expansion) reached in the steam explosion. Taleyarkhan uses the Redlick-Kwong equation of state for water:

$$P = \frac{RT_e}{(v_m - a_r)} - \frac{b_r}{[T_e^{1/2}\, v_m\, (v_m + a_r)]} \qquad (13)$$

where

P = pressure
R = gas constant for steam
a_r, b_r = constants; $a_r = 0.00117$ and $b_r = 43961$

He reports good agreement between his calculations and experimental data.

Two additional points must be made with respect to the use of this model. The calculation of the equilibrium temperature using Eq. (11) requires that a determination be made as to the mass of fuel and the mass of coolant that "participate" in the steam explosion. The individual masses actually need not be known, but their ratio is required. Experimental evidence indicates that the total amount of corium present

in the pool of water may not participate in the explosion. The amount of coolant involved may also be less than the total mass in the pool. The FDI package contains equations to determine the mixing volume and the amount of coolant mass involved in the mixing phase, although these equations are not presently accessed when FDI is executed. However, there is insufficient data at this point to judge whether the current FDI models for these quantities will produce pressures, using the Corradini-Taleyarkhan equations, that agree with experimental results. Some modification of the code may be required to allow MELCOR to calculate coolant and corium masses, or at least coolant-to-corium mass ratio, that is appropriate for use in the peak pressure model. The second point is that the peak pressure calculated by this model may be of extremely short duration and in an area away from structures. Therefore, the actually pressure experienced by structures in and around the water pool can be considerably smaller than the calculated peak. Experimental data reported by Corradini show peak pressure pulses of durations as short as 200 μs. The pressures measured at transducers a short distance from the "center" of the steam explosion were as much as an order of magnitude less than the calculated peak. Nevertheless, this model may be valuable in allowing the user to compare steam explosions in various systems, using a quantitative measure of the potential damage of which an explosion is capable.

Recommendations for Experimental Work

As previously stated in this Appendix, the data available on steam explosions are in general very limited. The availability of steam explosion data involving molten corium and concrete is virtually nonexistent. It is therefore almost impossible to render even a qualitative judgment as to whether steam explosions in Mark-II wetwells involving molten corium, molten concrete, and concrete decomposition products are more or less probable than explosions involving only corium. It is also almost impossible to determine whether the destructive potential of the former would be greater or less than that of the latter. Steam explosions appear to require contact of water with molten high temperature material. The presence of concrete might therefore increase the probability of an explosion, since the presence of concrete in mixed oxides would tend to lower the solidus point and allow the mixture to remain molten longer. A counter argument can be made, however, that the concrete might lower the equilibrium temperature of a melt-coolant mixture, thus offsetting the lower solidus temperature.

It can also be speculated that a concrete-corium mixture could fall to the floor of a water pool, with the concrete solidifying and insulating the corium from the surrounding coolant, in a configuration somewhat similar to that reported in the SWISS tests. This configuration is also similar to that observed in smelt-water steam explosions, raising the question of the possibility of such explosions in nuclear systems after substantial delays, as reported for the smelt-water systems.

The conjectures discussed above will require that experimental data be obtained to resolve them, and to answer other questions about the probability and processes of steam explosions in Mark II wetwells. Such data will also permit the development of quantitative models for some of the processes involved.

It is recommended that experiments be performed to acquire data in the following areas:

1. Interaction of molten corium with concrete.
2. Melt-through of concrete slabs using corium mixtures.
3. Behavior of molten concrete when dropped into water pools.
4. Behavior of molten corium-concrete mixtures when dropped into water pools.
5. Integrated experiments involving melt-through of a concrete slab by a molten corium pool, with subsequent entry of the molten corium-concrete mixture into a water pool.

The data acquired in these experiments would shed considerable light on the issue of steam explosions in Mark II containments. They would also permit more accurate modeling of the processes involved in corium-concrete-water interactions in codes such as MELCOR. Even if steam explosions are found to be unlikely in such events, it must be noted again that the gases evolved during corium-concrete interactions and the steam generated when the molten material falls into the water pool will pressurize the containment, possibly causing it to fail in a non-energetic fashion.

Summary and Conclusions

This Appendix has presented information relevant to the issue of severe accidents in boiling water reactors having Mark II containments. In particular, the interaction of molten corium with concrete, as would occur in the event a core melt accident followed by reactor vessel failure, has been discussed. The possibility of a steam explosion in a Mark II wetwell, caused by melt-through of the concrete drywell floor, and the potential effects of molten concrete on steam explosion dynamics have been explored.

The major models in the Fuel Dispersal Interaction package of the MELCOR computer code have been reviewed, and improvements to the code have been proposed. Finally, an experimental outline has been presented to permit acquisition of data.

Because of the lack of experimental data in this area, it is not possible to reach definite conclusions regarding steam explosion phenomena in Mark II containments. However, given experiences with steam explosions in other types of systems, it does not appear to be possible to rule out this type of event in a Mark II wetwell. Since a steam explosion in a Mark II has the potential for producing a sudden failure of the containment and resuspending fission products previously deposited in the containment, this area should be the focus of substantial investigation.

REFERENCES FOR APPENDIX D

1. S. R. Greene, *Realistic Simulation of Severe Accidents in BWRs - Computer Modeling Requirements*, NUREG/CR-2940, Oak Ridge National Laboratory (April 1984).

2. M. L. Corradini, "Analyses and Modeling of Large-Scale Steam Explosion Experiments," *Nuclear Science and Engineering*, 82, 429-447 (1982).

3. L. S. Nelson and L. D. Buxton, *Steam Explosion Triggering Phenomena: Stainless Steel and Corium-E Simulants Studied with a Floodable Arc Melting Apparatus*, Sandia National Laboratories, NUREG/CR-1022 (May 1978)

4. L. S. Nelson et al., *Steam Explosion Triggering Phenomena; Part 2: Corium-A and Corium-E Simulants and Oxides of Iron and Cobalt Studied with a Floodable Arc Melting Apparatus*, NUREG/CR-0633, Sandia National Laboratories (May 1980).

5. L. D. Buxton and W. B. Benedick, *Steam Explosion Efficiency Studies; Part I*, NUREG/CR-0947, Sandia National Laboratories (October 1980).

6. M. L. Corradini, "Molten Fuel/Coolant Interactions: Recent Analysis of Experiments, *Nuclear Science and Engineering*, 86, 372-387 (1986).

7. C. Long, "Explosion of Molten Aluminum in Water - Causes and Prevention," *Metal Progress*, 71 (1957)

8. T. M. Grace and R. R. Robinson, *Energetics of Smelt/Water Explosions*, NUREG/CR-4745, IIT Research Institute (October 1986).

9. J. E. Gronager et al., *TURC1: Large Scale Metallic Melt-Concrete Interaction Experiments and Analysis*, NUREG/CR-4420, Sandia National Laboratories (January 1986).

10. D. A. Powers et al., *Exploratory Study of Molten Core Material/Concrete Interactions, July 1975-March 1977*, SAND77-2042, Sandia National Laboratories (February 1978).

11. J. E. Gronager et al., *TURC2 and 3: Large Scale $UO_2/ZrO_2/Zr$ Melt-Concrete Interaction Experiments and Analysis*, NUREG/CR-4521, Sandia National Laboratories (June 1986).

12. D. A. Powers and F. E. Arellano, *Large Scale, Transient Tests of the Interaction of Molten Steel with Concrete*, NUREG/CR-2282, Sandia National Laboratories (January 1982).

13. R. E. Blose et al., *SWISS: Sustained Heated Metallic Melt/Concrete Interactions with Overlying Water Pools*, NUREG/CR-4727, Sandia National Laboratories (July 1987).

14. S. A. Hodge et al., *Primary Containment Response Calculations for Unmitigated Short-Term Station Blackout at Peach Bottom*, Oak Ridge National Laboratory (November 1988).

15. F. E. Haskin et al., "Development and Status of MELCOR," presented at the Fourteenth Water Reactor Safety Information Meeting, Gaithersburg, MD (October 1988).

16. R. P. Taleyarkhan, *Steam Explosion Safety Concerns for the Advanced Neutron Source Reactor at ORNL: An Issue Paper*, to be published.

APPENDIX E:

CODE INPUT DECKS

MARK II CONTAINMENT CALCULATIONS

E.1 BWR-LTAS Code Input

This Section provides a set of representative code input for the Boiling Water Reactor Long Term Accident Simulation (BWR-LTAS) code. This input was used to generate the first 35 minutes of the short-term station blackout accident sequence for the Mark II containment calculations. The BWRSAR severe accident response calculation (Section E.2) was initiated at accident time 35 minutes from the results of this BWR-LTAS calculation.

INPUT DATA AFTER MODIFICATIONS

acop	=	191.993
acor	=	144.939
acpf	=	1.
admet	=	16570.
adsovr	=	1.
advent	=	0.
awvent	=	1.75
aleak0	=	0.
apmet	=	7847.7
art	=	42.332
asspw	=	5277.
atwsf	=	0.
a0cp	=	975.8
a1cp	=	3.025e-03
a2cp	=	-1.72304e-06
bdwc0	=	2800.
bdwsp0	=	1250.
bc100	=	27000.
bhot10	=	0.
bhot04	=	430.
blpmin	=	8500.
bm	=	20.
brdpc	=	2.5
brhrp	=	22.2
brhrpd	=	22.2
bspdw0	=	2000.
bsump	=	50.
cdmet	=	19346.9
cpmet	=	9075.6
cpref	=	3293.
cpst	=	0.1259
cp0	=	3293.
cvvent	=	0.833
daleak	=	0.
delt	=	0.5
dkdtcr	=	-1.e-05
dm	=	80000.
dmin	=	0.2
dphp	=	190.
dplp	=	75.
dtrvhl	=	423.
dzs	=	21.2
dzv	=	35.
erhrr	=	0.375
ewsdc	=	234.
fcstsp	=	0.7
fflash	=	5.e-04
ffrec	=	2.e-02
fintim	=	2103.
fldwg	=	3.12e-08

```
flspg    =    1.e-08
ftstab   =    2000.
hboaf    =    18.025
hci0     =    539.
hcst     =    58.
hpcimx   =    694.167
hpcipc   =    0.
href     =    522.
hscsf    =    16.2
hsrhrf   =    15.6
hudwci   =    20.
humdw0   =    50.
humsp0   =    99.
h0       =    3816.
h1       =    1.552
h2       =    -2.517e-02
jetpmp   =    0.
kcrdch   =    4.47e-02
kcrdtv   =    5.07e-02
kptb     =    1.e-02
ksu      =    5.157e-04
lbase    =    0.
lbot     =    26.392
lcore    =    12.5
lcstss   =    0.
lcstuv   =    8.266e-05
ldcr     =    27.58
ldcset   =    560.
ldc0     =    28.32
lheder   =    23.4
lhpin    =    476.
lhpmin   =    490.
lhpmt    =    540.
lhpt     =    582.
llpi     =    413.5
llpit    =    575.
lop      =    5.167
lrcin    =    476.5
lrcmin   =    550.
lrcmt    =    582.
lrct     =    582.
lrt      =    11.033
lrvads   =    397.
lspss    =    7.
ltcrd    =    581.
ltrdwc   =    99.
ltrjp    =    490.
mint     =    477000.
mrvst    =    1500000.
ncs      =    4.
nlpci    =    4.
nsorv    =    0.
ntrhr    =    4.
ntrhrd   =    4.
```

```
obrvd     =    120.
ocbpc     =    60.
odcs      =    1000000.
odlpci    =    1000000.
oervd     =    720.
ohpman    =    1000000.
ohpt      =    0.
ohptr     =    1000000.
oocbp     =    1000000.
ooptb     =    1000000.
ootv      =    1000000.
opchrc    =    60.
opchsv    =    30.
orcman    =    1000000.
orct      =    0.
orctr     =    1000000.
ordwc     =    1000000.
osbor     =    300.
oscri     =    300.
oscs      =    1000000.
osdlev    =    1000000.
osdpc     =    1000000.
oslpci    =    1000000.
osscrd    =    1000000.
ossdc     =    1000000.
ossubp    =    1000000.
osvman    =    120.
otcbp     =    0.
otcrdp    =    1000000.
otdwc     =    1000000.
pc        =    1015.7  1017.7  1025.7  1027.7  1029.7  1031.7
               1035.7  1036.7  1037.7  1038.7  1045.7  1046.7
               1047.7
pcdwv     =    15.
pcor      =    6693.37
pdcvp     =    5.05
pdhosv    =    1.e-02
pdlpi     =    16.95
pdocsv    =    2.e-02
pdwads    =    16.42
pehpis    =    165.
pelct     =    40.
pfmosv    =    110.
pfodp     =    765.
phcovr    =    1.
phpin     =    16.95
phpis     =    115.
pidwv     =    1000000.
pldwca    =    1.389e-03
pmxdpc    =    1.35
pmndpc    =    1.1
po        =    1090.7  1092.7  1100.7  1102.7  1104.7  1106.7
               1110.7  1111.7  1112.7  1113.7  1120.7  1121.7
               1122.7
```

```
prated          =    1196.
prcis           =    65.
prelr           =    0.32
prr             =    1020.
ptdwg0          =    14.95
ptrdwc          =    16.95
ptspg0          =    14.95
pvlpi           =    480.
pvlpiv          =    480.
pvtdwc          =    465.
p0              =    1034.7
qdwcr           =    1389.
qoph10          =    298.3
qrvh10          =    1583.3
rcicmx          =    83?3
sboflg          =    2.
sdvflg          =    0.
tadwci          =    145.
taulen          =    2.5
tauoh1          =    600.
tbase           =    85.
tbgrhr          =    1800.
tdgrhr          =    1000000.
trerhr          =    2000000.
tblein          =    0.
$

tcfail          =    2.5
tdiesl          =    1000000.
tdmet0          =    126.
tfdwc           =    200.
tfdwca          =    1000000.
tgdw0           =    126.
tgsp0           =    85.
thpis           =    194.
tpair           =    90.
tpmet0          =    85.
trcf            =    190.
trcis           =    194.
tslc            =    1000000.
tslein          =    1000000.
tsorv           =    1000000.
tsquen          =    10.
tstrat          =    0.
tsw             =    90.
tswd            =    90.
twdwci          =    100.
t0              =    36.
uairv           =    33.
vann            =    1177.51
vcst0           =    362000.
vcstmx          =    375000.
vcstsp          =    135000.
vhotmu          =    97000.
```

```
vhotw0      =     113000.
vdiff       =     189.076
vfree       =     14580.074
vgdw        =     239600.
vjet        =     95.195
vojp        =     1535.473
volp        =     2428.636
vrec        =     1150.
vsl         =     2100.907
vrsop       =     3864.149
vtsp        =     276831.4
vuv1        =     1061.371
vuv2        =     2042.338
wbslc       =     0.1826
wdleak      =     0.24
wquess      =     0.
wrated      =     239.6
wref        =     9111.
wrhrr       =     1389.
wrhrsd      =     625.
wrhrsw      =     625.
wswr        =     625.
wtehp0      =     45.12
wterc0      =     5.41
wwdwc       =     143.4
x11         =     0.
x12         =     8.483
x13         =     18.858
x14         =     32.6
x15         =     35.85
x16         =     37.85
x17         =     44.058
xref        =     0.133
$

abio        =     4207.6
adflr       =     4715.8
admm        =     60080.
aped        =     1998.6
awmm        =     28969.6
cbiol       =     20119.
cdmm        =     288277.
cpcor       =     0.
cwmm        =     109739.1
dxbio       =     1.75
dxgbic      =     0.
dxgdw       =     1.e-04
dxgww       =     1.e-04
dxs         =     1.e-02
kcon        =     1.917e-04
mk          =     2.
rhocon      =     140.8
$
```

```
aspl      =    11925.5
cpspl     =    13791.4
aspmm     =    4062.4
cpspmm    =    6186.4
$

asbic     =    1.e-02
lsbic     =    312.
tisbic    =    1000000.
wdwsmp    =    0.
$

idecay    =    44
dtim      =    0.  1.  1.5  2.  3.  4.  6.  8.  10.  15.  20.  30.  40.
               60.  80.  100.  150.  200.  300.  400.  600. 800.  1000.
               1500.  2000.  3000.  4000.  6000.  8000.  10000.  15000.
               20000.  30000.  40000.  60000.  80000.  100000.  150000.
               200000.  300000.  400000.  600000.  800000.  1000000.
decay     =    6.000e-02   5.715e-02   5.552e-02   5.437e-02   5.204e-02
               5.040e-02   4.807e-02   4.619e-02   4.473e-02   4.205e-02
               4.015e-02   3.756e-02   3.572e-02   3.313e-02   3.137e-02
               3.000e-02   2.777e-02   2.619e-02   2.428e-02   2.293e-02
               2.102e-02   1.965e-02   1.859e-02   1.662e-02   1.522e-02
               1.354e-02   1.235e-02   1.067e-02   9.815e-03   9.152e-03
               8.193e-03   7.512e-03   6.764e-03   6.232e-03   5.484e-03
               5.039e-03   4.693e-03   4.141e-03   3.749e-03   3.275e-03
               2.940e-03   2.466e-03   2.187e-03   1.971e-03
```

E.2 BWRSAR Code Input

This Section provides a set of representative code input for the Mark II calculations performed with the Boiling Water Reactor Severe Accident Response (BWRSAR) code. This input was used to calculate the events of the short-term station blackout accident sequence (with ADS actuation) from accident time 35 minutes to time 905 minutes. The MELCOR containment response calculation (Section E.3) was driven by the results of this BWRSAR calculation.

```
susquehanna short term station blackout with ads actuation, 08/12/89
steel     concrete
dwliner   dwfloor   dwpdstl   sldwall   dwsteel   wwliner   wwpedst   wwspcle
wwvnpip   wwroof    qdot-ps
 &change
       check=0.   cpstp=300.0.   trst=905.01.
 &end
 &nlmar
  atime= 35.00.   fptmon=2000.0.   tap=5.256e5.
       ibrk= 0.        icbrk= 0.    iecmxx=  0.
      ifpem= 2.        ipdtl= 0.      ispra= 0.
 &end
 &ntslab
  dwn(1)=489.0,140.0,3*0.0.
  dtdx(1)=0.0,0.0,0.0,0.0,0.0,0.0,0.0,0.0,0.0,0.0,0.0,0.0,0.0,0.0,0.0,0.0,5*0.0.
  fc1xxx=0.450,  fc2xxx=0.105,  fc4xxx=0.049.
  fract1=0.0, fract2=0.96.
  hc(1)=0.1124,0.3107,3*0.0.
  hif(1)=1000.,1000.,0.,1000.,0.,1000.,1000.,0.,0.,1000.,5*0.0.
  iblat1=2, iblat2=3, igas=2.
  ivl(1)=1,1,1,1,1,2,2,2,2,2,1,4*0.
  ivr(1)=1,1,1,1,1,2,2,2,2,2,1,4*0.
  mat1(1)=1,1,2,1,1,1,1,1,1,1,1,4*0.
  mat2(1)=2,2,2,2,1,2,2,1,1,2,1,4*0.
  nmat=2.
   nno1(1)=2,2,9,3,3,2,2,4,3,2,5*0.
  nn=2(1)=13,9,0,7,0,13,9,0,0,9,5*0.
  nod(1)=1,16,36,27,49,46,64,75,79,82.
  nodes=10.    nslab=11.
  sarea(1)=17571.6,5227.0,3997.1,8415.3,60080.,7531.,4111.7,3500.6.
  sarea(9)=14502.3,5290.4,0.01,4*0.0.
  tc(1)=8.0,1.05,5*0.0.
  tchi=1472.,  tclo=1022.,
 temp(1)=2*131.80.
 temp(3)=131.2,130.3,128.8,127.0,126.1,124.0,121.2,116.2,110.8,103.2.
 temp(13)=95.5,87.8,80.0.
 temp(16)=2*129.6.
 temp(18)=129.3,128.8,127.8,126.7,126.1,123.4,118.6,111.1,105.5.
 temp(27)=132.3,131.3,129.5,127.3,126.1,4*126.0.
 temp(36)=129.6,129.5,129.4,129.2,128.6,127.6,126.5,126.0,2*126.0.
 temp(46)=132.22,132.15,132.08.
 temp(49)=2*87.2).
 temp(51)=87.0,86.5,85.9,85.2,85.0,84.7,84.5,83.9,83.35.
 temp(60)=82.5,81.7,80.85,80.0.
 temp(64)=87.3,87.2,87.0,86.5,85.9,85.2,5*85.0.
 temp(75)=87.6,87.5,87.4,87.2.
 temp(79)=3*87.6.
 temp(82)=87.3,87.3,87.0,86.5,85.9,85.9,86.8,88.65,92.4,99.9,105.5.
 temp(93)=108*0.0.
  twhi=958.0,  twlo=190.0,
 x(1)=0.000,0.0208,
 x(5)=.022,.032,.052,.092,.172,.332,.652,1.292,2.0,3.0,4.0,5.0,6.021.
 x(16)=0.000,0.0208,
 x(18)=.022,.032,.052,.092,.172,.332,.652,1.292,1.771,
 x(27)=0.000,0.010,0.030,0.070,0.15,0.31,0.63,1.27,2.250,
 x(36)=0.00,0.040,0.086,0.087,0.100,0.120,0.160,0.260,0.500,0.961,
 x(46)=0.00,0.040,0.0863,
 x(49)=0.000,0.0208,
 x(51)=.022,.032,.052,.092,.172,.332,.652,1.292,2.0,3.0,4.0,5.0,6.021,
 x(64)=0.00,0.021,0.032,0.032,0.052,0.092,0.172,0.332,0.652,1.292,2.542,
 x(75)=0.00,0.035,0.070,0.10417,
 x(79)=0.00,0.040,0.089,
 x(82)=0.000,0.00625,
 x(84)=.010,.020,.040,.080,.160,.320,.640,1.280,1.768,108*0.0
  uzrv=13604.0,
&end
```

```
&nlecc
 cxprc=0.0,
 dt    =.100.0,
 ec    =.01,
 rwstm=1870438.,
 trwstx=85.0,
 wtcavx=1.0,
 npump=7,
 ivaloc(1)=     2,       3,       3,       1,       1,       1,       2,
  npsuc(1)=     2,       2,       3,       3,       3,       3,       3,
  nptyp(1)=     3,       3,       3,       3,       1,       1,       3,
       pf(1)=  289.0,   289.0,  1250.0,  403.0,  1250.0,  1250.0,  131.5,
    pio(1)=    0.1,     0.1,     0.0,     0.1,     115.0,    65.0,    0.0,
     stp(1)=  1.0e8,   1.1e8,   1.2e8,   1.3e8,   1.4e8,   1.5e8,  1.6e6,
      tm(1)=  1.0e8,   1.1e8,   1.2e8,   1.3e8,   1.4e8,   1.5e8,  1.6e6,
     wac(1)=    0.0,     0.0,     0.0,     0.0,  5000.0,   600.0,    0.0,
 pgpm(1,1)= 41148.,  40000.,  38200.,  36000.,  32000.,  28000.,  24000.,
 phead(1,1)=     0.,     20.,   46.9,    81.1,   133.7,   182.1,   222.1,
 pgpm(0,1)= 18000.,  10000.,      0.,
 phead(0,1)= 263.5,   309.0,   331.5,
 pgpm(1,2)= 15240.,  14000.,  12500.,  12000.,  10000.,   8000.,   6000.,
 phead(1,2)=     0.,    57.8,    120.,   137.3,   200.9,   254.1,   292.6,
 pgpm(0,2)=  4000.,   2000.,      0.0,
 phead(0,2)= 319.5,   336.3,   343.6,
 pgpm(1,3)=  180.0,   168.4,   156.2,   143.0,   128.5,   112.0,    92.6,
 phead(1,3)=    0.0,   215.0,   415.0,   615.0    815.0,  1015.0,  1215.0,
 pgpm(0,3)=    67.6,    21.7,     0.0,
 phead(0,3)= 1415.,   1615.,   1635.,
 pgpm(1,4)= 30347.,  29399.,  28023.,  26739.,  25385.,  16033.,  10689.,
 phead(1,4)=    0.0,     27.,     60.,     91.,    202.,    288.,    351.,
 pgpm(0,4)=  5145.,   2672.,     0.0,
 phead(0,4)=  389.,    396.,    403.,
 pgpm(1,7)=  580.0,   450.0,   350.0,   300.0,   250.0,   200.0,   150.0,
 phead(1,7)=    0.0,    30.5,    50.0,    58.5,    65.1,    71.0,    76.0,
 pgpm(0,7)=  100.0,    50.0,     0.0,
 phead(0,7)=   79.0,    80.5,    81.0,
 wshpci= 3360.0,   wercic=  444.0,   zjl=470.0,   zjh=585.0,
&end
ipci    ce      crd     cbp     hpci    rcic    fire
&nlecx
      eqr=0.0,     atpir=0.0,     atsir=0.0,      awpr=0.0,      awsr=0.0,
&end
&nlcax
      eqr=0.0,     atpir=0.0,     atsir=0.0,      awpr=0.0,      awsr=0.0,
&end
&nlccol
 cqr=7.2806,    ctpr=135.0,    ctsr=50.0,    cvap=0.693,
cwpr=112000.0,   cwsr=6190.3,       jcool=0,   tcool=1.9e8,
&end
&nlleak
 nlc=1,    ilkp=1,    ilkt=0,    kleak=1,
 dpleak(1)=126.,128.0,130.0,133.0,136.0,140.0,145.0,152.5,160.0,200.0,
  qleak(1)=000.,0.007,0.015,0.026,0.037,0.050,0.070,0.097,0.124,0.271,
 a1=0.0,    a2=0.0,    t1=0.0,    t2=0.0,    test=0.0,
 clk=0.503,    nhyst=3,    indx=10,    fctr(1)=10*0.0,
&end
&nlmece
 area(1)=5227.2,5572.65,
 c1(1)=500.0,174.0,8*0.0,
 c2(1)=0.593,0.593,8*0.0,
 c3(1)=0.196,1.10,8*0.0,
 c4(1)=0.0,0.0,8*0.0,
 dcf=1000.0,   dto=0.05,   dtpnt=19.99,   tpntm=155.01,   dtpnt2=29.99,
  hmaxx=200.0,
  hum(1)=0.1234,0.9262,
 kt(1,1)=0,kt(2,1)=2,
```

```
 kt(1,2)=.5,kt(2,2)=0.
 n=2,   nc(1)=2,2,8*0.
 ns(1)=2,2,9*0,   nt(1)=7,7,8*0.
 po(1)=37.09,15.81,
 press(1,1)=0.0,press(2,1)=0.5,
 press(1,2)=5.293,press(2,2)=0.0,
 sumps=256.0,  tdwsmp=110.0,  tempo(1)=199.13,9a.70,
 tpool=174.17, vc(1)=239600.0,143709.87,0.0,
 vcav=24.06, vflr=7345.0, wdwsmp=327.43, wflash=2000.0, wpool=8192443.0,
  wcdo(1)=0.0,0.0,
  wcmo(1)=0.0,0.0,
  whyd(1)=0.0,0.0,
  wntr(1)=-.965,-.965,
  woxy(1)=-.035,-.035,
 &end
 &nlhoil
  abr(1)=-1.0,-1.0,-1.0,-1.0,-1.0,-1.0,-1.0,-1.0,-1.0,-1.0,
         -1.0,-1.0,-1.0,-1.0,-1.0,0.1091,
  abrk=2.29e-5,
  ah(1)=651.0,9230.2,673.5,4*0.0,
  ahu(1)=1620.0,426.0,1270.0,1270.0,1270.0,1270.0,19010.0,13*0.0,
  arstr(1)=0.0,-7.87,-12.22,4*0.0,
  arstru(1)=148.04,148.04,42.33,42.33,42.33,42.33,128.4,13*0.0,
  clad=0.0025,  cladwr=0.00254,
  cm(1)=2337.0,15310.2,21653.6,4*0.0,
  cpu(1)=29280.0,37973.0,26486.0,26486.0,26486.0,26486.0,78000.0,13*0.0,
  cond=4.7,        d=0.0353,       dcrdod=0.8958,
  dd(1)=0.125,0.0208,0.635,4*0.0,
  ddu(1)=0.160,1.00,0.5054,0.5054,0.5054,0.5054,0.071,13*0.0,
  df=0.0297,       dh=0.0423,    dpart=.01177,     drgap=3.125e-4,
    tpn(1)=20.0,40.1,280.1,1.0e6,2.0e6,3.0e6,4.0e6,5.0e6,
   dtpn(1)=5.00,10.0,20.00,100.0,101.0,102.0,103.0,104.0,
  dr=id=20.91667,     dshdid=16.96,    fcfail=0.75,
  duo2=0.0297,  dwrod=0.0354,     fcol=0.256,    fdfuel=0.92,
  fid=0.0, fpv(1)=0.00,0.50,3.10,0.65,0.03,0.02,0.50,13*0.0,
  fwsscr=0.18,    fwssfe=0.[illegible],    fwssni=0.08,    fwuzr(1)=0.20,19*0.0,
  fz(1)=0.66006,0.9004,0.96607,1.02872,1.07198,1.12138,1.1916,1.22818,
  fz(9)=1.22008,1.15422,0.97839,0.49386,13*0.0,
  fl2=0.01,    hz=12.500,    hnf=0.914,
  hfse=114.7,    hfue2=118.0,    hfzirc=108.0,    htmtoc=600.0,
          ibxxx=1,        ibedc=2,        ibeds=3,
          ifp=2,           ihc=0,          imwe=3,
          ipowar=1,   ir1=1,ir2=2,ir3=3,   istm=1,
          istr=3,        istru=7,        mwornl=1,
          ndzf=12,       nnt=61084,        nr=60356,     ndzn=1,
  pf(1)=1.14375,1.14375,1.072,1.072,0.853,0.853,0.582,0.582,
  pitch=0.0477,  porb=0.4,  pval=980.4,  q235u=193.0, qzerox=1.1236e10,
  rhocld=408.9,    rhofu1=646.7,   r1=1,  r2=0,   r239u=0.0,    sfactr=2.0,
    tb(1)=1.0e8,15*1.0e8,
     tcormb=1.e4, tfailx=2100.0, tfail2=2100.0, tfus=4600.0,
  tfpcld=1800.0,    thkrx=0.5417,    thkshd=0.166667,
  thku(1)=0.042,0.166667,0.025,0.025,0.025,0.025,0.01,13*0.0,
    tmeltt=4900.0,  tmwzof=4175.0,  tmybk=1.0e6,  tpm=1.0,
   t=h(1)=.050,.025,0.100,.020,0.050,0.020,0.100,0.200,
  tsct(1)=10.0,77.50,100.0,124.,180.6,220.0,265.0,280.0,
  ttu(1)=542.2,542.2,542.2,542.2,542.2,542.2,542.2,13*0.0,
  vf(1)=.311515,.311515,.062825,.062825,.06021,.06021,.065445,.065445,
  xan=6.233e-6,
 ybr(1)=-1.0,-1.0,-1.0,-1.0,-1.0,-1.0,-1.0,
        -1.0,-1.0,-1.0,-1.0,-1.0,-1.0,-1.0,20.00,
   ybrk=-100.0,  ybrk2=1000.0,
 &end
t guide shr.heads/spip 1s/spip 2s/spip 3s/spip 4dryers
 &nburin
 farin=86.48, farout=61.56, pbox=1.7543,xbox=0.006667,xboxz1=0.333e-6,
 xboxzn=0.333e-6, f12bx=0.010,   f22bx=0.010,   f22rd=0.010,  frdbx=0.25,
```

```
 fhscb=0.25, dhbxct=0.016583, tmelmx=3365.0, tfbox=4175.0,
   ifrbox=1,    nboxs=764,       imbox=1,    thkcb=0.0217, tmsef=1126.0,
 ic    1,1)=1,1,1,1,1,1,1,1,1,1,1,1,
 ic    1,2)=0,0,0,0,0,0,0,0,0,0,0,0,
 iocb(1,3)=1,1,1,1,1,1,1,1,1,1,1,1,
 iocb(1,4)=0,0,0,0,0,0,0,0,0,0,0,0,
 iocb(1,5)=1,1,1,1,1,1,1,1,1,1,1,1,
 iocb(1,6)=0,0,0,0,0,0,0,0,0,0,0,0,
 iocb(1,7)=1,1,1,1,1,1,1,1,1,1,1,1,
 iocb(1,8)=0,0,0,0,0,0,0,0,0,0,0,0,
 xlcb=.40625, thkgap=0.00467, xcbdp=3.35e-6,  ncbled=185,   fllcb=0.010,
 fllcb=0.010,  tmelcb=2450.0,  tfcbd=3126.0,    imwss=1,
 xlcpst=0.065083,  thkwal=0.002083,  diab4c=0.0115,  thkgap=0.0005,
 rhob4c=110.0,  rhoss=496.0,  nabrod=76,  imwb4c=2,    fb4cmx=0.03,
&end
&nbwrlv
   nbaf=216.3125,  nbgb=121.5,  ndead=205.3125
 hinitl=367.68, hilel=646.5,
  hajjp=205.3125,  htef=568.3125,  htjp=317.1875,
   htop=876.0,    hts=607.5,     ns=50,
hh(1)=0.0,6.0,11.0,16.0,21.0,26.0,32.0,37.0,42.0,48.0,
hh(11)=51.0,58.0,64.0,69.0,74.0,79.0,85.0,90.0,95.0,101.0,
hh(21)=106.,111.,116.,121.5,127.5,151.125,216.312,317.187,360.125,379.125,
hh(31)=411.625,414.,417.,420.,423.,426.,429.,431.,434.,437.,
hh(41)=440.,442.625,514.,533.5,564.,577.87,607.5,635.,749.,876.,
vcore(1)=0.0,7.95,26.36,55.07,93.48,
vcore(6)=141.3,210.42,277.29,352.1,451.74,
vcore(11)=505.38,633.48,753.11,859.14,970.43,
vcore(16)=1086.55,1231.61,1352.72,1485.2,1643.17,
vcore(21)=1777.45,1913.64,2051.28,2203.82,2296.69,
vcore(26)=3334.98,3712.77,4924.898,5440.129,5671.609,
vcore(31)=6347.52,6393.289,6546.238,6493.691,6535.551,
vcore(36)=6571.719,6602.129,6619.160,6639.762,6654.328,
vcore(41)=6662.871,6665.262,6933.539,7117.27,7470.629,
vcore(46)=7613.559,7789.031,0.0,0.0,0.0,0.0,
vshrd(1)=20*0.0,
vshrd(21)=0.0,0.0,0.0,0.0,0.0,0.0,58.72,
vshrd(26)=74>.37,982.48,1946.08,2367.92,2507.69,
vshrd(31)=2745.15,2762.74,2790.40,2824.23,2864.32,
vshrd(36)=2910.77,2963.68,3082.59,3066.48,3173.92,
vshrd(41)=3214.52,3287.95,4784.517,5193.379,5832.891,
vshrd(46)=6113.609,6713.301,0.0,0.0,0.0,0.0,
vtot(1)=0.0,7.95,26.36,55.07,93.48,
vtot(6)=141.3,210.42,277.29,352.1,451.74,
vtot(11)=505.38,633.48,753.11,859.14,970.43,
vtot(16)=1086.55,1231.61,1352.72,1485.2,1643.17,
vtot(21)=1777.45,1913.64,2051.28,2203.82,2355.41,
vtot(26)=4078.35,4695.25,6870.98,7808.121,9178.699,
vtot(31)=9092.672,9156.031,9236.641,9317.922,9399.871,
vtot(36)=9487.488,9565.809,9621.750,9706.238,9828.250,
vtot(41)=9877.391,9953.211,11718.051,12510.648,13303.520,
vtot(46)=13727.172,14502.328,15308.719,18651.578,21134.289,
&end
&nbwrrv
   dpvdyc=20.0,   dpvdyo=50.0,
   iads(1)=0,0,0,0,0,0,0,0,0,0,1,1,1,1,1,0,4*0,
     nvalve=17,       ntperv=1,      pdwca=100.0,
 psrvo(1)=1090.7,1092.7,1100.7,1102.7,1104.7,1106.7,1110.7,1112.7,
 psrvo(9)=1114.7,1116.7,1120.7,1122.7,1124.7,1130.7,1132.7,1134.7,
 psrvo(17)=25.0,
 psrvc(1)=1015.7,1017.7,1025.7,1027.7,1029.7,1031.7,1035.5,1037.7,
 psrvc(9)=1039.7,1041.7,1045.7,1047.7,1049.7,1055.7,1057.7,1059.7,
 psrvc(17)=20.0,
 ratflo(1)=2*867400.0,
 ratflo(3)=4*883950.0,
 ratflo(7)=4*891380.0,
```

```
 ratflo(11)=3*898800.0,
 ratflo(16)=3*906250.0,
 ratflo(17)=8000.0,
 ratpre(1)=2*1196.0,
 ratpre(3)=4*1225.3,
 ratpre(7)=4*1235.7,
 ratpre(11)=1246.0,1246.0,1246.0,1246.0,
 ratpre(14)=1256.3,1256.3,1256.3,
 ratpre(17)=1050.0,
 ratrho(1)=2*2.75,
 ratrho(3)=4*2.83,
 ratrho(7)=4*2.86,
 ratrho(11)=2.88,2.88,2.88,2.90,2.90,2.90,
 ratrho(17)=2.35,
  tmsvlk=60.0,
 manval=1,  pmnset=1005.0,  pmnban=70.0,  topchk=0.10,  tmsnon=35.0,
 tmsnof=77.99,  tmdson=79.49,  nscrv=1,  tsorvo=77.99,
&end
&nbwrqb
  h23=207.4,   h35=389.6,   djp=11.86,   ajp=20,
 tmssso(1)=500.39,
 tmssso(2)=505.05,
 tmssso(3)=542.21,
 tmssso(4)=542.21,
 tmssso(5)=542.21,
 tmssso(6)=542.21,
&end
&nthead
 dbh=0.10,  thead=0.060,  fopen=0.532,  dthead=10.0,  nlmax=2.50,
 condex=2.02,  condss=11.3,  hdld2=3.64,  hrvdw=0.625,  hskirt=6.02,
 nmeltx=0,  sfcrdb=2.0,   thkcrs=0.500,
 thkhd1=0.708,   thkhd2=0.505,   nps=26,
 hpipes=180.0,  th46=2250.0,  th460=2050.0,  tshlet=2660.0,
 smtmel(1)= 2750.,2750.,2750.,2750.,
 smtmel(10)=4800.,4800.,4800.,4800.,4800.,4800.,4800.,4800.,
 ioutec=2
 frckey(1)=0.579,0.830,8*0.0,
 loukey(1)=2.10,8*0,
 tmltow(1)=2750.,4800.,8*0.,
 iwu(1,1)=1,1,1,1,0,0,0,0,0,0,0,0,0,0,0,0,0,0,0,0,
 iwu(1,2)=0,0,0,0,0,0,0,0,0,0,0,1,0,0,0,0,0,0,1,0,0,
 ioutyp(1)=2,2,8*0,
 xrnkey(1,1)=0.210,0.579,0.151,0.060,
 xrnkey(11,2)=3.170,
 xrnkey(18,2)=0.830,
&end
```

E.3 MELCOR Code Input

This Section provides a set of representative code input as processed by the MELGEN package of MELCOR for the Mark II Containment response calculations. This MELCOR input was used for the short-term station blackout accident sequence with ADS actuation. It provides a single drywell cavity for the representation of debris/concrete interactions. This is the basic code input deck to which variations were made as required to perform the MELCOR calculations discussed in Chapter 2.

```
*************************************************************************
*************************************************************************
*
* CPI Plant primary containment model
*
* Case 1 - SISB w/ADS, no vent, no sprays, no scrb, no head flooding &
*          NO PRIMARY CONTAINMENT FAILURE ALLOWED
*
* Updated to incorporate PPL's comments of 7/6/89,7/13/89,7/18/89
*   and 9/14/89--should be final CPI deck
*
*  added degassing 10/25/89
*
*************************************************************************
*************************************************************************
title      e1
jobid      e1
*
tstart    2100.    *  35 min, end of burites
*
restartf  e1rst
outputf   e1gout
diagf     e1gdia
plotf     e1ptf
crtout
dttime     0.1
*
*sc0000 10 1.       1   * cpu weighting factor
*sc0001 10 0.22     2   * i/o weighting factor
*sc0002 10 0.225    3   * memory weighting factor
*
*
*************************************************************************
*************************************************************************
***                                                                   ***
***                                                                   ***
***                  CPI Primary Containment Model                    ***
***                                                                   ***
***                                                                   ***
***          Total Drywell Volume =  228627 ft**3 =  6474 m**3        ***
***          Total Downcomer Volume = 11675 ft**3 =   331 m**3        ***
***          Total Wetwell Volume =  280141 ft**3 =  7933 m**3        ***
***             Total P. C. Volume = 520443 ft**3 = 14738 m**3        ***
***                                                                   ***
***                                                                   ***
***                                                                   ***
*************************************************************************
*************************************************************************
*  cont.     cont. volume     connects
* vol. #        name          via ft#  to cont. volume    (#)
*  -----  ------------------  -----  ------------------  -----
*
*   200    drywell inpedestal   201    drywell 705-723       (201)
*                               202    drywell 705-723       (201)
*                               203    drywell 723-758       (202)
*
*   201    drywell 705-723      210    drywell 723-758       (202)
*                               250    downcomers            (300)
*                               290    RB via 2" vent        (900)
*                               291    RB via 18" vent       (900)
*
*   202    drywell 723-758      220     drywell 758-779      (204)
*
*   203    rx/shield annulus    204     drywell 723-758      (202)
*                               205     drywell 758-779      (204)
*                               240     drywell 779-809      (205)
```

```
*
*   204    drywell 758-779          230     drywell 779 809      (205)
*
*   2      drywell 779-809          260     head leakage         (600)
*
*   300    downcomers               300     wetwell pool         (401)
*
*   400    wetwell pedestal         401     wetwell pool         (401)
*                                   402     wetwell pool         (401)
*                                   403     wetwell airspace     (401)
*
*   401    wetwell                  430     VB(1) to downcomer   (300)
*                                   440     VB(4) to downcomer   (300)
*                                   490     ENV via 2" vent      (900)
*                                   491     ENV via 18" vent     (900)
*                                   495     LEAK to ENV          (900)
*
*   600    reactor pit              600     Pit to env           (900)
*
*   900    environment
*
*************************************************************************
*************************************************************************
*
*************************************************************************
*************************************************************************
*      ncg input
*************************************************************************
*************************************************************************
*
ncg004     h2  4  * hydrogen
ncg005     n2  5  * nitrogen
ncg006     co  6  * carbon monoxide
ncg007     co2 7  * carbon dioxide
ncg008     ch4 8  * methane
ncg009     o2  9  * oxygen
*
*
*ppppppppppppppppppppppppppppppppppppppppppppppppppppppppppppppppppppppppp
*ppppppppppppppppppppppppppppppppppppppppppppppppppppppppppppppppppppppppp
*pp
*pp    DEFINE EXTERNAL DATA FILES
*pp
*ppppppppppppppppppppppppppppppppppppppppppppppppppppppppppppppppppppppppp
*ppppppppppppppppppppppppppppppppppppppppppppppppppppppppppppppppppppppppp
*
* ----- BWRSAR SRV FLOWS -----  time  cum water  cum steam  cum h2  temperature
*         edfname      channels     direct
edf10000     'sar-srv-flows'      4          read
*         filename
edf10001  sarsrv
*           format
edf10002   10f8.1
*
* ----- BWRSAR VESSEL LEAKAGE FLOWS -  time cum water cum steam cum h2 temp
*
*         edfname      channels     direct
edf20000     'sar-brk-flows'      4          read
*         filename
edf20001  sarbrk
*           format
edf20002   10f8.1
*
*  ---- BWRSAR DEBRIS POURS -----  time & 16 variables
*             edfname      channels     direct
edf90000     'debris pour'      16          read
```

```
*           filename
edf90001  serpour
*            format
edf90002   5e15.8
edf90003     0.0   * pour offset
*
* ----- BWRSAR CAVITY DECAY HEAT ----- time, decay heat(watts)
*                 edfname      channels      direct
edf70000    'cav decay heat'      1           read
*           filename
edf70001  serdecay
*            format
edf70002   4e15.8
edf70003     0.0  * decay heat offset
*pppppppppppppppppppppppppppppppppppppppppppppppppppppppppppppppp
*pppppppppppppppppppppppppppppppppppppppppppppppppppppppppppppppp

*
*--------------------- SRV source tables for testing model ---------------
*
*     Steam and hydrogen sources taken from Steve's Susquehanna
*     BWRSAR calculation.
*
*     Source steam as vapor into a dummy control volume, and
*     then into the PSP pool via a flow path terminating below the
*     pool surface.
*
*     Source hydrogen into a dummy control volume, and thence into
*     the PSP pool via a flow path terminating below the pool
*     surface.
*
*
*
*   h2o liquid source table: time (s) vs  integrated flow (kg)
*
cv100c0   mass.1   800   1 * source into pool
cv100c1        to   895   9
cf80000   h2o-pool-src   equals   1   1.  0.
cf80010   1.   0.   edf.100.1
*
*
*   h2o vapor source table: time (s) vs  integrated flow (kg)
*
cv100c2   mass.3   810   1 * source into atmosphere
cv100c3        te   890   9
cf81000   h2o-vapor-src   equals   1   1.  0.
cf81010   1.   0.   edf.100.2
*
**
**   hydrogen source table: time (s) vs  integrated flow (kg)
**
cv100c6   mass.4   830   1
cv100c7        te   890   9
cf83000   h2-mass-src   equals   1   1.   0.
cf83010   1.   0.   edf.100.3
**
*****************************************************************
*****************************************************************
**
**   temperature table: time (s) vs  temp (k)
**
cf89000   temp-src   equals   1   1.   0.
cf89001  564.3  *  initialize at tsat (1100 psia) = 556.28 f = 564.3 k
cf89010   1.   0.   edf.100.4
*********************************************************************
******  **********************************************************
```

```
**
**   temperature table: time (s) vs  temp (k)
**
**      s table is limited to sub-critic temperature bounds for u
**   with mass.1 (liquid water) mass sources
**
cf89500   temp-src   equals   1   1.   0.
cf89501   564.3  *  initialize at tsat(1100 psia) = 556.28 f < 564.3 k
cf89502  3  273.15  647.2
cf89510   1.   0.   edf.100.4
*******************************************************************
*******************************************************************

*
* ------------- Vessel Break source tables for testing model ---------------
*
*
*   h2o liquid source table: time (s) vs  integrated flow (kg)
*
cv200c0   mass.1   200   1 * source into pool
cv200c1       te   295   9
cf20000   h2o-pool-src   equals   1   1.   0.
cf20010   1.   0.   edf.200.1
*
*
*   h2o vapor source table: time (s) vs  integrated flow (kg)
*
cv200c2   mass.3   210   1 * source into atmosphere
cv200c3       te   290   9
cf21000   h2o-vapor-src   equals   1   1.   0.
cf21010   1.   0.   edf.200.2
*
**
**   hydrogen source table: time (s) vs  integrated flow (kg)
**
cv200c6   mass.4   230   1
cv200c7       te   290   9
cf23000   h2-mass-src   equals   1   1.   0.
cf23010   1.   0.   edf.200.3
**
*******************************************************************
*******************************************************************
**
**   temperature table: time (s) vs  temp (k)
**
cf29000   temp-src   equals   1   1.   0.
cf29010   1.   0.   edf.200.4
*******************************************************************
*******************************************************************
**
**   temperature table: time (s) vs  temp (k)
**
**   this table is limited to sub critic temperature bounds for use
**   with mass.1 (liquid water) mass sources
**
cf29500   temp-src   equals   1   1.   0.
cf29502  3  273.15  647.2 * limits on liq water temp
cf29510   1.   0.   edf.200.4
*******************************************************************
*******************************************************************
*pppppppppppppppppppppppppppppppppppppppppppppppppppppppppppppppppppp
*pppppppppppppppppppppppppppppppppppppppppppppppppppppppppppppppppppp
*
*
*******************************************************************
************************  source volume  ************************
```

```
*****************************************************************
***                                                           ***
***  this volume is required to provide a pathway for the BWRSRB ***
***  h2 and h2o gas flows to enter the pressure suppression pool ***
***  below the surface of the pool--like actual srv discharge ***
***                                                           ***
*****************************************************************
*
*
cv10000      source-volume     2   2   3
cv10001      0     0
cv100a0      3
cv100a1      pvol     117831.        rhum      .93    *  17.09 psia
cv100a2      tatm     365.85           tpol     324.11
cv100a3      zpol     204.52
cv100a4      mlfr.4   0.0             mlfr.5    0.96       mlfr.6    0.0
cv100a5      mlfr.7   0.0             mlfr.8    0.0        mlfr.9    0.04
cv100b1      190.          0.0   *
cv100b2      210.          500.    *  extend cv above the 16.4592 ele -- erg
*
*  ------------------------ flow paths ------------------------------
*
f1100000    steam-line-srv     100   401   198.6   198.6
f1100001    3.0000   41.3122   1.0 1.95 1.95
f1100002    3 0 0 1 * horizontal flow path, active, def, sparc
f1100a1     3.0000   41.3122    1.95      5.e-6
*
*
*****************************************************************
************************ drywell in-pedestal ********************
*****************************************************************
*
*
cv20000      'in-ped-drywell'     2   2   2
cv20001      0     0
cv200a0      3
cv200a1      pvol     117831.        rhum      .12    *  17.09 psia
cv200a2      tatm     365.85
*cv200a3      mass.1    1269.0    * seal leakage of 350/min for 2175 sec
cv200a4      mlfr.4   0.0             mlfr.5    0.96       mlfr.6    0.0
cv200a5      mlfr.7   0.0             mlfr.8    0.0        mlfr.9    0.04
*    to Sallo cavity is 9' 6.5" deep = 2.91 m
*    Start volume @ 703'11" - 9'6.5" = 694'4.5" = 211.65 m
cv200b1        214.55             0.0    * excludes to Sallo cavity volume
cv200b5        274.97           225.6    * excludes to Sallo cavity volume
*cv200b1        211.65             0.0    * includes to Sallo cavity volume
*cv200b5        222.44           312.0    * includes to Sallo cavity volume
*
*
* direct openings between reactor cavity and drywell
*
f1200100       'loped-drywell'    200    201    215.63    215.63
f1200101       2.79      1.35     1.0      2.40     2.40    * door & 2 circular ports
f1200102       3    0    0    0    * horizontal flow
f1200103       1.     1.     1.     1.
f1201a0        2.79    1.35     1.24      5.0e-5
*
f1200200       'midped-drywell'    200    201    218.24    218.24
f1200201       1.45      1.35     1.0      2.04      2.04       * crd removal hatch
f1200202       3    0    0    0    * horizontal flow
f1200203       1.     1.     1.     1.
f1202a0        1.45    1.35     1.05      5.0e-5
*
f1200300       'hiped-drywell'    200    202    221.13    221.13
f1200301       3.04     1.62     1.0      0.864    0.864         * crd line portals
f1200302       3    0    0    0     *  horizontal flow
```

```
ff2f0s0       3.84   1.62    0.5      5.0e-5
*
*
*      Note: to Solid cavity walls below drywell floor elevation are
*            not modeled as heatslabs
*
*
*  hs20001xnn =  heat  slab for  drywell inpedestal floor
*                 elevation=700'6" to 704'= 213.51 m to 214.59 m
*                 thickness = .081" steel + 3'6"concrete +  1/4" steel
*                 id=20'3"
*                 tot thick=3.52758 ft = 1.07521 m
*
hs20001000  20  1  1  0    * rectangular
hs20001001  'dw-inped floor'
hs20001002  213.5  0.0   * elevation = 700'6"
hs20001003  1.0 * multiplicity
hs20001100  -1  1  0.0
hs20001102  0.00100  2   *  0.039"  steel
hs20001103  0.00206  3   *  0.081"  steel/concrete
hs20001104  0.00254  4   *   0.1"  concrete
hs20001105  0.00508  5   *  0.2"  concrete
hs20001106  0.01016  6   *  0.4"  concrete
hs20001107  0.02032  7   *  0.8"  concrete
hs20001108  0.04064  8   *  1.6"  concrete
hs20001109  0.08128  9   *  3.2"  concrete
hs20001110  0.16256  10   *  6.4"  concrete
hs20001111  0.32512  11   * 12.8"  concrete
hs20001112  0.536575  12   *21.125"  concrete
hs20001113  0.748030  13   *29.450"  concrete
hs20001114  0.910590  14   *35.850"  concrete
hs20001115  0.991870  15   *39.050"  concrete
hs20001116  1.032510  16   *40.650"  concrete
hs20001117  1.052030  17   *41.450"  concrete
hs20001118  1.068857  18   *42.00 "  concrete/steel
hs20001119  1.070610  19   *42.15"   steel
hs20001120  1.075207   20   *42.25"  steel
hs20001200  -1
hs20001201  'carbon steel'  2
hs20001202  'concrete'      17
hs20001203  'carbon steel' 19
hs20001300  0
hs20001400  1  400  'ext'  1.0  1.0
hs20001401  0.5   'equiv band'  5.    * steel surface
hs20001500  29.921  3.0861   1
hs20001600  1  200  'ext'  1.0  1.0
hs20001601  0.5   'equiv band'  5.    * steel surface
hs20001700  29.921  3.0861   1
hs20001800  -1
hs20001801  298.76  20 * room temp =70f
hsdg000010  -20001  17  'h2o-vap'
hsdg000020  -20001  17  'h2o-vap'
hsdg000030  -20001  17  'co2'
hsdg000011    59.68  2.250e6  360.0  378.0
hsdg000021    44.27  6.065e6  378.0  793.0
hsdg000031   473.06  4.157e6  823.0 1073.0
*
*
*
*  hs20002xnn  = drywell pedestal wall
*                 elevation= 703'11" to 723'5 3/4"
*                 id=20'3"
*                 thickness = 4'5" = 1.3462 m
*
hs20002000  19  2  1  0     *  cylindrical
```

```
hs20002001  'dw-pedestal-wall'
hs20002002  214.5538  1.0  *elevation=703'11"
hs20002003  1.0 * multiplicity
hs20002100  -1  1  3.0861  *id=20'3"
hs20002102  3.08864  2  *0.1" concrete
hs20002103  3.09118  3  *0.2" concrete
hs20002104  3.09676  4  *0.4" concrete
hs20002105  3.10647  5  *0.8" concrete
hs20002106  3.12674  6  *1.6" concrete
hs20002107  3.16738  7  *3.2" concrete
hs20002108  3.24866  8  *6.4" concrete
hs20002109  3.41122  9  *12.8" concrete
hs20002110  3.75920  10  *26.5" concrete
hs20002111  4.10718  11  *40.2" concrete
hs20002112  4.26974  12  *46.6" concrete
hs20002113  4.35102  13  *49.8" concrete
hs20002114  4.39166  14  *51.4" concrete
hs20002115  4.41198  15  *52.2" concrete
hs20002116  4.42214  16  *52.6" concrete
hs20002117  4.42722  17  *52.8" concrete
hs20002118  4.42976  18  *52.9" concrete
hs20002119  4.43230  19  *53.0" concrete
hs20002700  -1
hs20002701  'concrete'  18
hs20002300  0
hs20002400  1  200  'int'  1.0  1.0
hs20002401  0.6  'equiv band'  5.  * concrete surface
hs20002500  1.0  6.1722  5.96265
hs20002600  1  201  'ext'  1.0  1.0
hs20002601  0.6  'equiv band'  5.  * concrete surface
hs20002700  1.0  7.52  5.96265
hs20002800  -1
hs20002801  294.26  19 *room temp=70'
hsdg000040  +20002  18  'h2o-vap'
hsdg000050  +20002  18  'h2o-vap'
hsdy000060  +20002  18  'co2'
hsdg000041  59.68  2.258e6  360.0  378.0
hsdg000051  44.27  6.065e6  378.0  793.0
hsdg000061  473.06  4.157e6  823.0 1073.0
*
*
*
*
*  hs20003xnn =  reactor pedestal wall  drywell portion
*                from elevation  723' 5 3/4"  to  729'9 5/8"
*                wall  thickness =  5'4"
*                id=  18'5"
*
hs20003000  20  2  1  0  * cylindrical
hs20003001  'dw-pedestal-wall'
hs20003002  220.51645  1.0 *elevation =7  '5 3/4"
hs20003003  1.0 * multiplicity
hs20003100  -1  1  2.8067  *radius=9' 2 1/2"
hs20003102  2.80924  2  *  0.1"  concrete
hs20003103  2.81178  3  *  0.2"  concrete
hs20003104  2.81686  4  *  0.4"  concrete
hs20003105  2.82702  5  *  0.8"  concrete
hs20003106  2.84734  6  *  1.6"  concrete
hs20003107  2.88798  7  *  3.2"  concrete
hs20003108  2.96926  8  *  6.4"  concrete
hs20003109  3.13182  9  *  12.8"  concrete
hs20003110  3.45694 10  *  25.6"  concrete
hs20003111  3.61950 11  *  32.0"  concrete
hs20003112  4.10718 12  *  51.2"  concrete
hs20003113  4.26974 13  *  57.6"  concrete
hs20003114  4.35102 14  *  60.8"  concrete
```

```
hs20003115  4.39166 15  * 62.4"  concrete
hs20003116  4.41198 16  * 63.2"  concrete
hs200     7  4.42214 17  * 63.6"  concrete
hs200L   18  4.42722 18  * 63.8"  concrete
hs20003119  4.42976 19  * 63.9"  concrete
hs20003120  4.43230 20  * 64.0"  concrete
hs20005200  -1
hs20003201  'concrete' 19
hs20003300  0
hs20003400  1  200  'int'  1.0  1.0
hs20003401  0.6   'equiv bond'   5.    * concrete surface
hs20003500  1.0  5.89  1.9
hs20003600  1  202  'ext'  1.0  1.0
hs20003601  0.6   'equiv bond'   5.    * concrete surface
hs20003700  1.0  7.52  1.9
hs20003800  -1
hs20003801  294.26  20  *room temperature=70f
hsdg000070  -20003  19  'h2o-sap'
hsdg000080  -20003  19  'h2o-vap'
hsdy000090  -20003  19  'co2'
hsdg000071   59.68  2.258e6  360.0  378.0
hsdy000081   44.77  6.065e6  378.0  793.0
hsdg000091  473.06  8.157e6  823.0 1073.0
*
*
*    RPV bottom head (hemisphere)
*    hs20004xxx
*    thick=7.25 inches = .18415 m
hs20004000  8  4  0  0
hs20004001  'low-rpv-head'
hs20004002  221.0  *  lowermost elevation
hs20004003   1.0 *  multiplicity
hs20004100  -1  1  3.1877  * tr = 125.5 inches = 3.1877 m
*              x(1)  1
hs20004102     3.2387  2
hs20004103     3.2895  3
hs20004104     3.3149  4
hs20004105     3.3339  5
hs20004106     3.3529  6
hs20004107     3.3656  7
hs20004108     3.3719  8
hs20004200  -1
hs20004201  'carbon steel'  7
hs20004300  0  *  no heat generation
hs20004400  8898  *  use cf898 (srv gas temp) to define the boundary condition
hs20004600  1  200  'ext'  1.0  1.0  *  all atm heat xfer
hs20004601  .3  'equiv bond'  3.0
hs20004700  71.44  3.37  4.77
hs20004800  -1  *  enter nodal temps
hs20004801  533.0  8  *  500 f
*
*
*****************************************************************************
*****************    drywell ex-pedestal 705'-723'  *********  *********
*****************************************************************************
*
*
cv20100      drywell-bot    2    2    2
cv20101      0    0
cv201a0      3
cv201a1     pvol    117831.       rhum     .12  *  17.09 psia
cv201a2     tatm    365.85
cv201a3     vpol    0.
cv201a4     mlfr.4  0.0           mlfr.5   0.96       mlfr.6   0.0
cv201a5     mlfr.7  0.0           mlfr.8   0.0        mlfr.9   0.0e
cv20161       214.5         0.0   * 703.7'
```

```
cv201b4        220.52       1860.    * 722.99*
*
*
*
f121000       '201-to-202'     201    202    219     221.
f121001       164.     2.     1.0     0.001     0.001
f121002       0    0    0    0    * vertical flow
f121003       1.    1.    1.    1.
f1210s0       164.    2.    13.4     5.0e-5
*
f125000       'downcomer inlet'     201    300    215.04    215.04
f125001       23.88    13.87    1.0     0.001     0.001
*NOTE: DOWNCOMER ID = 24*(2*(3/8)*)=23.25*
*NOTE: FLOW AREA = 23.88 = 85*PI*(23.25*.0349/12)**2/4
f125002       0    0    0    0    * vertical flow
f125003       1.    1.    1.    1.
f1250s0       23.88    13.87    0.59     5.0e-5
*
*NOTE: FOLLOWING NI INERTING LINE INPUT IS LA SALLE-SPECIFC !!
*
*       DOES NOT APPLY TO SUSQUEHANNA !  (re C.R. 6/16/89)
*
* nitrogen inerting system has a 1-1/2 inch line which is normally open
* and remains open during station blackout (see 2vq15e,16e,18e,19e) which
* directly connects the drywell and wetwell between levels e20 and e66.
*f102900       'n2-bypass'              201    401      14.9     -9.2
*f102901       0.00114      30.0      1.0      0.0381      0.0381
*f102902       0    0    0    0
*f102903       0.0     0.0     0.0    0.0
*f1029s0       0.00114      30.0      0.0381       5.0e-5
*
*NOTE: containment venting flow path input from LA SALLE
*
f129000    dw-2-inch     201      900      217.    217.
f129001    0.302027       1.0      0.0
f129002    3
f129003    15.0    15.0
f1290s1    0.002027       1.0     0.0508
f1290v1    -1     171     171
*
           cf17100    dw-2-valve    equals    1     1.0    0.0
           cf17101    0.0
           cf17111    0.0    0.0    time
*
f129100    dw 10 inch    201     900      217.    217.
f129101    0.1642         20.0      0.0
f129102    3
f129103    10.0     10.0
f1291s1    0.1642        20.0     0.4572
f1291v1    -1     172     172
*
           cf17200    dw-10-valve    equals    1     1.0    0.0
           cf17201    0.0
           cf17211    0.0     0.0    time
*
*
*
*   hs20101xnn = lowest drywell cell floor
*                thickness= 0.081" steel + 3'6"concrete  +  1/4" steel
*                 od=86'3"
*                 id=29'1"
*                 delta r =8.7122e
*                 elevation begins  at 700' 6"
*
hs20101000   20   1   1   0    * rectangular
hs2010'701   'low-dw-floor'
```

```
hs20101002  213.5124  0.0  *elevation=700'6"
hs20101003  1.0
hs201   30  20001  1  0.0
hs201   30  20001
hs20101300  0
hs20101400  1  401  'ext'  1.0  1.0
hs20101401  0.3   'equiv band'  5.    * steel surface
hs20101500  401.00  0.7122  0.1
hs20101600  1  201  'ext'  1.0  1.0
hs20101601  0.3   'equiv band'  5.    * steel surface
hs20101700  401.00  0.7122  0.1
hs20101800  -1
hs20101801  294.26  20  *room temp = 70f
hsdg000100  -20101  17  'h2o-vap'
hsdy000110  -20101  17  'h2o-vap'
hsdg000120  -20101  17  'co2'
hsdy000101   59.68  2.258e6  360.0  378.0
hsdg000111   44.27  6.065e6  378.0  793.0
hsdg000121  473.06  4.157e6  823.0 1073.0
*
*hs20105xnn =  heat slab for lowest drywall cell wall
*
hs20102000  13  1  1  0   * rectangular
hs20102001  'low-dw-cell-wall'
hs20102002 214.5792  0.2734 *elevation=704'
hs20102003  1.0 * multiplicity
hs20102100   1  1  0.0
hs20102102  0.00254  2  *0.1" steel
hs20102103  0.00508  3  *0.20" steel
hs20102104  0.00635  4  *0.25" steel
hs20102105  0.01270  5  *0.50" steel
hs20102106  0.02540  6  *1.0"  concrete
hs20102107  0.05080  7  *2.0"  concrete
hs20102108  0.10160  8  *4.0"  concrete
hs20102109  0.20320  9  *8.0"  concrete
hs20102110  0.40640  10 *16.0"  concrete
hs20102111  0.81280  11 *32.0"  concrete
hs20102112  1.62560  12 *64.0"  concrete
hs20102113  1.83515  13 *72.25"  concrete
hs20102200  -1
hs20102201  'carbon steel'  3
hs20102202  'concrete'  12
hs20102300  0
hs20102400  1  201  'ext'  1.0  1.0
hs20102401  0.3   'equiv band'  5.    * steel surface
hs20102500  477.05  8.17242  8.17242
hs20102600  0 * insulated
hs20102800  -1
hs20102801  294.26  13  *room temperature =  70f
*
*
*   hs20103xnn = lowest dw cell misc. steel
*
hs20103000  9  1  1  0
hs20103001  'low-dw-misc-st'
hs20103002  214.580   1.0  *
hs20103003  1.0 * multiplicity
hs20103100  -1  1  0.0  *slab  1" thick
hs20103102  0.00254  2  *0.1" steel
hs20103103  0.00508  3  *0.2" steel
hs20103104  0.01016  4  *0.4" steel
hs20103105  0.01270  5  *0.5" steel
hs20103106  0.01524  6  *0.6" steel
hs20103107  0.02032  7  *0.8" steel
hs20103108  0.02286  8  *0.9"  steel
hs20103109  0.02540  9  *1.0" steel
```

```
hs20103000  -1
hs20103001  'carbon steel'  0
hs20103308  0
hs20103409  1  201  'ext'  1.0  1.0
hs20103401  0.5  'equiv band'  5.  * steel surface
hs20103500  961.2  5.9375  5.9375
hs20103600  1  201  'ext'  1.0  1.0
hs20103601  0.5  'equiv band'  5.  * steel surface
hs20103700  961.2  5.5375  5.9375
hs20103800  -1
hs20103801  296.26  9 *room temp
*
*
*****************************************************************
*****************  drywell ex-pedestal 723' 758'  ***************
*****************************************************************
*
*
cv20200      drywell-2   2    2    2
cv20201      0    0
cv207a0      3
cv207e1      cvol    117931.      rhom     17  *  17.09 pcf
cv207e2      tatm    385.85
cv207e3      vpol    0.
cv207e4      mlfr.4  0.0          mlfr.5   0.96      mlfr.6   0.0
cv207e5      mlfr.7  0.0          mlfr.8   0.0       mlfr.9   0.04
cv20761        720.37        0.0    * 723'
cv207b4        741.0       2596.    * 758'
*
*
*
f1220000     '202-to-204'    202   204   230   232
f1220001     93.   2.      1.0    0.001    0.001
f1220h2      0   0   0   0   * vertical flow
f1220003     1.   1.   1.   1.
f1220s0      93.   2.  0.59687    5.0e-5
*
*
*
*  hs20202xnn = heat slab for 2nd drywell  cell  exterior wall
*
hs20202000  13  1  1  0
hs20202001  '2nd-dw-cell-wall'
hs20202002  720.5164  0.2734  *elevation=723'5  3/4"
hs20202003  1.0 * multiplicity
hs20202100  20102  1  0.0
hs20202200  20102
hs20202300  0
hs20202400  1  202  'ext'  1.0  1.0
hs20202401  0.5  'equiv band'  5.  * steel surface
hs20202500  684.67  10.94  10.94
hs20202600  0
hs20202800  -1
hs20202801  294.26  13  *room temperature = 70f
*
*
*  hs20201xnn =  lower shield wall
*                  1/2"steel + 1'9"concrete + 1.5"steel
*                  elevation =729' 9 5/8" to 758'
*                  height  = 8.59473 m
*                  thickness = 1.9167 ft = .5842 m
*                  ir=12.7917 ft = 3.8989 m
*                  or=14.7084 ft = 4.4831 m
*
hs20201000  19  2  1  0
hs20201001  'low-shield wall'
```

```
hs20201002  722.4440  1.0  "elevation=729'9 5/8"
hs2020'203 1.0 * multiplicity
hs202!    6  -1  1  3.8989  "id-25' )"
hs2020..02  3.90144  2  " 0.1" steel
hs2C201103  3.90398  3  "0.2"  steel
hs20201104  3.90906  4  "0.4"  steel
hs20201105  3.91160  5  "0.5"  steel/concrete
hs20201106  3.92430  6  "  concrete
hs20201107  3.9497   7  "  concrete
hs20201108  4.0005   8  "  concrete
hs20201109  4.10210  9  "  concrete
hs20201110  4.16560 10  "  concrete
hs20201111  4.22910 11  "  concrete
hs20201112  4.33070 12  "  concrete
hs20201113  4.38150 13  "  concrete
hs20201114  4.4450  14  "  concrete/steel
hs20201115  4.4500  15  "  steel
hs20201116  4.4600  16  "  steel
hs20201117  4.4700  17  "  steel
hs20201118  4.4750  18  "  steel
hs20201119  4.4831  19  "  steel
hs20201200  -1
hs20201201  'carbon steel'  4
hs20201202  'concrete'  13
hs20201203  'carbon steel'  18
hs20201300  0
hs20201400  1  203  'int'  1.0  1.0 " c 203 is the
hs20201401  0.3   'equiv band'  5    " steel surface
hs20201500  1.0  7.7978  8.5
hs20201600  1  202  'ext'  1.0  1.0 " ev202 is rhs
hs20201601  0.3   'equiv band'  5    " steel surface
hs20201700  1.0       8.38       8.3
hs20201800  -1
hs20201801  294.26  19 "room  temp - 70f
hsdg000130  +20201  13  'h2o-vap'
hsdg000140  +20201  13  'h2o-vap'
hsdg000150  +20201  13  'co2'
hsdg000131   59.68  2.250e6  360.0  378.0
hsdg000141   44.27  6.065e6  378.0  793.0
hsdg000151  473.06  4.157e6  823.0 1073.0
*
*
*    hs20203xnn = 2nd drywell cell misc. steel
*
hs20203000  9  1   1  0
hs20203001  '2nd-dw-misc-st'
hs20203002  220.51645  1.0  "elevation=723' 5 3/4"
hs20203003  1.0 * multiplicity
hs20203100  20103  1  0.0  "slab-1"thick
hs20203200  20103
hs20203300  0
hs20203400  1  202  'ext'  1.0  1.0
hs20203401  0.3   'equiv band'  5    " steel surface
hs20203500  1123.8  10.48  10.48
hs20203600  1  202  'ext'  1.0  1.0
hs20203601  0.3   'equiv band'  5    " steel surface
hs20203700  1123.8  10.48  10.48
hs20203800  -1
hs20203801  294.26  9  "room temp
*
*
*
*****************************************************************
*****************  reactor/shield wall annulus  *****************
*****************************************************************
*
```

```
*
cv20300      shield-annulus    2    2    2
cv20301      0    0
cv20300      3
cv203a1      pvol     117831.       rhum     .12   *   17.09 psia
cv203a2      tatm     365.85
cv203a3      vpol     0.
cv203a4      mlfr.4   0.0           mlfr.5    0.96       mlfr.6    0.0
cv203a5      mlfr.7   0.0           mlfr.8    0.0        mlfr.9    0.04
cv203b1        222.4          0.0   * 729'9"
cv203b4        237.363        18.4  * elev  & vol. includes DW head*
*
*
*
f120400    annulus-to-202     203      202      227.37    227.37
f120401    15.78      584     1.       89       89
f120402    3    * horizontal flow
f120403    1.0     1.0    1.0    1.0
f1204s1    15.78      .584      .295     5.0e-5
*
f120500    annulus-to-204     203      204      234.19    234.19
f120501    11.01      .584     1.      3.37     3.37
f120502    3    * horizontal flow
f120503    1.0     1.0    1.0    1.0
f1205a1    11.01      .584     1.     5.0e-5
*
f124000    'annulus-to-head'     203    205    237     238
f124001    1.24        50        1.0     0.001     0.001  * assume 2" annular
*                                                           gap @ 12'9.5" rad
f124007    0    0    0    0    * vertical flow
f124003    1.     1.     1.     1.
f1240a9    1.24      .50    1.0     5.0e-5
*
*
*  hs20302xnn = upper shield wall
*               elevation =758' to 778'9"
*               height = 6.3246 m
*               id=25'7"
*               od=29'1"
*               thickness = 1.75'
*
hs20302000  19   2   1   0
hs20302001  'upper-shld-wall'
hs20302002  231.0384   1.0   *elevation=758'
hs20302003  1.0 * multiplicity
hs20302100  20201   1   3.8989 *id=25'7"
hs20302200  20201
hs20302300  0
hs20302400  1   203   'int'   1.9   1.0
hs20302401  0.3     'equiv band'    .15     * steel surface
hs20302500  1.0   7.7978   6.3246
hs20302600  1   204   'ext'   1.0   1.0
hs20302601  0.3     'equiv band'   5.     * steel surface
hs20302700  1.0   8.38   6.3246
hs20302800  1
hs20307801   294.26   19   *room temp = 70f
hsdg000160  +20302   13   'h2o-vap'
hsdg000170  +20302   13   'h2o-vap'
hsdg000180  +20302   13   'co2'
hsdg000161    59.68   2.258e6   360.0   378.0
hsdg000171    44.27   6.065e6   378.0   793.0
hsdg000181   473.06   4.157e6   823.0  1073.0
*
*
*
*     heat slab for reactor vessel (wall insulation neglected)
```

```
*     average wall thickness = 6.85"
*     hs20305xnn = rx vessel wall
*       vssel id =  20.9'
*
hs20305000  8  2  1  0
hs20305001  'rx-vessel-wall'
hs20305002   727.944  1.0  *elevation=729' 9 5/8"
hs20305003  1.0 * multiplicity
hs20305100  -1  1  3.18516  *id=20.9 ft
hs20305102  3.26136  2  *3" thick
hs20305103  3.31216  3  *5" thick
hs20305104  3.33756  4  *6" thick
hs20305105  3.35026  5  *6.5" thick
hs20305106  3.35661  6  *6.75" thick
hs20305107  3.35788  7  *6.80" thick
hs20305108  3.35915  8  *6.85" thick
hs20305200  -1
hs20305201  'carbon steel'  7
hs20305300  0 * no volumetric power
hs20305400  8890 * use cf890 (srv gas temp) to define the boundary temp
hs20305600  1  203  'ext'  1.0  1.0
hs20305601  0.3   'equiv band'   .15   * steel surface
hs20305700  1.0  6.37032  14.9
hs20305800  -1
hs20305801  310.93  0  *initial temp=100f
*
*
*****************************************************************
*****************  drywell ex-pedestal 758'-779'  ***************
*****************************************************************
*
*
cv20400       drywell-3    2    2    2
cv20401       0    0
cv204a0       3
cv204a1      pvol     117831.       rhum     .12  *  17.09 psia
cv204a2      tatm     365.85
cv204a3      vpol     0.
cv204a4      mlfr.4  0.0           mlfr.5   0.96       mlfr.6   0.0
cv204a5      mlfr.7  0.0           mlfr.8   0.0        mlfr.9   0.04
cv204b1        231.0        0.0    * 758'
cv204b4        237.44        722    * 779'
*
*
f1230000 '204-to-205'   204   205   237.   238.
f1230001  55.    2.    1.    .001    .001
f1230002   0    0    0    0    * vertical flow
f1230003  1.    1.    1.    1.
f1230b0  55.    2.    5.9   5.0e-5
*
*
*    hs20403xnn  = 3rd drywell cell misc. steel
*
hs20403000  9  1  1  0
hs20403001  '3rd-dw-misc-st'
hs20403002 231.0384  1.0  *  elevation = 758'
hs20403003  1.0 * multiplicity
hs20403100  20103  1  0.0  'slab=1'thick
hs20403200  20103
hs20403300  0
hs20403400  1  204  'ext'  1.0  1.0
hs20403401  0.3   'equiv band'  5.    * steel surface
hs20403500  388.75  6.3246  6.3246
hs20403600  1  204  'ext'  1.0  1.0
hs20403601  0.3   'equiv band'  5.    * steel surface
hs20403700  388.75  6.3246  6.3246
```

```
hs20401800  -1
hs20403801  294.26  9  *room temp
*
* hs20401xnn =  heat slab for 3rd drywell cell exterior wall
*                 elevation=758' to 791' 9"
*
*
hs20401000  13  1  1  0
hs20401001  '3rd dw cell wall'
hs20401002  231.0384  1.0  *elevation=758'
hs20401003  1.0 * multiplicity
hs20401100  20102  1  0.0
hs20401200  20102
hs20401300  0
hs20401400  1  204  'ext'  1.0  1.0
hs20401401  0.3   'equiv band'  5.    * steel surface
hs20401500  312.64   6.4    6.4
hs20401600  0
hs20401800  -1
hs20401801  294.26  13  *  room  temperature = 70f
*
*
*****************************************************************
*****************  drywell ex-pedestal 779'-809' (top)   ********************
*****************************************************************
*
*
cv20500      drywell-top    2    2    2
cv20501      0    0
cv205a0      3
cv205a1     pvol    117831.       :hum     .12  *  17.09 psia
cv205a2     tatm    365.85
cv205a3     vpol    0.
cv205a4     mlfr.4  0.0           mlfr.5   0.96       mlfr.6   0.0
cv205a5     mlfr.7  0.0           mlfr.8   0.0        mlfr.9   0.04
cv205b1       237.363         0.0      * 779'
cv205b4       246.5878        1052.    * 806.7'
**
** drywell head leak flow path -- DEACTIVATED FOR CB RUN
**
** Start leaking if drywell head temp has ever > Cf245 and if gauge pressure >
** than the value set in Cf246
*
* --- Maximum leakage area based on CBI Peach Bottom study for case
*     with no gasket springback
*
*   -- use Susquehanna head dimensions for hydraulic diameter : 4A/P
* ---  P = Pi * 37'-7.5" = 36.0281 m  Dhyd = 4 (.04)/ 36.0281 =  .00444
*      Assume flow path length = flange thickness = 4" =  .1016
*
*f126000       'dw hd failure'          205    600     741.7    741.7
*f126001       0.04    .1016    1.        * maximum open area = .04
*f126002       3
*f126003       1.0  1.0
*f126040       0.04    .1016    0.00444     1.0e-4     16.0
*f126050       -1     470    470
*
              cf47000       dwhead-fail-frac      1.a ifte  3    1.0    0.0
              cf47001       0.0
              cf47011       1.0    0.0    cfvalu 450
              cf47012       1.0    0.0    cfvalu 600
              cf47013       0.0    0.0    time
*
              cf45000       'dwhead-fail'  1.and     2      1.0     0.0
              cf45001        false.
              cf45011       1.0      0.0      cfvalu 245   * temperature criterion
```

```
*              cf45012      1.0      0.0      cfvalu.246   * psid criterion
*
               cf24500      'temp-criterion'     1-gt    2      1.0    t
               cf24501      .false.
               cf24505      latch
               cf24511      1.0        0.0    hs-temp.2050408 * midpoint flange temp
               cf24512      0.0     644.3     time   *  head fail temp = 700 f
*
               cf24600      'dp-criterion'    1-gt     2    1.0    0.0
               cf24601      .false.
               cf24611      1.0         0.0    cfvalu.197    * dw head dp
               cf24612      0.0   565370.     time   * head fail dp = 82 psid
*
               cf19700      'diff-pressure'     add     2      1.0     0.0
               cf19711      1.0       0.0      cvh.p.205   *  DP = P(205) - Env
               cf19712     -1.0       0.0      cvh.p.600
*
               cf40000     'frac-open-cf'  tab fun    1    1.0    0.0
               cf40003      252
               cf40011      1.0     0.0    cfvalu.197

* base on data from CBI Peach Bottom Study for case of no gasket springback
*
               tf25200    'area-vs-dp'      4     1.0     0.0
               tf25211        -1.e9        0.0     *
               tf25212     565370.07       0.0     *   82 psid    0.0 sq meters
               tf25213    1378951.4        1.0     * 200 psid    0.04 sq meters
               tf25214         1.e9        1.0     *hold area constant above 200 psid
*
*
*
*
*    hs20501xnn = rx vessel head
*    thickness varies form 3.5" to 4 15/16" avg =4.25"
*
hs20501000   10   5   1   0
hs20501001   'rx-vessel-head'
hs20501002   241.3254   *elevation = 791'9"
hs20501003   1.0 * multiplicity
hs20501100   -1   1   3.1877   *radius=125.5"
hs20501102   3.2258   2   *1.5" steel
hs20501103   3.2512   3   *2.0" steel
hs20501104   3.2639   4   *3.0" steel
hs20501105   3.27025   5   *3.25" steel
hs20501106   3.27660   6   *3.50" steel
hs20501107   3.28295   7   *3.75" steel
hs20501108   3.28930   8   *4.0" steel
hs20501109   3.29311   9   *4.15" steel
hs20501110   3.29565   10  *4.25" steel
hs20501200   -1
hs20501201   'carbon steel'   9
hs20501300   0
hs20501400   8890   *   use cf890 (srv gas temp) to define ths boundary condition
hs20501600   1.205   'ext'   1.0   1.0
hs20501601   0.3    'equiv band'   3.     * steel surface
hs20501700   1.0   3.1877   1.0
hs20501800   -1
hs20501801   310.93   10   *initial temp=100f*
*
*
*   hs20502xnn =upper head region external  wall
*              elevation = 770'9" to 791'9"
*
hs20502000   13   1   1   0
hs20502001   'upper-head-wall'
hs20502002   237.363   0.2734   *elevation = 778'9"
```

```
hs20502003   1.0
hs20502100   20102  1  0.0
hs20502200   20102
hs20502300   0
hs20502400   1  205  'ext'  1.0  1.0
hs20502401   0.3   'equiv band'  2.    * steel surface
hs20502500   158.03  4.1194  4.1194
hs20502600   0
hs20502800   -1
hs20502801   294.26  13  *room temperature = 70f
*
*
*hs20503  is retangular approximation of drywell head
*
hs20503000   9  1  1  0
hs20503001   'dw head retang'
hs20503002   246.58  0.  * horizontal slab, bottom at 246.58 m
hs20503003   1.0 * multiplicity
hs20503100   -2  1  0.0
hs20503102   0.00254  2  *0.1" steel
hs20503103   0.00508  3  *0.2" steel
hs20503104   0.01016  4  *0.4" steel
hs20503105   0.01905  5  *0.75" steel
hs20503106   0.02794  6  *1.1" steel
hs20503107   0.03302  7  *1.3" steel
hs20503108   0.03556  8  *1.4" steel
hs20503109   0.03810  9  *1.5" steel
hs20503200   -1
hs20503201   'carbon steel'  8
hs20503300   0
hs20503400   1  205  'int'  1.0  1.0
hs20503401   0.3   'equiv band'  5.    * steel surface
hs20503500   317.65   5.7243   1.0   * use Steve's calculated area
hs20503600   1  609  'ext'  0.1   0.1
hs20503601   0.3   'equiv band'  5.    * steel surface
hs20503700   317.65   5.7243  1.0
hs20503800   -1
hs20503801   294.29  9  *room temp = 70f
*
*
*  hs20504xnn     = drywell head flange
*                   elevation 791'9" to  797' 1-3/8"
*                   thickness = 4" = 0.1016 m
*                   1.0  = 37' 7-1/2"  =  11.4681 m
*                   radius = 5.73405 m
*
hs20504000   15   2   0   0   * cylindrical slab
hs20504001   'dw head flange'
hs20504002   241.3254   1.0   * bottom @ 791' 9", vertical structure
hs20504003   1.0 * multiplicity
hs20504100   -1   1   5.73405
hs20504102   5.73659   2   * 0.1" steel
hs20504103   5.73913   3   * 0.2" steel
hs20504104   5.74421   4   * 0.4"
hs20504105   5.75437   5   * 0.8"
hs20504106   5.76453   6   * 1.2"
hs20504107   5.77469   7   * 1.6"
hs20504108   5.78485   8   * 2.0"
hs20504109   5.79501   9   * 2.4"
hs20504110   5.80517  10   * 2.8"
hs20504111   5.81533  11   * 3.2"
hs20504112   5.82549  12   * 3.6"
hs20504113   5.83057  13   * 3.8"
hs20504114   5.83311  14   * 3.9"
hs20504115   5.83565  15   * 4.0"
hs20504200   -1
```

```
hs20504701   'carbon steel'  14
hs20504300   0
hs20504     30    1   205   'ext'   1.0   1.0
hs205.   01  0.3   'equiv bond'  2.    * steel surface
hs20504500   1.0   1.635   1.635
hs20504600   1   600   'ext'   0.1   0.1
hs20504601  0.3   'equiv bond'  2.    * steel surface
hs20504700   1.0   1.635   1.635
hs20504800   -1
hs20504801   311.    15   * initial temp. = 100 f *
*
*
*hs20505xnn  = drywell head misc steel
*
hs20505000  9  1  1  0
hs20505001  'dw-head-misc-st'
hs20505002  237.363  1.0 * elevation=778'9"
hs20505003  1.0 * multiplicity
hs20505100  20103  1  0.0  *slab-1"thick
hs20505200  20103
hs20505300  0
hs20505400  1  205  'ext'  1.0  1.0
hs20505401  0.3   'equiv bond'  2.    * steel surface
hs20505500  158.25  3.9624  3.9624
hs20505600  1  205  'ext'  1.0  1.0
hs20505601  0.3   'equiv bond'  2.    * steel surface
hs20505700  158.25  3.9624  3.9624
hs20505800  -1
hs20505801  294.26  9  *room temp
*
*
*
*************************************************************************
************************      downcomers      ************************
*************************************************************************
*
*
cv30000      downcomers    2    .   3
cv30001      0    0
cv300a0      3
cv300a1      pvol     117831.        rhum     .93    *  17.09 psia
cv300a2      tatm     340.11           tpol    324.11
cv300a3      zpol     204.52
cv300a4      mlfr.4  0.0             mlfr.5   0.96       mlfr.6   0.0
cv300a5      mlfr.7  0.0             mlfr.8   0.0        mlfr.9   0.04
cv300b1       201.16           0.0
cv300b2       215.04         330.6   * volume = all 87 downcomers
*
*-------------------------  flow paths  -------------------------
*
f130100       'downcomer exit'      300    a01    201.16    201.16
f130101       22.4     7.6   1.0    0.001     0.001 * use small opening heights
*   82 uncapped downcomer pipes
*    5    capped downcomer pipes with 3 inch drains to ww pool
*NOTE: 22.4 = 82*Pi*(0.59**2)/4+(5*Pi*(3*.3048/12)**2/4)
f130102       0    0    0    1    * vertical flow, sparc physics
f130103       1.0     1.0    1.0    1.0
f1301a0       22.4      6.94    0.59    5.0e-5
*
*
*
*
*   hs30002xnn  down comer wall air portion
*
hs30002000  5  2  1  0
hs30002001  'downcomers air'
```

```
hs30002002   204.5208   1.0   *elevation=671 ft
hs30002003   87.0 * multiplicity
hs30002100   -1   1   0.295275
hs30002102   0.299720   2       *0.175"    steel
hs30002103   0.302260   3       *0.275" steel
hs30002104   0.302895   4       *0.30" steel
hs30002105   0.304800   5       *0.375" steel
hs30002200   -1
hs30002201   'carbon steel'   4
hs30002300    0
hs30002400    1   300   'int'   1.0   1.0
hs30002401   0.3    'equiv band'   .5      * steel surface
hs30002500    1.0      0.59055    8.9792
hs30002600    1   401   'ext'   1.0   1.0
hs30002601   0.3    'equiv band'   5      * steel surface
hs30002700     1.0    0.60960    8.9792
hs30002800   -1
hs30002801   294.26   5   *room   temperature=70f
*
*    hs30001xnn   downcomers submerged
*
hs30001000   5   2   1   0
hs30001001   'downcomers outer'
hs30001002   201.168   1.0* elevation=660'
hs30001003   87.0 * multiplicity
hs30001100   30002    1   0.295275
hs30001200   30002
hs30001300   0
hs30001400    1   300   'int'   0.0   0.0
hs30001500   1.0   0.59055   3.3528
hs30001600    -1   401   'ext'   0.0   0.0
hs30001700   1.0   0.69060    3.3528
hs30001800   -1
hs30001801   294.26 5 *   room   temperature =70f
*
*
*
*
*
*
*
*********************************************************************
*********************** wetwell in-pedestal *************************
*********************************************************************
*
*
cv40000      'wetwell cavity'     2   1   2     3
cv40001      0     0
cv40040      5
cv40041      pvol      109006.         rhuo      .93     *   15.81 psia
cv40042      tatm      307.83            tpol    324.11
cv40043      zpol      204.52
cv40044      mass 2    0.0
cv40045      mlfr.4   0.0             mlfr.5    0.96        mlfr.6    0.0
cv40046      mlfr.7   0.0             mlfr.8    0.0         mlfr.9    0.04
cv40061       197.5              0.0     *   648'
cv40062       213.5124          447.7   *   701'11"   -  3.5' =  700.42 = 213.5124 m
*                                        *   pedestal ID = 19'7"
*
f140100    ped-to-WW bottom   400    401    198.91    198.91
f140101    1.167      1.55    1.0      609      609
f140102    3 * horizontal flow path
f140103    1.5      1.5 * kfor=krev
f1401c1    1.167      1.55     .61      5.e-6
*
f140200    ped-to-WW middle   400    401    202.41    202.41
```

```
r1402?01    1.167      1.55    1.0      .609      .609
r1402?02    3 * horizontal flow path
r1402?      1.5        1.5 * bfore+brev
r1402?      1.167      1.55    .61      5.e-6
*
r1406300    ped-to-ww-top  400    401    208.65    208.65
r1403?01    1.55       1.55     1.0      .914      .914
r1403?02    3 * horizontal flow path
r1403?03    1.5        1.5
r1403?41    1.53       1.55     .71      5.e-6
*
*
*
*      hs40002xnn  wetwall inpedestal  wall-pool
*        25 inch steel inside
*     60.00 inches concrete
*        50 inch steel outside
*
hs40002000  19  2  1  0
hs40002001  'ww ped-wall-wet'
hs40002002  197.5108    1.0 'water begins at 648'
hs40002003  1.0 * multiplicity
hs40002100  -1  1  2.9845  'id=19'?'
hs40002102  2.99704  2  '0.1     steel
hs40002103  2.99695  3  '0.25'  steel/concrete
hs40002104  2.99720  4  '0.5'  concrete
hs40002105  3.00790  5  '1.0' concrete
hs40002106  3.03530  6  '2.0' concrete
hs40002107  3.08610  7  '4.0' concrete
hs40002108  3.18770  8  '8.0' concrete
hs40002109  3.39090  9  '16.0' concrete
hs40002110  3.75920 10  '30.5' concrete
hs40002111  4.12750  11  'a5.0' concrete
hs40002112  4.33070  12  '53.0' concrete
hs40002113  4.03230  13  '57.0' concrete
hs40002114  4.09310  14  '59.0' concrete
hs40002115  4.50850  15  '60.0' concrete
hs40002116  4.52120  16  '60.5' concrete/steel
hs40002117  4.52755  17  '60.75' steel
hs40002118  4.53136  18  '60.90' steel
hs40002119  4.53390  19  '61.0' steel
hs40002200  -1
hs40002201  'carbox st301'  2
hs40002202  'concrete'  15
hs40002203  'carbon steel'  18
hs40002300  0
hs40002400  -1  400  'int'  0.0  0.0 * ht to pool only
hs40002500  1.0  5.969    7.0104
hs40002600  -1  401  'ext'  0.0  0.0 * ht to pool only
hs40002700  1.0  9.0678  7.0704
hs40002800  -1
hs40002801  294.26  19*   room  temperature=70f
*
*   hs40031xnn  wet wall in pedestal - air
*                 length of air portion=29.5'
*
*
hs40003000  19  2  1  0
hs40003001  'ww-ped-wall-air'
hs40003002  204.5208  1.0' air  begins at   671'
hs40003003  1.0 * multiplicity
hs40003100  40002  1  2.9845  'id=19'?'
hs40003200   40002
hs40003300   5
hs40003400   1  400  'int'  1.0  0.0
hs40031401  0.3   'equiv band'  5.   * steel surface
```

```
hs40001500  1.0   5.969     8.9192
hs40001600   1  401  'ext'  1.0  1.0
hs40001601  0.3   'equiv band'  5.    * steel surface
hs40001700  1.0  9.9678  8.9192
hs40001800  -1
hs40001801  294.26  19 * room  temperature  = 70f
hsdg000190  +40003  15  'h2o-vap'
hsdg000200  +40003  15  'h2o-vap'
hsdg000210  +40003  15  'co2'
hs*sg000191   59.68  2.258e6  360.6  379.9
hs*sg000201   44.27  6.065e6  370.0  393.9
hsdg000211  473.66  8.157e6  823.0 1873.0
*
*hs4C001nnn   wet  wall inpedestal floor is 8'thick with 1/4" liner
*
hs40001000  12  1  1  0
hs40001001  'ww inped floor'
hs40001007  195.8616   0.0  * bottom elevation=640' (=648'-8')
hs40001003  1.0 * multiplicity
hs40001100  -5  2  0.0    * ww=0.0 begins at elevation  640' and points upwards
hs40001102  0.012800  2  * 32" concrete
hs40001103  1.625600  3  * 32" concrete
hs40001104  2.032000  4  * 16" concrete
hs40001105  2.235200  5  *  8" concrete
hs40001106  2.336800  6  *  4" concrete
hs40001107  2.387600  7  *  2" concrete
hs40001108  2.413000  8  *  1" concrete
hs40001109  2.425700  9  *0.5" concrete
hs40001110  2.432050 10  *.25" concrete
hs40001111  2.435860 11  *.15" steel
hs40001112  2.438400 12  *0.1" steel  slab thickness =8'
hs40001200  -1
hs40001201  'concrete'  9
hs40001202   'carbon steel' 11
hs40001300  0
hs40001400    0
hs40001600  1  400  'ext'  0.0  0.0
hs40001700  27.98  5.97   0.1 * floor dia  = 19'7" (5.97 m)
hs40001800  -1 * nodal temps
hs40001801  294.26  11        * room temperature  =  70f
hs40001802   285.8   12       *  average  room temperature=55f
*
*
*
*
*
*------------------------------------------------------------------------
*------------------------- wetwell ex-pedestal ---------------------------
*------------------------------------------------------------------------
*
*
cv40100      wetwell    2    2    3
cv40101      0    0
cv40103      498.25    * control volume area used for velocity calc
cv401a0      3
cv401a1      pvol     109006.        thum     .95     *  15.81 psia
cv401a2      tatm     307.83           tpol    324.11
cv401a3      zpol     204.52
cv401a4      mlfr.4  0.0             mlfr.5   0.96       mlfr.6   0.0
cv401a5      mlfr.7  0.0             mlfr.8   0.0        mlfr.9   0.04
cv401b1       197.5          0.0
cv401b3       213.5124        7e05
*
*------------------------- vacuum breakers -------------------------
*
* --- this breaker represents the first 25 % of the first vb
```

```
*
*  --- this is done to aid in determining the fraction of the flow path
*      ich opens each time the vacuum breakers actuate
*
*  Use PPL data for vacuum breakers:
*                7467.0 pa-diff(1.083 psid) to crack the breakers
*               16182.0 pa-diff(2.347 psid) to fully open breakers
*          max opening area at 65 degrees is .175 m**2(1.885 ft**2)
*
f143000    vac-brk-1a   401    300    211.76    211.76
f143001    0.04375      0.9144    0.0      .5  .5 * initially closed
f143002    3 * horizontal flow path
f143003    8.47       1.0e6 * PPL kforward, large kreverse
f1430s1    0.04375      0.9144    1.       5.e-6
f1430v0    -1   102   102
*
*          control functions for vacuum breakers
           cf10100    'dp-401-300'  add 2  1.0  0.0
           cf10110    1.0  0.0  cvb-p 401 * not corrected for cool elev
           cf10111   -1.0  0.0  cvb-p 300
*
           cf10200    'vb-1a-tab'  tab-fun  1  1.0  0.0
           cf10203    11  * tabular function number
           cf10210    1.0  0.0  cfvalu 101
*
           tf01100    'vb-1a-fract-open'  4  1.0  0.0
*                     delta-p    fraction-open
           tf01110     -1.0e6    0.0
           tf01111     7467.     0.0     * start opening @ 1.083 psid
           tf01112     7902.75   1.0     * full open @ 1.146 psid
           tf01113     +1.0e6    1.0
*
*      this breaker represents the second 25 % of the first vb
*
f143100    vac-brk-1b   401    300    211.76    211.76
f143101    0.04375      0.9144    0.0      .5  .5 * initially closed
f143102    3 * horizontal flow path
f143103    8.47       1.0e6
f1431s1    0.04375      0.9144    1.       5.e-6
f1431v0    -1   103   103
*
           cf10300    'vb-1b-tab'  tab-fun  1  1.0  0.0
           cf10303    12  * tabular function number
           cf10310    1.0  0.0  cfvalu 101
*
           tf01200    'vb-1b-fract-open'  4  1.0  0.0
*                     delta-p    fraction-open
           tf01210      -1.0e6    0.0
           tf01211     7902.76    0.0     * start opening @ 1.146 psid
           tf01212     8538.5     1.0     * full open @ 1.209 psid
           tf01213      +1.0e6    1.0
*
*
*  --- this breaker represents the third 25 % of the first vb
*
f143200    vac-brk-1c   401    300    211.76    211.76
f143201    0.04375      0.9144    0.0      .5  .5 * initially closed
f143202    3 * horizontal flow path
f143203    8.47       1.0e6
f1432s1    0.04375      0.9144    1.       5.e-6
f1432v0    -1   104   104
*
           cf10400    'vb-1c-tab'  tab-fun  1  1.0  0.0
           cf10403    13  * tabular function number
           cf10410    1.0  0.0  cfvalu 101
*
```

```
          tf01300   'vb-1c fract open'  4  1.0  0.0
*                   delta-p   fraction-open
          tf01310     -1.0e6    0.0
          tf01311    8330.58    0.0     * start opening @ 1.209 psid
          tf01312    8774.25    1.0     * full open @ 1.273 psid
          tf01313     +1.0e6    1.0
*
*  --- this breaker represents the last 25 % of the first vb
*
f143400   vac-brk-1d  401   300   211.76   211.76
f143401   0.04375    0.9144   0.0     .5  .5 * initially closed
f143402   3 * horizontal flow path
f143403   8.47      1.0e6
f143ea1   0.04375    0.9144   1.      5.e-6
f143ev0   -1  105  105
*
          cf10500   'vb-1d-tab'  tab-fun  1  1.0  0.0
          cf10503   18  * tabular function number
          cf10510   1.0  0.0  cfvalu.101
*
          tf01400   'vb-1d-fract-open'  4  1.0  0.0
*                   delta-p   fraction-open
          tf01410     -1.0e6    0.0
          tf01411    8774.26    0.0     * start opening @ 1.273 psid
          tf01412    9210.9     1.0     * full open @ 1.336 psid
          tf01413     +1.0e6    1.0
*
*  ------ this vacuum breaker represents the 2nd of 5 breakers
*
*  --- this vacuum breaker will only be allowed to open after the first
*  --- vacuum breaker is fully open
*
f144000   vac-brk-2of5  401   300   211.76   211.76
f144001   0.175     0.9144   0.0     .5  .5 * initially closed
f144002   3 * horizontal flow path
f144003   8.47      1.0e6
f144a51   0.175     0.9144   1.      5.e-6
f144ev0   -1  109  109
*
          cf10900   'vb-2-tab'  tab-fun  1  1.0  0.0
          cf10903   19 * tabular function number
          cf10910   1.0  0.0  cfvalu.101
*
          tf01900   'vb-2 frac-op'  4  1.0  0.0
*                   delta-p   fraction-open
          tf01910     -1.0e6    0.0
          tf01911     9210.1    0.0     * start opening @ 1.336 psid
          tf01912    10953.0    1.0     * full open @ 1.389 psid
          tf01913     +1.0e6    1.0
*
*
*   this vacuum breaker represents the final 3 breakers combined
f145000   'vac-brk-345' 401   300   211.76   211.76
f145001   0.525   0.9144   0.0   0.5   0.5   * initially closed
f145002   3   * horizontal flow path
f145003   8.47   1.0e6
f145a51   0.525   0.9144   1.0   5.0e-6
f145ev0   -1   451   451
*
          cf45100   'vb-345-tab'  tab-fun  1  1.0  0.0
          cf45103   451   *  tab function number
          cf45110   1.0  0.0  cfvalu.101
*
          tf45100   'vb-345-frac-op'  4  1.0  0.0
*                   delta-p  frac-open
          tf45110     -1.0e6      0.0
```

```
            tf45111  10953.1      0.0  *  start open @ 1.569 psid
            tf45112  16187.0      1.0  *  full open @ 2.347 psid
            tf45113    +1.0e6     1.0
*
*
f1a9000   ww-2-inch     401       900       210       210
f1a9001   0.002027      1.0     0.0
f1a9002   3
f1a9003   15.0     15.0
f1a90s1   0.002027     1.0     0.0509
f1a90v1   -1     173       173
*
          cf17300   ww-2-valve     equals     1     1.0   0.0
          cf17301   0.0
          cf17311   0.0     0.0     time
*
f1a9100   ww-10-inch    401       900       210       210
f1a9101   0.1662      20.0     0.0
f1a9102   3
f1a9103   10.0     10.0
f1a91s1   0.1662      20.0     0.4572
f1a91v1   -1     102     102
*
          cf10200   ww-10-valve    equals    1    1.0    0.0
          cf10201   0.0
          cf10211   0.0    0.0      time
***
* wetwell leak flow path - DEACTIVATED FOR CO RUN
*
* Start leaking if wetwell gauge pressure > value set in Cf 150
*
* leakage is from wetwell about half way between the water and ceiling
*f149500       'ww-failure'          401    900      210      210
*f149501       0.00929023    1.219    0.0                        * 0.1 ft2
*f149502       3
*f149503       1.0   1.0
*f149504       0.00929023    1.219    0.109     1.0e-4     16.0
*f1495v0       -1     151    151
*
              cf15100       ww-fail-frac      1.e-1fte   3    1.0    0.0
              cf15101       0.0
              cf15111       1.0    0.0    cfvalu.150
              cf15112       0.0    1.0    time
              cf15113       0.0    0.0    time
*
              cf15000       'ww-fail'    1-gt     2      1.0     0.0
              cf15001       .false.
              cf15005       latch
              cf15011       1.0      0.0      cfvalu.149
              cf15012       0.0      935792.      time   * fail wetwell at 135 psig
*
              cf14900       'diff-pressure'    add     2      1.0     0.0
              cf14911       1.0      0.0      cvh p.401   *  DP - ww - inv
              cf14912      -1.0      0.0      cvh p.900
*
*  ----------  deactivate SMI to SAlle ww failure ffo  ----------------*
*
*             cf29300       'liner fail'     1-gt    2      1.0    0.0
*             cf29301       .false.
*             cf29305       latch
*             cf29311       1.0       0.0    hg-temp.4010301
*             cf29312       0.0    1273.0    time * ww liner fail temp (K)
*
*             cf29600       ww-fail thresh    1 gt     2    1.0    0.0
*             cf29601       .false.
*             cf29605       latch
```

```
*              cf29611       1.0    0.0    cfvalu.[5]
*              cf29612       1.0    0.0    cfvalu.297
*
* calculate ww leak failure pressure
*              cf29700     'fail-pres'  tab-fun    1    1.0    0.0
*              cf29701      1.3445e6
*              cf29702      3        4.8263e5     1.3445e6
*              cf29703      299
*              cf29711      1.0     0.0     cfvalu.298
*
* containment failure pressure  vs.  average ww wall temperature
* base on data from expert opinions
*              tf29900    'p.vs.t fail'     4     1.0     0.0
*              tf29911       0.0       1.3445e6      *
*              tf29912     533.33      1.3445e6      *   588 f    195 psig
*              tf29913     700.00      1.0342e6      *   806 f    150 psig
*              tf29914     922.22      4.8263e5      *  1208 f     70 psig
*
* average wetwell wall concrete temperature
*
*              cf29800      'tave-ww-wall'     add      9    0.824544    0.0
*              cf29812       0.06326          0.0      hs-temp.4010304
*              cf29813       0.00653          0.0      hs-temp.4010305
*              cf29814       0.03308          0.0      hs-temp.4010306
*              cf29815       0.02852          0.0      hs-temp.4010307
*              cf29816       0.05849          0.0      hs-temp.4010308
*              cf29817       0.10673          0.0      hs-temp.4010309
*              cf29818       0.21020          0.0      hs-temp.4010310
*              cf29819       0.45538          0.0      hs-temp.4010311
*              cf29820       0.11780          0.0      hs-temp.4010312
*
*
*
*heat slab input for  cv  401
*
*   hs4010ixnn    wet   wall    floor
*
hs40101000  12  1  1  0
hs40101001  'wet-well-floor'
hs40101002  195.0616    0.0  *  bottom elevation=648' (=648'-0')
hs40101003  1.0 * multiplicity
hs40101100  40001  1  0.5 * slab geometry
hs40101200  c0001
hs40101300  0
hs40101400   0
hs40101600   1  401 'ext' 0.0 0.0 0.0
hs40101700   500.47  0.0773   1   1
hs40101800  -1
hs40101801  294.26  11    *  room    temperature    =70f
hs40101802  285.90  12    *  ground    temperature=55f
*
*ht40104xxnn    air    portion of  dry well  floor support  columns
*
hs40104000  6  2  1  0
hs40104001  'support  cols-air'
hs40104002  104.5209  1.0  *air  portion begins  at  671'  elevation
hs40104003  12.0 * multiplicity
hs40104100  -1  1  0.50165     *id=39 5*
hs40104102  0.50419    2  *    steel
hs40104103  0.50927    3  *    steel
hs40104104  0.51689    4  *    steel
hs40104105  0.52451    5  *    steel
hs40104106  0.53740    6  *    steel
hs40104200    -1
hs40104201  'carbon steel'  5
hs40104300  0
```

```
hs40104600    1  401    ext'  1.0  1.0 * ht to atm
hs401   01  0.3    'equiv band'  5.    * steel surface
hs401    00      1.0  1.0668  8.9792
hs40104800 -1
hs40104801    294.26  6  * room  temperature =70f
*
*    hs40105xnn  water portions of support  columns
*
hs40105000  5  2  0  0
hs40105001  'support colm-water'
hs40105002  197.5104  1.0 *  water  begins at 648'
hs40105003   12.0 * multiplicity
hs40105100    40104  1  0.50165  * id=39.5
hs40105200   40104
hs40105300     0
hs40105400    0  -401
hs40105600     -1  401  'ext'  0.0  0.0
hs40105700     1.0  1.0668  7.0104
hs40105800   -1
hs40105801   294.26  6    *room  temperature = 70f
*
*hs40103xnn    wet-well-wall-air
*
hs40103000   12  2  1  0
hs40103001   'ww-wall-air'
hs40103002   204.5208  1.0  *  elevation at 671'
hs40103003   1.0 * multiplicity
hs40103100   -1  1 13.4112  *  id=88'
hs40103102   13.41374  2  *0.1"  steel
hs40103103   13.41755  3  *0.25"  steel
hs40103104   13.42390  4  *0.5"  concrete
hs40103105   13.43660  5  * 1.0" concrete
hs40103106   13.46200  6  *2"    concrete
hs40103107   13.51720  7  *4 " concrete
hs40103108   13.61460  8  *8"    concrete
hs40103109   13.81760  9  *16"    concrete
hs40103110   14.22400  10  *32"     concrete
hs40103111   15.03680  11  *64" concrete
hs40103112   15.24000  12  *72'x6' concrete
hs40103200      -1
hs40103201   'carbon steel'  2
hs40103202   'concrete'  11
hs40103300   0
hs40103400    1  401 'ext'  1.0 1.0
hs40103401   0.3    'equiv band'  5.    * steel surface
hs40103500   1.0  26.8224  8.9792
hs40103600   0     -401
hs40103800     -1
hs40103801   294.25  12  * o'r portion of well at 70f
*
*     hs40102xnn    wetwell -  -wall
*
hs40102000   12  2  0     0
hs40102001   'ww-well-water'
hs40102002   197.5104  1.0  * elevation=648'
hs40102003   1.0 * multiplicity
hs40102100   40103  1  13.4112  *id=88'
hs40102200   40103
hs40102300   0
hs40102400      -1  401  'ext'  0.0     0.0
hs40102500   1.0  26.8224  7.0104
hs40102600     0    -401
hs40102800   -1
hs40102801   294.25  12  *  pool temperature=70f
*
```

```
*
*
*
*****************************************************************
****************** reactor well above drywell head **********************
*****************************************************************
*
*
************ temporary data ********** verify volume/altitude table with PPL
*
cv600000     rf/rx-well  2  2  a
cv600a0       3
cv600a1      pvol  1 vi300a5
cv600a2      vpol  0.          rhum     0.5     tatm  316.  * initial temp=110f
cv600a3      mlfr.5  0.79     mlfr.9  0.21
cv600b1        241.1         0.0    *  assume bottom of well is at 791' for now
cv600b2        247.5       316.0    * assume top of well is at 812' for now
*
*          Assumed vol = pit vol - dw head vol
*          Assumed vol = Pi*(48'10")**2*(812'-791')/4
*
*                  - (1/2) * (4/3) * Pi (37.75/2)**3   (approximately)
*               = 39532 - 28168 ft**3 = 11164 ft**3 = 316 m**3
*
*
f160000       'rxwell-to-rf'     600    900    247.    249.4
*  assume 1/8" annular gap around outer perimeter of shield plug
*  A = Pi/4*(48'10-1/8"**2 - 48'10"**2) = 0.79972 ft**2 = 0.0742 m**2
f160001       0.0742     5.      1.0     0.001     0.001   * check length
f160002       0    0    0    0    * vertical flow
f160003       1.    1.    1.    1.
f1600a0       0.0742    5.    13.4     5.0e-5  * check length, hyd. dia. & loss fact
*
*
*hs60101xnn    reactor well cylindrical wall
*
hs60101000  12  2  1  0    * cylindrical
hs60101001  'wall-well-air'
hs60101002  241.1  1.0   *  elevation at 791'
hs60101003  1.0 * multiplicity
hs60101100  -1  1  7.4427
hs60101102  7.44855   2    *  steel/concrete
hs60101103  7.47395   3    * concrete
hs60101104  7.52475   4    * concrete
hs60101105  7.62635   5    * concrete
hs60101106  7.82955   6    * concrete
hs60101107  8.03275   7    * concrete
hs60101108  8.23595   8    * concrete
hs60101109  8.54075   9    * concrete
hs60101110  8.84555   10   * concrete
hs60101111  9.0       11   * concrete
hs60101112  9.2711    12   * concrete
hs60101200     -1
hs60101201  'carbon steel'    1
hs60101202  'concrete'   11
hs60101300  0 * no heat source
hs60101400 1 600 'int' 1  1 * hx to pool if it covers more than 10% of structure
hs60101401  0.3    'equiv band'   5.    * steel surface
hs60101500  1.   14.888   6.4
hs60101600  0     -600 * insulated rhs
hs60101800     1 * nodal temps
hs60101801  294.25   12   * air portion of well at 70f
*
*
*   hs60201xnn =  reactor well shield plugs
*
```

```
hs60201001  'shield plugs'
hs602   02  747.5  0.0  * elevation = 812'
hs60    03  1.0
hs60201100  -1  1  0.0
hs60201104  0.00254  2  *   0.1"  concrete
hs60201105  0.00508  3  *  0.2"  concrete
hs60201106  0.01016  4  *  0.4"  concrete
hs60201107  0.02032  5  *  0.8"  concrete
hs60201108  0.04064  6  *  1.6"  concrete
hs60201109  0.08128  7  *  3.2"  concrete
hs60201110  0.16256  8  *  6.4"  concrete
hs60201111  0.32512  9  * 12.8"  concrete
hs60201112  0.536575  10  *21.125"  concrete
hs60201113  0.748030  11  *29.450"  concrete
hs6020111A  0.910590  12  *35.850"  concrete
hs60201115  0.991870  13  *39.050"  concrete
hs60201116  1.032510  14  *40.650"  concrete
hs60201117  1.052830  15  *41.450"  concrete
hs60201200  -1
hs60201202  'concrete'      14
hs60201300  0
hs60201400  1  600  'ext'  1.0  1.0
hs60201401  0.6   'equiv band'   5    * concrete surface
hs60201500  174.  4.  .1
hs60201600  1  900  'ext'  1.0  1.0
hs60201601  0.6   'equiv band'  5    * concrete surface
hs60201700  174.  4.  .1
hs60201800  -1
hs60201801  294.26  15 * room temp =70f
*
*************************************************************************
************************      environment      ************************
*************************************************************************
*
*
*  outer environment
cv90000    environment  1  2  6
cv900a0      3
cv900a1     pcal  1.013508e5
cv900a2     vpol  0.          rhum    0.5    tatm  305.
cv900a3     mlfr.5  0.79    mlfr.9  0.21
cv900b1       190.        0.0
cv900b2       300.        1.0e8
*
*
*--   the following heat slab is here to facilitate the
*     RN package aerosol settling calculations
*
hs90001000  4  1  1  0
hs90001001  'env-conc-floor'
hs90001002  213.5124  0.0  *elevation=700'6"
hs90001003  1.0 * multiplicity
hs90001100  -1   1  0.
hs90001101  0.00635  2  *0.25" concrete
hs90001102  0.00889  3  *0.35" concrete
hs90001103  0.01143  4  *0.45"  concrete
hs90001200  -1
hs90001202  'concrete'  3
hs90001300  0
hs90001400  0
hs90001600  1  900  'ext'  1.0  1.0
hs90001700  481.08  10.0  1.0
hs90001800  -1
hs90001801  305.      4  *room temp = 80f
*
```

```
*
*
*
*
*****************************************************  ******  ******
*
*
*********************************************************************
*********************************************************************
* material properties data
*********************************************************************
*********************************************************************
* tabular function input for thermal conductivity, heat capacity, and
* density of heat structure materials
*
*********************************************************************
* carbon steel
*********************************************************************
mpmat10000 'carbon steel'
mpmat10001 thc 100
mpmat10002 cps 101
mpmat10003 rho 102
*
tf10000    'thc carbon steel'  10          1.0         0.0
tf10010                        273.15      55.0        373.15     52.0
tf10011                        473.15      48.0        573.15     45.0
tf10012                        673.15      42.0        873.15     35.0
tf10013                       1073.15      31.0       1273.15     29.0
tf10014                       1473.15      31.0       1973.15     31.0
*
tf10100    'cp carbon steel '  2          1.0         0.0
tf10110                        273.15     0.465e3    5000.0     0.465e3
*
tf10200    'rho carbon steel'  2          1.0         0.0
tf10210                        273.15     7833.0     5000.0     7833.0
*********************************************************************
* drywell head air space gap properties
*********************************************************************
mpmat20000    'air gap 1'
mpmat20001    thc  200
mpmat20002    cps  201
mpmat20003    rho  202
*
tf20000       'thc air gap 1'   2      1.0     0.0
tf20011          273.15      17.0        10000.0       17.0
*
tf20100       'cps air gap 1'   2      1.0     0.0
tf20111          273.15     1005.0        10000.0      1005.0
*
tf20200       'rho air gap 1'   2      1.0     0.0
tf20211          273.15      1.18         10000.0       1.18
*********************************************************************
* thermal properties for limestone / common sand concrete
*********************************************************************
mpmat30000    'concrete'
mpmat30001    thc  300
mpmat30002    cps  301
mpmat30003    rho  302
*
tf30000       'thc concrete'     2      1.0      0.0
tf30011          273.15      1.3         10000.0       1.3
*
tf30100       'cps concrete'     2      1.0      0.0
tf30111          273.15    1200.0        10000.0     1200.0
*
tf30200       'rho concrete'     2      1.0      0.0
```

```
trshzii          273.15     2540.0      10000.0       2540.0
*****************************************************************
*
*
*
*****************************************************************
*****************************************************************
*     decay heat input
*****************************************************************
*****************************************************************
*
* --- the dchdefcls0 card must be specified for cases in which
* --- the RN package is calculating aerosol behavior, even if
* --- no fission products are being tracked
*
dchreactor  bwr
dchshut     -1   0.
dchdecpow   origen
*
dchdefcls9    'all'
dchclsnorm yes
sc00001 3210  0.92  1    * derate power to 3293 mw.  .92 = 3293/3578
*
*****************************************************************
*****************************************************************
*     transfer process input
*****************************************************************
*****************************************************************
*
*   'in' transfer process for core package
*           nmsin    nthrm
tpin10100   6        9
tpin10101     read     900
*
*    'out' transfer process for cavity package
*           nmsot    npotoi   iotmtx
tpot10200   5        101      uin 103
*
*     cor-cav translation matrix
*     *** note *** control poison mass is not conserved
*           nrow     ncol
tpm1030000  5        6
*           nrow/ncol  value
tpm1030001  1/1          1.0      * uo2 mass
tpm1030002  2/2          1.0      * zro2 mass
tpm1030003  3/3          1.0      * steel mass    * ????????
tpm1030004  4/4          1.0      * zr mass
tpm1030005  5/5          1.0      * steel oxide mass
*     transfer processes for radionuclide transfer
tpin60100   15       1
tpot60200   15       601     def 1
*
*
*
*****************************************************************
*****************************************************************
**     dw cavity input
*****************************************************************
*****************************************************************
*
*
*    La Salle Cavity:  Depth = 9' 6 1/2" = 2.91 m
*                      I.D.  = 20' 3" = 6.17 m
*                      O.D.  = 29' 11" = 9.12 m
*                      Approximate cavity volume = 3051 ft**3 = 86.41 m**3
*                      Sidewall thickness = 4' 10" = 1.47 m
```

```
*                       floor thickness = 3' 9" = 1.14 m
*
*  -- WNP-2 Cavity:      Depth = 6' 10" = 2.08 m
*                       I.D.  = 20' 3" = 6.17 m
*                       O.D.  = 30' 4" = 9.25 m
*                       Approximate cavity volume = 2196 ft**3 = 62.19 m**3
*                       Sidewall thickness = 5' 0.5" = 1.54 m
*                       floor thickness = 5' = 1.52 m
*
*
cav0100     200     dw-cavity      *  drywell inpedestal cavity
cav01dh     117   118  119         * cf #'s for decay heat, oxide & metal splits
cav01tp     102                    *  transfer process number
*
cf11700   dw-cav-decay-ht   equals   1   1   0.
cf11710     1         0.    edf.200.1
*
cf11800   oxide-dh-fract    tab-fun   1   1   0.
cf11803   118
cf11810     1.        0.    time
tf11800   oxide-dh-fract    2   1.    0.
tf11810       0.            .98      *  put 98% of decay heat in oxide layer
tf11811     1.0e7           .98
*
cf11900   metal-dh-fract    tab-fun   1   1   0.
cf11903   119
cf11910     1.        0.    time
tf11900   metal-dh-fract      2   1.    0.
tf11910       0.            .02      *  put  2% of decay heat in metal layer
tf11918     1.0e7           .02
*
cav01g0   corcon  2                  *  flat bottom cylinder geometry
*
*         nrays    r0    z0
cav01g1     50      0.    0.
*         zt    rad    hit    radc    rw    hbb   nbot   ncorn
cav01g2   0.   3.086   7.91    0.1   4.56   1.14    23       3 * use in Sallie cavity
*
cav01ra    -1     * stop calculation when debris melts through floor
cav01rr    -1     * stop calculation when debris melts through side wall
*
*    15452.3 kg of stainless steel are added initially to the cavity
*    to account for the sump tank, gratings, liners, pipes and
*    supports melted by the corium
*
cav0110       temp         305.0
cav0111       fe         11434.7
cav0112       cr          2781.4
cav0113       ni          1236.2
*
* test test test --- add a bit of uo2 to the debris
* this is necessary to prevent vaness from bombing the first time it
* is called.  It is first called at the onset of concrete ablation
*
cav0120       temp         305.0
cav0121       uo2           11.0
*
*    limestone / common sand concrete (mix446) with 0.056 kg/kg rebar
*
cav01c0   mix446
cav01c1   sio2        0.36982          tio2       0.00013
cav01c2   mno         0.00005          mgo        0.09214
cav01c3   cao         0.27255          na2o       0.00059
cav01c4   k2o         0.00148          fe2o3      0.00210
cav01c5   al2o3       0.00902          cr2o3      0.00002
cav01c6   co2         0.20173          h2oevap    0.02549
```

```
                                                    fe          0 05e00
cav01cs   densct     2348.0     * concrete density
cav0      tsolct     1420.0     * concrete solidus temperature
cav0      tliqct     1670.0     * concrete liquidus temperature
cav01cd   tablct     1503.0     * concrete ablation temperature
cav01ce   tinct       310.0     * concrete initial temperature
cav01cf   emisct        0.82    * emissivity
sc01000  2303  2920.0   4   * solidus temp  of high melting group
sc01001  2303  2920.0   5   * liquidus temp  of high melting group
*
*
*
*****************************************************************
*****************************************************************
**      radionuclide input
*****************************************************************
*****************************************************************
**
rn1000 0
rn1001 5 1 15 14 11 0 0
rn1100 1.0e-6 50.e-6 1000.
*
rnacoef   1   * calculate aerosol coefficients
*      ----      settling areas
*           fr    to      elev      area
rnset001   100   401     198.6       1.1      * f1100
rnset002   205   204     237.44     55.0      * f1230
rnset003   204   202     251.0      93.0      * f1220
rnset004   203   202     227.3       4.1      * f1204 (horizontal projection)
rnset005   202   201     220.52    164.0      * f1210
rnset006   300   401     261.16     20.6      * f1301 (conservatively high)
*


   -- setup ww pool scrubbing for downcomer flow paths

 s1400     301

*; ***************************************************
*; *******  special output control functions ***********
*; ***************************************************
*
   e one-shot control functions for cf161,cf178,cf179,cf180,cf181
   771,cf774,and cf342 so that the editcf, restartcf, and the plotcf
  meicor features will produce one and only output as each of the
* above control functions switches from false to true, ie as each
* event occurs.
*
*
*****************************************************************
* write edit when user specified (meicor input) pressures are reached
* pressure 1
cf16000     pressure-1    equals     1     1.0    0.0
cf16001     1.0e8
cf16011     0.0     105489.78    time * pressure-1 = 15.3 psig (vent trigger)
*
cf16100     del-p-ww      add      2     1.0     0.0
cf16101     0.0
cf16111     1.0       0.0    cvh-p 401   *  dp = WW - Env
cf16112    -1.0       0.0    cvh-p 900
*                                        ,
cf16200     set-pflag-1     1-gt       2      1.0    0.0
cf16201      false
cf16211     1.0       0.0      cfvalu 161
cf16212     1.0       0.0      cfvalu 160
*
cf16300     vent-mes-1        1 equals      1      1.0    0.0
```

```
cf16501     .false.
cf16505     one-shot
cf16506     2          'wetwell exceeded 15.3 psig'
cf16511     1.0     0.0        cfvalu.162
*
* pressure 2
cf16400     pressure-2   equals     1     1.0   0.0
cf16401     1.0e8
cf16411     0.0     310264.1    time    * pressure-2 = 45 psig = Low MX If Dos  Pres
*
cf17400     set-pflag-2     1-gt      2      1.0   0.0
cf17401     .false.
cf17411     1.0       0.0       cfvalu.161
cf17412     1.0       0.0       cfvalu.164
*
cf17800     vent-mes-2        1-equals      1      1.0   0.0
cf17801     .false.
cf17805     one-shot
cf17806     2          'wetwell exceeded 45 psig'
cf17811     1.0     0.0        cfvalu.174
*
* pressure 3
cf16500     pressure-3   equals     1     1.0   0.0
cf16501     1.0e8
cf16511     0.0       758423.    time     * pressure-3 = 110 psig
*
cf17500     set-pflag-3     1-gt      2      1.0   0.0
cf17501     .false.
cf17511     1.0       0.0       cfvalu.161
cf17512     1.0       0.0       cfvalu.165
*
cf17900     vent-mes-3        1-equals      1      1.0   0.0
cf17901     .false.
cf17905     one-shot
cf17906     2          'wetwell exceeded 110 psig'
cf17911     1.0     0.0        cfvalu.175
*
* pressure 4
cf16600     pressure-4   equals     1     1.0   0.0
cf16601     1.0e8
cf16611     0.0     827371.      time     * pressure-4 = 120 psig
*
cf17600     set-pflag-4     1-gt      2      1.0   0.0
cf17601     .false.
cf17611     1.0       0.0       cfvalu.161
cf17612     1.0       0.0       cfvalu.166
*
cf18000     vent-mes-4        1-equals      1      1.0   0.0
cf18001     .false.
cf18005     one-shot
cf18006     2          'wetwell exceeded 120 psig'
cf18011     1.0     0.0        cfvalu.176
*
* pressure 5
cf16700     pressure-5   equals     1     1.0   0.0
cf16701     1.0e8
cf16711     0.0     965266.      time     * pressure-5 = 140 psig
*
cf17700     set-pflag-5     1-gt      2      1.0   0.0
cf17701     .false.
cf17711     1.0       0.0       cfvalu.161
cf17712     1.0       0.0       cfvalu.167
*
cf18100     vent-mes-5        1-equals      1      1.0   0.0
cf18101     .false.
cf181       one-shot
```

```
cf18100     2          'wetwell exceeded 140 psig'
cf18111     1.0    0.0       cfvalu.177
*
*
*
*
* -- flag debris presence in cavity
*
cf77100      'debris-in-cav'   1-equals     1     1.0      0.0
cf77101      .false.
cf77105      one-shot
cf77106      2          'mass of SIFEL pour in cavity 1 > 0.0 kg'
cf77111      1.0         0.0      cfvalu.081
*
*  cavity flag active when > 0.0 kg SIFEL has poured from bwtear
*
cf08100      cav-steel     1-gt    2     1.0   0.0
cf08101      .false.
cf08111      1.0    0.0    edf 900.3  *  steel mass on floor
cf08112      0.0    0.0    time
*
*
* --- trap time of first drywell head leakage
*
*
cf77400  dwl-edit  1-equals  1  1.  0.
cf77401   .false.
cf77405  one-shot
cf77406  2  'drywell head leakage begins (dwl)'
cf77411  1.  0.  cfvalu.450
*
*
* --- trap time of first wetwell leakage
*
*
cf34200  twl-edit  1-equals  1  1.  0.
cf34201  .false.
cf34205  one shot
cf34206  2  'the wetwell leaked (twl)'
cf34211  1.  0.  cfvalu.150
*
*
*******  write edits using input editcf in meicor input
cf99100  edits  1-or  0  1.  0.
cf99101  .false.
cf99125  1.  0.  cfvalu.771 *melt in drywell cavity
cf99126  1.  0.  cfvalu.163 *wetwell exceeded pressure 1
cf99127  1.  0.  cfvalu.178 *wetwell exceeded pressure 2
cf99128  1.  0.  cfvalu.179 *wetwell exceeded pressure 3
cf99129  1.  0.  cfvalu.180 *wetwell exceeded pressure 4
cf99130  1.  0.  cfvalu.181 *wetwell exceeded pressure 5
cf99131  1.  0.  cfvalu.774 *drywell head leaked  (dwl)
cf99135  1.  0.  cfvalu.342 *wetwell leaked       (twl)
*****************************************************
******* write restarts using restartcf in meicor input
cf99200  restarts  1-or  0   1.  0.
cf99201  .false.
cf99214  1.  0.    cfvalu.771 *melt in drywell cavity
cf99215  1.  0.    cfvalu.163 *wetwell exceeded pressure 1
cf99216  1.  0.    cfvalu.178 *wetwell exceeded pressure 2
cf99217  1.  0.    cfvalu.179 *wetwell exceeded pressure 3
cf99218  1.  0.    cfvalu.180 *wetwell exceeded pressure 4
cf99219  1.  0.    cfvalu.181 *wetwell exceeded pressure 5
cf99231  1.  0.    cfvalu.774 *drywell head leaked  (dwl)
cf99232  1.  0.    cfvalu.342 *wetwell leaked (twl)
*****************************************************
```

```
*******  write plot dump using plotcf in melcor input
cf99300  plots  1 or  0  1.  0.
cf99301   false
cf99331  1.   0.   cfvalu 771 *melt in drywell cavity
cf99332  1.   0.   cfvalu 163 *wetwell exceeded pressure 1
cf99333  1.   0.   cfvalu 178 *wetwell exceeded pressure 2
cf99334  1.   0.   cfvalu 179 *wetwell exceeded pressure 3
cf99335  1.   0.   cfvalu 180 *wetwell exceeded pressure 4
cf99336  1.   0.   cfvalu 181 *wetwell exceeded pressure 5
cf99337  1.   0.   cfvalu 774 *drywell head leaked  (dwl)
cf99338  1.   0.   cfvalu 342 *wetwell leaked       (twl)
  * that is all
```

APPENDIX F:

CODE INPUT DECKS

MARK III CONTAINMENT CALCULATIONS

F.1 BWR-LTAS Code Input

This Section provides a set of representative code input for the Boiling Water Reactor Long Term Accident Simulation (BWR-LTAS) code. This input was used to generated the first five minutes of the short-term station blackout accident sequence for the Mark III containment calculations. The BWRSAR severe accident response calculation (Section F.2) was initiated at accident time 5.0 minutes from the results of this BWR-LTAS calculation.

INPUT DATA AFTER MODIFICATIONS

acop	=	191.993
acor	=	144.939
acpf	=	1.
admet	=	16570.
adsovr	=	1.
advent	=	0.
awvent	=	1.75
aleak0	=	0.
apmet	=	7847.7
art	=	42.332
asspw	=	5277.
atwsf	=	0.
a0cp	=	975.8
a1cp	=	3.025e-03
a2cp	=	-1.72304e-06
bdwc0	=	2800.
bdwsp0	=	1250.
bc1u0	=	27000.
bhot10	=	0.
bhot04	=	430.
blpmin	=	8500.
bm	=	20.
brdpc	=	2.5
brhrp	=	22.2
brhrpd	=	22.2
bspdw0	=	2000.
bsump	=	50.
cdmet	=	19346.9
cpmet	=	9075.6
cpref	=	3293.
cpst	=	0.1259
cp0	=	3293.
cvvent	=	0.833
daleak	=	0.
delt	=	0.5
dkdtcr	=	-1.e-05
dm	=	80000.
dmin	=	0.2
dphp	=	190.
dplp	=	75.
dtrvhl	=	423.
dzs	=	21.2
dzv	=	35.
erhrr	=	0.375
ewsdc	=	234.
fcstsp	=	0.7
fflash	=	5.e-04
ffrec	=	2.e-02
fintim	=	310.
fldwg	=	3.12e-08

```
flspg    =    1.e-08
ftstab   =    2000.
hboaf    =    18.025
hci0     =    539.
hcst     =    58.
hpcimx   =    694.167
hpcipc   =    0.
href     =    522.
hscsf    =    16.2
hsrhrf   =    15.6
hudwci   =    20.
humdw0   =    50.
humsp0   =    99.
h0       =    3816.
h1       =    1.952
h2       =    -2.517e-02
jetpmp   =    0.
kcrdch   =    4.47e-02
kcrdtv   =    5.07e-02
kptb     =    1.e-02
ksu      =    5.157e-04
lbase    =    0.
lbot     =    26.392
lcore    =    12.5
lcstss   =    0.
lcstuv   =    8.266e-05
ldcr     =    27.58
ldcset   =    560.
ldc0     =    28.32
lheder   =    23.4
lhpin    =    476.
lhpmin   =    490.
lhpmt    =    540.
lhpt     =    582.
llpi     =    413.5
llpit    =    575.
lop      =    5.167
lrcin    =    476.5
lrcmin   =    550.
lrcmt    =    582.
lrct     =    582.
lrt      =    11.033
lrvads   =    397.
lspss    =    7.
ltcrd    =    581.
ltrdwc   =    99.
ltrjp    =    490.
mint     =    477000.
mrvst    =    1500000.
ncs      =    4.
nlpci    =    4.
nsorv    =    0.
ntrhr    =    4.
ntrhrd   =    4.
```

```
obrvd     =    120.
ocbpc     =    60.
odcs      =    1000000.
odlpci    =    1000000.
oervd     =    720.
ohpman    =    1000000.
ohpt      =    0.
ohptr     =    1000000.
oocbp     =    1000000.
ooptb     =    1000000.
ootv      =    1000000.
opchrc    =    60.
opchsv    =    30.
orcman    =    1000000.
orct      =    0.
orctr     =    1000000.
ordwc     =    1000000.
osbor     =    300.
oscri     =    300.
oscs      =    1000000.
osdlev    =    1000000.
osdpc     =    1000000.
oslpci    =    1000000.
osscrd    =    1000000.
ossdc     =    1000000.
ossubp    =    1000000.
osvman    =    120.
otcbp     =    0.
otcrdp    =    1000000.
otdwc     =    1000000.
pc        =    1015.7  1017.7  1025.7  1027.7  1029.7  1031.7
               1035.7  1036.7  1037.7  1038.7  1045.7  1046.7
               1047.7
pcdwv     =    15.
pcor      =    6693.37
pdcvp     =    5.05
pdhosv    =    1.e-02
pdlpi     =    16.95
pdocsv    =    2.e-02
pdwads    =    16.42
pehpis    =    165.
perct     =    40.
pfmosv    =    110.
pfodp     =    765.
phcovr    =    1.
phpin     =    16.95
phpis     =    115.
pidwv     =    1000000.
pldwca    =    1.389e-03
pmxdpc    =    1.35
pmndpc    =    1.1
po        =    1090.7  1092.7  1100.7  1102.7  1104.7  1106.7
               1110.7  1111.7  1112.7  1113.7  1120.7  1121.7
               1122.7
```

```
prated          =    1196.
prcis           =    65.
prelr           =    0.32
prr             =    1020.
ptdwg0          =    14.95
ptrdwc          =    16.95
ptspg0          =    14.95
pvlpi           =    480.
pvlpiv          =    480.
pvtdwc          =    465.
p0              =    1034.7
qdwcr           =    1389.
qoph10          =    298.3
qrvh10          =    1583.3
rcicmx          =    83.3
sboflg          =    2.
sdvflg          =    0.
tadwci          =    145.
taulen          =    2.5
tauoh1          =    600.
tbase           =    85.
tbgrhr          =    1800.
tdgrhr          =    1000000.
trerhr          =    2000000.
tblein          =    0.
$

tcfail          =    2.5
tdiesl          =    1000000.
tdmet0          =    126.
tfdwc           =    200.
tfdwca          =    1000000.
tgdw0           =    126.
tgsp0           =    85.
thpis           =    194.
tpair           =    90.
tpmet0          =    85.
trcf            =    190.
trcis           =    194.
tslc            =    1000000.
tslein          =    1000000.
tsorv           =    1000000.
tsquen          =    10.
tstrat          =    0.
tsw             =    90.
tswd            =    90.
twdwci          =    100.
t0              =    36.
uairv           =    33.
vann            =    1177.51
vcst0           =    362000.
vcstmx          =    375000.
vcstsp          =    132000.
vhotmu          =    97000.
```

```
vhotw0      =     113000.
vdiff       =     189.076
vfree       =     14580.074
vgdw        =     239600.
vjet        =     95.195
vojp        =     1535.473
volp        =     2428.636
vrec        =     1150.
vsl         =     2100.907
vssop       =     3864.149
vtsp        =     276831.4
vuv1        =     1061.371
vuv2        =     2042.338
wbslc       =     0.1826
wdleak      =     0.24
wquess      =     0.
wrated      =     239.6
wref        =     9111.
wrhrr       =     1389.
wrhrsd      =     625.
wrhrsw      =     625.
wswr        =     625.
wtehp0      =     45.12
wterc0      =     5.41
wwdwc       =     143.4
x11         =     0.
x12         =     8.483
x13         =     18.850
x14         =     32.6
x15         =     35.85
x16         =     37.85
x17         =     44.058
xref        =     0.133
$

abio        =     4207.6
adflr       =     4715.8
admm        =     60080.
aped        =     1998.6
awmm        =     28969.6
cbiol       =     20119.
cdmm        =     288277.
cpcor       =     0.
cwmm        =     109739.1
dxbio       =     1.75
dxgbic      =     0.
dxgdw       =     1.e-04
dxgww       =     1.e-04
dxs         =     1.e-02
kcon        =     1.917e-04
mk          =     2.
rhocon      =     140.8
$
```

```
aspl      =    11925.5
cpspl     =    13791.4
aspmm     =    4062.4
cpspmm    =    6186.4
$

asbic     =    1.e-02
lsbic     =    312.
tisbic    =    1000000.
wdwsmp    =    0.
$

idecay    =    44
dtim      =    0.  1.  1.5  2.  3.  4.  6.  8.  10.  15.  20.  30.  40.
               60.  80.  100.  150.  200.  300.  400.  600. 800.  1000.
               1500.  2000.  3000.  4000.  6000.  8000.  10000.  15000.
               20000.  30000.  40000.  60000.  80000.  100000.  150000.
               200000.  300000.  400000.  600000.  800000.  1000000.
decay     =    6.000e-02   5.715e-02   5.552e-02   5.437e-02   5.204e-02
               5.040e-02   4.807e-02   4.619e-02   4.473e-02   4.205e-02
               4.015e-02   3.756e-02   3.572e-02   3.313e-02   3.137e-02
               3.000e-02   2.777e-02   2.619e-02   2.428e-02   2.293e-02
               2.102e-02   1.965e-02   1.859e-02   1.662e-02   1.522e-02
               1.354e-02   1.235e-02   1.067e-02   9.815e-03   9.152e-03
               8.193e-03   7.512e-03   6.764e-03   6.232e-03   5.484e-03
               5.039e-03   4.693e-03   4.141e-03   3.749e-03   3.275e-03
               2.940e-03   2.466e-03   2.187e-03   1.971e-03
```

F.2 BWRSAR Code Input

This Section provides a set of representative code input for the Mark III calculations performed with the Boiling Water Reactor Severe Accident Response (BWRSAR) code. This input was used to calculate the events of the short-term station blackout accident sequence (with ADS actuation) from accident time 5.0 minutes to time 900 minutes. The MELCOR containment response calculation (Section F.3) was driven by the results of this BWRSAR calculations.

```
grand gulf slsb with aps actuation, two   eutectics, 10/10/89
steel     concrete
dufloor   uufloor   shldwall  pedestal  uuwall    dwetop    dwebot    miscconc

 &change
       check=0.    cpstp=300.0.    trst=900.01.
 &end
 &nlmar
  atime= 5.00.    fptmon=2000.0.    tap=5.256e5.
       ibrk= 0.          icbrk= 0.     iaccxx=  0.
     ifpsm= 2.          ipdti= 1.       ispra= 0.
 &end
 &nlslab
  don(1)=489.0,140.0,3*0.0,
  dto=(1)=0.0,0.0,0.0,0.0,0.0,0.1,0.1,0.1,0.1,0.1,0.1,0,7*0.0,
  fc1xxx=0.450,  fc2xxx=0.105,  fc4xxx=0.049,
  fract1=0.0, fract2=0.96,
  hcf(1)=0.1124,0.3107,3*0.0,
  hif(1)=0.,100.,0.,0.,0.,0.,100.,0.,7*0.0,
  iblat1=1, iblat2=4, igas=2,
  ivl(1)=1,2,1,1,2,1,1,2,7*0,
  ivr(1)=1,2,1,1,2,2,2,2,7*0,
  mat1(1)=2,1,2,2,1,2,1,2,7*0,
  mat2(1)=2,2,2,2,1,2,2,2,7*0,
  nmat=2,
  nno1(1)=18,5,9,11,9,19,5,17,7*0,
  nno2(1)=0,10,0,0,0,0,17,0,7*0,
  nod(1)=63,1,54,43,54,104,
  nodes=5,   nslab=8,
  sarea(1)=3402.,5900.,9603.,3150.,80488.,25923.,6333.,16878.,
  tc(1)=0.0,1.05,3*0.0,
  tch=1472.,  tclo=1022.,
 temp(1)=18*135.0,
 temp(19)=15*90.0,
 temp(34)=9*135.00,
 temp(43)=11*135.0,
 temp(54)=9*90.0,
 temp(63)=135.,134.9,134.8,134.6,134.3,133.5,132.1,129.2,123.5,112.5,
 temp(75)=101.5,95.7,92.9,91.4,90.7,90.4,90.2,90.1,90.0,
 temp(82)=5*135.0,134.8,133.7,131.6,127.2,122.4,
 temp(92)=113.4,104.4,99.9,95.4,93.1,
 temp(97)=92.0,91.2,90.9,90.5,90.3,90.1,90.0,
 temp(104)=17*135.0,
  twhi=968.0, twlo=190.0,
 x(1)=0.,.01,.02,.04,.08,.16,.32,.64,1.,2.,4.,6.,8.,12.,16.,20.,24.,26.,
 x(19)=.0,.01,.02,.04,.08,.16,.32,.64,1.28,2.56,
 x(29)=5.12,8.0,11.,14.,16.,
 x(34)=.0,.01,.02,.04,.08,.16,.32,.64,1.0,
 x(43)=.0,.01,.02,.04,.08,.16,.32,.64,1.28,2.0,3.0,
 x(54)=.0,.01,.02,.04,.06,.08,.10,.12,.14,
 x(63)=.0,.01,.02,.04,.08,.16,.32,.64,1.28,2.5,
 x(75)=3.72,4.36,4.68,4.84,4.92,4.96,4.98,4.99,5.0,
 x(82)=.0,.01,.02,.04,.08,.12,.24,.48,.96,1.5,
 x(92)=2.50,3.5,4.0,4.5,4.75,4.88,4.96,5.0,5.04,5.07,5.09,5.1,
 x(104)=.0,.01,.02,.04,.08,.16,.32,.64,1.0,1.36,1.68,1.84,1.92,
 x(117)=1.96,1.98,1.99,2.0,
  vary=10982.4,
 &end
 &nlacc
  csprc=0.0,
  dtsubx=-100.0,
  eccrc=.01,
  rwstm=1870438.,
  trwstx=85.0,
  wtcavx=1.0,
  npump=7,
```

```
 ienject(1)=    2.      3.      3.      1.      1.      1.      2.
  npspc(1)=    2.      2.      3.      3.      3.      3.      3
  n    ):(1)=    3.      3.      3.      3.      1.      1.      -
       p(1)=  789.0,  789.0,  1250.0,  403.0,  1250.0,  1250.0, 13  ,
     plo(1)=   0.1,    0.1,    0.0,    0.1,    115.0,    65.0,   0.0,
     etp(1)=  1.0e8,  1.1e8,  1.2e8,  1.3e8,  1.4e8,  1.5e8,  1.6e6,
      te(1)=  1.0e8,  1.1e8,  1.2e8,  1.3e6,  1.4e8,  1.5e8,  1.6e6,
     wec(1)=    0.0,    0.0,    0.0,    0.0,  5000.0,   600.0,   0.0,
  pgpm(1,1)= 41148.,  40000.,  38200.,  36000.,  32000.,  28000.,  24000.,
  phead(1,1)=    0.,     20.,   46.9,   81.1,  133.7,  182.1,  222.1,
  pgpm(0,1)= 18000.,  10000.,     0.,
  phead(0,1)= 263.5,  309.8,  331.5,
  pgpm(1,2)= 15240.,  14000.,  12500.,  12000.,  10000.,   8000.,   6000.,
  phead(1,2)=    0.,   57.8,   120.,   137.3,  200.9,  254.1,  292.6,
  pgpm(0,2)=  4000.,  2000.,     0.0,
  phead(0,2)= 319.5,  336.3,  343.6,
  pgpm(1,3)=  180.0,  168.4,  156.2,  143.0,  128.5,  112.0,   92.6,
  phead(1,3)=   0.0,  215.0,  415.0,  615.0,  815.0, 1015.0, 1215.0,
  pgpm(0,3)=   67.6,   21.7,    0.0,
  phead(0,3)= 1415.,  1615.,  1635.,
  pgpm(1,4)= 30347.,  29399.,  28023.,  26730.,  21385.,  16033.,  10689.,
  phead(1,4)=   0.0,    27.,    60.,    91.,    202.,    288.,    351.,
  pgpm(0,4)=  5345.,  2672.,    0.0,
  phead(0,4)=  389.,   396.,   403.,
  pgpm(1,7)=  580.0,  450.0,  350.0,  300.0,  250.0,  200.0,  150.0,
  phead(1,7)=   0.0,   30.5,   50.0,   58.5,   65.1,   71.0,   76.0,
  pgpm(0,7)=  100.0,   50.0,    0.0,
  phead(0,7)=  79.0,   80.5,   81.0,
  wshpci= 3368.0,   wsrcic=  444.0,   zjl=470.0,   zjh=583.0,
 &end
lpci    cs      crd     cbp     hpci    rcic    fire
 &nlocx
      eqr=0.0,      etplr=0.0,      etslr=0.0,      ewpr=0.0,      ewsr=0.0,
 &end
 &nlcsx
      eqr=0.0,      etplr=0.0,      etslr=0.0,      ewpr=0.0,      ewsr=0.0,
 &end
 &nlcool
  cqr=7.28e6,    ctpr=135.0,    ctsr=50.0,    cvap=0.693,
 cwpr=112000.0,   cwsr=6190.3,       jcool=0,   tcool=1.0e8,
 &end
 &nlleak
  nlc=1,    llkp=1,    llkt=0,    kleak=1,
  dpleak(1)=126.,128.0,130.0,133.0,136.0,140.0,145.0,152.5,160.0,200.0,
   aleak(1)=000.,0.007,0.015,0.026,0.037,0.054,0.070,0.097,0.124,0.271,
  a1=0.0,    a2=0.0,    t1=0.0,    t2=0.0,    test=0.0,
  clk=0.583,    nhyst=1,    indx=10,    fctr(1)=10*0.0,
 &end
 &nlmace
  area(1)=4000.,12000.,
  c1(1)=500.0,174.0,8*0.0,
  c2(1)=0.593,0.593,8*0.0,
  c3(1)=0.196,1.10,8*0.0,
  c4(1)=0.0,0.0,8*0.0,
  dcf=1000.0,  dto=0.05,  dtpnt=14.99,  tpntm=20.01,  dtpnt2=19.99,
   hmaxx=200.0,
   hum(1)=0.50,0.90,
  kt(1,1)=0,kt(2,1)=2,
  kt(1,2)=2,kt(2,2)=0,
  n=2,    nc(1)=2,2,8*0,
  ns(1)=2,2,8*0,    nt(1)=2,2,8*0,
  po(1)=14.8,14.7,
  press(1,1)=0.0,press(2,1)=5.0,
  press(1,2)=5.293,press(2,2)=0.0,
  sumpa=256.0,  tdwsmp=110.0,  tempo(1)=155.0,90.0,
  tpool=102.0, vc(1)=270100.0,1400000.0,0.0,
```

```
 vcav=24.86, vflr=2145.8, wdwsep=327.45, wflash=2000.0, wpool=8513000.,
  wcdo(1)=0.0,0.0,
  wcwo(1)=0.0,0.0,
  whyo(1)=0.0,0.0,
  wntr(1)= .790,-.790,
  woxy(1)=-.210,-.210,
 &end
 &nlbail
  abr(1)=-1.0,-1.0,-1.0,-1.0,-1.0, 1.0, 1.0,-1.0,-1.0,-1.0,
         -1.0,-1.0,-1.0,-1.0,-1.0,0.1091,
  abrk=3.71e-5,
  wh(1)=651.0,8230.2,673.5,4*0.0,
  whu(1)=1620.0,426.0,1270.0,1270.0,1270.0,1270.0,19010.0,13*0.0,
  arstr(1)=0.0,-7.87,-12.22,4*0.0,
  arstru(1)=148.04,1**0.04,42.33,42.33,42.33,42.33,128.4,13*0.0,
  clad=0.0025,  cladwr=0.00254,
  cmt(1)=2337.0,15310.2,21653.6,4*0.0,
  cmu(1)=29280.0,37973.0,26486.0,26486.0,26486.0,26486.0,78080.0,13*0.0,
  conh=4.7,     d=0.0353,    dc=300.0,    dcrdod=0.8950,
  dd(1)=0.125,0.0200,0.635,4*0.0,
  ddu(1)=0.160,1.00,0.3354,0.5054,0.5054,0.5054,0.5054,0.071,13*0.0,
  df=0.0297,       dh=0.0423,    dpart=.01177,     drgap=3.125e-4,
    tpn(1)=0.00,10.1,280.1,1.0e6,2.0e6,3.0e6,4.0e6,5.0e6,
   dtpn(1)=5.00,10.0,20.00,100.0,101.0,102.0,103.0,104.0,
  dtsld=20.91667,     dshdld=17.65667,    fcfail=0.75,
  duo2=0.0297,   dwrad=0.0354,     fco1=0.250,    fdfuel=0.92,
  fld=0.0, fpv(1)=0.00,0.50,0.10,0.05,0.03,0.02,0.50,13*0.0,
  fwsscr=0.18,    fwssfe=0.74,    fwsshi=0.08,    fwuzr(1)=0.20,19*0.0,
  fz(1)=0.62566,1.18552,1.2094,1.21355,1.2229,1.22817,1.19982,1.12935,
  fz(9)=1.02916,0.911,0.736,0.30952,13*0.0,
  fl7=0.01,    hz=12.500,    hwf=0.814,
  hfss=114.7,    hfuo2=110.0,    hfzirc=108.0,    htmtoc=600.0,
         iaxxx=1,        ibodc=2,        ibeds=3,
         ifp=2,          ihc=0,          imws=3,
         ipower=1,   ir1=1,ir2=2,ir3=3,   istm=1,
         istr=3,         istru=7,         mworn1=1,
         ndzf=12,        nnt=64800,       nr=65200,     ndzn=1,
  pf(1)=1.2846,1.2846,1.18024,1.18024,1.03725,1.03725,0.83162,0.83162,
  pf(9)=0.35245,0.35245,
  pitch=0.0477,   porb=0.4,   pvol=944.4,   q235u=193.0, qzero=1.30787e10,
  rhocld=408.9,    rhofu1=646.7,   r1=1,  r2=10,   r239u=0.0,    sfactr=2.0,
    tb(1)=1.0e8,15*1.0e8,
     tcrmh=1.e4, tfail1=2100.0, tfail2=2100.0, tfus=4600.0,
  tfpcld=1800.0,    thkrx=0.5150,    thkshd=0.166667,
  thku(1)=0.047,0.166667,0.025,0.025,0.025,0.025,0.01,13*0.0,
    tmelt=4900.0,   tmzof=4175.0,   tmybk=1.0e6,   tpm=1.0,
   tsb(1)=.100, .025,0.100, .020, .050,0.020,0.100, .200,
  tsct(1)=0.00,75.0,100.0,124.,180.,220.0,265.0,280.,
  ttu(1)=542.7,542.7,542.7,542.7,542.7,542.7,542.7,542.7,13*0.0,
  vf(1)=0.18500,0.18500,0.08500,0.08500,0.0500,0.0500,0.0975,0.0975,
  vf(9)=0.08250,0.08250,
  xgc=6.733e-6,
 ybr(1)= 1.0,-1.0,-1.0,-1.0,-1.0, 1.0,-1.0, 1.0,
        -1.0,-1.0,-1.0,-1.0,-1.0,-1.0,-1.0,20.00,
   ybrk=-100.0,   ybrk2=1000.0,
 &end
t guide shr heads/spip 1s/spip 2s/spip 3s/spip 4dryers
 &nbwrin
 farin=90.55, farout=69.061, pbox=1.7543,xbox=0.006667,xboxri=0.333e-6,
 xboxzo=0.333e-6, f12bx=0.010,    f22bx=0.010,    f22rd=0.010,   frdbx=0.25,
  fhxcb=0.25, dhbxcb=0.016583, tmelbx=3365.0, tfbox=4175.0,
    ihrbox=1,     nboxs=800,     ionbox=1,    thkcb=0.0217, tmxof=3126.0,
  iocb(1,1)=1,1,1,1,1,1,1,1,1,1,1,1,1,
  iocb(1,2)=0,0,0,0,0,0,0,0,0,0,0,0,0,
  iocb(1,3)=1,1,1,1,1,1,1,1,1,1,1,1,1,
  iocb(1,4)=0,0,0,0,0,0,0,0,0,0,0,0,0,
```

```
 tocbt(1,5)=1.1,1,1,1,1,1,1,1,1,1,1,1,
 tocb(1,6)=0.0,0,0,0,0,0,0,0,0,0,0,0,
 to    1,7)=1,1,1,1,1,1,1,1,1,1,1,1,
 to    1,8)=0,0,0,0,0,0,0,0,0,0,0,0,
 xicb=.40625, thksso=0.00467, xcbdo=3.33e 6,  ncblad=193,   f12cb=0.010,
 f22cb=0.010,  tmelcb=2450.0,  tfcbo=3126.0,   imwsk=1,
 xicpst=0.065083,  thkssl=0.002083,  diab4c=0.0115,  thkgap=0.0005,
 rhob4c=110.0,  rhoss=496.0,  nabrod=76,  imwb4c=2,    fb4cmx=0.03,
&end
&nbwriv
   hbaf=216.3125,  hbsb=121.5,  hdead=205.3125
 hinitl=523.7, hilel=646.5,
  hsjjp=205.3125,  htaf=366.3125,  htjp=317.1875,
   htop=876.0,   hts=607.5,    ns=68,
 vcore(27)=5059.794,5125.852,5333.171,5499.033,5672.669,5702.475,
 vcore(33)=5730.216,5942.848,6297.522,6420.069,6578.238,6761.331,
 vcore(39)=6836.506,6879.832,6906.501,6934.814,7073.277,7094.618,
 vcore(45)=7118.959,7156.706,7186.338,7243.134,7457.265,7486.520,
 vcore(51)=7528.514,
 vshrd(27)=1411.916,1441.521,1560.923,1664.499,1774.587,1787.697,
 vshrd(33)=1799.122,1905.354,2021.045,2059.128,2107.254,2206.967,
 vshrd(39)=2290.443,2366.673,2436.593,2576.067,3502.217,3664.096,
 vshrd(45)=3831.064,4078.139,4281.405,4654.862,6048.046,6208.381,
 vshrd(51)=6440.216,
 vtot(27)=6471.710,6567.373,6894.094,7163.532,7447.256,7490.167,
 vtot(33)=7529.338,7848.202,8318.567,8479.197,8685.492,8968.298,
 vtot(39)=9126.949,9246.705,9343.094,9510.881,10572.49,10758.71,
 vtot(45)=10958.02,11234.85,11467.74,11898.00,13506.11,13694.91,
 vtot(51)=13968.73,14142.33,
&end
&nbwrrv
   dpvdyc=20.0,   dpvdyo=50.0,
   lads(1)=1,1,1,1,0,0,0,0,0,0,0,0,0,0,0,1,1,1,1,0,
     nvalve=20,       ntpsrv=1,      pdwca=100.0,
 psrvo(1)=1153.4,1156.7,1160.0,1163.3,1166.7,1170.0,1173.3,1176.6,
 psrvo(9)=1160.2,1172.9,1177.6,1182.4,1187.1,1191.8,
 psrvo(15)=1178.1,1182.9,1187.6,1192.4,1197.1,10.0,
 psrvc(1)=1053.4,1056.7,1060.0,1063.3,1066.7,1070.0,1073.3,1076.6,
 psrvc(9)=1068.2,1072.9,1077.6,1082.4,1087.1,1091.8,
 psrvc(15)=1078.1,1082.9,1087.6,1092.4,1097.1,1.0,
 ratflo(1)=8*895000.,
 ratflo(9)=6*906000.,
 ratflo(15)=5*913000.,
 ratflo(20)=8000.0,
 ratprs(1)=8*1180.0,
 ratprs(9)=6*1195.0,
 ratprs(15)=5*1205.0,
 ratprs(20)=1050.0,
 ratrho(1)=8*2.7084,
 ratrho(9)=6*2.7477,
 ratrho(15)=5*2.7730,
 ratrho(20)=2.35,
  tmsvlk=60.0,
 manval=0,  pmnset=1005.0,  pmnban=70.0,  topchk=0.10,  tmanon=1.0e6,
 tmanof=1.0e7,  tmdaon=75.0,  nsorv=0,  tsorvo=1.0e6,
&end
&nbwrgb
  h23=207.4,   h35=380.6,   djp=11.26,   ajp=20,
 tmasso(1)=537.9,
 tmasso(2)=537.9,
 tmasso(3)=537.8,
 tmasso(4)=537.8,
 tmasso(5)=537.8,
 tmasso(6)=537.8,
&end
&nlhead
```

```
 dbk=0.10,  fhead=0.060,  fopen=0.932,  dthead=10.0,  hlmax=2.50,
 condox=2.02,  condes=11.3,  hold2=3.64,  hrvdw=0.625,  hskirt=6.02,
 nmeltx=0,  afcrdb=2.0,  thkcrs=0.500,
 thkhd1=0.700,  thkhd2=0.585,  nps=26,
 hpipes=100.0,  thk6=2750.0,  thk60=2850.0,  tablat=2660.0,
 zmtmel(1)= 2750.,2750.,2750.,2750.,
 zmtmel(10)=4800.,4800.,4800.,4800.,4800.,4800.,4800.,4800.,4800.,
 teutec=2
 frckey(1)=0.579,0.630,8*0.0,
 teukey(1)=2.18,8*0,
 tmlteu(1)=2750.,4800.,8*0.,
 teu(1,1)=1.1,1.1,0.0,0.0,0.0,0.0,0.0,0.0,0.0,0.0,0.0,0.0,
 teu(1,2)=0.0,0.0,0.0,0.0,0.0,0.0,0.0,0.0,1.0,0.0,0.0,0.0,0.0,0.0,1.0,0.0,
 teutyp(1)=2,2,8*0,
 xrnkey(1,1)=0.210,0.579,0.151,0.860,
 xrnkey(11,2)=0.170,
 xrnkey(18,2)=0.830,
&end
```

1

IMAGE EVALUATION TEST TARGET (MT-3)

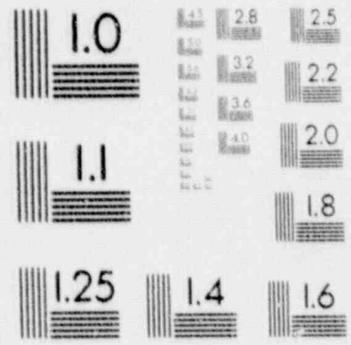

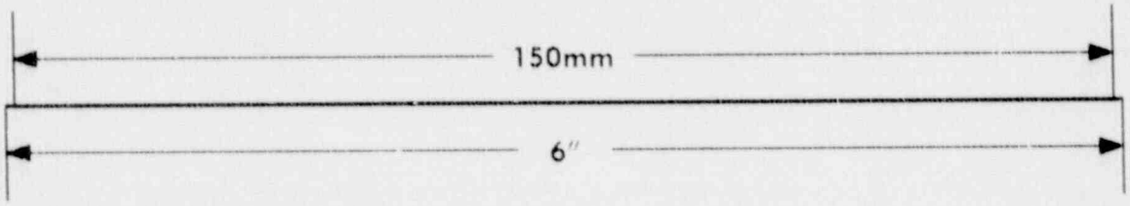

1

IMAGE EVALUATION TEST TARGET (MT-3)

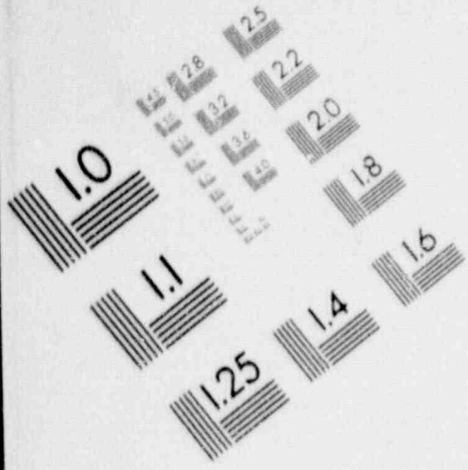

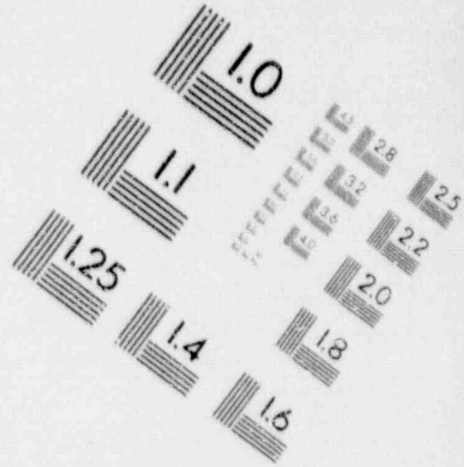

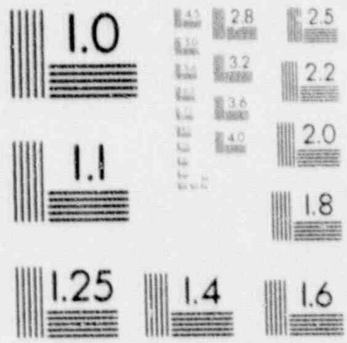

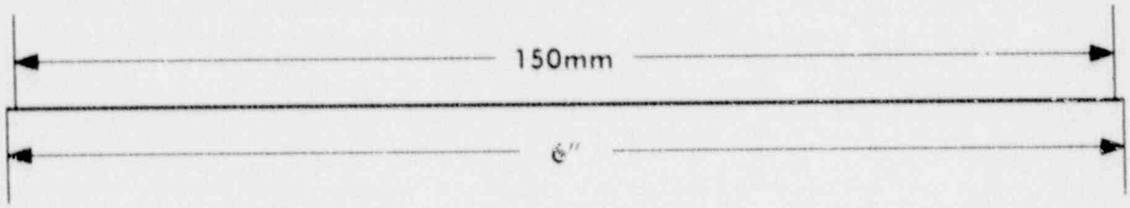

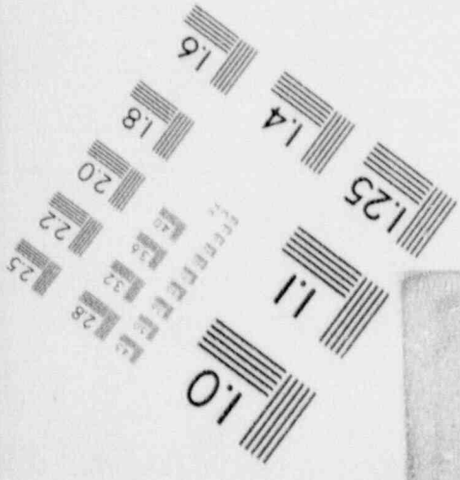

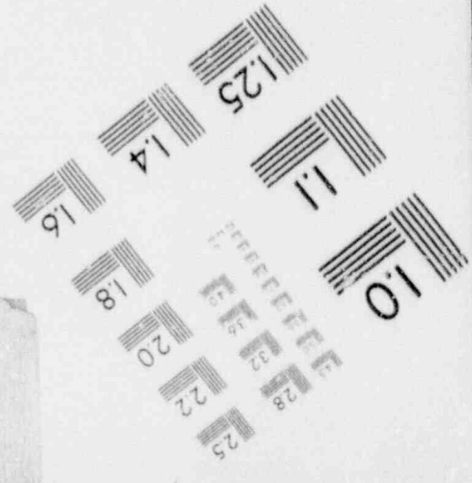

1

IMAGE EVALUATION TEST TARGET (MT-3)

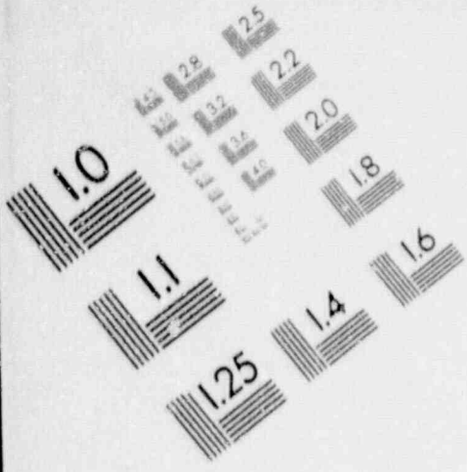

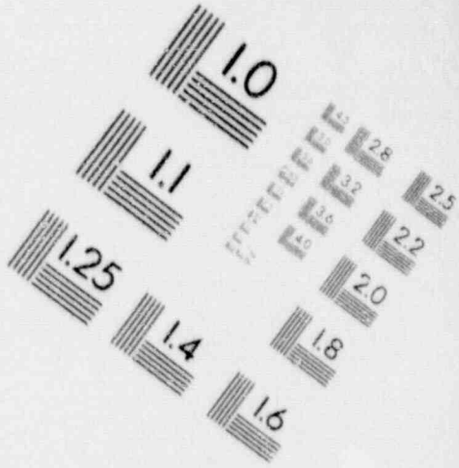

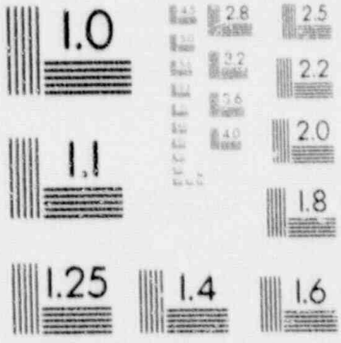

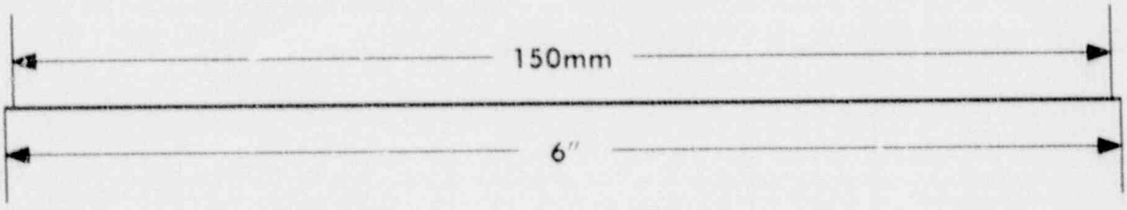

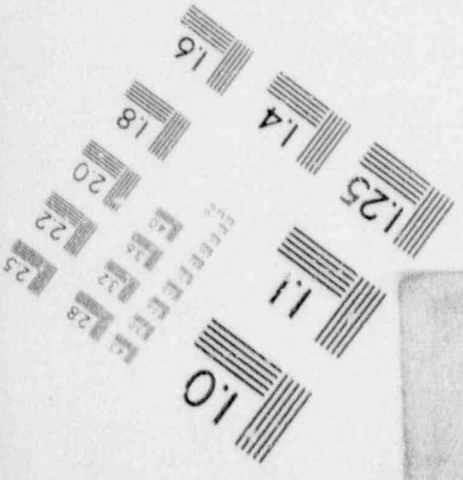

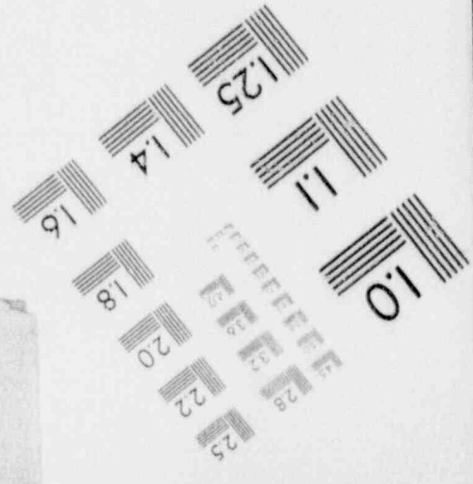

1

IMAGE EVALUATION TEST TARGET (MT-3)

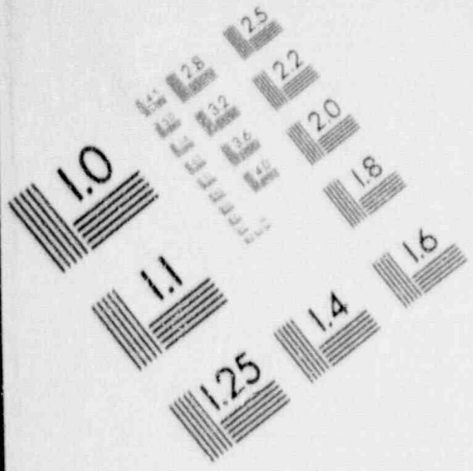

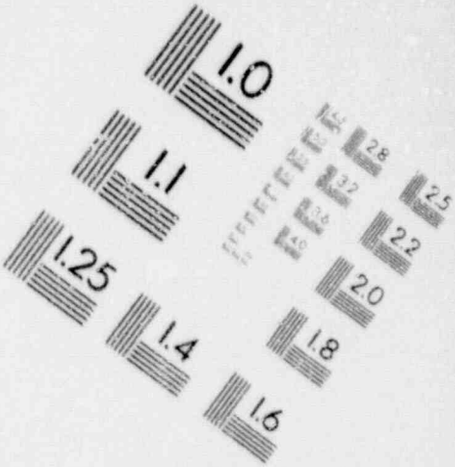

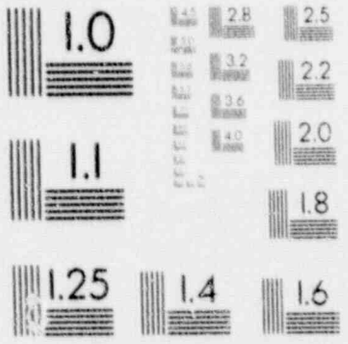

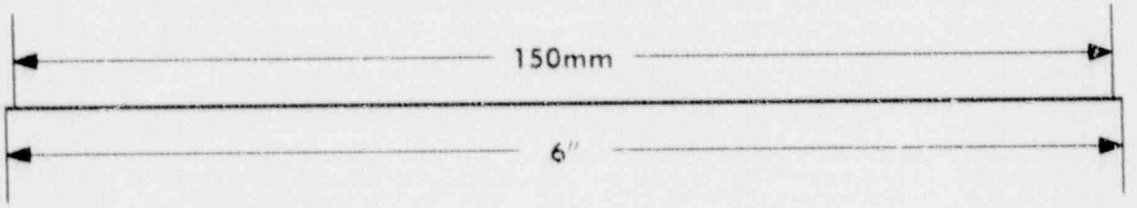

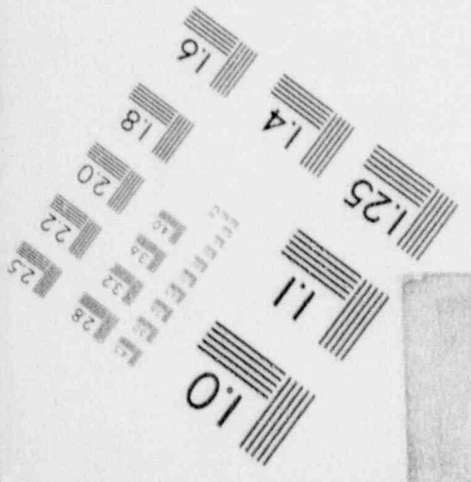

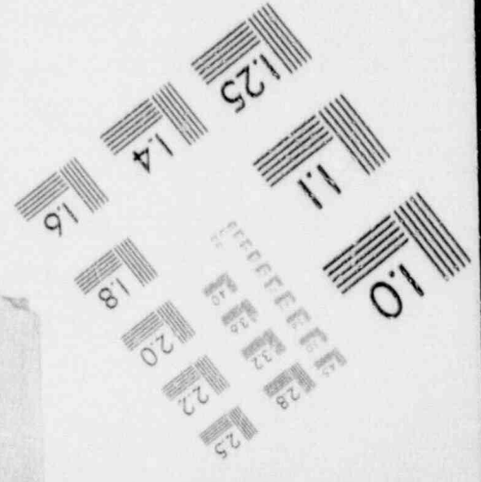

F.3 MELCOR Code Input

This Section provides a set of respresentative code input as processed by the MELGEN package of MELCOR for the Mark III containment response calculations. This MELCOR input was used for the short-term station blackout accident sequence with ADS actuation. This is the basic code input deck to which variations were made as required to perform the MELCOR calculations discussed in Chapter 3.

```
*******************************************************************
*
*       CASE: ggl - ADS based SAR files, No containment failure or burns
*
*       reactor:        grand gulf
*       sequence:       station blackout - low pressure
*                       initial conditions at 300s in ltes run
*       nodalization    rpv(6), cont(18), sec(1)
*
*   ---- this file date:  Oct 23, 1989
*
*******************************************************************
*
title       'grand gulf mk iii containment model'
jobid       'ggl'
*
tstart    300.
*
restartf ggirst
outputf   gglgout
diagf     gglgdia
plotf     gglptf
crtout
dttime     0 1
*
c:tou
*******************************************************************
*******************************************************************
*       ncg input
*******************************************************************
*******************************************************************
*
ncg004     n2   4   * hydrogen
ncg005     n2   5   * nitrogen
ncg006     co   6   * carbon monoxide
ncg007     co2  7   * carbon dioxide
ncg008     ch4  8   * methane
ncg009     o2   9   * oxygen
*
*
*
*******************************************************************
*       cvh input
*******************************************************************
*
*
*
*****************************************************************
*    cv 201 - region between top of shield wall and drywell
*             head seals
*             begins elevations at 173' 3" = 52.8066 m
*             ends elevation at 183' 10" = 56.030 m
*             inner radius = 134 5/16" = 3.412 m  (rpv od =268 7/8")
*             outer radius = 16'4" = 4.9784 m
*             vol = pi *(ro**2-ri**2)*h
*                 = 133.075 m**3
*****************************************************************
*
cv20100    dry head-seal  2  2  2
cv20101    0  0
cv20102    0.0  0.0
cv201a0    3
cv201a1    pvol  1.01353e5  tatm  330.72
cv201a2    mlfr.5  0.79  mlfr.9  0.21
cv201a3    rhum  0.5
cv201b0    52.8066  0.0
```

```
cv20101    36.0328  155.075
*
*****  ************************************************************
*    c    02 - pedestal cavity region
*              begins at elevation = 94' 6" = 28.8036 m
*              ends at elevation = 121' 4 1/2" =36.9951 m
*              volume = 259.420 m**3  (includes sumps)
*              initial water from burltas in sumps = 327 & lbs=148.5kg
*               r1= 10' 7"
*               r2= 9' 5"
*************************************************************************
*
cv20200  pedestal-cavity  2  2  2
cv20201  0  0
cv20202  0.0  0.0
cv202a0  3
cv202a1  pvol 1.01353e5  tatm 330.72
cv202a2  rhum 0.5  mlfr.5  0.79
cv202a3  mlfr.9  0.21 mass 1 148.51
cv202b0  27.8892  0.0
cv202b1  28.8036  4.7714
cv202b2  34.9123  208.47
cv202b3  35.2679  214.88
cv202b4  36.9951  259.42
*
*************************************************************************
*     cv 203- weir wall annulus
*              begins at elevation = 93' 0 1/4"= 28.3528 m
*              ends at elevation = 117' 8" = 35.7632 m
*              inside radius = 34' 0" = 10.3632 m
*              outside radius = 36' 6" = 11.1252 m
*              volume = 381.198 m**3
*              vent volume = 81.722 m**3  (table a-10 ufsar)
*              total volume = 462.92 m**3
*************************************************************************
*
cv20300  weir-wall-ann.     2  2  2
cv20301  0  0
cv20302  0.0  0.0
cv203a0  3
cv203a1  pvol  1.01353e5  tatm  330.72
cv203a2  zpol  34.1078  tpol  312.04  mlfr.5  0.79
cv203a3  mlfr.9  0.21
cv203b0  28.3528  0.0
cv203b1  35.7632  462.92
*
*************************************************************************
*    cv 204 - drywell annular region from 161' 6" to 180' 3"
*              begins at elevation = 161' 6" = 49.2252 m
*              ends at elevation = 180' 3" = 54.9402 m
*              inside radius = 16' 4" = 4.9784 m
*              outside radius = 36' 6" = 11.1252 m
*              vol = 1777.208 m**3
*************************************************************************
*
cv20400  drywell-ann-A      2  2  2
cv20401  0  0
cv20402  0.0  0.0
cv204a0  3
cv204a1  pvol  1.01353e5  tatm  330.72
cv204a2  rhum  0.5  mlfr.5  0.79
cv204a3  mlfr.9  0.21
cv204b0  49.2252  0.0
cv204b1  54.9402  1777.208
*
*************************************************************************
```

```
*   cv 205   rpv shield wall annular region
*            rpv midplane outside radius = 133 1/8" = 3.3814 m
*            shield wall inside radius = 14'4" = 4.3688 m
*            begins at elevation = 121' 4 1/2" = 36.995 m
*            ends at elevation = 173' 3" = 52.807 m

*            vol = 380.139 m**3
*
*************************************************************
*
cv20500  shield-wall-ann.  2  2  2
cv20501  0  0
cv20502  0.0  0.0
cv205a0  3
cv205a1  pvol 1.01353e5 tatm 330.72
cv205a2  mlfr.5  0.79  mlfr.9  0.21
cv205a3  rhum  0.5
cv205b0  36.995  0.0
cv205b1  52.807  380.139
*
*************************************************************
*  cv 206  drywell annular region from top of grating at 147'7"
*          level to top of grating at 161'6"
*
*          begins at elevation = 147'7"= 44.9834 m
*          ends at elevation = 161'6" = 49.2252 m
*          ri = 16'4" = 4.9784 m
*          ro = 36'6" = 11.1252 m
*          vol = pi*(ro**2-ri**2)*(height) = 1319.083 m**3
*
*************************************************************
cv20600   drywell-ann.-3  2  2  2
cv20601   0  0
cv20602   0.0  0.0
cv206a0   3
cv206a1   pvol 1.01353e5  tatm  330.72
cv206a2   rhum  0.5  mlfr.5  0.79
cv206a3   mlfr.9  0.21
cv206b0   44.9834  0.0
cv206b1   49.2252  1319.083
*
*****************************************************************
*  cv207  drywell annular region form top of weir wall to grating at
*         147'7"
*
*         begins at elevation = 117'4" = 35.7632 m
*         ends at elevation = 147' 7" = 44.9834 m
*         inside radius = 16'4" = 4.9784 m
*         outside radius = 36'6" = 11.1252 m
*         vol=pi*(ro**2-ri**2)*(height) = 2867.228 m**3
*****************************************************************
cv20700   drywell-ann.-2  2  2  2
cv20701   0  0
cv20702   0.0  0.0
cv207a0   3
cv207a1   pvol 1.0135e5  tatm  330.72
cv207a2   rhum  0.5  mlfr.5  0.79
cv207a3   mlfr.9  0.21
cv207b0   35.7632  0.0
cv207b1   44.9834  2867.228
*
*****************************************************************
*   cv208  drywell annulus region next to weir wall
*
*          begins at elevation  =  100'9" =30.7086
*          ends at elevation =  117'4" = 35.7632 m
```

```
*            ro = 24'6"  = 7.7088 m
*            ri = 16'4"  = 4.9784 m
*            vol = pi*(ro**2-ri**2)*(height)
*****  ***************************************************  ******
cv208bu   drywell-ann.-1  2  2  2
cv20801   0  0
cv20802   0.0  0.0
cv208a0   3
cv208a1   pvol  1.01353e5   tatm  330.72
cv208a2   rhum  0.5  mlfr.5  0.79
cv208a3   mlfr.9  0.21
cv208b0   30.7086  0.0
cv208b1   55.7632  1164.672
*
*****************************************************************
*   cv 209 - rpv head -drywell head region
*            begins at elevation = 183'10" = 56.032 m
*            ends at elevation = 200' 6" = 61.1112 m
*            vol= 161.460
******* ********************************************************
*
cv20900  drywell-head    2  2  2
cv20901  0  0
cv20902  0.0  0.0
cv20903  35.873
cv209a0  3
cv209a1  pvol  1.01353e5  tatm 330.72
cv209a2  rhum 0.5  mlfr.5  0.79
cv209a3  mlfr.9  0.21
cv209b0  56.032  0.0
cv209b1  58.674  100.730
cv209b2  61.112  161.460
*
*****************************************************************
*   cv 310  suppression pool
*           begins at elevation = 93'0 1/4" = 28.3528 m
*           ends at elevation = 135' 4" = 41.2496 m
*           outside radius = 62' 0" = 18.8976 m
*           inside  radius = 41' 6" = 12.649 m
*           pool elevation = 34.1078 at t= 300.0 due to steam from srv's
*           top of pool at 111'7 1/6" = 34.015m
*           vol= 7986.6954 m**3
*****************************************************************
*
cv31000  suppression-pool  2  2  3
cv31001  0  0
cv31002  0.0  0.0
cv310a0  3
cv310a1  pvol 1.01353e5  tatm 308.45
cv310a2  rhum 0.60  mlfr.5  0.79  mlfr.9  0.21
cv310a3  zpol  34.1078  tpol  312.04
cv310b0  28.3528  0.0
cv310b1  34.0150  3507.80
cv310b2  41.2496  7986.7
*
*****************************************************************
*   cv 311 - wetwell- drywell annulus
*            begins at elevation = 135' 4" = 41.2496 m
*            ends at elevation = 161' 6" = 49.225 m
*            inside radius = 41' 6" = 12.649 m
*            outside radius = 62' 0" = 18.8976 m
*            vol = 4274.897 m**3
*            vol(cv 311)-vol (equip hatch)= 4274.897-563.277 =3711.62m**3
*****************************************************************
*
cv31100  wetwell ann-1  2  2  3
```

```
cv31101  0  0
cv31102  0.0  0.0
cv31103  548.639
cv311a0  3
cv311a1  pvol  1.01353e5  tatm  308.15
cv311a2  mlfr.5  0.79  mlfr.9  0.21
cv311a3  rhum  0.6
cv311b0  41.2496  0.0
cv311b1  49.2252  3711.62
*
*-----------------------------------------------------------------------
*    cv312 - upper-pool-annulus-1
*          - begins at elevation = 161'6" = 49.2252 m
*          - ends at elevation = 184'6" = 56.2356 m
*          - area = 3254.72 ft**2 = 302.3734 m**2
*          - area=area(cv312)-area(equip hatch)=302.3724-70.625=231.7484m**2
*          - vol = area *h =(302.3734m**2)*(56.2356 49.2252)m
*                = 2119.7584 m**3
*          -vol=vol(cv 31.,-vol(equip hatch)=2119.7584-495.1096=1624.649m**3
*
*-----------------------------------------------------------------------
*
cv31200  upper-pool-ann-1  2  2  3
cv31201  0  0
cv31202  0.0  0.0
cv31203  231.7484
cv312a0  3
cv312a1  pvol 1.01353e5 tatm  308.15
cv312a2  rhum 0.6  mlfr.5  0.79  mlfr.9  0.21
cv312b0   49.2252  0.0
cv312b1   56.2356  1624.649
*
*-----------------------------------------------------------------------
*    cv 313 - refueling pool/ upper containment pool
*           - begins at elevation = 208'10" = 63.6524 m
*           - begins at elevation = 167' 6 1/4" = 51.0604 m
*           - midpoint elevation = 184'6 1/4" = 56.242 m
*           - total volume = 73000 ft**3 = 2067.13 m**3
*           - normal water level = 207' 10" = 63.3476 m
*           - total volume = vol pool + vol air
*                          = 2067.13 + 86.70
*                          = 2154.09 m**3
*           - 36,380 ft**3 can be dumped (1030.167 m**3)
*
*-----------------------------------------------------------------------
*
cv31300     refueling-pool  2  2  1
cv31301     0  0
cv31302     0.0  0.0
cv313a0     3
cv313a1     pvol 1.01353e5  tatm  308.15
cv313a2     rhum 0.6  mlfr.5  0.79  mlfr.9  0.21
cv313a3     zpol  63.3476
cv313b0     51.0604    0.0
cv313b1     56.2420    102.0
cv313b2     63.3476    2067.13
cv313b3     63.6524    2154.10
*
*-----------------------------------------------------------------------
*    cv314 - upper containment region 1 above upper pool
*          - begins at elevation = 208'10" = 63.6524 m
*          - ends at elevation = 226'2" = 68.9356 m
*          - r1 = 47'10.5766" = 14.5942 m
*          - area = 7202.5 ft**2 = 669.134 m**2
*          - vol = 669.134m**2 * 5.2832 m = 3535.1695 m**3
*
```

```
*-----------------------------------------------------------------------
*
cv31      upper-ctmt reg-1  2  2  3
cv314     0  0
cv31402   0.0  0.0
cv31403   669.134
cv314a0   3
cv314a1   pvol 1.01353e5  tatm  308.15
cv314a2   mlfr.5  0.79  mlfr.9  0.21  rhum 0.6
cv31460   63.6524  0.0
cv314b1   68.9356  3535.1695
*
*-----------------------------------------------------------------------
*   cv315 - upper containment region 2 above uppper pool
*         - begins at elevation = 226'2" = 68.9356 m
*         - ends at elevation = 243'6" = 74.2188 m
*         - vol = 3535.1695 m**3
*
*-----------------------------------------------------------------------
*
cv31500   upper-ctmt-reg 2  2  2  3
cv31501   0  0
cv31502   0.0  0.0
cv31503   669.134
cv315a0   3
cv315a1   pvol 1.01353e5  tatm 308.15
cv315a2   mlfr.5 0.79  mlfr.9 0.21  rhum 0.6
cv31560   68.9356  0.0
cv315b1   74.2188  3535.1695
*
*-----------------------------------------------------------------------
*   cv316     hemispherical portion of dome
*             begins at el 243'-6" = 74.2188 m
*             ends at el  299'-9" = 91.3638 m
*             thickness = 2'-6"= 0.762 m
*             inside radius = 56'3" = 17.145 m
*             volume= 1/2 * (4/3*pi*r**3) = 10555.312 m**3
*
*-----------------------------------------------------------------------
*
cv31600   dome-hemisphere  2  2  3
cv31601   0  0
cv31602   0.0  0.0
cv316a0   3
cv316a1   pvol 1.0135e5  tatm 294.26  rhum  0.75
cv316a2   mlfr.5  0.79  mlfr.9  0.21
cv316b0   74.2188  0.0
cv316b1   91.3638  10555.3122
*
*-----------------------------------------------------------------------
*   cv317 - wetwell containment annuler region (lower)
*         - begins at elevation = 208'10" = 63.6524 m
*         - ends at elevation = 226'2" = 68.9356 m
*         - ro = 62' 0" = 18.8976 m
*         - ri = 47' 10.5766" = 14.5942 m
*         - vol = 2392.2224 m**3
*         - delta r = 4.3034 m
*         - area = pi*ro**2 - pi*ri**2 = 452.7980 m**2
*
*-----------------------------------------------------------------------
*
cv31700     ww-annulus-lower  2  2  3
cv31701     0  0
cv31702     0.0  0.0
cv31703     452.7980
cv317a0     3
```

```
cv317a1     pvol  1.01353e5  tatm  308.15
cv317a2     mlfr.5 0.79  mlfr.9  0.21  rhum 0.6
cv317b0     63.6524  0.0
cv317b1     68.9356  2392.2224
*
*****************************************************************
*    cv 318 - wetwell containment annular region - upper
*           -begins at elevation = 226'2" = 68.9356 m
*           - ends at elevation = 243'6" = 74.2188 m
*           - ro = 62'0" = 18.8976 m
*           - ri = 47' 10.5766" = 14.5942 m
*           _ vol = area *h = 2392.2224 m**3
*           - delta r = 4.3034 m
*           - area = 452.7980 m**2
*
*****************************************************************
*
cv31800    ww-annulus-upper  2  2  3
cv31801    0  0
cv31802    0.0  0.0
cv31803    452.7980
cv318a0    3
cv318a1    pvol 1.01353e5  tatm 308.15
cv318a2    rhum  0.6   mlfr.5  0.79  mlfr.9  0.21
cv318b0    68.9356  0.0
cv318b1    74.2188  2392.2224
*
*****************************************************************
*  cv319 - upper pool annulus 2
*         - begins at elevation = 184'6" = 56.2356 m
*         - ends at elevation = 208' 10" = 63.6524 m
*         - area = 270.8598 m**2
*         - area=area(cv319)-area(equip hatch)=200.2338 m**2
*         - vol = 2230.717 m**3
*         - vol=vol(cv 319)-vol(equip hatch) =2230.717-523.812=1706.905m**3
*
*****************************************************************
*
cv31900  upper-pool-ann-2  2  2  3
cv31901  0  0
cv31902  0.0  0.0
cv31903  200.2338
cv319a0  3
cv319a1  pvol 1.01353e5  tatm 308.15  rhum 0.6
cv319a2  mlfr.5  0.79  mlfr.9  0.21
cv319b0  56.2356  0.0
cv319b1  62.4332   1240.969
cv319b2  63.6524   1706.9050
*
*****************************************************************
*    cv 320 - rwcu holding pump & sampling room
*           - figure 6.2.56-57 fsar
*           - begins at elevation = 184'6" = 56.2356 m
*           - ends at elevation =204'10" = 62.4332 m
*           - vol = 12525 ft**3 = 354.67  m**3
*
*****************************************************************
*
cv32000  pump-sampling  1  1  3
cv32001  0  0
cv32002  0.0  0.0
cv320a0  3
cv320a1  pvol  1.01353e5  tatm 330.72
cv320a2  mlfr.5  0.79  mlfr.9  0.21  rhum 1.0
cv320b0  56.2356  0.0
cv320b1  62.4332  354.67
```

```
*****************************************************************
*  c    21 - main steam tunnel
*          - vol = 16,800 ft**3 = 475.723 m**3
*          - begins at elevation =140'0" = 42.672m
*          - ends at elevation = 166'0" = 50.5968 m
*
*****************************************************************
*
cv32100  main-steam-room  1  2  3
cv32101  0  0
cv32102  0.0   0.0
cv321a0  3
cv321a1  pvol 1.01353e5  tatm 299.82
cv321a2  mlfr.5  0.79  mlfr.9  0.21  rhum  0.5
cv321b0  42.672    0.0
cv321b1  50.5968  475.723
*
*****************************************************************
*  cv 322 - rwcu hx room
*          - vol = 10,500 ft**3 = 297.327 m**3
*          - begins at elevation = 170' = 51.816 m
*          - ends at elevation = 205'10" = 62.738 m
*          - initial temp = 80 f
*
*****************************************************************
*
cv32200  rwcu-hx-room  1   2   3
cv32201  0  0
cv32202  0.0  0.0
cv322a0  3
cv322a1  pvol  1.01353e5  tatm  299.82
cv322a2  mlfr.5  0.79  mlfr.9  0.21  rhum  0.5
cv322b0  51.8160  0.0
cv322b1  62.7380  297.327
*
*****************************************************************
*  cv 323 - valve nest room (combine compt's 1,2,3 - fig 6.2-62)
*          - vol = 2686 ft**3 + 367 ft**3 + 154 ft**3 = 3207 ft**3
*                = 90.812 m**3
*          - begins at elevation = 173'2" = 52.7812 m
*          - ends at elevation = 180'6" = 55.0164 m
*
*****************************************************************
*
cv32300  valve-nest-room  1  1  3
cv32301  0  0
cv32302  0.0  0.0
cv323a0  3
cv323a1  pvol 1.01353e5 tatm 299.82
cv323a2  mlfr.5  0.79  mlfr.9  0.21  rhum 1.0
cv323b0  52.7812  0.0
cv323b1  55.0164  90.812
*
*****************************************************************
*  cv 324  - rwcu filter/demineralizer rooms 1 & 2
*          - vol = 4578 ft**3 = 129.52 m**3
*          - begins at elevation = 184'6" = 56.2356 m
*          - ends at elevation = 204'10" = 62.4332 m
*
*****************************************************************
*
cv32400  rcwu-filter-dem   1  1  3
cv32401  0  0
cv32402  0.0  0.0
cv324a0  3
```

```
cv324a1  pvol 1.01353e5  tatm  299.82
cv324a2  mlfr.5  0.79  mlfr.9  0.21  rhum 0.50
cv324b0  56.2356  0.0
cv324b1  62.4332  129.52
*
*************************************************************************
*    cv 325 - rwcu pump room
*           - begins at elevation = 161'10" = 49.3268 m
*           - ends at elevation = 166'10" = 50.8508 m
*           - vol = 771.7 ft**3 = 21.852 m**3
*
*************************************************************************
*
cv32500  rwcu-pump-room  1  2  3
cv32501  0  0
cv32502  0.0  0.0
cv325a0  3
cv325a1  pvol 1.01353e5  tatm 299.82
cv325a2  mlfr.5  0.79   mlfr.9  0.21  rhum  1.0
cv325b0  49.3268  0.0
cv325b1  50.8508  21.852
*
*************************************************************************
*   cv 326  - rwcu backwash recieving tank room
*           - begins at elevation = 161'10"= 49.3268 m
*           - ends at elevation = 170'10" = 52.0700 m
*           - vol = 3446.8 ft**3 = 97.603 m**3
*
*************************************************************************
*
cv32600  rcwu-tank-room  1  2  3
cv32601  0  0
cv32602  0.0  0.0
cv326a0  3
cv326a1  pvol  1.01353e5  tatm  299.82
cv326a2  mlfr.5  0.79  mlfr.9  0.21   rhum 1.0
cv326b0  49.3268  0.0
cv326b1  52.0700  97.603
*
*************************************************************************
*
*   cv 327 - control volume representing equipment hatch space in
*            the drywell-wetwell annular region
*          - area = 760.2 ft**2 = 70.625 m**2
*          - begins at 135'4" (41.2496 m)
*          - ends at 208'10" (63.6524 m)
*          - vol = (70.625m**2)*(22.4028m) = 1582.198 m**3
*
*************************************************************************
cv32700  'equip hatch'  2  2  3
cv32701  0  0
cv32702  0.0  0.0
cv32703  70.625
cv327a0  3
cv327a1  pvol 1.01353e5  tatm 308.15  rhum 0.6
cv327a2  mlfr.5  0.79   mlfr.9  0.21
cv327b0  41.2496  0.0       * 135'4"
cv327b1  63.6524  1582.198 * 208'10"
*
*************************************************************************
*
* environment
*
*************************************************************************
*
cv40000      environment  1  2  6
```

```
cv400a0     )
cv400a1     pvol  1.01353e5    rhum  0.5    tatm   300.0
cv40r       mlfr.5  0.79      mlfr.9  0.21
cv40          28.3528         0.0
cv400b1       95.1738         1.0e7
*
*****************************************************************
*
*    flow path input
*
*****************************************************************
*  f1201 - flowpath between cv 207 and cv 208
*        - area = 1681.75 ft**2 = 156.2397 m**2 (per table 6.2-31)
*        - begins at elevation = 117'4" = 35.7632 m
*        - delta r =4.9276 m
*        - length = midpoint cv207 to midpoint 208 =132'5.5"-108'10.75"
*                 = 23.5625 ' = 7.1819 m
*        - seg 1: p=2*pi*(ri+ro)=93.5214 m; a'=230.418m**2  ;4a'/p=9.8552m
*        - seg 2: p=2*pi*ri=31.280; a'=230.418 m**2; 4a'/p=29.465m
*
*****************************************************************
*
f120100   f1201  208  207  35.7632  35.7632
f120101   156.2397  7.1819  1.0  4.9276  4.9276
f120102   0  0  1  1
f120103   1.0  1.0  1.0  1.0
f120104   0.0  0.0
f1201s1   156.2387  2.5718  9.8522  * seg 1 100'9" -117'4"
f1201s2   156.2387  4.6101  29.465  * seg 2 117'4" -132'5.5"
*
*****************************************************************
*   f1202 - flowpath between cv207 and cv206
*         - area =2356.80 ft**2 = 218.9539 m**2 (per fear table 6.2-31)
*         - begins at elevation = 147'7" =44.9834 m
*         - delta r = 6.1468 m
*         - 4*a'/p = 4(310.972)/(2*pi*(11.1252+4.9784)=12.2936m
*
*****************************************************************
*
f120200   f1202  207  206  44.9834  44.9834
f120201   218.9539  6.7818  1.0  6.1469  6.1469
f120202   0  0  1  1
f120203   1.0  1.0  1.0  1.0
f120204   0.0  0.0
f1202s1   218.9539  6.7818  12.2936
*
*****************************************************************
*   f1203 - flowpath between cv 206 and cv 204 (per table 6.2-31 fear)
*         - area = 2354.84 ft**2 = 218.7718 m**2
*         - begins at elevation = 161'10" = 49.3268 m
*         - length = midpoint cv204 - midpoint cv206 = 171'1/2"-154'7.5"
*                  = 16'4" = 4.9784 m
*
*****************************************************************
*
f120300   f1203  206  204  49.2252  49.2252
f120301   218.7718  4.9784  1.0  6.1468  6.1468
f120302   1  0  0  0
f120303   1.0  1.0  1.0  1.0
f120304   0.0  0.0
f1203s1   218.7718  4.9784  12.2936
*
*****************************************************************
*   f1204 - flowpath between cv204 and cv201
*         - begins at elevation =  173'3"
*         - ends at elevation = 180'3"
```

```
*          - area = 67.07+174.15+447.01 ft**2 = 63.9387m**2
*          - note:meicer cv201 = vol 1 + vol 2 + vol 3 of foar(table 6.2-31)
*          - opening diameter = 7"= 2.1336 m
*          - length = 1.72 m
*          - k eff = 1/.93 = 1.08
*          - 4a/p = 2*1 =4.2672 m
*
*****************************************************************************
*
f120400  f1204  204  201  53.8734  53.8734
f120401  63.9387  1.720  1.0  2.1336  2.1336
f120402  3  0  0  0
f120403  1.08  1.08  999.0  999.0
f120404  0.0  0.0
f1204a1  63.9387  1.720  4.2672  0.5e-5  0.0
*
*****************************************************************************
*   f1205 - flowpath between cv205 and cv201
*          - begins at elevation = 173'3" = 52.8066 m
*          - ends at elevation = same
*          - area = 25.03+62.57+162.69 ft**2 = 23.2527 m**2
*          - length = 9.22 m
*          - k eff = 1/.92 = 1.087
*          - delta r = 0.5548 m
*          - 4a/p= 1.975 m
*
*****************************************************************************
*
f120500  f1205  205  201  52.8066  52.8066
f120501  23.2527  9.220  1.0  0.5548  0.5548
f120502  0  0  0  0
f120503  1.087  1.087  999.0  999.0
f120504  0.0  0.0
f1205a1  23.2527  9.220  1.975  0.5e-5  0.0
*
*****************************************************************************
*   f1 206 - flowpath between cv 209 and cv201
*          - elevation = 183'10"=56.0324m
*          - area = 1/2 * 0.72 ft**2 = 0.405m**2
*          - length = 2.488 m
*          - orifice , therefore k= 1.0
*
*****************************************************************************
*
f120600   f1206  209  201  56.0324  56.0324
f120601   0.405 2.488  1.0
f120602   1  0  0  0
f120603   1.0  1.0  1.0  1.0
f120604   0.0  0.0
f1206a1   0.405 2.488  1.016  0.5e-5  0.0
*
*****************************************************************************
*   f1 207 - horizontal flowpath between cv 202 and cv 205
*          - centerline elevation = 122' 10" = 37.4396 m
*          - area = 1.824 m**2 (30 " o.d.)
*          - length = midpoint cv 202 - midpoint cv 205 at 122'10"
*                   ' = 3.875 m (midpoint of shield wall ann.)
*          - le = thickness = 0.25 " = 0.108 m
*          - 30" manholes (2/4 in skirt; currently using 4)
*          - 4a/p = o.d. = 30" = 0.762 m
*
*****************************************************************************
*
f120700  f1207  202  205  36.995  37.4396
f120701  1.824  3.875  1.0  0.762  0.762
f1207[illegible]  3  0  0  0
```

```
f120703  1.0  1.0  1.0  1.0
f12070a  0.0  0.0
f120     1.824  0.108  0.762
*f12(  ,
*
*****************************************************************
*
*  f1 208  - vertical flowpath between cv 208 and cv 202
*          -  centerline elevation = 104' 3" = 31.7754 m
*          - wall thickness = ls = 5.75' = 1.7526 m
*          - l = midpoint cv 208 to midpoint cv 202
*            = 24' 5" = 7.4422 m
*          - area = 7' x 3' = 21 ft**2 = 1.951 m**2
*          - 4*a/p = 4.2' = 1.2802 m
*
*****************************************************************
*
f120800  f1208  208  202  31.7754  31.7754
f120801  1.951  7.4422  1.0  0.9144  0.9144
f120802  3  0  0  0
f120803  1.0  1.0  1.0  1.0
f120804  0.0  0.0
f1208s1  1.951  1.7526  1.2802  0.5e-5
*
*****************************************************************
*   f1209  - drain flowpath between cv208 and cv202
*          - begins at elevation = 100'9"=30.7086m
*          - ends at elevation = 96'10.5"=29.5275m
*          - flowpath area = 2-8" pipes =2*?:*16 in**2 = 0.06486m**2
*          - elevation opening height = o.d. of circle with area
*            = 2-6" o.d. pipes and 2-8" o.d. pipes = 157.08 in**2
*            = 0.10134 m**2 , therefore o.d. = 0.3592m
*
*****************************************************************
*
f120900  f1209  208  202  30.7086  29.5275
f120901  0.06486  17.222  1.0  0.3592  0.28206
f120902  3  0  1  1
f120903  1.0  1.0  1.0  1.0
f120904  0.0  0.0
f1209s1  0.05067  1.2802  0.1814  *8" & 6" lines parallel for 42'
f1209s2  0.06486  2.8956  0.2032  * 2 -8" lines parallel for 9.5'
f1209s3  0.03243  1.5240  0.2032  *8" single line for 5'
*
*****************************************************************
*   f1 210 - drywell vacuum breaker flowpath
*          - begins at elevation = 179'2" = 54.610 m
*          - ends at elevation = 194' 0" = 59.1312 m
*          - id =10.02"
*          - od = 10.75"   (10" sch 40 pipe)
*          - a/sqrt(k) = 0.225 ft**2  , therefore k =5.93
*
*****************************************************************
*
*
*  valve = closed for task 3c.1
*
f121000  f1210  204  319  54.610  55.1312
f121001  5.0903e-2  6.985  1.0  0.1273  0.2545
f121002  0  0  1  1
f121003  5.93  5.93  1.0  1.0
f121004  0.0  0.0
f1210s1  0.050903  4.4704  0.2545  *vertical section
f1210s2  0.10186  1.3462  0.2545  *53" parallel segment
f1210s3  0.050903  1.1684  0.2545  *rest of 93" segment
f1210v1  -250  250  250
```

```
*
cf25000  vac-bkr-open  1-a-ifte  3  1.0  0.0
cf25010  1.0  0.0  cfvalu.251
cf25011  0.0  1.0  time
cf25012  0.0  0.0  time
*
cf25100  dual-test-logic  1-and  2  1.0  0.0
cf25110  1.0  0.0     cfvalu.252
cf25111  1.0  0.0     cfvalu.253
*
cf25200  vac-open-start  1-gt  2  1.0  0.0
cf25210  1.0  0.0     time
cf25211  0.0  1.0e9   time
*
cf25300  ww-dw-dp  1-ge  2  1.0  0.0
cf25310  -1.0  0.0       cfvalu 311
cf25311   0.0  3.4474e3  time
*
*****************************************************************
*   f1211 - top row of vents
*         - centerline at elevation = 104'4" = 31.8008 m
*
*****************************************************************
*
f121100  top-row-vents  203  310  31.8008  31.8008
f121101  0.37987  1.524  1.0  0.69546  0.69546
f121102  3  0  1  1
f121103  1.48  1.48  1.48  1.48
f121104  0.0  0.0
f1211s1  12.17055  1.524  2.2311  0.5e-5  0.0
*
*****************************************************************
*   f1212 - middle row of vents
*         - centerline at 100'2" = 30.5308 m
*
*****************************************************************
*
f121200  mid-row-vents  203  310  30.538  30.5308
f121201  0.37987  1.524  1.0  0.69546  0.69546
f121202  3  0  1  1
f121203  1.48  1.48  1.0  1.0
f121204  0.0  0.0
f1212s1  12.17055  1.524  2.2311  0.5e-5  0.0
*
*****************************************************************
*  f1213 - bottom row of vents
*        - centerline at elevation = 96'0" = 29.2608 m
*
*****************************************************************
*
f121300  bottom-row-vents  203  310  29.2608  29.2608
f121301  0.37987  1.524  1.0  0.69546  0.69546
f121302  3  0  1  1
f121303  1.48  1.48  1.0  1.0
f121304  0.0  0.0
f1213s1  12.17055  1.524  2.2311  0.5e-5  0.0
*
*****************************************************************
*  f1 214 - flowpath between cv207 and cv203
*         - elevation = 117'4" = 35.7632 m
*         - area = 51.4409 m**2
*         - ri = 10.3632 m
*         - ro = 11.1252 m
*         - delta r = 0.762 m
*         - length = midpoint of air portion of cv 203 to midpoint
*                    of cv 207 =131'1/2" 11' 10 5/12" = 18'1/2" =5.4885 m
```

```
*           neglect friction losses fs= 0.0
*         - A*a/p = 1.524 m
*         - ls = 117'4" - 111'7 1/6" = 1.7484 m
*****   ***************************************************   *******
*
f121400  f1211  207  203  35.7632  35.7632
f121401  51.4409  5.4885  1.0  0.762  0.762
f121402  1  0  1  1
f121403  1.0  1.0  1.0  1.0
f121404  0.0  0.0
f1214s1  51.4409  1.7484  1.524  0.5e-5  0.0
*
*****************************************************************
*  f1215  - drywell-wetwell leakage
*         - a/sqrt(k)=0.048ft**2=4.46e-03 ; (fig 6.2-16 fsar)
*         - therefore set k=1.0, and area =0.048ft**2
*         - assume elevation = 135' = 44.148m (horizontal flowpath)
*         - ls = 5' =1.524 m
*         - ds = 4*a/p =2*(ro-ri) for concentic circles
*         - assume ro-ri=1/4" ; ds=0.013 m
*         - note  a/sqrt(k) = 0.048 no spray
*                           = 0.9  for spray
*
*****************************************************************
*
f121500  f1215  207  310  41.148  41.148
f121501  4.46e-3  1.524  1.0
f121502  3  0  0  0
f121503  1.0  1.0  1.0  1.0
f121504  0.0  0.0
f1215s1  4.46e-3  1.524  0.013  0.5e-5  0.0 * f=0.0 since a/sqrt(k) known
*
*****************************************************************
*   f1 216 - flowpath between cv 209 and cv201
*         - elevation = 183'10"=56.0324m
*         - area = 1/2 * 8.72 ft**2 = 0.405 m**2
*         - length = 2.488 m
*         - orifice , therefore k= 1.0
*
*****************************************************************
*
f121600   f1216  209  201  56.0324  56.0324
f121601   0.405  2.488  1.0
f121602   1  0  0  0
f121603   1.0  1.0  1.0  1.0
f121604   0.0  0.0
f1216s1   0.405  2.488  1.016  0.5e-5  0.0
*
*****************************************************************
*   f1301 - flowpath between cv 310 and cv311
*         - elevation = 135'4"=41.2496m
*         - grating area = 2883 ft**2 = 267.8395 m**2
*         - ctmt annulus area = 6663.7 ft**2 =619.2638 m**2
*         - no communication area =  3783 ft**2 = 351.5422 m**2
*         - assume orifice , therefore k=1.0
*         - 73% of grating area open, therefore area =2104.6 ft**2
*           = 195.523 m**2
*         - length = midpoint cv311 - midpoint cv310
*                  =148'5"-114'1.875"=34'3.125"=10.4426m
*        -segment 1:ls=131'4"-114'1.875"=5.2356m;area=619.277m**2
*                   ds=4a/p=12.497
*        -segment 2:ls=4'=1.2192m; area=197.2145m**2; ds=4a/p=6.23
*        -segment 3:ls=148'5"-135'4"=3.9878m; area=619.277m**2
*                   ds=4a/p=12.497m
*         - p (seg 2)= 126.63m  (measured)
*         - reduce area of flow 302 by area of hatch (267.8395-70.625=197.2145)
```

```
*
*****************************************************************
*
f130100  f1301  310  311  41.2496  41.2496
f130101  197.2145  10.4426  0.73  6.2486  6.2486
f130102  0  0  1  1
f130103  1.0  1.0  1.0  1.0
f130104  0.0  0.0
f1301a1  619.277  5.2356  12.497
f1301a2  197.2145  1.2192  6.23
f1301a3  619.277  3.9878  12.497
*
*****************************************************************
*    f1302 - flowpath  between cv311 and cv312
*          - grating area = 3254.2 ft**2 = 302.3251 m**2
*          - ctmt annulus area =6665.7 ft**2
*          -  no communication area = 3411.5 ft**2
*          - 73% open
*          - elevation = 161'6"=49.2252m
*          - segment 1: la=161'6"-140'5"=3.9878m; area=619.277 m**2
*                       da=12.497 m
*          - segment 2: la=173'-161'6"=11'6"=3.5052m
*                       area=231.700m**2
*                       da=Aa/p=6.73       (p measured = 137.7m)
*          - reduce area of f1302 by area of hatch=302.3251-70.625=231.7m**2
*
*****************************************************************
*
f130200  f1302  311 312  49.2252  49.2252
f130201  231.700  7.493  0.73  6.2486  6.2486
f130202  0  0  1  1
f130203  1.0  1.0  1.0  1.0
f130204  0.0  0.0
f1302a1  619.277  3.9878  12.497
f1302a2  231.700  3.5052  6.73
*
*****************************************************************
*    f1303 -flow path between cv319 and cv317
*          - elevation =208'10" = 63.6524 m
*          - containment area = 12.076.3 ft**2 = 1121.925 m**2
*          - no communication area = 7202.5 ft**2 = 669.1342 m**2
*          - grating area = 4091.6 ft**2 = 380.1221 m**2
*          - open area = 760.2 ft**2 = 70.6249 m**2
*          - total open area = 760.2 ft**2 + 0.73 *(4091.6 ft**2)
*                            = 3747.068 ft**2 = 348.114 m**2
*          - length = midpoint cv317 to midpoint cv319 = 217'6"-196'8"
*                   = 20' 10"
*          - 4*a/p=  = 6.86
*          - delta r = 62' - ri = 4.3034 m
*          - length (segment) = 208'10"-184'6"=7.4168 m
*          - reduce f1303 area by area of hatch (70.625 m**2)
*
*****************************************************************
*
f130300  f1303  319  317  63.6524  63.6524
f130301  277.489  6.350  1.0  4.3034  4.3034
f130302  0  0  1  1
f130303  1.0  1.0  1.0  1.0
f130304  0.0  0.0
f1303a1  277.489  7.4168  6.86
*
*****************************************************************
*    f1304 - flow path between cv317 and cv318
*          - elevation = 226'2" = 68.9356 m
*          - area = 4873.8 ft**2 =452.7908 m**2
*          - delta r = 62'-47'10.5766"=4.3034m m
```

```
*           - length = midpoint cv318 to midpoint cv317
*                    = 5.2832 m
*           - 4a/p = 4(452.7908)/2*pi*ro = 15.2536 m
*
*****************************************************************
*
f130400  f1304  317  318  68.9356  68.9356
f130401  452.7908  5.2832  1.0  4.3034  4.3034
f130402  0  0  1  1
f130403  1.0  1.0  1.0  1.0
f130404  0.0  0.0
f1304s1  452.7908  5.2832  15.2536
*
*****************************************************************
*   f1305 - horizontal flowpath between cv317 and cv314
*           -elevation = 216' 8" =66.040 m
*           -length = midpoint cv317 to midpoint cv314
*                   = 54.9407 ft = 16.7459 m
*           -area = 2*pi*ri*l' = 2*pi*(47.8814')*(17'4")
*                 =484.4609 m**2
*           -4*a/p= 4*(2*pi*ri)*l'/(2*2*pi*ri) = 2*l'=10.5664 m
*
*****************************************************************
*
f130500   f1305  317  314  66.040  66.040
f130501   484.4609  16.7459  1.0  5.2832  5.2832
f130502   3  0  0  0
f130503   1.0  1.0  1.0  1.0
f130504   0.0  0.0
f1305s1   484.4609  16.7459  10.5664  0.5e-5  0.0
*
*****************************************************************
*
*   f1306 - horizontal flowpath between cv318 and cv315
*           - elevation = 235'8" = 71.5264 m
*           - length = midpoint cv318 to midpoint cv315 = 16.7459
*           - area = 484.4609 m**2
*
*****************************************************************
*
f130600   f1306  318  315  71.5264  71.5264
f130601   484.4609  16.7459  1.0  5.2832  5.2832
f130602   3  0  0  0
f130603   1.0  1.0  1.0  1.0
f130604   0.0  0.0
f1306s1   484.4609  16.7459  10.5664  0.5e-5  0.0
*
*****************************************************************
*   f1307 - flowpath between cv318 and cv316
*           - elevation = 243'6" = 74.2188 m
*           - area = 4873.0 ft**2 = 452.7908 m**2
*           - delta r = 4.3034 m
*           - length = midpoint cv318 to midpoint cv316 = 19.1576
*           - 4*a/p = 15.2536 m
*
*****************************************************************
*
f130700  f1307  318  316  74.2188  74.2188
f130701  452.7908  19.1576  1.0  4.3034  4.3034
f130702  0  0  1  1
f130703  1.0  1.0  1.0  1.0
f130704  0.0  0.0
f1307s1  452.7908  19.1576  15.2536
*
*****************************************************************
*   f1308 - vertical flowpath between cv315 and cv316
```

```
*         - elevation = 243'6" = 74.2188 m
*         - length = midpoint cv316 to midpoint cv315
*                  = 272' 10.5" - 234' 10"
*                  =38' 1/2" = 11.5951 m
*         - area = 669.1346 m**2
*         - diameter = 29.1885 m
*
*****************************************************************
*
f130800  f1308  315  316  74.2188  74.2188
f130801  669.1346  11.5951  1.0  29.1885  29.1885
f130802  0  0  1  1
f130803  1.0  1.0  1.0  1.0
f130804  0.0  0.0
f1308s1  669.1346  11.591  29.1885  0.5e-5  0.0
*
*
*****************************************************************
*   f1309 - vertical flowpath between cv314 and cv315
*         - elevation = 226'2" = 68.9356 m
*         - length = 5.2832 = midpoint cv314 to midpoint cv315
*         - area =pi*ri**2 = 669.1346 m
*         - diameter = 29.1885 m
*
*****************************************************************
*
f130900  f1309  314  315  68.9356  68.9536
f130901  669.1346  5.2832  1.0  29.1885  29.1885
f130902  0  0  1  1
f130903  1.0  1.0  1.0  1.0
f130904  0.0  0.0
f1309s1  669.1346  5.2832  29.1885  0.5e-5  0.0
*
*****************************************************************
*f1310 - vertical flowpath between cv313 and cv314
*       -elevation = 208'10"=63.6524 m
*       -length = 217'6"-207'11"=2.921 m
*       -area=pi*(47.8814')**2=7202.505ft**2=669.1346m**2
*       -diameter = 29.1885 m
*
*****************************************************************
*
f131000  f1310  313  314  63.6524  63.6524
f131001  669.1346  2.921  1.0  29.1885  29.1885
f131002  0  0  1  1
f131003  1.0  1.0  1.0  1.0
f131004  0.0  0.0
f1310s1  669.1346  2.921  29.1885  0.5e-5  0.0
*
*
*****************************************************************
*   f1311 - flow path between cv312 and c319
*         - elevation = 184'8" = 56.2356 m
*         - ctmt annulus area = 6665.7 ft**2= 619.2638 m**2
*         - no communication area = 3750.2 ft**2 = 348.405 m**2
*         - grating area = 1909.37 ft**2 = 177.3816 m**2
*         - open area = 1006.18 ft**2 = 93.4772 m**2
*         - total area =open + 0.73 *grating area = 222.9658 m**2
*         - length = midpoint 310 - midpoint 312 = 196'8" - 173'0"
*                  = 23'8" = 7.2136 m
*         - ro = 10.8976 m
*         - 4*a/p = 7.708
*         - delta r = 1.9817
*         - length (segment) = 184'6"-161'6" = 23' =7.0104 m
*         - reduce area of f1311 by area of hatch(222.9658-70.625=152.3408)
*
```

```
*-----------------------------------------------------------------------
*
f131     f131if  312  319  56.2356  56.2356
f131     152.3408  7.2136  1.0  1.9817  1.9817
f1311u2  0  0  1  1
f131105  1.0  1.0  1.0  1.0
f131104  0.0  0.0
f131161  152.3408  7.0104  2.708
*
*-----------------------------------------------------------------------
*   f1 312 - horizontal flowpath between cv 312 and cv 400
*          - installed 20" vent line exhaust
*          - area = pi*(d/2)**2 = 0.18777 m**2
*          - elevation = 177'9" = 54.1782 m
*          - length = 5' =1.524 m
*          - wall thickness = 0.375 "
*          - id = 19.25 " = 0.48895 m
*          - both supply and exhaust vents open per epg
*
*-----------------------------------------------------------------------
*
* note : for task 3c.1 srd cases with no vents valve = closed
*
f131200  f1312  312  400  54.1782  54.1782
f131201  0.37554  1.524  1.0  0.48895  0.48895
f131202  3  0  1  1
f131203  1.0  1.0  1.0  1.0
f131204  0.0  0.0
f1312a1  0.37554  1.524  0.48895
f1312v1  -550  350  350
*
cf35000  vent-line-open  1-a-ifte  3  1.0  0.0
cf35010  1.0  0.0  cfvalu.351
cf35011  0.0  1.0  time
cf35012  0.0  0.0  time
*
cf35100  vent-open-start  1-gt  2  1.0  0.0
cf35110  1.0  0.0  time
cf35111  0.0  1.0e9  time
*
*-----------------------------------------------------------------------
*  f1 313 - horizontal flowpath between cv 320 and cv319
*         - midpoint of elevation = 188'= 57.3024 m
*         - area = 28 ft**2 = 2.6013 m**2
*         - k eff = 1.205
*          - wall thickness = 1s =4 1/2' = 1.3716 m
*         - p = 2 * 4' + 2 * 7' = 11.5824 m
*         - 4*a/p = ds = 0.8984
*         - f = 0.0
*         - door = 4' x 7' x 4 1/2' thick
*         - 1/a = 0.0511 ft-1 , therfore l = 0.4361 m
*
*-----------------------------------------------------------------------
*
f131300  f1313  319  320  57.3024  57.3024
f131301  2.6013  0.4361  1.0  2.1336  2.1336
f131302  3  0  1  1
f131303  1.205  1.205  999.0  999.0
f131304  0.0  0.0
f1313a1  2.6013  0.4361  0.8984  0.5e-5  0.0
*
*-----------------------------------------------------------------------
*  f1314 - vertical flowpath between cv 321 and cv322
*        - k tot = 1.42, keff = f/c = 1.192
*        - area = 33.75 ft**2 = 3.1355 m**2
*        - 1/a=0.1898 ; therefore l = 6.4058 ft = 1.9525 m
```

```
*          elevation opening = 170' = 51.816 m
*        - exit elevation = 166' = 50.5968 m
*        - friction loss =0.0
*        - p = 4'6" + 6'3" = 6.5532 m
*        - 4a/p = 1.914 m
*
*************************************************************************
*
f131400  f1314  322  321  51.816  50.5968
f131401  3.1355  1.9525  1.0  1.905  1.905
f131502  1  0  0  0
f131403  1.192  1.192  999.0  999.0
f131404  0.0  0.0
f1314s1   3.1355  1.9525  1.914  0.5e-5  0.0
*
*************************************************************************
*  f1 315 - flowpath between cv322 and cv319
*        - area = 20.93 ft**2 = 1.9445 m**2
*        - k tot = 1.9 ; keff = 1/c = 1/0.82 = 1.22
*        - 1/s = 0.1953 ; therefore l = 4.888 ft = 1.246 m
*        - f =0.0
*        - assume elevation = 187' 8.5" = 57.2135 m
*        - 4a/p = 1.246
*
*************************************************************************
*
f131500  f1315  319  322  57.2135  57.2135
f131501  1.9445  1.246  1.0  0.7867  0.7867
f131502  3  0  0  0
f131503  1.22  1.22  999.0  999.0
f1315s1  1.9445 1.246  1.5734  0.5e-5  0.0
*
*************************************************************************
*   f1 316 - suppression pool dump (30" dump lines)
*          - vertical flowpath between cv 313
*          - begins at elevation = 187' 10"=57.2516 m
*          - opening = 30" o.d. pipe
*          - ends at elevation = 120'10" = 36.830 m
*          - 2 - 30" lines in parallel
*          - segment area 9.8175 ft**2 = 0.9121 m**2
*          - length = 20.422m = 20.5 m
*
*************************************************************************
*
*   for task 3c.1 case valve = closed
*
f131600  f1316  313  310  57.3516  36.830
f131601  0.4561  20.500  1.0  0.381  0.381
f131602  2  0  0  0
f131603  1.0  1.0  1.0  1.0
f131604  0.0  0.0
f1316s1  0.9121  20.500  0.762  * 2- 30" parallel lines
f1316v1  -316  316  316
*
cf31600 supp-pool-dump   1-e-lfto 3  1.0  0.0
cf31610  1.0  0.0   cfvalu 317
cf31611  0.0  1.0   time
cf31612  0.0  0.0   time
*
cf31700  dump-start  1-gt  2  1.0  0.0
cf31710  1.0  0.0    time
cf31711  0.0  1.0e9  time
*
*************************************************************************
*   f1 317 - horizontal flowpath from cv 312 to cv 323
*          - area = 3.6ft**2 + 16.8ft**2 = 20.4ft**2 = 1.895m**2
```

```
*           -1/e=0.177 (area weighted) , therefore l =3.61 ft = 1.101m
*            k eff=1/c = 1.63
*           - f = 0.0
*           - elevation = 173'2"+(7'/2)=176'8"=53.848m
*           - opening height = 3' = 0.9144m
*           - 3' x 7' opening each side, therefore p = 40'=0.6218m
*
*****************************************************************
*
f131700  f1317  312  323  53.848  53.848
f131701  1.895  1.101  1.0  0.9144  0.9144
f131702  1  0  0  0
f131703  1.63  1.63  999.0  999.0
f131704  0.0  0.0
f1317e1  1.895  1.101  0.6218  0.5e-5  0.0
*
*****************************************************************
*  f1 318 - flowpath between cv 324 (rucu demin room) and cv 319
*           vent area = 2 x 15ft**2 = 30ft**2 = 0.8495m**2
*           - k = 1.44, f=0.0; keff = 1/.833 = 1.200
*           - centerline elevation = 204'4" = 62.2808m
*           - vent = 12" x 15'
*           - p = 32' = 9.7536 m
*           - 4a/p = 0.3484 m
*           - 1/e = 0.1812 ft-1 , therefore l =5.436' = 1.657 m
*
*****************************************************************
*
f131800  f1318  319  324  62.2808  62.2808
f131801  0.8495  1.657  1.0  0.3048  0.3048
f131802  3  0  0  0
f131803  1.200  1.2000  999.0  999.0
f131804  0.0  0.0
f1318e1  0.8495  1.657  0.3048  0.5e-5  0.0
*
*****************************************************************
*  f1 319 - vertical flowpath between cv 325 and cv 312
*           area = 21 ft**2 = 1.95096 m**2
*           - k tot = 1.304 ; k eff = 1/c = 1/.82 =1.22
*           - f = 0.0
*           - 1/e = 0.54; therefore l = 1.85352 m
*           - assume centerline elevation = 170'10" = 52.070 m
*           - assume exit elevation = 166'10" = 50.8508 m
*
*****************************************************************
*
f131900  f1319  312  325  52.070  50.8508
f131901  1.951  1.0535  1.0  0.788  0.788
f131902  1  0  0  0
f131903  1.22  1.22  999.0  999.0
f131904  0.0  0.0
f1319e1  1.951  1.0535  1.576  0.5e-5  0.0
*
*****************************************************************
*
*  f1 320 - horizontal flowpath between cv 325 and cv 326
*           - assume elevation = 164'4" = 50.0888 m
*           - area = 21 ft**2 = 1.950964 m**2 = 1.9510 m**2
*           - k eff = 1/c =1/0.84 = 1.19
*           - 1/e = 0.499 ft-1 ; l = 0.9735 m
*           - f = 0.0
*
*****************************************************************
*
f132008  f1320  325  326  50.0888  50.0888
f132001  1.9510  0.9735  1.0  0.788  0.788
```

```
f132002  3  0  0  0
f132003  1.19  1.19  999.0  999.0
f132004  0.0  0.0
f1320s1  1.9510  0.9735  1.576  0.5e-5  0.0
*
*-----------------------------------------------------------------
*     the  following flowpaths represent the equipment hatch
*     to dw-ww annular regions
*
*-----------------------------------------------------------------
*
f132500  hatch-dome  327  317  63.6524  63.6524
f132501  70.625  13.043  1.0  6.1  6.1
f132502  0  0  0  0
f132503  1.0  1.0
f1325s1  70.625  13.043  10.0  0.5e-5  0.0
*
f132400  hatch-uppann  327  319  59.944  59.944
f132401  127.73  49.55  1.0  17.22  17.22
f132402  3  0  0  0
f132403  1.5  1.5
f1324s1  127.73  49.55  10.0  0.5e-5  0.0
*
f132300  hatch-uppann  327  312  52.7304  52.7304
f132301  120.73  49.55  1.0  17.22  17.22
f132302  3  0  0  0
f132303  1.5  1.5
f1323s1  120.73  49.55  10.0  0.5e-5  0.0
*
f132200  hatch-lowann  327  311  45.2374  45.2374
f132201  137.35  49.55  1.0  17.22  17.22
f132202  3  0  0  0
f132203  1.0  1.0
f1322s1  137.35  49.55  10.0  0.5e-5  0.0
*
f132100  hatch-ww  310  327  41.7496  41.2496
f132101  70.625  17.656  1.0  6.1  6.1
f132102  0  0  0  0
f132103  1.0  1.0
f1321s1  70.625  17.656  10.0  0.5e-5  0.0
*
*-----------------------------------------------------------------
*
*     radionuclide input
*
*-----------------------------------------------------------------
*
rn1000 0
rn1001 5 1 16 14 13 0 0
rn1100 1.0e-6 50.e-6 1000.
*
* use default radionuclides plus csi class 16
*
dchdefcls0 all
*
* csi class
*
dchnem0100 ci 1.0e-6
dchnem0101    0.  5.0211e5    6.12 4.0919e5    11.88 3.0675e5    18.  3.5494e5
dchnem0102   29.88 3.1747e5      61.2 2.0612e5     118.8 2.4439e5
dchnem0103   241.2 2.3141e5      612.  2.1557e5    1188.  1.9989e5
dchnem0104   3600.  1.5937e5     5400.  1.3421e5     7200.  1.2565e5
dchnem0105  14400.  8.3485e4    21600.  6.9352e4    28800.  5.8241e4
dchnem0106  36000.  5.1511e4    43200.  4.3972e4    54000.  3.8938e4
dchnem0107  72000.  3.1424e4    86400.  2.6405e4   129600.  1.7206e4
dchnem0108 172800.  1.3019e4   259200.  8.8275e3   345600.  6.4804e3
```

```
dchmem0109 518400.  4.5686e3  691200.  3.5678e3  864000.  3.0797e3
dchcls0160 cei
dchc'    61 ci
*
dchclsnorm yes
*
rncls0100 16
rncls0101 2 1.0 *cs
rncls0102 4 0.5 *12
*
*   vanesa to class map
*
rnvnc101   25 16
*
* core fission product inventories
*
* based on 3578 mwft bwr inventories
*
*
* aerosol coefficients
*
rnscoef 1
*
*   default values for the aerosol
*   parameters are used
*
*   deposition surfaces
*
*
*   settling areas
*
*            fr    to      elev          area
*
rnset001   204    206     49.2252     218.7718
rnset002   206    207     44.9834     218.9539
rnset003   207    208     35.7632     156.2397
rnset004   207    203     35.7632      51.4409
rnset005   316    315     74.2188     669.1346
rnset006   315    314     68.9356     669.1346
rnset007   314    313     63.6524     669.1346
rnset008   316    318     74.2188     452.7908
rnset009   318    317     68.9356     452.7908
rnset010   317    319     63.6524     277.489
rnset011   319    312     56.2356     222.9658
rnset012   312    311     49.2252     302.3251
rnset013   311    310     41.2496     197.2145
rnset014   201    205     52.8066      23.2527
rnset015   100    310      29.8768     0.5067
rnset016   201    205      52.8066     23.2527
rnset017   205    202      36.9951    34.10
rnset018   209    201      56.0320     0.8100
rnset019   314    313      63.6524     669.1346
rnset020   317    327      63.6524       70.625
rnset021   327    310      41.2496       70.625
*
*
*
*  pool scrubbing - rn package
*     01-suppression pool
*     02-pedestal cavity
*
rn2pls01   100  0.005  1.5  0.20  1.16
rn2pls02 1001  0.005  1.5  0.20  1.16
*
*
*      rn spray parameters
```

```
*
rn2spr00    4
rn2spr02  01    392.0
*
*******************************************************************
*
* heat structure input
*
*******************************************************************
*
*****************************************************************
*   hs20145xnn - misc steel horizontal heat slab for cv 210
*              - elevation = 176'9" = 53.8734 m
*              - area = 1490.2 ft**2 = 138.43 m**2
*              - length = delta r = 1.5664 m
*              - assume thickness = 1/8" = 0.003175 m
*
*****************************************************************
*
hs20145000  5  1  -1  0
hs20145001  misc-steel-cv201
hs20145002  53.8734  0.0
hs20145003  1.0
hs20145100  -1  2  0.0
hs20145102  0.00794  1 * 1/32" steel
hs20145103  0.001589 1  * 2/32" steel
hs20145104  0.002381 1  * 3/32 " steel
hs20145105  0.003175 1  * 4/32 " steel
hs20145200  -1
hs20145201  carbon-steel  4
hs20145300  0
hs20145400  1  201  'int'  1.0  1.0
hs20145500  138.43  1.5664  1.5664
hs20145600  1  201  'ext'  1.0  1.0
hs20145700  138.43  1.5664  1.5664
hs20145800  -1
hs20145801  299.82  5
*
*****************************************************************
*    hs20215xnn -pedestal cavity wall
*               begins at elevation = 94' 6" =28.806 m
*               ends at elevation = 100' 9" = 30.7086 m
*               length = 1.905 m
*               ri = 10' 7" =3.2258 m
*               ro = 16' 4" = 4.978e m
*****************************************************************
*
hs20215000   15   2   -1   0
hs20215001  ped-cavity-wall
hs20215002  28.8036  1.0
hs20215003  1.0
hs20215100  -1  1  3.2258
hs20215102  3.2283  2 * 1/10" concrete
hs20215103  3.2309  3 * 2/10" concrete
hs20215104  3.2360  4 * 4/10" concrete
hs20215105  3.2512,  5 * 1"    concrete
hs20215106  3.3528  6 * 5"    concrete
hs20215107  3.6068  7 * 15"   concrete
hs20215108  4.1071  8 * 34.5" concrete
hs20215109  4.5974  9 * 54"   concrete
hs20215110  4.8514 10 * 64"   concrete
hs20215111  4.9530 11 * 68"   concrete
hs20215112  4.9682 12 * 68.6" concrete
hs20215113  4.9733 13 * 68.8" concrete
hs20215114  4.9759 14 * 68.9" concrete
```

```
hs20215115  4.9784 15 * 69.0" concrete
hs20215200  -1
hs20    201  concrete                14
hs20.   500  0
hs20215e00  1  202  'int'  1.0  1.0
hs20215500  1.0  6.4516  1.905
hs20215600  0
hs20215800  -1
hs20215801  330.72  15
*
*****************************************************************
*    hs20216xnn - pedestal cavity  wall
*                 begins at elevation = 114' 9" = 34.9758 m
*                 ends at elevation = 117' 4" = 35.7632 m
*                 ri=  9'5" = 2.8702 m
*                 ro = 16'4" = 4.9784 m
*                 wall thickness = 83" concrete
*****************************************************************
*
hs20216000  17  2  -1  0
hs20216001  ped-cavity-wall
hs20216002  34.9758  1.0
hs20216003  1.0
hs20216100  -1  1  2.8702
hs20216102  2.8727  2 * 1/10"   concrete
hs20216103  2.8753  3 * 2/10"   concrete
hs20216104  2.8804  4 * 4/10"   concrete
hs20216105  2.9856  5 * 1 "     concrete
hs20216106  2.9972  6 * 5 "     concrete
hs20216107  3.2512  7 *15 "     concrete
hs20216108  3.6322  8 *30 "     concrete
hs20216109  3.9243  9 *41.5"    concrete
hs20216110  4.2164 10 *53  "    concrete
hs20216111  4.5074 11 *68 "     concrete
hs20216112  4.8514 12 *78 "     concrete
hs20216113  4.9530 13 *82 "     concrete
hs20216114  4.9682 14 *82.6"    concrete
hs20216115  4.9733 15 *82.8"    concrete
hs20216116  4.9759 16 *82.9"    concrete
hs20216117  4.9784 17 *83.0"    concrete
hs20216200  -1
hs20216201  concrete                16
hs20216300  0
hs20216400  1  202  'int'  1.0  1.0
hs20216500  1.0 5.7404  0.7874
hs20216600  1  200  'ext' 1.0  1.0
hs20216700  1.0  9.9568  0.7874
hs20216800  -1
hs20216801  330.72  17
*
*****************************************************************
*    hs20226xnn - pedestal cavity floor
*                 begins at elevation = 83'6" = 25.4508 m
*                 ends at elevation = 94' 8" = 28.8036 m
*                  r = 10' 7" = 3.2258 m
*                 delta z =length = 3.3528 m
*                 area = pi*r**2 = 32.691m**2
*****************************************************************
*
hs20226000  12  1  -1  0
hs20226001  ped-cavity-floor
hs20226002  25.4508  0.0
hs2022600?  1.0
hs20226100  -1  1  25.4508
hs20226102  27.1272  2  *5.5'  concrete
hs20226103  28.1534  3  *6' 8.8" concrete
```

```
hs20226104  28.4785   4   '8' 10.4" concrete
hs20226105  28.6410   5   '9' 11.2" concrete
hs20226106  28.7232   6   '10'5.6" concrete
hs20226107  28.7629   7   '10' 8.8" concrete
hs20226108  28.7833   8   '10' 10.4" concrete
hs20226109  28.7934   9   '10' 11.6" concrete
hs20226110  28.7985 10   '10' 11.8" concrete
hs20226111  28.8010 11   '10' 11.9" concrete
hs20226112  28.8036 12   '11' 0"     concrete
hs20226200  -1
hs20226201  concrete                11
hs20226300  0
hs20226400  0
hs20226600  1  202  'ext'  0.5  0.5
hs20226700  32.691  3.2258  3.2258
hs20226800  -1
hs20226801  295.0  12
*
*-----------------------------------------------------------------------
*   hs202228xnn = cavity  pedestal wall
*                 similar to hs20215xnn
*                 begins at elevation = 100'9" = 30.7086 m
*                 ends at elevation = 114'9" =34.9758 m (midpoint of
*                 tapered region
*-----------------------------------------------------------------------
*
hs20228000  15  2  -1  0
hs20228001  ped-cavity-wall
hs20228002  30.7086  1.0
hs20228003  1.0
hs20228100  20215  1  3.2258
hs20228200  20215
hs20228300  0
hs20228400  1  202  'int'  1.0  1.0
hs20228500  1.0  6.4516  4.2672
hs20228600  1  208  'ext'  1.0  1.0
hs20228700  1.0  9.9568  4.2672
hs20228800  20215
*
*-----------------------------------------------------------------------
*  hs20229xnn - same as hx20216
*               begins at elevation = 117'4" = 35.7632 m
*               ends at  elevation = 121'4" = 36.9824 m
*-----------------------------------------------------------------------
*
hs20229000  17  2  -1  0
hs20229001  ped-cavity-wall
hs20229002  35.7632  1.0
hs20229003  1.0
hs20229100  20216  1  2.8702
hs20229200  20216
hs20229300  0
hs20229400  1  202  'int'  1.0  1.0
hs20229500  1.0  5.7404  1.2192
hs20229600  1  207  'ext'  1.0  1.0
hs20229700  1.0  9.9568  1.2192
hs20229800  20216
*
*-----------------------------------------------------------------------
*   hs20330 - weir wall annulus floor
*           - begins at elevation = 83'6" = 25.4508 m
*           - ends at elevation = 93' 0 1/4" = 28.3578 m
*           - ri = 10.3632 m
*           - ro = 11.1252 m
*           - similar to hs 31027
*           - area = 51.4409 m**2
```

```
*
hs20[illegible]00  11  1  -1  0
hs20[illegible]01  weir-wall-enn-f1
hs20330002  25.4508  0.0
hs20330003  1.0
hs20330100  31027  1  25.4508
hs20330200  31027
hs20330300  0
hs20330400  0
hs20330600  1  203  'ext'  0.0  0.0
hs20330700  51.4409  0.762  67.5078
hs20330800  31027
*
*...........................................................
*   hs20421 - drywell wall
*             begins at elevation = 161'6" = 49.2252 m
*             ends at elevation = 180' 3" = 54.9402 m
*             length = 5.7150 m
*             same as heat slab 20717
*...........................................................
*
hs20421000  18  2  -1  0
hs20421001  drywell-wall-21
hs20421002  49.2252  1.0
hs20421003  1.0
hs20421100  20717  1  11.1252
hs20421200  20717
hs20421300  0
hs20421400  1  208  'int'  1.0  1.0
hs20421500  1.0  22.2504  5.7150
hs20421600  1  312 'ext'  1.0  1.0
hs20421700  1.0  25.2900  5.7150
hs20421800  20717
*
*...........................................................
*   hs20446xnn - misc steel horizontal heat slab for cv 204
*              - area = 19926.97 ft**2 = 1851.2  m**2
*              - elevation = 170' 4.5" = 51.9303 m
*              - same as hs20145xnn
*              - length = delta r = 6.1468 m
*
*...........................................................
*
hs20446000  5  1  -1  0
hs20446001  misc-steel-cv204
hs20446002  51.9303  0.0
hs20446003  1.0
hs20446100  20145  2  0.0
hs20446200  20145
hs20446300  0
hs20446400  1  204  'int'  1.0  1.0
hs20446500  1851.2  6.1468  6.1468
hs20446600  1  204  'ext'  1.0  1.0
hs20446700  1851.2  6.1468  6.1468
hs20446800  20145
*
*...........................................................
*  hs20524xnn - heat slab for top spherical head of reactor
*             - begins at elevation = 184' 1" = 56.1086 m
*             - ri = 124 3/4" = 3.1687 m
*             - thickness = 3 1/8" = 0.08255 m
*
*...........................................................
*
hs20524000   6  5  -1  0
```

```
hs20524001  rx vessel head
hs20524002  56.1086
hs20524003  1.0
hs20524100  -1  2  3.1687
hs20524102  0.06255  5
hs20524200  -1
hs20524201  carbon-steel  5
hs20524300  0
hs20524400  8890 -205  'int'  1.0  1.0
hs20524500  1.0  3.1687  3.1687
hs20524600  1  209  'ext'  1.0  1.0
hs20524700  1.0  3.2513  3.2513
hs20524800  -1
hs20524801  550.0  6
*
*****************************************************************
*     hs20527xnn - cylindrical portion of reactor vessel
*                - begins at elevation = 128' 8.66" = 39.2344 m
*                - ends at elevation = 184' 1" = 56.1086 m
*                - ri = 126.6875 " = 3.2179 m
*                - length = 16.87424 m
*
*****************************************************************
*
hs20527000  6  2  -1  0
hs20527001  rx-vessel-cylin.
hs20527002  39.2344  1.0
hs20527003  1.0
hs20527100  -1  2  3.2179  *od = 253 3/8"
hs20527102  0.32703  5  *steel
hs20527200  -1
hs20527201  carbon-steel  5  *steel
hs20527300  0
hs20527400  8890 -205 'int' 1.0  1.0
hs20527500  1.0  13.5726  13.5726
hs20527600  1  205  'ext'  1.0  1.0
hs20527700  1.0  13.5726  13.5726
hs20527800  -1
hs20527801  550.0  6
*
*****************************************************************
*     hs20526xnn - heat slab for bottom spherical head of pressure
*                  vessel
*                - begins at elevation = 133' 97652 " = 40.7864 m
*                - ri = 138 3/16 " = 3.510 m
*                - thickness = 7.672 " = 0.1949 m
*
*****************************************************************
*
hs20526000  6  4  -1  0
hs20526001  rx-vessel-bot
hs20526002  40.7864
hs20526003  1.0
hs20526100  -1  2  3.510
hs20526102  0.1949  5  *carbon steel
hs20526200  -1
hs20526201  carbon-steel  5
hs20526300  0
hs20526400  8890  -205  'int'  1.0  1.0
hs20526500  1.0  3.510  3.510
hs20526600  1  205  'ext'  1.0  1.0
hs20526700  1.0  3.7050  3.7050
hs20526800  -1
hs20526801  550.0  6
*
*****************************************************************
```

```
*   hs20547xnn - misc steel horizontal heat slab for cv 205
*              - area = 3465.6 ft**2 = 321.965  m**2
*              - elevation = 147' 3.75" = 44.90090 m
*              - same as hs20145xnn
*              - length = delta r = 0.9874 m
*
*****************************************************************
*
hs20547000  5  1  -1  0
hs20547001  misc-steel-cv205
hs20547002  44.90090  0.0
hs20547003  1.0
hs20547100  20145  2  0.0
hs20547200  20145
hs20547300  0
hs20547400  1  205  'int'  1.0  1.0
hs20547500  321.965  0.9874  0.9874
hs20547600  1  205  'ext'  1.0  1.0
hs20547700  321.965  0.9874  0.9874
hs20547800  20145
*
*****************************************************************
*   hs20850xnn - misc steel horizontal heat slab for cv 208
*              - area = 13056.51 ft**2 = 1213.0  m**2
*              - elevation = 109' 0.5" = 33.2359 m
*              - same as hs20145xnn
*              - length = delta r = 4.9276 m
*
*****************************************************************
*
hs20850000  5  1  -1  0
hs20850001  misc-steel-cv208
hs20850002  33.2359  0.0
hs20850003  1.0
hs20850100  20145  2  0.0
hs20850200  20145
hs20850300  0
hs20850400  1  208  'int'  1.0  1.0
hs20850500  1213.0  4.9276  4.9276
hs20850600  1  208  'ext'  1.0  1.0
hs20850700  1213.0  4.9276  4.9276
hs20850800  20145
*
*****************************************************************
*   hs20951xnn - misc steel horizontal heat slab for cv 209
*              - area = 1818.767 ft**2 = 168.23  m**2
*              - elevation = 192' 2" = 58.5724 m
*              - same as hs20145xnn
*              - length = delta r = 9.7536 m
*
*****************************************************************
*
hs20951000  5  1  -1  0
hs20951001  misc-steel-cv209
hs20951002  58.5724  0.0
hs20951003  1.0
hs20951100  20145  2  0.0
hs20951200  20145
hs20951300  0
hs20951400  1  209  'int'  1.0  1.0
hs20951500  168.23  9.7536  9.7536
hs20951600  1  209  'ext'  1.0  1.0
hs20951700  168.23  9.7536  9.7536
hs20951800  20145
*
*****************************************************************
```

```
*    hs20648xnn   misc steel horizontal heat slab for cv 206
*                 - area = 14780.62 ft**2 = 1373.17  m**2
*                 - elevation = 153' 11.5" = 46.9265 m
*                 - same as hs20145xnn
*                 - length = delta r = 6.1468 m
*
*******************************************************************
*
hs20648000  5  1  -1  0
hs20648001  misc-steel-cv206
hs20648002  46.9265  0.0
hs20648003  1.0
hs20648100  20145  2  0.0
hs20648200  20145
hs20648300  0
hs20648400  1  206  'int'  1.0  1.0
hs20648500  1373.17  6.1468  6.1468
hs20648600  1  206  'ext'  1.0  1.0
hs20648700  1373.17  6.1468  6.1468
hs20648800  20145
*
*******************************************************************
*    hs20749xnn - misc steel horizontal heat slab for cv 207
*                 - area = 32134.41 ft**2 = 2985.38  m**2
*                 - elevation = 132' 5.5" = 40.3733 m
*                 - same as hs20145xnn
*                 - length = delta r = 6.1468 m
*
*******************************************************************
*
hs20749000  5  1  -1  0
hs20749001  misc-steel-cv207
hs20749002  40.3733  0.0
hs20749003  1.0
hs20749100  20145  2  0.0
hs20749200  20145
hs20749300  0
hs20749400  1  207  'int'  1.0  1.0
hs20749500  2985.38  6.1468  6.1468
hs20749600  1  207  'ext'  1.0  1.0
hs20749700  2985.38  6.1468  6.1468
hs20749800  20145
*
*******************************************************************
*    hs31052xnn - misc steel horizontal heat slab for cv 310
*                 - area = 117885.8 ft**2 = 10951.95  m**2
*                 - elevation = 123' 0" = 37.7444 m
*                 - same as hs20145xnn
*                 - length = delta r = 6.2484 m
*
*******************************************************************
*
hs31052000  5  1  -1  0
hs31052001  misc-steel-cv310
hs31052002  37.7444  0.0
hs31052003  1.0
hs31052100  20145  2  0.0
hs31052200  20145
hs31052300  0
hs31052400  1  310  'int'  1.0  1.0
hs31052500  10951.95  6.2484  6.2484
hs31052600  1  310  'ext'  1.0  1.0
hs31052700  10951.95  6.2484  6.2484
hs31052800  20145
*
*******************************************************************
```

```
*   hs31153xnn - misc steel horizontal heat slab for cv 311
*                - area = 78296.3 ft**2 = 7273.96  m**2
*                - elevation = 148' 5" = 45.2374 m
*                - same as hs20145xnn
*                - length = delta r = 6.2484 m
*
*****************************************************************
*
hs31153000  5  1  -1  0
hs31153001  misc-steel-cv311
hs31153002  45.2374  0.0
hs31153003  1.0
hs31153100  20145  2  0.0
hs31153200  20145
hs31153300  0
hs31153400  1  311  'int'  1.0  1.0
hs31153500  7273.96  6.2484  6.2484
hs31153600  1  311  'ext'  1.0  1.0
hs31153700  7273.96  6.2484  6.2484
hs31153800  20145
*
*****************************************************************
*   hs31254xnn - misc steel horizontal heat slab for cv 312
*                - area = 31546.3 ft**2 = 2930.75  m**2
*                - elevation = 173' 0" = 52.7304 m
*                - same as hs20145xnn
*                - length = delta r = 1.9817 m
*
*****************************************************************
*
hs31254000  5  1  -1  0
hs31254001  misc-steel-cv312
hs31254002  52.7304  0.0
hs31254003  1.0
hs31254100  20145  2  0.0
hs31254200  20145
hs31254300  0
hs31254400  1  312  'int'  1.0  1.0
hs31254500  2930.75  1.9817  1.9817
hs31254600  1  312  'ext'  1.0  1.0
hs31254700  2930.75  1.9817  1.9817
hs31254800  20145
*
*****************************************************************
*  hs31308xnn - upper pool vertical walls (slab)
*               - begins at elevation = 167'6.25" = 51.0604 m
*               - ends at elevation = 208' 10" = 63.6524 m
*               - lined with 1/4" steel plate
*               - model wall as 2' thick concrete with insulated boundary
*               - area = 9303 ft**2 = 964.3 m**2
*
*****************************************************************
*
hs31308000  11  1  -1  0
hs31308001  upper-pool-wall
hs31308002  51.0604  1.0
hs31308003  1.0
hs31308100  -1  1  0.0
hs31308102  0.00254  2  * 1/10" steel
hs31308103  0.00508  3  * 2/10" steel
hs31308104  0.00635  4  * 1/4"  steel
hs31308105  0.01270  5  * 1/2"  concrete
hs31308106  0.02540  6  * 1 "   concrete
hs31308107  0.05080  7  * 2"    concrete
hs31308108  0.10160  8  * 4 " concrete
hs31308109  0.20320  9  * 8 " concrete
```

```
hs31308110  0.40640 10   * 16" concrete
hs31308111  0.01280 11   * 24" concrete
hs31308200  -1
hs31308201  carbon-steel  3
hs31308202  concrete  10
hs31308300  0
hs31308400  1  313 'int'  0.0  0.0
hs31308500  964.3  7.32  7.32
hs31308600  0
hs31308800  -1
hs31308801  294.3  11
*
*****************************************************************
*     hs31309xnn - upper pool floor horizontal slab
*                - begins at elevation = 180'3" = 54.9402 m
*                - ends at elevation = 184' 6.25" = 56.2420 m
*                - area = 3652 ft**2 (measured) = 339.3 m**2
*                - thickness = 4'3" = 1.2954 m
*                - 1/4 " steel plate next to pool and drywall
*                - 106.25' x 34.375'
*
*****************************************************************
*
hs31309000  19  1  -1  0
hs31309001  upper-pool-floor
hs31309002  54.9402  0.0
hs31309003  1.0
hs31309100  -1  1  0.0
hs31309102  0.00254  2   * 1/10" steel
hs31309103  0.00635  3   * 1/4 " steel
hs31309104  0.01270  4   * 1/2 " concrete
hs31309105  0.02540  5   * 1"  concrete
hs31309106  0.05080  6   * 2 " concrete
hs31309107  0.10160  7   * 4 " concrete
hs31309108  0.20320  8   * 8 " concrete
hs31309109  0.40640  9   * 16" concrete
hs31309110  0.64770 10   * 25.5" concrete
hs31309111  0.88900 11   * 35"  concrete
hs31309112  1.09220 12   * 43" concrete
hs31309113  1.19380 13   * 47" concrete
hs31309114  1.24460 14   * 49" concrete
hs31309115  1.27000 15   * 50" concrete
hs31309116  1.28270 16   * 50.5" concrete
hs31309117  1.28905 17   * 50.75" steel
hs31309118  1.29286 18   * 50.90" steel
hs31309119  1.29540 19   * 51.00" steel
hs31309200  -1
hs31309201  carbon-steel  2
hs31309202  concrete  14
hs31309203  carbon-steel  18
hs31309300  0
hs31309400  1  204  'int' 1.0  1.0
hs31309500  339.3  10.48  10.48
hs31309600  1  313  'ext'  0.0  0.0
hs31309700  339.3  10.48  10.48
hs31309800  -1
hs31309801  294.3  19
*
*****************************************************************
*   hs31955xnn - misc steel horizontal heat slab for cv 319
*              - area = 38307.67 ft**2 = 3558.9  m**2
*              - elevation = 196' 8" = 59.9440 m
*              - same as hs20145xnn
*              - length = delta r = 4.3034 m
*
*****************************************************************
```

```
hs31955000  5  1  -1  0
hs31[illegible]001  misc-steel-cv319
hs31    02  59.9440  0.0
hs319>>003  1.0
hs31955100  20145  2  0.0
hs31955200  20145
hs31955300  0
hs31955400  1  319  'int'  1.0  1.0
hs31955500  3558.9  4.3034  4.3034
hs31955600  1  319  'ext'  1.0  1.0
hs31955700  3558.9  4.3034  4.3034
hs31955800  20145
*
*****************************************************************
*   hs32056xnn - misc steel horizontal heat slab for cv 320
*              - area = 4447.88 ft**2 = 413.15  m**2
*              - elevation = 194' 8" = 59.3344 m
*              - same as hs20145xnn
*              - length = delta r = 10.140 m
*
*****************************************************************
*
hs32056000  5  1  -1  0
hs32056001  misc-steel cv320
hs32056002  59.3344  0.0
hs32056003  1.0
hs32056100  20145  2  0.0
hs32056200  20145
hs32056300  0
hs32056400  1  320  'int'  1.0  1.0
hs32056500  413.15  10.140  10.140
hs32056600  1  320  'ext'  1.0  1.0
hs32056700  413.15  10.140  10.140
hs32056800  20145
*
*****************************************************************
*   hs32157xnn - misc steel horizontal heat slab for cv 321
*              - area = 5967.24 ft**2 = 554.4  m**2
*              - elevation = 153' 0" = 46.6344 m
*              - same as hs20145xnn
*              - length = delta r = 6.2484 m
*
*****************************************************************
*
hs32157000  5  1  -1  0
hs32157001  misc-steel-cv321
hs32157002  46.6344  0.0
hs32157003  1.0
hs32157100  20145  2  0.0
hs32157200  20145
hs32157300  0
hs32157400  1  321  'int'  1.0  1.0
hs32157500  554.4  6.2484  6.2484
hs32157600  1  321  'ext'  1.0  1.0
hs32157700  554.4  6.2484  6.2484
hs32157800  20145
*
*****************************************************************
*   hs32258xnn - misc steel horizontal heat slab for cv 322
*              - area = 3743.72 ft**2 = 347.80  m**2
*              - elevation = 187' 11" = 57.277 m
*              - same as hs20145xnn
*              - length = delta r = 4.064 m
*
*****************************************************************
```

```
*
hs32250000  5  1  -1  0
hs32250001  misc-steel-cv322
hs32250002  52.277  0.0
hs32250003  1.0
hs32250100  20145  2  0.0
hs32250200  20145
hs32250300  0
hs32250400  1  322  'int'  1.0  1.0
hs32250500  347.80  4.064  4.064
hs32250600  1  322  'ext'  1.0  1.0
hs32250700  347.80  4.064  4.064
hs32250800  20145
*
*---------------------------------------------------------------------
*   hs32359xnn - misc steel horizontal heat slab for cv 323
*              - area = 1134.46 ft**2 = 1134.46  m**2
*              - elevation = 176' 10" = 53.8988 m
*              - same as hs20145xnn
*              - length = delta r = 3.81 m
*
*---------------------------------------------------------------------
*
hs32359000  5  1  -1  0
hs32359001  misc-steel-cv323
hs32359002  53.8988  0.0
hs32359003  1.0
hs32359100  20145  2  0.0
hs32359200  20145
hs32359300  0
hs32359400  1  323  'int'  1.0  1.0
hs32359500  105.395  3.81  3.81
hs32359600  1  323  'ext'  1.0  1.0
hs32359700  105.395  3.81  3.81
hs32359800  20145
*
*---------------------------------------------------------------------
*   hs32460xnn - misc steel horizontal heat slab for cv 324
*              - area = 1633.62 ft**2 = 151.77  m**2
*              - elevation = 194' 8" = 59.3344 m
*              - same as hs20145xnn
*              - length = 30' = 9.144 m
*
*---------------------------------------------------------------------
*
hs32460000  5  1  -1  0
hs32460001  misc-steel-cv324
hs32460002  59.3344  0.0
hs32460003  1.0
hs32460100  20145  2  0.0
hs32460200  20145
hs32460300  0
hs32460400  1  324  'int'  1.0  1.0
hs32460500  151.77  9.144  9.144
hs32460600  1  324  'ext'  1.0  1.0
hs32460700  151.77  9.144  9.144
hs32460800  20145
*
*---------------------------------------------------------------------
*   hs32561xnn - misc steel horizontal heat slab for cv 325
*              - area = 274.58 ft**2 = 25.506  m**2
*              - elevation = 164' 4" = 50.0888 m
*              - same as hs20145xnn
*              - length = 7.5' (measured) = 2.286 m
*
*---------------------------------------------------------------------
```

```
hs32561000  5  1  -1  0
hs325  1001  misc-steel-cv325
hs32   002  50.0000  0.0
hs32561003  1.0
hs32561100  20145  2  0.0
hs32561200  20145
hs32561300  0
hs32561400  1  325  'int'  1.0  1.0
hs32561500  25.506  2.296  2.296
hs32561600  1  325  'ext'  1.0  1.0
hs32561700  25.506  2.296  2.296
hs32561800  20145
*
*****************************************************************
*   hs32662xnn - misc steel horizontal heat slab for cv 326
*              - area = 1225.21 ft**2 = 113.825  m**2
*              - elevation = 166' 4" = 50.6984 m
*              - same as hs20145xnn
*              - length = 13.333' (measured) = 4.064 m
*
*****************************************************************
*
hs32662000  5  1  -1  0
hs32662001  misc-steel-cv326
hs32662002  50.6984  0.0
hs32662003  1.0
hs32662100  20145  2  0.0
hs32662200  20145
hs32662300  0
hs32662400  1  326  'int'  1.0  1.0
hs32662500  113.825  4.064  4.064
hs32662600  1  326  'ext'  1.0  1.0
hs32662700  113.825  4.064  4.064
hs32662800  20145
*
*****************************************************************
*   hs20519 - shield wall
*             begins at elevation = 121' 4 1/2" = 36.995 m
*             ends at elevation = 167'7" = 44.983m m
*             ri = 14'4" = 4.3688 m
*             ro = 16'0" = 4.8768 m
*             length = 7.9884 m
*             3/4" steel plate on internal surface , 1 1/4" plate
*             on outer surface, thickness = 24" (22" concrete  )
*
*****************************************************************
*
hs20519000  15  2  -1  0
hs20519001  shield-wall-19
hs20519002  36.995  1.0
hs20519003  1.0
hs20519100  -1  1  4.3688
hs20519102  4.37308  2  "2/10"  steel
hs20519103  4.37896  3  "4/10"  steel
hs20519104  4.39705  4  "3/4"   steel
hs20519105  4.40690  5  "1.5"   concrete
hs20519106  4.44500  6  "5"     concrete
hs20519107  4.52120  7  "6"     concrete
hs20519108  4.67360  8  "12"    concrete
hs20519109  4.82600  9  "18"    concrete
hs20519110  4.90720 10  "21"    concrete
hs20519111  4.90930 11  "22.5"  concrete
hs20519112  4.98665 12  "22.75" concrete
hs20519113  4.96570 13  "23.50" steel
hs20519114  4.97205 14  "23.75  steel
```

```
hs20518115  4.97840 15  "24.0"  steel
hs20518200  -1
hs20518201  carbon-steel          3
hs20518202  concrete              11
hs20518203  carbon-steel          14
hs20518300  0
hs20518400  1  205  'int'  1.0  1.0
hs20518500  1.0  8.7376  7.9884
hs20518600  1  207  'ext'  1.0  1.0
hs20518700  1.0  9.9568  7.9884
hs20518800  -1
hs20518801  330.72  15
*
*-------------------------------------------------------------
*   hs20520 - shield wall
*             begins at elevation = 147' 7" = 44.9834 m
*             ends at elevation = 161' 6" = 49.2252 m
*             length = 4.2418 m
*             same as heat slab 20518xnn
*-------------------------------------------------------------
*
hs20520000  15  2  -1  0
hs20520001  shield-wall-20
hs20520002  44.9834  1.0
hs20520003  1.0
hs20520100  20518  1  4.3688
hs20520200  20518
hs20520300  0
hs20520400  1  205  'int'  1.0  1.0
hs20520500  1.0  8.7376  4.2418
hs20520600  1  206  'ext'  1.0  1.0
hs20520700  1.0  9.9568  4.2418
hs20520800  20518
*
*-------------------------------------------------------------
*   hs20522 - shield wall
*             begins at elevation = 161'10" = 49.3268 m
*             ends at elevation = 173' 3" = 52.807 m
*             length = 3.4802 m
*             same as heat slab 20518
*-------------------------------------------------------------
*
hs20522000  15  2  -1  0
hs20522001  shield-wall-22
hs20522002  49.3268  1.0
hs20522003  1.0
hs20522100  20518  1  4.3688
hs20522200  20518
hs20522300  0
hs20522400  1  205  'int'  1.0  1.0
hs20522500  1.0  8.7376  3.4802
hs20522600  1  204  'ext'  1.0  1.0
hs20522700  1.0  9.9568  3.4802
hs20522800  20518
*
*-------------------------------------------------------------
*   hs20615xnn - drywell wall
*                begins at 147' 7" = 44.9834 m
*                ends at 161'6" = 49.2752 m
*                ri = 36' 6" = 11.1252 m
*                ro = 41' 6" = 12.6492 m
*                length = 4.2418 m
*                same as hs20717xnn
*-------------------------------------------------------------
*
hs20615000  18  2  -1  0
```

```
hs20615001  drywall-wall-15
hs20615002  ac 9834  1.0
hs20[illegible]03  1.0
hs20[illegible]30  20717  1  11.1252
hs20615200  20717
hs20615300  0
hs20615400  1  20[illegible]  'int'  1.0  1.0
hs20615500  1.0  22.2504  4.2418
hs20615600  1  311  'ext'  1.0  1.0
hs20615700  1.0  25.2906  4.2418
hs20615900  20717
*
*************************************************************
*     hs20717 - drywall wall
*               begins at elevation = 117'4" = 35.7632 m
*               ends at elevation = 135'4" = 41.2496 m
*               length = 5.4864 m
*               1/4" thick steel plate on inside surface
*               ri= 36'6" = 11.1252 m
*               ro= 41'6" = 12.6492 m
*************************************************************
*
hs20717000  10  2  -1  0
hs20717001  drywall-wall-17
hs20717002  35.7632  1.0
hs20717003  1.0
hs20717100  -1  1  11.1252
hs20717102  11.12776  2  "1/10" steel
hs20717103  11.13020  3  "2/10" steel
hs20717104  11.13155  4  " 1/4" steel
hs20717105  11.15060  5  "1"    concrete
hs20717106  11.17600  6  "2"    concrete
hs20717107  11.22680  7  "4"    concrete
hs20717108  11.32840  8  "8"    concrete
hs20717109  11.53160  9  "16"   concrete
hs20717110  11.90720 10  "30"   concrete
hs20717111  12.20200 11  "44"   concrete
hs20717112  12.40600 12  "52"   concrete
hs20717113  12.54760 13  "56"   concrete
hs20717114  12.59840 14  "58"   concrete
hs20717115  12.62380 15  "59"   concrete
hs20717116  12.63650 16  "59.5" concrete
hs20717117  12.64290 17  "59.75" concrete
hs20717118  12.64920 18  "60"   concrete
hs20717200  -1
hs20717201  carbon-steel          3
hs20717202  concrete              17
hs20717300  0
hs20717400  1  207  'int'  1.0  1.0
hs20717500  1.0  22.2504  5.4864
hs20717600  1  310  'ext'  1.0  1.0
hs20717700  1.0  25.2906  5.4864
hs20717900  -1
hs20717901  320.0  10
*
*************************************************************
*   hs 20729 - drywall -wall
*            - begins at elevation = 135'0" = 41.2496 m
*            - ends at elevation = 147'7" = 44.9834 m
*            - length = 3.7338 m
*            - same as hs20717
*
*************************************************************
*
hs20729000  10  2  -1  0
hs20729001  drywall-wall-29
```

```
hs20729002  41.2496  1.0
hs20729003  1.0
hs20729100  20717  1  11.1252
hs20729200  20717
hs20729300  0
hs20729400  1  207  'int'  1.0  1.0
hs20729500  1.0  22.2504  3.7338
hs20729600  1  311  'ext'  1.0  1.0
hs20729700  1.0  25.2984  3.7338
hs20729800  20717
*
*-----------------------------------------------------------------------
*   hs20813 - weir wall heat slab
*             ri = 32'6" = 9.906 m
*             ro = 34'0" = 10.3632 m
*             begins at elevation = 100'9"
*             ends at elevation = 117' 6"
*             3/8" plate on suppression pool side
*
*-----------------------------------------------------------------------
*
hs20813000  17  2  -1  0
hs20813001  weir-wall
hs20813002  30.7086  1.0 * elevation = 100'9"
hs20813003  1.0
hs20813100  -1  1  9.906
hs20813102  9.90854  2  "1/10"   concrete
hs20813103  9.91108  3  "2/10"   concrete
hs20813104  9.91616  4  "4/10"   concrete
hs20813105  9.92632  5  "8/10"   concrete
hs20813106  9.94664  6  "1.6"    concrete
hs20813107  9.98728  7  "3.2"    concrete
hs20813108  10.06856 8  "6.4"    concrete
hs20813109  10.15460 9  "9.0"    concrete
hs20813110  10.20064 10 "11.6"   concrete
hs20813111  10.28192 11 "14.8"   concrete
hs20813112  10.32256 12 "16.4"   concrete
hs20813113  10.34288 13 "17.2"   concrete
hs20813114  10.35304 14 "17.6"   concrete
hs20813115  10.35685 15 "17.75"  steel
hs20813116  10.35939 16 "17.85"  steel
hs20813117  10.36320 17 "18.00"  steel
hs20813200  -1
hs20813201  concrete              13
hs20813202  carbon-steel          16
hs20813300  0
hs20813400  1  208  'int'  1.0  1.0
hs20813500  1.0  19.8120  5.0546
hs20813600  1  203  'ext'  0.5  0.5
hs20813700  1.0  20.7264  5.0546
hs20813800  -1
hs20813801  308.15  17
*
*-----------------------------------------------------------------------
*   hs 20814 - drywell floor
*              begins at elevation = 83'6" = 25.4508 m
*              ends at elevation = 100'9" = 30.7086 m
*              ri = 16'6" = 4.9784 m
*              ro = 32'6" = 9.9060 m
*              delta r = 4.9276 m
*              area = 230.418 m**2
*-----------------------------------------------------------------------
*
hs20814000  9  1  -1  0
hs20814001  drywell-floor
hs20814002  25.4508  0.0
```

```
hs20814003  1.0
hs20814100  -1  1  25.0509
hs208   02  28.11700  2  * 92'1 1/2" concrete
hs209   03  29.39415  3  *96' 5 1/4"  concrete
hs20814104  30.05140  4  *98' 7.125" concrete
hs20814105  30.40300  5  *99'9"      concrete
hs20814106  30.55670  6  *100'3"     concrete
hs20814107  30.63240  7  *100'6"     concrete
hs20814108  30.68320  8  *100'8"     concrete
hs20814109  30.70860  9  *100'9"     concrete
hs20814200  -1
hs20814201  concrete  0
hs20814300  0
hs20814400  0
hs20814600  1  208  'ext'  0.5  0.5
hs20814700  230.418  4.9276  4.9276
hs20814800  -1
hs20814901  294.3  9
*-------------------------------------------------------------------
*   hs20923 - drywall head cylindrical portion
*           - thickness = 1 1/2" = 0.0381 m
*           - inside radius = 16' =4.8768 m
*           - outside radius = 16' 1 1/2" = 4.9149 m
*           - begins at elevation = 183' 10" = 56.032 m
*           - ends at elevation = 192' 6" = 58.674 m
*           - length = 2.6416 m
*
*-------------------------------------------------------------------
*
hs20923000  0  2  -1  0
hs20923001  dw-head-cylinder
hs20923002  56.032  1.0
hs20923003  1.0
hs20923100  -1  1  4.8768
hs20923102  4.87934  2  *1/10" ss
hs20923103  4.88188  3  *2/10" ss
hs20923104  4.88696  4  *4/10" ss
hs20923105  4.89712  5  *8/10" ss
hs20923106  4.90728  6  *1 2/10" ss
hs20923107  4.91236  7  *1 4/10" ss
hs20923108  4.91490  8  *1 5/2" ss
hs20923200  -1
hs20923201  'stainless steel'  7
hs20923300  0
hs20923400  1  209  'int'  1.0  1.0
hs20923500  1.0  9.7536  2.6416
hs20923600  1  313  'ext'  0.0  0.0
hs20923700  1.0  9.8298  2.6416
hs20923800  -1
hs20923801  294.3  8
*
*-------------------------------------------------------------------
*  hs20925  - drywall head elliptical portion
*           - thickness = 1 2/16" = 0.020575
*           - ellipsoid surface area = 2*pi*b**2 + 2*pi*a*b*sin-1(e)/e
*                                    = 127.706 m**2
*           - b = 8' = 2.0384 m
*           - a = 2*b = 16' = 4.8768 m
*           - eccentricity (e) = sqrt((a**2-b**2)/a**2) = .866
*           - equal as semi-spherical shell and require equal surface areas
*           - s (semi-sphere) = 2*pi*r**2 = 127.706 m**2
*           - r = 4.509 m
*           - ends at elevation = 208'6" - 61.1120 m
*           - require beginning elevation = 61.11240 - 4.508 m =56.60440
*
*-------------------------------------------------------------------
```

```
*
hs20925000  9  5  -1  0
hs20925001  dw-head ellipse
hs20925002  56.604
hs20925003  1.0
hs20925100  -1  1  4.508
hs20925102  4.51054  2  "1/10" ss
hs20925103  4.51308  3  "2/10" ss
hs20925104  4.51816  4  "4/10" ss
hs20925105  4.52229  5  "9/16" ss
hs20925106  4.52642  6  "0.725" ss
hs20925107  4.53150  7  "0.925" ss
hs20925108  4.53404  8  "1.025" ss
hs20925109  4.53658  9  "1.125" ss
hs20925200  -1
hs20925201  'stainless steel'  0
hs20925300  0
hs20925400  1  209  'int'  1.0  1.0
hs20925500  1.0  4.8768  2.4384
hs20925600  1  313  'ext'  0.0  0.0
hs20925700  1.0  4.93395  2.466975
hs20925800  -1
hs20925801  294.3  9
*
*******************************************************************
*     hs31007xnn - wetwell wall - suppression pool water
*                  begins at elevation = 93' 01/4" = 28.3528 m
*                  ends at elevation = 111' 7 1/6" = 34.015 m
*                  ri = 62'0" = 18.8976 m
*                  ro = 65'6" = 19.9644 m
*                  1/4 " steel plate on inside surface
*                  3' 6" thick wall
*******************************************************************
*
hs31007000  11  2  -1  0
hs31007001  wetwell-wall-h20
hs31007002  28.3528  1.0
hs31007003  1.0
hs31007100  -1  1  18.8976
hs31007102  18.90014  2  "1/10" steel
hs31007103  18.90268  3  "2/10" steel
hs31007104  18.90776  4  "1/4"  steel
hs31007105  18.92300  5  "1"    concrete
hs31007106  18.94840  6  "2"    concrete
hs31007107  18.99920  7  "4"    concrete
hs31007108  19.10080  8  "8"    concrete
hs31007109  19.30400  9  "16"   concrete
hs31007110  19.71040 10  "32"   concrete
hs31007111  19.9644  11  "42"   concrete
hs31007200  -1
hs31007201  carbon-steel              3
hs31007202  concrete  10
hs31007300  0
hs31007400  1  310  'int'  0.0  0.0
hs31007500  1.0  37.7952  5.6622
hs31007600  1  400  'ext'  1.0  1.0
hs31007700  1.0  37.7952  5.6622
hs31007800  -1
hs31007801  308.15  11
*
*******************************************************************
*    hs31006xnn - wetwell-wall-air
*                 same as 31007
*                 begins at elevation = 111' 7 1/6" = 34.015 m
*                 ends at elevation = 135' 4" = 41.2496 m
*******************************************************************
```

```
*
hs31006000  11  7  -1  0
hs310   '01  wetwall-wall-air
hs310   .02  30.015  1.0
hs31006003  1.0
hs31006100  31007  1  10.9976
hs31006200  31007
hs31006300  0
hs31006400  1  310  'int'  1.0  1.0
hs31006500  1.0  37.7952  7.2346
hs31006600  1  400  'ext'  1.0  1.0
hs31006700  1.0  37.7952  7.2346
hs31006800  31007
*
*****************************************************************
*   hs31011 - drywall wall - pool side
*             begins at elevation = 93' 0 1/4" = 28.3520 m
*             ends at elevation = 117' 4" = 35.7632 m
*             ri = 36'6" = 11.1252 m
*             ro = 41'6" = 12.6492 m
*             wall thickness = 60"
*             1/8" thick steel plate on each side
*****************************************************************
*
hs31011000  17  7  -1  0
hs31011001  drywall-wall-11
hs31011002  28.3520  1.0
hs31011003  1.0
hs31011100  -1  1  11.1252
hs31011102  11.12770  2  "1/10"   steel
hs31011103  11.13155  3  "1/4"    steel
hs31011104  11.13790  4  "1/2"    concrete
hs31011105  11.15060  5  "1"      concrete
hs31011106  11.20140  6  "3"      concrete
hs31011107  11.35380  7  "9"      concrete
hs31011108  11.58240  8  "18"     concrete
hs31011109  11.88720  9  "30"     concrete
hs31011110  12.19200 10  "42"     concrete
hs31011111  12.42060 11  "51"     concrete
hs31011112  12.57300 12  "57"     concrete
hs31011113  12.62390 13  "59"     concrete
hs31011114  12.63650 14  "59.5"   concrete
hs31011115  12.64290 15  "59.75"  concrete
hs31011116  12.64670 16  "59.90"  steel
hs31011117  12.64920 17  "60.0 "  steel
hs31011200  -1
hs31011201  carbon-steel              2
hs31011202  concrete  14             1
hs31011203  carbon-steel              16
hs31011300  0
hs31011400  1  203  'int'  0.5  0.5
hs31011500  1.0 22.2504  7.4104
hs31011600  1  310  'ext'  0.5  0.5
hs31011700  1.0  25.2984  7.4104
hs31011800  -1
hs31011801  315.0   17
*
*****************************************************************
*   hs31027 - suppression pool floor - wetwall side
*             ri = 12.6490 m
*             ro = 10.9976 m
*             delta r = 6.2906 m
*             begins at elevation = 83'6"
*             ends at elevation = 93'0 1/4"
*
*****************************************************************
```

```
*
hs31027000  11  1  -1  0
hs31027001  supp-pool-floor
hs31027002  25.4508  0.0
hs31027003  1.0
hs31027100  -1  1  25.4508
hs31027102  26.89860  2  "53"  concrete
hs31027103  27.62250  3  "85 1/2" concrete
hs31027104  27.98445  4  "99 3/4"  concrete
hs31027105  28.16860  5  "107"  concrete
hs31027106  28.25750  6  "110.5" concrete
hs31027107  28.30850  7  "112.5" concrete
hs31027108  28.34640  8  "114.0" concrete
hs31027109  28.3489  9  "114.1" steel
hs31027110  28.35148 10  "114.2" steel
hs31027111  28.35280 11  "114.25" steel
hs31027200  -1
hs31027201  concrete  7
hs31027202  'stainless steel'  10
hs31027300  0
hs31027400  0
hs31027600  1  310  'ext'  0.0  0.0
hs31027700  619.278  6.2486  99.1066
hs31027800  -1
hs31027801  308.15  11
*
*****************************************************************
*   hs31105 - wetwell containment wall from 135'4" to 161'6"
*             ri = 62'0"
*             ro = 65'6"
*
*****************************************************************
*
hs31105000  11  2  -1  0
hs31105001  cont-wall-cv311
hs31105002  41.2496  1.0
hs31105003  1.6
hs31105100  31007  1  18.8976
hs31105200  31007
hs31105300  0
hs31105400  1  311  'int'  0.0  0.0
hs31105500  1.0  37.7952  7.9756
hs31105600  1  400  'ext'  0.6  0.0
hs31105700  1.0  37.7952  7.9756
hs31105800  31007
*
*****************************************************************
*   hs31204 - wetwell containment wall from 161'6" to 184'6"
*             (49.2252 m to 56.2356 m)
*
*****************************************************************
hs31204000  11  2  -1  0
hs31204001  cont-wall-cv312
hs31204002  49.2252  1.0
hs31204003  1.0
hs31204100  31007  1  18.8976
hs31204200  31007
hs31204300  0
hs31204400  1  312  'int'  0.0  0.0
hs31204300  1.0  37.7952  7.0104
hs31204600  1  400  'ext'  0.0  0.0
hs31204700  1.0  37.7952  7.0104
hs31204800  31007
*
*****************************************************************
*    hs31601 - dome portion of well containment wall
```

```
*               thickness = 2'6"
*               begins at elevation =243'6"
*         -radius of 62' based on elevation = 237'9"
*****  ***************************************************   ***
*
hs31601000  10  5  -1  0
hs31601001  cont-wall-dome
hs31601002  74.2188
hs31601003  1.0
hs31601100  -1  1  17.1450
hs31601102  17.14754  2  "1/10" steel
hs31601103  17.15008  3  "2/10" steel
hs31601104  17.15516  4  "1/4 " steel
hs31601105  17.17040  5  "1"    concrete
hs31601106  17.19580  6  "2"    concrete
hs31601107  17.24660  7  "4"    concrete
hs31601108  17.34820  8  "8"    concrete
hs31601109  17.55140  9  "16"   concrete
hs31601110  17.9070 10  "30"   concrete
hs3160120 '  -1
hs31601201  carbon-steel       3
hs31601202  concrete  9
hs3160:300  0
hs31601400  1  316  'int'  0.0  0.0
hs31601500  1.0  17.1450  17.1450
hs31601600  1  400  'ext'  0.0  0.0
hs31601700  1.0  17.1450  17.1450
hs31601800  -1
hs31601801  308.15  10
*
*****************************************************************  *****
*   hs31703 - wetwell containment wall from 208'10" to 226'2"
*             (63.6524 m to 68.9356 m)
*
*****************************************************************
*
hs31703000  11  2  -1  0
hs31703001  cont-wall-cv317
hs31703002  63.6524  1.0
hs31703003  1.0
hs31703100  31007  1  18.8976
hs31703200  31007
hs31703300  0
hs31703400  1  317  'int'  0.0  0.0
hs31703500  1.0  37.7952  5.2832
hs31703600  0
hs31703800  31007
*
*****************************************************************
*   hs31802 - wetwell containment wall from 226'2"  to 243'6"
*             (68.9356 m to 74.2188 m)
*
*****************************************************************
*
hs31802000  11  2  -1  0
hs31802001  cont-wall-cv318
hs31802002  68.9356  1.0
hs31802003  1.0
hs31802100  31007  1  18.8976
hs31802200  31007
hs31802300  0
hs31802400  1  318  'int'  0.0  0.0
hs31802500  1.0  37.7952  5.2832
hs31802600  0
hs31802800  31007
*
```

```
*-----------------------------------------------------------------------
*    concrete    degassing input
*    degassing values provided by c.r. hyman (ctd, ornl) 10-26-89
*-----------------------------------------------------------------------
hsdg000110      -20215        10     'h2o-vap'      * 360.0-378 k
hsdg000120      -20215        10     'h2o-vap'     * 378-793 k
hsdg000130      -20215        10     'co2'           * 823-1073 k
hsdg000111      59.68      2.258e6        360.0        378.0
hsdg000121      44.27      6.065e6        378.0        793.0
hsdg000131      473.06     4.157e6        823.0       1073.0
*-----------------------------------------------------------------------
hsdg000210      20226         11     'h2o-vap'      * 360.0-378 k
hsdg000220      20226         11     'h2o-vap'     * 378-793 k
hsdg000230      20226         11     'co2'           * 823-1073 k
hsdg000211      59.68      2.258e6        360.0        378.0
hsdg000221      44.27      6.065e6        378.0        793.0
hsdg000231      473.06     4.157e6        823.0       1073.0
*-----------------------------------------------------------------------
hsdg000310      -20228        10     'h2o-vap'      * 360.0-378 k
hsdg000320      -20228        10     'h2o-vap'     * 378-793 k
hsdg000330      -20228        10     'co2'           * 823-1073 k
hsdg000311      59.68      2.258e6        360.0        378.0
hsdg000321      44.27      6.065e6        378.0        793.0
hsdg000331      473.06     4.157e6        823.0       1073.0
*-----------------------------------------------------------------------
*
* ---------------------------------------------------------------------
* tabular function for pressure vessel temperatures vs time
* ---------------------------------------------------------------------
*
*
*     the values of temperature vs time were taken from the bwr sar srv run
*     of october 10, 1989. the steam/h2 temperature vs time in the srv
*     file was used as the basis of the pressure vessel temperature.  the
*     inside surface of the pressure vessel is set equal to the control
*     fun.  see hs 20527xnn, hs20528xnn, hs20526xnn for use of cf 898
*
*
*
*
* ---------------------------------------------------------------------
* tabular function input for vessel insulation
* ---------------------------------------------------------------------
*
tf12000    'htc out vess'       2          1.0         0.0
tf12010                         273.15     10.0        5000.0      10.0
*-----------------------------------------------------------------------
* ---------------------------------------------------------------------
* tabular function input for thermal conductivity, heat capacity, and
* density of heat structure materials
* ---------------------------------------------------------------------
*-----------------------------------------------------------------------
* carbon-steel
mpmat10000 carbon-steel
mpmat10001 thc 100
mpmat10002 cps 101
mpmat10003 rho 102
*
tf10000    'thc carbon-steel'  10         1.0         0.0
tf10010                        273.15     55.0        373.15      52.0
tf10011                        473.15     48.0        573.15      45.0
tf10012                        673.15     42.0        873.15      35.0
tf10013                       1073.15     31.0       1273.15      29.0
tf10014                       1473.15     31.0       9973.15      31.0
*
tf10100    'cp carbon-steel '  2          1.0         0.0
```

```
tf10110                         273.15     0.465e3    5000.0     0.465e3
*
tf102      'rho carbon-steel'   2          1.0        0.0
tf102                           293.15     7833.0     5000.0     7833.
*****************************************************************
* drywell head air space gap properties
mpmat20000    'air gap 1'
mpmat20001    thc  200
mpmat20002    cps  201
mpmat20003    rho  202
*
tf20000       'thc air gap 1'   2      1.0     0.0
tf20011           273.15      17.0         10000.0       17.0
*
tf20100       'cps air gap 1'   2      1.0     0.0
tf20111           273.15     1005.0        10000.0      1005.0
*
tf20200       'rho air gap 1'   2      1.0     0.0
tf20211           273.15      1.18         10000.0       1.18
*****************************************************************
* thermal properties for limestone / common sand concrete
mpmat30000    concrete
mpmat30001    thc  300
mpmat30002    cps  301
mpmat30003    rho  302
*
tf30000       'thc concrete'    2      1.0     0.0
tf30011           273.15      1.3         10000.0       1.3
*
tf30100       'cps concrete'    2      1.0     0.0
tf30111           273.15    1200.0        10000.0     1200.0
*
tf30200       'rho concrete'    2      1.0     0.0
tf30211           273.15    2340.0        10000.0     2340.0
*****************************************************************
cf31100   ww-dw-dp  add  2  1.  0.
cf31101   0.
cf31110   1.   0.   cvh-p.310
cf31111   -1.   0.   cvh-p.204
*
cf31200   ww-dp  max  2  1.  0.
cf31201   0.
cf31210   1.   0.   cfvalu.311
cf31211   1.   0.   cfvalu.312
*
cf31300   ww-ww-p  max  2  1.  0.
cf31301   0.
cf31310   1.    0.    cvh-p.310
cf31311   1.    0.    cfvalu.313
*
cf31400   ww-ww-t  max  2  1.  0.
cf31401   0
cf31410   1.    0.    cvh-tvap.310
cf31411   1.    0.    cfvalu.314
*
*****************************************************************
*****************************************************************
*    3 spray headers at elevations 294' 0", 282' 10", and 264' 0"
*    with a total flow rate of 5650 gpm (0.3565 m**3/sec)
*    all 3 headers located in cv 316
*    based on a mean drop fall height of 65.5 m, an elevation of
*    208'10" + 65.5' = 274'4" is used
*
*****************************************************************
sprsr0100  cont-spray  316  83.6168  333
sprsr0101  335.93  0.3565
```

```
sprsr0102  2.30e-04    1.0
sprjun01   316   315   0.6
sprjun02   316   318   0.4
sprjun03   315   314   1.0
sprjun04   318   317   1.0
sprjun05   314   313   1.0
sprjun06   317   319   1.0
sprjun07   319   312   1.0
sprjun08   312   311   1.0
sprjun09   311   310   1.0
sprsump0    310
*
cf33300     sprey-start  1-gt  2  1.   0.
cf33310     1.   0.   time
cf33311     0.  1.e9 time      * sprays inactive for task 3c.1
*
*************************************************************************
*************************************************************************
*
* burn package set to default values
* igniters  off for task 3c.1 (on card  bur000, 0=active,1=inactive)
*
bur000    1
*          xh2ign    xcoign    xh2igy    xcoigy    xo2ig   xmeig
bur001      0.10     0.167     0.015     0.129     0.05    0.55
bur002      0.14      0.09       0.3
*          xh2cc     xcocc    xh2pup    xcopup
bur003     0.08     0.148     0.041     0.125     0.06     0.138    0.09    0.150
*          icvnum   igntr  cdim   tfrac
bur101      311        -777
bur102      312        -777
bur103      207        -777
bur104      204        -777
bur105      206        -777
bur106      316        -777
bur107      319        -777
bur108      320        -777
bur109      321        -777
bur110      322        -777
bur111      323        -777
bur112      324        -777
bur113      325        -777
bur114      326        -777
burcc00   -1   0
burfs00   -1   0
*                   flame speed
*sc00001     2200         4.5          1
*sc00002     2200         0.           2
*
*
*  control function  to turn igniters on/off
*
cf77700 igniters-start  1-gt  2  1.0  0.0
cf77710  1.0  0.0    time
cf77711  0.0  1.0e9   time
*
*************************************************************************
*************************************************************************
***
*
***     DEFINE EXTERNAL DATA FILES
***
*************************************************************************
*************************************************************************
*
* ------ RWRSAR SRV files -----   time  cum-water  cum-steam  cum-h2  temperature
```

```
*          edfname     channels     direct
edf10000    'ser-srv-flows'      4          read
*          filename
edf10.     dp3srv
*            format
edf10002   10f8.1
*
* ----- BWRSAR VESSEL LEAKAGE FLOWS -  time cum-water cum-steam cum-h2 temp
*
*          edfname     channels     direct
edf20000    'ser-brk-flows'      4          read
*          filename
edf20001   dp3brk
*            format
edf20002   10f8.1
*
* ----- BWRSAR DEBRIS POURS -----  time & 16 variables
*              edfname      channels     direct
edf90000    'debris pour'      16          read
*          filename
edf90001   dp3pour
*            format
edf90002   5e15.8
*
* ----- BWRSAR CAVITY DECAY HEAT ----- time, decay heat(watts)
*                edfname      channels     direct
edf70000    'cav decay heat'      1          read
*          filename
edf70001   dp3decay
*            format
edf70002   4e15.8
*************************************************************************
*************************************************************************

*
*------------------------ SRV source tables for testing model ---------------
*
*     Steam and hydrogen sources taken from Steve's Grand Gulf
*     BWRSAR calculation.
*
*     Source steam as vapor into a dummy control volume, and
*     then into the PSP pool via a flow path terminating below the
*     pool surface.
*
*     Source hydrogen into a dummy control volume, and thence into
*     the PSP pool via a flow path terminating below the pool
*     surface.
*
*
*
*   h2o liquid source table: time (s) vs  integrated flow (kg)
*
cv100c0   mass 1   000   1 * source into pool
cv100c1       to   095   9
cf00000   h2o-pool-src   equals   1   1.   0
cf00010   1.   0.   edf.100.1
*
*
*   h2o vapor source table: time (s) vs  integrated flow (kg)
*
cv100c2   mass 3   010   1 * source into atmosphere
cv100c3       to   090   9
cf01000   h2o-vapor-src   equals   1   1.   0.
cf01010   1.   0.   edf.100.2
*
**
```

```
**   hydrogen source table: time (s) vs  integrated flow (kg)
**
cv100c6   mass 4   830   1
cv100c7       te   890   9
cf83000   h2-mass-src   equals   1   1.   0.
cf83010   1.   0.   edf.100.3
**
*****************************************************************
*****************************************************************
**
**   temperature table: time (s) vs  temp (k)
**
cf89000   temp-src   equals   1   1.   0.
cf89001  558.1
cf89010   1.   0.   edf.100.4
*****************************************************************
*****************************************************************
**
**   temperature table: time (s) vs  temp (k)
**
**   this table is limited to sub-critical temperature bounds for use
**   with mass.1 (liquid water) mass sources
**
cf89500   temp-src   equals   1   1.   0.
cf89502  3  273.15  647.2
cf89510   1.   0.   edf.100.4
*****************************************************************
*****************************************************************

*
*-------------- Vessel Break source tables for testing model ---------------
*
*
*   h2o liquid source table: time (s) vs  integrated flow (kg)
*
cv202c0   mass.1   200   1 * source into pool
cv202c1       te   295   9
cf20000   h2o-pool-src   equals   1   1.   0.
cf20010   1.   0.   edf.200.1
*
*
*   h2o vapor source table: time (s) vs  integrated flow (kg)
*
cv202c2   mass.3   210   1 * source into atmosphere
cv202c3       te   290   9
cf21000   h2o-vapor-src   equals   1   1.   0.
cf21010   1.   0.   edf.200.2
*
**
**   hydrogen source table: time (s) vs  integrated flow (kg)
**
cv202c6   mass.4   230   1
cv202c7       te   290   9
cf23000   h2-mass-src   equals   1   1.   0.
cf23010   1.   0.   edf.200.3
**
*****************************************************************
*****************************************************************
**
**   temperature table: time (s) vs  temp (k)
**
cf29000   temp-src   equals   1   1.   0.
cf29010   1.   0.   edf.200.4
*****************************************************************
*****************************************************************
**
```

```
*..    temperature table: time (s) vs  temp (k)
*..
*..       a table is limited to sub-critical temperature bounds for
*..    ..h mass.l (liquid water) mass sources
*..
cf29500    temp-src    equals    1    1    0.
cf29502   3  273.15  647.2
cf29510    1.     0.     edf.200.4
*************************************************************************
*************************************************************************
*************************************************************************
*************************************************************************
*
*
*************************************************************************
************************  source volume  ************************
*************************************************************************
***                                                                   ***
***  this volume is required to provide a pathway for the BWRSAR      ***
***  hydrogen flows to enter the pressure suppression pool            ***
***                                                                   ***
*************************************************************************
*
*************************************************************************
*    cv100 - safety relief valves/spargers volume
*          - centerline elevation = 98'- 0 1/4" = 29.8768 m
*          - volume = 1138.25 ft**3  (all 20 srv's per table e-1 fsar)
*          - assume 10 srv's open at time of sds  (8 + 2 = 10)
*          - assume volume of air and water partitioned according to
*            elevation
*          - elevation = 96.5' to 147' 10 5/8"
*            - use volume of all 20 srv's to aid in code run time
*
*************************************************************************
*
cv100000      sr-values-volume    2    2    3
cv100001   0   0
cv100002   0.0   0.0
cv100a0   3
cv100a1   pvol 1.01353e5  tatm 330.72
cv100a2   mlfr.5   0.79   mlfr.9   0.21   rhum 0.6
cv100a3   zpol   34.1070
cv100b0   79.4132   0.0
cv100b1   45.0755   32.232
*
*
*  ------------------------ flow paths ------------------------------
*
*    f1100 - flowpath between cv100 and cv310
*          - vertical flowpath
*          - elevation = 98'0 1/4" = 29.8768 m
*          - area =pi*r**2 = 2.9186 m**2 (10 srv's * 4 12"od pipes  per srv)
*          - avg segment length = 27.123 m = 72.582'
*          - length = midpoint cv100 to 98'0 1/4"
*          - friction loss term f1/d = 2.3 incorporated into 8* term
*            therefore  f=0.0
*
*************************************************************************
*
f1100000    f1100   100   310   29.8768   29.8768
f1100001    2.9186   27.123    1.0
f1100002    5   0   1   1
f1100003    9.2   9.2   1.0   1.0
f1100004    0.0   0.0
f1100a1    2.9186   27.123   0.254   0.50e-6   0.0
*
```

```
*
*
*
*
*******************************************************************************
*******************************************************************************
*     decay heat input
*******************************************************************************
*******************************************************************************
*
*     the dchdefcls0 card must be specified for cases in which
*     the RN package is calculating aerosol behavior, even if
*     no fission products are being tracked
*
dchreactor  bwr
dchehot     -1   0.
dchdecpow   origen
*
dchdefcls0     'all'
dchctenorm yes
sc00001 3210  1.0713  1    * upgrade power to 3833 mw, 1.0713 = 3833/3578
*
*******************************************************************************
*******************************************************************************
*     transfer process input
*******************************************************************************
*******************************************************************************
*
*    'in' transfer process for core package
*           nmsin    nthre
tpin10100   6        9
tpin10101     read     900
*
*    'out' transfer process for cavity package
*           nmsot    npotot   iotmtx
tpot10200   5        101      vin.103
*
*     cor-cav translation matrix
*     *** note *** control poison mass is not conserved
*           nrow     ncol
tpm1030000  5        6
*           nrow/ncol   value
tpm1030001  1/1         1.0      * uo2 mass
tpm1030002  2/2         1.0      * zro2 mass
tpm1030003  3/3         1.0      * steel mass    * ????????
tpm1030004  4/4         1.0      * zr mass
tpm1030005  5/5         1.0      * steel oxide mass
*     transfer processes for radionuclide transfer
tpin60100   15       1
tpot60200   15       601     do? 1
*
*
*
*******************************************************************************
*******************************************************************************
**     dw cavity input
*******************************************************************************
*******************************************************************************
*
*
*  -- Grand Gulf Cavity:
*                       1.0    = 18' 10" = 5.7404 m
*                       0.0    = 21' 2"  = 6.4516 m
*                       Approximate cavity volume  =  254.648 m**3
*                       Sidewall thickness = 5' 9" = 1.7526 m
*                       Floor thickness = 11' 0" = 3.3528 m
```

```
*
*
*
cav01s      702     dw-cavity      *  drywell impedestal cavity
cav01dh     117   118  119         * cf #'s for decay heat, oxide & metal splits
*
cf11700   dw-cav-decay-ht   aquale   1   1.   0.
cf11710    1.       0.    adf.700.1
*
cf11000   oxide-dh-fract   tab-fun   1   1.   0.
cf11003   118
cf11010    1.       0.    time
tf11000   oxide-dh-fract   2   1.    0.
tf11010       0.            .98     *  put 98% of decay heat in oxide layer
tf11011    1.0e7            .98
*
cf11900   metal-dh-fract   tab-fun   1   1.   0.
cf11903   119
cf11910    1.       0.    time
tf11900   metal-dh-fract     2   1.    0.
tf11910       0.            .02     *  put  2% of decay heat in metal layer
tf11918    1.0e7            .02
*
*
* test test test --- add a bit of material to the debris
* this is necessary to prevent vaness from bombing the first time it
* is called.  it is first called at the onset of concrete ablation
*
cav0110       temp        300.0
cav0111       uo2     0.05
cav0112       nio     0.05
cav0113       cr2o3   0.05
cav0114       zro2    0.05
cav0115       feo     0.05
*
cav0120       temp     300.0
cav0121       fe       0.05
cav0122       ni       0.05
cav0123       zr       0.05
cav0124       cr       0.05
*.....................................................................
*
*     cavity concrete properties
*
*.....................................................................
*
*
*   limestone / common sand concrete (mix#6) with 0.135 kg/kg rebar
cav01c0   user-input
cav01c1   sio2       0.30300        tio2      0.00075
cav01c2   ano        0.00020        ago       0.10000
cav01c3   cao        0.18700        no2o      0.00330
cav01c4   k2o        0.00829        fe2o3     0.01100
cav01c5   al2o3      0.05052        cr2o3     0.00011
cav01c6   co2        0.20500        h2oevap   0.02970
cav01c7   h2ochem    0.02130
cav01c8   fe         0.13500    * 0.135 kg/kg rebar
cav01ca   densct     2340.0     * density
cav01cb   tsolct     1420.0     * solidus temperature
cav01cc   tliqct     1670.0     * liquidus temperature
cav01cd   tablct     1503.0     * ablation temperature
cav01ce   tinct       310.0     * initial temperature
cav01cf   emisct        0.82    * emissivity
*
cav01g0   corcon  2              *  flat bottom cylinder geometry
*
```

```
*          nrayo    r0    z0
cav01g1     55       0.    0.6
*          zt     rad       nit       radc      rw      hbh          nbet   ncorn
cav01g2    0.0   5.7250   2.0596   0.01    4.9784    3.3528    32       3
*
cav01tp          102                 *  transfor process number
*
  ** end of file*
```